2024

Development of a Ni-Catalyzed Enantioselective Intramolecular Mizoroki- Heck Reaction for the Synthesis of Phenanthridinone Derivatives

Diana Rachii
Bryn Mawr College

Development of a Ni-Catalyzed Enantioselective Intramolecular Mizoroki-Heck Reaction for the Synthesis of Phenanthridinone Derivatives

by Diana Rachii

2024

Submitted to the Faculty of Bryn Mawr College
in partial fulfillment of the requirements for
the degree of Doctor of Philosophy
in the Department of Chemistry

Doctoral Committee:

William Malachowski, Advisor
Ashlee Plummer-Medeiros
Yan Kung
Patrick Melvin
Sharon Burgmayer
Victor Donnay

Abstract

The Birch reduction-alkylation coupled to the desymmetrizing Mizoroki-Heck reaction is a novel synthetic tool to form potentially bioactive phenanthridinone analogs from inexpensive and easily available starting materials. This work describes a rare example of the direct replacement of palladium for nickel in our previously reported enantioselective intramolecular Heck reaction. A Ni-catalyzed enantioselective intramolecular Mizoroki-Heck reaction has been developed to transform symmetrical 1,4-cyclohexadienes with attached aryl halides to phenanthridinone analogs containing quaternary stereocenters. Moreover, this approach provides direct access to six-member ring heterocyclic systems bearing all-carbon quaternary stereocenters, which have been much more challenging to form enantioselectively with nickel-catalyzed Heck reactions. The first part of this project describes important advances in reaction optimization enabling control of unwanted proto-dehalogenation and alkene reduction side products. The second section focuses on the development of enantioselective strategy with a newly synthesized chiral *i*Quinox-type bidentate ligand. In the third section, we describe efforts to explore the substrate scope and to subsequently transform the 1,3-diene Heck products into molecules with potentially greater therapeutic relevance. In the last project chapter, mechanistic investigations and a computational study of the key 1,2-migratory insertion step shed light on the catalytic cycle and the basis for the enantioselectivity. Altogether,

this work presents a very attractive alternative to the palladium-catalyzed process and should facilitate the application of Ni catalysis to traditional Heck transformations.

Dedication

In loving memory of my grandmother, Yaroslava Kraikivska, who taught me to be resilient and patient.

Acknowledgements

I would like to express a special gratitude to my advisor, Dr. William Malachowski, for providing me with the opportunity to pursue this research work. His enthusiasm and thoughtful guidance have consistently motivated me and kept me curious about my research. His mentorship and extensive knowledge of chemistry, generously shared with me during my time at Bryn Mawr, have played a pivotal role in shaping me into the chemist I am today. I would also like to extend my special gratitude to Maria Winters, PhD'14, whose encouragement motivated me to pursue chemistry at the graduate level at Bryn Mawr College. I still vividly recall the note she wrote to me on the last day of sophomore organic chemistry class, saying, "I hope you remember me when you become a doctor". I also thank Dr. Sharon Burgmayer for helpful discussions and advice, as well as the rest of my committee members: Dr. Yan Kung, Dr. Patrick Melvin, Dr. Ashlee Plummer-Medeiros, and Dr. Victor Donnay. I also thank other faculty members, Dr. Lisa Watkins, Dr. Olga Karagiaridi, and Dr. Ariana Hall for their guidance and support in my teaching experience at Bryn Mawr. I would also like to thank Paul Hintz for his dedicated care and maintenance of the instruments essential to my research. I would also like to express my appreciation to Dean Cheng for her unwavering support and valuable advice throughout the program.

I would like to thank the Department of Chemistry for financial support, research facilities and recourses it provided for this project. Additionally, I would like to gratefully acknowledge the financial support from National Institutes of Health (National Institute of General Medical Sciences, 1-R15-GM123475-01A1). I am also grateful for the financial support from the GSAS office.

My deep gratitude goes to my parents, Oksana and Wasyl, for their love, support, and encouragement. I thank them for giving me with the opportunity to discover my passion and for instilling in me the confidence to believe in myself and my abilities. To my fiancé, Brian, I express my heartfelt thanks for his love, care, patience, and kindness. Your constant presence and encouragement in pursuing my academic goals mean the world to me. I also want to acknowledge my fiancé's parents, Diane and Brian, for their love and support. A special thank you goes out to all my friends who helped me maintain a healthy work-life balance throughout graduate school.

Lastly, I want to express my gratitude to all the graduate students, including Mary Sexton, Cassie Gates, Jim Vogel, Greg Feldman, Rich Davis, Edwin Ragwan, Kim McCaskey, as well as the undergraduate students, including Yelin Jung, Alex Matei, Sam Peterson, Mia Tran, Lynn Chen, Kalyn Wiley, Reece Carew-Lyons, Christina Douglas, Dana Caldwell, Yui Kosukegawa, and Lana Giha, with whom I had the pleasure of working. Their collective contributions have truly made this journey a memorable and pleasant experience.

Table of Contents

Acronyms and Abbreviations

α – alpha
Å – angstrom
ACN - acetonitrile
AcO – acetate
APT – attached proton test
Aq. – aqueous
Ar – aryl
β – beta
BET – bromodomain and extraterminal domain
BINAP – 2,2'-Bis(diphenylphosphino)-1,1'-binaphthyl
Biox – bioxazoline
Bipy – bipyridine
Bn – benzyl
Bu -butyl
Boc – *tert*-butoxycarbonyl
Box – bis(oxazoline)
BPin – boronic pinacol ester
bs – broad singlet
°C – degrees Celsius
cat. – catalyst
$CDCl_3$ – deuterated chloroform
compd. – compound
COD – 1,5-cyclooctadiene
CN- nitrile
COD – 1,5-cyclooctadiene
Cy – cyclohexyl
d – doublet or day(s)
dd – doublet of doublets
ddd – doublet of doublets of doublets
dq – doublet of quartets
dt – doublet of triplets
Δ – reflux
δ – peak
DAD – diode array detector
DAST – diethylaminosulfur trifluoride
DCM – dichloromethane
DDQ – 2,3-dichloro-5,6-dicyano-1,4-benzoquinone
DFT – density functional theory

DIBAL – diisobutylaluminium hydride
DMA – dimethylacetamide
DMAP – 4-dimethylaminopyridine
DMF – *N*,*N*-dimethylformamide
DMS – dimethyl sulfide
DMSO – dimethyl sulfoxide
DMSO-d_6 – dimethyl sulfoxide
DNA – deoxyribonucleic acid
D_2O – deuterium oxide
Dr. – doctor
E° – the cell potential
EC_{50} – half maximal effective concentration
EDG – electron-donating group
EI-MS – electron-impact ionization mass spectrometry
e.r. – enantiomeric ratio
ee – enantiomeric excess
eq. – equation
equiv. – equivalent
EI – electron impact
ESI – electrospray ionization
Et – ethyl
et al. – and others
Et_2Zn – diethyl zinc
EtOAc – ethyl acetate
EWG - electron-withdrawing groups
FT – Fourier transform
γ-gamma
g – gram(s)
GC – gas chromatography
GCMS – gas chromatography-mass spectrometry
h – hour(s)
hept – heptet
HPLC – high performance liquid chromatography
HRMS – high resolution mass spectrometry
Hz – hertz
i – iso
in situ – in the reaction mixture
*i*Quinox – isoquinoline
J – coupling constant
k – a rate constant
kcal – kilocalorie(s)
L – ligand
LAH – lithium aluminium hydride
LIFDI – liquid field desorption ionization
LiHMDS – lithium bis(trimethylsilyl)amide
LIMR – Lankenau Institute of Medical Research
log – logarithm

m – multiplet or meta
μ – micro
M – metal or molarity
m-CPBA – meta-chloroperoxybenzoic acid
Me – methyl
MHz – megahertz
min. – minute(s)
mL – milliliter(s)
μL – microliter(s)
mm – millimeter(s)
μm – micrometer(s)
mol – mole(s)
mmol – millimole(s)
MOM – methoxymethyl
m.p. – melting point
MS – mass spectrometry
m/z – mass to charge ratio
MW – molecular weight or microwave
n – normal
n – number of units
NaHMDS – sodium bis(trimethylsilyl)amide
NCI – National Cancer Institute
n.d. – not determined
NHAc – acetamide
Ni-H – nickel hydride
NIH – The National Institutes of Health
nm – nanometer
NMM – N-methylmorpholine
NMR – nuclear magnetic resonance
NR – no reaction
o – ortho
OD – optical density
OMe – methoxy
OTf – triflate (trifluoromethanesulfonate)
p – para
π – pi
PARP – poly-adenosyl ribosyl polymerase
PDC – pyridinium dichromate
Pin_2B_2 – bis(pinacolato)diboron
Ph – phenyl
pH – hydrogen ion concentration in aqueous solution
Phox – phosphinooxazoline(s)
PMB – para-methoxybenzyl
ppm – parts per million
Pr – propyl
Prof. – professor

psi - pounds per square inch
Pybox – pyridine-bis(oxazoline)
Pyox – pyridine-oxazoline
q – quartet
Quinox – 2-(4,5-dihydro-2-oxazolyl)quinoline
R – alkyl or aryl group
R – rectus
r.t. – room temperature
s – singlet
S – sinister
sec – second(s)
S – sinister
S.A. – sacrificial alkene
SHE – the standard hydrogen electrode
s.m. – starting material
S_NAr – nucleophilic aromatic substitution
SRB – sulforhodamine B
t – tert
t – triplet
TBS – *tert*-butyldimethylsilyl
td – triplet of doublets
TDAE – tetrakis(dimethylamino)ethylene
TDP – tyrosyl-DNA phosphodiesterase
TEMPO – (2,2,6,6-tetramethylpiperidinyloxy or 2,2,6,6-tetramethylpiperidine 1-oxyl)
THF – tetrahydrofuran
TLC – thin layer chromatography
TM – transition metal
TMS – trimethylsilyl
t_R – retention time
UV – ultra violet
vacuo – vacuum via rotary evaporation
VWD – variable wavelength detector
X – halide or pseudohalide / halide or pseudohalide anion

List of Figures

List of Schemes

List of Tables

Chapter 1: Background and Introduction

1.1 Quaternary Carbon Stereocenters

The discovery of successful drug candidates highly correlates to the frequency of sp^3 carbons and chiral centers.[1, 2 3] Recent surveys of the most successful drugs over the past three decades show that sp^3-rich small molecule drugs have higher likelihood of success in clinical trials and gain approval from the Food and Drug Administration. Enhanced molecular complexity and conformational constraints improve the pharmaceutical profile of sp^3-rich and chiral drug candidates due to increased solubility[4] and less promiscuous binding behavior.[2] Quaternary carbon stereocenters are sp^3 carbon centers with four distinct carbon substituents. They are commonly encountered in natural products, bioactive compounds, and drugs. Their unique properties are influenced by their shapes, which are dictated by the three-dimensional orientation of carbon substituents.[5] Consequently, the construction of all-carbon quaternary centers has become an effective strategy to increase the fraction of sp^3 carbons and improve the pharmaceutical properties of drug molecules.[6]

Phenanthridinone is an example of a planar aromatic tricyclic structure that is widely encountered in bioactive molecules. In fact, according to a PubChem search, the phenanthridinone core is found in over 360 bioactive compounds.[7] Phenanthridinone and its derivatives are reported to show anti-cancer bioactivity by targeting poly-adenosyl ribosyl polymerase (PARP) and tankyrase,[8] DNA topoisomerase 1B and tyrosyl-DNA

phosphodiesterase 1 (TDP1),[9] progesterone receptor,[10] Aurora kinase,[11] and BET bromodomain.[12] In addition, phenanthridinone analogs have shown anti-bacterial,[13] anti-viral,[14] anti-plasmodial,[15] and anti-inflammatory bioactivity.[16] Despite the broad range of phenanthridinone bioactivity, its promiscuous binding behavior contributes to low selectivity, poor pharmacokinetic profile, and potential side effects. Alternatively, three-dimensional phenanthridinone derivatives with sp^3 carbon centers have the potential for uniquely accessing unoccupied space both above and below the flat tricyclic structure (**Figure 1.1**), which, in theory, should have greater selectivity and therapeutic potency.[1, 2, 6] The enantioselective generation of all-carbon quaternary carbon centers is a challenging process as proven by chemical libraries with predominantly flat sp^2 structures. In fact, an analysis of chemical reactions used in modern medicinal chemistry revealed that the most frequently used reactions were amide formation, Suzuki-Miyaura coupling, and nucleophilic aromatic substitution (S_NAr) reactions, all of which generate flat sp^2 structures.[17]

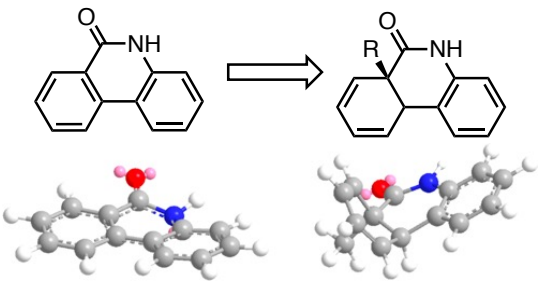

Figure 1.1 Phenanthridinone analog with a quaternary carbon stereocenter.

1.2 The Birch-Heck Sequence

Desymmetrization of prochiral molecules with a quaternary carbon is one of the common synthetic strategies to all-carbon quaternary stereocenters.[18] This process, however, creates two main challenges for chemical synthesis: an increased steric

repulsion between all carbon substituents and less enantiofacial discrimination due to higher steric similarity between carbon substituents versus a carbon substituent and a hydrogen atom. The emergence of enantioselective methods in transition metal (TM) catalysis facilitated the development of asymmetric transformations and desymmetrization reactions for the synthesis of complex molecules.[18] The Mizoroki-Heck reaction has become one of the most powerful and efficient methods for producing quaternary stereocenters.[19, 20] The Malachowski group recently developed the Birch-Heck sequence as a novel and efficient synthetic tool to enantioselectively generate complex phenanthridinone derivatives with all-carbon quaternary stereocenters from inexpensive and easily available benzoic acid (**Scheme 1.1**).[21, 22] This short four-step sequence yields asymmetric quaternary carbon-containing phenanthridinone derivatives, in contrast to one earlier report which had limited scope and was not enantioselective.[23]

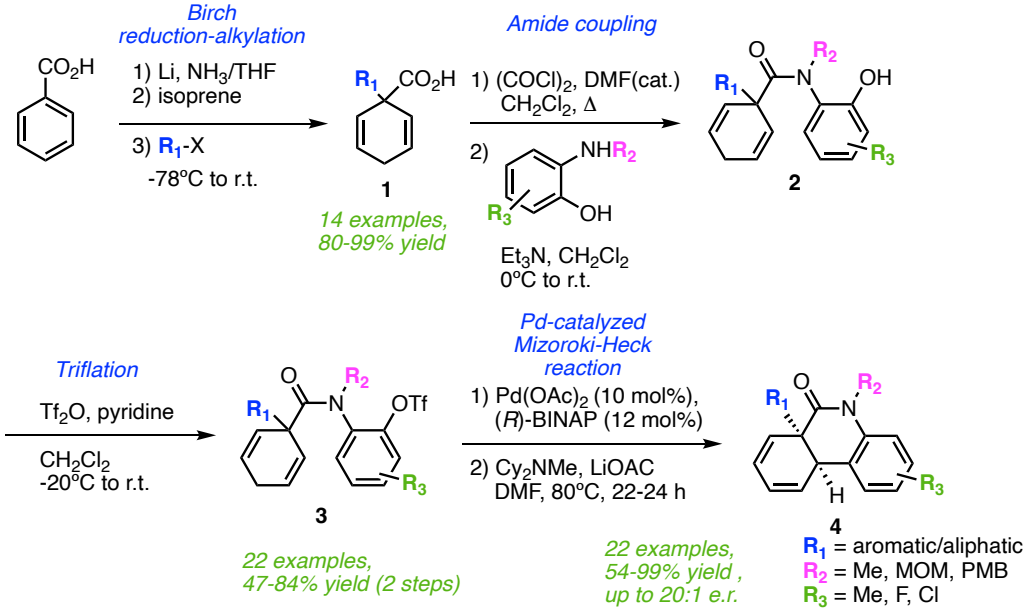

Scheme 1.1 Precedent Birch-Heck sequence to phenanthridinone derivatives with the palladium catalyst.

The Birch-reduction[24] is the first important step which affords 1,4-cyclohexadiene product **1** with the prochiral quaternary center in consistently high yields and purity without chromatographic purification. The carboxylic acids **1** were converted to the corresponding amides **2** through standard acyl chloride formation followed by the coupling with the appropriate primary or secondary amine.[22] The amides **2** were used in the subsequent triflation reaction to provide the substrates **3** for the Mizoroki-Heck reaction in 47-84% yields over the two-step process. Unfortunately, the secondary amide substrates **3** were unsuccessful for the Heck reaction and had to be protected as the methoxymethyl (MOM) tertiary amides. We believe it is the result of a stable Pd complex from an intramolecular reaction: a six-member ring chelation between the amide oxygen and palladium after the oxidative addition. The optimal conditions for the enantioselective Pd-catalyzed Mizoroki-Heck reaction were established using $Pd(OAc)_2$ as the source of palladium, (*R*)-BINAP as the chiral ligand, Cy_2NMe as the base, LiOAc as the additive in DMF at 80°C. Notably, the role of the LiOAc salt was critical to accelerate the formation of the allylic acetate intermediate in the preferred pathway to the desired 1,3-diene product.[25] The substrate scope exploration demonstrated compatibility with a wide range of aromatic and aliphatic (R_1) groups at the quaternary center; the amide nitrogen (R_2) groups of methyl, methoxymethyl (MOM), and para-methoxybenzyl (PMB); and aryl triflate (R_3) groups of Me, F, Cl in good yield and with good to very good enantioselectivity (**Scheme 1.1**).[22]

1.3 Palladium-Catalyzed Mizoroki-Heck Reaction

The second critical transformation in the sequence is the Mizoroki-Heck reaction which involves the cross-coupling of an unsaturated halide or triflate with an alkene in

the presence of a base and a TM catalyst, typically palladium (**Scheme 1.2**).[26] The reaction was discovered by Tsutomu Mizoroki[27] in 1971 and later improved by Richard Heck.[28] Since then, both the inter- and intramolecular Heck reactions have been used as a valuable tool for asymmetric and desymmetrization processes.[19] The discovery and development of this powerful synthetic transformation was awarded the 2010 Noble Prize in Chemistry.

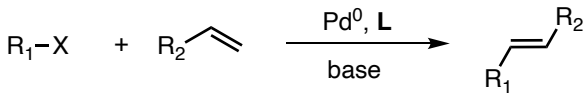

Scheme 1.2 Traditional Heck reaction

Traditional Heck reactions undergo a Pd^0/Pd^{II} catalytic cycle. The mechanism begins with oxidative addition of the electrophile to the Pd center, coordination to the alkene, *syn* migratory insertion, internal rotation (only relevant to acyclic substrates) , β-hydride elimination, and reductive elimination to regenerate active Pd^0 species (**Scheme 1.3**).[29]

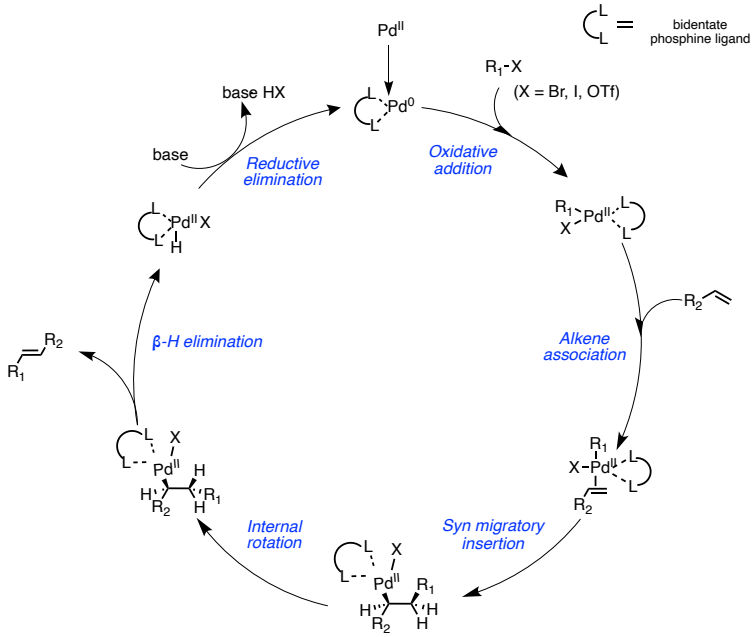

Scheme 1.3 The general mechanism of Pd-catalyzed Heck reaction.

To account for the differences in reactivity, regioselectivity, and enantioselectivity of unsaturated triflates and halides, the general mechanism can be termed either "neutral" or "cationic".[29, 30] In the absence of Ag(I) or Tl(I) salts, unsaturated vinyl or aryl halides undergo a neutral mechanism. This process involves the formation of a neutral palladium complex, where the halide ion ligand remains strongly coordinated to the metal. The neutral complex poses a challenge for the weak alkene ligand to coordinate to palladium, often necessitating the dissociation of a phosphine ligand. This partial ligand dissociation can decrease stereochemical control in the neutral pathway. On the other hand, in the cationic mechanism, the abstraction of halide by Ag(I) or Tl(I) salts or the use of easily dissociated triflate counterion creates an extra site of coordinative unsaturation on palladium throughout the cycle. The cationic complex is more electron-deficient than the neutral and can facilitate faster insertion into the alkene. Thus, optimal efficiency and enantioselectivity in the asymmetric Heck reactions can be achieved via the cationic pathway.[30] In our previous research work on the Pd-catalyzed Heck reaction, the use of the aryl triflate substrates for the asymmetric synthesis of phenanthridinone analogs was effective in promoting the cationic mechanism and enhancing stereochemical control.[21, 22]

1.4 Recent Developments in Nickel Catalysis

While palladium has shown excellent performance and unique versatility in a range of organometallic reactions,[31-33] its high cost prompted an extensive search for the replacement of palladium with an alternative and cheaper earth-abundant transition metal catalysts.[34-38] Nickel, a group 10 metal located just above palladium in the periodic table, has recently gained significant attention as a sustainable, cheaper, and attractive

alternative to palladium. Both metals show notable similarities in organometallic catalysis,[35] however, the cost of nickel in its elemental form is almost 2000 times lower than palladium.[38, 39]

Nickel was first isolated as an element from the mineral niccolite (NiAs) in 1751 by the Swedish chemist Axel Fredrik Cronstedt. It was named after the German word "kupfernickel", which means "devil's copper" because of unsuccessful efforts to recover copper from this ore.[38] In the late nineteenth century, Ludwig Mond observed nickel's unusual reactivity toward carbon monoxide (CO) at room temperature to form $Ni(CO)_4$, which can be used for nickel purification.[40] Shortly after, Paul Sabatier developed a new method of hydrogenating organic compounds in the presence of nickel, for which he was awarded the 1912 Noble Prize in Chemistry.[41] However, one of the most significant early contributions to homogeneous nickel catalysis was the development of useful nickel complexes, such as $Ni(COD)_2$, $Ni(allyl)_2$, $Ni(C_2H_4)_3$, and their application for the oligomerization of dienes by Günther Wilke.[42] Since the 1970s, nickel has been extensively used in a wide range of organometallic reactions.[43]

Despite some similarities shared with palladium, nickel has many different and unique properties.[35, 38, 44, 45] Nickel has lower electronegativity (1.91 for Ni and 2.20 for Pd), lower first ionization energy, lower reduction potential, and a smaller atomic radius than palladium. Thus, oxidative addition tends to be faster than with palladium. The facile oxidative addition allows for the use of less reactive electrophiles (e.g. ether C-O[46] and amide C-N[47], sp^3 C-Cl[48] bonds) than in palladium catalysis. However, this also makes Ni(0) species less stable and more prone to oxidation than Pd(0) species, which

requires the use of special reductants with Ni(II) pre-catalysts to generate active Ni(0) or Ni(I) species.[35, 38, 45]

In contrast to facile oxidative addition, reductive elimination with Ni(II) species is more challenging than with palladium. In addition, Ni(II) alkyl complexes are more stable against β-hydride elimination relative to palladium for the following reasons: 1) the lower electronegativity of nickel weakens an agostic interaction with the β-hydrogen; 2) the smaller atomic radius results in a more strained transition state of β-hydride elimination; 3) the higher energy barrier for Ni-C bond rotation required for the β-hydride elimination in acyclic structures.[49]

Ni complexes are capable of adapting both high- and low-spin configurations and can access a wide range of stable oxidation states spanning from Ni(0) to Ni(IV).[50] On the other hand, Pd complexes tend to be predominantly low-spin and are most frequently encountered as diamagnetic Pd(0), Pd(II), and Pd(IV) species. The tendency of Ni to adopt stable open-shell electronic configurations (e.g. Ni(I) and Ni(III)) can be attributed to the higher pairing energy of Ni compared to Pd. As a result, Ni can activate electrophiles through two-electron oxidative addition, leading to organonickel intermediates, or by single-electron pathways, resulting in the formation of radicals and more diverse catalysis mechanisms. Therefore, the differences in reactivity between Ni and Pd have been used to enable a variety of catalytic transformations where both metals have their own application niches.[35]

The contrasting reactivity and selectivity of Ni versus Pd in alkene functionalization and other Heck-type reactions have been leveraged to develop a variety of impressive reports on alkene hydroarylation, hydroalkylation, and

dicarbofunctionalization reactions.[50-53] Alkene dicarbofunctionalization has been at the center of the most challenging area of intramolecular enantioselective reactions for the creation of quaternary stereocenters.[54-57] The more popular Ni-catalyzed reductive Heck-type reactions offer an alternative pathway to traditional palladium-catalyzed Heck reactions and help to overcome the difficulty of nickel complexes undergoing β-hydride elimination.

While there was early work in the late 1980s demonstrating traditional Ni-catalyzed Heck reactions for the coupling of activated alkenes with organic halides,[58, 59] there has been a notable decrease in the number of reports describing the traditional intramolecular or intermolecular Heck transformations[60] likely due to harsh reaction conditions, including high temperatures, metal additives, and prolonged reaction times, that are often required to unable the thermodynamically unfavorable β-hydride elimination. Herein, we provide seminal examples of the Ni-catalyzed Heck reaction that have been influential and inspiring for this work.

The first intermolecular example of a Ni-catalyzed Heck reaction of aryl triflates with vinyl ethers under mild reaction conditions that are comparable to the analogous palladium version was reported by Gøgsig and co-workers in 2012 (**Scheme 1.4 A**).[61] In that work, they also describe and support by density functional theory (DFT) calculations the formation of a critical cationic nickel complex responsible for a favorable β-hydride elimination.

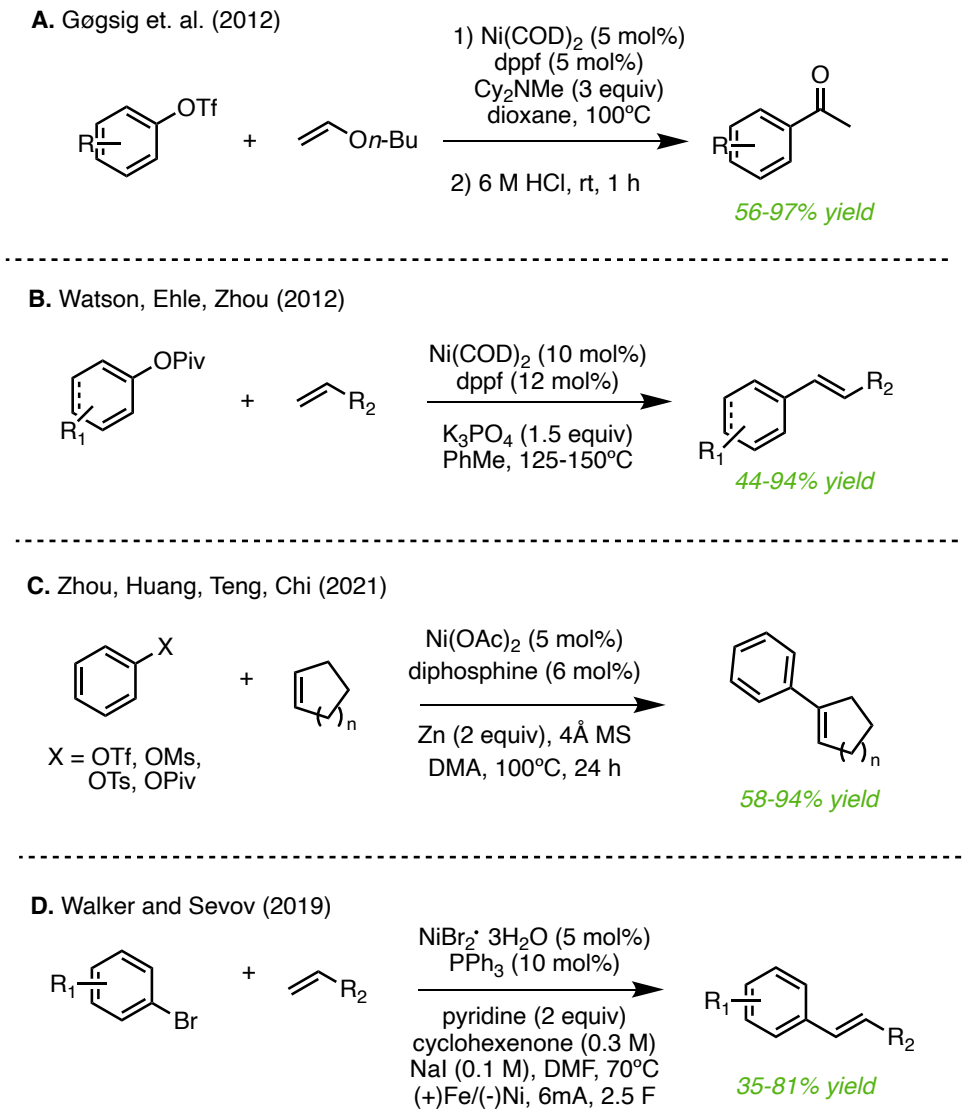

Scheme 1.4 Advances in intermolecular Ni-catalyzed Mizoroki-Heck Reaction.

In a different work by Watson et. al., an intermolecular Ni-catalyzed Heck reaction was reported as the first example of a C-C cross-coupling via activation of a strong C-O bond in aryl and vinyl pivalates to be coupled with both styrenes and α-olefins (**Scheme 1.4 B**).[62] Another report on the intermolecular Heck reaction of cycloalkenes using less reactive aryl sulfonates and pivalates to deliver unusual conjugated arylated isomers has been disclosed by Zhou and co-workers (**Scheme 1.4 C**).[63] Interestingly, in this approach they deliberately excluded the use of external bases

to enable extensive olefin isomerization of the initial non-conjugated Heck product by nickel hydride species. The last example by Walker and Sevov features the Ni-catalyzed Heck reaction of aryl halides and a broad range of alkenes by utilizing electrochemistry to promote the reaction under mild conditions (**Scheme 1.4 D**).[64]

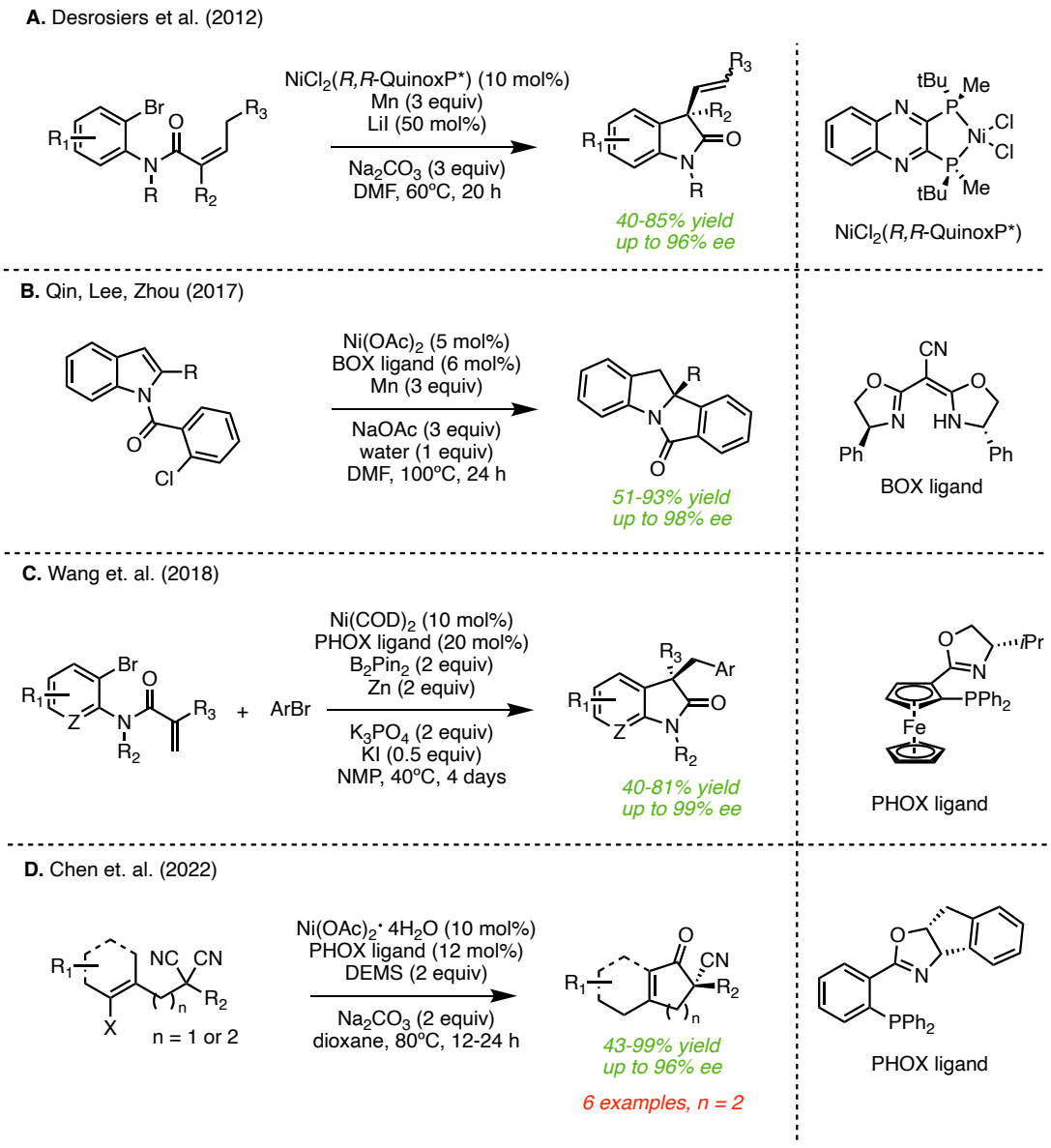

Scheme 1.5 Seminal intramolecular Ni-catalyzed Mizoroki-Heck Reactions.

In a particular and highly demanding field of enantioselective intramolecular reactions aimed at generating quaternary stereocenters, most examples feature

asymmetric reductive Ni-catalyzed Heck reactions due to the challenges with β-hydride eliminations. The development of enantioselective Ni-catalyzed Heck cyclization by Desrosiers and coworkers was the first and only prior intramolecular example of the traditional Heck reaction that demonstrates that β-hydride elimination can be accomplished with the use of nickel as the catalyst (**Scheme 1.5 A**).[65] The first example of nickel-catalyzed asymmetric reductive Heck cyclization of aryl chlorides that affords substituted indolines with high enantioselectivity was reported by Qin and co-workers in 2017 (**Scheme 1.5 B**).[66] Inspired by this work, Wang and co-workers presented the first example of Ni-catalyzed enantioselective reductive diarylation of alkenes to provide direct access to various bis-heterocycles bearing all-carbon quaternary centers in good yields and with excellent enantioselectivity (**Scheme 1.5 C**).[67]

Another limitation observed in recent reports of intramolecular nickel-catalyzed Heck reactions, including alkene difunctionalization, is the scarcity of examples involving the formation of six-membered rings with high degree of enantioselectivity. Numerous reports have emerged demonstrating exceptional enantioselectivity to form five-membered rings,[65, 68-79] with indolinone and oxindole structures as the most frequently observed products. Conversely, there is only one recent report by Chen et.al.[80] featuring a collection of six-membered substrates with excellent enantioselectivity (**Scheme 1.5 D**) and two additional reports having just one successful enantioselective six-membered ring formation.[81, 82] In other cases, the previously published communications have either reported relatively moderate enantioselectivities below 50% enantiomeric excess (e.r. = 3:1) or reported no enantioselectivity for the six-membered ring formations.[68, 83-85] Considering the significance of six-membered rings in organic

chemistry and drug development,[86, 87] the limited number of examples demonstrating enantioselective six-membered ring formation appears to be a significant oversight. Thus, we envisioned that we could build upon the previously reported advances in Ni-catalyzed Heck reaction (**Scheme 1.4-1.5**) and substitute nickel for palladium in an analogous Heck reaction that was recently published by our group.[22] Apart from identifying and highlighting the differences between the Ni-catalyzed conditions and the identical palladium Heck reaction, we wanted to provide direct access to six-membered ring heterocyclic systems bearing all-carbon quaternary stereocenters, which have been much more challenging to form with nickel-catalyzed Heck reactions. Seminal literature reports outlined in **Scheme 1.5** provided several significant factors of nickel's characteristic modes of reactivity for us to consider as we embarked on our research work:

1) Since nickel has significantly lower reduction potential for $M^{2+} + 2e^- = M^0$ transformations than Pd (−0.257 V for Ni and 0.951 V for Pd),[35] Ni(0) species are less stable than Pd(0) species and more prone to oxidation. In addition, Ni(II) precatalysts often require the use of special metal reductants, such as Zn or Mn, or electric current to be reduced to active Ni(0) or Ni(I) species. Alternative additives, such as Pin_2B_2[67] and sacrificial alkenes,[88] have been reported to facilitate the reduction of Ni(II) species.
2) The addition of an external iodide source, such as LiI or KI, has been shown to improve the reactivity of Ni-catalyzed transformations.[61, 67, 89]
3) Lower reduction potential and electronegativity (1.91) than Pd (2.20)[35] allows for facile oxidative addition to less reactive cross-coupling electrophiles that would be less prone to oxidative addition with palladium. This provides the opportunity

to substitute an expensive triflate group with a more readily available aryl halide substrate.[38]

4) The easy accessibility of Ni(I) and Ni(III) oxidation states enables various avenues of reactivity and facilitates radical mechanisms. Additional mechanistic and computational studies are usually required to understand the more diverse catalysis mechanisms.
5) A significant portion of asymmetric Ni-catalyzed reactions employ bidentate and tridentate N-ligands, including bipyridine (Bipy), bis(oxazoline) (Biox), terpyridine (Terpy), pyridine-oxazoline (Pyox), and pyridine-bis(oxazoline) (Pybox), which will be considered for the development of our enantioselective process.[45, 90]

1.5 Project Overview

In this work, we describe four main areas (Chapters 2-5) of an enantioselective intramolecular Ni-catalyzed reaction development and optimization with the overall goal of demonstrating a direct and valuable comparison of the performance of nickel and palladium catalysts, which should facilitate the utilization of Ni catalysis in traditional Heck transformations (**Scheme 1.6**).[91] In addition, we aim to portray a rare case where a Ni-catalyzed intramolecular Heck reaction has been successfully employed to construct a six-membered ring featuring an all-carbon quaternary center with the broadest substrate scope to date and good to very good levels of enantioselectivity.

In Chapter 2, we describe significant progress in optimizing the reaction conditions to effectively control undesired proto-dehalogenation and alkene reduction side products by integrating the Heck reaction with a transfer hydrogenation step

involving a sacrificial alkene and by introducing an external iodide source to the reaction conditions.

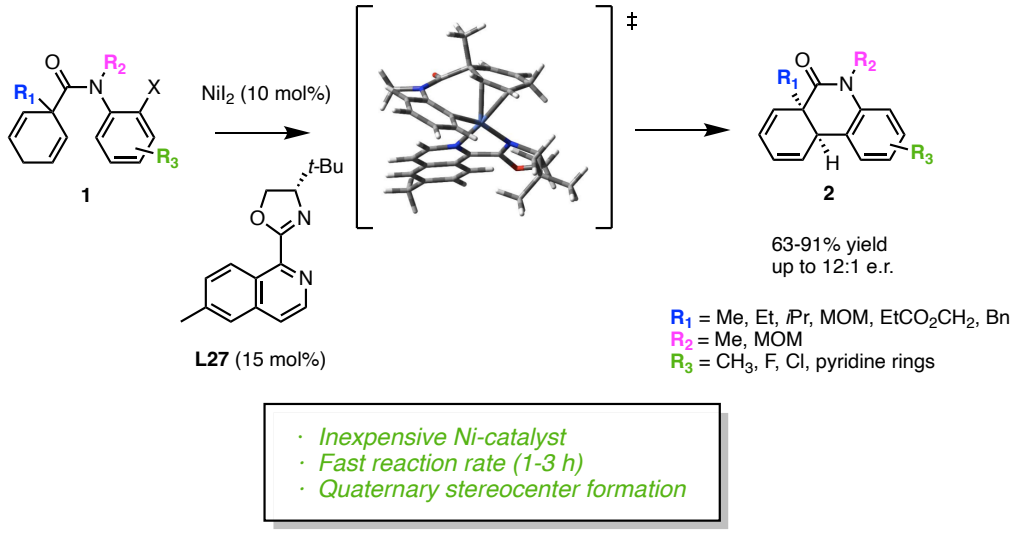

Scheme 1.6 Ni-catalyzed enantioselective intramolecular Mizoroki−Heck reaction.

In Chapter 3, the focus is on the development of an enantioselective strategy. We initially perform a survey of chiral ligands commonly used in Ni-catalyzed cross-coupling reactions to search for optimal enantioselective results. Among the collection of commercially available bidentate and tridentate N- or P,N-ligands, *t*Bu-pyox- and *t*Bu-iQuinox-type ligands become the focus of our subsequent studies which involve the synthesis and testing of novel *t*Bu-pyox and *t*Bu-iQuinox chiral ligands. The overall process leads to the improved enantioselectivity with (*S*)-*t*Bu-*i*Quinox **L27** (**Scheme 1.6**), likely due to the favorable π-stacking interaction between the aryl group of the substrate and the isoquinoline ring of the *i*Quinox ligand.

Chapter 4 details the results of our substrate scope investigation with variations at the quaternary center (R_1), the amide nitrogen (R_2), and the aryl halide (R_3) (**Scheme 1.6**). Herein, we report good to excellent yields and good enantioselectivities with a

variety of aryl bromides and aryl iodides, highlighting the tolerance of heterocycle rings which was not observed with the Pd-catalyzed conditions. Subsequently, we show a variety of further transformations of the 1,3-diene Heck products that illustrate the possibility of transforming these molecules into potentially more viable drug molecules.

In the final part of this work (Chapter 5), we describe mechanistic investigations that support a traditional two-electron Heck reaction mechanism. Additionally, we explore the roles of the reducing metal (Mn and Zn) and the sacrificial alkene (2-cyclohexenone). To shed light on the basis for the enantioselectivity in the catalytic cycle, we collaborated with Dr. Paul Rablen from Swarthmore College to perform a computational study of the key 1,2-migratory insertion step, which is assumed to be rate-determining and stereo-determining. The results of this analysis confirm the presence of dynamic kinetic resolution which has been previously observed in intramolecular asymmetric Heck reactions.[92] Moreover, the presence of atropisomers in the tertiary amides used in this transformation can be confirmed by NMR analysis.[22] Overall, the computational analysis provides two useful insights into the reaction process. First, it explains the discrepancy between predicted and experimentally observed enantiomeric ratios. Second, it suggests potential ways to improve the stereoselectivity of this reaction.

1.6 References

1. Lovering, F.; Bikker, J.; Humblet, C. Escape from Flatland: Increasing Saturation as an Approach to Improving Clinical Success. *J. Med. Chem.* **2009**, *52* (21), 6752–6756.
2. Lovering, F. Escape from Flatland 2: complexity and promiscuity. *Med. Chem. Commun.* **2013**, *4* (3), 515–519.
3. Silvestri, I. P.; Colbon, P. J. J. The Growing Importance of Chirality in 3D Chemical Space Exploration and Modern Drug Discovery Approaches for Hit-ID. *ACS Med. Chem. Lett.* **2021**, *12*, 1220.

4. Ishikawa, M.; Hashimoto, Y. Improvement in Aqueous Solubility in Small Molecule Drug Discovery Programs by Disruption of Molecular Planarity and Symmetry. *J. Med. Chem.* **2011**, *54*, 1539–1554.
5. Quasdorf, K.; Overman, L. Catalytic Enantioselective Synthesis of Quaternary Carbon Stereocenters. *Nature* **2014**, *216*, 181–191.
6. Talele, T. T. Opportunities for Tapping into Three-Dimensional Chemical Space through a Quaternary Carbon. *J. Med. Chem.* **2020**, *63* (22), 13291–13315.
7. PubChem substructure search for 6(5H)-Phenanthridinone with filter for bioassay active hits in PubMed. (accessed January 29, 2023).
8. Wahlberg, E.; Karlberg, T.; Kouznetsova, E.; Markova, N.; Macchiarulo, A.; Thorsell, A.-G.; Pol, E.; Frostell, A.; Ekblad, T.; Oncu, D.; et al. Family-wide chemical profiling and structural analysis of PARP and tankyrase inhibitors. *Nat Biotech* **2012**, *30*, 283–288.
9. Zhang, X.-R.; Wang, H.-W.; Tang, W.-L.; Zhang, Y.; Yang, H.; Hu, D.-X.; Ravji, A.; Marchand, C.; Kiselev, E.; Ofori-Atta, K.; et al. Discovery, Synthesis, and Evaluation of Oxynitidine Derivatives as Dual Inhibitors of DNA Topoisomerase IB (TOP1) and Tyrosyl-DNA Phosphodiesterase 1 (TDP1), and Potential Antitumor Agents. *J. Med. Chem.* **2018**, *61*, 9908–9930.
10. Nishiyama, Y.; Mori, S.; Makishima, M.; Fujii, S.; Kagechika, H.; Hashimoto, Y.; Ishikawa, M. Novel Nonsteroidal Progesterone Receptor (PR) Antagonists with a Phenanthridinone Skeleton. *ACS Med. Chem. Lett.* **2018**, *9*, 641–645.
11. Karra, S.; Xiao, Y.; Chen, X.; Liu-Bujalski, L.; Huck, B.; Sutton, A.; Goutopoulos, A.; Askew, B.; Josephson, K.; Jiang, X.; et al. SAR and evaluation of novel 5H-benzo[c][1,8]naphthyridin-6-one analogs as Aurora kinase inhibitors. *Bioorganic Med. Chem. Lett.* **2013**, *23*, 3081–3087.
12. Zhi, Y.; Wang, S.; Huang, W.; Zeng, S.; Liang, M.; Zhang, C.; Ma, Z.; Wang, Z.; Zhang, Z.; Shen, Z. Novel phenanthridin-6(5H)-one derivatives as potent and selective BET bromodomain inhibitors: Rational design, synthesis and biological evaluation. *Eur. J. Med. Chem.* **2019**, *179*, 502–514.
13. Nair, J. J.; Wilhelm, A.; Bonnet, S. L.; van Staden, J. Antibacterial constituents of the plant family Amaryllidaceae. *Bioorganic Med. Chem. Lett.* **2017**, *27*, 4943–4951.
14. Aoyama, H.; Sugita, K.; Nakamura, M.; Aoyama, A.; Salim, M. T. A.; Okamoto, M.; Baba, M.; Hashimoto, Y. Fused heterocyclic amido compounds as anti-hepatitis C virus agents. *Bioorg. Med. Chem.* **2011**, *19*, 2675–2687.
15. Yapi, A.-D.; Desbois, N.; Chezal, J.-M.; Chavignon, O.; Teulade, J.-C.; Valentin, A.; Blache, Y. Design and preparation of aza-analogues of benzo[c]phenanthridine framework with cytotoxic and antiplasmodial activities. *Eur. J. Med. Chem.* **2010**, *45*, 2854–2859
16. Borbély, G.; Szabadkai, I.; Horváth, Z.; Markó, P.; Varga, Z.; Breza, N.; Baska, F.; Vántus, T.; Huszár, M.; Geiszt, M.; et al. Small-Molecule Inhibitors of NADPH Oxidase 4. *J. Med. Chem.* **2010**, *53*, 6758–6762.

17. Brown, D. G.; Boström, J. Analysis of Past and Present Synthetic Methodologies on Medicinal Chemistry: Where Have All the New Reactions Gone? *J. Med. Chem.* **2016**, *59*, 4443–4458.
18. Zeng, X.; Cao, Z.; Wang, Y.; Zhou, F.; Zhou, J. Catalytic Enantioselective Desymmetrization Reactions to All-Carbon Quaternary Stereocenters. *Chem. Rev.* **2016**, *116* (12), 7330–7396.
19. Mc Cartney, D.; Guiry, P. J. The asymmetric Heck and related reactions. *Chem. Soc. Rev.* **2011**, *40*, 5122–5150.
20. Büschleb, M.; Dorich, S.; Hanessian, S.; Tao, D.; Schenthal, K. B.; Overman, L. E. Synthetic Strategies toward Natural Products Containing Contiguous Stereogenic Quaternary Carbon Atoms. *Angew. Chem. Int. Ed.* **2016**, *55* (13), 4156–4186.
21. Krasley, A. T.; Malachowski, W. P.; Hannah, T. M.; Tran Tien, S. Catalytic Enantioselective Birch–Heck Sequence for the Synthesis of Tricyclic Structures with All-Carbon Quaternary Stereocenters. *Org. Lett.* **2018**, *20* (7), 1740–1743.
22. Sexton, M.; Malachowski, W. P.; A., G. Y. P.; Rachii, D.; Feldman, G.; Krasley, A.; Chen, Z.; Tran, M.; Wiley, K.; Matei, A.; et al. Catalytic Enantioselective Birch−Heck Sequence for the Synthesis of Phenanthridinone Derivatives with an All-Carbon Quaternary Stereocenter. *J. Org. Chem.* **2022**, *87* (2), 1154–1172.
23. Fujita, R.; Watanabe, K.; Yoshisuji, T.; Kabuto, C.; Matsuzaki, H.; Hongo, H. Diels-Alder Cycloadditions of 2(1H)-Quinolones Having an Electron-Withdrowing Group at the 3-Position Acting as Dienophiles with Dienes. *Chem. Pharm. Bull.* **2011**, *49*, 893.
24. Schultz, A. G. The asymmetric Birch reduction and reduction–alkylation strategies for synthesis of natural products. *Chem. Commun.* **1999**, (14), 1263–1271.
25. Larock, R. C.; Han, X. Palladium-Catalyzed Cross-Coupling of 2,5-Cyclohexadienyl-Substituted Aryl or Vinylic Iodides and Carbon or Heteroatom Nucleophiles. *J. Org. Chem.* **1999**, *64* (6), 1875–1887.
26. Drahl, C. In Names, History and Legacy. *Chem. Eng. News* **2010**, *88* (22), 31–33.
27. Mizoroki, T.; Mori, K.; Ozaki, A. Arylation of Olefin with Aryl Iodide Catalyzed by Palladium. *Bull. Chem. Soc. Jpn.* **1971**, *44* (2), 581.
28. Heck, R. F.; Nolley, J. P. Palladium-catalyzed vinylic hydrogen substitution reactions with aryl, benzyl, and styryl halides. *J. Org. Chem.* **1972**, *37* (14), 2320–2322.
29. Wang, S.; Yang, G. Recent developments in low-cost TM-catalyzed Heck-type reactions (TM = transition metal, Ni, Co, Cu, and Fe). *Catal. Sci. Technol.* **2016**, *6*, 2862–2876
30. Dounay, A. B.; Overman, L. E. The Asymmetric Intramolecular Heck Reaction in Natural Product Total Synthesis. *Chem. Rev.* **2003**, *103*, 2945–2964.

31. Nicolaou, K. C.; Bulger, P. G.; Sarlah, D. Palladium-Catalyzed Cross-Coupling Reactions in Total Synthesis. *Angew. Chem. Int. Ed.* **2005**, *44* (29), 4442–4489.
32. Wu, X.-F.; Anbarasan, P.; Neumann, H.; Beller, M. From Noble Metal to Nobel Prize: Palladium-Catalyzed Coupling Reactions as Key Methods in Organic Synthesis. *Angew. Chem. Int. Ed.* **2010**, *49* (48), 9047–9050.
33. Gildner, P. G.; Colacot, T. J. Reactions of the 21st Century: Two Decades of Innovative Catalyst Design for Palladium-Catalyzed Cross-Couplings. *Organometallics* **2015**, *34* (23), 5497–5508.
34. Bhakta, S.; Ghosh, T. Emerging Nickel Catalysis in Heck Reactions: Recent Developments. *Adv. Synth. Catal.* **2020**, *362* (23), 5257–5274.
35. Chernyshev, V. M.; Ananikov, V. P. Nickel and Palladium Catalysis: Stronger Demand than Ever. *ACS Catal.* **2022**, *12* (2), 1180–1200.
36. Poremba, K. E.; Dibrell, S. E.; Reisman, S. E. Nickel-Catalyzed Enantioselective Reductive Cross-Coupling Reactions. *ACS Catal.* **2020**, *10* (15), 8237–8246.
37. Standley, E. A.; Tasker, S. Z.; Jensen, K. L.; Jamison, T. F. Nickel Catalysis: Synergy between Method Development and Total Synthesis. *Acc. Chem. Res.* **2015**, *48* (5), 1503–1514.
38. Tasker, S. Z.; Standley, E. A.; Jamison, T. F. Recent advances in homogeneous nickel catalysis. *Nature* **2014**, *509* (7500), 299–309.
39. Daily Metal Prices, https://www.dailymetalprice.com/ (accessed 2023 February 6).
40. Mond, L.; Langer, C.; Quincke, F. Action of Carbon Monoxide on Nickel. *J. Chem. Soc., Trans.* **1890**, *57*, 749–753.
41. *Paul Sabatier - Facts*. NobelPrize.org, https://www.nobelprize.org/prizes/chemistry/1912/sabatier/facts/ (accessed 2023 February 7).
42. Wilke, G. Contributions to Organo-Nickel Chemistry. *Angew. Chem. Int. Ed. Engl.* **1988**, (27), 185–206.
43. Tamaru, Y. *Modern Organonickel Chemistry*; Wiley-VCH, 2006.
44. Ananikov, V. P. Nickel: The "Spirited Horse" of Transition Metal Catalysis. *ACS Catal.* **2015**, *5*, 1964−1971.
45. Diccianni, J. B.; Diao, T. Mechanisms of Nickel-Catalyzed Cross-Coupling Reactions. *Trends in Chemistry* **2019**, *1* (9), 830–844.
46. Rosen, B. M.; Quasdorf, K. W.; Wilson, D. A.; Zhang, N.; Resmerita, A.-M.; Garg, N. K.; Percec, V. Nickel-Catalyzed Cross-Couplings Involving Carbon-Oxygen Bonds. *Chem. Rev.* **2011**, *111*, 1346−1416.
47. Weires, N. A.; Baker, E. L.; Garg, N. K. Nickel-catalyzed Suzuki−Miyaura coupling of amides. *Nat. Chem.* **2016**, *8*, 75.
48. Li, Y.; Luo, Y.; Peng, L.; Li, Y.; Zhao, B.; Wang, W.; Pang, H.; Deng, Y.; Bai, R.; Lan, Y.; et al. Reaction scope and mechanistic insights of nickel-catalyzed migratory Suzuki-Miyaura cross-coupling. *Nat. Commun.* **2020**, *11*, 417.

49. Lin, B. L.; Liu, L.; Fu, Y.; Luo, S. W.; Chen, Q.; Guo, Q. X. Comparing nickel- and palladium-catalyzed Heck reactions. *Organometallics* **2004**, *23* 2114−2123.
50. Diccianni, J.; Lin, Q.; Diao, T. Mechanisms of Nickel-Catalyzed Coupling Reactions and Applications in Alkene Functionalization. *Acc. Chem. Res.* **2020**, *53* (4), 906−919.
51. Dhungana, R. K.; Kc, S.; Basnet, P.; Giri, R. Transition Metal-Catalyzed Dicarbofunctionalization of Unactivated Olefins. *Chem. Rec.* **2018**, *18*, 1314−1340.
52. García-Domínguez, A.; Li, Z.; Nevado, C. Nickel-Catalyzed Reductive Dicarbofunctionalization of Alkenes. *J. Am. Chem. Soc.* **2017**, *139*, 6835−6838.
53. Watson, M. P.; Jacobsen, E. N. Asymmetric Intramolecular Arylcyanation of Unactivated Olefins via C–CN Bond Activation. *J. Am. Chem. Soc.* **2008**, *130* (38), 12594–12595.
54. Reznikov, A. N.; Ashatkina, M. A.; Klimochkin, Y. N. Recent developments in asymmetric Heck type cyclization reactions for constructions of complex molecules. *Org. Biomol. Chem.* **2021**, *19* (26), 5673–5701.
55. Oxtoby, L. J.; Vasquez, A. M.; Kang, T.; Li, Z.-Q. Metal-Mediated and Catalyzed Difunctionalization of Unsaturated Organics. In *Comprehensive Organometallic Chemistry IV*; Parkin, G., Meyer, K., O'Hare, D., Eds.; Elsevier, **2022**; pp 132–193.
56. Zhu, S.; Zhao, X.; Li, H.; Chu, L. Catalytic three-component dicarbofunctionalization reactions involving radical capture by nickel. *Chem. Soc. Rev.* **2021**, *50* (19), 10836–10856.
57. Li, Y.; Wang, K.; Ping, Y.; Wang, Y.; Kong, W. Nickel-Catalyzed Domino Heck Cyclization/Suzuki Coupling for the Synthesis of 3,3-Disubstituted Oxindoles. *Org. Lett.* **2018**, *20* (4), 921–924.
58. Boldrini, G. P.; Savoia, D.; Tagliavini, E.; Trombini, C.; Ronchi, A. U. Nickel-catalyzed coupling of activated alkenes with organic halides. *J. Organomet. Chem.* **1986**, *301* (3), C62–C64.
59. Lebedev, S. A.; Lopatina, V. S.; Petrov, E. S.; Beletskaya, I. P. Condensation of organic bromides with vinyl compounds catalysed by nickel complexes in the presence of zinc. *J. Organomet. Chem.* **1988**, *344* (2), 253–259.
60. Alisha, M.; Philip, R. M.; Anilkumar, G. Low-Cost Transition Metal-Catalyzed Heck-Type Reactions: An Overview. *Eur. J. Org. Chem.* **2022**, *7*, e202101384.
61. Gøgsig, T. M.; Kleimark, J.; Lill, S. O. N.; Korsager, S.; Lindhardt, A. T.; Norrby, P. O.; Skrydstrup, T. Mild and Efficient Nickel-Catalyzed Heck Reactions with Electron-Rich Olefins. *J. Am. Chem. Soc.* **2012** *134* (1), 443–452.
62. Ehle, A. R.; Zhou, Q.; Watson, M. P. Nickel(0)-Catalyzed Heck Cross-Coupling via Activation of Aryl C–OPiv Bonds. *Org. Lett.* **2012**, *14* (5), 1202–1205.

63. Zhou, J. S.; Huang, X.; Teng, S.; Chi, Y. R. Nickel-catalyzed Heck reaction of cycloalkenes using aryl sulfonates and pivalates. *Chem. Commun.* **2021**, *57*, 3933–3936.
64. Walker, B. R.; Sevov, C. S. An Electrochemically Promoted, Nickel-Catalyzed Mizoroki–Heck Reaction. *ACS Catal.* **2019**, *9* (8), 7197–7203.
65. Desrosiers, J.-N.; Wen, J.; Tcyrulnikov, S.; Biswas, S.; Qu, B.; Hie, L.; Kurouski, D.; Wu, L.; Grinberg, N.; Haddad, N.; et al. Enantioselective Nickel-Catalyzed Mizoroki–Heck Cyclizations To Generate Quaternary Stereocenters. *Org. Lett.* **2017**, *19* (13), 3338–3341.
66. Qin, X.; Lee, M. W. Y.; Zhou, J. S. Nickel-Catalyzed Asymmetric Reductive Heck Cyclization of Aryl Halides to Afford Indolines. *Angew. Chemie - Int. Ed.* **2017**, *56* (41), 12723–12726.
67. Wang, K.; Ding, Z.; Zhou, Z.; Kong, W. Ni-Catalyzed Enantioselective Reductive Diarylation of Activated Alkenes by Domino Cyclization/Cross-Coupling. *J. Am. Chem. Soc.* **2018**, *140* (39), 12364–12368.
68. Yang, F.; Jin, Y.; Wang, C. Nickel-Catalyzed Asymmetric Intramolecular Reductive Heck Reaction of Unactivated Alkenes. *Org. Lett.* **2019** *21* (17), 6989–6994.
69. Qin, X.; Yao Lee, M. W.; Zhou, J. S. Asymmetric Hydroarylation of Enones via Nickel-Catalyzed 5-Endo-Trig Cyclization. *Org. Lett.* **2019**, *21* (15), 5990 –5994.
70. Wang, K.; Kong, W. Enantioselective Reductive Diarylation of Alkenes by Ni-Catalyzed Domino Heck Cyclization/Cross Coupling. *Synlett* **2019**, *30* (9), 1008–1014.
71. Wu, J.; Wang, C. Nickel-Catalyzed Asymmetric Reductive Dicarbamoylation of Alkenes. *Org. Lett.* **2021**, *23* (16), 6407–6411.
72. Marchese, A. D.; Wollenburg, M.; Mirabi, B.; Abel-Snape, X.; Whyte, A.; Glorius, F.; Lautens, M. Nickel-Catalyzed Enantioselective Carbamoyl Iodination: A Surrogate for Carbamoyl Iodides. *ACS Catal.* **2020**, *10* (8), 4780–4785.
73. Wu, X.; Qu, J.; Chen, Y. Quinim: A New Ligand Scaffold Enables Nickel-Catalyzed Enantioselective Synthesis of α-Alkylated γ-Lactam. *J. Am. Chem. Soc.* **2020**, *42* (37), 15654–15660.
74. Yoon, H.; Marchese, A. D.; Lautens, M. Carboiodination Catalyzed by Nickel . *J. Am. Chem. Soc.* **2018**, *140* (35), 10950–10954.
75. Li, Y.; Zhang, F.-P.; Wang, R.-H.; Qi, S.-L.; Luan, Y.-X.; Ye, M. Carbamoyl Fluoride-Enabled Enantioselective Ni-Catalyzed Carbocarbamoylation of Unactivated Alkenes. *J. Am. Chem. Soc.* **2020**, *142* (47), 19844–19849.
76. Wu, X.; Luan, B.; Zhao, W.; He, F.; Wu, X.-Y.; Qu, J.; Chen, Y. Catalytic Desymmetric Dicarbofunctionalization of Unactivated Alkenes. *Angew. Chem., Int. Ed.* **2022**, *61* (26), e202111598.
77. Ping, Y.; Wang, K.; Pan, Q.; Ding, Z.; Zhou, Z.; Guo, Y.; Kong, W. Ni-Catalyzed Regio- and Enantioselective Domino Reductive Cyclization: One-Pot Synthesis of 2,3-Fused Cyclopentannulated Indolines. *ACS Catal.* **2019**, *9* (8), 7335–7342.

78. Wang, G.; Shen, C.; Ren, X.; Dong, K. Ni-Catalyzed enantioselective reductive arylcyanation/cyclization of N-(2-iodo-aryl) acrylamide. *Chem. Commun.* **2022**, *58* (8), 1135–1138.
79. Fang, K.; Huang, W.; Shan, C.; Qu, J.; Chen, Y. Synthesis of 3,3-Dialkyl-Substituted Isoindolinones Enabled by Nickel-Catalyzed Reductive Dicarbofunctionalization of Enamides. *Org. Lett.* **2021**, *23* (14), 5523–5527.
80. Chen, Z.-H.; Sun, R.-Z.; Yao, F.; Hu, X.-D.; Xiang, L.-X.; Cong, H.; Liu, W.-B. Enantioselective Nickel-Catalyzed Reductive Aryl/Alkenyl–Cyano Cyclization Coupling to All-Carbon Quaternary Stereocenters. *J. Am. Chem. Soc.* **2022**, *144* (11), 4776–4782.
81. Tian, Z.-X.; Qiao, J.-B.; Xu, G.-L.; Pang, X.; Qi, L.; Ma, W.-Y.; Zhao, Z.-Z.; Duan, J.; Du, Y.-F.; Su, P. Highly Enantioselective Cross-Electrophile Aryl-Alkenylation of Unactivated Alkenes. *J. Am. Chem. Soc.* **2019**, *141* (18), 7637–7643.
82. Li, H.; Chen, J.; Dong, J.; Kong, W. Ni-Catalyzed Reductive Arylcyanation of Alkenes. *Org. Lett* . **2021**, *23* (16), 6466–6470.
83. Jin, Y.; Wang, C. Nickel-Catalyzed Asymmetric Reductive Arylalkylation of Unactivated Alkenes. *Angew. Chem., Int. Ed.* **2019**, *58* (20), 6722–6726.
84. Jin, Y.; Yang, H.; Wang, C. Nickel-Catalyzed Asymmetric Reductive Arylbenzylation of Unactivated Alkenes. *Org. Lett.* **2020**, *22* (7), 2724–2729.
85. Pan, Q.; Ping, Y.; Wang, Y.; Guo, Y.; Kong, W. Ni-Catalyzed Ligand-Controlled Regiodivergent Reductive Dicarbofunctionalization of Alkenes. *J. Am. Chem. Soc.* **2021**, *143* (27), 10282–10291.
86. Taylor, R. D.; MacCoss, M.; Lawson, A. D. G. Rings in Drugs. *Med. Chem.* **2014**, *57* (14), 5845–5859.
87. Aldeghi, M.; Malhotra, S.; Selwood, D. L.; Chan, A. W. E. Two- and Three-dimensional Rings in Drugs. *Chem. Bio. Drug Des.* **2014**, *83* (4), 450–461.
88. Lv, H.; Kang, H.; Zhou, B.; Xue, X.; Engle, K. M.; Zhao, D. Nickel-catalyzed intermolecular oxidative Heck arylation driven by transfer hydrogenation. *Nat. Commun.* **2019** *10* (1), 5025.
89. Colon, I.; Kelsey, D. R. Coupling of aryl chlorides by nickel and reducing metals. *J. Org. Chem.* **1986**, *51* (14), 2627–2637.
90. Yang, G.; Zhang, W. Renaissance of pyridine-oxazolines as chiral ligands for asymmetric catalysis. *Chem. Soc. Rev.* **2018**, *47*, 1783–1810.
91. Rachii, D.; Caldwell, D. J.; Kosukegawa, Y.; Sexton, M.; Rablen, P.; Malachowski, W. P. Ni-Catalyzed Enantioselective Intramolecular Mizoroki–Heck Reaction for the Synthesis of Phenanthridinone Derivatives. *J. Org. Chem.* **2023**, *88* (13), 8203–8226.
92. McDermott, M. C.; Stephenson, G. R.; Hughes, D. L.; Walkington , A. J. Intramolecular Asymmetric Heck Reactions: Evidence for Dynamic Kinetic Resolution Effects. *Org. Lett.* **2006** *8*(14), 2917–2920.

Chapter 2: Synthesis of the Heck Substrates and Reaction Optimization

2.1 Introduction

The Heck substrates **1** and **1-I** for the Ni-catalyzed Heck reactions were prepared using a well-established three-step sequence[1] that entails a Birch reduction-alkylation process followed by coupling with a corresponding primary or secondary aniline derivative (**Scheme 2.1**). Similar to the Pd-catalyzed case, the use of tertiary amides was necessary for the reactivity in the Ni-catalyzed Heck reactions. Specifically, N-methyl and N-methoxymethyl (N-MOM) amides were selected for this study. The choice of N-MOM amides allows for subsequent deprotection, revealing the critical hydrogen-bond donor in the secondary amide of the parent phenanthridinone structure.

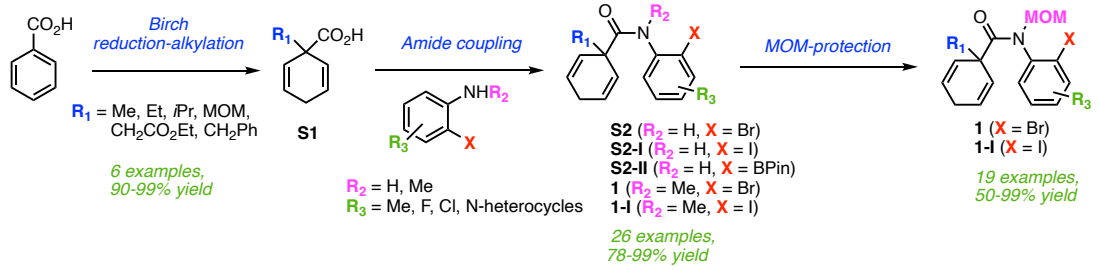

Scheme 2.1 Synthesis of the Heck substrates.

In our earlier research involving the Pd-catalyzed enantioselective desymmetrizing Heck reaction, we observed that the presence of bulkier alkyl groups at the quaternary center (e.g., $\mathbf{R_1}$ = -*i*Pr, -*i*Bu, and -Cy) led to diminished levels of enantioselectivity. Therefore, we started our investigations into the use of nickel as an alternative catalyst to potentially enhance enantioselectivity when dealing with these

more sterically demanding substrates. Our preliminary screening of reaction parameters was initiated by Dr. Mary Sexton.[2] While it showed some success in delivering the desired 1,3-diene Heck product, further optimization was undertaken to increase product yield and reduce the formation of side-product. When the initial reaction conditions (**Scheme 2.2**) using $NiCl_2$ as the catalyst, bipyridine (bipy) as the ligand, and Zn as the reducing agent, were applied to tertiary aryl bromide (**1d**) in dimethylformamide (DMF) at 80°C, we were pleased to observe promising results with an impressively fast reaction rate (10 min).[3] These preliminary findings motivated us to continue further optimization studies.

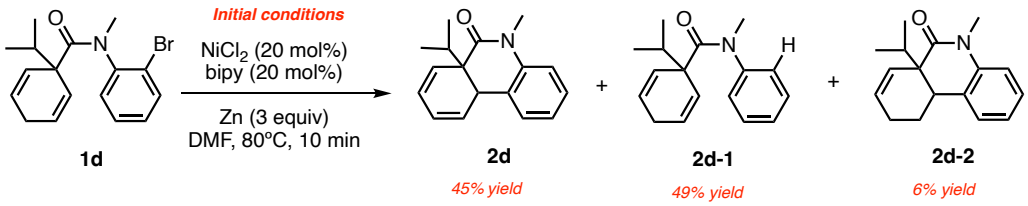

Scheme 2.2 Preliminary Ni-catalyzed Mizoroki-Heck reaction conditions.

2.2 Heck Substrate Synthesis

2.2.1 Synthesis of secondary and tertiary amides

The first step in our Birch-Heck sequence involves the reduction of inexpensive benzoic acids or esters by dissolving Li metal in liquid ammonia. The enolate anion intermediate is quenched with an alkyl halide to form 1,4-diene systems with prochiral quaternary carbon centers. The Birch reduction-alkylation, which has been thoroughly optimized by Dr. Andrew Krasley,[4] plays a pivotal role in our sequence due to its ability to introduce a quaternary center and generate a symmetrical 1,4-cyclohexadiene structure. Consequently, it establishes the foundation for the key enantioselective Heck desymmetrization and cyclization reaction. **Table 2.1** outlines the Birch products used to

synthesize the Heck precursors for the Ni-catalyzed Mizoroki-Heck reaction. The reactions employing benzoic acid as a classic Birch reaction substrate with a corresponding choice of alkyl halide, successfully afforded the 1,4-cyclohexadiene products in consistently high yields and high purity for the subsequent use without chromatographic purification (**entries 1-6**).[1] To provide examples of 6-5-6 and 6-6-6 tricarbocyclic systems using the Ni-catalyzed Mizoroki-Heck reaction, we used the Birch products **S1g** and **S1h** prepared by Andrew Kraskey, PhD'17 from benzoate esters (**entries 7-8**).[4] The precursor for the tricyclic 6-5-6 ring system **1g** was formed in very good yield (**entry 7**). However, the Birch product for the 6-6-6 carbocyclic system **1h** underwent significant yield loss due to the competing bimolecular elimination (E2) side reaction that resulted in the formation of a styrene derivative.[5]

Table 2.1 Birch Products.

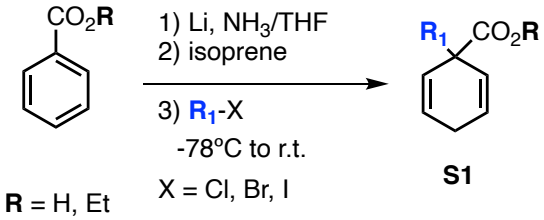

entry	R	R_1-X	yield (%)	compound
1	H	iodomethane	94	**S1a**
2	H	bromoethane	99	**S1b**
3	H	2-iodopropane	96	**S1c**
4	H	methyl chloromethyl ether	90	**S1d**
5	H	ethyl 2-chloroacetate	99	**S1e**
6	H	benzyl chloride	94	**S1f**
7	Et	2-iodobenzyl bromide	85	**S1g**
8	Et	1-(2-bromoethyl)-2-iodobenzene	26	**S1h**

Optimal efficiency and enantioselectivity in our previous Pd-catalyzed method were achieved by promoting the cationic catalytic cyclic[6] with the use of an aryl triflate electrophile.[1] However, previous literature reports supporting a cationic Ni-catalyzed Heck pathway have been limited to intermolecular approaches regarding regioselective

olefination of aryl triflates.[7-9] The enhanced catalytic activity in these transformations was explained by the generation of a critical cationic nickel complex in the catalytic cycle, which was responsible for promoting a favorable β-hydride elimination step and subsequent reductive elimination.[8] Regarding intramolecular Ni-catalyzed Heck reactions, a previous study by Desrosiers and coworkers is particularly pertinent to this work.[10] Their research provided a comparison of reactivity between the neutral and cationic pathways, with the neutral pathway demonstrating enhanced yield and enantioselectivity.[11] Moreover, our initial efforts to subject aryl triflate to the Ni-catalyzed Heck conditions had proven unsuccessful in delivering any cyclized Heck product. Thus, our research became focused on utilizing aryl halides rather than aryl triflates to facilitate a neutral catalytic pathway with nickel.

The carboxylic acid Birch products **S1a-f** were converted to amide using standard acid chloride formation with $(COCl)_2$/DMF (cat.) followed by reaction with the appropriate corresponding primary or secondary aniline derivative (**Table 2.2**). The yields for this step ranged from 51-99% after chromatographic purification with the lowest yield obtained from the amide coupling of **S1a** with 4-amino-5-bromopyrimidine due to low solubility of pyrimidine in dichloromethane (DCM) and poor nucleophilicity of the amine group on the electron-deficient pyrimidine ring. An improved yield for this substrate was obtained when using THF instead of DCM and changing 4-amino-5-bromopyrimidine to a limiting reagent (**entry 24**).

Table 2.2 Amide Formation.

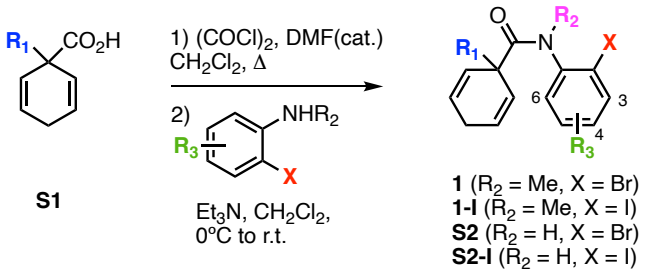

entry	R_1	R_2	R_3	X	yield (%)	compound
1	Me, **S1a**	Me	H	Br	93	**1a**
2	Me, **S1a**	Me	H	I	79	**1a-I**
3	Me, **S1a**	H	H	Br	95	**S2b**
4	Me, **S1a**	H	H	I	99	**S2b-I**
5	Et, **S1b**	H	H	I	95	**S2c-I**
6	*i*-Pr, **S1c**	Me	H	Br	90	**1d**
7	*i*-Pr, **S1c**	Me	H	I	84	**1d-I**
8[a]	*i*-Pr, **S1c**	Me	H	OTf	81	**1d-II**
9	*i*-Pr, **S1c**	H	H	Br	79	**S2e**
10	*i*-Pr, **S1c**	H	H	I	84	**S2e-I**
11	*i*-Pr, **S1c**	H	H	BPin	87	**S2e-II**
12	CH_2OCH_3, **S1d**	H	H	I	97	**S2f-I**
13	CH_2CO_2Et, **S1e**	Me	H	I	83	**1g-I**
14	CH_2Ph, **S1f**	H	H	Br	88	**S2h**
15	CH_2Ph, **S1f**	H	H	I	90	**S2h-I**
16	*i*-Pr, **S1c**	H	4-F	Br	90	**S2i**
17	*i*-Pr, **S1c**	H	4-F	I	91	**S2i-I**
18	*i*-Pr, **S1c**	H	4-Cl	Br	93	**S2j**
19	*i*-Pr, **S1c**	H	4-Cl	I	82	**S2j-I**
20	*i*-Pr, **S1c**	H	4-Me	Br	96	**S2k**
21	*i*-Pr, **S1c**	H	5-Me	I	99	**S2l-I**
22	Me, **S1a**	H	C_3=N	Br	85	**S2m**
23	Me, **S1a**	H	C_6=N	Br	81	**S2n**
24	Et, **S1b**	H	C_6=N	Br	78	**S2o**
25	Et, **S1b**	H	C_6=N	I	89	**S2o-I**
26[b]	Me, **S1a**	H	$C_{4,6}$=N	Br	51	**S2p**
27	CH_2CO_2Et, **S1e**	H	H	Br	93	**S2r**

[a]Initially synthesized for the Pd-catalyzed Heck reaction; yield (%, 2 steps).[1] [b]Used THF instead of CH_2Cl_2 in step 2; acid chloride intermediate used in excess (1.5 equiv).

Despite the preliminary results indicating that the aryl triflate substrate was unreactive with the Ni-catalyzed system, we decided to include aryl triflate **1d-II** (initially synthesized for the previous Pd-catalyzed Heck reaction) in the list of amides for the substrate scope exploration in this work (**entry 8**). We also included aryl boronic

ester **S2e-II** in **Table 2.2**, **entry 11**, which was used in our attempts to investigate the oxidative boron Heck reactions in Chapter 5.

While conducting NMR analysis of the tertiary benzamides in deuterated chloroform, we observed signal broadening, indicative of atropisomer formation, which was similar to what we observed with aryl triflates used in the palladium-catalyzed Heck reaction.[2] Atropisomerism arises from restricted rotation around a single bond, typically because of steric or electronic hindrances.[12] This constraint leads to slow interconversion between two or more conformers at lower temperatures.[13, 14] Therefore, peak broadening and complex NMR spectra were caused by the restricted rotation around the N-aryl or the amide N-(C=O) bond due to steric hindrance with the N-Me or N-MOM groups and slow atropisomer interconversion at room temperature. Peak coalescence was achieved at elevated temperatures using deuterated dimethylsulfoxide (DMSO-d_6). This effect was attributed to the increased rate of atropisomer interconversion, achieved by overcoming the rotational barrier between the conformers. Besides impacting NMR resolution, atropisomerism can also have several important implications in the Heck reaction. The reaction is likely to experience some degree of dynamic kinetic resolution, which may influence enantioselectivity.[14, 15] The presence of atropisomers can also offer the potential for controlling the temperature-dependent equilibrium of isomer interconversion to foster chiral induction from the chiral catalyst.

Conversely, the existence of atropisomerism was not observed with secondary benzamides due to unrestricted rotation around the N-aryl and the amide N-(C=O) bonds because hydrogen is a small atom, allowing for facile rotation around the single bond. Unfortunately, as with the previous Pd-catalyzed method, our preliminary results showed

that secondary amide substrates **S2** and **S2-I** were not successful substrates for the Ni-catalyzed Heck reaction conditions and had to be protected as the methoxymethyl tertiary amides by treatment with a base (LiHMDS) and alkylation with methoxymethyl chloride or bromide (MOM-Cl/Br) (**Table 2.3**). We hypothesized it was the result of a stable Ni complex from an intramolecular reaction: a six-member ring chelation between the amide oxygen and nickel after the oxidative addition.[1] The use of N-MOM benzamides allows for a later deprotection step, unveiling the significant hydrogen-bond donor in the secondary amide of the parent phenanthridinone.

The average yields for the secondary amide MOM-protection ranged from 50-96% for most substrates (**Table 2.3**). The alkylation of the secondary amide containing the aryl boronic ester group **S2e-II** failed to produce the MOM-protected tertiary amide **1e-II**, potentially due to steric hindrance caused by the boronic ester group (**entry 6**). The pyrimidine-based secondary amide **S2p** was difficult to alkylate with either MOM-Cl or MOM-Br due to weak nucleophilicity of the six membered heterocycle rings. Pyrimidine rings are more electron deficient compared to benzene due to the presence of two nitrogen atoms that reduce π-electron density. Even after multiple attempts with alternative bases (e.g., NaHMDS, NaH) or large access of MOM-Br (10 equiv), the highest yield of the desired product **1p** was only 8% (**entry 20**). Thus, we turned to alternative methods to synthesize the tertiary N-Me amide **1q** containing a pyrimidine moiety instead (**Scheme 2.3**).

Table 2.3 Secondary Amide Protection.

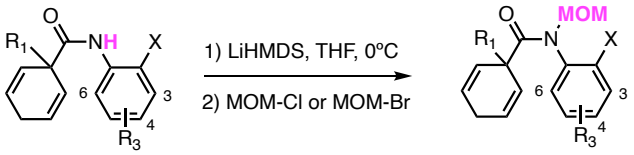

S2 (X = Br)
S2-I (X = I)

1 (X = Br)
1-I (X = I)

entry	R_1	R_3	X	yield (%)	compound
1	Me, **S2b**	H	Br	76	**1b**
2	Me, **S2b-I**	H	I	88	**1b-I**
3	Et, **S2c-I**	H	I	79	**1c-I**
4	*i*-Pr, **S2e**	H	Br	81	**1e**
5	*i*-Pr, **S2e-I**	H	I	72	**1e-I**
6	*i*-Pr, **S2e-II**	H	BPin	NR[a]	**1e-II**
7	CH_2OCH_3, **S2f-I**	H	I	90	**1f-I**
8	CH_2Ph, **S2h**	H	Br	92	**1h**
9	CH_2Ph, **S2h-I**	H	I	85	**1h-I**
10	*i*-Pr, **S2i**	4-F	Br	87	**1i**
11	*i*-Pr, **S2i-I**	4-F	I	96	**1i-I**
12	*i*-Pr, **S2j**	4-Cl	Br	79	**1j**
13	*i*-Pr, **S2j-I**	4-Cl	I	87	**1j-I**
14	*i*-Pr, **S2k**	4-Me	Br	77	**1k**
15	*i*-Pr, **S2l-I**	5-Me	I	84	**1l-I**
16	Me, **S2m**	C_3=N	Br	84	**1m**
17	Me, **S2n**	C_6=N	Br	65	**1n**
18	Et, **S2o**	C_6=N	Br	78	**1o**
19	Et, **S2o-I**	C_6=N	I	50	**1o-I**
20	Me, **S2p**	$C_{4,6}$=N	Br	8	**1p**
21	CH_2CO_2Et, **S2r**	H	Br	NR	**1r**

[a]NR = no reaction

In our first strategy, **5-bromo-*N*-methylpyrimidin-4-amine** was synthesized in 89% yield via a nucleophilic aromatic substitution (S_NAr) on 5-bromo-4-chloropyrimidine in the presence of methylamine in ethanol (**Scheme 2.3 A**). Unfortunately, the amide coupling of the resulting amine with the carboxylic acid **S1a** had failed to deliver the desired tertiary N-Me amide **1q**. Thus, we turned to the next strategy, where **S1a** was coupled with methylamine via an acyl chloride intermediate to yield **S2q** in 63% yield (**Scheme 2.3 B**). Following this, our efforts to employ **S2q** in the alternative S_NAr on 5-bromo-4-chloropyrimidine were not fruitful. This was primarily due to reduced nucleophilicity of the amide nitrogen via resonance stabilization by the

carbonyl group or the presence of bromine in the ortho position to the chlorine, leading to steric hindrance near the site of nucleophilic attack.

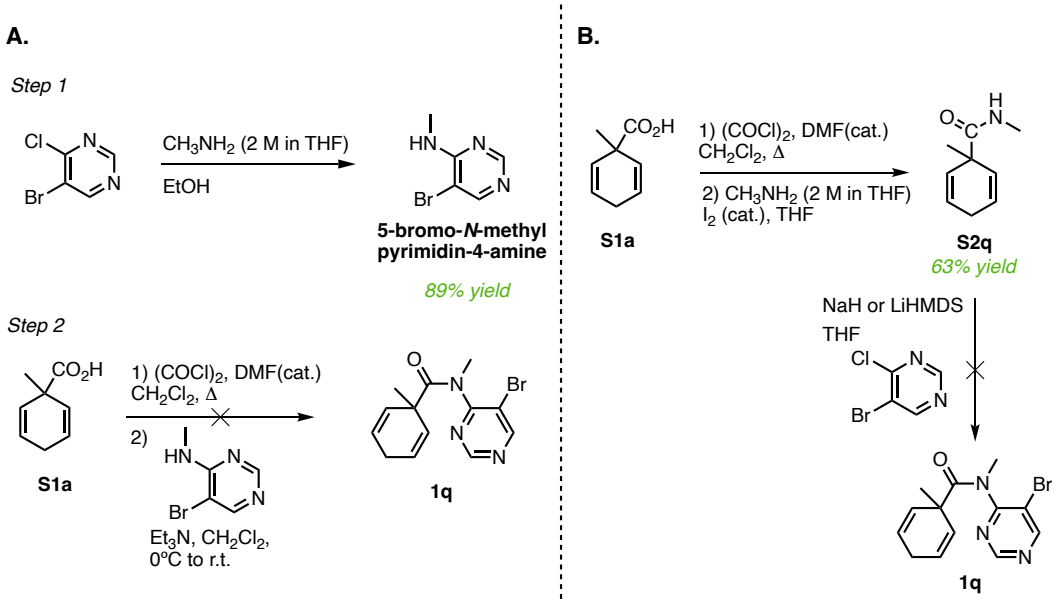

Scheme 2.3 Alternative approaches for the formation of a tertiary N-Me amide **1q**.

Another unsuccessful substrate for the MOM-protection was an ester containing secondary amide **S2r**, resulting in the predominant formation of a cyclic imide **1r-1,** due to an intramolecular nucleophilic acyl substitution involving the deprotonated nitrogen of the amide and the ester carbonyl group (**Table 2.3**, **entry 21**; **Scheme 2.4**). Since the MOM protection of **S2r** had failed to deliver the desired product **1r**, we decided to exclusively focus on the tertiary N-Me amide **1g-I** with the ester containing R_1 group for the Ni-catalyzed Heck reaction (**Table 2.2**).

Previous attempts to increase the size of the central 6-membered ring in our series of tricarbocyclic ring systems with palladium were not successful.[4] Therefore, we decided to investigate the possibility of using nickel to create a 6-7-6 triheterocyclic ring system with a quaternary center. The Heck substrate **1u** was successfully synthesized in

excellent yield through the standard amide formation protocol, followed by the MOM-protection (**Scheme 2.5**)

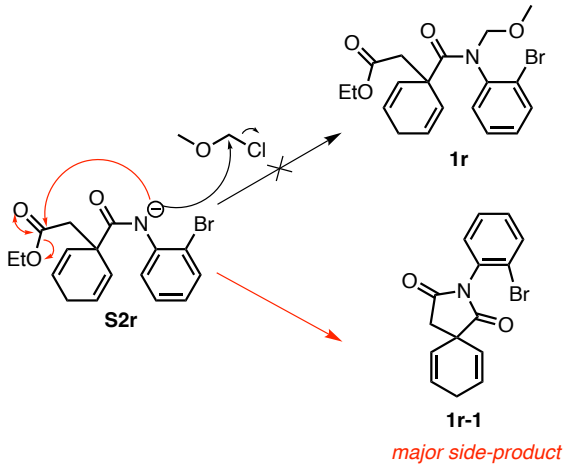

Scheme 2.4 Formation of the cyclic imide side-product.

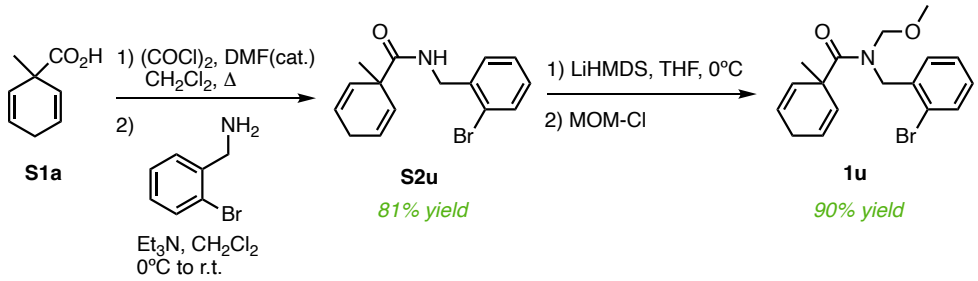

Scheme 2.5 Synthesis of the Heck substrate **1u** for the 6-7-6 ring system formation.

In addition to our efforts in forming tricyclic ring systems in the Ni-catalyzed Heck reaction, we also explored the possibility of creating a bicyclic 6-6 system that includes a terminal alkene that could potentially serve as a versatile handle for further functionalization, leading to a broader range of molecular scaffolds. To access the Heck precursor for this transformation, we initially synthesized a vinyl bromide amine intermediate by reacting 2,3-dibromopropene with methyl amine in the presence of the base (Et_3N) (**Scheme 2.6, step 1**). The crude product was coupled with the acid chloride intermediate of **S1a** following the general procedure for amide formation to yield the Heck substrate **1v** in excellent yield (**Scheme 2.6, step 2**).

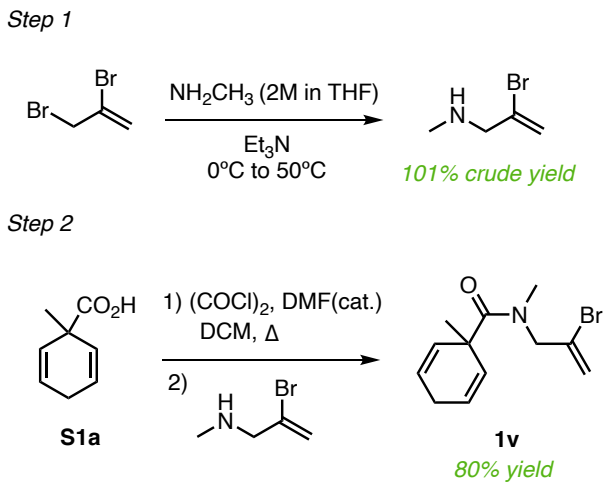

Scheme 2.6 Synthesis of the Heck substrate **1v** for the 6-6 bicyclic ring system.

2.2.1 Amine Synthesis by Amide Reduction

One potential solution to address atropisomerism in our tertiary amide structures was to reduce the tertiary N-methyl amide group to the corresponding tertiary amine. The absence of the carbonyl group alleviates steric hindrance with the nitrogen substituent, allowing for the free rotation around the CH_2-N(R) bond. Building on our previous experience with the Pd-catalyzed enantioselective Heck reaction, we hypothesized that there might be a dynamic kinetic resolution process at play, where one atropisomer reacts faster in the critical 1,2-migratory insertion step that determines both the rate and stereochemistry of the reaction. If the rate of amide twist interconversion is competitive with the reaction leading to the minor stereoisomer, it could result in reduced enantioselectivity. As a result, we suggested that eliminating atropisomerism in our tertiary amides could improve the stereoselectivity of the Ni-catalyzed Heck reaction. Furthermore, by exposing amines to the reaction conditions with the nickel catalyst, we aimed to explore the possibility of *ortho* effect involvement, which suggests the carbonyl group can chelate to the oxidative addition Ni-complex and stabilize it in the (II) oxidation step.[16] This phenomenon was observed with the secondary amides in our

previous work with palladium. The reduction of tertiary amide **1a** was accomplished with DIBAL (di-isobutyl aluminum hydride), a strong and bulky reducing agent (**Scheme 2.7**). Tertiary amine **1w** was obtained in satisfactory yield and subsequently used in the optimized Ni-catalyzed Heck reaction as part of the substrate scope analysis.

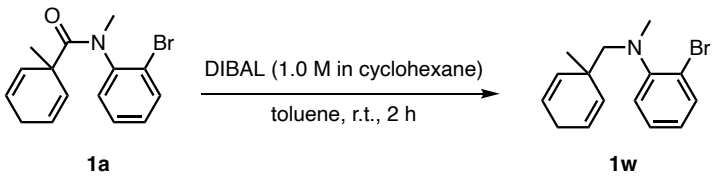

1a **1w**

62% yield

Scheme 2.7 Reduction of tertiary amide **1a** using DIBAL.

In addition to assessing the compatibility of tertiary N-methyl amines in our Ni-catalyzed system. Unfortunately, when we attempted to reduce secondary amide **S2b-I** to the corresponding secondary amine **S1x-I** using DIBAL, the reaction was incomplete and required a large excess of the reducing reagent (>10 equiv) (**Scheme 2.8**). While the product was formed in fair yield, the formation of over-reduced side-products made the purification process very difficult. The inefficiency of this method forced us to search for an alternative protocol for the reduction of secondary amides.

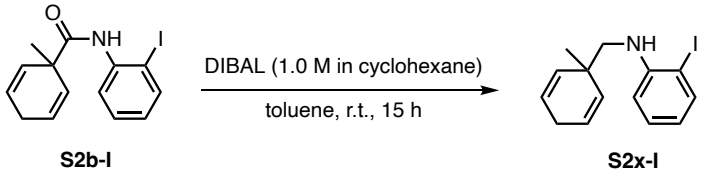

S2b-I **S2x-I**

59% yield

Scheme 2.8 Reduction of secondary amide **S2b-I** using DIBAL.

In the search for the most optimal reaction conditions to accomplish this challenging reduction procedure, we used secondary amide **S2e-I** (**Table 2.4**). We started with one of the most traditional methods for the reduction of secondary amides using BH_3-DMS (borane dimethyl sulfide)[17] complex (**entries 1-2**). The mechanism involves

activation of the carbonyl by Lewis acidic boron, followed by hydride transfer and subsequently cleavage of the C-O bond. The initial product of an amide reduction with borane reagents is the amine-borane complex, which must be decomposed to release the free amine product. One of the main challenges we experienced with our substate was the cleavage of the resulting borane-amine adduct during the workup procedures. Multiple attempts using strongly acidic conditions (e.g., refluxing aqueous 3 or 6 N HCl) were unsuccessful.[18] Next, we tried to utilized a triethylborane (BF_3)-base catalytic system with hydrosilane ($PhSiH_3$) reported more recently by Yao and co-workers (**entry 3**).[19] The preliminary data of their study suggests that the alkaline metal base facilitates the hydride transfer from silicon to boron, resulting in the formation of an active borane/silane complex for the amide reduction. Unfortunately, our secondary amide **S2e-I** did not show reactivity under these conditions, affording predominantly the starting material, with a minor formation of the amine-borane complex. Likewise, the secondary amide was completely unreactive toward a mixture of sodium borohydride ($NaBH_4$) in the presence of Lewis acid BF_3-OEt_3[20] (**entry 4**) and zinc-catalyzed hydrosilylation conditions[21] (**entry 5**). Using the even stronger reducing agent lithium aluminum hydride (LAH), led to a mixture of protodehalogenated and reduced protodehalogenated side products, along with a substantial amount of starting material (**entry 6**). Ultimately, we managed to obtained secondary amine **S2y-I** in good yield by reducing it with alane (AlH_3), one of the most powerful reducing agents prepared in situ by the reaction of LAH with aluminum chloride ($AlCl_3$) in ether solution (**entry 7**).[22] The absence of protodehalogenation with alane versus LAH is likely due to alane's electrophilic nature

versus LAH's nucleophilic reduction mechanism which makes aryl halides vulnerable to cleavage.

Table 2.4 Secondary amide reduction conditions.

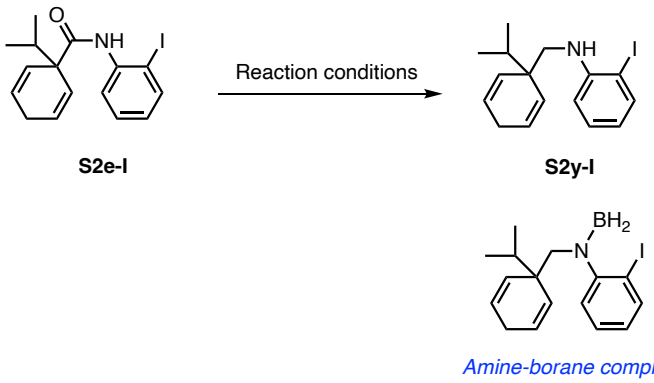

S2e-I **S2y-I**

entry	conditions	product yield (%)[a]
1	BH_3-DMS (1M in THF), 0°C to r.t.	-
2	1) BF_3-OEt_2, BH_3-DMS, THF, Δ 2) 3 or 6 N HCl, Δ	-
3	cat. BEt_3/NaOMe, $PhSiH_3$, THF, 50°C	-
4	$NaBH_4$, BF_3-OEt_2 THF, 0°C to r.t.	NR[b]
5	cat. $Zn(OTf)_2$, TMDS, toluene, 100°C	NR
6	LAH, THF, r.t.	-
7	LAH/$AlCl_3$, THF/ether, 0°C to r.t.	78

[a]Isolated yield. [b]NR = no reaction.

To explore the reactivity of various tertiary N-protected amines, we considered using a selection of protecting groups for our secondary amine substate **S2y-I** (**Table 2.5**). The standard conditions for the MOM-protection with LiHMDS and MOM-Cl or MOM-Br did not work for the secondary amine **S2y-I** (**entries 1-2**). Subsequent attempts to install silyl-protective groups[23] (e.g., tert-butyldimethylsilyl (TBS), trimethylsilyl (TMS) groups) were equally unsuccessful (**entries 3-5**). Following this, we chose to protect the amine with carbamate protecting groups. While employing the *t*-butyloxycarbonyl (Boc) protecting group failed to yield the desired N-Boc protected amine **1yd-I** (**entry 6**), we successfully obtained the tertiary amine **1ye-I**, protected with the methyl carbamate group,[24] in excellent yield (**entry 7**). Lastly, we were able to access the N-benzyl protected amine **1yf-I** in good yield (**entry 8**).

Table 2.5 Secondary amine protection reactions.

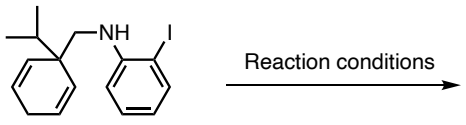

S2y-I

1ya-I (R = MOM)
1yb-I (R = TBS)
1yc-I (R = TMS)
1yd-I (R = BOC)
1ye-I (R = CO_2CH_3)
1yf-I (R = Bn)

entry	R	conditions	Compound	% yield[a]
1	MOM	LiHMDS, MOM-Cl, THF, 0°C to r.t.	**1ya-I**	NR[b]
2	MOM	LiHMDS, MOM-Br, THF, 0°C to r.t.	**1ya-I**	NR
3	TBS	imidazole, TBS-Cl, DMF, 0°C to r.t.	**1yb-I**	NR
4	TBS	LiHMDS, TBS-Cl, THF, 0°C to r.t.	**1yb-I**	NR
5	TMS	Et_3N, TMS-Cl, DCM, r.t.	**1yc-I**	NR
6	Boc	DMAP, Boc_2O, DCM, r.t.	**1yd-I**	NR
7	CO_2CH_3	LiHMDS, DMAP, $ClCO_2CH_3$, THF, 0°C to r.t.	**1ye-I**	91
8	Bn	LiHMDS, Bn-Br, THF, 0°C to r.t.	**1yf-I**	77

[a]Isolated yield. [b]NR = no reaction.

2.3 Optimization of the Ni-catalyzed Mizoroki-Heck Reaction

The main focus of this section was to develop conditions for a new nickel-catalyzed intramolecular Heck reaction that substitutes nickel for palladium in a Heck transformation that was identical to a similar phenanthridinone synthesis recently reported by our group.[1] In addition to contrasting the nickel-catalyzed conditions for the identical palladium Heck reaction, the primary goal of this work was to achieve high levels of enantioselectivity with nickel as an alternative catalyst choice. Herein, we describe our efforts to optimize the reaction conditions by employing an achiral method with bipy as our standard ligand.[3] In Chapter 3, we provide further exploration of an enantioselective version of this reaction.

Table 2.6 Optimization of the Heck reaction.[a]

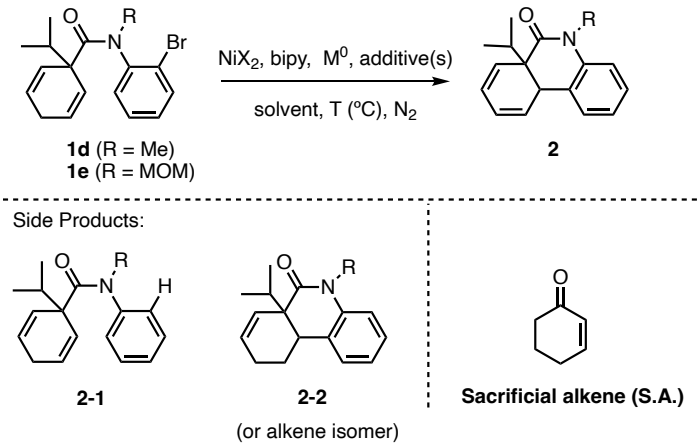

entry	1	time	T (˚C)	NiX_2 (mol %)	M^0 (equiv.)	additive(s) (equiv.)	solvent	2 (%)[b]	2-1 (%)[b]	2-2 (%)[b]
1	**1d**	10 min	80	$NiCl_2$ (20)	Zn (3)	-	DMF	45	49	6
2	**1d**	10 min	80	$NiCl_2$ (20)	Zn (3)	LiI (1)	DMF	56	40	5
3	**1d**	10 min	80	$NiCl_2$ (20)	Zn (3)	NaI (1)	DMF	61	32	7
4	**1d**	10 min	80	$NiCl_2$ (20)	Zn (3)	KI (1)	DMF	67	33	5
5	**1d**	1.5 h	80	$NiCl_2$ (20)	Zn (3)	K_3PO_4 (1)	DMF	59	33	8
6	**1d**	1 h	80	$NiCl_2$ (20)	Zn (1.5)	KI (1)	DMF	63	29	9
7	**1d**	10 min	120	$NiCl_2$ (20)	Zn (3)	KI (1)	DMF	62	28	11
8	**1d**	2 h	60	$NiCl_2$ (20)	Zn (3)	KI (1)	DMF	57	36	7
9	**1d**	6h	80	$NiCl_2$ (20)	Zn (3)	KI (1)/ LiOAc (1)	DMF	55	38	7
10	**1d**	20 min	80	$NiCl_2$ (20)	Zn (3)	KI (1)	DMA	60	34	6
11	**1d**	1h	80	$NiCl_2$ (20)	Zn (3)	KI (1)	DMSO	61	29	10
12	**1d**	20 min	80	$NiCl_2$ (20)	Zn (3)	KI (1)/ S.A. (2)	DMF	85	9	6
13	**1d**	18 h	80	$NiCl_2$ (20)	TDAE (3)	KI (1)/ S.A (2)	DMF	80	4	10
14	**1e**	1.5 h	80	$NiCl_2$ (20)	Zn (3)	KI (1)/ S.A (2)	DMF	72	0.2	22
15	**1e**	3 h	80	$NiCl_2$ (20)	Mn (3)	KI (1)/ S.A (2)	DMF	73	0.3	25
16	**1e**	24 h	80	$Ni(acac)_2$ (20)	Mn (3)	KI (1)/ S.A (3)	DMF	79	7	14
17	**1e**	1 h	80	$NiBr_2$ (20)	Mn (3)	KI (1)/ S.A (3)	DMF	73	-	27
18	**1e**	1.5 h	80	NiI_2 (10)	Mn (3)	KI (1)/ S.A (3)	DMF	93	-	7

[a]Conditions: NiX_2 (10-20 mol %), bipy (15-20 mol %), M^0 (3 equiv), additives (1-3 equiv), DMF (12 mL/mmol ArX). [b]Determined by GC analysis.

Given that the presence of sterically bulky alkyl groups at the quaternary center led to reduced enantioselectivities in the palladium-catalyzed Heck reaction, our initial investigation of reaction conditions focused on tertiary aryl bromide **1d** (with R = -*i*Pr) with an ultimate objective to achieve higher levels of enantioselectivity in the nickel-catalyzed process (**Table 2.6**).

Although promising results were achieved when employing $NiCl_2$ as the catalyst, bipy as the ligand, and Zn as the reducing agent, we observed significant formation of two major side products: a protodehalogenated **2-1** species and a cyclized alkene **2-2** species (**entry 1**). Remarkably, the reaction was completed in an impressively short time (10 min), a notable contrast to the palladium-catalyzed reaction, which required 24-48 h. Since we suspected that both side-products were the result of Ni-H intermediates, we performed further optimization using aryl bromide **1d** as the model substrate to increase product yield and decrease the amount of the major side products.

Initially, we improved the catalytic system outcome with the addition of 1 equiv of LiI (**entry 2**). Replacing LiI with NaI as an external iodide source resulted in a slight decrease in the amount of unwanted protodebromination product **2-1** (**entry 3**). Consequently, we observed even further increase in the product formation with the addition of KI, the most ionic halide salt (**entry 4**). To test whether the KI improvement was more the result of the potassium cation than the iodide anion, we used K_3PO_4 as the additive (**entry 5**). The absence of iodide significantly prolonged the reaction time and increased the amount of cyclized alkene **2-2** versus the desired cyclized diene.

Iodide has been demonstrated to enhance the reactivity of Ni-catalyzed reactions,[10, 25-28] although the precise mechanism behind this improvement is not definitely known. Prior literature explanations highlight several important benefits of the exogenous halide source.[10, 25-33] For instance, Desrosiers and co-workers[10] reported the use of exogenous halides to improve product yields and enantioselectivity in their studies, primarily by facilitating a neutral Heck mechanism. Wang and co-workers demonstrated improved reactivity without sacrificing the enantioselectivity by the addition of KI in

domino cyclization/cross-coupling of two aryl bromides. In their discussion, they refer to a more comprehensive investigation by Colon and Kelsey into the kinetic effect of the added halide salts on Ni-catalyzed coupling of aryl chlorides with excess reducing metal.[26] In this study, the researchers reported that halide salts accelerated the reduction of $NiCl_2$ to an active catalyst species in the following sequence of effectiveness I>Br>Cl> no salt. Their hypothesis suggested the formation of a pentacoordinate nickelate complex through the association of halide with Ni (**Scheme 2.9**). The nickelate intermediate could form a bridged Zn complex, with the added halide serving as a bridging ligand and facilitating the transfer of electrons from Zn to Ni. Another work supporting the formation the nickelate species and improved reduction of the nickel catalyst with the simple addition of sub-stoichiometric NaI (50 mol%) was reported by Prinsell et al.[27]

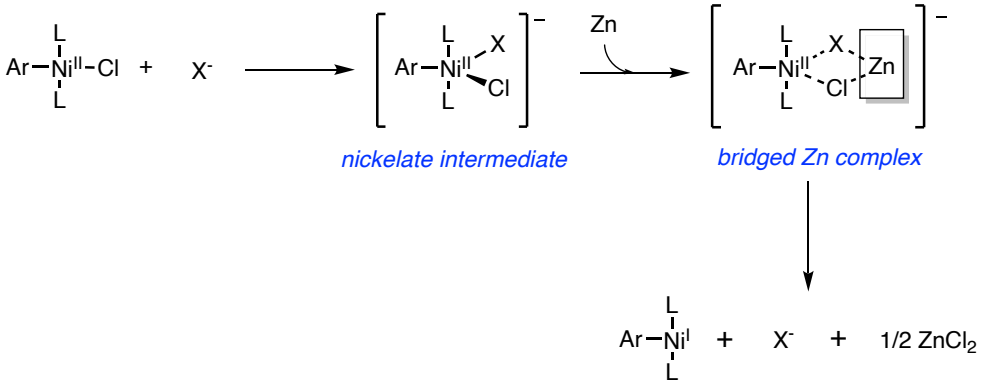

Scheme 2.9 Formation of nickelate intermediate and bridged Zn complex.

Alternatively, nickel-catalyzed halogen exchange[28] of the aryl bromide for iodide with the addition of exogeneous iodide can facilitate substrate reactivity toward oxidative addition of the nickel catalyst. Nevertheless, this mechanism has not been supported by the GCMS analysis of our system as the halogen-exchanged starting material was not present at any point in the reaction mixture.

Reducing the amount of Zn led to a decreased catalyst turnover rate (**entry 6**). Increasing or decreasing the temperature had a minimal impact on product yield (**entry 4** vs **entries 7-8**). In our previous work with the Pd-catalyzed Heck reaction, we discovered the resting state Pd-allyl catalyst complex to be the preferred pathway to the desired 1,3-diene product (**Scheme 2.10**). The formation of this complex was the result of chain walking by the Pd catalyst. We also hypothesized that the formation of the allylic acetate intermediate was the result of nucleophilic addition of the acetate anion (from the $Pd(OAc)_2$ catalyst) to the resting allylic Pd complex.[34-36] Similar to LaRock's report on the isolation of allylic acetate products in related achiral intramolecular Heck reactions involving cyclohexadiene substrates,[34] we were able to isolate and fully characterize the acetate intermediate.[1] To further promote the preferred catalytic pathway, we added LiOAc to the reaction to increase the amount of acetate and accelerate the formation of the allylic acetate intermediate. To our delight, the addition of LiOAc not only promoted the formation of the 1,3-diene product, but also improved enantioselectivity of the Pd-catalyzed reaction. Unfortunately, a similar benefit with the addition of 1 equiv. of LiOAc was not observed with our Ni-catalyzed reaction, eliminating the possibility of the Ni-allyl complex formation (**entry 9**). This can be explained by reluctance of Ni to chain walking reactions due to slower β-hydride elimination and reinsertion steps than with the Pd catalyst.[37]

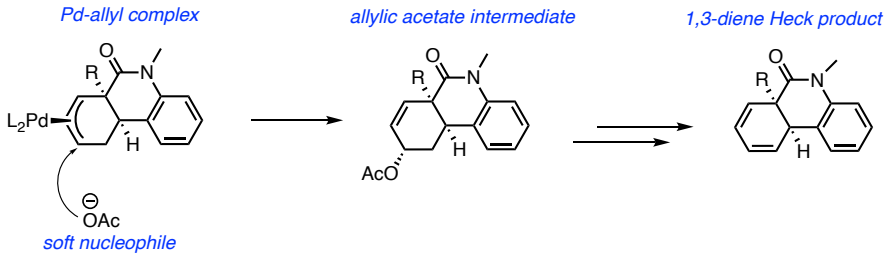

Scheme 2.10 Preferred Pd-catalyzed pathway through acetate intermediate.

Replacing DMF by DMA decreased the amount of 1,3-diene formed (**entry 10** vs **4**). The formation of cyclized alkene **2-2** was increased when using DMSO as a solvent (**entry 11** vs **4**). Since both side products, **2-1** and **2-2**, are likely the result of Ni−H intermediates, we explored the use of acceptor olefin additives to consume the hydride species. Prior work by Lv[38] elegantly demonstrated that the addition of a sacrificial acceptor olefin (S.A.) facilitated the Ni(0)-catalyzed oxidative Heck arylation via a transfer hydrogenation process (**Scheme 2.11**).

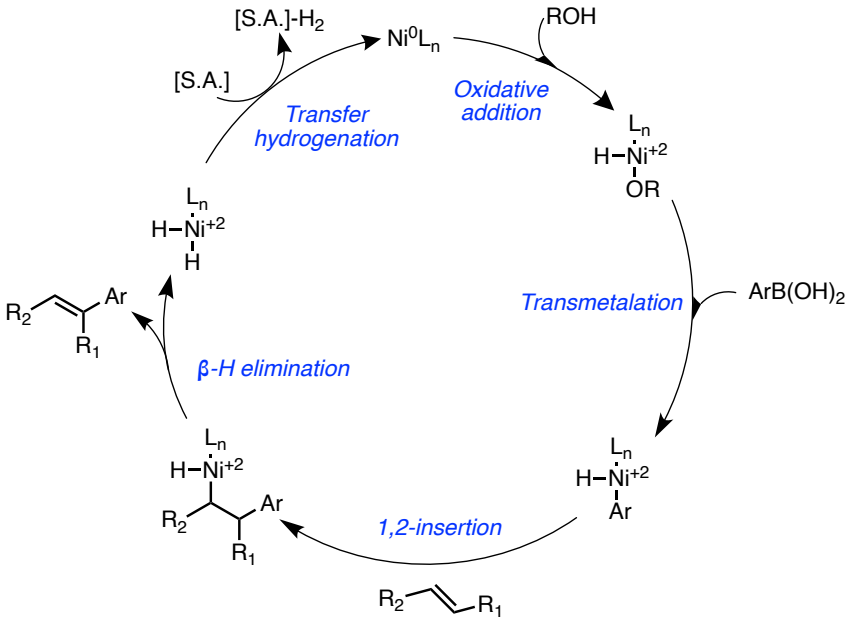

Scheme 2.11 Ni-catalyzed oxidative Heck arylation driven by transfer hydrogenation by Lv et al.[38]

We were pleased to find that the reaction efficiency was considerably enhanced by incorporating 2 equiv. of 2-cyclohexen-1-one as a sacrificial alkene (**entry 12**). Since the full reduction of 2-cyclohexen-1-one requires not only the nickel hydride species, but also a proton source, we proposed the process was facilitated through a nickel-enolate intermediate. In this mechanism, N(II)−XH species can not only acts as the hydride to form the enolate, but also as the proton source to fully reduce the enone system (**Scheme**

2.12). Indeed, cyclohexanone was detected and quantified (1 equiv) in the gas chromatographic analysis of the reactions, demonstrating that the enone system was reduced.

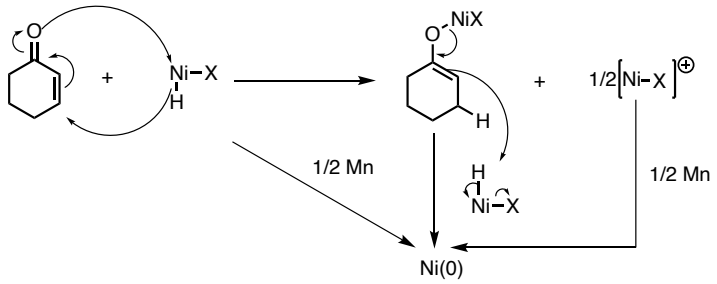

Scheme 2.12 Proposed mechanism for the reduction of 2-cyclohexen-1-one.

Replacing Zn with tetrakis(dimethylamino)ethylene (TDAE) as an organic reductant resulted in a significantly longer reaction time (**entry 13**). Unfortunately, after employing our initially optimized conditions to a MOM-protected tertiary amide **1e** (**entry 14**), we observed an increased level of formation of cyclized alkene side product **2-2**, so further optimization through additional screening of the Ni source, reductants, and additives was performed (**entries 15−18**). The reaction efficiency was dramatically improved with NiI_2 (10 mol %) as the catalyst and Mn as the reductant (**entry 18**). Because Mn is a stronger two-electron reductant [$E° = -1.18$ V vs the standard hydrogen electrode (SHE) in water] than Zn ($E° = -0.76$ V vs SHE in water), it likely accelerates catalyst turnover by reducing the Ni(II)-H species faster, if the Ni(II)-H is not consumed by the sacrificial alkene.

2.4 Conclusions

In this chapter, we discussed the synthesis of tertiary amide substrates for the Ni-catalyzed Mizoroki-Heck reaction aiming to form tricyclic or bicyclic ring systems. A wide range of Heck precursors was successfully prepared using the standard Birch

reduction/alkylation, amide formation, and MOM-protection protocols. To address atropisomerism in the tertiary amides and investigate the possibility of the ortho effect in the Heck reaction, we identified efficient procedures for the reduction of tertiary and secondary amides to their corresponding tertiary and secondary amines, using DIBAL or alane reducing agents, respectively. The secondary amine products were protected as the methyl carbamate or benzyl tertiary amines.

The optimal conditions for the Ni-catalyzed Heck reaction were established using NiI_2 as the nickel source, bipy as the achiral ligand, Mn as the reductant, KI and 2-cyclohexenone as additives in DMF at 80°C. Through important advances in reaction optimization, we were able to control unwanted protodehalogenation and alkene reduction side products with the addition of an external iodide source (KI) and a sacrificial alkene (2-cyclohexenone) to consume the hydride species.

2.4 References

1. Sexton, M.; Malachowski, W. P.; A., G. Y. P.; Rachii, D.; Feldman, G.; Krasley, A.; Chen, Z.; Tran, M.; Wiley, K.; Matei, A.; et al. Catalytic Enantioselective Birch−Heck Sequence for the Synthesis of Phenanthridinone Derivatives with an All-Carbon Quaternary Stereocenter. *J. Org. Chem.* **2022**, *87* (2), 1154–1172.
2. Sexton, M. Exploration of the use of Palladium and Nickel to Catalyze Enolate Cross-coupling and the Enantioselective Mizoroki-Heck Reaction. Bryn Mawr College, Scholarship, Research, and Creative Work at Bryn Mawr College., 2021.
3. Rachii, D.; Caldwell, D. J.; Kosukegawa, Y.; Sexton, M.; Rablen, P.; Malachowski, W. P. Ni-Catalyzed Enantioselective Intramolecular Mizoroki–Heck Reaction for the Synthesis of Phenanthridinone Derivatives. *J. Org. Chem.* **2023**, *88* (13), 8203–8226.
4. Krasley, A. T.; Malachowski, W. P.; Hannah, T. M.; Tran Tien, S. Catalytic Enantioselective Birch–Heck Sequence for the Synthesis of Tricyclic Structures with All-Carbon Quaternary Stereocenters. *Org. Lett.* **2018**, *20* (7), 1740–1743.
5. Krasley, A. T. Exploration of Synthetic Pathways to Quaternary Carbon Stereocenters and Fused Ring Systems via Birch Reductions. Bryn Mawr College, Scholarship, Research, and Creative Work at Bryn Mawr College, **2017**
6. Dounay, A. B.; Overman, L. E. The Asymmetric Intramolecular Heck Reaction in Natural Product Total Synthesis. *Chem. Rev.* **2003**, *103*, 2945–2964.
7. Tasker, S. Z.; Gutierrez, A. C.; Jamison, T. F. Nickel-catalyzed Mizoroki-Heck reaction of aryl sulfonates and chlorides with electronically unbiased terminal olefins: high selectivity for branched products. *Angew. Chem. Int. Ed.* **2014**, *53* (7), 1858–1861.
8. Gøgsig, T. M.; Kleimark, J.; Lill, S. O. N.; Korsager, S.; Lindhardt, A. T.; Norrby, P. O.; Skrydstrup, T. Mild and Efficient Nickel-Catalyzed Heck Reactions with Electron-Rich Olefins. *J. Am. Chem. Soc.* **2012** *134* (1), 443–452.
9. Kampmann, S. S.; Man, N. Y. T.; McKinley, A. J.; Koutsantonis, G. A.; Stewart, S. G. Exploring the Catalytic Reactivity of Nickel Phosphine–Phosphite Complexes. *Aust. J. Chem.* **2015**, *68* (12), 1842–1853.
10. Desrosiers, J.-N.; Wen, J.; Tcyrulnikov, S.; Biswas, S.; Qu, B.; Hie, L.; Kurouski, D.; Wu, L.; Grinberg, N.; Haddad, N.; et al. Enantioselective Nickel-Catalyzed Mizoroki–Heck Cyclizations To Generate Quaternary Stereocenters. *Org. Lett.* **2017**, *19* (13), 3338–3341.
11. Desrosiers, J.-N.; Senanayake, C. H. Development of a Nickel-Catalyzed Enantioselective Mizoroki–Heck Coupling. In *Organometallic Chemistry in Industry*, John Wiley & Sons, Ltd, 2020; pp 91–119.

12. Bringmann, G.; Mortimer, A. J. P.; Keller, P. A.; Gresser, M. J.; Garner, J.; Breuning, M. Atroposelective Synthesis of Axially Chiral Biaryl Compounds. *Angew. Chem. Int. Ed.* **2005**, *44* (34), 5384–5427.
13. Hosoi, S. O., M.Nakano, M.Arimitsu, K.Kajimoto, T.Kojima, N. Iwasaki, H. Miura, T.; Kimura, H.; Node, M.; Yamashita, M. Mechanistic aspects of asymmetric intramolecular Heck reaction involving dynamic kinetic resolution: flexible conformation of the cyclohexenylidene -benzene system. *Tetrahedron* **2015** *71*, 2317–2326.
14. McDermott, M. C.; Stephenson, G. R.; Hughes, D. L.; Walkington , A. J. Intramolecular Asymmetric Heck Reactions: Evidence for Dynamic Kinetic Resolution Effects. *Org. Lett.* **2006** *8*(14), 2917–2920.
15. Lapierre, A. J. B. G., S. J.Curran, D. P. Low-Temperature Heck Reactions of Axially Chiral o-Iodoacrylanilides Occur with Chirality Transfer: Implications for Catalytic Asymmetric Heck Reactions. *J. Am. Chem. Soc.* **2007**, *129*, 494–495.
16. Marchese, A. D.; Kersting, L. L., M. Diastereoselective Nickel-Catalyzed Carboiodination Generating Six-Membered Nitrogen-Based Heterocycles. *Org. Lett.* **2019**, *21* (17), 7163–7168.
17. *Boranes (Dimethylsulfide Borane, Borane-Tetrahydrofuran Complex)* https://www.organic-chemistry.org/chemicals/reductions/boranes.shtm (accessed 2023 October 17).
18. Brown, H. C.; Narasimhan, S.; Choi, Y. M. Improved Procedure for Borane Dimethyl Sulfide Reduction of Tertiary and Secondary Amides in the Presence of Boron Trifluoride Etherate. *Synthesis* **1981**, *12*, 996–997.
19. Yao, W.; Fang, H.; He, Q.; Peng, D.; Liu, G.; Huang, Z. A BEt_3-Base Catalyst for Amide Reduction with Silane. *J.Org.Chem.* **2019**, *84* (10), 6084–6093.
20. Campeau, L.-C.; Dolman, S. J.; Gauvreau, D.; Corley, E.; Liu, J.; Guidry, E. N.; Ouellet, S. G.; Steinhuebel, D.; Weisel, M.; O'Shea, P. D. Convergent Kilo-Scale Synthesis of a Potent Renin Inhibitor for the Treatment of Hypertension. *Org. Process Res. Dev.* **2011**, *15* (5), 1138–1148.
21. Das, S.; Addis, D.; Junge, K.; Beller, M. Zinc-Catalyzed Chemoselective Reduction of Tertiary and Secondary Amides to Amines. *Chem. Eur. J.* **2011**, *17*, 12186–12192.
22. Brower, F. M.; Matzek, N. E.; Reigler, P. F.; Rinn, H. W.; Roberts, C. B.; Schmidt, D. L.; Snover, J. A.; Terada, K. Preparation and properties of aluminum hydride. *J. Am. Chem. Soc.* **1976**, *98* (9), 2450–2453.
23. Tinsley, J. M.; Roush, W. R. Total Synthesis of Asimicin via Highly Stereoselective [3 + 2] Annulation Reactions of Substituted Allylsilanes. *J. Am. Chem. Soc.* **2005**, *127* (31), 10818–10819.
24. Beemelmanns, C.; Reissig, H.-U. A Short Formal Total Synthesis of Strychnine with a Samarium Diiodide Induced Cascade Reaction as the Key Step. *Angew. Chem. Int. Ed.* **2010**, *49* (43), 8021–8025.
25. Wang, K.; Ding, Z.; Zhou, Z.; Kong, W. Ni-Catalyzed Enantioselective Reductive Diarylation of Activated Alkenes by Domino Cyclization/Cross-Coupling. *J. Am. Chem. Soc.* **2018**, *140* (39), 12364–12368.

26. Colon, I.; Kelsey, D. R. Coupling of aryl chlorides by nickel and reducing metals. *J. Org. Chem.* **1986**, *51* (14), 2627–2637.
27. Prinsell, M. R.; Everson, D. A.; Weix, D. J. Nickel-catalyzed, sodium iodide-promoted reductive dimerization of alkyl halides, alkyl pseudohalides, and allylic acetates. *Chem. Commun.* **2010**, *46*, 5743–5745.
28. Arvela, R. K.; Leadbeater, N. E. Fast and Easy Halide Exchange in Aryl Halides. *Synlett* **2003**, *2003* (08), 1145–1148.
29. Maitlis, P. M.; Haynes, A.; James, B. R.; Catellani, M.; Chiusoli, G. P. Iodide effects in transition metal catalyzed reactions. *Dalton Trans.* **2004**, 3409–3419.
30. Cassar, L.; Foà, M. Nickel-catalyzed carbonylation of aromatic halides at atmospheric pressure of carbon monoxide. *J. Organomet. Chem.* **1973**, *51*, 381–393.
31. Bergamini, P.; Costa, E.; Ganter, C.; Orpen, A. G.; Pringle, P. G. The reaction of trimethylsilyldiazomethane with complexes of the type [PtX(CH3)(diphosphine)] (X = Cl, Br, I). Some observations on β-hydrogen migrations in PtCHRCH3 species and organoplatinum(II)-catalysts for alkene formation from trimethylsilyldiazomethane. *J. Chem. Soc., Dalton Trans.* **1999**, *6*, 861–866.
32. Fagnou, K.; Lautens, M. Halide Effects in Transition Metal Catalysis. *Angew. Chem., Int. Ed.* **2002**, *41* (1), 26–47.
33. Cherney, A. H.; Reisman, S. E. Nickel-Catalyzed Asymmetric Reductive Cross-Coupling Between Vinyl and Benzyl Electrophiles. *J. Am. Chem. Soc.* **2014**, *136* (41), 14365–14368.
34. Larock, R. C.; Han, X. Palladium-Catalyzed Cross-Coupling of 2,5-Cyclohexadienyl-Substituted Aryl or Vinylic Iodides and Carbon or Heteroatom Nucleophiles. *J. Org. Chem.* **1999**, *64* (6), 1875–1887.
35. Sommer, H.; Juliá-Hernández, F.; Martin, R.; Marek, I. Walking Metals for Remote Functionalization. *ACS Cent. Sci.* **2018**, *4*, 153.
36. Larionov, E.; Li, H.; Mazet, C. Well-defined transition metal hydrides in catalytic isomerizations. *Chem. Commun.* **2014**, *50*, 9816.
37. Chernyshev, V. M.; Ananikov, V. P. Nickel and Palladium Catalysis: Stronger Demand than Ever. *ACS Catal.* **2022**, *12* (2), 1180–1200.
38. Lv, H.; Kang, H.; Zhou, B.; Xue, X.; Engle, K. M.; Zhao, D. Nickel-catalyzed intermolecular oxidative Heck arylation driven by transfer hydrogenation. *Nat. Commun.* **2019** *10* (1), 5025.

Chapter 3: Development of an Enantioselective Process

3.1 Introduction

The initial efforts at an enantioselective version of the nickel-catalyzed Heck reaction involved a survey of commercially available bidentate and tridentate N- or P,N-ligands commonly reported with asymmetric Ni-catalyzed reactions[1-4] (e.g., Pyox, Box, Pybox, Biox, diamine, Phox, Quinap, and Pinap) (**Scheme 3.1**). Nickel's unique reactivity, especially its greater range of accessible oxidation states and propensity to involve radical-type reactions via open-shell pathways, makes π-accepting N-based bidentate and tridentate ligands particularly well-suited for Ni catalysts. A lot of N-ligands are redox-active, resulting in a higher field splitting compared to more traditional phosphine-based ligands. Consequently, they increase the stabilization of open-shell paramagnetic Ni intermediates by delocalizing the unpaired electron into the ligand's π* orbital.[5] While there have been significant advancements in understanding the important advantages of N-ligands in Ni-catalyzed reactions involving radicals, there is still a need for more thorough investigation into the fundamental benefits of N-ligands in non-radical processes.[1, 6]

Most of the commercially available ligands we screened featured a chiral oxazoline group, which is a common component found in many ligands used for a wide range of important metal-catalyzed enantioselective transformations.[7] A "hybrid" pyridine-oxazoline-type ligand (Pyox) was the first oxazoline-containing ligand designed

by the Brunner group for a Cu-catalyzed desymmetrizing monophenylation of 1,2-diols. However, the unique properties of Pyox ligands have only been unveiled more recently and their use in asymmetric catalysts is now rapidly gaining popularity.[2]

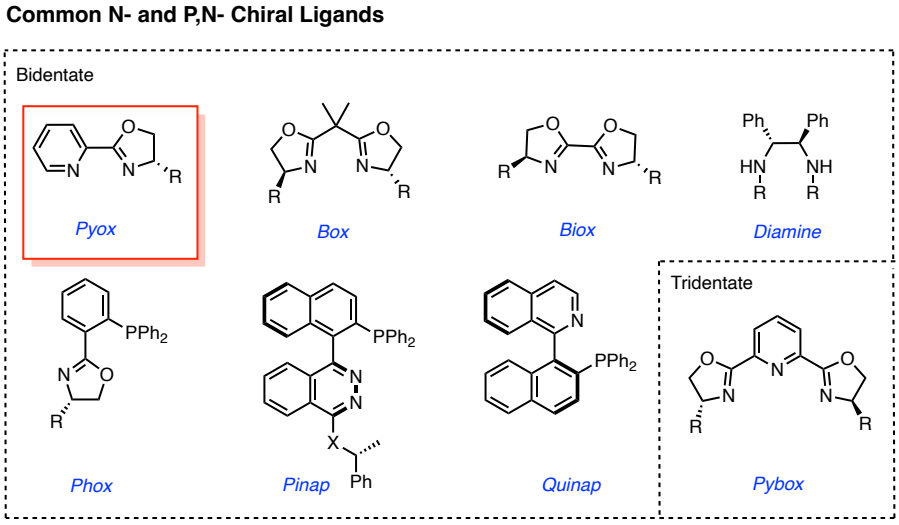

Scheme 3.1 Common N- and P,N- chiral ligands for asymmetric Ni-catalyzed reactions.

Pyox ligands (**Figure 3.1**) were widely used in this study on enantioselective Ni-catalyzed Heck reaction as it provides several important advantages:[2]

1) They are relatively cost-effective and stable to oxidative conditions.
2) A wide range of derivatives with different electronic and steric properties can be readily synthesized from a variety of commercially available pyridine derivatives and chiral amino alcohols.
3) They serve as good chiral analogues of bipyridine (bipy), which was used in our reaction optimization.
4) The nitrogen atom of the pyridine ring is relatively electron-poor and can facilitate a typically slow reductive elimination in Ni-catalyzed reactions.
5) The nitrogen atom of the oxazoline ring is relatively electron-rich due to p–π conjugation between the oxygen atom and the C=N bond. Thus, it can facilitate

oxidative addition. Alternatively, the C-sp^2 carbon is electron-deficient and can decrease the electron density of the adjacent pyridine ring.

6) Finally, the incorporation of chiral substituents on the oxazoline ring system significantly influences the activity of the ligand by establishing a chiral environment.

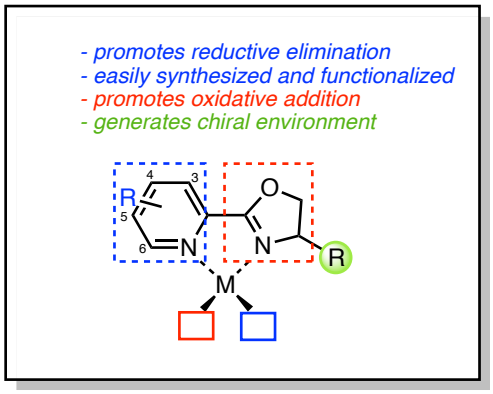

Figure 3.1 Analysis of pyridine-oxazoline-type ligands.

The results of our initial screening process did not provide optimal enantioselectivity values, however, we observed that *(S)*-*t*Bu-Pyox- and *(S)*-*t*Bu-iQuinox-type ligands were more enantioselective than other N- and P,N- chiral ligands. Therefore, subsequent studies were focused on these ligand types.

1.1 Screening of Commercially Available Chiral Ligands

We initiated a ligand screening process using *t*Bu-Pyox **L1** as a ligand. This led to the successful formation of the Heck product **2** in excellent yield but poor enantioselectivity (**Table 3.1**, **entry 1**). To address this issue and potentially enhance enantioselectivity, we conducted experiments at lower temperatures which, in theory, could amplify the small energy difference between the two diastereomeric complexes in an asymmetric catalytic reaction. Unfortunately, lowering the temperature to 60ºC had a negative impact on product yield and resulted in an increase in the amount of unwanted

protodebromination side product **2-1** (**entry 2**). We hypothesized that this could be due to a more significant difference in reactivity and a slower interconversion between the two atropisomers at lower temperatures, thereby making it more difficult to access the more efficient and enantioselective pathway.[8, 9]

Table 3.1 Screening of common N- and P,N- chiral ligands.

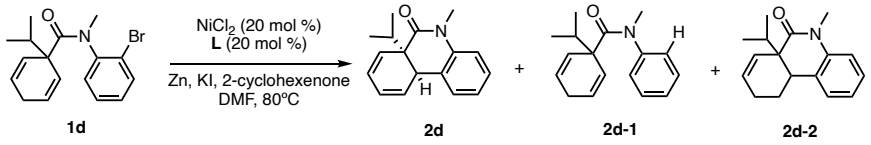

Commercially available ligands (**L1-18**)

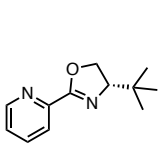

L1, *1:1 e.r.*

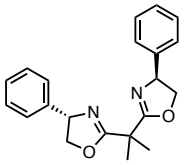

L2, *n.d.*

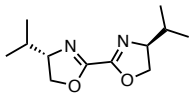

L3, *1:1 e.r.*

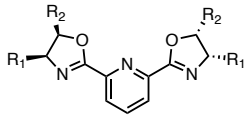

L4 (R_1 = *i*Pr, R_2 = H), *1:1 e.r.*
L5 (R_1 = Ph, R_2 = H), *2:1 e.r.*
L6 (R_1 = Bn, R_2 = H), *1:1 e.r.*
L7 (R_1 = *t*Bu, R_2 = H), *1:1 e.r.*
L8 (R_1 = Ph, R_2 = Ph), *1:1 e.r.*

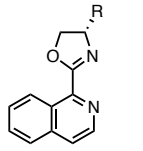

L9 (R = *t*Bu), *3:1 e.r.*
L10 (R = *i*Pr), *1:1 e.r.*

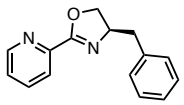

L11, *1:1 e.r.*

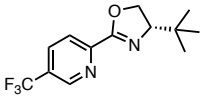

L12, *1:3 e.r.*

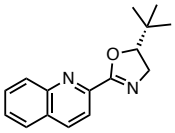

L13, *1:1 e.r.*

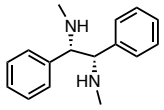

L14, *n.d.*

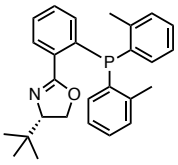

L15, *n.d.*

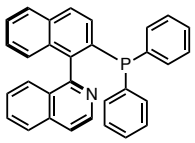

L16, *1:1 e.r.*

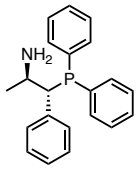

L17, *n.d.*

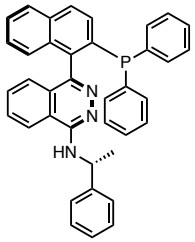

L18, *2:1 e.r.*

entry	Time	ligand	2(%)[a]	e.r.[b]	2-1(%)[a]	2-2(%)[a]
1	20 min	**L1**	94	1:1	-	6
2[c]	1.5 h	**L1**	62	1:1	33	5
3	24 h	**L2**	19	-	4	-
4	23 h	**L3**	48	1:1	9	43
5	1 h	**L4**	76	1:1	5	19
6	3 h	**L5**	72	2:1	25	3
7	3 h	**L6**	86	1:1	-	14
8	3 h	**L7**	100	1:1	-	-
9	3 h	**L8**	84	1:1	8	8
10	4 h	**L9**	71	3:1	14	15
11	24 h	**L10**	77	1:1	13	10
12	1 h	**L11**	84	1:1	10	6
13	2 d	**L12**	29	1:3	16	6
14	1.5 h	**L13**	69	1:1	12	19
15	24 h	**L14**	NR[d]	-	-	-
16	24 h	**L15**	NR	-	-	-
17	1.5 h	**L16**	77	1:1	5	18
18	24 h	**L17**	NR	-	-	-
19	24 h	**L18**	68	2:1	7	25

[a]Determined by GC analysis. [b]Determined by HPLC using a chiral stationary phase. [c]At 60 °C. [d]NR = no reaction.

The reaction employing box ligand **L2** did not go to completion and delivered the Heck product in very poor yield and undetermined enantioselectivity (**entry 3**). Likewise, the use of biox **L3** led to poor reaction efficiency and enantioselectivity (**entry 4**). These results suggest that the absence of the electron-deficient pyridine moiety could hinder the rate of reductive elimination.

Subsequently, we chose to explore tridentate pyridine-bis-oxazoline (Pybox) type ligands. The formation of a coordinatively saturated Ni-Pybox aryl halide complex could potentially enhance enantioselectivity by exerting more precise control over the steric environment around the nickel catalyst.[10] Conversely, the chelating nature of Pybox ligands that creates coordinative saturation can hinder β-hydride elimination.[3]

When we screened a selection of Pybox ligands **L4-8**, we observed good to excellent product yields (**entries 5-9**), suggesting that coordinative saturation around Ni does not affect the rate of the β-hydride elimination. Unfortunately, the enantioselectivities remained generally low, so we opted to explore alternative types of N- and P,N- chiral ligands.

Using isoquinoline derived ligand *i*Quinox **L9** with a bulky -*t*Bu chiral substituent on the oxazoline ring afforded the desired product in good yield and slightly improved enantioselectivity (**entry 10**). The isoquinoline ring has a similar effect to the substitution at the C-3 position on the pyridine ring (**Figure 3.1**). It has the potential to increase the dihedral angle with the oxazoline ring, which can influence catalytic activity and enantioselectivity. The isoquinoline may also exhibit stronger π–π interactions with the aryl ring on the substrate coordinated in the cis position compared to the pyridine ring. Alternatively, the presence of a less sterically demanding -*i*Pr chiral group in the *i*Quinox **L10** resulted in complete loss of e.r. achieved with **L9** (**entry 11**). When the -*t*Bu chiral substituent on the pyox ligand was replaced with a benzyl group in **L11**, the Heck product **2** was formed in very good yield, albeit giving poor enantioselectivity (**entry 12**). Thus, we concluded that the presence of a sterically bulky -*t*Bu group is necessary for chiral induction, and there appears to be no significant influence from a π - π interaction between the substrate and the aromatic substituent on the oxazoline ring.[2]

After establishing that Pyox ligands with the -*t*Bu substitution were more efficient and enantioselective than other types of N-ligands, we decided to explore whether having a functionalized pyridine ring could further improve the enantioselectivity. The ortho-hydrogen at the 6-position on the pyridine ring can form a non-classical hydrogen bond with the substrate group that coordinates to the metal in the cis position with pyridine, resulting in a stabilizing C6-H/π interaction (**Figure 3.2**).[11] Consequently, the presence of electron-withdrawing groups on the pyridine ring can increase the acidity of the ortho-hydrogen atom, resulting in a stronger hydrogen bond. These groups can also increase the

positive charge of the nickel cation and increase the electrophilicity of the group that coordinates with the metal at the trans position.[2, 4]

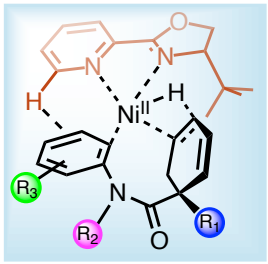

Figure 3.2 C6-H/π interaction during migratory insertion into nickel-*t*Bu-Pyox complex.

When the tBu-Pyox **L12**, featuring an electron-deficient CF_3 substituent at the C-5 position, was examined, we observed enhanced enantioselectivity. Unfortunately, the reaction was incomplete, yielding only 29% of the desired product (**entry 13**). Next, we wanted to investigate an ortho-substitution effect of Pyox ligands. The ortho-substituent can affect the asymmetric catalysis in two ways: 1) it can serve as a source of steric hindrance and push the bulky substrate or bulky group on the substrate to the cis position with oxazoline, creating site-selective coordination; 2) it may coordinate with the metal center via its C-H bond and block the trans coordination site of the oxazoline ring, placing the substrate in close proximity to the chiral substituent.[2] To introduce the ortho-substitution, the pyridine ring was replaced with a quinoline in **L13**, which provides a similar effect to having an ortho-substituent at the C-6 position of the pyridine ring. Unfortunately, the use of **L13** as a ligand did not afford the desired enantioselectivity (**entry 14**). Consequently, these preliminary results suggested that ortho-functionalization does not promote the enantioselectivity and the stabilizing C6-H/π interaction or favorable π- π interactions could influence the stereochemical outcome of the reaction.

These emerging trends were subjected to further investigation during the screening of a collection of synthesized Pyox- and *i*Quinox-type ligands.

Lastly, other categories of N- and P,N- chiral ligands were screened in a search of favorable enantioselectivity trends. Diamine **L14**, Phox **L15**, and aminophosphine **L17** classes of ligands were unreactive in our system (**entries 15-16**, **18**). Both Quinap **L16** and Pinap **L18** delivered the product in good yields, albeit low enantioselectivities.

3.2 Synthesis and Screening of Chiral *(S)-t*Bu-Pyox and *(S)-t*Bu-*i*Quinox Ligands

With less-than-optimal enantioselective results from commercially available bidentate and tridentate *N*- or P,*N*-ligands, we decided to pursue the synthesis and testing of novel functionalized *(S)-t*Bu-Pyox and *(S)-t*Bu-*i*Quinox ligands. A general procedure for the synthesis of (*S*)-tBu-Pyox ligands was adapted from Stoltz et al.[12] and is outlined in **Scheme 3.2**.

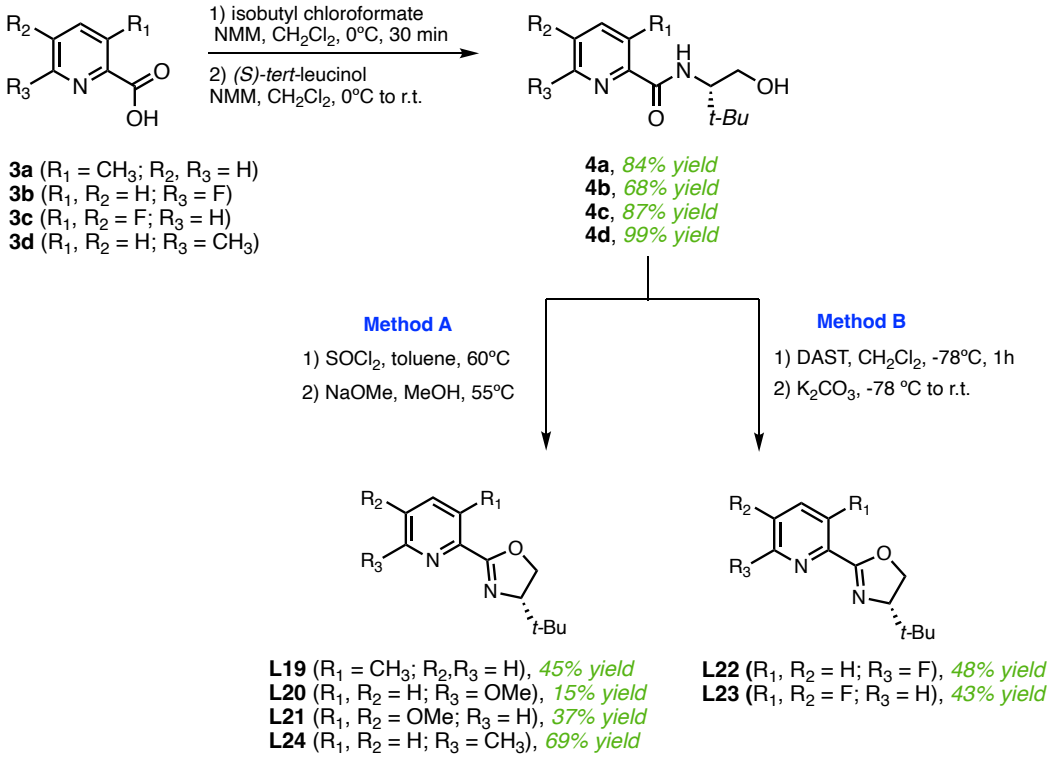

Scheme 3.2 Synthesis of functionalized (*S*)-tBu-Pyox ligands.

Since we observed the highest e.r. with the isoquinoline-containing ligand **L9**, we decided to start with the C-3 functionalization (R_1 = Me) of the pyridine ring that would have a similar effect to having the isoquinoline ring by increasing the dihedral angle between the pyridine ring and the oxazoline ring. The picolinic acid **3a** (R_1 = Me) was converted to the amide intermediate **4a** in very good yield via mixed anhydride formation with isobutyl chloroformate followed by the reaction with *(S)-tert*-leucinol (**Scheme 3.2**). The alcohol group of **4a** was converted to an alkyl chloride using thionyl chloride. The crude material was used in the next cyclization step (**Method A**) in the presence of sodium methoxide in methanol to afford **L19** in fair yield. When **L19** was tested with **1d**, the product was delivered in very good yield but with poor enantioselectivity (**Table 3.2**, **entry 1**).

Table 3.2 Screening of synthesized tBu-Pyox ligands.

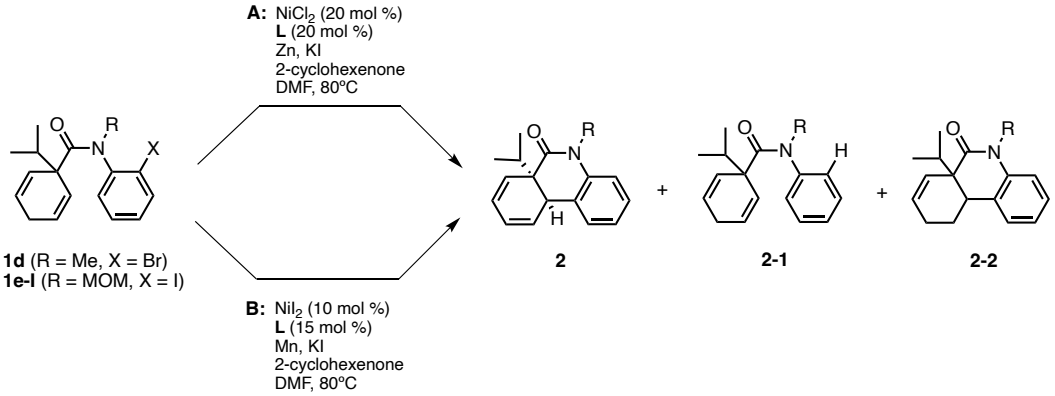

Synthesized ligands (**L19-30**):

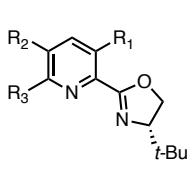

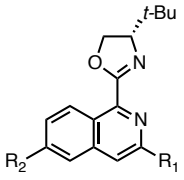

L19 (R_1 = CH_3; R_2, R_3 = H), *1:1 e.r.*
L20 (R_1, R_2 = H; R_3 = OMe), *1:1 e.r.*
L21 (R_1, R_2 = OMe; R_3 = H), *1:1 e.r.*
L22 (R_1, R_2 = H; R_3 = F), *1:1 e.r.*
L23 (R_1, R_2 = F; R_3 = H), *2:1 e.r.*
L24 (R_1, R_2 = H; R_3 = CH_3), *1:1 e.r.*

L25 (R_1 = CH_3, R_2 = H), *1:1 e.r.*
L26 (R_1 = H, R_2 = F), *9:1 e.r.*
L27 (R_1 = H, R_2 = CH_3), *11:1 e.r.*
L28 (R_1 = H, R_2 = *i*-Pr), *12:1 e.r.*
L29 (R_1 = H, R_2 = OMe), *9:1 e.r.*
L30 (R_1 = H, R_2 = CF_3), *13:1 e.r.*

entry	1	conditions	Time	ligand	2(%)[a]	e.r.[b]	2-1(%)[a]	2-2(%)[a]
1	**1d**	A	30 min	**L19**	85	1:1	10	5
2	**1d**	A	19 h	**L20**	89	1:1	4	7
3	**1d**	A	1 h	**L21**	85	1:1	9	6
4	**1d**	A	2 d	**L22**	14	1:1	4	-
5	**1d**	A	22 h	**L23**	81	2:1	19	-
6	**1d**	A	30 min	**L24**	94	1:1	-	6
7	**1d**	A	2.5 h	**L25**	100	1:1	-	-
8	**1e-I**	B	4 h	**L26**	95	9:1	2	3
9	**1e-I**	B	3 h	**L27**	94	11:1	1	5
10[c]	**1e-I**	B	22 h	**L27**	68	3:1	1	31
11	**1e-I**	B	1 h	**L28**	88	12:1	2	10
12	**1e-I**	B	3 h	**L29**	93	9:1	2	5
13	**1e-I**	B	24 h	**L30**	49	13:1	5	46

[a]Determined by GC analysis. [b]Determined by HPLC using a chiral stationary phase. [c]At 60 °C.

Following this, we decided to investigate the electronic properties of the pyridine ring derivatives, with a particular focus on the influence of electron-withdrawing groups (EWGs). Building upon our previous observations with **L12,** where a strong EWG group like the trifluoromethyl group (-CF_3) at the C-5 position of the pyridine ring resulted in a modest positive effect on enantioselectivity, yet slow and inefficient reaction, we decided to explore the influence of a weaker EWG, such as fluorine. We first attempted to functionalize the pyridine ring with fluorine substituents at the C-6 or the C-3 and C-4 positions. Using substrates **3b** (R_3 = F) and **3c** (R_1, R_2 = F) the amide intermediate **4b** and **4c** were synthesized in good to very good yields (**Scheme 3.2**). However, the subsequent cyclization step using Method A resulted in the formation of different *t*Bu-Pyox ligand **L20** and **L21**, respectively, featuring an electron-donating (EDG) methoxy group at the C-6, C-3, C4 positions. This unexpected outcome was attributed to a nucleophilic aromatic substitution involving the electron-deficient pyridine ring, with sodium methoxide acting as the nucleophile. When both **L20** and **L21** was used in the Heck reactions with the substrate **1d**, the Heck products were formed in very good yields. However, neither of them resulted in enantioselectivity and the use of **L20** led to prolonged reaction time (**Table 3.2**, **entries 2-3**).

Since the Stoltz's protocol (**Scheme 3.2**, **Method A**) failed to deliver the desired fluoro-substituted *t*Bu-Pyox ligands, we decided to use an alternative method for intermediates **4b** (R_3 = F) and **4c** (R_1, R_2 = F), which was adapted from Hickey et al. (**Scheme 3.2**, **Method B**).[13] This approach employs the use of a common fluorinating agent, diethylaminosulfur trifluoride (DAST), to fluorinate the alcohol group. The oxazoline ring was successfully formed upon the addition of potassium carbonate. Thus, we were able to synthesize **L22** and **L23** ligands with the functionalized fluoro-substitutions at the C-6, C-3, and C-4 positions in fair yields. When the ortho-fluoro-substituted **L22** was screened in the Heck reaction with substrate **1d**, the reaction did not go to completion, resulting in poor yield of the product and low enantioselectivity (**Table 3.2**, **entry 4**). Similarly, when the difluoro-substituted **L23** was employed, the enantioselectivity was low. Despite the extended reaction time, the reaction proceeded to completion, delivering the desired product in good yield (**entry 5**). The final functionalization of the pyridine ring involved the introduction of a methyl group at the C-6 position (R_3 = Me). **L24** was synthesized in good yield using Method A (**Scheme 3.2**). Interestingly, the Heck reaction rate was fast (30 min), delivering the 1,3-diene product in excellent yield, in contrast to the other two ortho-substituents (e.g. -OMe, F), which resulted in sluggish reactivity (**Table 3.2**, **entry 6** vs **2** and **5**). Consistent with our previous findings regarding ortho functionalization of the pyridine core, the enantioselectivity was not improved, which was presumably due to the lack of a stabilizing C6-H/π interaction or favorable π-stacking of the substrate aryl group and the pyridine ring.

Subsequently, our focus shifted to the functionalization of *(S)-t*Bu-iQuinox ligands (**Scheme 3.3**). This decision was driven by the fact that the highest enantioselectivity, while maintaining system reactivity, was achieved with **L9**, an unsubstituted version of *(S)-t*Bu-iQuinox (**Table 3.1**, **entry 10**). A general three-step procedure is summarized in Scheme 3.3. The first two steps of a regioselective cyanation of isoquinoline N-oxides were adapted from Sarmah and co-workers.[14] Their work highlights the dual role of trimethylsilyl cyanide, serving both as a source of nitrile and as an activating agent. The final step was inspired by the work of Pezzetta and co-workers.[15] In their method, they introduced zinc triflate to facilitate a Lewis acid catalyzed coupling of *(S)-tert*-leucinol with isoquinoline-1-carbonitrile and the subsequent cyclization of the oxazoline ring.

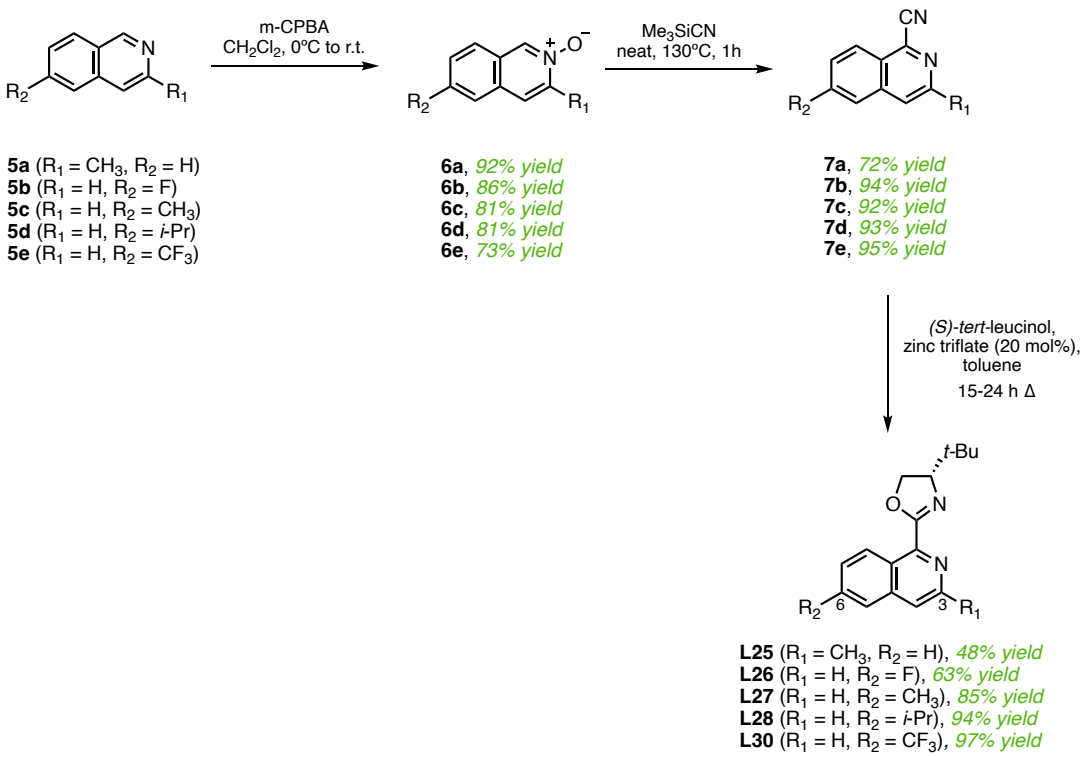

Scheme 3.3 Synthesis of functionalized (S)-tBu-iQuinox ligands.

The first functionalization of the isoquinoline ring involved the ortho-methyl-substitution to assess whether the lack of a C3-H/π interaction can have the same negative influence on enantioselectivity as the absence of the C6-H/π interaction of the pyridine ring with our Heck substrate. The N-oxidation of isoquinoline **5a** (R_1 = Me**)** with meta-chloroperoxybenzoic acid (mCPBA) resulted in the formation of the isoquinoline N-oxide derivative **6a** in excellent yield (**Scheme 3.3**). The substrate **6a** was taken forward to the cyanation reaction with trimethylsilyl cyanide at 130ºC for 1 h to afford the N-heteroaromatic nitrile **7a** in good yield. We were pleased to obtain **L25** after the final cyclization reaction in the presence of *(S)-tert*-leucinol and zinc triflate. The yield of **L25** was fair but lowed than reported by Pezzetta. The reaction did not proceed to completion and even after heating the reaction mixture under reflux for 48 h, 35% of the starting material **7a** was recovered after chromatographic purification. The most likely explanation of such poor reactivity was the presence of moisture in our zinc triflate. Moving forward, we started using a freshly opened bottle of zinc triflate and subjected the reagent to thorough drying under high vacuum at 90ºC for several hours before starting the reaction. When **L25** was tested with **1d**, the product **2d** was delivered in excellent yield, albeit significantly lower enantioselectivity than with the unsubstituted, commercially available *i*Quinox ligand **L9** (**Table 3.2, entry 7**). Therefore, we reached the conclusion that ortho-functionalization of the isoquinoline ring is detrimental to the enantioselectivity of our system.

Further functionalization of the isoquinoline ring was performed to investigate whether the improvement in enantioselectivity with **L9** was by the C3-H/π interaction with the aryl ring of the Heck substrate or by π-stacking of the substrate aryl group and

the isoquinoline ring (**Table 3.1**). Initially, we attempted to incorporate a fluorine substituent at the C-6 position to determine whether by increasing the acidity of the ortho-hydrogen, we can create a stronger C3-H/π interaction, leading to improved enantioselectivity.

Starting with isoquinoline **5b** (R_2 = F), both N-oxide **6b** and nitrile **7b** were obtained in very good yields. The final reaction delivered **L26** in good yield. To our delight, when **L26** was screened with MOM-protected aryl iodide **1e-I** under improved reaction conditions with 10 mol% of NiI_2 instead of 20 mol% of $NiCl_2$ and Mn in place of Zn, the Heck product was formed in excellent yield and the enantioselectivity was improved to 9:1 (**Table 3.2, entry 8**). Encouraged by this advance in enantioselectivity, we decided to further investigate substitution at the 6-position of the isoquinoline ring with the aim to identify a trend that would promote the enantioselectivity in our system.

Towards this effort, we synthesized a range of functionalized *(S)-t*Bu-iQuinox ligands with electron-donating and electron-withdrawing groups at the C-6 position and tested them with the Heck substrate **1e-I**. Using isoquinoline derivative **5c** (R_3 = Me), the methyl group at the 6-position of the isoquinoline ring was successfully incorporated to deliver **L27** in good yield (**Scheme 3.3**). Subsequent screening of **L27** resulted in an even further increase in enantioselectivity, with the enantiomeric ratio reaching to 11:1 (**Table 3.2**, **entry 9**). Again, lowering the temperature to 60ºC with **L27** resulted in much lower enantioselectivity (3:1 vs 11:1), longer reaction time (22 h vs 3 h) and an increase and in an increase in the amount of cyclized alkene side product 2-1. (**Table 3.2**, **entry 10**). Introducing a more sterically demanding -*i*Pr group at the C-6 position resulted in **L28**, which was formed in excellent yield (**Scheme 3.3**). The enantioselectivity with **L28** was

not significantly different than with the methyl-substituted **L27** (**Table 3.2**, **entry 11**). When *t*Bu-iQuinox was functionalized at C-6 position with a strong electron-donating methoxy group by a former undergraduate student, Yui Kosukegawa, the enantioselectivity was slightly decreased (**Table 3.2**, **entry 12**). Lastly, we decided to synthesize the trifluoromethyl-substituted (-CF_3) *(S)*-*t*Bu-*i*Quinox **L30** and test it in our Ni-catalyzed Heck reaction.

The synthesis of **L30** presented more challenges compared to the other *i*Quinox ligands. The main reason for this was the higher cost of 6-(trifluoromethyl)isoquinoline in comparison to the other isoquinoline derivatives we had previously used. Consequently, we designed our own two-step synthetic route to make this costly starting material from inexpensive and readily available 6-bromoisoquinoline **8e** (**Scheme 3.4**).

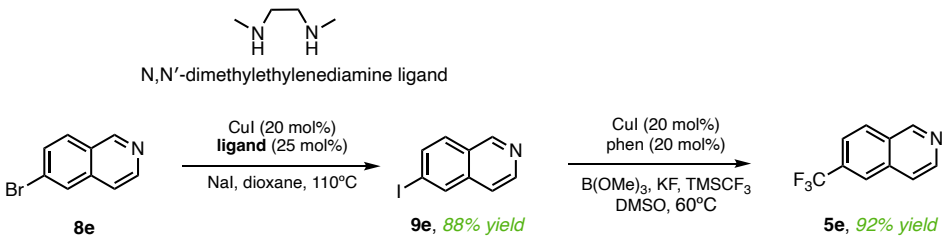

Scheme 3.4 Synthesis of 6-(trifluoromethyl)isoquinoline **5e**.

The first step in this sequence involves copper-catalyzed halogen exchange of isoquinoline bromide **8e** into the corresponding iodide **9e**. In general, preparation of functionalized aryl iodides can be difficult to accomplish.[16] One of the most common preparative methods is copper-catalyzed conversion of more available aryl bromides into aryl iodides. However, this process can be limited by the harsh reaction conditions that traditionally require high temperatures (>150 °C), polar solvents and excess of copper(I) iodide. In our own experience, a first attempt to carry out this transformation under the harsh conditions outlined in a patent protocol from Eli Lilly and Company proved

unsuccessful, yielding only 10% the desired product **9e**. (**Scheme 3.5**).[17] After prolonged heating for 7 days using a mineral oil bath set to 150°C, the reaction was still incomplete. While we were able to isolate the desired product **9e** in 57% yield, chromatographic purification proved to be difficult due to the similar size and polarity of **8e** and **9e**. Thus, we shifted our focus to searching for an alternative and milder method to accomplish this transformation.

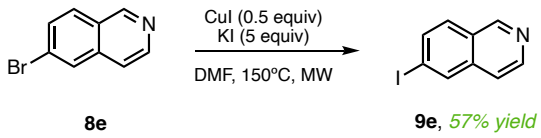

8e **9e**, *57% yield*

Scheme 3.5 Copper-catalyzed halogen exchange using harsh reaction conditions.

To this end, we were pleased to find the most optimal reaction conditions using the method reported by Klapars and Buchwald (**Scheme 3.4**).[16] According to their study, a high concentration of the halide salts in the solution inhibits the desired halogen exchange reaction by forming poorly reactive halocuprate complexes. Acceleration of the copper-catalyzed halogen exchange reaction was achieved by selecting the appropriate 1,2-diamine ligand and using sodium iodide in dioxane to maintain an optimal halide concentration. Using this method, we achieved 99% conversion of heteroaryl bromide **8e** to the corresponding heteroaryl iodide **9e**, which was isolated in good yield following column purification (**Scheme 3.4**).

The second step in our sequence to form 6-(trifluoromethyl)isoquinoline **5e** was adapted from Gonda and co-workers.[18] Their method describes copper-catalyzed trifluoromethylation of aromatic and heteroaromatic iodides with $TMSCF_3$ in the presence of trimethylborate ($B(OMe)_3$). The efficiency of this transformation was achieved by using $B(OMe)_3$ as the Lewis acid to reversibly quench the *in situ* generated

trifluoromethyl anion and prevent it from rapid decomposition before entering the relatively slow catalytic cycle with copper(I) iodide. Applying this strategy to substrate **9e**, we successfully obtained 6-(trifluoromethyl)isoquinoline **5e** in excellent yield (**Scheme 3.4**).

Following the general sequence for the synthesis of *i*Quinox ligands, **L30** was delivered in excellent yield (**Scheme 3.3**) and subsequently used in the Heck reaction with **1e-I** (**Table 3.2**, **entry 13**). Like the trifluoromethyl-substituted *t*Bu-Pyox **L12** used in our initial screening process (**Table 3.1**, **entry 13**), the use of **L30** led to slow reaction rate and a notable formation of cyclized alkene **2e-2**. While the enantioselectivity in the reaction was good (13:1), it was not significantly higher than with more efficient *(S)-t*Bu-*i*Quinox ligands (e.g., **L27**, **L28**). Therefore, we decided not to pursue further investigations with **L30**.

3.3 Conclusions

Unfortunately, the results of our initial screening process did not provide optimal levels of enantioselectivity to proceed with an evaluation of the substrate scope (**Table 3.1**). Nevertheless, it did offer valuable insights and led us in new directions focusing on *(S)-t*Bu-Pyox and *(S)-t*Bu-*i*Quinox chiral ligands. Due to the ease of synthesizing various derivatives with distinct electronic and steric properties, we embarked on the preparation and screening of novel functionalized Pyox and *i*Quinox ligands (**Table 3.2**). We had two remaining questions to investigate: 1) Does ortho-functionalization of the pyridine or isoquinoline ring have a negative effect on the enantioselectivity? 2) Which of the following interactions between the substrate aryl group and the isoquinoline or pyridine ring is more influential, the ortho-H/π or π-stacking?

Based on the screening of a collection of synthesized Pyox- and *i*Quinox-type ligands, we confirmed that ortho-functionalization does not promote the enantioselectivity. The initial assumption regarding the importance of ortho-H/π interactions was not supported by our findings since the enantioselectivity was not significantly improved in the presence of chiral ligands with more acidic ortho-hydrogens. Instead, we proposed that *i*Quinox-type ligands were more enantioselective than Pyox ligands, likely due to favorable π -stacking interactions. Subsequent computational studies supported these conclusions (see Chapter 5). Considering these results, we selected *(S)-t*Bu-*i*Quinox **L27** with a methyl-substituted C-6 position of the isoquinoline ring as the optimal ligand for achieving enantioselectivity without compromising the reactivity of our system.

3.4 References

1. Diccianni, J. B.; Diao, T. Mechanisms of Nickel-Catalyzed Cross-Coupling Reactions. *Trends in Chemistry* **2019**, *1* (9), 830–844.
2. Yang, G.; Zhang, W. Renaissance of pyridine-oxazolines as chiral ligands for asymmetric catalysis. *Chem. Soc. Rev.* **2018**, *47*, 1783–1810.
3. Hu, X. Nickel-catalyzed cross coupling of non-activated alkyl halides: a mechanistic perspective. *Chem. Sci.* **2011**, (10), 1867–1886.
4. Oliveira, C. C.; Pfaltz, A.; Correia, C. R. D. Quaternary Stereogenic Centers through Enantioselective Heck Arylation of Acyclic Olefins with Aryldiazonium Salts: Application in a Concise Synthesis of (R)-Verapamil. *Angew. Chemie - Int. Ed.* **2015** *54* (47), 14036–14039.
5. Chernyshev, V. M.; Ananikov, V. P. Nickel and Palladium Catalysis: Stronger Demand than Ever. *ACS Catal.* **2022**, *12* (2), 1180–1200.
6. (6) Diccianni, J.; Lin, Q.; Diao, T. Mechanisms of Nickel-Catalyzed Coupling Reactions and Applications in Alkene Functionalization. *Acc. Chem. Res.* **2020**, *53* (4), 906–919.
7. Connon, R.; Roche, B.; Rokade, B. V.; Guiry, P. J. Further Developments and Applications of Oxazoline-ContainingLigands in Asymmetric Catalysis. *Chem. Rev.* **2021**, *121* (11), 6373–6521.
8. Hosoi, S. O., M.Nakano, M.Arimitsu, K.Kajimoto, T.Kojima, N. Iwasaki, H. Miura, T.; Kimura, H.; Node, M.; Yamashita, M. Mechanistic aspects of asymmetric intramolecular Heck reaction involving dynamic kinetic

resolution: flexible conformation of the cyclohexenylidene -benzene system. *Tetrahedron* **2015** *71*, 2317–2326.
9. McDermott, M. C.; Stephenson, G. R.; Hughes, D. L.; Walkington , A. J. Intramolecular Asymmetric Heck Reactions: Evidence for Dynamic Kinetic Resolution Effects. *Org. Lett.* **2006** *8*(14), 2917–2920.
10. Babu, S. A.; Krishnan, K. K.; Ujwaldev, S. M.; Anilkumar, G. Applications of Pybox Complexes in Asymmetric Catalysis. *Asian J. Org. Chem.* **2018**, *7*, 1033–1053.
11. Dang, Y.; Shuanglin, Q.; Wang, Z.-X.; Wang , X. A Computational Mechanistic Study of an Unprecedented Heck-Type Relay Reaction: Insight into the Origins of Regio- and Enantioselectivities. *J. Am. Chem. Soc.* **2014** *136* (3), 986–998.
12. Stoltz, B. M.; Holder, J. C.; Shockley, S. E.; Wiesenfeldt, M. P.; Shimizu, H. Preparation of (S)- t*ert* -ButylPyOx and Palladium-catalyzed Asymmetric Conjugate Addition of Arylboronic Acids. *Organic Synth.* **2016**, *92*, 1–16.
13. Hickey, D. P.; Rhodes, C. S. Z.; Gensch, T.; Fries, L.; Sigman, M. S.; Minteer, S. D. Investigating the Role of Ligand Electronics on Stabilizing Electrocatalytically Relevant Low-Valent Co(I) Intermediates. *J. Am. Chem. Soc.* **2019**, *141* (3), 1382–1392.
14. Sarmah, B. K.; Konwar, M.; Bhattacharyya, D.; Adhikari, P.; Das, A. Regioselective Cyanation of Six-Membered N -Heteroaromatic Compounds Under Metal-, Activator-, Base- and Solvent-Free Conditions. *Adv. Synth. Catal.* **2019**, *361*, 5616–5625.
15. Pezzetta, C.; Bonifazi, D.; Davidson, R. W. M. Enantioselective Synthesis of N-Benzylic Heterocycles: A Nickel and Photoredox Dual Catalysis Approach. *Org. Lett.* **2019**, *21* (22), 8957–8961.
16. Klapars, A.; Buchwald, S. L. Copper-Catalyzed Halogen Exchange in Aryl Halides: An Aromatic Finkelstein Reaction. *J. Am. Chem. Soc.* **2002**, *124* (50), 14844–14845.
17. W., B. D.; P., B. T.; Decollo, R. V.; Godfrey, A. G.; Heap, C. R.; King, C.-H. R.; Li, H.-Y.; McMillen, W. T.; Sawyer, J. S.; Wang, Y. Novel compounds as pharmaceutical agents. United States 2004.
18. Gonda, Z.; Kovács, S.; Wéber, C.; Gáti, T.; Mészáros, A.; Kotschy, A.; Novák, Z. Efficient Copper-Catalyzed Trifluoromethylation of Aromatic andHeteroaromatic Iodides: The Beneficial Anchoring Effect of Borates. *Org. Lett.* **2014**, *16* (16), 4268–4271.

Chapter 4: Substrate Scope, Transformations of the Heck Products, and Biological Studies

4.1 Introduction

After establishing the optimal reaction conditions (**Table 2.4**, **entry 18**) and achieving the enantioselectivity with *(S)-t*Bu-*i*Quinox **L27** (**Table 3.2**, **entry 9**), we proceeded to evaluate the substrate scope of the enantioselective intramolecular Ni-catalyzed Heck reaction with variations at the quaternary center (R_1), the amide nitrogen (R_2), and the aryl halide (R_3) (**Table 4.1**).[1] We were pleased to find that a variety of aryl bromides and aryl iodides could undergo this Ni-catalyzed Heck cyclization to furnish the phenanthridinone derivatives in good to excellent yields with good enantioselectivities.

Moreover, most reactions were completed within 3 h, which is roughly 7 times faster than with the Pd catalyst. Both aryl halides **1** and **1-I** demonstrated compatibility with a simple achiral ligand such as bipy; however, aryl iodides **1-I** showed better reactivity when employing chiral ligand **L27**. The higher reactivity of aryl iodides is consistent with the weaker C−I bond being more susceptible to oxidative addition than the C−Br bond of the aryl bromides.[2] Oxidative addition is often the slowest step in cross-coupling reactions.[3] In addition, we believe it correlates to the complex nature of the iodide effect that seems to increase substrate reactivity.[4-6] Followed by the substrate scope, we also showed that the Heck products could be further transformed into molecules with potentially more viable drug-like properties.[7] Lastly, a variety of phenanthridinone derivatives were tested for cytotoxicity by our collaborators at the

Lankenau Institute of Medical Research and for anti-cancer activity by The National Cancer Institute 60.

4.2 Substrate Scope

Table 4.1 Substrate scope.[a]

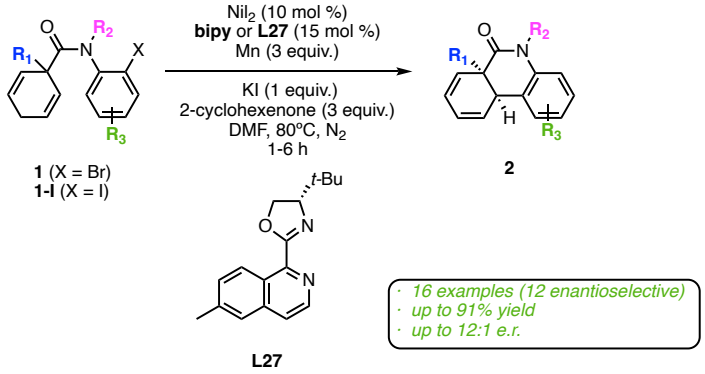

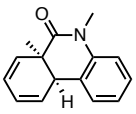

2a

bipy: 85%, from X = Br
bipy: 98%, from X = I
L27: 79%, 10:1 e.r., from X = I

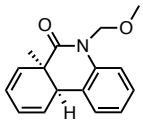

2b

bipy: 76%, from X = Br
bipy: 75%, from X = I
L27: 85%, 10:1 e.r., from X = I

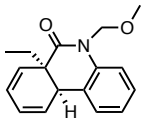

2c

bipy: 86%, from X = I
L27: 82%, 12:1 e.r., from X = I
L27: 1 mmol scale, 53%, 9:1 e.r.

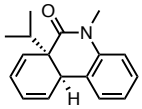

2d

bipy: 85%, from X = Br
bipy: 90%, from X = I
L27: 83%, 9:1 e.r., from X = I

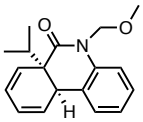

2e

bipy: 90%, from X = Br
bipy: 91%, from X = I
L27: 67%, 11:1 e.r., from X = I

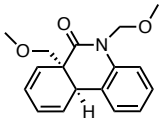

2f

bipy: 91%, from X = I
L27: 91%, 12:1 e.r., from X = I

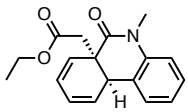

2g

bipy: 74%, from X = I
L27: 71%, 3:1 e.r., from X = I

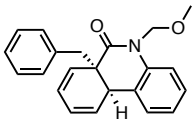

2h

bipy: 90%, from X = Br
bipy: 97%, from X = I
L27: 66%, 11:1 e.r., from X = I

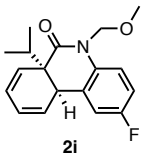

2i

bipy: 85%, from X = Br
bipy: 61%, from X = I
L27: 87%, 10:1 e.r., from X = I

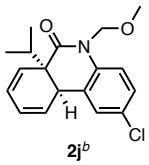

2j[b]

bipy: 67%, from X = Br
bipy: 91%, from X = I
L27: 68%, 7:1 e.r., from X = I

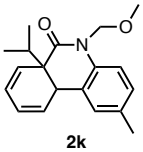

2k

bipy: 87%, from X = Br

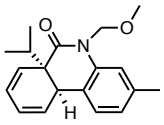

2l

bipy: 81%, from X = I
L27: 63%, 10:1 e.r., from X = I

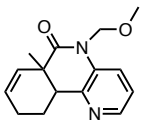

2m-2

bipy: 85%, from X = Br

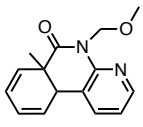

2n

bipy: 80%, from X = Br

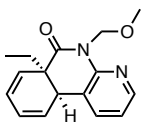

2o[c]

bipy: 76%, from X = Br
bipy: 82%, from X = I
L26: 76%, 7:1 e.r., from X = I

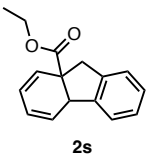

2s

bipy: 73%, from X = I

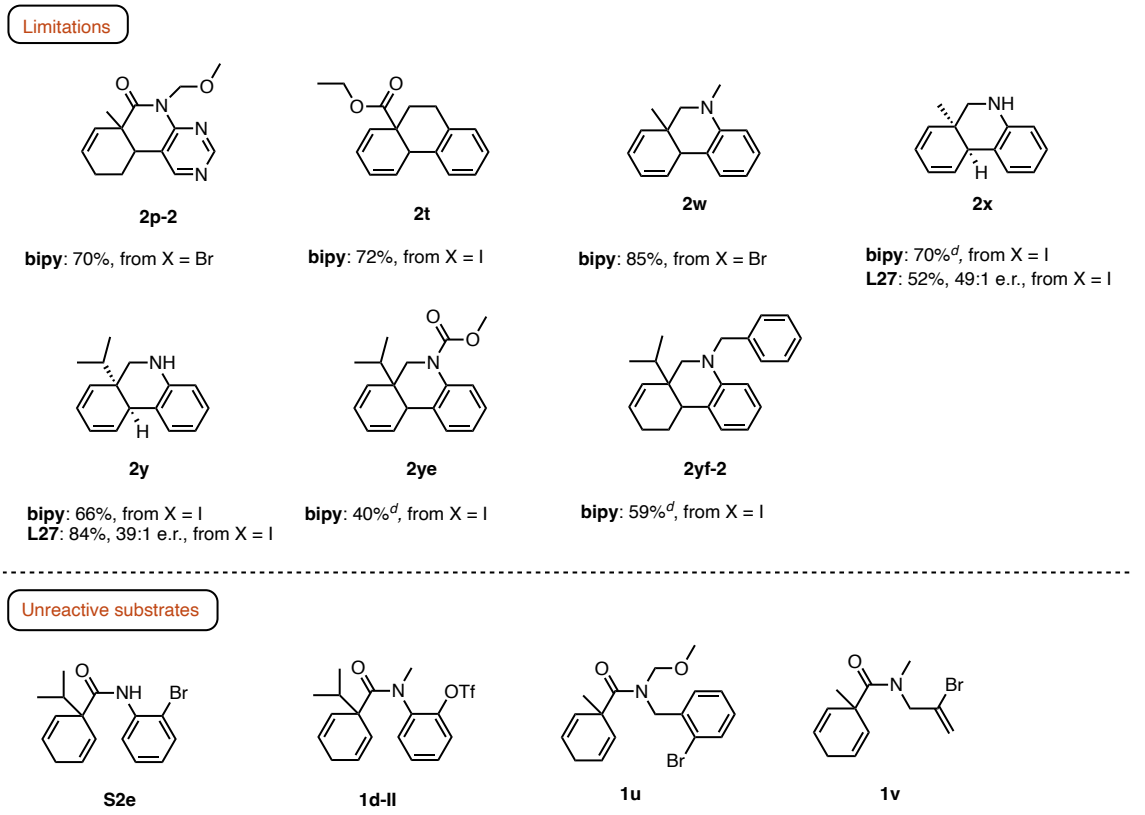

[a]Unless otherwise noted, the reaction of aryl halide **1** or **1-I** (1 equiv) was carried out with NiI_2 (10 mol %), bipy or **L27** (15 mol %), Mn (3 equiv), KI (1 equiv), 2-cyclohexenone (3 equiv), and DMF (0.08 M) at 80°C. The yield of **2** is the isolated yield. [b]At 65°C. [c]With **L26** (R = F). [d]Determined by GC analysis.

Our analysis of the substrate scope for the Ni-catalyzed enantioselective desymmetrizing intramolecular Heck reaction demonstrated that variations at the quaternary center (R_1), the amide nitrogen (R_2), and the aryl halide (R_3) were compatible with the reaction.[1] A range of alkyl (R_1) groups were well-tolerated and showed reactivity comparable to that of the analogous Pd version,[7] including methyl (**2a**, **2b**, **2m**, and **2n**), ethyl (**2c** and **2o**), and isopropyl (**2d**, **2e**, and **2i**–**l**) groups. A larger scale (1 mmol) enantioselective Heck reaction converting **1c-I** to **2c** demonstrated a slight reduction in reaction yield and a modest decrease in enantioselectivity. We were particularly delighted to achieve higher enantioselectivity for the isopropyl (**2e**) derivative (11:1) than with our previous Pd-catalyzed method (7:1). Functional groups such as ether (**2f**) and ester (**2g** and **2s**) and large benzyl groups (**2h**) were generally well-

tolerated. As with the Pd catalyst report,[7] only tertiary amides (R_2 = Me or MOM) were successful in this intramolecular Heck reaction. The reaction with the secondary amide **S2e** afforded a mixture of the starting material and a side product resulting from protodebromination. Our previous experimental work with palladium[7] suggested the secondary amides experience an *ortho* effect[8-11] in which the carbonyl group chelates to the metal, forming a stable complex that is resistant to catalysis. It was proposed to be due to an intramolecular reaction that forms a six-member ring chelation between the amide oxygen and the metal (Pd or Ni) after the oxidative addition. The evidence supporting this intramolecular phenomenon was obtained when the addition of acetanilide (Ph-NHAc, 1 equiv) had no impact on the reaction outcome, indicating that the secondary amide needs to be part of the actual substrate structure.[7] In contrast, tertiary amides are less prone to experience stabilization from the carbonyl oxygen due to steric hindrance created by the nitrogen substituent.

Next, we examined aryl halide substitution (R_3) and found a variety of aryl ring substituents were tolerated, including the 4-F, 4-Cl, 4-Me, and 5-Me derivatives (**2i–l**, respectively). The formation of a protodechlorinated side product was observed with the chloro analogue (**2j**) in 22% yield for X = Br, which results from oxidative addition of nickel into the C–Cl bond. Formation of this side product was decreased by decreasing the reaction temperature to 65°C. When X = Br for **2j**, a 67% yield was obtained at the lower temperature, and when X = I for **2j**, a 91% yield was achieved. The higher yield of the iodo derivative is likely due to the greater difference in reactivity of the Ar–I and Ar–Cl bonds versus the Ar–Br and Ar–Cl bonds. The enantiomeric ratio for **2j** was

lower, but a similar lower enantiomeric ratio was seen in our studies of the same enantioselective desymmetrizing Heck reaction with palladium.[7]

Noteworthy was the tolerance of pyridine rings, which afforded **2m−o** derivatives in very good yields, albeit with lower er (**2o**). Interestingly, pyridine bromide **1m** delivered exclusively the cyclized alkene product (**2m-2**). We speculate this may be the result of the initial 1,3-diene product isomerizing to the 1,4-diene product and the resulting conjugation with the pyridine ring promoting reduction with the Ni−H complex before reaction with the cyclohexenone sacrificial alkene. It must be noted that, in our phenanthridinone substrate, the presence of heterocyclic rings was not compatible with the Pd-catalyzed conditions,[7] thereby illustrating another benefit of the Ni-catalyzed Heck version. Although enantioselectivity was not studied with bromopyridine derivatives **2m-2** and **2n**, iodopyridine **2o** afforded higher enantioselectivity with **L26** (R = F) than with **L27** (7:1 vs 4:1). Unfortunately, the compatibility with pyrimidine rings was limited, resulting mainly in the formation of the cyclized alkene product (**2p-2**), which proved challenging to separate from the mixture of other side-products. Due to the challenges involved in synthesizing pyrimidine-based tertiary amides, we made the decision not to pursue further investigations into the reactivity of this substrate.

Following this, we proceeded to explore the reactivity of carbocyclic ring systems. The 6-5-6 system **2s** was efficiently formed in good yield. However, lower tolerance was observed for the 6-6-6 carbocyclic system **2t**, leading to the significant formation of cyclized alkene isomers that could not be separated from the diene product **2t**. Unlike with the Pd-catalyzed conditions, aryl triflate **1d-II** was completely unreactive in the Ni-catalyzed Heck reaction.

Next, we employed the Heck substrate **1u** to investigate the potential of using nickel to create a 6-7-6 heterocyclic ring system. Regrettably, we only obtained the protodehalogenated side-product **2u-1** in this case. We also explored the possibility of generating a 6-6 bicyclic system with vinyl bromide **1v**. Interestingly, Ni catalyst promoted the dimerization of vinyl bromide **1v**, rather than catalyzing the intramolecular cyclization. Even when the reaction was conducted at a more dilute concentration (in DMF, 0.008 M vs. 0.08 M) to promote intramolecular transformation, it still did not yield the desired bicyclic product.

Finally, the reactivity of amine substrates was evaluated. Gratifyingly, both secondary and tertiary amines successfully underwent the intramolecular cyclization with the nickel catalyst, affording **2w, 2x, 2y**, **2ye** and **2yf-2** in fair to good yields, albeit with higher formation of unwanted side-products, which complicated chromatographic purification and isolation of the desired product. The tertiary N-methyl carbamate-protected amine **1ye-I** and N-benzyl amine **1yf-I** had lower reactivity compared to the tertiary N-methyl amine **1w**. Specifically, the methyl carbamate protecting group resulted in much lower reactivity and led to significant formation of protodehalogenated side product **2ye-1** (>40%) in addition to the desired 1,3-diene product **2ye**. The N-benzyl amine **1yf-I** delivered a complex mixture of cyclized alkene isomers **2yf-2**. While enantioselectivity was not studied for the tertiary amines, a significant improvement in enantioselectivity was observed with the secondary amines **2x** and **2y**. This observation suggests that the elimination of atropisomerism can lead to improved stereoselectivity in the Ni-catalyzed Heck reaction. Additionally, the reactivity of amines further supported the *ortho* effect that limits the reactivity of secondary amides. In the case of secondary

and tertiary amines, the oxidative addition Ni-complex is not subject to additional stabilization from the carbonyl oxygen, allowing for facile intramolecular cyclization to take place.

4.3 Transformations of the Heck Products

Focusing on expanding the potential drug-like molecules derived from the Heck product, we subjected the 1,3-diene products to a series of further transformations (**Scheme 4.1**).

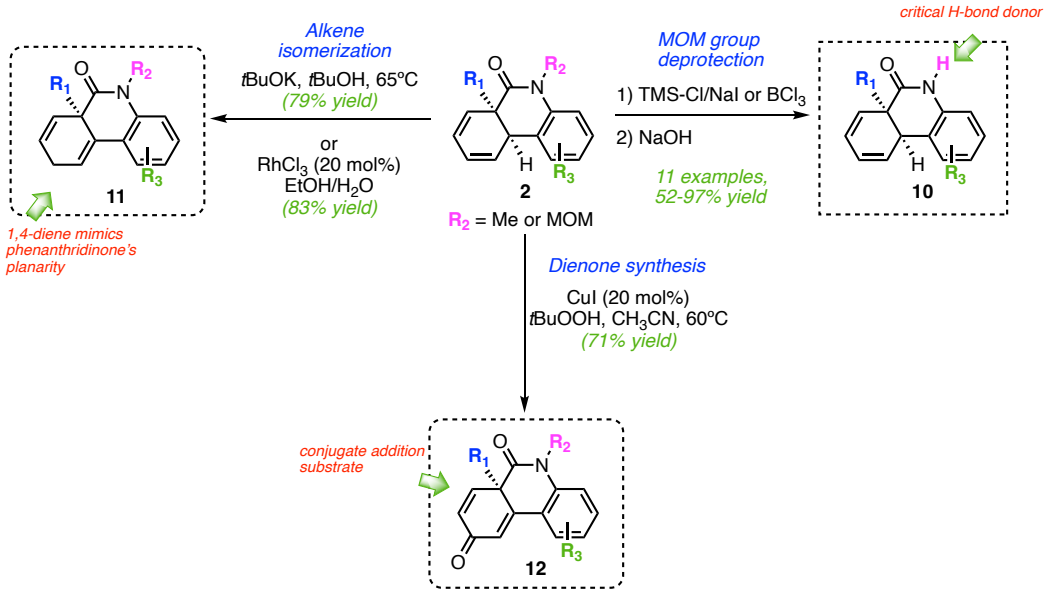

Scheme 4.1 Transformations of the Heck products.

Prior efforts in our group to cleave the N-methyl amide and yield a secondary amide were not successful.[7] Nonetheless, removal of the MOM amide protecting group facilitated the conversion of the tertiary amide **2** into a secondary amide **10**, which can potentially act as a critical hydrogen bond donor for interactions with target proteins and nucleic acids. The cis ring junction of the 1,3-diene Heck products have a convex shape, which stands in sharp contrast to the planar structure of phenanthridinone. This observation has been confirmed by molecular modeling. We carried out two

transformations of the 1,3-diene **2** to generate analogues that replicate the planar structure of phenanthridinone while preserving the quaternary center: 1) alkene isomerization to a planar 1,4-diene **11**; 2) oxidation to dienone **12**, a potential substrate for covalent inhibition through conjugate addition.

Removal of the MOM amide protecting group was achieved with TMS-I[12] generated in situ for most Heck products **10a-k** (**Table 4.2**, **entries 1-8**), except for pyridine analogues **10m-o** for which BCl_3 was used to deprotect the MOM group (**entries 9-11**). The yields for this reaction ranged from 52-97%.

Table 4.2 MOM Group Deprotection.

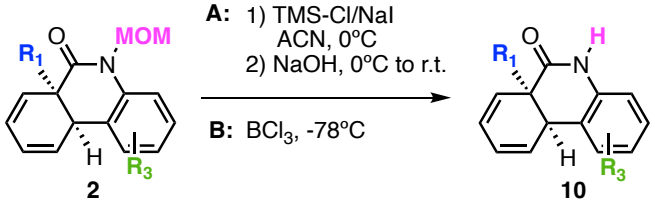

entry	R_1	R_3	conditions	yield (%)	compound
1	Me, **2b**	H	A	81	**10b**
2	Et, **2c**	H	A	82	**10c**
3	*i*-Pr, **2e**	H	A	81	**10e**
4	MOM, **2f**	H	A	97	**10f**
5	Bn, **2h**	H	A	71	**10h**
6	*i*-Pr, **2i**	2-F	A	52	**10i**
7	*i*-Pr, **2j**	2-Cl	A	62	**10j**
8	*i*-Pr, **2k**	2-Me	A	85	**10k**
9	Me, **2m-2**	C_1=N	B	63	**10m-2**
10	Me, **2n**	C_4=N	B	73	**10n**
11	Et, **2o**	C_4=N	B	79	**10o**

To identify the optimal conditions for alkene isomerization, we used the methyl derivative **2a**. After subjecting **2a** to the basic conditions derived from *tert*-butoxide (6 equiv) and water (2 equiv) in ether,[13] no isomerization of the 1,3-diene was observed (**Table 4.3**, **entry 1**). However, by following a slightly modified procedure by Ringold and Malhotra[14] for the deconjugation of α,β-unsaturated ketones, we managed to achieve

the isomerization and isolate the 1,4-diene product **11a** in very good yield (**entry 2**). Alternatively, the $RhCl_3$-mediated isomerization method[15] demonstrated comparable efficiency in delivering **11a** (**entry 3**).

Table 4.3 Alkene Isomerization.

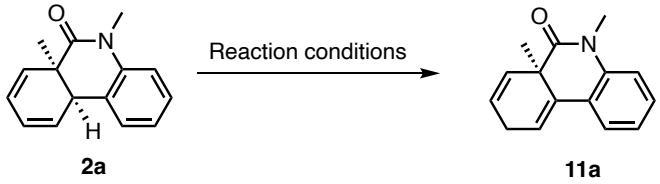

entry	conditions	product yield (%)[a]
1	*t*-BuOK, H_2O, diethyl ether, r.t.	NR[b]
2	*t*-BuOK, *t*-BuOH, 65°C	79
3	$RhCl_3$ (20 mol%), EtOH/H_2O (10:1), 65°C	83

[a]Isolated yield. [b]NR = no reaction.

Our initial approach to synthesize the 2,5-cyclohexadienone **12** via allylic oxidation of the 1,3-diene **2a** using pyridinium dichromate (PDC) and *tert*-butyl hydroperoxide (*t*-BuOOH) resulted in an inseparable mixture of enone and dienone products (**Scheme 4.2**, **Part I**, **method A**).

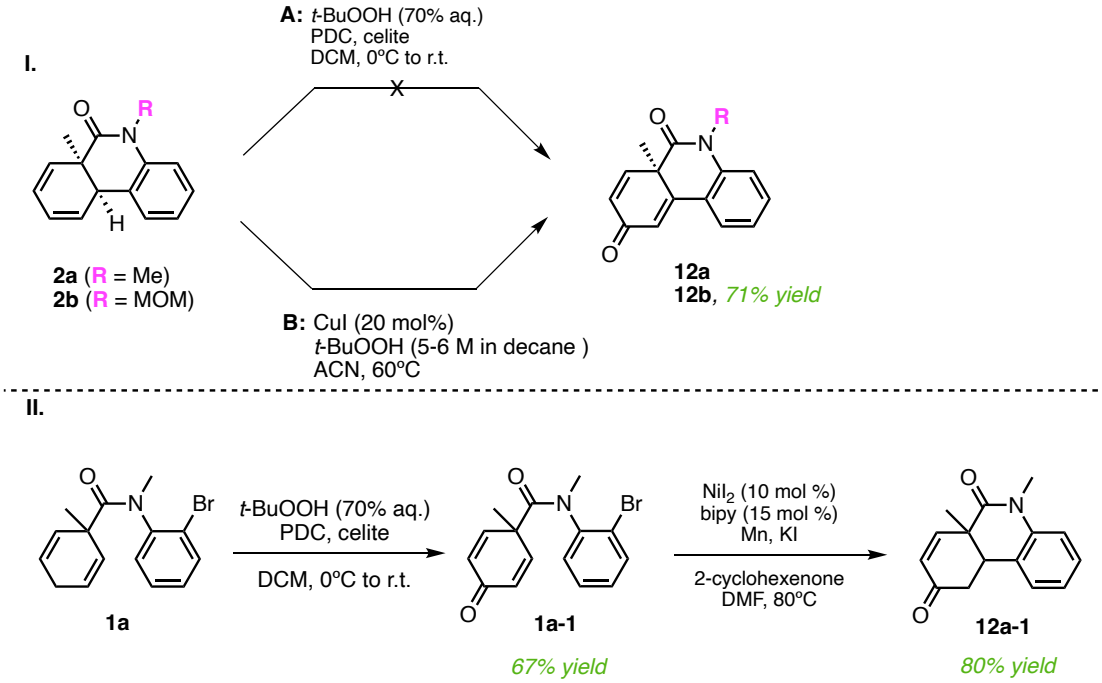

Scheme 4.2 Dienone synthesis.

Therefore, we decided to pursue an alternative route to access the dienone system **12** (**Scheme 4.2**, **Part I**). This involved initially subjecting the tertiary amide **1a** to the oxidation conditions with PDC/*t*-BuOOH and subsequently using the resulting dienone substrate **1a-1** for the Ni-catalyzed the Heck reaction. However, this alternative synthetic pathway delivered exclusively the cyclized enone system **12a-1**.

The second method for allylic oxidation of the 1,3-diene Heck product was adapted from Dr. Krasley's previous research on the development of an intramolecular oxidative Heck-type C-H activation of dienone systems.[16] We were pleased to discover that by using catalytic (20 mol%) CuI, an excess of *t*BuOOH, and heating the reaction at 65°C, we successfully synthesized dienone **12b** in good yield from the Heck product **2b** (**Scheme 4.2**, **Part II**).

4.4 Biological Evaluation of Phenanthridinone Derivatives

A wide selection of thirty-four phenanthridinone derivatives synthesized by the Malachowski group members was evaluated for cytotoxicity by our biological collaborators at the Lankenau Institute of Medical Research (LIMR). Two human cell lines were employed in this study: WI-38, a diploid human cell line composed of fibroblasts derived from lung tissue, which served as the normal cell line; and MCF-7, a breast cancer cell line. The compounds were screened using the Sulforhodamine B (SRB) assay.[17] Unfortunately, out of the 34 compounds submitted, only four compounds (13, 14, 16, 33) induced cell death (**Table 4.4**). Our collaborators at LIMR were also unable to successfully conduct the PARP assay on the most potent compounds from their initial screen.

Table 4.4 Cytotoxicity screening.[a, b]

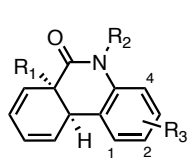

2j, 10e, 10i

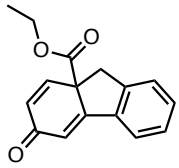

12s

compd	R_1	R_2	R_3	EC_{50} (μM)	
				MCF-7	**WI-38**
13	*i*-Pr, **2j**	MOM	2-Cl	53.70	120.5
14	*i*-Pr, **10e**	H	H	35.55	104.5
16	*i*-Pr, **10i**	H	2-F	35.66	68.63
33	CO_2Et, **12s** dienone	6-5-6	H	7.687	27.82

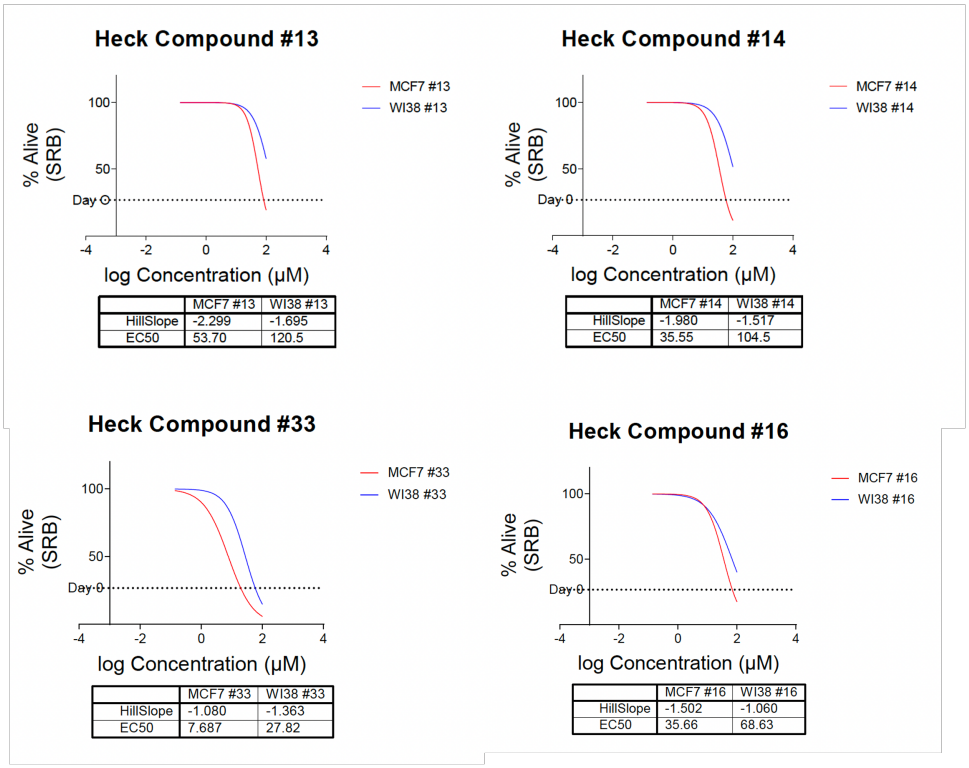

[a]SRB assay, WI-38 and MCF-7 human cell lines, 48 h incubation. [b]Day 0 corresponds to the optical density (OD) when the cells were incubated.

Following the cytotoxicity studies, we submitted 10 additional compounds for evaluation in the National Cancer Institute 60 (NCI-60) cell line screen to assess their anti-cancer activity.[18] Unfortunately, none of these compounds advanced to further testing as they displayed insufficient activity in the initial screening process. In fact, it was observed that certain compounds seemed to marginally stimulate cancer activity.

4.5 Conclusions

In summary, we evaluated the substrate scope of the enantioselective intramolecular Ni-catalyzed Heck reaction with variations at the quaternary center (R_1), the amide nitrogen (R_2), and the aryl halide (R_3). A wide range of substates worked in good to excellent yields and good enantioselectivities comparable to that of the analogous Pd version. This method allowed us to achieve higher enantioselectivity for the isopropyl derivatives, which was one of the primary objectives of this project. While pyridine rings were found to be compatible, pyrimidine rings showed limited reactivity. Lower tolerance was also observed for the 6-6-6 carbocyclic system and for both secondary and tertiary amines. Interestingly, the use of secondary amines led to a substantial improvement in enantioselectivity in the Ni-catalyzed Heck reaction, likely attributed to the absence of atropisomerism. The lack of reactivity with the secondary amides due to the ortho effect was consistent with our findings with palladium. Additionally, efforts to create the 6-7-6 and 6-6 ring systems were unsuccessful.

Removal of the MOM amide protecting group was achieved with TMS-I generated in situ for most Heck products, except for pyridine analogues for which BCl_3 was used to deprotect the MOM group. Alkene isomerization of the 1,3-diene to a planar 1,4-diene was achieved under either basic (*t*-BuOK/*t*-BuOH) or transition-metal-catalyzed ($RhCl_3$) conditions. Oxidation of the 1,3-diene with CuI (cat.)/*t*-BuOOH afforded the 2,5-cyclohexadienone, a potentially valuable conjugate addition substrate. Unfortunately, the results of the biological studies showed that the phenanthridinone derivatives do not exhibit significant cytotoxicity or anti-cancer activity.

4.6 References

1. Rachii, D.; Caldwell, D. J.; Kosukegawa, Y.; Sexton, M.; Rablen, P.; Malachowski, W. P. Ni-Catalyzed Enantioselective Intramolecular Mizoroki–Heck Reaction for the Synthesis of Phenanthridinone Derivatives. *J. Org. Chem.* **2023**, *88* (13), 8203–8226.
2. Anjali, B. A.; Suresh, C. H. Interpreting Oxidative Addition of Ph–X (X = CH 3 , F, Cl, and Br) to Monoligated Pd(0) Catalysts Using Molecular Electrostatic Potential. *ACS Omega* **2017**, *2* (8), 4196–4206.
3. Labinger, J. A. Tutorial on Oxidative Addition. *Organometallics* **2015**, *34*, 4784−4795.
4. Maitlis, P. M.; Haynes, A.; James, B. R.; Catellani, M.; Chiusoli, G. P. Iodide effects in transition metal catalyzed reactions. *Dalton Trans.* **2004**, 3409–3419.
5. Wang, K.; Ding, Z.; Zhou, Z.; Kong, W. Ni-Catalyzed Enantioselective Reductive Diarylation of Activated Alkenes by Domino Cyclization/Cross-Coupling. *J. Am. Chem. Soc.* **2018**, *140* (39), 12364–12368.
6. Colon, I.; Kelsey, D. R. Coupling of aryl chlorides by nickel and reducing metals. *J. Org. Chem.* **1986**, *51* (14), 2627–2637.
7. Sexton, M.; Malachowski, W. P.; A., G. Y. P.; Rachii, D.; Feldman, G.; Krasley, A.; Chen, Z.; Tran, M.; Wiley, K.; Matei, A.; et al. Catalytic Enantioselective Birch−Heck Sequence for the Synthesis of Phenanthridinone Derivatives with an All-Carbon Quaternary Stereocenter. *J. Org. Chem.* **2022**, *87* (2), 1154–1172.
8. Marchese, A. D.; Kersting, L. L., M. Diastereoselective Nickel-Catalyzed Carboiodination Generating Six-Membered Nitrogen-Based Heterocycles. *Org. Lett.* **2019**, *21* (17), 7163–7168.
9. Mohadjer Beromi, M.; Nova, A.; Balcells, D.; Brasacchio, A. M.; Brudvig, G. W.; Guard, L. M.; Hazari, N.; Vinyard, D. J. Mechanistic Study of an Improved Ni Precatalyst for Suzuki–Miyaura Reactions of Aryl Sulfamates: Understanding the Role of Ni(I) Species. *J. Am. Chem. Soc.* **2017**, *139* (2), 922–936.
10. Bajo, S.; Laidlaw, G.; Kennedy, A. R.; Sproules, S.; Nelson, D. J. Oxidative Addition of Aryl Electrophiles to a Prototypical Nickel(0) Complex: Mechanism and Structure/Reactivity Relationships. *Organometallics* **2017**, *36* (8), 1662–1672.
11. Wada, M.; Kusabe, K.; Oguro, K. Aryl(pentachlorophenyl)nickel(II) complexes. Lack of free rotation about tolyl-nickel bonds and lack of ″ortho effect″ in carbonylation. *Inorg. Chem.* **1977**, *16* (2), 446–449.
12. Fukuyama, T.; Liu, G. Stereocontrolled Total Synthesis of (±)-Gelsemine. *J. Am. Chem. Soc.* **1996**, *118*, 7426–7427.
13. Gassman, P. G.; Hodgson, P. K. G.; Balchunis, R. J. Base-promoted hydrolysis of amides at ambient temperatures. *J. Am. Chem. Soc.* **1976**, *98* (5), 1275–1276.
14. Ringold, H. J.; Malhotra, S. K. Deconjugation of α,β-unsaturated ketones. *Tetrahedron Lett.* **1962**, *3* (15), 669–672.

15. Taniguchi, T.; Tanabe, G.; Muraoka, O.; Hiroyuki, I. Total Synthesis of (±)-Stemonamide and (±)-Isostemonamide Using a Radical Cascade. *Org. Lett.* **2008**, *10* (2), 197–199.
16. Krasley, A. T. Exploration of Synthetic Pathways to Quaternary Carbon Stereocenters and Fused Ring Systems via Birch Reductions. Bryn Mawr College, Scholarship, Research, and Creative Work at Bryn Mawr College, **2017**
17. Skehan, P.; Storeng, R.; Scudiero, D.; Monks, A.; McMahon, J.; Vistica, D.; Warren, J. T.; Bokesch, H.; Kenney, S.; Boyd, M. R. New Colorimetric Cytotoxicity Assay for Anticancer-Drug Screening. *J Natl Cancer Inst* **1990**, *82* (13), 1107–1112.
18. *Cell Lines in the In Vitro Screen.* National Cancer Institute, 2015. https://dtp.cancer.gov/discovery_development/nci-60/cell_list.htm (accessed 2023 October 23).

Chapter 5: Alternative Heck-type Transformations, Mechanistic and Computational Studies

5.1 Introduction

The distinctive characteristics of Ni catalysts provide opportunities for a wide array of mechanisms in cross-coupling reactions. Given the ability of Ni to adopt a range of oxidation states, spanning from Ni(0) to Ni(IV), both single-electron and two-electron pathways can be mediated through different types of Ni intermediates.[1]

In this chapter, we initially investigated the possibility of accessing different modes of reactivity with Ni for our Heck substrates. This includes explorations of alkene dicarbofunctionalization and oxidative Heck-type reactions. We also performed mechanistic studies to gain insights into the traditional intramolecular Ni-catalyzed reaction relevant to our system, which leads to the formation of 1,3-diene phenanthridinone analogues. Our mechanistic investigations, which included exploring the possibility of a radical pathway and examining the roles of the reducing metal and the sacrificial alkene, contributed to the proposal of a plausible mechanism for this traditional Ni-catalyzed reaction. To better understand the factors governing enantioselectivity in the catalytic cycle, we collaborated with a computational chemist from Swarthmore College, Prof. Paul Rablen, to conduct a computational analysis of the critical 1,2-migratory insertion step.

5.2 1,2-Dicarbofunctionalization of alkenes

Transition-metal-catalyzed 1,2-dicarbofunctionalization of alkenes, which combines a domino cyclization and cross-coupling process, has become a robust technique for accessing a diverse range of cyclic compounds fused with benzene rings.[2, 3] This method involves coupling tethered alkenes to a range of simple and readily available electrophiles (e.g., organohalides and triflates) or nucleophiles (e.g., organometallic reagents). In particular, the field of nickel-catalyzed alkene difunctionalization is currently experiencing rapid advancements.[1, 4-6] This progress is driven by the higher tendency of nickel-alkyl intermediates to undergo cross-coupling with another electrophile or nucleophile compared to that observed in palladium-catalyzed reactions due to the intrinsically slower β-H elimination rate with nickel. In the nickel-catalyzed alkene difunctionalization reaction, two distinct mechanisms are possible: a classic two-electron pathway and a radical pathway.[7, 8]In the two-electron pathway, reactions are initiated by transmetalation of a nucleophile or oxidation addition of a C(sp^2) electrophile to afford organometallic nickel species that can undergo migratory insertion with an alkene. Ni-catalyzed alkene-functionalization via a radical mechanism involves the formation of radicals from C(sp^3) electrophiles. Both redox-neutral and reductive approaches have been widely utilized in this transformation.[3] Redox-neutral dicarbofunctionalization necessitates the use of an electrophile and a nucleophile, whereas reductive dicarbofunctionalization occurs in the presence of two electrophiles and requires the use of reductants. Reductive difunctionalization is considered a cost-effective method as it prevents the use of expensive and air-sensitive stoichiometric organometallic reagents.[8-10] In particular, the Ni-catalyzed enantioselective reductive

dicarbofunctionalization of alkenes represents a valuable strategy for the rapid synthesis of important (hetero)cyclic structures commonly present in bioactive compounds.[11] However, the developed methods are primarily limited to the use of terminal alkenes that are tethered to an electrophile.[4] Working with internal alkenes poses a distinctive challenge for nickel-catalyzed reductive difunctionalization due to the lower reactivity and affinity of the internal alkene for nickel that frequently hinder migratory insertion step. Additionally, the tendency of acyclic 1,2-disubstituted alkenes to undergo β-hydride elimination often leads to the formation of Heck side-products.[12] Another complicating factor is the homolytic nature of the alkylnickel intermediate, which can give rise to issues related to diastereoselectivity. As a result, there have been significantly fewer reports on the difunctionalization of internal alkenes.[11, 13-15] To help address this deficiency, we endeavored to investigate the feasibility of dicarbofunctionalizing one of the internal alkenes present in our Heck substrate.

Initially, we explored the use of diethylzinc (Et_2Zn) as a nucleophile in a redox-neutral dicarbofunctionalization of tertiary amide **1d** (**Scheme 5.1**, **eq 1**). The dialkylzinc reagents have been previously reported[3] for both intramolecular[16, 17] and intermolecular[15, 18] 1,2-difunctionalization. By adding excess of Et_2Zn (6 equiv), we envisioned to difunctionalize one of the internal alkenes, forming the arylalkylated product **13d-1**. Given that diethylzinc is known to act as a stoichiometric reducing agent,[19, 20] we hypothesized that it can reduce the Ni(II) precatalyst to Ni(0). This catalytically active Ni(0) species would initiate oxidative addition with the aryl bromide, followed by migratory insertion into the alkene. At this stage, we proposed that Et_2Zn might intercept the Ni(II) alkyl intermediate through a transmetalation event and generate the desired

product via C(sp^3)–C(sp^3) reductive elimination.[18] Unfortunately, the use of Et_2Zn for the formation of the difunctionalized alkene product **13d-1** was unsuccessful. The major isolated product was likely the result of an unwanted side reaction: transmetalation between the Ni(II) oxidative addition complex and Et_2Zn, followed by C(sp^2)–C(sp^3) reductive elimination.

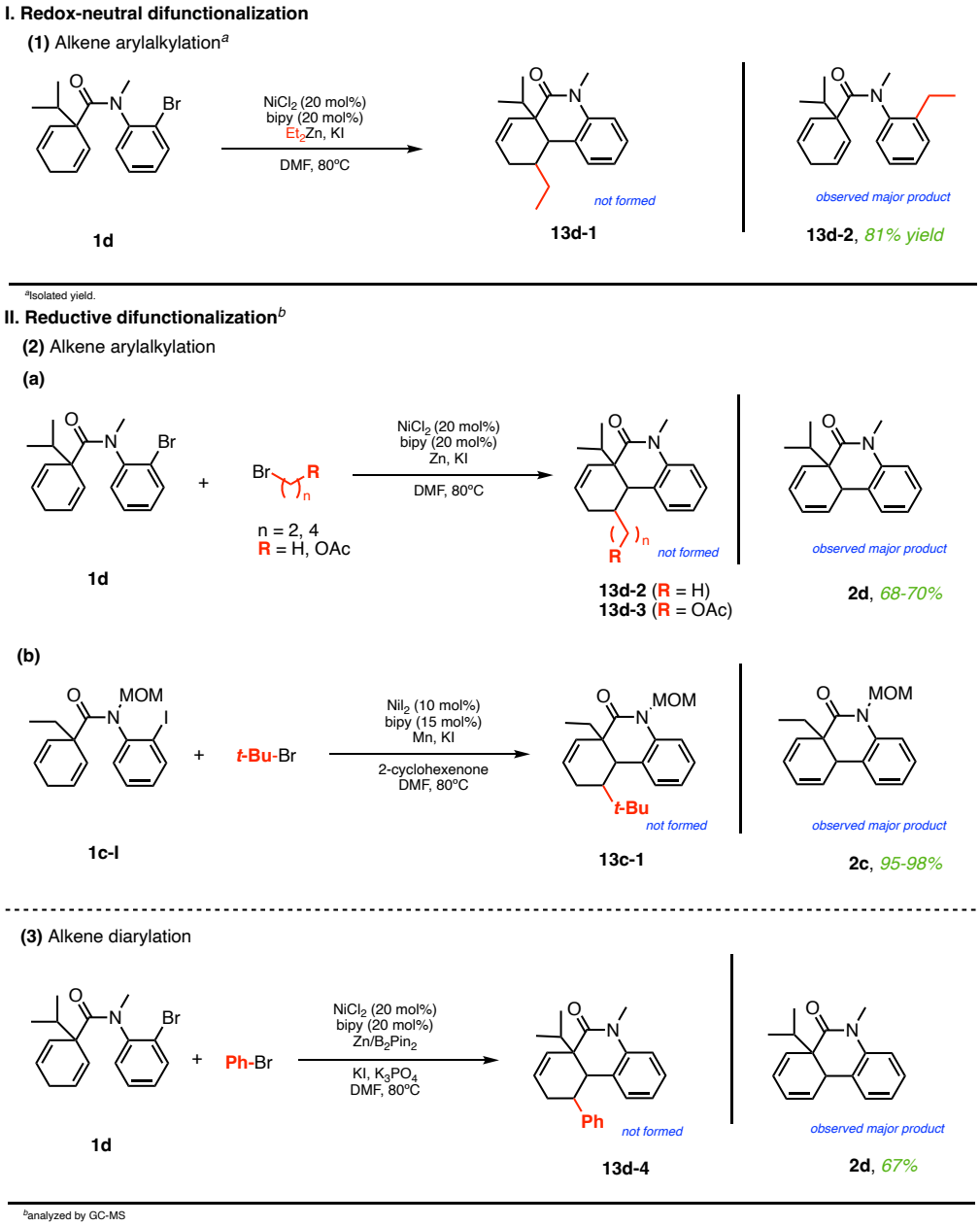

Scheme 5.1 Efforts toward dicarbofunctionalization of an internal alkene.

In our subsequent attempts to achieve reductive alkene dicarbofunctionalization, we employed C(sp^3) electrophiles. Informed by a related report by Jin and Wang,[21] we decided to perform a coupling reaction involving aryl bromide **1d** and either of two electrophiles, bromobutane or 2-bromoethyl acetate (**Scheme 5.1**, **eq 2-a**). The reaction was carried out in the presence of $NiCl_2$, bipy, Zn, and KI. In both cases, we observed the formation of the Heck product **2d** as the major species, which can suggest that the resultant nickel intermediates do not mediate the formation of radicals from C(sp^3) electrophiles and do not engage in radical mechanisms in the context of this transformation. Similarly, the attempt to perform alkene arylalkylation using tert-butyl bromide as a C(sp^3) alkyl electrophile in the reaction with substrate **1c-1** (as shown in **Scheme 5.1**, **eq 2-b**) was also unsuccessful. Hence, we made the decision to transition to using the C(sp^2) aryl electrophile and proceeded with reductive alkene diarylation instead (**Scheme 5.1**, **eq 3**).

Inspired by the work of Wang and co-workers,[22] who presented a Ni-catalyzed reductive diarylation of activated alkenes by domino cyclization/cross-coupling of two aryl bromides, all without the need for preformed organometallic reagents, we decided to apply similar conditions to our aryl bromide substrate **1d**. Our hypothesis was that following the oxidative addition and migratory insertion steps involving **1d**, the resulting Ni(II) alkyl species could be reduced to the corresponding Ni(I) alkyl intermediate in the presence of Zn/Pin_2B_2. Subsequently, the Ni(I) alkyl species generated in situ can be captured by phenyl bromide, which serves as a second electrophile. Unfortunately, the reaction still proceeded with the major formation of the 1,3-diene Heck product **2d**. Further attempts to accomplish alkene diarylation via a domino Heck cyclization/Suzuki

coupling[23] with phenylboronic acid did not yield any promising results either (**Scheme 5.2**).

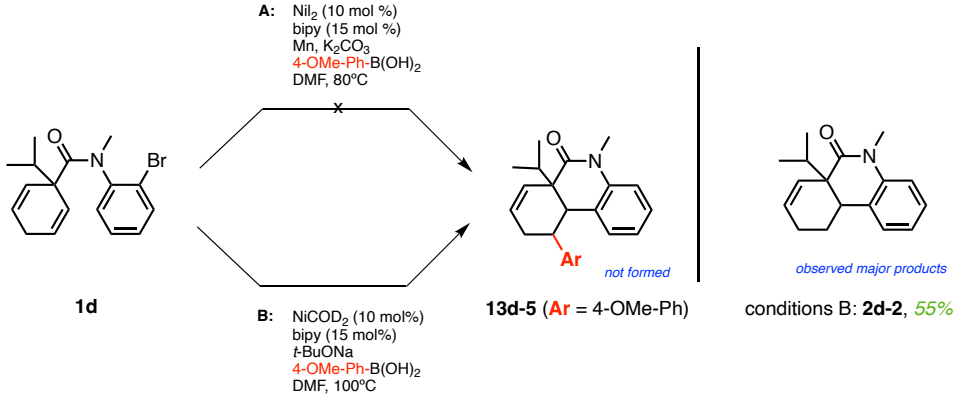

Scheme 5.2 Alkene diarylation via domino Heck cyclization/Suzuki coupling

5.3 Oxidative Boron Heck reactions

Recently, the development of enantioselective Pd-catalyzed oxidative boron Heck reactions has become an attractive alternative to the traditional Heck reaction.[24] Oxidative boron Heck reactions are typically catalyzed by Pd(II) instead of Pd(0) and replace the use of halides or triflates by organoboronic acids. These transformations are recognized for their efficiency, mild reaction conditions, tolerance to air and moisture, and their ability to engage more challenging alkene substrates. Additionally, the absence of a halide-Pd intermediate in the oxidative reactions promote the cationic pathway, which can be critical for achieving enantioselectivity. The important distinction between the traditional Heck reaction and the oxidative Heck catalytic cycle lies in the initial step. In the oxidative Heck cycle, the transmetalation between the organoboronic acid and the Pd(II) catalyst takes place as the first step. In contrast, in the traditional Heck reaction, the initial step involves the oxidative addition of Pd(0) into the halide or triflate substrate. Another critical difference is the requirement of an oxidant (typically O_2, air, benzoquinone, Cu(II) salts etc.) to re-oxidize Pd(0) to Pd(II) and turn over the catalytic

cycle. The use of nitrogen-based ligands, which are cheaper, and more air and moisture stable compared to phosphine ligands, has been demonstrated to facilitate efficient reoxidation of Pd(0).[25] Specifically, the chiral *t*Bu-substituted Pyox ligand with a CF_3 group at the 5-position appears to play a pivotal role in many of the recent enantioselective developments.[24]

Table 5.1 Oxidative boron Heck reactions.

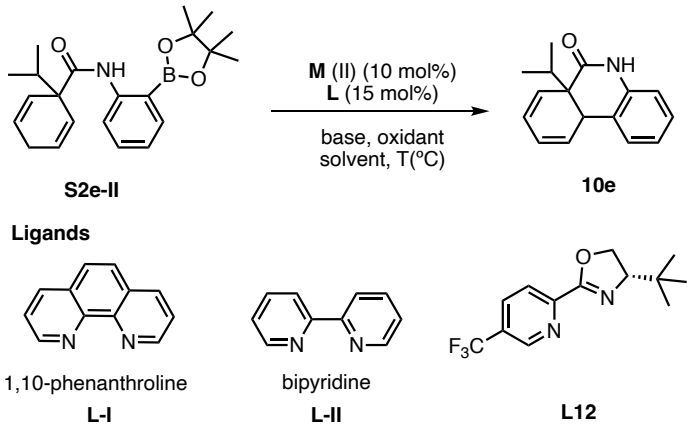

entry	conditions	product yield (%)
1	$Pd(OAc)_2$, **L-I**, Na_2CO_3, O_2, DMF, 70°C	NR[a]
2	$Pd(TFA)_2$, **L12**, Na_2CO_3, O_2, DCE, 50°C	NR
3	NiI_2, **L-II**, Cs_2CO_3, DDQ, DMF, 80°C	NR

[a]NR = no reaction.

The first example of the Pd(II)-catalyzed enantioselective intermolecular organoboron-mediated Heck-type reaction was reported by Mikami and co-workers in 2005.[26] Since then, the field of oxidative enantioselective intermolecular Heck-type transformations has seen significant progress, allowing for couplings of more challenging systems that include quaternary centers, cyclic enones, and acyclic alkenes.[24] Although there have been significant advances in intermolecular couplings, there has been just one reported example of an asymmetric intramolecular oxidative Heck reaction, also by Mikami and co-workers in 2007.[27] To address this limitation, we attempted to subject our

aryl boronic ester **S2e-II** to oxidative Pd(II)- or Ni(II)-catalyzed conditions using both achiral (**L-I** and **L-II**) and chiral (**L12**) nitrogen-based ligands (**Table 5.1**).

In the Pd(II)-catalyzed system, we added sodium carbonate as the base and used an O_2 balloon as the source of oxidant (**entries 1-2**). After unsuccessful attempts using the Pd catalyst, we decided to replace palladium with nickel and introduce 2,3-Dichloro-5,6-dicyano-1,4-benzoquinone (DDQ) as the oxidant (**entry 3**). Regrettably, the Ni(II)-catalyzed system also proved unsuccessful in delivering the desired product.

5.4 Mechanistic Studies

We performed several control experiments to gain a better understanding of the mechanism of our traditional Ni-catalyzed Heck reaction.[28] We first analyzed the role of the reducing metal, Mn primarily, but also the Zn used in the early reaction development. When manganese was removed from the reaction mixture, the reaction was completely hindered, suggesting the catalytic cycle is not initiated by a Ni(II) catalyst (**Scheme 5.3**, **eq 1**). Using 10 mol% of $Ni(COD)_2$ in the absence of Mn afforded the cyclized diene in low yield (8%) (**eq 2**), the expected result for one round of catalyst activity. Under identical reaction conditions with the addition of 3 equiv of Mn, 78% of product was formed, which indicates the importance of Mn to turn over the catalytic cycle.

In the context of this catalytic process, we speculated that an arylmanganese intermediate (ArMnBr or ArMnI),[29,30] if formed, could create an aryl−Ni intermediate via nucleophilic addition instead of direct oxidative addition of Ni into the aryl halide. In addition, insertion of Mn into the Ar−X bond could facilitate the formation of protodehalogenated species. To assess the possibility of ArMnX intermediates, both aryl bromide **1e** and aryl iodide **1e-I** were used as substrates for stoichiometric reactions with

Mn powder (**eq 3a**). Both reactions were quenched with deuterium oxide (D_2O) after 3 h, and the mixtures allowed to stir for an additional 18 h. Deuterated dehalogenated side product **$D_1$2e-1** was formed in only 13% yield and presumably from an ArMnI intermediate (**Scheme 5.4**). When stoichiometric reactions were performed with Zn, we observed deuterated side product **$D_1$2e-I** in 82% yield (**Scheme 5.3**, **eq 3b**). The additional unknown side product was presumed to be the cyclized alkene, based on the GC retention time and the MS data. The basis for this cyclization is unclear but may be the result of minor Ni or Pd contamination of the commercial Zn reagent.

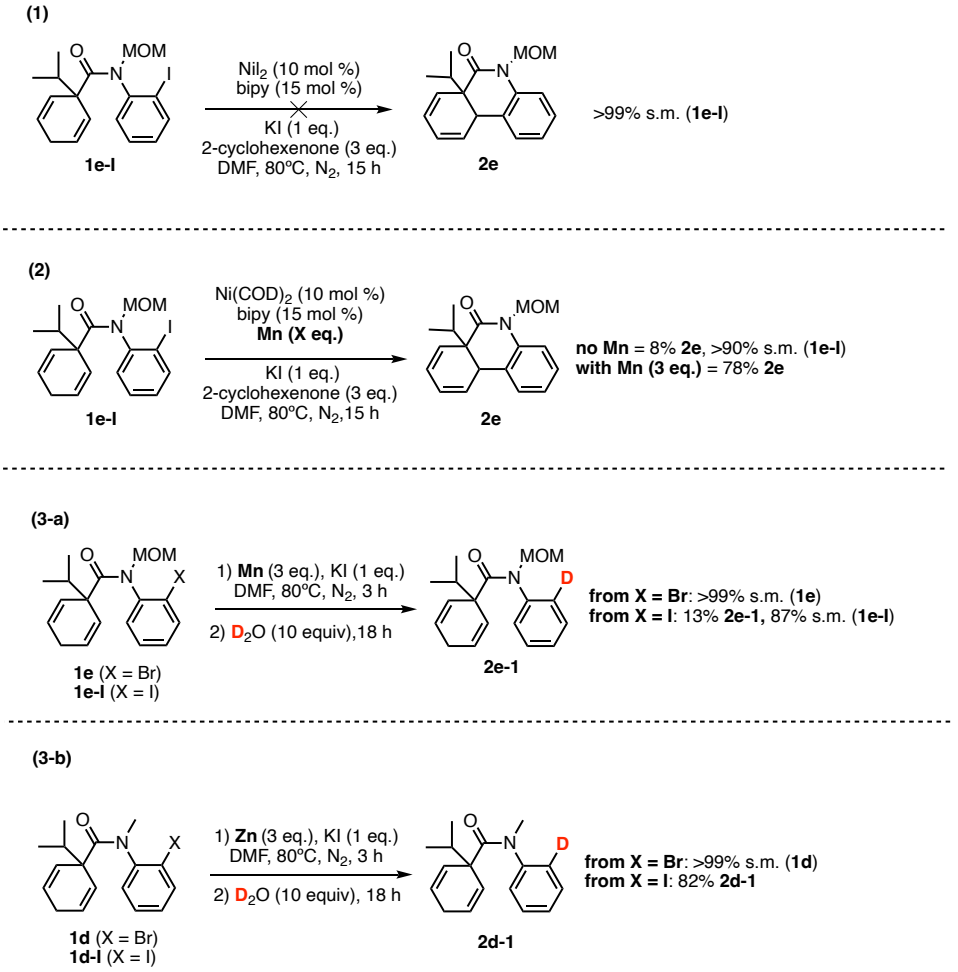

[a]Reactions were run on a 20–25 mg scale of aryl halide **1** or **1-I** and analyzed by GC-MS. s.m. = starting material.

Scheme 5.3 Control experiments of aryl halides with Mn and Zn.[a]

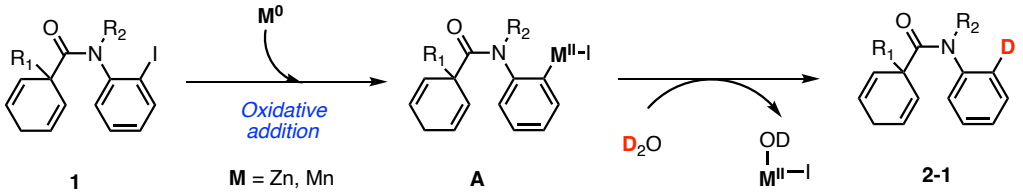

Scheme 5.4 Proposed reductant mediated formation of deuterated side product.

Overall, these results illustrate protodehalogenation reactions are likely with the aryl iodide substrates, but less relevant to the aryl bromide reactions. Given the short reaction times, it is likely the Mn oxidative addition has a limited impact in hampering the desired Heck product formation. However, insertion of Zn into the Ar−I reaction is likely contributing to some of the protodeiodination side product, **2e-1**.[31-33] Therefore, the main function of Mn in our reaction is to create a reducing environment for Ni(II) salts to form the necessary zerovalent nickel species, thus making it a better reductant.

The role of 2-cyclohexenone as a sacrificial alkene was the next reaction component to be analyzed. As noted earlier, it was introduced to remove Ni−H intermediates and reduce the amount of protodehalogenation (**2-1**) and alkene (**2-2**) side products. Cyclohexanone was detected and quantified (1 equiv) in the gas chromatographic analysis of the reactions using chlorobenzene as the internal standard, demonstrating that the enone system was reduced. To test for a potential competing reduction of the sacrificial alkene by Mn,[34] 2-cyclohexenone was stirred and heated at 80°C with Mn in DMF (**Scheme 5.5**). The formation of cyclohexanone was not observed, which confirms that the Mn is not responsible for the enone reduction.

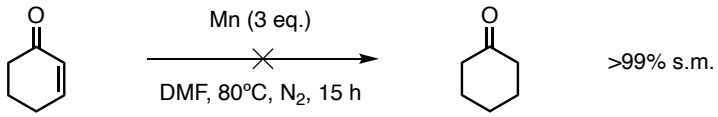

Scheme 5.5 Control experiment with the sacrificial alkene and Mn.

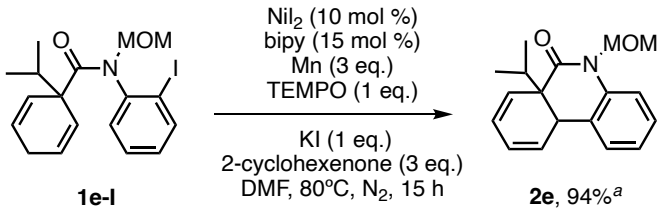

Scheme 5.6. Control reaction with TEMPO.

Ultimately, we considered the possibility of a single-electron pathway that could lead to the formation of an alkyl Ni(I) radical intermediate following the migratory insertion step. However, the addition of TEMPO (1 equiv) did not impact the reaction, suggesting that the formation of cyclized diene product **2e** occurs through a nonradical two-electron pathway (**Scheme 5.6**).

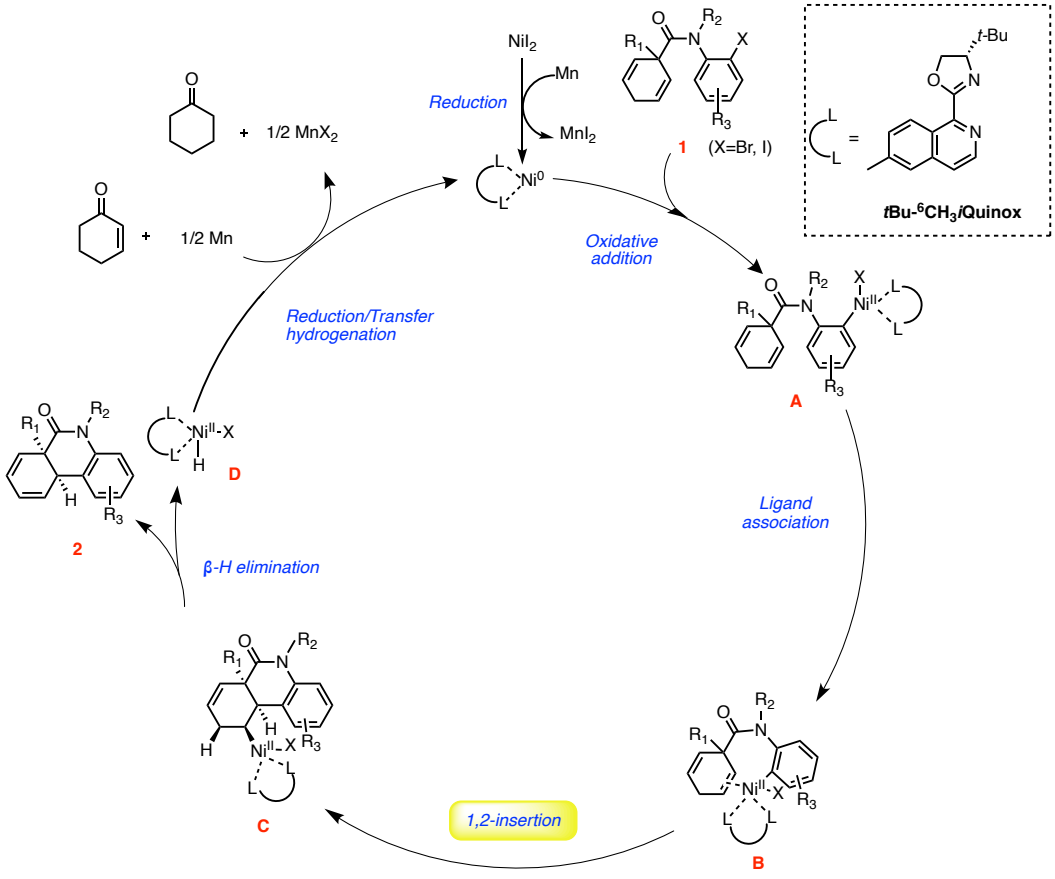

Scheme 5.7 Proposed Reaction Mechanism

According to the results from our mechanistic investigations, we propose a traditional two-electron Heck reaction mechanism (**Scheme 5.7**). The low-valent Ni(0) species generated under reductive conditions undergoes oxidative addition with aryl halide **1** to afford Ni(II) intermediate **A**. Ligand association of intermediate **A** followed by an intramolecular migratory insertion produces alkyl-Ni(II)-Ar species **C**. A syn-coplanar position of nickel with a β-hydrogen allows for efficient *β*-hydride elimination to afford product **2** and N(II)−XH species **D**. The Ni(0) catalyst is regenerated upon Mn reduction. Some of the Ni(II)−H is presumably converted to a Ni−enolate by reaction with 2-cyclohexenone and then subsequently reduced with Mn to Ni(0). Formation of the cyclohexanone, which was detected in our mechanistic studies, could occur by protonation of the Ni−enolate intermediate via a Ni(II)−H complex also present in solution.[35]

5.5 Computational Study

To gain insight into the basis for the enantioselectivity in the catalytic cycle, we engaged in collaboration with a computational chemist, Prof.Paul Rablen, to conduct a computational analysis of the key 1,2-migratory insertion step from proposed complex **B** to form **C** (**Scheme 5.7**) for substrate **2a** (R_1 and R_2 = Me; R_3 = H).[28] Initially, we hypothesized that this step would serve as rate- and stereo-determining. We found that the Gibbs free energy of activation for this step, when using bipyridine ligand, was calculated to be notably low at 1.9 kcal/mol. Additionally, the reaction is highly exothermic (17.5 kcal/mol), suggesting that it is unlikely to be reversible.

To develop a more comprehensive understanding of asymmetric induction, we conducted a study on the transition state of the 1,2-migratory insertion using ligand **L27**

(**Figure 5.1**). During this analysis, we considered eight possible geometries: the bidentate chiral ligand in either of two possible binding positions rotated by 180° degrees ("**F**"), the addition of the aryl group to either of the alkene positions in the cyclohexadiene ("**A**", *pro-R* or *pro-S*), and the two possible helical twists of the amide in the transition state ("**T**"). We explored these variations for both intermediates **B** and **C**, as well as the transition structure between them.

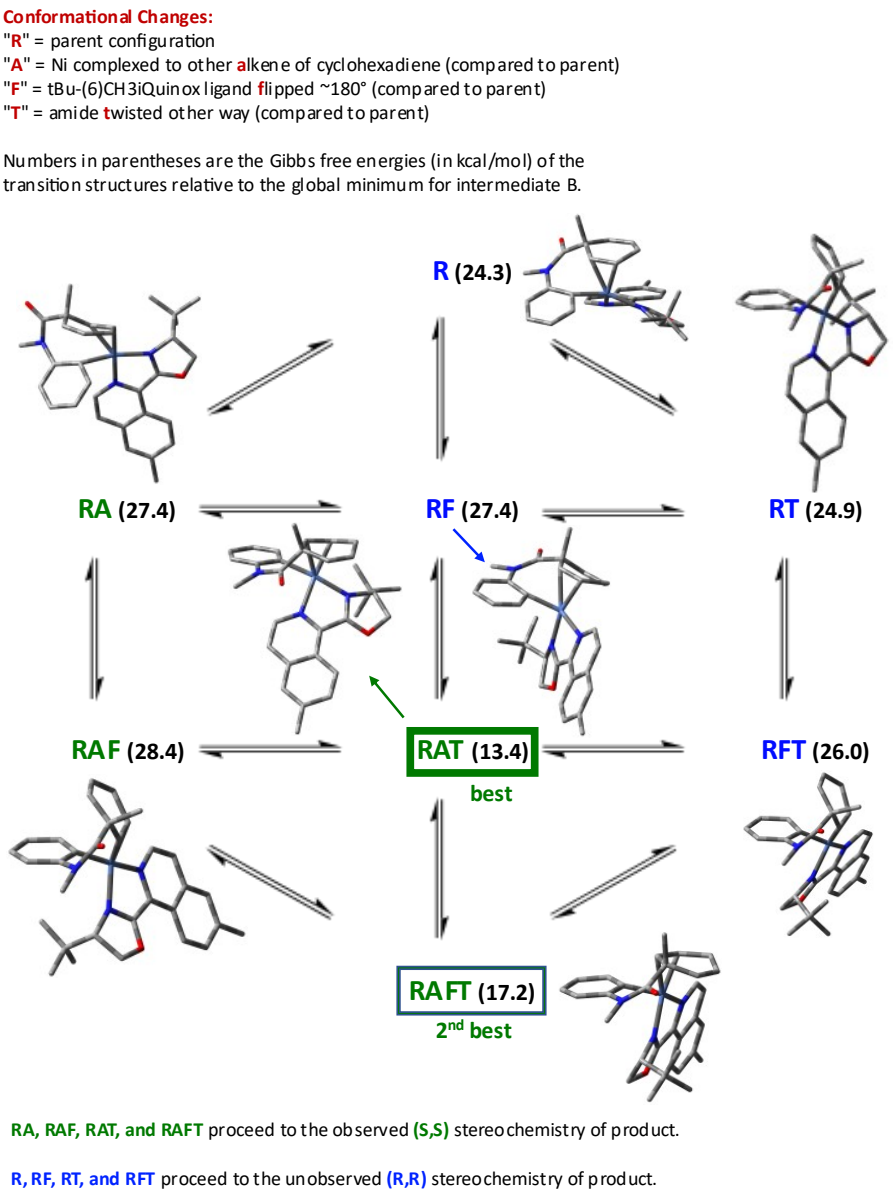

Figure 5.1 Conformation Images and Relative Energy.

The lowest-energy structures for intermediate **B** resulted in high energy barriers. In fact, out of the eight stereoisomeric transition structures, only two exhibited energies of less than 24 kcal/mol above the global minimum. These two transition structures were positioned 13.4 and 17.2 kcal/mol above the global minimum for intermediate **B**. Interestingly, they were only 2.2 and 6.0 kcal/mol, respectively, above the corresponding stereoisomers of intermediate **B**, which both happened to be 11.2 kcal/mol above the global minimum. These two pathways were distinguished only by a 180° rotation of the bidentate chiral ligand **L27** and, as a result, led to the same stereochemical outcome of the reaction. Furthermore, the exothermic nature of these pathways (16.3 kcal/mol) closely resembled that of the achiral bipyridine case. If we assume that the barriers for the reaction steps preceding the formation of intermediates **B** are minimal and that the migratory insertion is the rate-determining step, then the pathway with the lowest overall barrier to migratory insertion should be the predominant one. Even if the pathway with the second highest barrier were to have some influence, it would not alter the stereochemical outcome of the reaction. The remaining pathways, which result in different stereochemical outcomes, all entail substantially higher overall barriers.

The anticipated stereochemical result from the computational analysis involving **2a** (R for the quaternary carbon and R for the tertiary bridgehead carbon) using the *(S)*-**L27** ligand (**Figure 5.2**), coincided with the stereochemistry observed in our prior Pd-catalyzed Heck intramolecular desymmetrizing reactions.[36] In both reactions, the resulting products had the same major enantiomer as determined by chiral HPLC retention times. However, the calculated energy difference between the favored pathway leading to the observed major product and the lowest-energy alternative pathway

resulting in the opposite stereochemistry is notably large (10.9 kcal/mol). If our initial assumption that the 1,2-migratory insertion from **B** to **C** (**Scheme 5.7**) was the only factor in determining the stereochemical outcome was true, then the observed selectivity would have been much higher. Therefore, we recognized that the stereochemical result cannot be simply explained by the calculated energy difference between the two diastereomeric transition state complexes, which forced us to consider the possibility of dynamic kinetic resolution in this Heck reaction.[37]

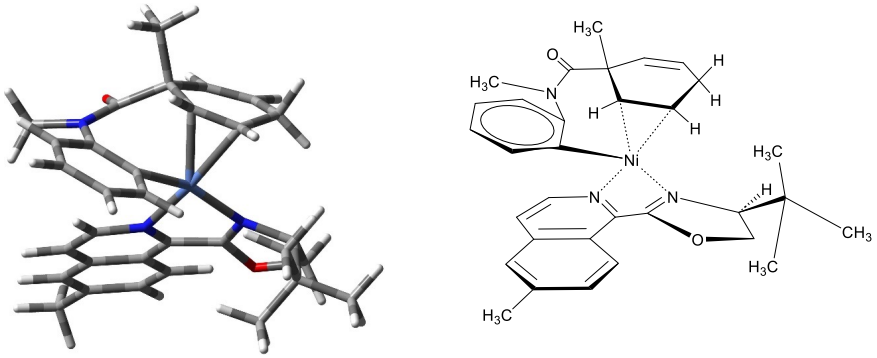

Figure 5.2 Lowest-energy transition state for 1,2-migratory insertion of **B** to **C**.

In the abovementioned analysis, we assumed that interconversion of the different possible conformations of the initial amide **1** occurs rapidly in comparison to the reaction rate, a scenario commonly referred to as the Curtin–Hammett condition.[38] Nonetheless, this hindered amide is twisted and axially chiral, although presumably racemic. Additionally, the interconversion of the enantiomers is likely to involve a relatively high energy barrier, potentially around 20 kcal/mol.[39] Consequently, the reaction is likely to undergo a degree of dynamic kinetic resolution, a previously observed phenomenon in similar Heck reactions.[37] To recall, the eight conformations of intermediate **B** (**Figure 5.1**) vary in terms of the nickel coordination to alkene ("**A**"), the orientation of **L27** ("**F**"), and the twist of the amide ("**T**"). Assuming that isomerization of the two

parameters "A" and "F" is rapid, and the amide twist interconversion is slow, we proposed the following kinetics of the reaction (**Scheme 5.8**). Given that it is not important for the purpose of this study and to streamline our analysis, we did not specify if the amide twist isomerization takes place in free amide **1**, in intermediate **A**, and/or in intermediate **B**. The series of structures **1**, **A**, and **B** share the same amide twist and the intermediate **B** represent the four calculated isomers of **B** that have this twist (**R**, **RA**, **RF**, and **RAF**, **Figure 5.1**). The series of structures **1T**, **AT**, and **BT** have the opposite amide twist and the intermediate **BT** includes the other four calculated isomers (**RT**, **RAT**, **RFT**, and **RAFT**, **Figure 5.1**). The global minimum corresponds to the lowest energy of the four "**BT**" structures and the lowest energy of the four "**B**" structures is 1.6 kcal/mol higher. The **BT** structures have low energy barriers (13.4 or 17.2 kcal/ mol) to the major observed stereochemistry of the product (*S,S*) and much higher barriers to the minor stereoisomer (*R,R*). On the other hand, the **B** structures lead preferentially to the minor observed stereochemistry via much higher barriers (24.3 or 27.4 kcal/mol), although lower than the barriers yielding the major stereoisomer (27.4 or 28.4 kcal/mol).

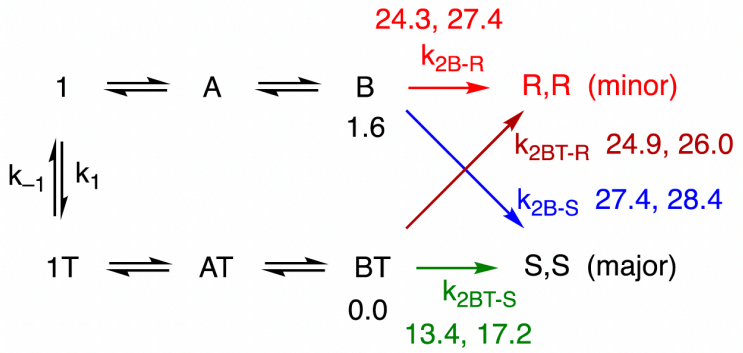

[a]Calculated energies are shown in kilocalories per mole (transition state energies for $k_{2B\text{-}R}$, $k_{2BT\text{-}S}$, $k_{2B\text{-}S}$, and $k_{2BT\text{-}R}$, minima for **B** and **BT**). [b]The amide isomerization (k_1/ k_{-1} process) is assumed to be slow.

Scheme 5.8 Kinetics of the Reaction in **Scheme 5.7**.[a,b]

If the rate of amide twist interconversion (k_1 and k_{-1}) is faster than the rate of the reaction leading to the minor stereoisomer (k_{2R}) (e.g., the k_1 process has a barrier << 24 kcal/mol), then according to the initially assumed Curtin−Hammett condition, the reaction would predominantly follow the pathway with the lowest overall barrier, as indicated in green, leading exclusively to one stereoisomer product (*S,S*) (**Scheme 5.8**). Alternatively, if the amide twist interconversion is slow, having a barrier considerably higher than 24 kcal/mol, there would be hardly any stereoselectivity observed overall.

In this case, we would expect that the 50% of molecules initially having the desired twist (**1T**) would primarily result in the (*S,S*) stereochemistry, while the remaining 50% with the opposite twist (**1**) would preferentially yield the (*R,R*) product. If the rate of amide twist interconversion is competitive with that of the reaction forming the minor product (the k_1 has a barrier ∼24 kcal/mol), we would expect reduced enantioselectivity, to the extent that **1** cannot isomerize to **1T** before reacting through **B** to yield the (*R,R*) product. Overall, this analysis provides two valuable insights into the reaction process. First, it explains why higher enantiomeric ratios are not attained despite the significantly large, calculated energy difference (∼11 kcal/mol) between the two diastereomeric transition state complexes in the 1,2-migratory insertion. In theory, one would expect that such a difference would result in enantiomeric ratios of >99:1. Secondly, the stereoselectivity of this reaction could be improved by increasing the barriers for the migratory insertion or, alternatively, by reducing the barriers for the amide bond rotation. If both the amide rotamer barrier and the migratory insertion barrier were to change simultaneously and to an equal extent, it would not help to improve the enantioselectivity. This explains why our experimental attempts to increase the

enantiomeric ratios by simply decreasing the temperature have been unsuccessful. Conversely, eliminating atropisomerism in our tertiary amide structures can be an efficient strategy for achieving higher levels of enantioselectivity, as supported by preliminary results showing significant improvement in enantioselectivity with the secondary amine substrates in the Heck reaction.

5.6 Conclusions

In this chapter, we conducted a preliminary exploration of alternative modes of reactivity with the nickel catalyst. Our investigation focused on the reactivity of tertiary amides in Ni-catalyzed alkene dicarbofunctionalization reactions using a selection of $C(sp^2)$ and $C(sp^3)$ electrophiles and nucleophiles. Regrettably, promising results could not be attained under either redox-neutral or reductive conditions for alkene dicarbofunctionalization. Similarly, we were unable to achieve reactivity with aryl boronic ester under oxidative Pd(II)- or Ni(II)-catalyzed conditions.

From our mechanistic studies, we derived several important conclusions that supported the proposed traditional two-electron Heck reaction mechanism. We established that Mn in our system primarily serves to create a reducing environment for Ni(II) salts, leading to the formation of the active low valent Ni(0) species and to reduce the Ni-hydride intermediate formed as the result of β-hydride elimination. Furthermore, our investigations confirmed that Mn is not responsible for the reduction of the sacrificial alkene. We observed the minor formation of arylmanganese intermediates when working with aryl iodide substrates, but it is likely to have a limited influence on the generation of protodehalogenated species. In contrast, Zn appears to be more susceptible to oxidative addition into the Ar-I bond, making it more likely to contribute to the formation of

unwanted protodehalogenation products. Lastly, a nonradical pathway was confirmed by the addition of a radical scavenger, TEMPO, and its failure to impact the cross-coupling reaction results.

During the computational study, we assumed that 1,2-migratory insertion is the rate- and stereo-determining step. Considering eight possible geometries with the bidentate chiral ligand **L27**, we identified the lowest energy transition state for the migratory insertion (intermediate **B**) with an energy of 13.4 kcal/mol above the global minimum. However, the calculated energy difference (10.9 kcal/mol) between the two diastereomeric transition state complexes did not correlate to the observed enantiomeric rations, leading us to consider the possibility of dynamic kinetic resolution as an explanation for this discrepancy. Based on the kinetics of this Heck reaction, we proposed that if the rate of amide twist interconversion is competitive with the reaction leading to the minor stereoisomer, it would result in reduced enantioselectivity. Overall, the computational study provided valuable insights into the basis for enantioselectivity, and it was confirmed experimentally that the presence of tertiary amide atropisomers leads to the lower experimental enantiomeric ratios by demonstrating higher enantioselectivity with two reduced amine substrate analogs.

5.7 References

1. Diccianni, J. B.; Diao, T. Mechanisms of Nickel-Catalyzed Cross-Coupling Reactions. *Trends in Chemistry* **2019**, *1* (9), 830−844.
2. Lan, Y.; Wan, C. Nickel-catalyzed enantioselective reductive carbo-acylation of alkenes. *Commun Chem* **2020**, *3* (45).
3. Qi, X.; Diao, T. Nickel-Catalyzed Dicarbofunctionalization of Alkenes. *ACS Catal.* **2020**, *10*, 8542−8556.
4. Wu, X.; Turlik, A.; Luan, B.; He, F.; Qu, J.; Houk, K. N.; Chen, Y. Nickel-Catalyzed Enantioselective Reductive Alkyl-Carbamoylation of Internal Alkenes. *Angew.Chem.Int.* **2022**, *61*, e2022075.

5. Ping, Y.; Kong, W. Ni-Catalyzed Reductive Difunctionalization of Alkenes. *Synthesis* **2020**, *52*, 979−992.
6. Derosa, J.; Apolinar, O.; Kang, T.; Tran, V.; Engle, K. Recent Developments in Nickel-Catalyzed Intermolecular Dicarbofunctionalization of Alkenes. *Chem. Sci.* **2020**, *11*, 4287−4296.
7. Tasker, S. Z.; Standley, E. A.; Jamison, T. F. Recent advances in homogeneous nickel catalysis. *Nature* **2014**, *509* (7500), 299−309.
8. Diccianni, J.; Lin, Q.; Diao, T. Mechanisms of Nickel-Catalyzed Coupling Reactions and Applications in Alkene Functionalization. *Acc. Chem. Res.* **2020**, *53* (4), 906–919.
9. García-Domínguez, A.; Li, Z.; Nevado, C. Nickel-Catalyzed Reductive Dicarbofunctionalization of Alkenes. *J. Am. Chem. Soc.* **2017**, *139*, 6835−6838.
10. Shu, W.; García-Domínguez, A.; Quirós, M. T.; Mondal, R.; Cárdenas, D. J.; Nevado, C. Ni-Catalyzed Reductive Dicarbofunctionalization of Nonactivated Alkenes: Scope and Mechanistic Insights. *J.Am.Chem.Soc.* **2019**, *141*, 13812−13821.
11. Wu, X.; Luan, B.; Zhao, W.; He, F.; Wu, X.-Y.; Qu, J.; Chen, Y. Catalytic Desymmetric Dicarbofunctionalization of Unactivated Alkenes. *Angew. Chem., Int. Ed.* **2022**, *61* (26), e202111598.
12. Bhakta, S.; Ghosh, T. Emerging Nickel Catalysis in Heck Reactions: Recent Developments. *Adv. Synth. Catal.* **2020**, *362* (23), 5257-5274.
13. Yang, T.; Chen, X.; Rao, W.; Koh, M. Broadly Applicable Directed Catalytic Reductive Difunctionalization of Alkenyl Carbonyl Compounds. *Chem.* **2020**, *6*, 738−751.
14. Lux, D. M.; Aryal, V.; Niroula, D.; Giri, R. Nickel-Catalyzed Regioselective Intermolecular Dialkylation of Alkenylarenes: Generation of Two Vicinal $C(sp^3)$ $C(sp^3)$ Bonds Across Alkene. *Angew. Chem. Int. Ed.* **2023**, *62*, e202305522.
15. Derosa, J.; van der Puyl, V. A.; Tran, V. T.; Liu, M.; Engle, K. Directed Nickel-Catalyzed 1,2-Dialkylation of Alkenyl Carbonyl Compounds.*Chem. Sci.* **2018**, *9*, 5278−5283.
16. Phapale, V. P.; Buñuel, E.; García-Iglesias, M.; Cárdenas, D. J. Ni-Catalyzed Cascade Formation of $C(sp^3)$-$C(sp^3)$ Bonds by Cyclization and Cross-Coupling Reactions of Iodoalkanes with Alkyl Zinc Halides. *Angew. Chemie - Int. Ed.* **2007** *46* (46), 8790–8795.
17. Vaupel, A.; Knochel, P. Stereoselective Synthesis of Heterocyclic Zinc Reagents via a Nickel-Catalyzed Radical Cyclization. *J. Org. Chem.* **1996**, *61*, 5743−5753.
18. Derosa, J.; Tran, V. T.; Boulous, M. N.; Chen, J. S.; Engle, K. M. Nickel-Catalyzed β,γ-Dicarbofunctionalization of Alkenyl Carbonyl Compounds via Conjunctive Cross-Coupling. *J. Am. Chem. Soc.* **2017**, *139*, 10657−10660.
19. Joensuu, P. M.; Murray, G. J.; Fordyce, E. A. F.; Luebbers, T.; Lam, H.-W. Diastereoselective Nickel-Catalyzed Reductive AldolCyclizations Using Diethylzinc as the StoichiometricReductant: Scope and Mechanistic Insight. *J. Am. Chem. Soc.* **2008**, *130*, 7328–7338.

20. Xiao, X.; Wang, H.; Huang, Z.; Yang, J.; Bian, X.; Qin, Y. Selective Diethylzinc Reduction of Imines in the Presence of Ketones Catalyzed by $Ni(acac)_2$. *Org. Lett.* **2006**, *8* (1), 139–142.
21. Jin, Y.; Wang, C. Ni-catalysed reductive arylalkylation of unactivated alkenes. *Chem. Sci.* **2019**, *10*, 1780−1785
22. Wang, K.; Kong, W. Enantioselective Reductive Diarylation of Alkenes by Ni-Catalyzed Domino Heck Cyclization/Cross Coupling. *Synlett* **2019**, *30* (9), 1008–1014.
23. Li, Y.; Wang, K.; Ping, Y.; Wang, Y.; Kong, W. Nickel-Catalyzed Domino Heck Cyclization/Suzuki Coupling for the Synthesis of 3,3-Disubstituted Oxindoles . *Org. Lett.* **2018**, *20* (4), 921–924.
24. Lee, A. L. Enantioselective oxidative boron Heck reactions. *Org. Biomol. Chem.* **2016**, *14*, 5357–5366.
25. Andappan, M. M. S.; Nilsson, P.; Larhed, M. The first ligand-modulated oxidative Heck vinylation. Efficient catalysis with molecular oxygen as palladium(0) oxidant. *Chem. Commun.* **2004**, (2), 218–219.
26. Akiyama, K.; Wakabayashi, K.; Mikami, K. Enantioselective Heck-Type Reaction Catalyzed by tropos-Pd(II) Complex with Chiraphos Ligand. *Adv. Synth. Catal.* **2005**, *347*, 1569–1575.
27. Akiyama, K.; Mikami, K. Pd(II)-Catalyzed Enantioselective Intramolecular Heck-Type Reaction to Construct Chiral Sulfonamide Rings. *Heterocycles* **2007**, *74* (1), 827–834.
28. Rachii, D.; Caldwell, D. J.; Kosukegawa, Y.; Sexton, M.; Rablen, P.; Malachowski, W. P. Ni-Catalyzed Enantioselective Intramolecular Mizoroki–Heck Reaction for the Synthesis of Phenanthridinone Derivatives. *J. Org. Chem.* **2023**, *88* (13), 8203–8226.
29. Peng, Z.; Knochel, P. Preparation of Functionalized Organomanganese(II) Reagents by Direct Insertion of Manganese to Aromatic and Benzylic Halides . *Org. Lett.* **2011**, *13* (12), 3198–3201.
30. Kakiya, H.; Nishimae, S.; Shinokubo, H.; Oshima, K. Preparation of organomanganese reagents from organic halides with activated manganese . *Tetrahedron* **2001**, *57* (42), 8807–8815.
31. Knochel, P. Organomagnesium and Organozinc Chemistry. *Organometallics in Synthesis* **2013**, 223–372 .
32. Knochel, P. *Organozinc Reagents in Science of Synthesis*. Vol. 3; Thieme, 2004.
33. Knochel, P.; Jones, P. O*rganozinc reagents: A practical approach.* Oxford University Press, **1999**.
34. Magnus, P.; Waring, M. J.; Scott, D. A. Conjugate reduction of α,β-unsaturated ketones using an MnIII catalyst, phenylsilane and isopropyl alcohol. *Tetrahedron Lett.* **2000**, *41* (50), 9731–9733.
35. Eberhardt, N. A.; Guan , H. Nickel Hydride Complexes. *Chem. Rev.* **2016** *116* (15), 8373–8426.
36. Sexton, M.; Malachowski, W. P.; A., G. Y. P.; Rachii, D.; Feldman, G.; Krasley, A.; Chen, Z.; Tran, M.; Wiley, K.; Matei, A.; et al. Catalytic Enantioselective Birch−Heck Sequence for the Synthesis of Phenanthridinone

Derivatives with an All-Carbon Quaternary Stereocenter. *J. Org. Chem.* **2022**, *87* (2), 1154–1172.
37. McDermott, M. C.; Stephenson, G. R.; Hughes, D. L.; Walkington , A. J. Intramolecular Asymmetric Heck Reactions: Evidence for Dynamic Kinetic Resolution Effects. *Org. Lett.* **2006** *8*(14), 2917–2920.
38. Seeman, J. I. Effect of conformational change on reactivity in organic chemistry. Evaluations, applications, and extensions of Curtin-Hammett Winstein-Holness kinetics. *Chem. Rev.* **1983**, *83* (2), 83–134.
39. Lapierre, A. J. B; Geib, S. J.; Curran, D. P. Low-Temperature Heck Reactions of Axially Chiral o-Iodoacrylanilides Occur with Chirality Transfer: Implications for Catalytic Asymmetric Heck Reactions. *J. Am. Chem. Soc.* **2007**, *129*, 494–495.

Chapter 6: Conclusions

6.1 Conclusions

In this work, we have developed the first example of an enantioselective intramolecular Ni-catalyzed synthesis of a heterocyclic system with a quaternary stereocenter using the Birch−Heck sequence.[1] This development represents a rare example of a Ni-catalyzed intramolecular Heck reaction to form a six-membered ring with an all-carbon quaternary center and demonstrates the broadest substrate scope to date with good to very good levels of enantioselectivity. Subsequently, we discovered a range of additional transformations of the 1,3-diene Heck products to demonstrate the potential for enhancing the drug-like properties of these molecules. Despite the outcomes of the biological studies indicating the lack of significant cytotoxicity or anti-cancer activity in the phenanthridinone derivatives, we believe that this new synthetic methodology can serve as an effective strategy for enantioselective introduction of all-carbon quaternary stereocenters to increase molecular complexity in other bioactive small-molecule inhibitors.[2-4]

In comparison with the Pd-catalyzed version of the reaction, the alternative Ni-catalyzed reaction is much faster (1 h vs 20 h) and cheaper (all reagents: \$0.73/mmol vs. \$2.02/mmol) than the analogous Pd version, and can be applied to a wide range of substrates giving good to excellent yields. It affords enantioselectivities comparable to that of the Pd/ BINAP Heck reaction[5] with the use of a newly synthesized chiral *i*Quinox-

type bidentate ligand **L27**. The chiral ligand likely creates chiral induction via favorable π-stacking interaction between the aryl group of the substrate and the isoquinoline ring of the *i*Quinox ligand.[6] Notably, during reaction optimization, we were able to control unwanted Ni−H reductions, including a protodehalogenation side reaction. This was achieved by integrating the Heck reaction with a transfer hydrogenation step[7] that utilized a sacrificial alkene and by introducing an external source of iodide source[8] into the reaction conditions. The proposed traditional two-electron Heck reaction mechanism was supported by the mechanistic studies. The computational study offered valuable insights into the basic for enantioselectivity and confirmed that the presence of tertiary amide atropisomers contributes to reduced enantioselectivity. As such, this work presents a direct and valuable comparison of the performance of nickel and palladium catalysts, which should facilitate the application of Ni catalysis to traditional Heck transformations.

6.2 References

1. Rachii, D.; Caldwell, D. J.; Kosukegawa, Y.; Sexton, M.; Rablen, P.; Malachowski, W. P. Ni-Catalyzed Enantioselective Intramolecular Mizoroki–Heck Reaction for the Synthesis of Phenanthridinone Derivatives. *J. Org. Chem.* **2023**, *88* (13), 8203–8226.
2. Lovering, F. Escape from Flatland 2: complexity and promiscuity. *Med. Chem. Commun.* **2013**, *4* (3), 515–519.
3. Lovering, F.; Bikker, J.; Humblet, C. Escape from Flatland: Increasing Saturation as an Approach to Improving Clinical Success. *J. Med. Chem.* **2009**, *52* (21), 6752–6756.
4. Quasdorf, K.; Overman, L. Catalytic Enantioselective Synthesis of Quaternary Carbon Stereocenters. *Nature* **2014** *216*, 181–191.
5. Sexton, M.; Malachowski, W. P.; A., G. Y. P.; Rachii, D.; Feldman, G.; Krasley, A.; Chen, Z.; Tran, M.; Wiley, K.; Matei, A.; et al. Catalytic Enantioselective Birch−Heck Sequence for the Synthesis of Phenanthridinone Derivatives with an All-Carbon Quaternary Stereocenter. *J. Org. Chem.* **2022**, *87* (2), 1154–1172.
6. Yang, G.; Zhang, W. Renaissance of pyridine-oxazolines as chiral ligands for asymmetric catalysis. *Chem. Soc. Rev.* **2018**, *47*, 1783–1810.

7. Lv, H.; Kang, H.; Zhou, B.; Xue, X.; Engle, K. M.; Zhao, D. Nickel-catalyzed intermolecular oxidative Heck arylation driven by transfer hydrogenation. *Nat. Commun.* **2019** *10* (1), 5025.
8. Colon, I.; Kelsey, D. R. Coupling of aryl chlorides by nickel and reducing metals. *J. Org. Chem.* **1986**, *51* (14), 2627–2637.

Chapter 7: Experimental

7.1 General experimental details

All reactants and reagents were commercially available and were used without further purification unless otherwise indicated. Anhydrous tetrahydrofuran (THF) was obtained by distillation from benzophenone-sodium under argon. All reactions were carried out under an inert atmosphere of argon in flame-dried glassware unless otherwise indicated. Concentrated refers to the removal of solvent with a rotary evaporator at normal water aspirator pressure. Concentrated under high vacuum refers to removal of solvent with a direct-drive rotary vane vacuum pump. Thin layer chromatography (TLC) was performed using silica gel 60 Å precoated aluminum backed plates (0.25 mm thickness) with fluorescent indicator. Developed TLC plates were visualized with UV light (254 nm) and $KMnO_4$ spray. Flash column chromatography was conducted with the indicated solvent system using normal phase silica gel 60 Å, 230-400 mesh. Yields refer to chromatographically and spectroscopically pure (> 95%) compounds, except as otherwise indicated.

^1H and ^{13}C NMR spectra were recorded on a Bruker Avance III 400 at 400 MHz and 100 MHz, respectively. Chemical shifts are reported in δ values (ppm) relative to an internal reference (0.05% v/v) of tetramethylsilane (TMS) for ^1H NMR or the solvent signal, chloroform ($CDCl_3$) or DMSO-d_6, for ^{13}C NMR. NMR analysis of the tertiary amides were conducted at elevated temperatures (77-100˚C) in DMSO-d_6 due to the presence of atropisomers. Peak splitting patterns in the ^1H NMR are reported as follows: s, singlet; bs, broad singlet; d, doublet; t, triplet; q, quartet; hept, heptet; dd, doublet of doublets; ddd, doublet of doublets of doublets; dt, doublet of triplets; dq, doublet of quartets; m, multiplet. ^{13}C NMR experiments were conducted with the attached proton test (APT) pulse sequence. ^{13}C multiplicities are reported as δ_u (up) for methyl and methine, and δ_d (down) for methylene and quaternary carbons.

GC-MS analyses were performed with an Agilent 6890 GC and a Hewlett-Packard 5973 EI-MS detector fitted with a 30 m x 0.25 mm column filled with crosslinked 5% PH ME siloxane (0.25 μm film thickness); gas pressure 7.63 psi He. Analysis of samples involved either heating from 70 to 250˚C (10˚C /min), then hold at 250˚C for 5 min. (method A) or heating from 175 to 250˚C (25˚C/min), then hold at 250˚C for 2 min. (method B). Melting points were measured on a Stanford Research Systems MPA160 melting point apparatus and are uncorrected. HPLC analysis was conducted using an Agilent 1100 fitted with a DAD at 254 nm using a CHIRACEL OD-H 4.6 mm x 250 mm, 5 μm column, run with the specified conditions. HRMS were collected at the University of Delaware using a Q-Exactive Orbitrap with an ESI source in positive mode or a

Waters GCT Premier equipped with a LIFDI (liquid field desorption ionization). Optical rotations were conducted on a Perkin Elmer 341 polarimeter at Villanova University at 589 nm and 20.0˚C.

7.2 Computational methods

All calculations were carried out with Gaussian 16[1] and using density functional theory (DFT) in the gas phase. We chose the specific configuration applied successfully by Houk, Chen, et. al. to a related Ni(II) migratory insertion.[2] This procedure involves geometry optimization using the B3LYP hybrid functional,[3] the def2-SVP basis set,[4, 5] and the Grimme D3 empirical dispersion correction[6] with Becke-Johnson damping,[7] followed by a single point energy correction using the TZVPP basis set. After each optimization (conducted with fopt=(calcfc,tight) or fopt=(calcfc,ts,tight)), a subsequent frequency calculation was performed in order to confirm the nature of the stationary point as a minimum (NImag=0) or a transition structure (NImag=1), and to obtain thermodynamic corrections. Gibbs free energies at 298 K were used for analysis, but essentially the same picture would be obtained using either enthalpies or electronic energies, as the thermodynamic corrections to the energy barriers and differences were small, as would be expected.

The structures computed were intermediates **B** and **C** in Scheme 5.7, and the transition structure between them, for the case $R_1 = R_2 = CH_3$, $R_3 = H$, and L–L = (*R*)-*t*Bu-$^6CH_3$-*i*Quinox. Eight major stereoisomers were computed, corresponding to the three major factors that could be varied one way or the other: (1) the orientation of the (*R*)-*t*Bu-$^6CH_3$-*i*Quinox ligand (a given orientation, or flipped 180° so as to transpose the positions of the two coordinating nitrogen atoms), (2) which of the two alkenes in the cyclohexadiene unit coordinates to nickel, and (3) whether to twist the amide out of plane in one sense or the other. In a few cases, there were additional orientations of the *i*Quinox ligand, leading to similar energies. In addition, of course, there would be another eight equivalent structures with the *S* configuration at the carbon bearing the *tert*-butyl group, but these would have the same energies and were not computed. The amide functionality was in all cases restricted to the *Z* conformation illustrated in Scheme 5.7. Conformation depictions and calculation details are available in below in section 7.19.

7.3 Birch reduction/alkylation general procedures and data

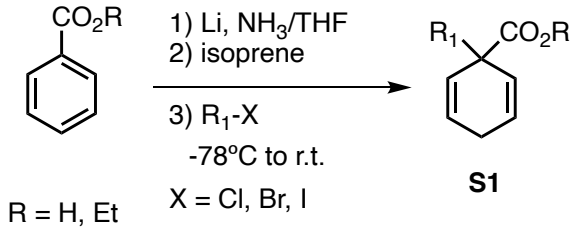

Scheme 7.1 Birch/reduction alkylation general reaction.

General procedure A

A flame dried 3-necked round bottom flask with a stir bar, connected to a Dewar condenser, under argon, was charged with benzoic acid (1.0 mmol, 1.0 equiv) which was dissolved in THF (0.4 mL, 2.5 M) and cooled to -78˚C. Ammonia (7 mL, 0.14 M) was distilled into the flask and lithium (4.0 mmol, 4.0 equiv) was added in small pieces until a dark blue color was maintained for 30 minutes. Isoprene was added dropwise to quench the excess lithium and produce a bright yellow opaque solution. Alkylating agent (2.0 mmol, 2.0 equiv) was added slowly dropwise. When the addition was complete the reaction was maintained at -78˚C while the color faded to white/off-white over 1h. The reaction was then warmed to room temperature and the ammonia was allowed to evaporate. Once evaporated the reaction was quenched with water and washed with diethyl ether. The aqueous layer was acidified with 6N HCl (until pH ~1), and then extracted with diethyl ether. The combined organic layers were washed $Na_2S_2O_4$ with brine, dried with $MgSO_4$, and concentrated in vacuo.

General procedure B

A flame dried flask with a stir bar, connected to a Dewar condenser, under argon, was charged with benzoate ester (1.0 mmol, 1.0 equiv), THF (0.4 mL, 2.5 M), and *t*-BuOH (1.1 mmol, 1.1 equiv) and cooled to -78˚C Ammonia (7 mL, 0.14 M) was distilled into the flask and lithium (2.0 mmol, 2.0 equiv) was added in small pieces until a dark blue color was maintained for 30 minutes. Isoprene was added dropwise to quench the lithium and produce a bright yellow opaque solution. Alkylating agent (1.1 mmol, 1.1 equiv) in THF (0.4 mL, 2.5 M) was added slowly dropwise. When the addition was complete the reaction was maintained at -78˚C while the color faded to white/off-white over 1 h. The reaction was then warmed to room temperature and the ammonia was allowed to evaporate under a stream of argon. Once evaporated the reaction was quenched with water and extracted with Et_2O (5 x 7 mL/mmol). The combined organic layers were washed with brine, dried with $MgSO_4$, concentrated in vacuo, and purified with flash chromatography on silica gel.

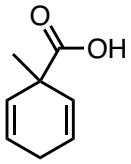

S1a

1-Methylcyclohexa-2,5-diene-1-carboxylic acid (S1a). Using Birch reduction-alkylation procedure A with benzoic acid (3.00 g, 24.6 mmol, 1.0 equiv) and iodomethane (3.06 mL, 49.1 mmol, 2.0 equiv) in THF (9.8 mL, 2.5 M) afforded **S1a** (3.18 g, 23.0 mmol) in 94% yield as a white solid, m.p. = 31.2 – 33.4˚C. Spectral data were in accordance with the literature.[8]

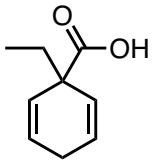

S1b

1-Ethylcyclohexa-2,5-diene-1-carboxylic acid (S1b). Using Birch reduction-alkylation procedure A with benzoic acid (3.03 g, 24.6 mmol, 1.0 equiv) and bromoethane (3.70 mL, 49.6 mmol, 2.0 equiv) in THF (9.8 mL, 2.5 M) provided **S1b** (3.74 g, 24.6 mmol) in 99% yield as a clear colorless oil. Spectral data were in accordance with the literature.[9]

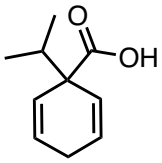

S1c

1-Isopropylcyclohexa-2,5-diene-1-carboxylic acid (S1c). Using Birch reduction-alkylation procedure A with benzoic acid (3.01 g, 24.6 mmol, 1.0 equiv) and 2-iodopropane (4.82 mL, 49.2 mmol, 2.0 equiv) in THF (9.8 mL, 2.5 M) afforded isopropyl diene acid S1c (7.07 g, 42.5 mmol) in 96% yield as a white solid, m.p. = 74.0-76.0˚C. Spectral data were in accordance with the literature.[10]

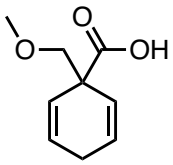

S1d

1-(Methoxymethyl)cyclohexa-2,5-diene-1-carboxylic acid (S1d). Using Birch reduction-alkylation procedure A with benzoic acid (3.02 g, 24.76 mmol, 1.0 equiv) and chloromethyl methyl ether (3.76 mL, 49.5 mmol, 2.0 equiv) in THF (9.9 mL, 2.5 M) afforded **S1d** (3.74 g, 22.2 mmol) in 90% yield as a white solid. m.p. = 66.9-70.5˚C. Spectral data were in accordance with a prior literature report.[10]

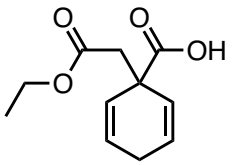

S1e

1-(2-Ethoxy-2-oxoethyl)cyclohexa-2,5-diene-1-carboxylic acid (S1e). Using Birch reduction-alkylation procedure A with benzoic acid (2.00 g, 16.4 mmol, 1.0 equiv) and ethyl 2-chloroacetate (3.51 mL, 32.8 mmol, 2.0 equiv) in THF (6.6 mL, 2.5 M) afforded **S1e** (3.41 g, 16.2 mmol) in 99% yield as a pale-yellow liquid that solidified to white crystals on cooling, m.p. = 63.5-66˚C. Spectral data were in accordance with a prior literature report.[10]

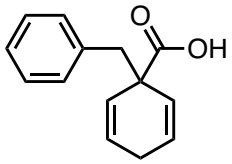

S1f

1-Benzylcyclohexa-2,5-diene-1-carboxylic acid (S1f). Using Birch reduction-alkylation procedure A (2.33 g, 19.1 mmol, 1.0 equiv) and benzyl chloride (4.38 mL, 38.1 mmol, 2.0 equiv) in THF (7.6 mL, 2.5 M) afforded **S1f** (3.83 g, 17.9 mmol) in 94% yield as a white crystalline solid, m.p. = 71.9-75.0˚C. Spectral data were in accordance with a prior literature report.[9]

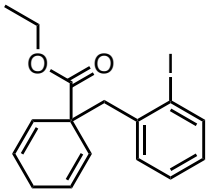

S1g

Ethyl-1-(2-iodobenzyl)cyclohexa-2,5-diene-1-carboxylate (S1g). Using Birch reduction-alkylation procedure B with ethyl benzoate (5.25 g, 35.0 mmol, 1.0 equiv) and 2-iodobenzyl bromide (11.4 g, 38.5 mmol, 1.1 equiv) in THF (14 mL, 2.5 M) afforded **S1g** (10.98 g, 29.82 mmol) in 85% yield as a clear colorless oil. Spectral data were in accordance with a prior literature report.[11]

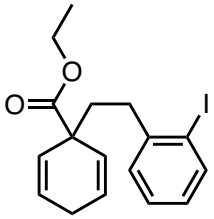

S1h

Ethyl-1-(2-iodophenethyl)cyclohexa-2,5-diene-1-carboxylate (S1h). Using Birch reduction-alkylation procedure B with ethyl benzoate (2.10 g, 14.0 mmol, 1.0 equiv) and 1-(2-bromoethyl)-2-iodobenzene (4.79 g, 15.4 mmol, 1.1 equiv) in THF (5.6 mL, 2.5 M) afforded crude product which was purified by column chromatography (silica, 4:1 hexanes: EtOAc) to afford pure **S1h** (1.39 g, 3.64 mmol) in 26% yield as clear colorless oil.[12]

^{1}H NMR (400 MHz, $CDCl_3$) δ 7.78 (dd, *J* = 7.9, 1.3 Hz, 1H), 7.30 – 7.20 (m, 1H), 7.18 (dd, *J* = 7.6, 1.8 Hz, 1H), 6.86 (td, *J* = 7.6, 1.8 Hz, 1H), 5.98 (dt, *J* = 10.5, 3.3 Hz, 2H), 5.87 (dt, *J* = 10.5, 2.0 Hz, 2H), 4.15 (q, *J* = 7.1 Hz, 2H), 2.70 (tt, *J* = 3.4, 2.0 Hz, 2H), 2.67 – 2.59 (m, 2H), 1.96 – 1.87 (m, 2H), 1.27 (d, *J* = 7.1 Hz, 3H).

^{13}C NMR (101 MHz, $CDCl_3$) δ_u 139.6, 139.5, 139.5, 129.5, 128.4, 127.8, 126.9, 126.3, 14.2; δ_d 174.5, 144.7, 100.4, 61.5, 60.9, 47.8, 39.7, 36.0, 26.3.

GC (Method B) t_R = 3.221 min. **EI-MS** m/z (%): 382.0 (M-56$^+$, 1), 309.0 (39), 231.0 (100), 216.9 (19), 181.1 (46), 167.1 (11), 152.1 (31), 105.1 (99), 94.1 (91), 77.1 (22), 51.1 (6).
HRMS (ESI) calculated for $C_{17}H_{20}O_2I$ $[M+H]^+$: 383.0508, found 383.0487.

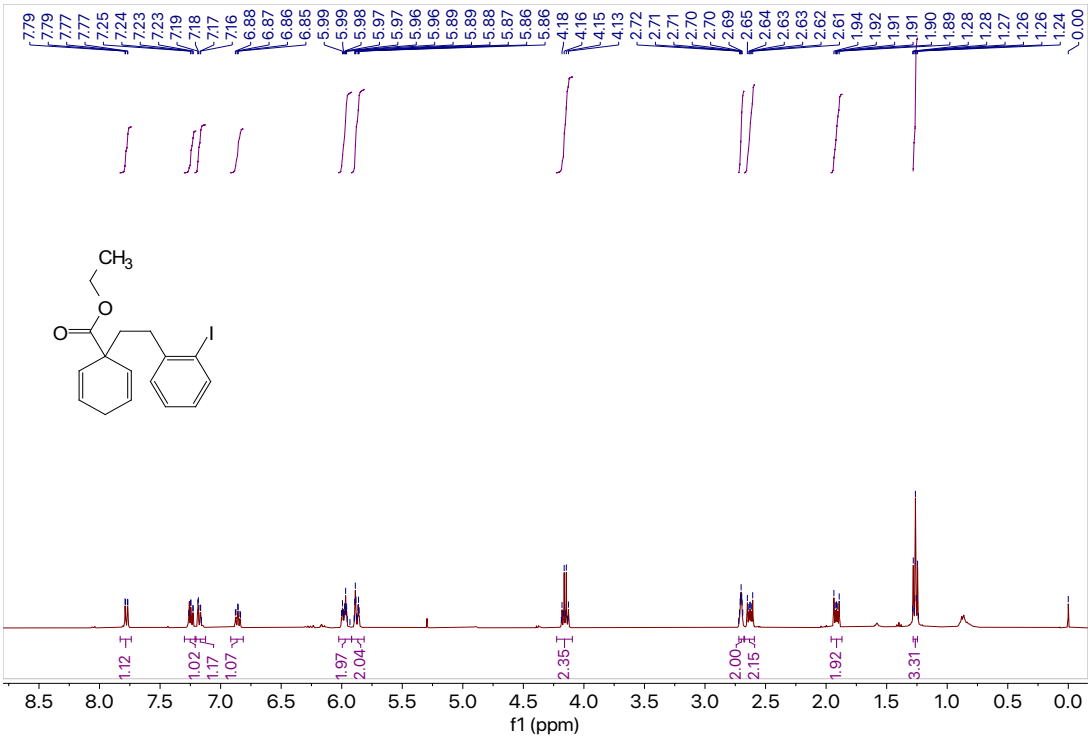

Figure 7.1 ^{1}H NMR (400 MHz, $CDCl_3$) of compound **S1h**.

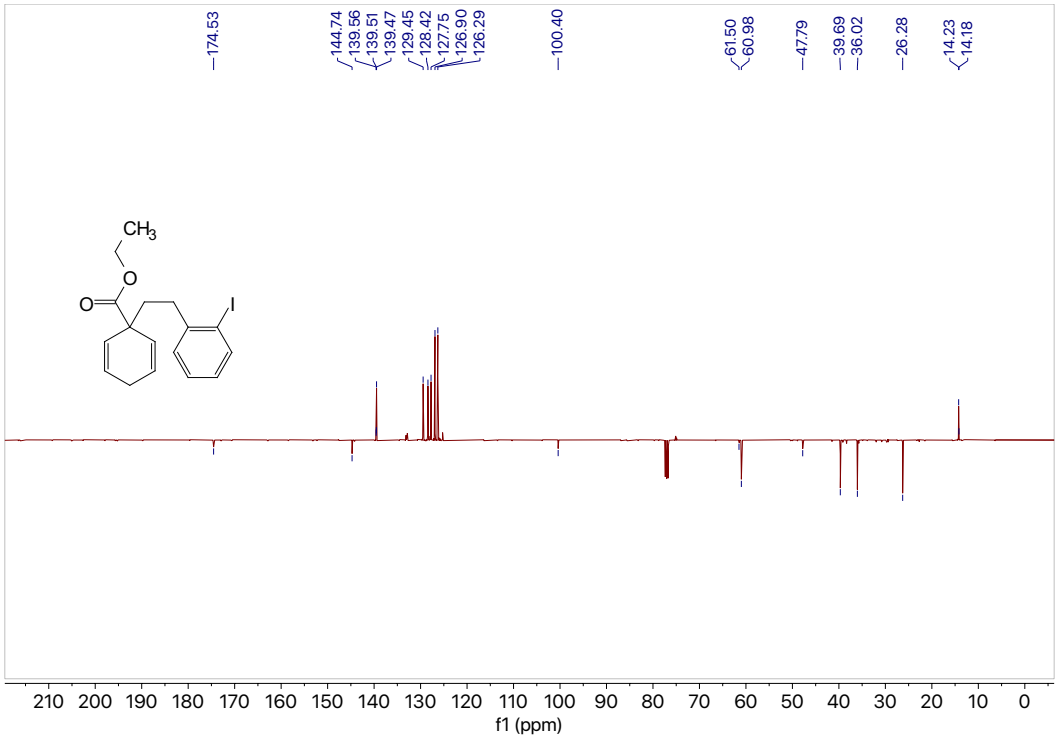

Figure 7.2 ^{13}C NMR (101 MHz) of compound **S1h**.

7.4 Synthesis of amine nucleophiles for amide bond formation

7.4.1 Aniline methylation general procedures and data

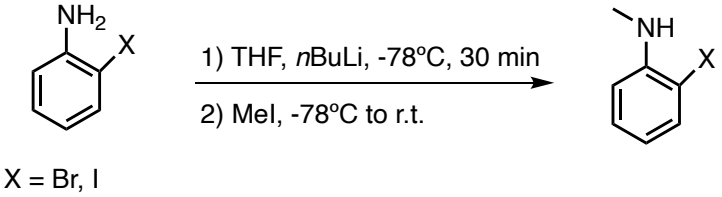

Scheme 7.2 Aniline methylation general reaction.

General procedure A

A flame dried round bottom flask with a stir bar, under argon, was charged with aniline (1.0 mmol, 1.0 equiv) in THF (2 mL, 0.5 M). The solution was cooled to -78˚C, then *n*BuLi (2.5 M in hexanes, 0.3 mL, 0.7 mmol, 0.7 equiv) was added slowly dropwise over 15 minutes. After the reaction mixture was stirred at -78˚C for 30 minutes, iodomethane (1.1 mmol, 1.1 equiv) was added over 5 minutes. The solution was stirred at -78˚C for 1 hour and then at room temperature overnight. The reaction was quenched with water and extracted with Et_2O (3 x 5 mL/mmol). The organic layers were combined and washed with brine, dried over $MgSO_4$, and concentrated in vacuo. The crude products were purified by column chromatography.

General procedure B

A flame dried round bottom flask with a stir bar, under argon, was charged with aniline (1.0 mmol, 1.0 equiv) in THF (2 mL, 0.5 M) and cooled to -78˚C. Using an automated syringe pump, MeLi (1.6 M in Et_2O, 0.6 mL, 1.0 mmol, 1.0 equiv) was added dropwise over 45 minutes. After the reaction mixture was stirred at -78˚C for 30 minutes, iodomethane (1.1 mmol, 1.1 equiv) was dissolved in THF (0.3 mL, 3.3 M) and added dropwise to flask over 10 minutes at -78 °C. The solution was stirred at -78˚C for 1 hour and then warmed to room temperature overnight. The reaction was quenched with saturated aqueous NH_4Cl (1.6 mL/mmol) and extracted with Et_2O (3 x 1.6 mL/mmol). The organic layers were combined and washed with brine, dried over $MgSO_4$, and concentrated in vacuo. The crude products were purified by column chromatography.

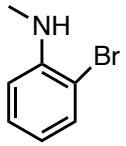

2-Bromo-*N*-methylaniline. Using the general aniline methylation procedure A with 2-bromoaniline (3.04 g, 17.7 mmol, 1.0 equiv) in THF (35 mL, 0.5 M) afforded crude product which was purified by column chromatography (silica, 10:1 hexanes: EtOAc) to afford pure 2-bromo-*N*-methylaniline (1.98 g, 10.6 mmol) in 60 % yield as a clear yellow oil. Spectral data were in accordance with a prior literature report.[13]

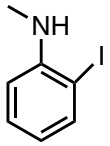

2-Iodo-*N*-methylaniline. Using the general aniline methylation procedure B with 2-iodoaniline (4.0 g, 18.3 mmol, 1.0 equiv) in THF (37 mL, 0.5 M) afforded crude product which was purified by column chromatography (silica, 60:1 hexanes: EtOAc) to afford pure 2-iodo-N-methylaniline (3.56 g, 15.3 mmol) in 83% yield as a yellow-orange oil. Spectral data were in accordance with a prior literature report.[13]

7.4.2 Synthesis of *N*-methyl pyrimidine general procedure and data

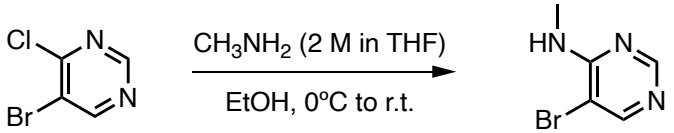

Scheme 7.3 N-methyl pyrimidine synthesis reaction.

General procedure and data

5-bromo-*N*-methylpyrimidin-4-amine. A flame dried round bottom flask with a stir bar, under argon, was charged with 5-bromo-4-chloropyrimidine (0.503 g, 2.59 mmol, 1.0 equiv) in ethanol (3.63 mL, 0.7 M) and cooled to 0˚C, then methylamine (2.0 M in THF, 12.9 mL, 25.9 mmol, 10.0 equiv) was added slowly, dropwise. Once completed, as

judged by GC-MS analysis, the reaction mixture was diluted with diethyl ether, filtered, and the filtrate was concentrated in vacuo. The crude product was purified by column chromatography (silica, 3:1 hexanes: EtOAc) to afford pure product (0.433 g, 2.30 mmol) in 89% yield as a white solid. Spectral data were in accordance with a prior literature report.[14]

7.4.3 Synthesis of vinyl bromide amine general procedure and data

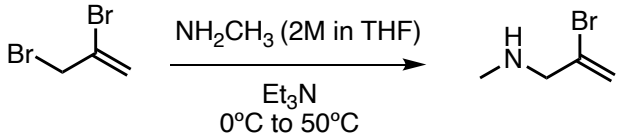

Scheme 7.4 Vinyl bromide amine synthesis reaction.

General procedure and data

2-bromo-*N*-methylprop-2-en-1-amine. A flame dried round bottom flask with a stir bar, under argon, was charged with methylamine (2 M in THF, 6.75 mL, 13.5 mmol, 3.0 equiv) and cooled to 0˚C, then triethylamine (0.63 mL, 4.50 mmol, 1.0 equiv) and 2,3-dibromoprop-1-ene (0.44 mL, 4.50 mmol, 1.0 equiv) were added. The solution was stirred at 50˚C. The reaction progress was monitored using ninhydrin stray for TLC. Upon completion, the reaction mixture was filtered using a pipet packed with silica gel and celite, then washed with excess DCM. The crude product was obtained (0.684 g, 4.56 mmol) in 101% yield as an orange oil and was used without further purification. Spectral data were in accordance with a prior literature report.[15]

7.5 Amide synthesis general procedure and data

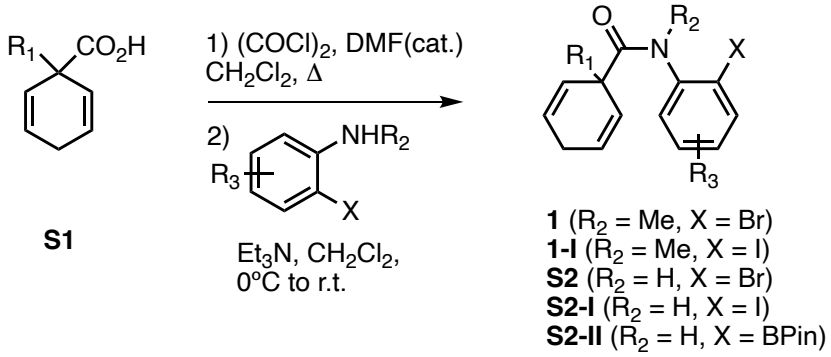

Scheme 7.5 Benzamide synthesis general reaction.

General procedure

In a round bottom flask with a stir bar, oxalyl chloride (2.2 mmol, 2.2 equiv) was dissolved in DCM (5.5 mL, 0.4 M) and a catalytic amount of DMF (1.4 µL, 0.02 equiv) was added. The Birch product (1.0 mmol, 1.0 equiv) was dissolved in DCM (2.5 mL, 0.4 M) and added dropwise to the flask. The reaction was refluxed under argon for an hour

until it turned deep yellow. Once completed, as judged by GC-MS analysis, the reaction was concentrated under vacuum to remove excess oxalyl chloride.

In a round bottom flask with a stir bar, 2-haloaniline or purified 2-halo-*N*-methylaniline (1.05-1.3 mmol, 1.05-1.3 equiv) was dissolved in DCM (2.5 mL, 0.4 M) and cooled to 0°C. Triethylamine (2.5 mmol, 2.5 equiv) was added dropwise followed shortly thereafter by the addition of the acid chloride (1.0 mmol, 1.0 equiv) in DCM (2.5 mL, 0.4 M). The mixture was allowed to warm to room temperature and react overnight. The reaction mixture was diluted with DCM and washed with saturated $NaHCO_3$, 1N HCl (not used for pyridine and pyrimidine containing substrates), brine and then dried with $MgSO_4$. The crude product was concentrated under vacuum and purified by column chromatography.

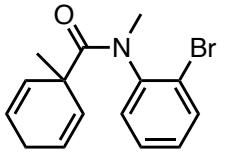

1a

***N*-(2-Bromophenyl)-*N*,1-dimethylcyclohexa-2,5-diene-1-carboxamide (1a).** Using the general benzamide synthesis procedure, diene acid **S1a** (1.15g, 7.33 mmol, 1.0 equiv) in DCM (18.3 mL, 0.4 M) reacted with 2-bromo-*N*-methylaniline (1.77 g, 9.53 mmol, 1.3 equiv) in DCM (23.8 mL, 0.4 M) to afford the crude product which was purified by column chromatography (silica, 4:1 hexanes: EtOAc) to afford pure **1a** (2.08 g, 6.79 mmol) in 93% yield as a white solid, m.p. = 42.2 – 44.4°C.
^{1}H NMR (400 MHz, $CDCl_3$) δ 7.46 (d, *J* = 7.5 Hz, 1H), 7.23 – 7.17 (m, 1H), 7.13 – 7.02 (m, 2H), 5.59 (d, *J* = 10.1 Hz, 1H), 5.48 – 5.38 (m, 2H), 4.94 (d, *J* = 10.1 Hz, 1H), 3.08 (s, 3H), 2.22 (d, *J* = 23.1 Hz, 1H), 1.83 (d, *J* = 23.0 Hz, 1H), 1.26 (s, 3H).
^{13}C NMR (101 MHz, $CDCl_3$) δ_u 133.1, 131.2, 131.1, 128.9, 128.3, 127.8, 123.5, 121.7, 39.0, 29.3; δ_d 174.2, 143.3, 124.6, 45.8, 25.9.
GC (Method B) t_R = 2.272 min. EI-MS m/z (%): 305 (M+, 1), 214 (45), 185 (18), 134 (100), 105 (13), 93 (53), 77 (46), 65 (8), 51 (8).
HRMS (ESI) calculated for $C_{15}H_{17}ONBr$ $[M+H]^+$: 306.0494, found 306.0493.

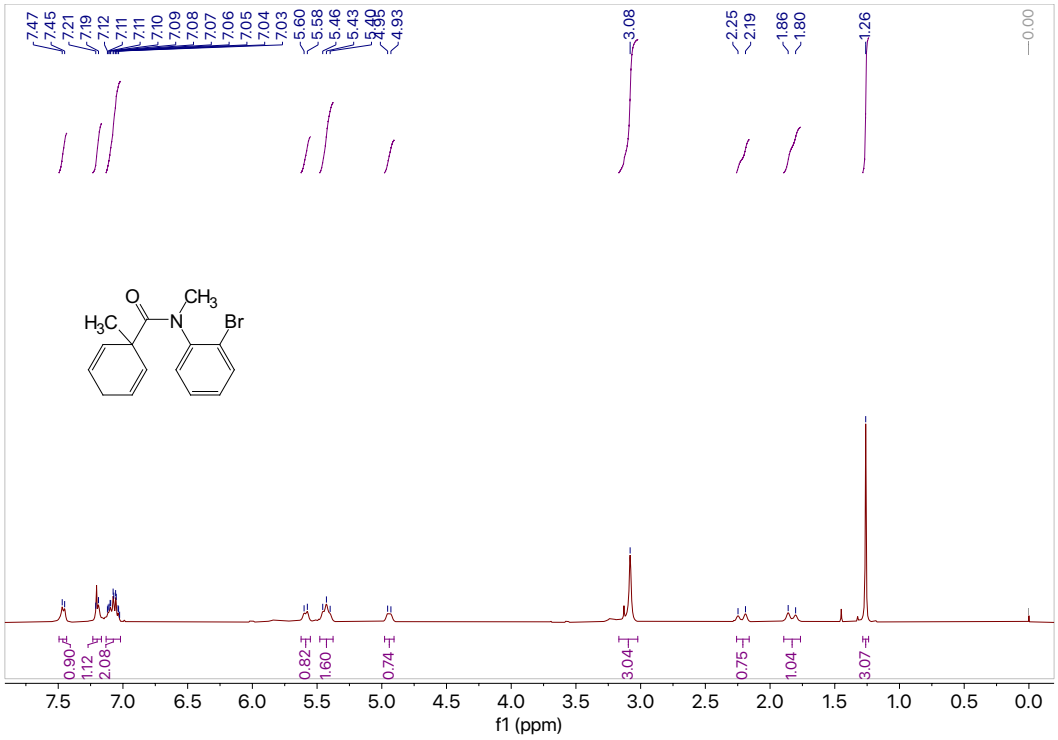

Figure 7.3 ^{1}H NMR (400 MHz, $CDCl_3$) of compound **1a**.

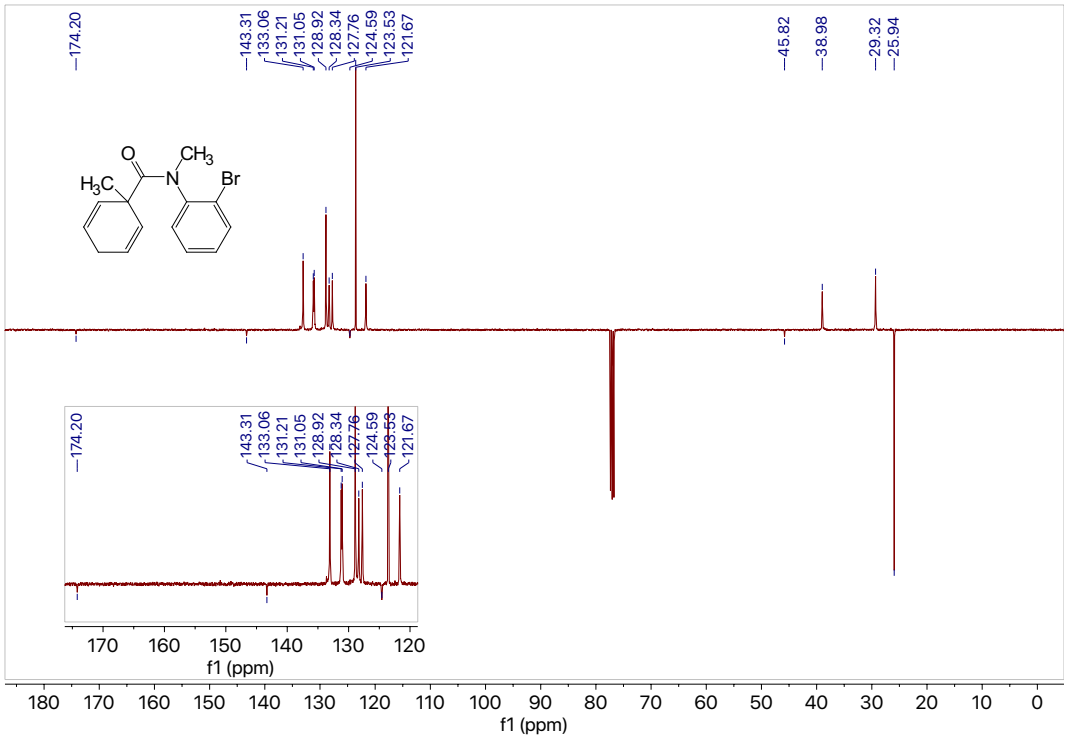

Figure 7.4 ^{13}C NMR (101 MHz, $CDCl_3$) of compound **1a**.

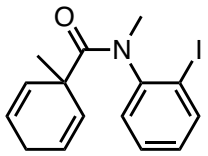

1a-I

***N*-(2-Iodophenyl)-*N*,1-dimethylcyclohexa-2,5-diene-1-carboxamide (1a-I).** Using the general benzamide synthesis procedure, diene acid **S1a** (1.16 g, 7.42 mmol, 1.0 equiv) in DCM (18.6 mL, 0.4 M) reacted with 2-iodo-*N*-methylaniline (2.25 g, 9.65 mmol, 1.3 equiv) in DCM (24.1 mL, 0.4 M) to afford the crude product which was purified by column chromatography (silica, 4:1 hexanes: EtOAc) to afford pure **1a-I** (2.07 g, 5.86 mmol) in 79% yield as a white solid, m.p. = 35.8 – 38.2°C.

^{1}H NMR (400 MHz, $CDCl_3$) δ 7.80 (d, *J* = 7.9 Hz, 1H), 7.27 – 7.18 (m, 2H), 6.96 (t, *J* = 7.9 Hz, 1H), 5.64 (s, 1H), 5.56 (d, *J* = 9.9 Hz, 1H), 5.49 (s, 1H), 5.01 (s, 1H), 3.14 (s, 3H), 2.30 (d, *J* = 23.2 Hz, 1H), 1.94 (d, *J* = 23.2 Hz, 1H), 1.35 (s, 3H).

^{13}C NMR (101 MHz, $CDCl_3$) δ_u 139.4, 131.2, 130.2, 128.9, 128.8, 123.6, 121.6, 39.4, 29.4; δ_d 174.2, 146.6, 101.8, 45.8, 26.0.

GC (Method B) t_R = 2.608 min. EI-MS m/z (%): 353.0 (M+, 1), 260.9 (92), 243.9 (19), 230.9 (20), 202.8 (7), 182.1 (1), 134.0 (100), 105.0 (30), 91.0 (47), 77.0 (47), 64.0 (11), 51.0 (12).

HRMS (ESI) calculated for $C_{15}H_{17}ONI$ $[M+H]^+$: 354.0355, found 354.0350.

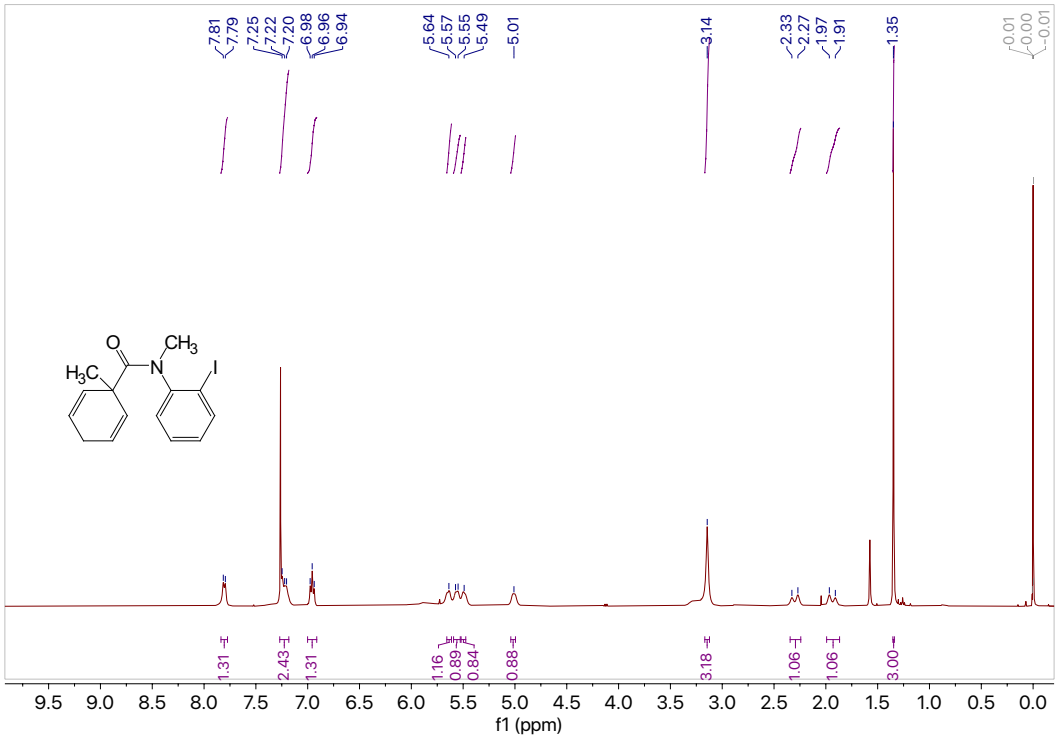

Figure 7.5 ^{1}H NMR (400 MHz, $CDCl_3$) of compound **1a-I**.

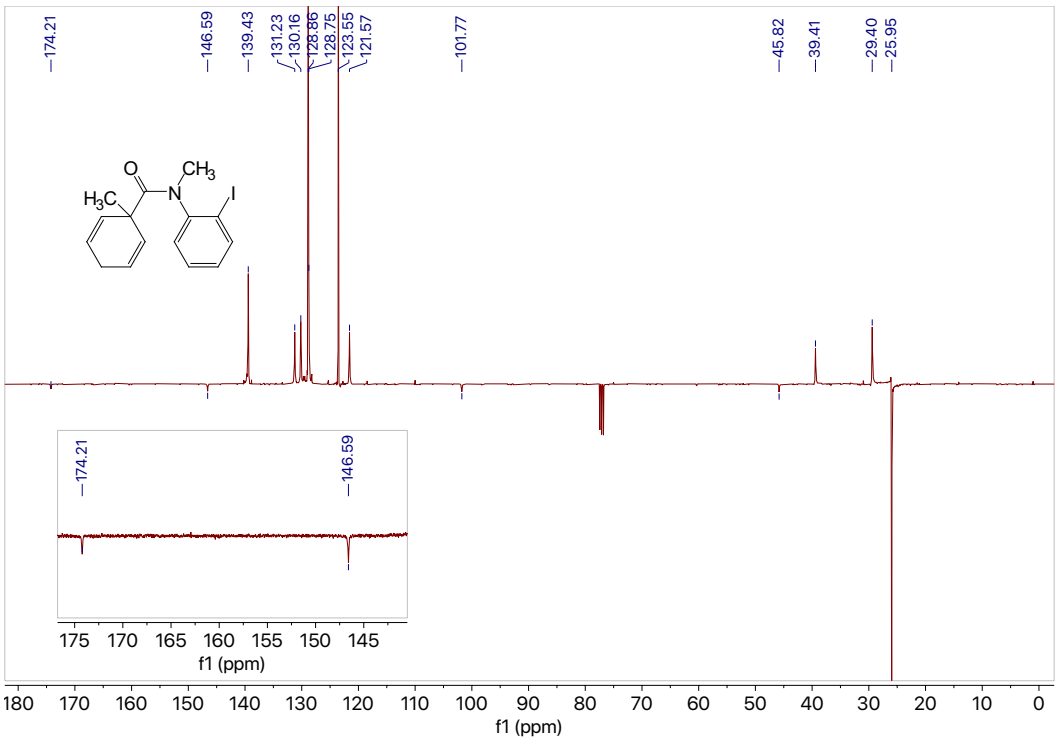

Figure 7.6 ^{13}C NMR (101 MHz, $CDCl_3$) of compound **1a-I**.

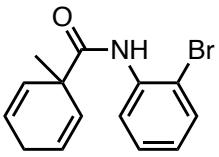

S2b

***N*-(2-Bromophenyl)-1-methylcyclohexa-2,5-diene-1-carboxamide (S2b).** Using the general benzamide synthesis procedure, diene acid **S1a** (0.505 g, 3.62 mmol, 1.0 equiv) in DCM (9.0 mL, 0.4 M) reacted with 2-bromoaniline (0.44 mL, 3.87 mmol, 1.1 equiv) in DCM (9.7 mL, 0.4 M) to afford the crude product which was purified by column chromatography (silica, 10:1 hexanes: EtOAc) to afford pure **S2b** (1.01 g, 3.46 mmol) in 95% yield as a clear colorless oil.

^{1}H NMR (400 MHz, $CDCl_3$) δ 8.32 (dd, J = 8.3, 1.6 Hz, 1H), 8.28 (s, 1H), 7.41 (dd, J = 8.1, 1.5 Hz, 1H), 7.25 – 7.16 (m, 1H), 6.89 – 6.80 (m, 1H), 5.97 – 5.87 (m, 2H), 5.76 – 5.67 (m, 2H), 2.86 – 2.65 (m, 2H), 1.34 (s, 3H).

^{13}C NMR (101 MHz, $CDCl_3$) δ_u 132.2, 129.7, 128.4, 126.1, 124.8, 120.9, 24.7; δ_d 172.8, 136.1, 113.1, 46.4, 26.0.

GC (Method B) t_R = 2.373 min. EI-MS m/z (%): 291.1 ($M+1^+$, 5), 276.0 (4), 198.9 (9), 171.0 (11), 120.0 (26), 93.1 (100), 77.1(35), 65.1 (10), 51.1 (5).

HRMS (ESI) calculated for $C_{14}H_{15}ONBr$ $[M+H]^+$: 292.0337, found 292.0331.

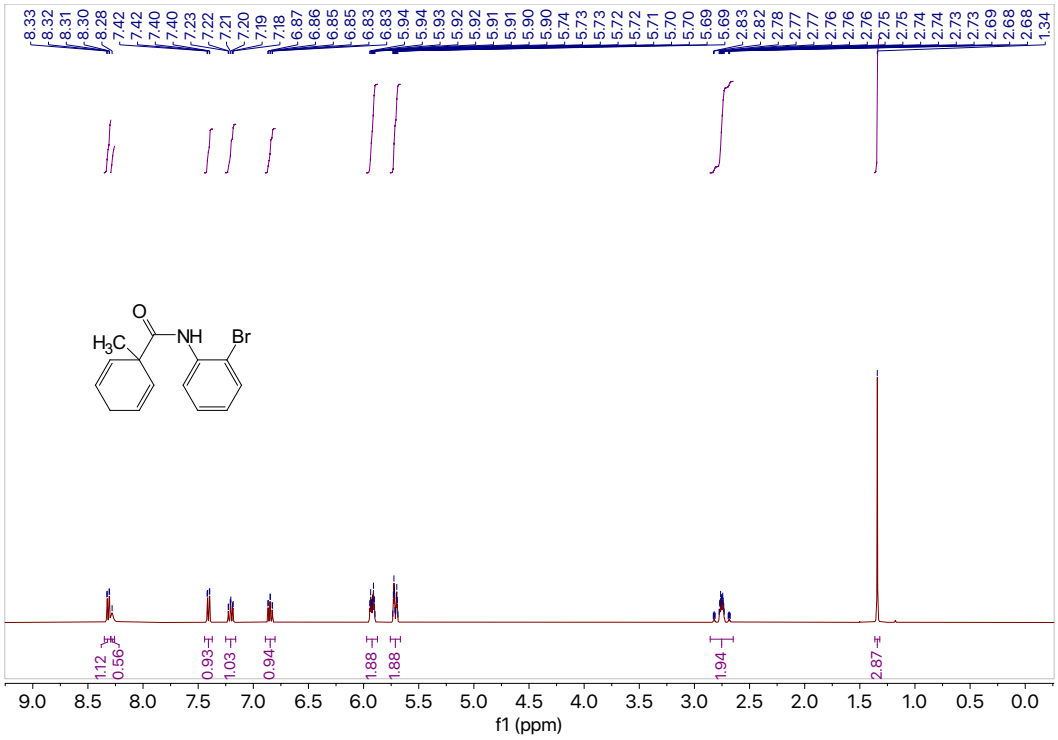

Figure 7.7 ^{1}H NMR (400 MHz, $CDCl_3$) of compound **S2b**.

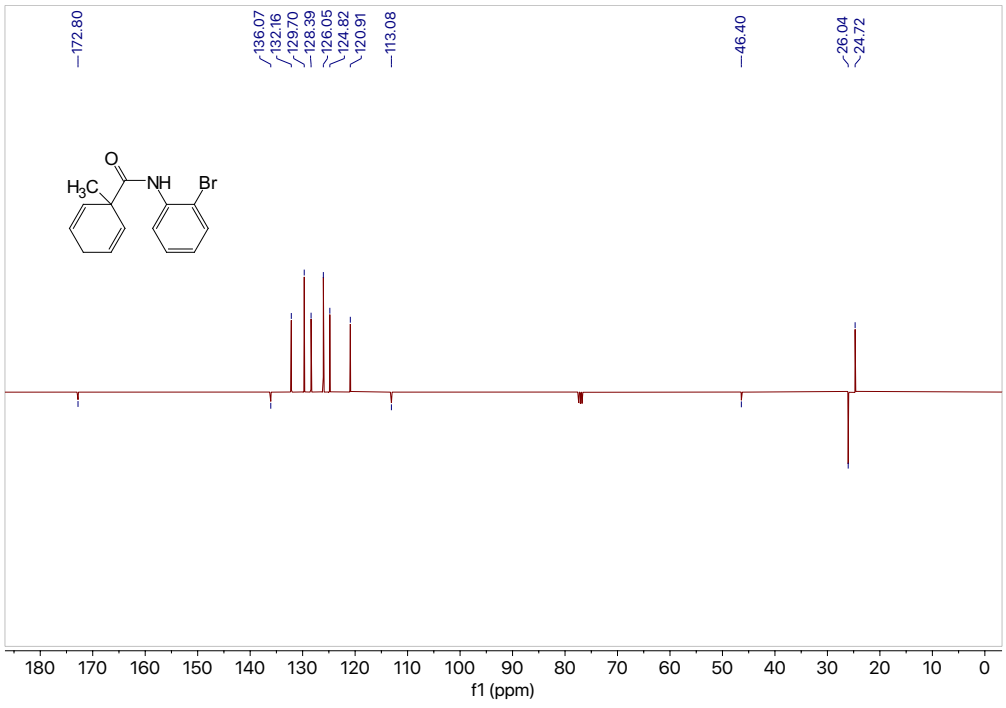

Figure 7.8 ^{13}C NMR (101 MHz, $CDCl_3$) of compound **S2b**.

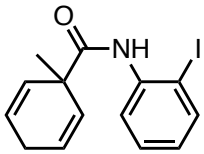

S2b-I

***N*-(2-Iodophenyl)-1-methylcyclohexa-2,5-diene-1-carboxamide (S2b-I).** Using the general benzamide synthesis procedure, diene acid **S1a** (0.299 g, 2.16 mmol, 1.0 equiv) in DCM (6.5 mL, 0.4 M) reacted with 2-iodoaniline (0.615 g, 2.81 mmol, 1.3 equiv) in DCM (7 mL, 0.4 M) to afford the crude product which was purified by column chromatography (silica, 9:1 hexanes: EtOAc) to afford pure **S2b-I** (0.694 g, 2.05 mmol) in 99% yield as an off-white solid, m.p. = 72.7 – 75.0°C.

^{1}H NMR (400 MHz, $CDCl_3$) δ 8.33 (dd, J = 8.2, 1.6 Hz, 1H), 8.17 (s, 1H), 7.76 (dd, J = 8.0, 1.5 Hz, 1H), 7.39 – 7.30 (m, 1H), 6.82 (td, J = 7.6, 1.6 Hz, 1H), 6.09 – 5.99 (m, 2H), 5.87 – 5.78 (m, 2H), 3.00 – 2.76 (m, 2H), 1.44 (s, 3H).

^{13}C NMR (101 MHz, $CDCl_3$) δ_u 138.8, 129.7, 129.3, 126.1, 125.5, 120.9, 24.8; δ_d 173.0, 138.6, 89.0, 46.3, 26.2.

GC (Method B) t_R = 2.792 min. EI-MS m/z (%): 339.0 (M+, 13), 324.0 (9), 246.9 (35), 218.9 (20), 202.9 (4), 120.0 (39), 93.0 (100), 77.0 (39), 64.0 (8), 51.0 (5).

HRMS (ESI) calculated for $C_{14}H_{15}ONI$ $[M+H]^+$: 340.0198, found 340.0197.

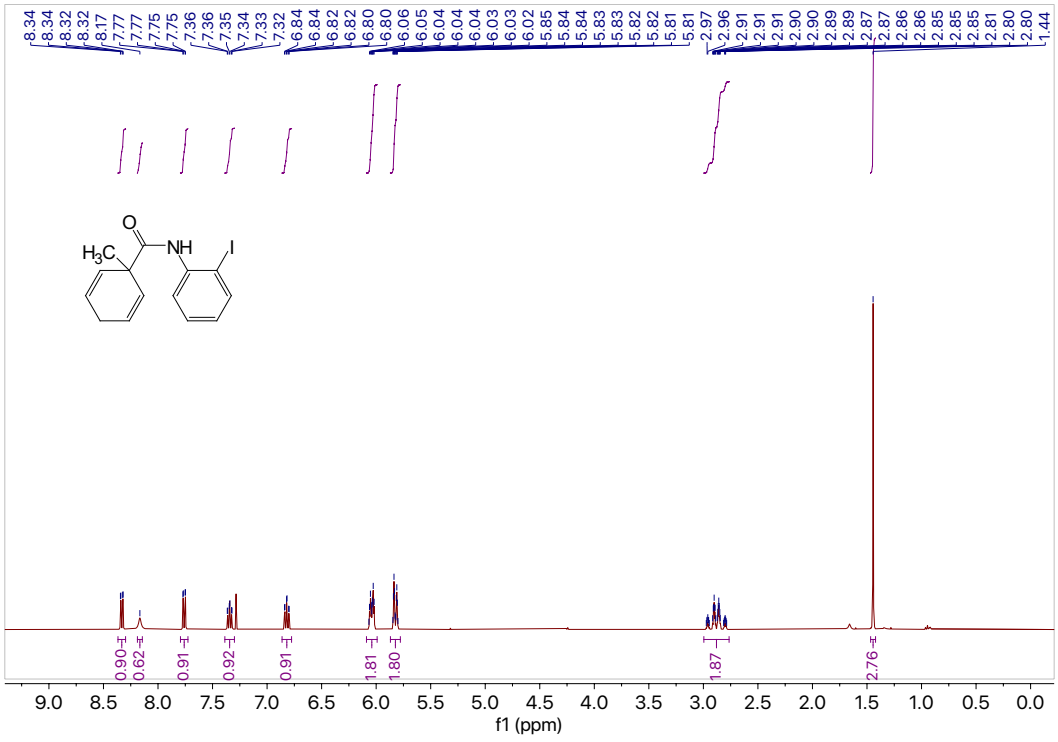

Figure 7.9 ^{1}H NMR (400 MHz, $CDCl_3$) of compound **S2b-I**.

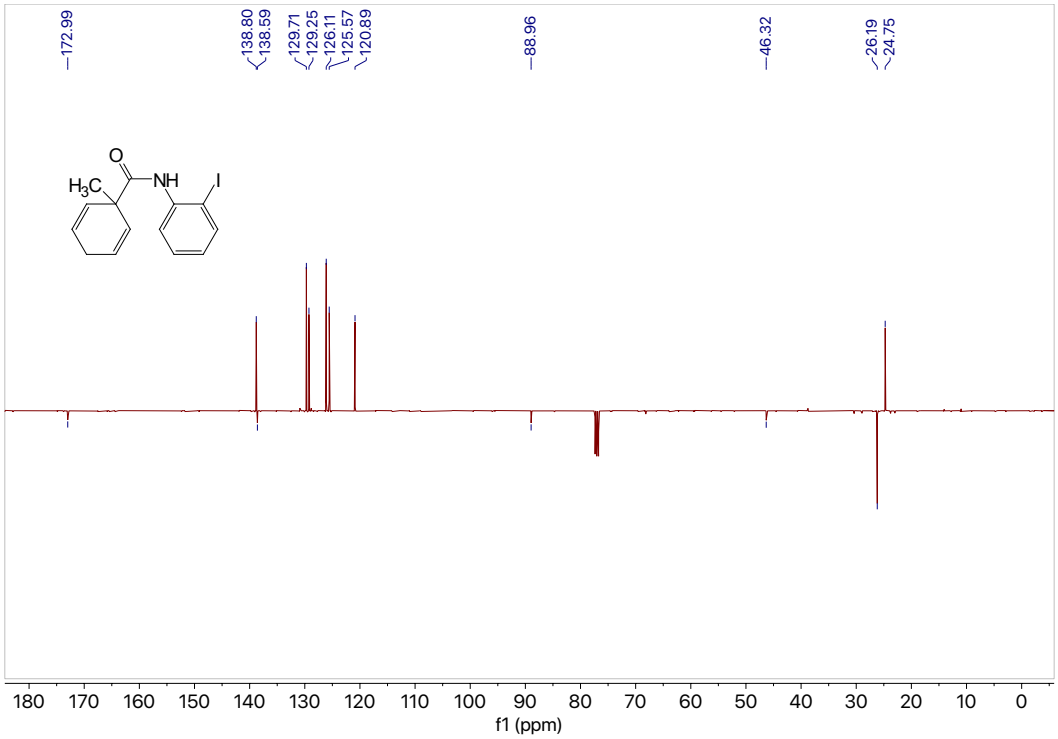

Figure 7.10 ^{13}C NMR (101 MHz, $CDCl_3$) of compound **S2b-I**.

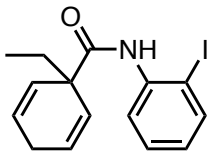

S2c-I

1-Ethyl-*N*-(2-iodophenyl)cyclohexa-2,5-diene-1-carboxamide (S2c-I). Using the general benzamide synthesis procedure, diene acid **S1b** (0.501 g, 3.26 mmol, 1.0 equiv) in DCM (8.2 mL, 0.4 M) reacted with 2-iodoaniline (0.935 g, 4.27 mmol, 1.3 equiv) in DCM (10.7 mL, 0.4 M) to afford the crude product which was purified by column chromatography (silica, 9:1 hexanes: EtOAc) to afford pure **S2c-I** (1.10 g, 3.11 mmol) in 95% yield as a white solid.

^{1}H NMR (400 MHz, $CDCl_3$) δ 8.31 (dd, J = 8.3, 1.6 Hz, 1H), 8.13 (s, 1H), 7.74 (dd, J = 7.9, 1.5 Hz, 1H), 7.32 (ddd, J = 8.5, 7.2, 1.5 Hz, 1H), 6.80 (td, J = 7.6, 1.6 Hz, 1H), 6.16 – 6.06 (m, 2H), 5.72 (dt, J = 10.4, 2.1 Hz, 2H), 2.96 – 2.73 (m, 2H), 1.87 (q, J = 7.5 Hz, 2H), 0.86 (t, J = 7.5 Hz, 3H).

^{13}C NMR (101 MHz, $CDCl_3$) δ_u 138.8, 129.2, 128.1, 127.8, 125.6, 121.1, 8.9; δ_d 172.8, 138.6, 89.1, 50.8, 29.5, 26.5.

GC (Method B) t_R = 3.101 min. EI-MS m/z (%): 353.1 (M+, 16), 324 (19), 246.9 (50), 218.9 (29), 202.9 (4), 120 (35), 107.0 (64), 91.0 (33), 79.0 (100), 65.0 (8).

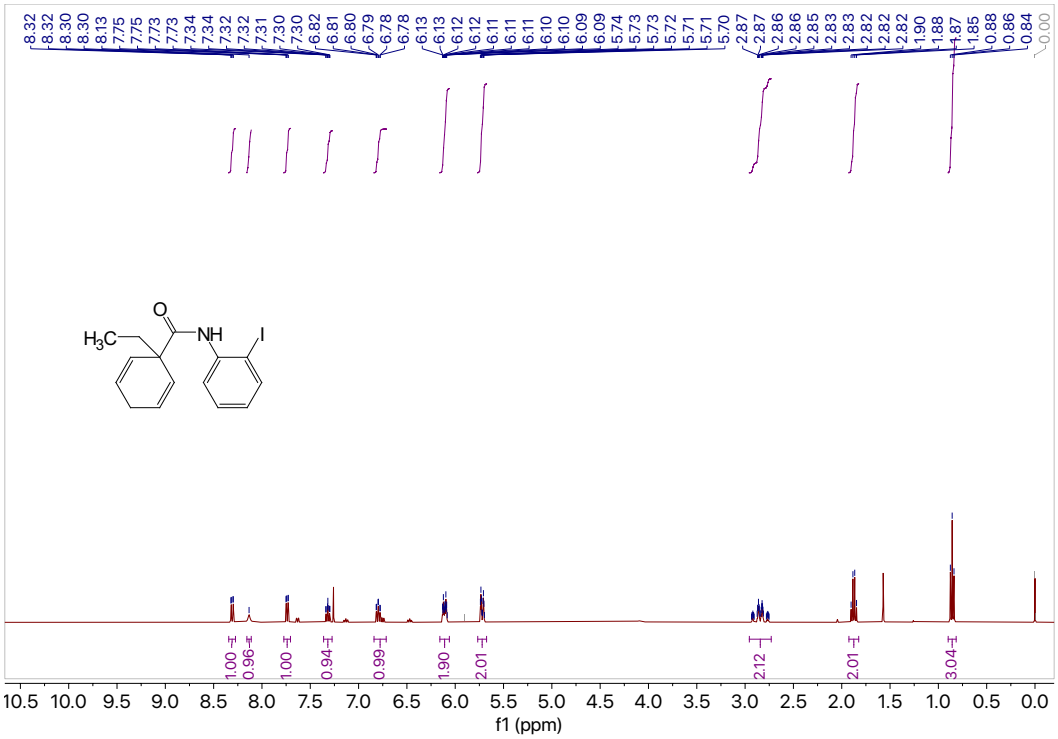

Figure 7.11 ^{1}H NMR (400 MHz, $CDCl_3$) of compound **S2c-I**.

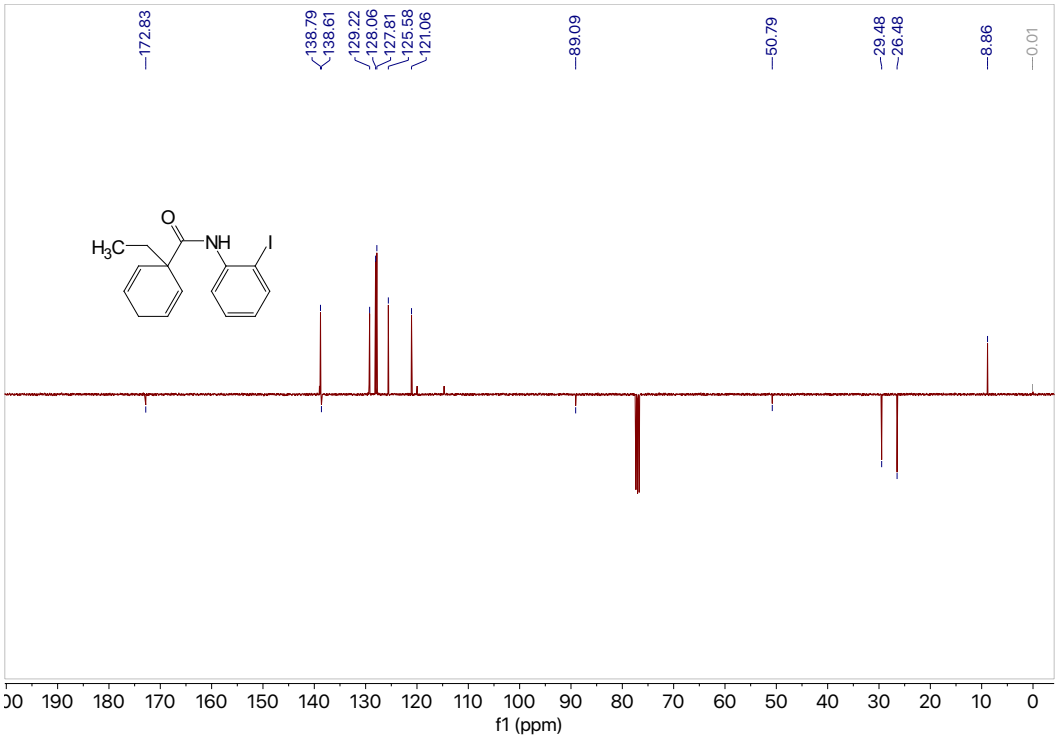

Figure 7.12 ^{13}C NMR (101 MHz, $CDCl_3$) of compound **S2c-I**.

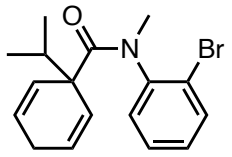

1d

***N*-(2-Bromophenyl)-1-isopropyl-*N*-methylcyclohexa-2,5-diene-1-carboxamide (1d).** Using the general benzamide synthesis procedure, diene acid **S1c** (0.501 g, 3.00 mmol, 1.0 equiv) in DCM (7.5 mL, 0.4 M) reacted with 2-bromo-*N*-methylaniline (0.587 g, 3.153 mmol, 1.05 equiv) in DCM (7.9 mL, 0.4 M) to afford the crude product which was purified by column chromatography (silica, 20:1 hexanes: EtOAc) to afford pure **1d** (0.897 g, 2.70 mmol) in 90% yield as a white solid, m.p. = 85.4 – 86.1°C.

^{1}H NMR (400 MHz, $CDCl_3$) δ 7.50 – 7.43 (m, 1H), 7.15 – 7.01 (m, 3H), 5.54 (d, *J* = 10.3 Hz, 1H), 5.43 (d, *J* = 10.4 Hz, 1H), 5.25 (d, *J* = 10.3 Hz, 1H), 5.02 (d, *J* = 10.7 Hz, 1H), 3.09 (s, 3H), 2.45 (hept, *J* = 6.8 Hz, 1H), 2.25 (d, *J* = 23.2 Hz, 1H), 2.01 (d, *J* = 20.1 Hz, 1H), 0.80 (d, *J* = 6.7 Hz, 3H), 0.61 (d, *J* = 7.0 Hz, 3H).

^{13}C NMR (101 MHz, $CDCl_3$) δ_u 133.0, 130.4, 130.1, 128.9, 128.9, 127.9, 124.9, 123.9, 38.9, 35.9, 17.8, 17.1; δ_d 174.7, 143.8, 124.3, 54.0, 26.6.

GC (Method B) t_R = 2.692 min. EI-MS m/z (%): 333.1 (M-1$^+$, 2), 290.0 (23), 214.0 (55), 185.0 (16), 134.0 (100), 121.1 (9), 105.0 (72), 91.0 (9), 77.1 (78), 51.0 (8).

HRMS (ESI) calculated for $C_{17}H_{21}ONBr$ $[M+H]^+$: 334.0807, found 334.0806.

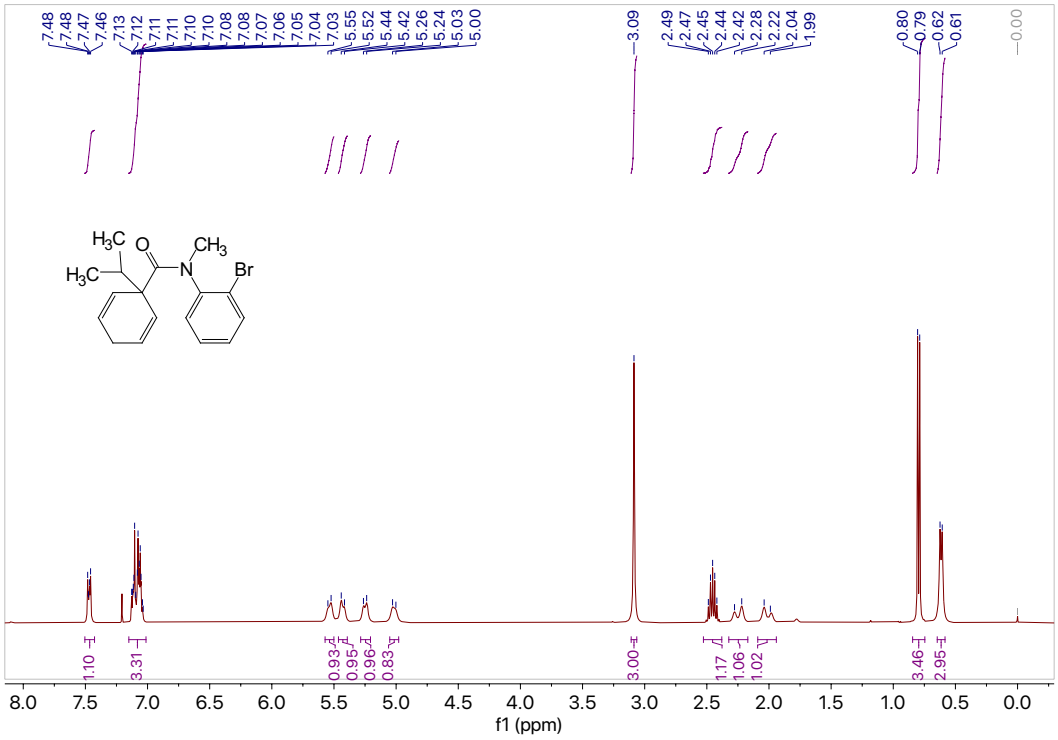

Figure 7.13 ^{1}H NMR (400 MHz, $CDCl_3$) of compound **1d**.

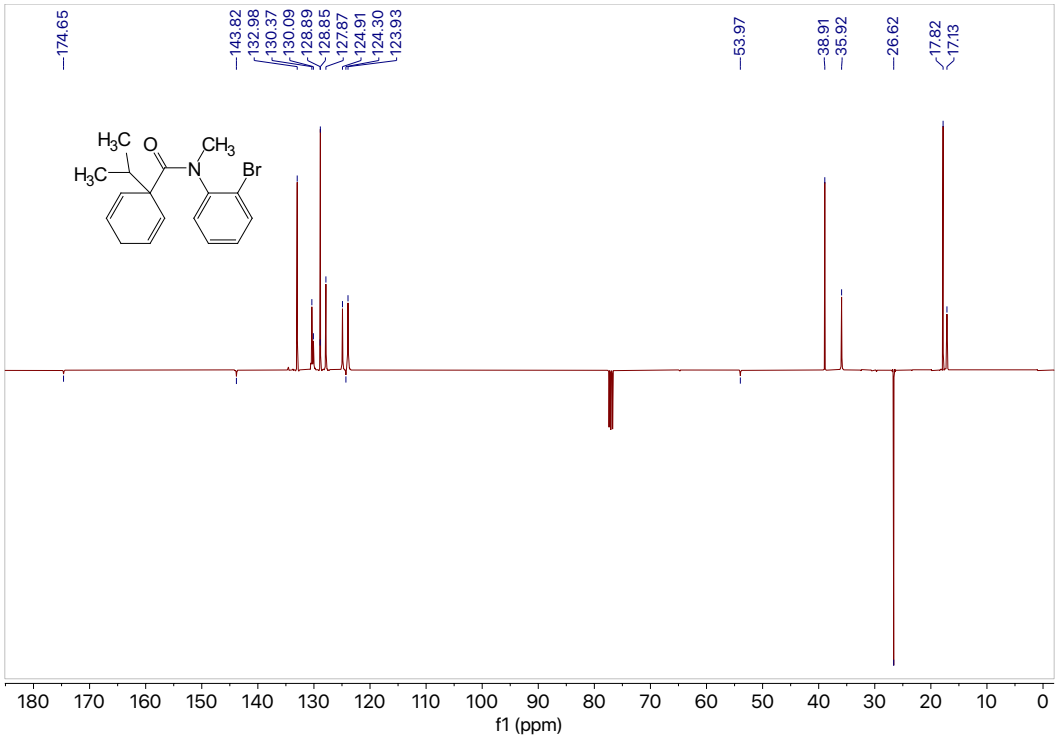

Figure 7.14 ^{13}C NMR (101 MHz, $CDCl_3$) of compound **1d**.

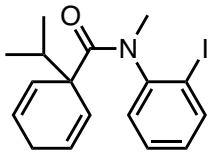

1d-I

***N*-(2-Iodophenyl)-1-isopropyl-*N*-methylcyclohexa-2,5-diene-1-carboxamide (1d-I).** Using the general benzamide synthesis procedure, diene acid **S1c** (0.340 g, 2.05 mmol, 1.0 equiv) in DCM (5.1 mL, 0.4 M) reacted with 2-iodo-*N*-methylaniline (0.620 g, 2.66 mmol, 1.3 equiv) in DCM (6.7 mL, 0.4 M) to afford the crude product which was purified by column chromatography (silica, 9:1 hexanes: EtOAc) to afford pure **1d-I** (0.267 g, 1.64 mmol) in 84% yield as a white solid, m.p. = 89.6 – 90.8°C.

^{1}H NMR (400 MHz, $CDCl_3$) δ 7.74 (d, J = 7.9 Hz, 1H), 7.11 (d, J = 3.9 Hz, 2H), 6.93 – 6.84 (m, 1H), 5.66 – 5.34 (m, 2H), 5.27 (d, J = 10.4 Hz, 1H), 5.01 (s, 1H), 3.08 (s, 3H), 2.46 (hept, J = 6.9 Hz, 1H), 2.31 – 1.94 (m, 2H), 0.83 (d, J = 6.8 Hz, 3H), 0.62 (d, J = 6.9 Hz, 2H).

^{13}C NMR (101 MHz, $CDCl_3$) δ_u 139.4, 130.3, 129.6, 128.8, 128.8, 125.0, 124.3, 123.8, 39.4, 36.0, 18.1, 17.1; δ_d 174.8, 147.1, 101.5, 54.0, 26.7.

GC (Method B) t_R =3.051 min. EI-MS m/z (%): 381.0 (M+, 2), 338.0 (20), 260.9 (75), 244.9 (5), 230.9 (15), 210.1 (14), 134.0 (100), 105.0 (80), 91.0 (9), 77.0 (39), 51.0 (8).

HRMS (ESI) calculated for $C_{17}H_{21}ONI$ $[M+H]^+$: 382.0668, found 382.0664.

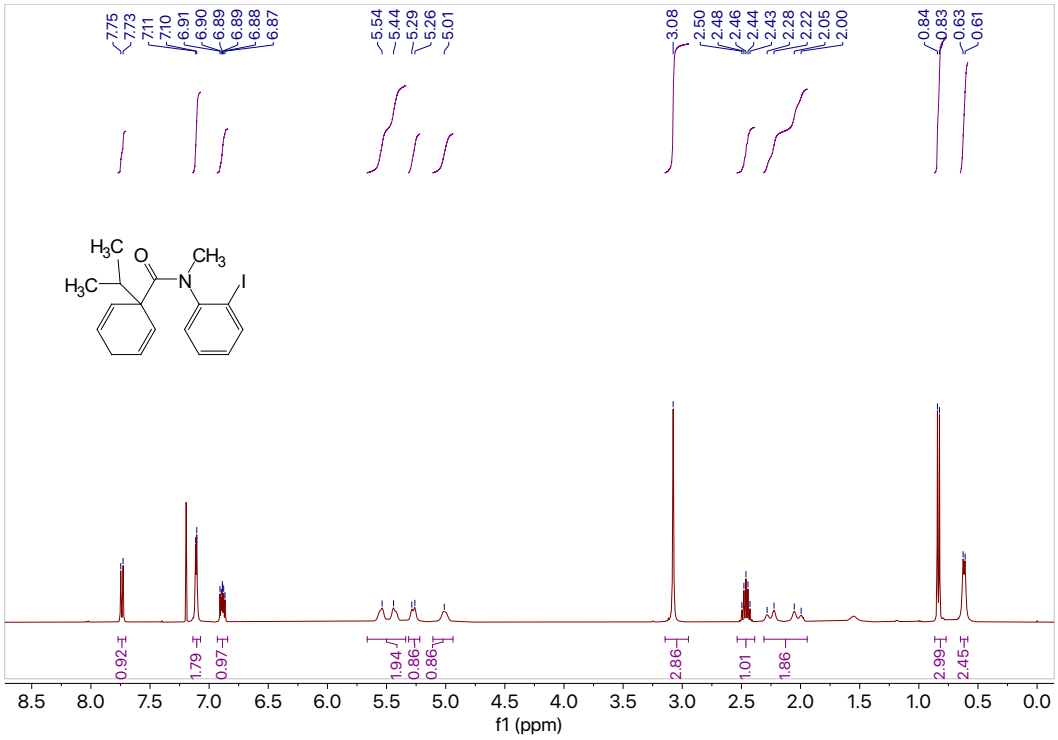

Figure 7.15 ^{1}H NMR (400 MHz, $CDCl_3$) of compound **1d-I**.

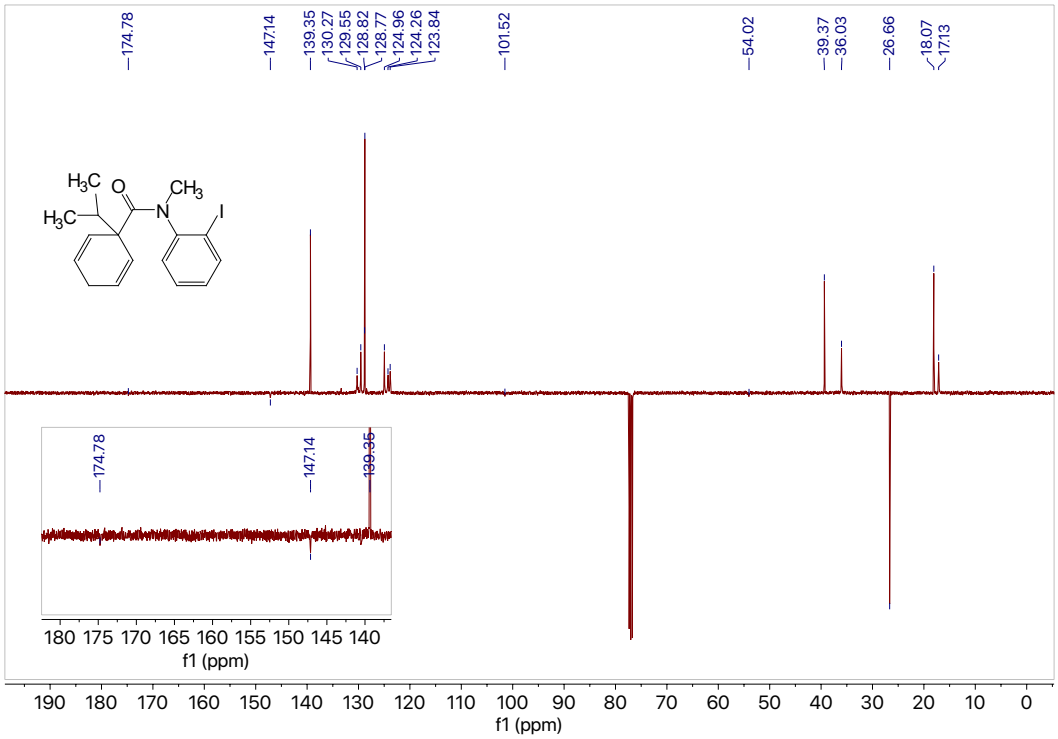

Figure 7.16 ^{13}C NMR (101 MHz, $CDCl_3$) of compound **1d-I**.

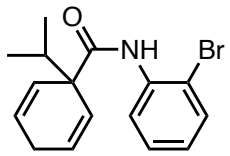

S2e

***N*-(2-Bromophenyl)-1-isopropylcyclohexa-2,5-diene-1-carboxamide (S2e).** Using the general benzamide synthesis procedure, diene acid **S1c** (0.800 g, 4.81 mmol, 1.0 equiv) in DCM (12.0 mL, 0.4 M) reacted with 2-bromoaniline (1.08 g, 6.25 mmol, 1.3 equiv) in DCM (15.6 mL, 0.4 M) to afford the crude product which was purified by column chromatography (silica, 9:1 hexanes: EtOAc) to afford pure **S2e** (1.18 g, 3.68 mmol) in 79% yield as a yellow oil.

^{1}H NMR (400 MHz, $CDCl_3$) δ 8.42 (dd, J = 8.3, 1.6 Hz, 1H), 8.35 (s, 1H), 7.50 (dd, J = 8.0, 1.5 Hz, 1H), 7.29 (ddd, J = 8.6, 7.4, 1.5 Hz, 1H), 6.94 (td, J = 7.7, 1.6 Hz, 1H), 6.17 – 6.07 (m, 2H), 5.78 (dp, J = 10.6, 2.1 Hz, 2H), 2.81 (qd, J = 3.3, 1.8 Hz, 2H), 2.48 (hept, J = 6.9 Hz, 1H), 0.90 (d, J = 6.9 Hz, 6H).

^{13}C NMR (101 MHz, $CDCl_3$) δ_u 132.2, 128.5, 128.4, 126.7, 124.9, 121.3, 33.4, 17.7; δ_d 172.5, 136.1, 113.4, 54.4, 26.8.

GC (Method B) t_R = 2.897 min. EI-MS m/z (%): 321.1 ($M+1^+$, 8), 277.9 (14), 198.9 (21), 170.9 (19), 121.0 (55), 105.0 (85), 91.0 (25), 79.0 (100), 65.1 (8), 51.0 (7).

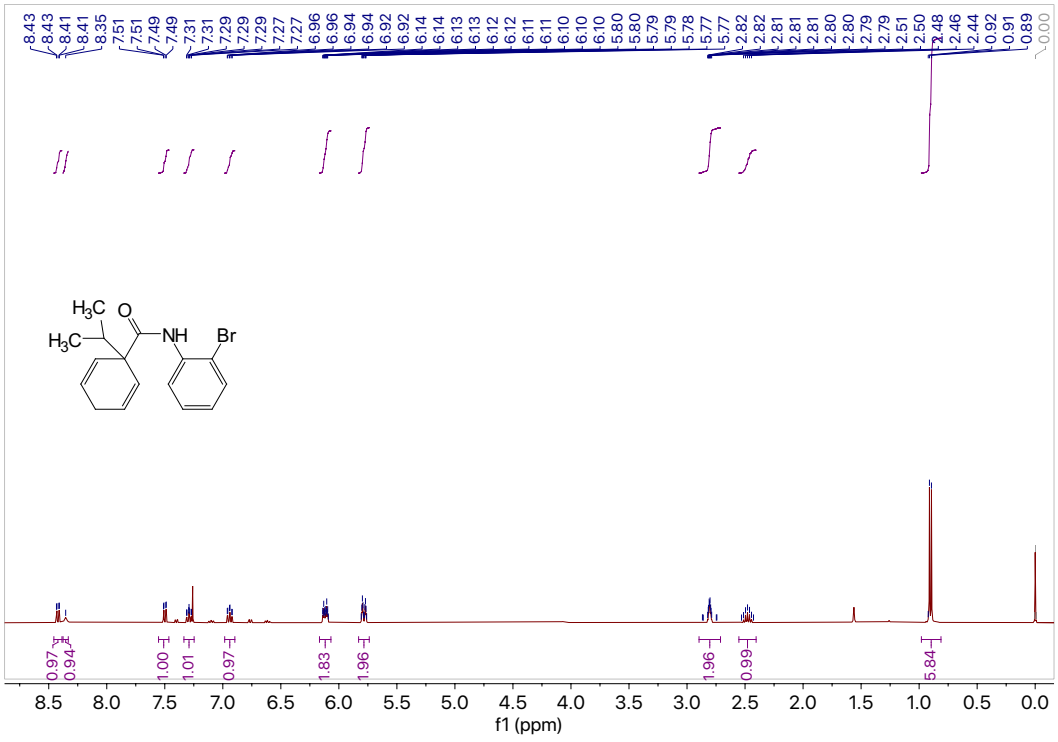

Figure 7.17 ^{1}H NMR (400 MHz, $CDCl_3$) of compound **S2e**.

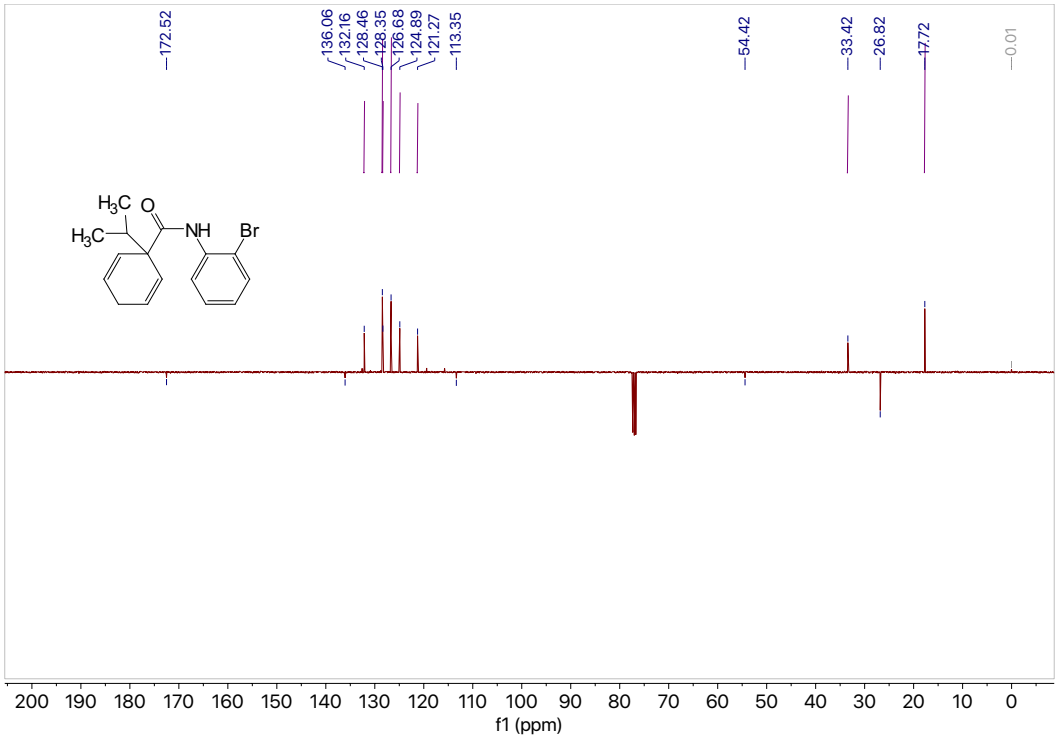

Figure 7.18 ^{13}C NMR (101 MHz, $CDCl_3$) of compound **S2e**.

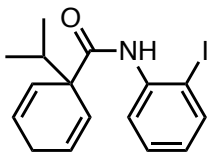

S2e-I

***N*-(2-Iodophenyl)-1-isopropylcyclohexa-2,5-diene-1-carboxamide (S2e-I).** Using the general benzamide synthesis procedure, diene acid **S1c** (0.497 g, 2.99 mmol, 1.0 equiv) in DCM (7.5 mL, 0.4 M) reacted with 2-iodoaniline (0.863 g, 3.94 mmol, 1.3 equiv) in DCM (9.9 mL, 0.4 M) to afford the crude product which was purified by column chromatography (silica, 4:1 hexanes: EtOAc) to afford pure **S2e-I** (0.93 g, 2.53 mmol) in 84% yield as a yellow oil.

^{1}H NMR (400 MHz, DMSO-d_6) δ 8.22 (s, 1H), 7.90 – 7.78 (m, 2H), 7.34 (t, J = 7.5 Hz, 1H), 6.93 – 6.84 (m, 1H), 6.09 (dt, J = 10.7, 3.4 Hz, 2H), 5.82 – 5.74 (m, 2H), 2.87 – 2.67 (m, 2H), 2.33 (m, 1H), 0.91 – 0.76 (d, 6H).

^{13}C NMR (101 MHz, DMSO-d_6) δ_u 139.3, 129.3, 128.4, 127.2, 126.7, 124.2, 33.9, 18.0; δ_d 172.5, 139.3, 93.9, 53.5, 26.9.

GC (Method B) t_R = 3.671 min. EI-MS m/z (%): 367.1 (M^+, 14), 324.0 (16), 247.0 (53), 218.9 (32), 197.1 (11), 121.1 (64), 105.1 (65), 91.0 (35), 79.1 (100), 65.1 (11), 51.0 (7).

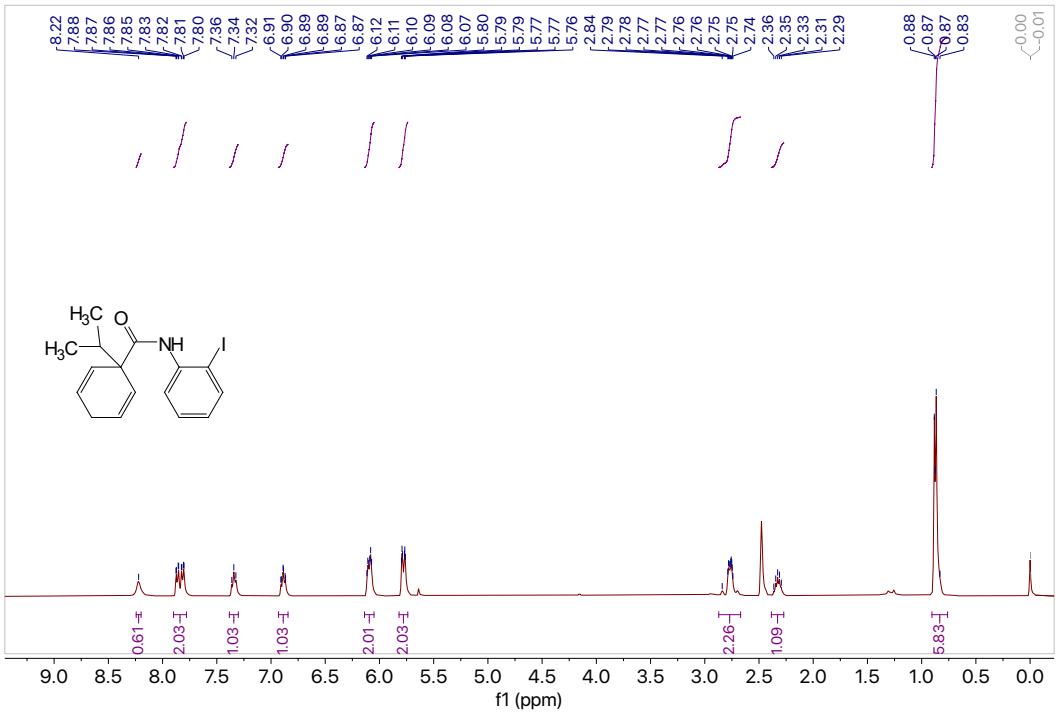

Figure 7.19 ^{1}H NMR (400 MHz, DMSO-d_6) of compound **S2e-I**.

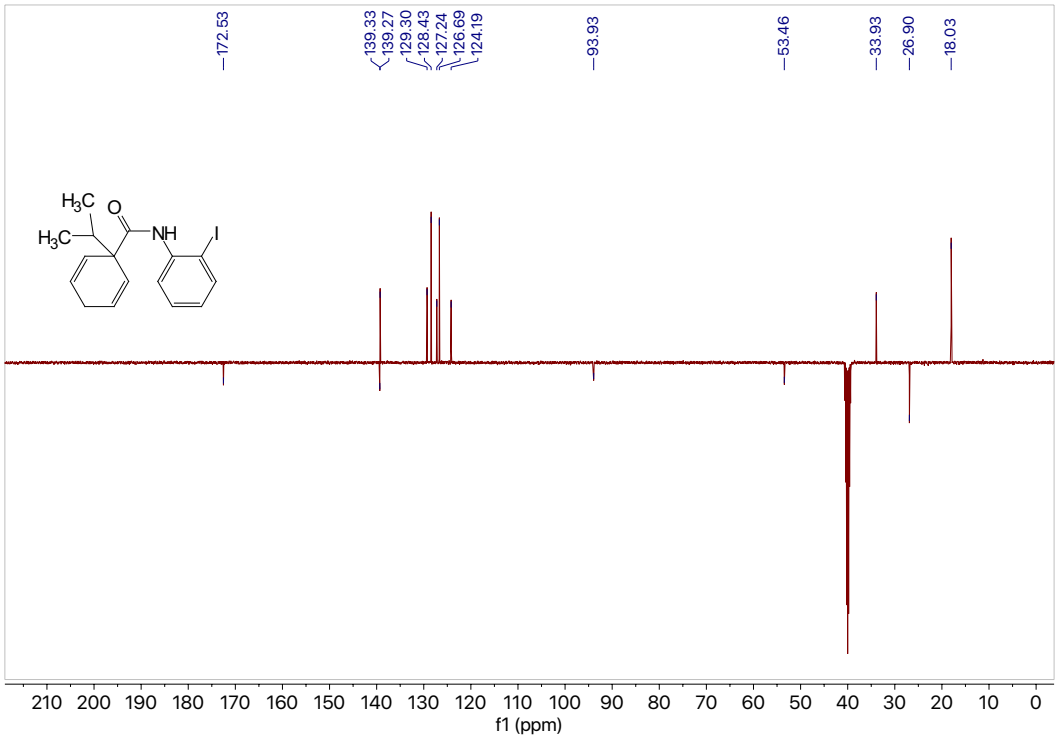

Figure 7.20 ^{13}C NMR (101 MHz, DMSO-d_6) of compound **S2e-I**.

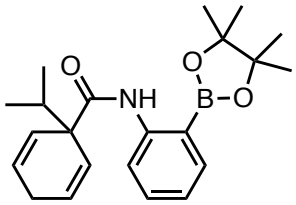

S2e-II

1-isopropyl-N-(2-(4,4,5,5-tetramethyl-1,3,2-dioxaborolan-2-yl)phenyl)cyclohexa-2,5-diene-1-carboxamide (S2e-II). Using the general benzamide synthesis procedure, diene acid **S1c** (0.550 g, 3.0 mmol, 1.0 equiv) in DCM (4.5 mL, 0.4 M) reacted with 2-aminophenylboronic acid pinacol ester (0.855 g, 3.90 mmol, 1.3 equiv) in DCM (9.8 mL, 0.4 M) to afford the crude product which was washed with $CuSO_4$ (aq.) and purified by column chromatography (silica, 9:1 hexanes: EtOAc) to afford pure **S2e-II** (0.96 g, 2.61 mmol) in 87% yield as an orange oil.

^{1}H NMR (400 MHz, $CDCl_3$) δ 9.31 (s, 1H), 8.52 (dd, J = 8.5, 1.0 Hz, 1H), 7.77 (dd, J = 7.4, 1.8 Hz, 1H), 7.43 (ddd, J = 8.7, 7.3, 1.8 Hz, 1H), 7.05 (td, J = 7.3, 1.1 Hz, 1H), 6.04 (dt, J = 10.4, 3.3 Hz, 3H), 5.84 (dt, J = 10.6, 2.0 Hz, 2H), 2.73 (tt, J = 3.4, 2.0 Hz, 2H), 2.48 – 2.33 (m, J = 7.2 Hz, 1H), 1.37 (s, 12H), 0.90 (s, 3H), 0.88 (s, 3H).

^{13}C NMR (101 MHz, $CDCl_3$) δ_u 136.3, 132.7, 126.6, 122.9, 119.7, 34.9, 24.9, 17.5; δ_d 173.7, 144.5, 84.1, 53.8, 26.9.

GC (Method A) t_R = 18.38 min. EI-MS m/z (%): 367.3 (M^+, 6), 308.2 (2), 266.1 (39), 246.1 (32), 224.0 (65), 208.1 (12), 189.0 (18), 164.0 (100), 146.0 (15), 122.1 (54), 101.1 (75), 83.0 (3), 55.0 (6).

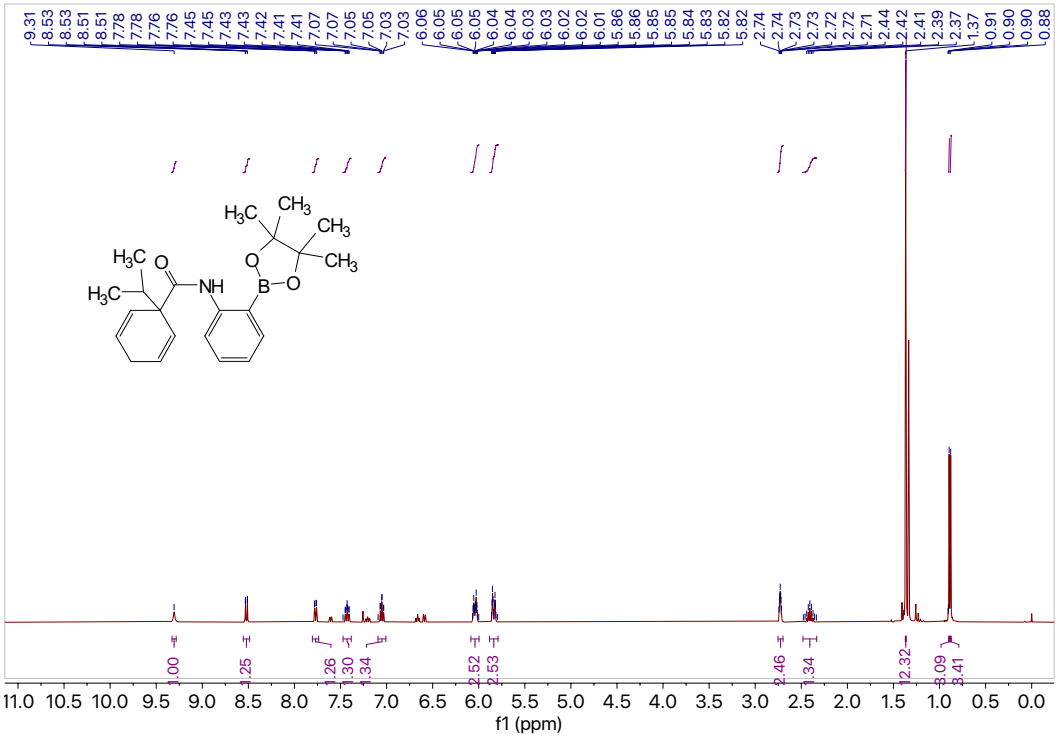

Figure 7.21 ^{1}H NMR (400 MHz, $CDCl_3$) of compound **S2e-II**.

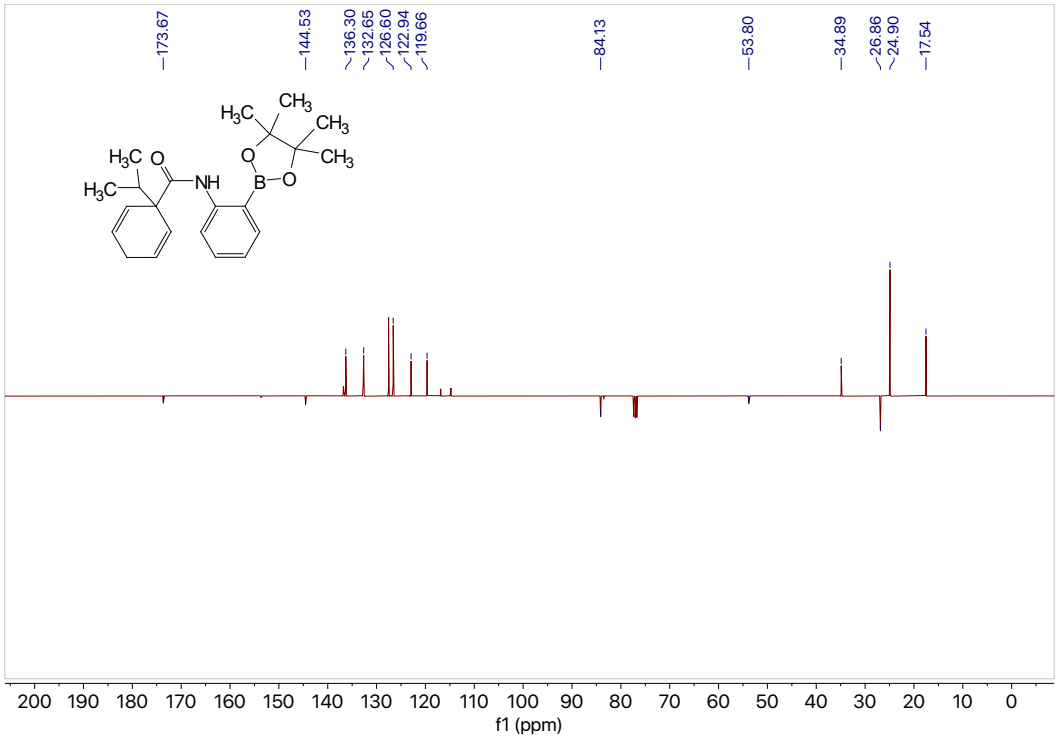

Figure 7.22 ^{13}C NMR (101 MHz, $CDCl_3$) of compound **S2e-II**.

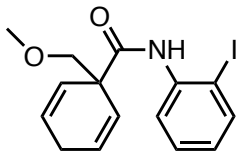

S2f-I

***N*-(2-Iodophenyl)-1-(methoxymethyl)cyclohexa-2,5-diene-1-carboxamide (S2f-I).** Using the general benzamide synthesis procedure, diene acid **S1d** (0.500 g, 2.97 mmol, 1.0 equiv) in DCM (7.4 mL, 0.4 M) reacted with 2-iodoaniline (0.781 g, 3.57 mmol, 1.2 equiv) in DCM (8.9 mL, 0.4 M) to afford the crude product which was purified by column chromatography (silica, 7:1 hexanes: EtOAc) to afford pure **S2f-I** (1.06 g, 2.87 mmol) in 97% yield as a yellow oil.

^{1}H NMR (400 MHz, $CDCl_3$) δ 8.25 (dd, J = 8.2, 1.6 Hz, 1H), 8.21 (s, 1H), 7.67 (dd, J = 8.0, 1.5 Hz, 1H), 7.28 – 7.20 (m, 1H), 6.73 (td, J = 7.6, 1.6 Hz, 1H), 6.11 – 6.01 (m, 2H), 5.89 – 5.79 (m, 2H), 3.62 (s, 2H), 3.33 (s, 3H), 2.92 – 2.68 (m, 2H).

^{13}C NMR (101 MHz, $CDCl_3$) δ_u 138.8, 129.2, 128.4, 125.9, 125.7, 121.3, 59.6; δ_d 171.1, 138.6, 89.1, 77.0, 51.1, 26.7.

GC (Method B) t_R = 3.353 min. EI-MS m/z (%): 369 (M+, 2), 336.0 (5), 227.9 (4), 262.9 (7), 244.9 (35), 232.0 (26), 218.8 (10), 210.0 (5), 196.0 (8), 150.9 (10), 118.9 (14), 105.0 (26), 92.0 (100), 77.0 (13), 63.0 (6).

HRMS (ESI) calculated for $C_{15}H_{17}INO_2$ $[M+H]^+$: 370.0304, found 370.0294.

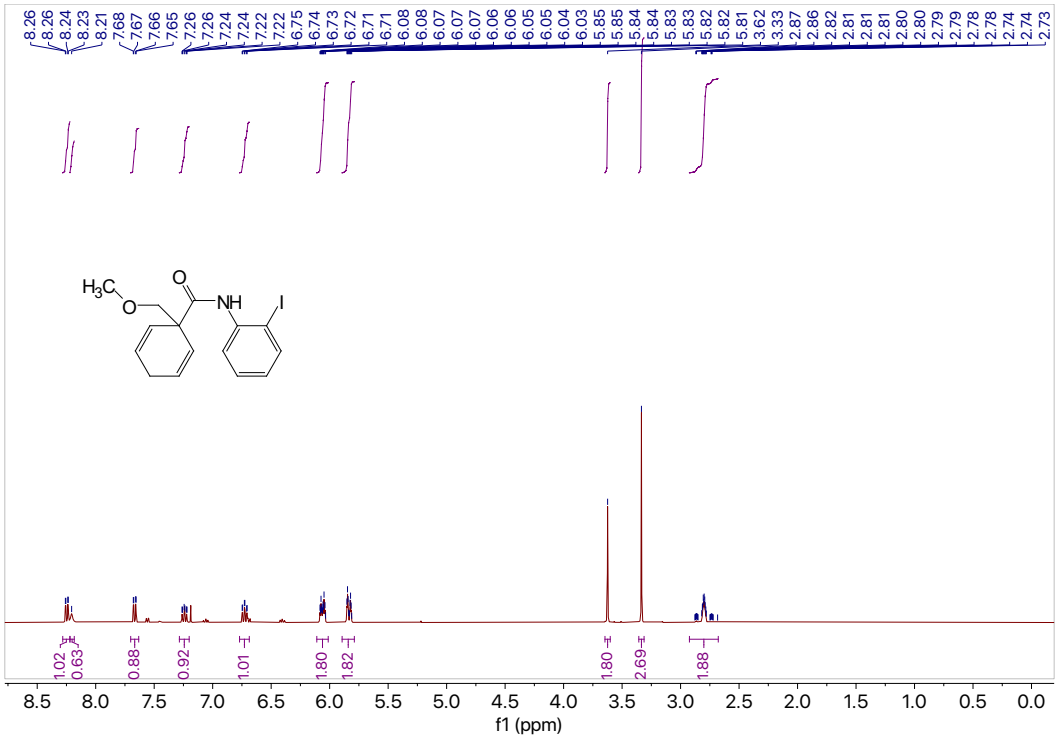

Figure 7.23 ^{1}H NMR (400 MHz, $CDCl_3$) of compound **S2f-I**.

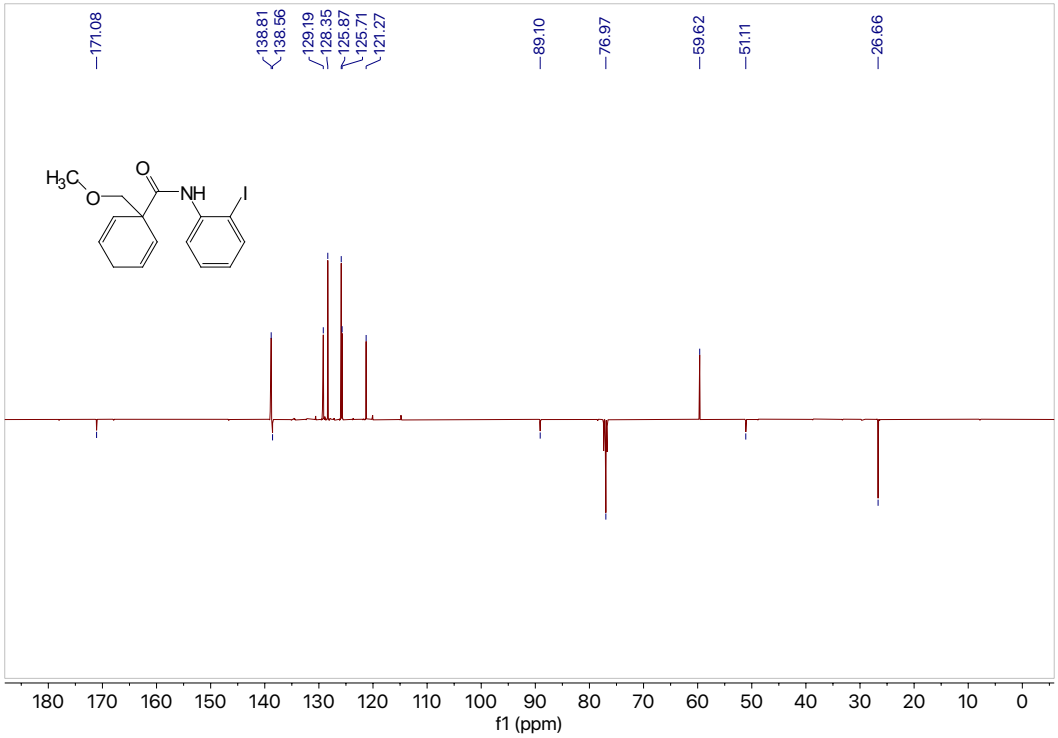

Figure 7.24 ^{13}C NMR (101 MHz, $CDCl_3$) of compound **S2f-I**.

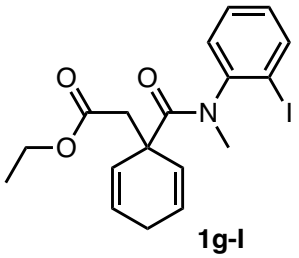

1g-I

Ethyl 2-(1-((2-iodophenyl)(methyl)carbamoyl)cyclohexa-2,5-dien-1-yl)acetate (1g-I). Using the general benzamide synthesis procedure, diene acid **S1e** (0.502 g, 2.38 mmol, 1.0 equiv) in DCM (6 mL, 0.4 M) reacted with 2-iodo-*N*-methylaniline (0.721 g, 3.09 mmol, 1.3 equiv) in DCM (7.7 mL, 0.4 M) to afford the crude product which was purified by column chromatography (silica, 4:1 hexanes: EtOAc) to afford pure **1g-I** (0.84 g, 1.97 mmol) in 83% yield as a tan solid, m.p. = 63.7 – 64.8°C.
^{1}H NMR (400 MHz, $CDCl_3$) δ 7.74 (d, *J* = 7.8 Hz, 1H), 7.23 (d, *J* = 7.7 Hz, 1H), 7.14 (d, *J* = 7.4 Hz, 1H), 6.89 (td, *J* = 7.6, 1.7 Hz, 1H), 5.78 (d, *J* = 10.3 Hz, 1H), 5.58 (d, *J* = 10.2 Hz, 1H), 5.41 (d, *J* = 10.1 Hz, 1H), 5.10 (d, *J* = 10.3 Hz, 1H), 4.05 (q, *J* = 7.1 Hz, 2H), 3.11 (s, 3H), 2.85 (d, *J* = 16.0 Hz, 1H), 2.52 (d, *J* = 16.1 Hz, 1H), 2.25 (d, *J* = 23.3 Hz, 1H), 1.94 (d, *J* = 22.8 Hz, 1H), 1.17 (t, *J* = 7.2 Hz, 3H).
^{13}C NMR (101 MHz, $CDCl_3$) δ_u 139.5, 130.5, 129.0, 129.0, 128.6, 126.9, 124.6, 123.7, 39.5, 14.3; δ_d 171.1, 146.4, 101.2, 60.2, 47.7, 46.6, 26.1.
GC (Method B) t_R = 4.145 min. EI-MS m/z (%): 380.1 (M+, 8), 260.0 (45), 232.9 (14), 210.1 (9), 165.1 (62), 134.0 (81), 119.0 (24), 105.0 (35), 91.1 (100), 77.0 (14).
HRMS (ESI) calculated for $C_{18}H_{21}O_3NI$ $[M+H]^+$: 426.0566, found 426.0580.

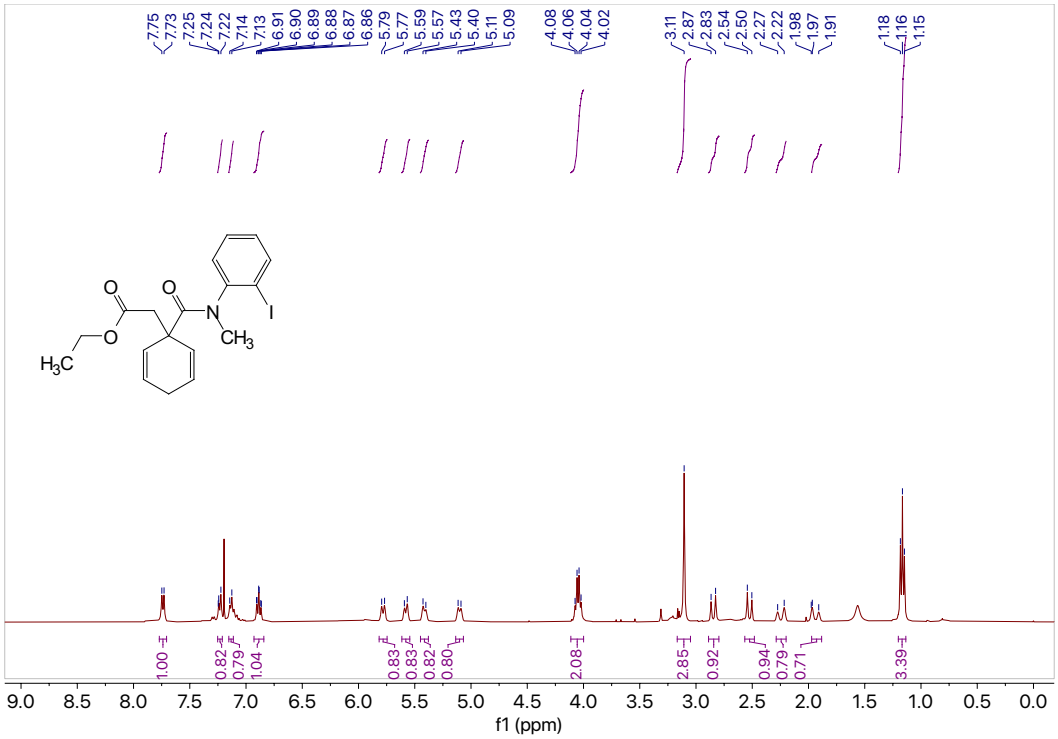

Figure 7.25 ^{1}H NMR (400 MHz, $CDCl_3$) of compound **1g-I**.

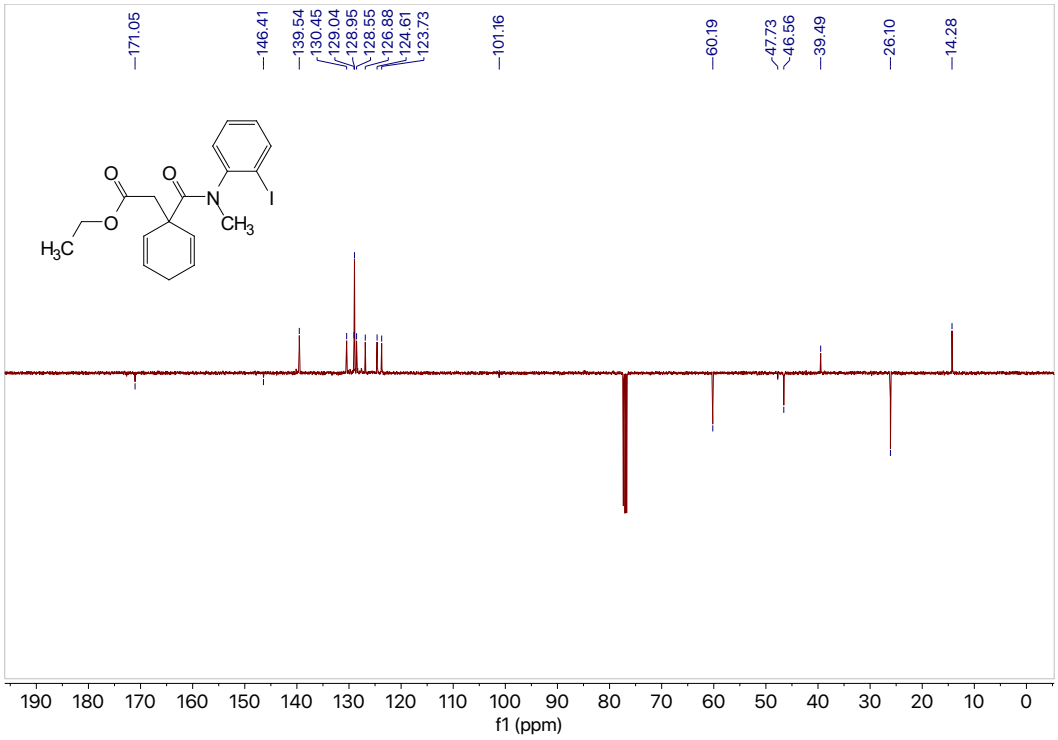

Figure 7.26 ^{13}C NMR (101 MHz, $CDCl_3$) of compound **1g-I**.

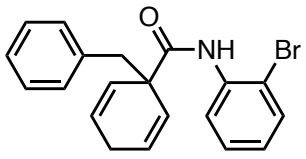

S2h

1-Benzyl-N-(2-bromophenyl)cyclohexa-2,5-diene-1-carboxamide (S2h). Using the general benzamide synthesis procedure, diene acid **S1f** (1.01 g, 4.71 mmol, 1.0 equiv) in DCM (11.8 mL, 0.4 M) reacted with 2-bromoaniline (1.05 g, 6.12 mmol, 1.3 equiv) in DCM (15.3 mL, 0.4 M) to afford the crude product which was purified by column chromatography (silica, 9:1 hexanes: EtOAc) to afford pure **S2h** (1.53 g, 4.15 mmol) in 88% yield as a yellow oil that solidified to white-yellow crystals on cooling, m.p. = 70.2 – 72.0°C.

^{1}H NMR (400 MHz, $CDCl_3$) δ 8.43 (dd, *J* = 8.3, 1.6 Hz, 1H), 8.31 (s, 1H), 7.48 (dd, *J* = 8.0, 1.5 Hz, 1H), 7.31 (ddd, *J* = 8.5, 7.5, 1.5 Hz, 1H), 7.27 – 7.14 (m, 4H), 6.95 (td, *J* = 7.7, 1.6 Hz, 1H), 5.99 (dt, *J* = 10.3, 3.3 Hz, 2H), 5.82 (dt, *J* = 10.4, 2.0 Hz, 2H), 3.21 (s, 2H), 2.73 (dddd, *J* = 23.4, 5.5, 3.1, 2.3 Hz, 1H), 2.56 (dtt, *J* = 23.4, 3.6, 1.8 Hz, 1H).
^{13}C NMR (101 MHz, $CDCl_3$) δ_u 132.2, 130.7, 128.4, 127.9, 127.8, 127.6, 126.3, 125.0, 121.2; δ_d 172.0, 137.4, 136.0, 113.3, 51.3, 43.4, 26.2.
GC (Method A) t_R = 19.251 min. EI-MS m/z (%): 367.1 (M+, 7), 276.0 (15), 196.1 (25), 170.1 (12), 152.1 (4), 120.0 (4), 105.0 (29), 91.1 (100), 77.1 (10), 63.1 (10).
HRMS (ESI) calculated for $C_{20}H_{19}ONBr$ $[M+H]^+$: 368.0650, found 368.0657.

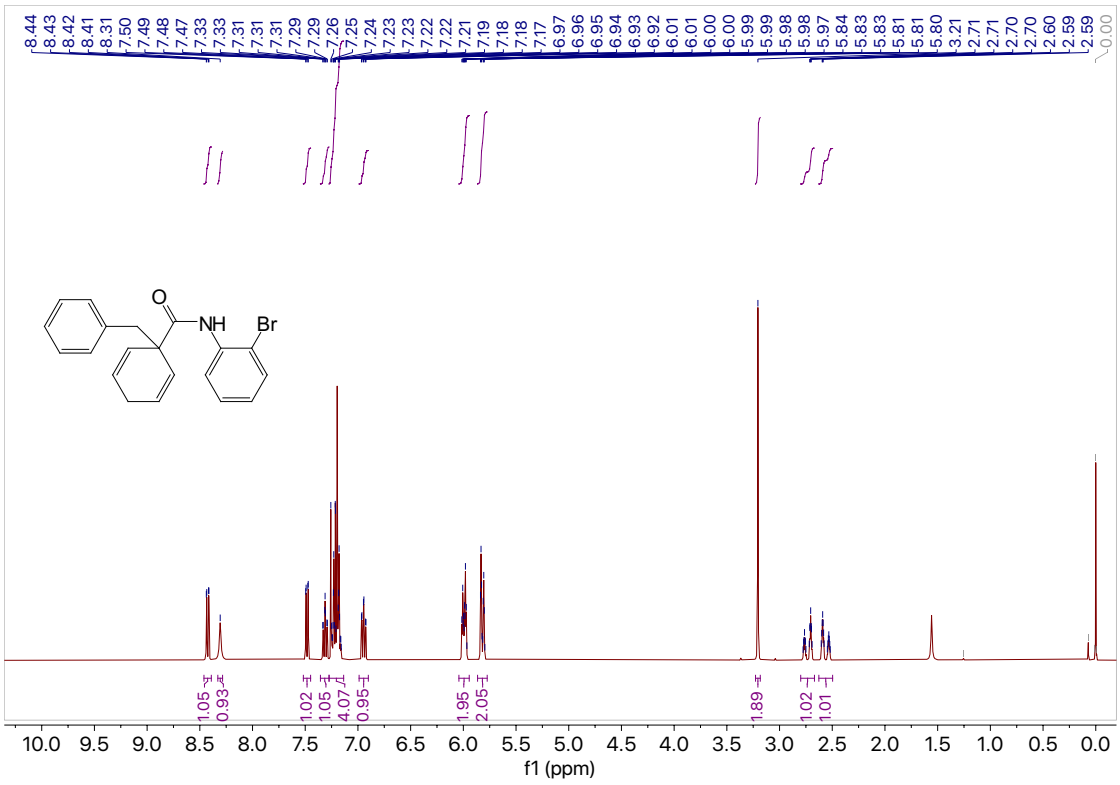

Figure 7.27 ^{1}H NMR (400 MHz, $CDCl_3$) of compound **S2h**.

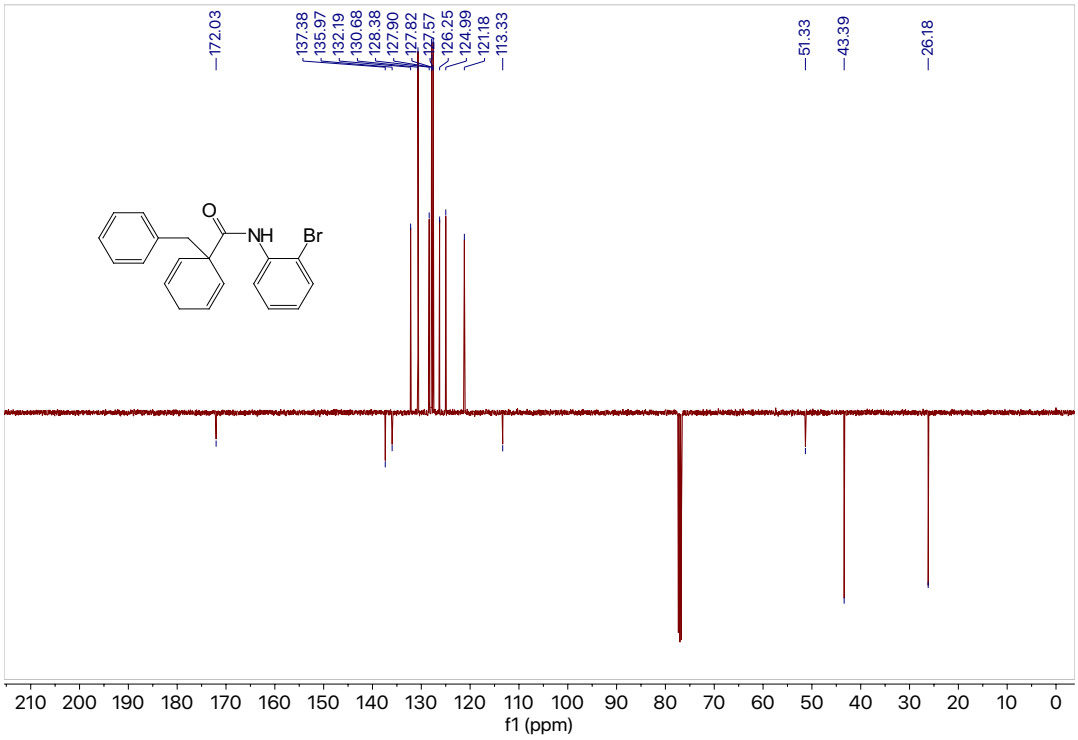

Figure 7.28 ^{13}C NMR (101 MHz, $CDCl_3$) of compound **S2h**.

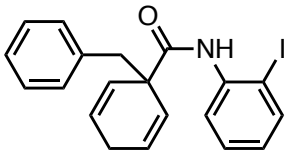

S2h-I

1-Benzyl-*N*-(2-iodophenyl)cyclohexa-2,5-diene-1-carboxamide (S2h-I). Using the general benzamide synthesis procedure, diene acid **S1f** (0.501 g, 2.33 mmol, 1.0 equiv) in DCM (5.8 mL, 0.4 M) reacted with 2-iodoaniline (0.665 g, 3.03 mmol, 1.3 equiv) in DCM (7.6 mL, 0.4 M) to afford the crude product which was purified by column chromatography (silica, 7:1 hexanes: EtOAc) to afford pure **S2h-I** (0.868 g, 2.09 mmol) in 90% yield as a yellow solid, m.p. = 68.6 – 70.4°C.

^{1}H NMR (400 MHz, $CDCl_3$) δ 8.35 (dd, *J* = 8.2, 1.6 Hz, 1H), 8.11 (s, 1H), 7.75 (dd, *J* = 8.0, 1.5 Hz, 1H), 7.41 – 7.32 (m, 1H), 7.27 – 7.16 (m, 5H), 6.84 (td, *J* = 7.6, 1.6 Hz, 1H), 6.03 (dt, *J* = 10.2, 3.4 Hz, 2H), 5.85 (dt, *J* = 10.4, 2.0 Hz, 2H), 3.23 (s, 2H), 2.85 – 2.73 (m, 1H), 2.66 – 2.53 (m, 1H).

^{13}C NMR (101 MHz, $CDCl_3$) δ_u 138.8, 130.7, 129.2, 127.9, 127.8, 127.6, 126.3, 125.8, 121.2; δ_d 172.2, 138.5, 137.4, 89.3, 51.2, 43.4, 26.3.

GC (Method B) t_R = 19.751 min. EI-MS m/z (%): 415.1 (M+,7), 324.0 (14), 245.9 (10), 218.9 (8), 196.0 (40), 170.0 (14), 119.0 (11), 105.0 (32), 91.0 (100), 77.1 (11), 65.0 (8).

HRMS (ESI) calculated for $C_{20}H_{19}ONI$ $[M+H]^+$: 416.0511, found 416.0508.

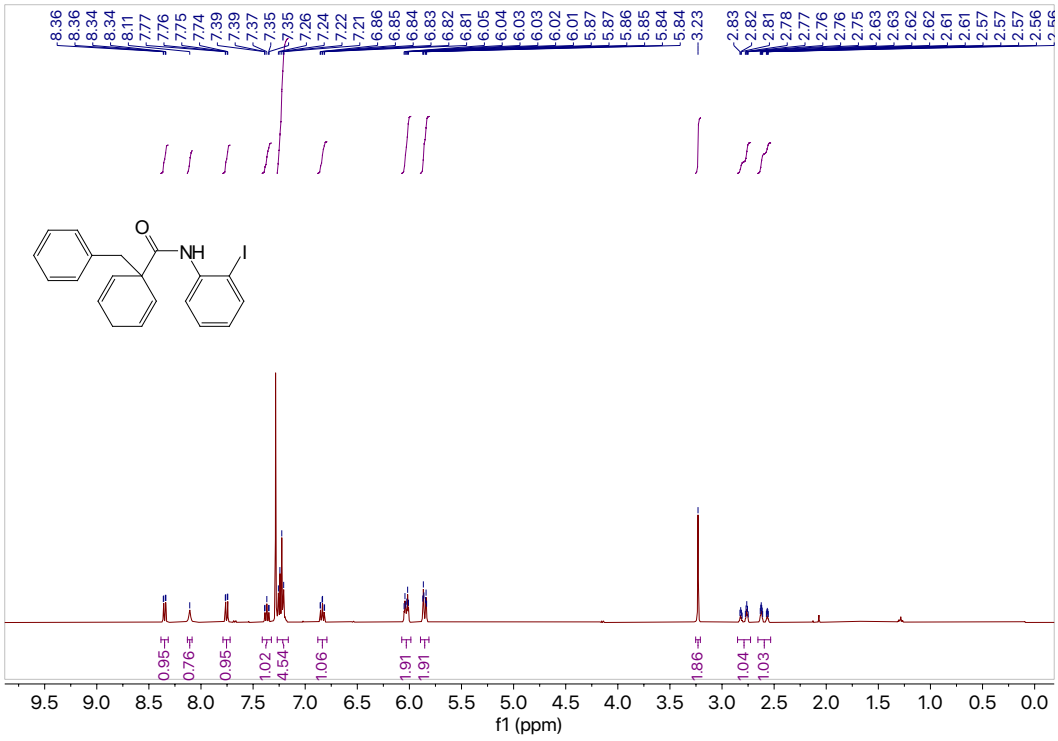

Figure 7.29 ^{1}H NMR (400 MHz, $CDCl_3$) of compound **S2h-I**.

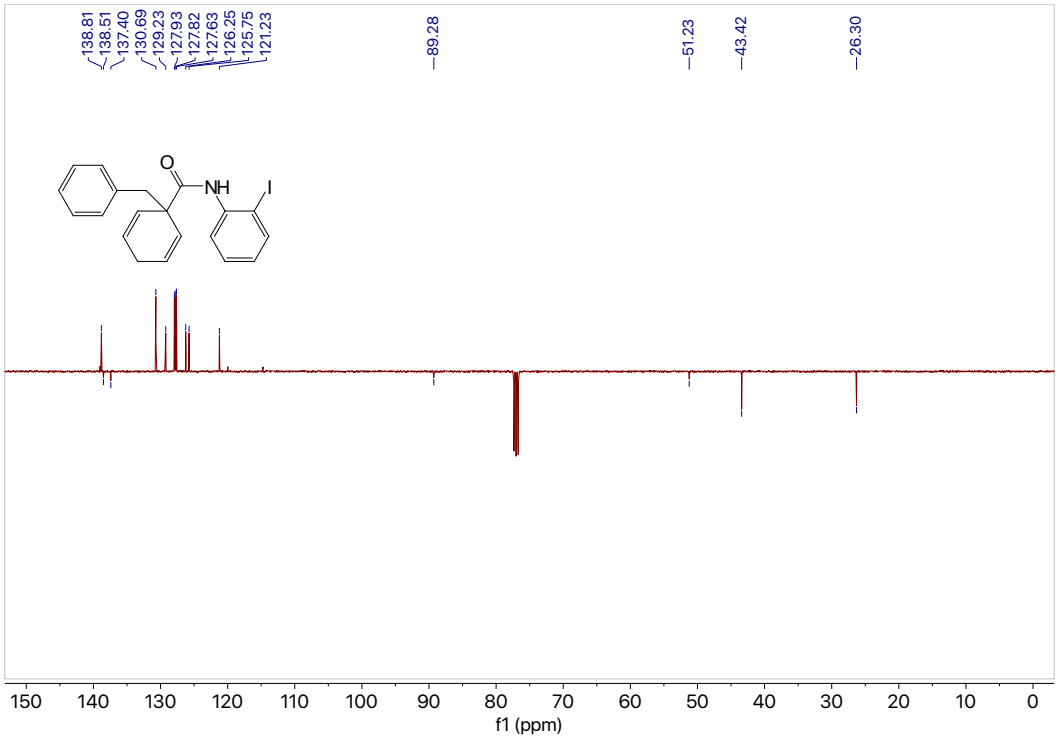

Figure 7.30 ^{13}C NMR (101 MHz, $CDCl_3$) of compound **S2h-I**.

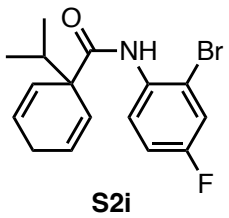

S2i

***N*-(2-Bromo-4-fluorophenyl)-1-isopropylcyclohexa-2,5-diene-1-carboxamide (S2i).** Using the general benzamide synthesis procedure, diene acid **S1c** (0.499 g, 3.00 mmol, 1.0 equiv) in DCM (7.5 mL, 0.4 M) reacted with 2-bromo-4-fluoroaniline (0.44 mL, 3.90 mmol, 1.3 equiv) in DCM (9.8 mL, 0.4 M) to afford the crude product which was purified by column chromatography (silica, 20:1 hexanes: EtOAc) to afford pure **S2i** (0.907 g, 2.68 mmol) in 90% yield as a clear colorless oil.

^{1}H NMR (400 MHz, $CDCl_3$) δ 8.37 (dd, J = 9.2, 5.6 Hz, 1H), 8.23 (s, 1H), 7.26 (dd, J = 7.9, 2.9 Hz, 1H), 7.03 (ddd, J = 9.2, 7.8, 2.9 Hz, 1H), 6.12 (dtd, J = 10.7, 3.4, 1.7 Hz, 2H), 5.77 (dt, J = 10.5, 2.0 Hz, 2H), 2.84 – 2.76 (m, 2H), 2.47 (hept, J = 6.9 Hz, 1H), 0.90 (d, J = 6.9 Hz, 6H).

^{13}C NMR (101 MHz, $CDCl_3$) δ_u 128.5, 126.6, 122.3 (d, $^3J_{C\text{-}F}$ = 8.1 Hz), 119.2 (d, $^2J_{C\text{-}F}$ = 26.3 Hz), 115.1 (d, $^2J_{C\text{-}F}$ = 22.2 Hz), 33.4, 17.7; δ_d 172.5, 158.3 (d, $^1J_{C\text{-}F}$ = 248.5 Hz), 132.6, 54.3, 26.8.

^{19}F NMR (376 MHz, $CDCl_3$) δ -116.66.

GC (Method B) t_R = 2.741 min. EI-MS m/z (%): 337.1 (M-1$^+$, 7), 294.0 (15), 216.9 (18), 188.9 (17), 138.0 (15), 121.1 (80), 105.0 (58), 79.1 (100), 51.0 (6).

HRMS (ESI) calculated for $C_{16}H_{18}ONBrF$ $[M+H]^+$: 338.0556, found 338.0560.

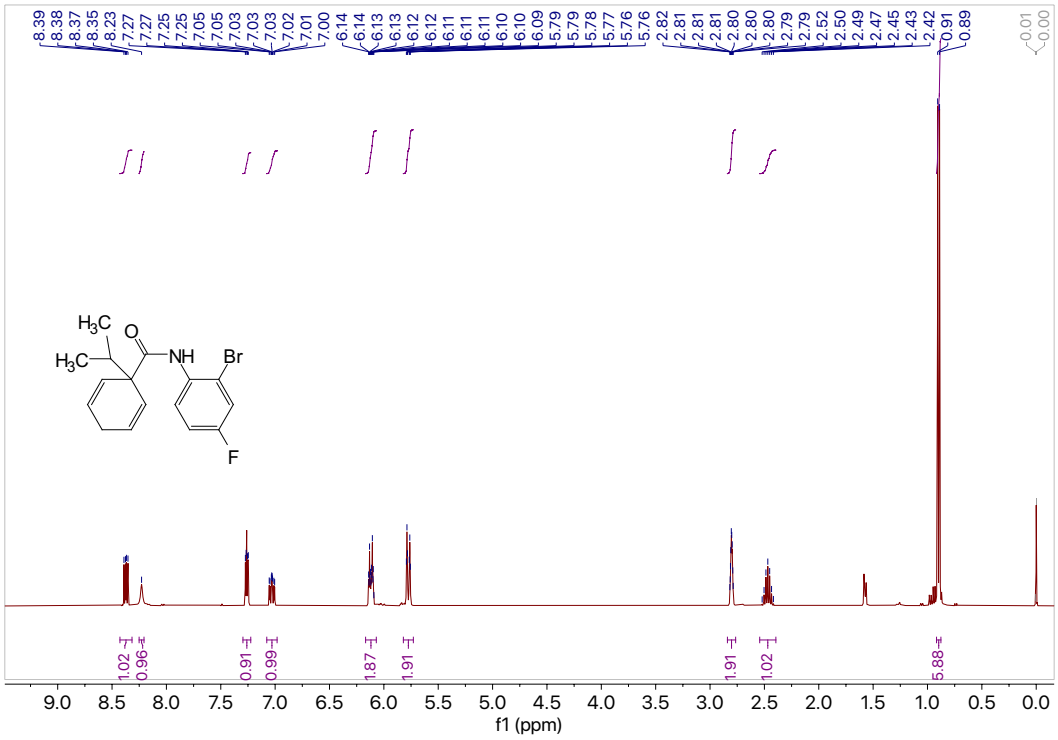

Figure 7.31 ^{1}H NMR (400 MHz, $CDCl_3$) of compound **S2i**.

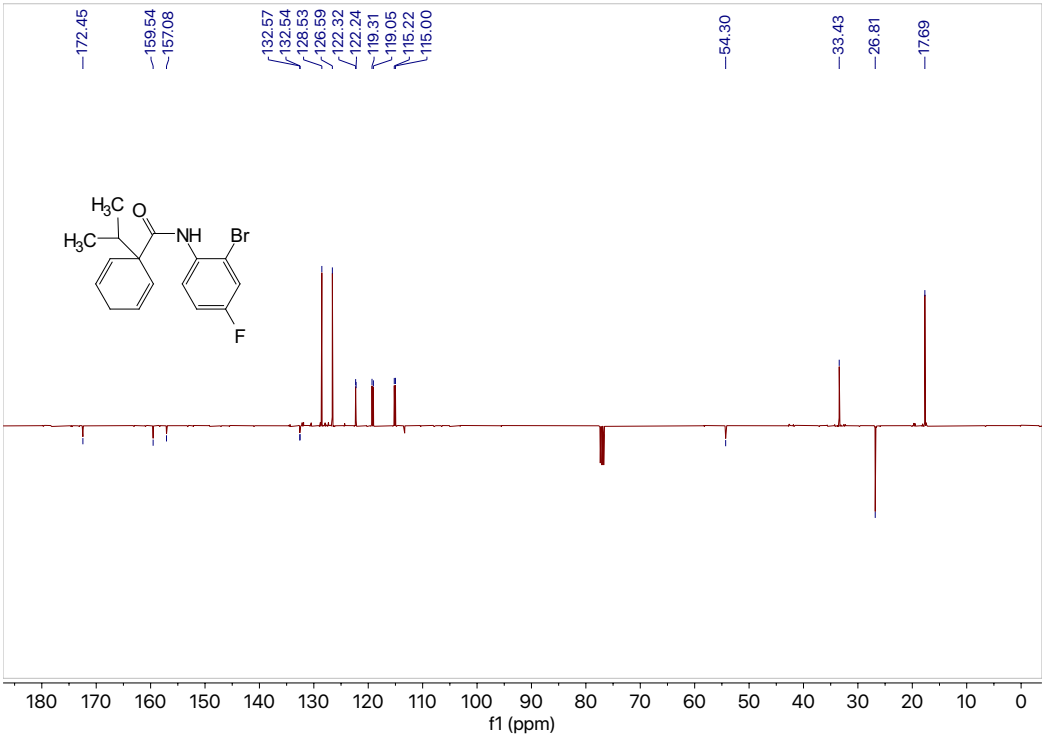

Figure 7.32 ^{13}C NMR (101 MHz, $CDCl_3$) of compound **S2i**.

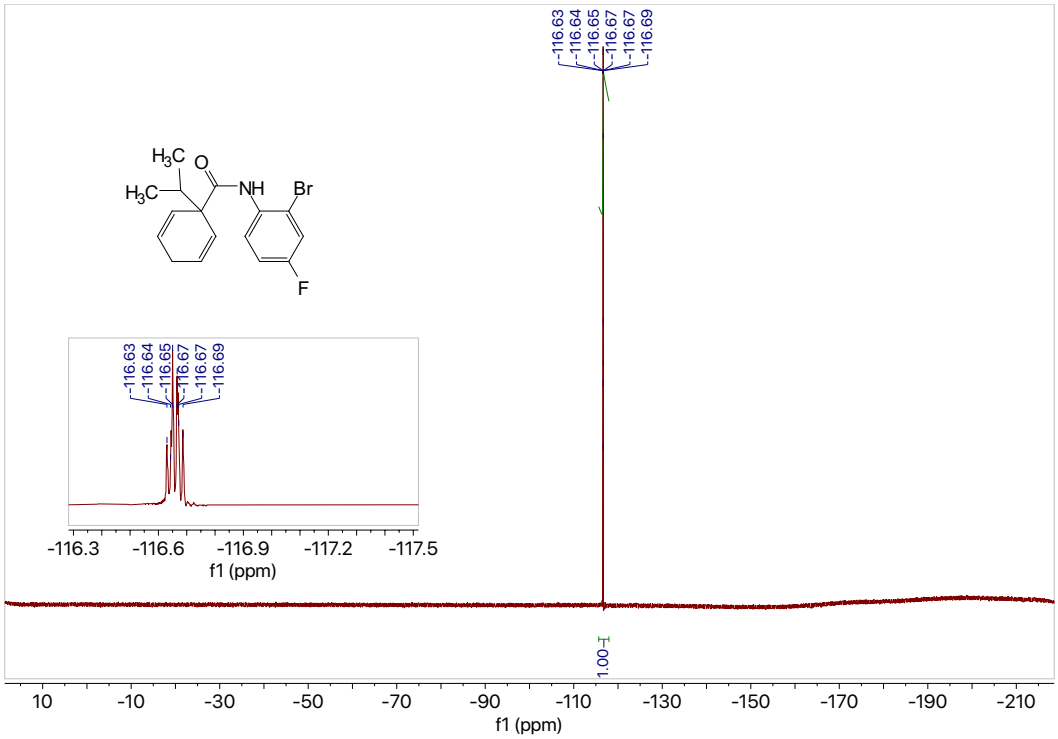

Figure 7.33 ^{19}F NMR (376 MHz, $CDCl_3$) of compound **S2i**.

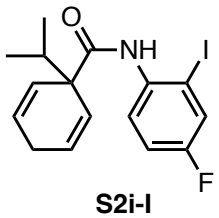

S2i-I

***N*-(4-Fluoro-2-iodophenyl)-1-isopropylcyclohexa-2,5-diene-1-carboxamide (S2i-I).** Using the general benzamide synthesis procedure, diene acid **S1c** (0.501 g, 3.01 mmol, 1.0 equiv) in DCM (7.5 mL, 0.4 M) reacted with 4-fluoro-2-iodoaniline (0.37 mL, 3.16 mmol, 1.05 equiv) in DCM (7.9 mL, 0.4 M) to afford the crude product which was purified by column chromatography (silica, 20:1 hexanes: EtOAc) to afford pure **S2i-I** (1.06 g, 2.74 mmol) in 91% yield as an orange solid, m.p. = 62.0 – 62.5°C.

^{1}H NMR (400 MHz, $CDCl_3$) δ 8.16 (dd, J = 9.1, 5.5 Hz, 1H), 7.95 (s, 1H), 7.40 (dd, J = 7.7, 2.9 Hz, 1H), 7.00 (ddd, J = 9.1, 7.8, 2.9 Hz, 1H), 6.06 (dt, J = 10.3, 3.3 Hz, 2H), 5.72 (dt, J = 10.5, 2.1 Hz, 2H), 2.84 – 2.65 (m, 2H), 2.40 (hept, J = 6.9 Hz, 1H), 0.83 (d, J = 6.9 Hz, 6H).

^{13}C NMR (101 MHz, $CDCl_3$) δ_u 128.6, 126.7, 125.3 (d, $^2J_{C\text{-}F}$ = 24.9 Hz), 122.2 (d, $^3J_{C\text{-}F}$ = 7.8), 115.9 (d, $^2J_{C\text{-}F}$ = 21.7 Hz), 33.4, 17.7; δ_d 172.6, 158.4 (d, $^1J_{C\text{-}F}$ = 248.6), 135.1, 88.7, 54.2, 26.9.

^{19}F NMR (376 MHz, $CDCl_3$) δ -116.70.

GC (Method B) t_R = 3.152 min. EI-MS m/z (%): 385.1 (M^+, 18), 342.0 (21), 264.9 (54), 236.9 (29), 215.0 (10), 138.0 (26), 121.1 (100), 105.0 (65), 85.1 (17), 79.0 (99) 51.0 (7).

HRMS (ESI) calculated for $C_{16}H_{18}ONFI$ $[M+H]^+$: 386.0417, found 386.0408.

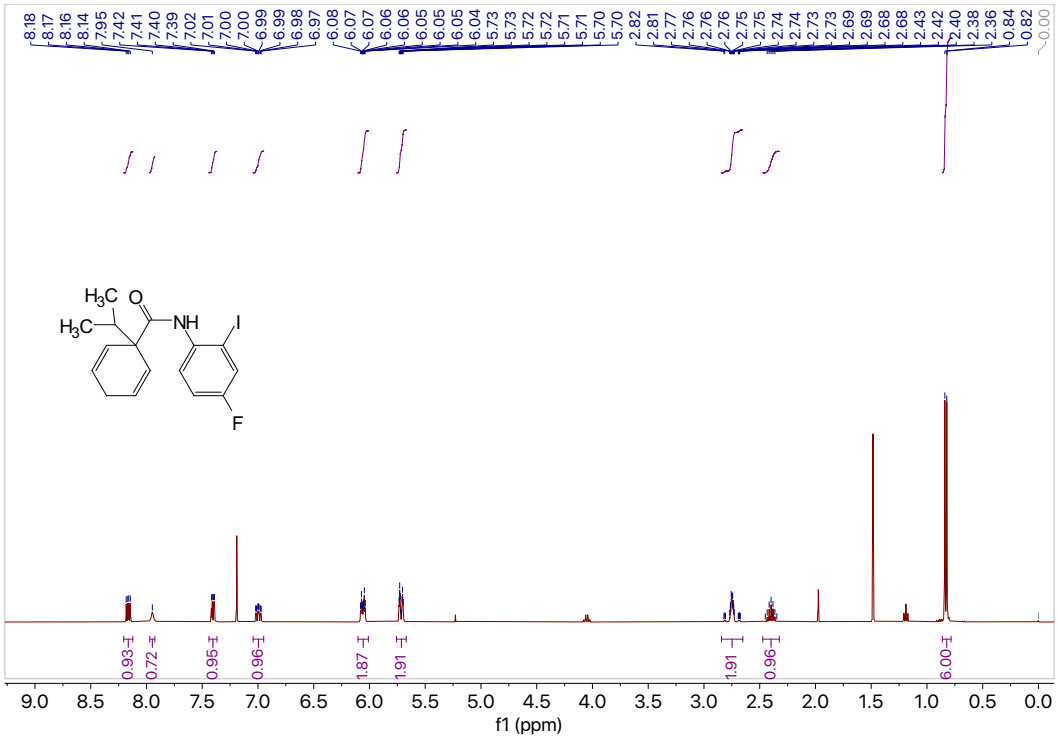

Figure 7.34 ^{1}H NMR (400 MHz, $CDCl_3$) of compound **S2i-I**.

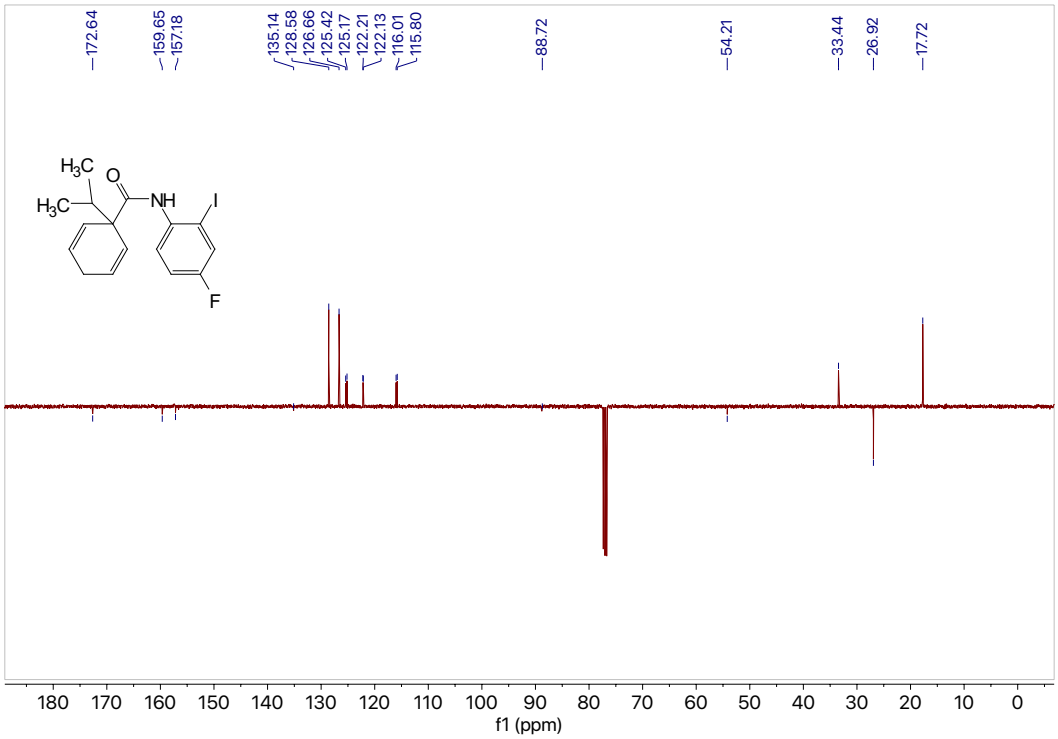

Figure.7.35 ^{13}C NMR (101 MHz, $CDCl_3$) of compound **S2i-I**.

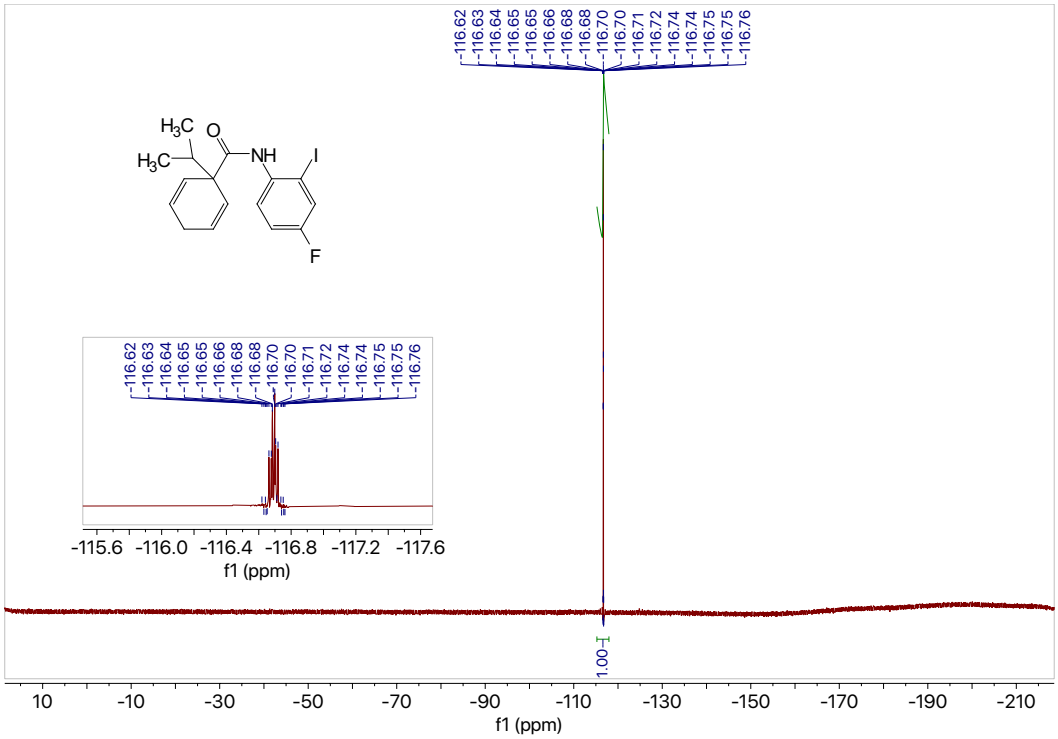

Figure 7.36 ^{19}F NMR (376 MHz, $CDCl_3$) of compound **S2i-I**.

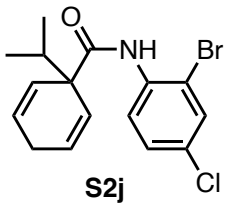

S2j

***N*-(2-Bromo-4-chlorophenyl)-1-isopropylcyclohexa-2,5-diene-1-carboxamide (S2j).** Using the general benzamide synthesis procedure, diene acid **S1c** (0.502 g, 3.02 mmol, 1.0 equiv) in DCM (7.6 mL, 0.4 M) reacted with 2-bromo-4-chloroaniline (0.804 g, 3.90 mmol, 1.3 equiv) in DCM (9.8 mL, 0.4 M) to afford the crude product which was purified by column chromatography (silica, 20:1 hexanes: EtOAc) to afford pure **S2j** (0.99 g, 2.79 mmol) in 93% yield as a yellow oil.

^{1}H NMR (400 MHz, $CDCl_3$) δ 8.39 (d, J = 8.9 Hz, 1H), 8.32 (s, 1H), 7.50 (d, J = 2.4 Hz, 1H), 7.27 (dd, 1H), 6.15 – 6.09 (m, 2H), 5.77 (dt, J = 10.5, 2.0 Hz, 2H), 2.82 – 2.78 (m, 2H), 2.46 (hept, J = 6.9 Hz, 1H), 0.89 (d, J = 6.9 Hz, 6H).

^{13}C NMR (101 MHz, $CDCl_3$) δ_u 131.6, 128.6, 128.4, 126.5, 121.8, 116.2, 33.4, 17.7; δ_d 172.5, 134.9, 129.0, 113.4, 54.4, 26.8.

GC (Method B) t_R = 3.515 min. EI-MS m/z (%): 355.1 ($M+1^+$, 6), 312.0 (13), 234.9 (16), 206.9 (16), 154.0 (11), 121.1 (90), 105.0 (51), 91.0 (12), 79.1 (100), 51.0 (6).

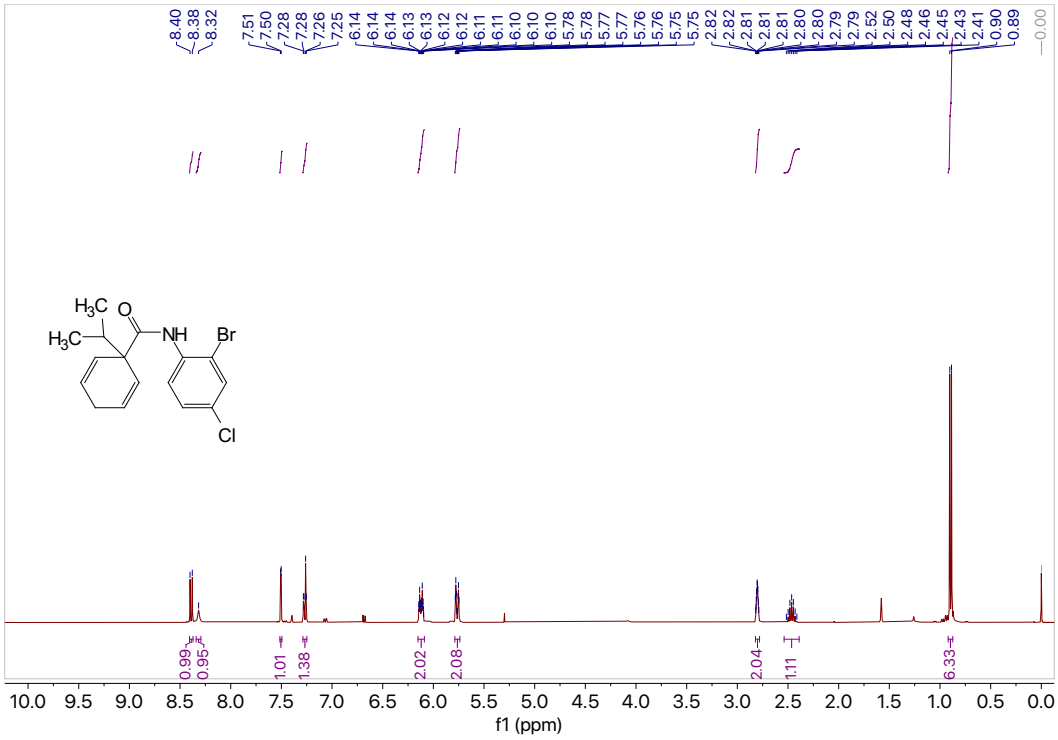

Figure 7.37 ^{1}H NMR (400 MHz, $CDCl_3$) of compound **S2j**.

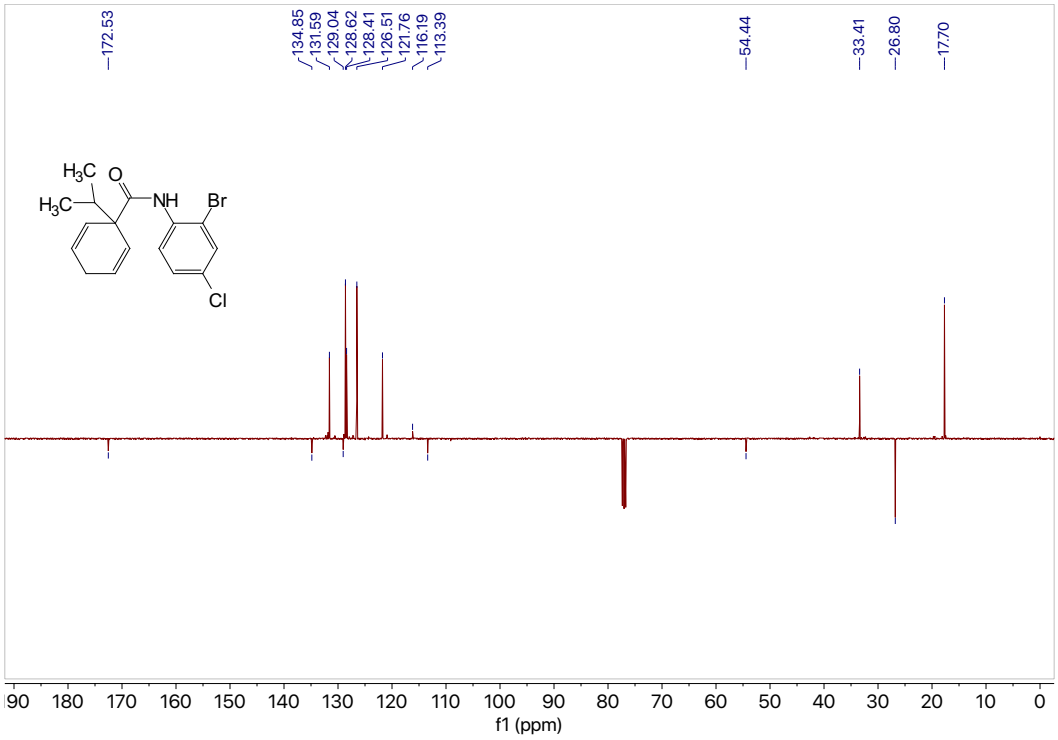

Figure 7.38 ^{13}C NMR (101 MHz, $CDCl_3$) of compound **S2j**.

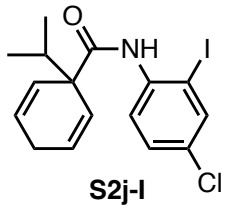

S2j-I

***N*-(4-Chloro-2-iodophenyl)-1-isopropylcyclohexa-2,5-diene-1-carboxamide (S2j-I):** Using the general benzamide synthesis procedure, diene acid **S1c** (0.505 g, 3.04 mmol, 1.0 equiv) in DCM (7.6 mL, 0.4 M) reacted with 4-chloro-2-iodoaniline (0.798 g, 3.15 mmol, 1.04 equiv) in DCM (7.9 mL, 0.4 M) to afford the crude product which was purified by column chromatography (silica, 20:1 hexanes: EtOAc) to afford pure **S2j-I** (0.998 g, 2.48 mmol) in 82% yield as a white solid, m.p. = 85.3 – 86.5°C.

^{1}H NMR (400 MHz, $CDCl_3$) δ 8.20 (d, J = 8.9 Hz, 1H), 8.04 (s, 1H), 7.66 (d, J = 2.4 Hz, 1H), 7.23 (dd, J = 8.9, 2.4 Hz, 1H), 6.06 (dt, J = 10.3, 3.4 Hz, 2H), 5.71 (dt, J = 10.5, 2.0 Hz, 2H), 2.84 – 2.65 (m, 2H), 2.39 (hept, J = 6.9 Hz, 1H), 0.83 (d, J = 6.9 Hz, 6H).

^{13}C NMR (101 MHz, $CDCl_3$) δ_u 137.8, 129.2, 128.7, 126.6, 121.6, 33.4, 17.7; δ_d 172.7, 137.5, 129.5, 89.0, 54.4, 26.9.

GC (Method B) t_R = 4.148 min. EI-MS m/z (%): 401.1 (M^+, 13), 358.0 (13), 280.9 (40), 252.9 (23), 231.0 (9), 154.0 (20), 121.1 (100), 105.0 (56), 91.0 (15), 79.0 (90), 63.0 (6), 51.0 (5).

HRMS (ESI) calculated for $C_{16}H_{18}ONClI$ $[M+H]^+$: 402.0122, found 402.0119.

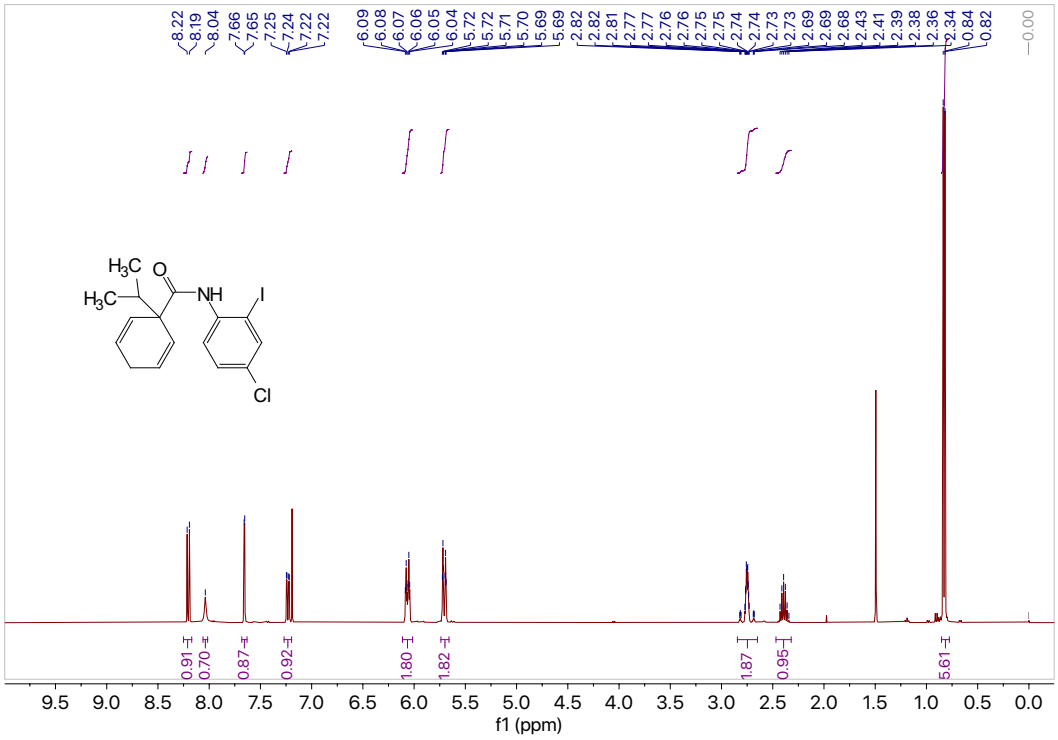

Figure 7.39 ^{1}H NMR (400 MHz, $CDCl_3$) of compound **S2j-I**.

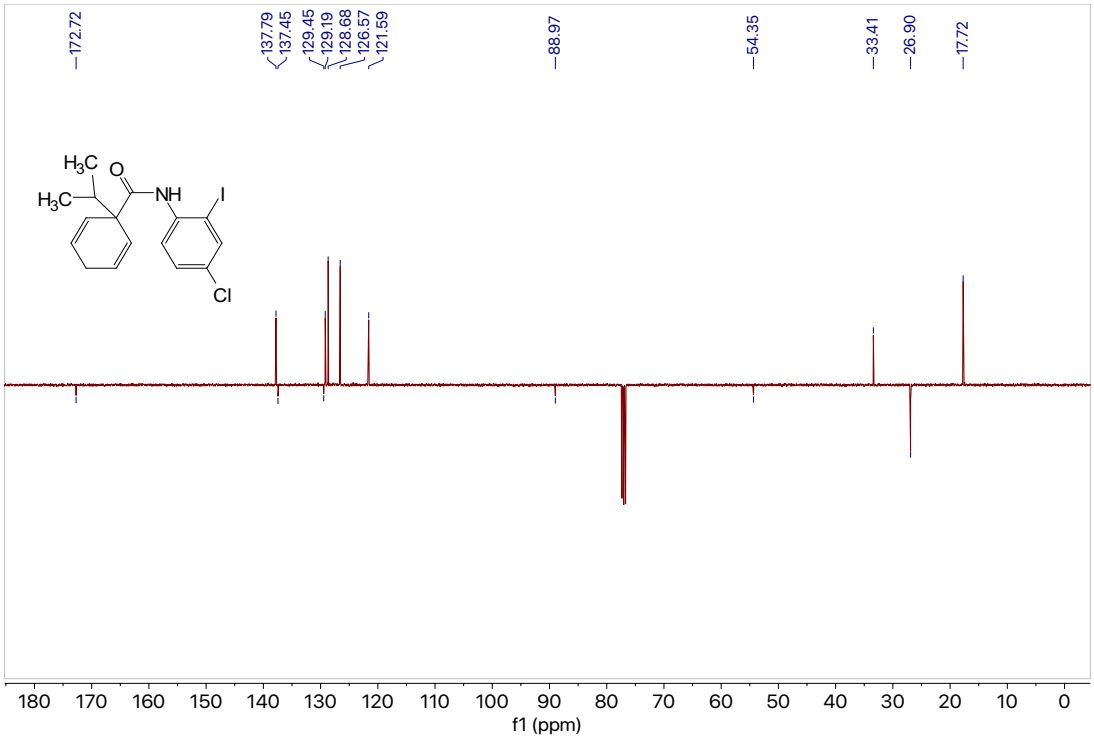

Figure 7.40 ^{13}C NMR (101 MHz, $CDCl_3$) of compound **S2j**.

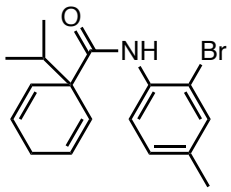

S2k

***N*-(2-Bromo-4-methylphenyl)-1-isopropylcyclohexa-2,5-diene-1-carboxamide (S2k).** Using the general benzamide synthesis procedure, diene acid **S1c** (0.504 g, 3.03 mmol, 1.0 equiv) in DCM (7.6 mL, 0.4 M) reacted with 2-bromo-4-methylaniline (0.48 mL, 3.94 mmol, 1.3 equiv) in DCM (9.9 mL, 0.4 M) to afford the crude product which was purified by column chromatography (silica, 10:1 hexanes: EtOAc) to afford pure **S2k** (0.966 g, 2.89 mmol) in 96% yield as a yellow oil.

^{1}H NMR (400 MHz, $CDCl_3$) δ ^{1}H NMR (400 MHz, $CDCl_3$) δ 8.26 (d, J = 8.3 Hz, 1H), 7.32 (dd, J = 2.0, 0.9 Hz, 1H), 7.09 (dd, J = 8.4, 2.0 Hz, 1H), 6.15 – 6.05 (m, 2H), 5.78 (dt, J = 10.5, 2.0 Hz, 2H), 2.80 (dp, J = 5.4, 1.9 Hz, 2H), 2.46 (h, J = 7.0 Hz, 1H), 2.28 (s, 3H), 0.90 (d, J = 6.9 Hz, 7H).

^{13}C NMR (101 MHz, $CDCl_3$) δ_u 132.4, 128.9, 128.3, 126.7, 121.2, 33.4, 20.5, 17.7; δ_d 172.4, 134.9, 133.5, 113.3, 54.3, 26.8.

GC (Method B) t_R = 3.296 min. EI-MS m/z (%): 333.1 (M-1$^+$, 13), 290.0 (19), 212.9 (22), 185.9 (24), 134.1 (60), 122.1 (62), 105.0 (65), 91.0 (15), 79.1 (100), 51.0 (8).

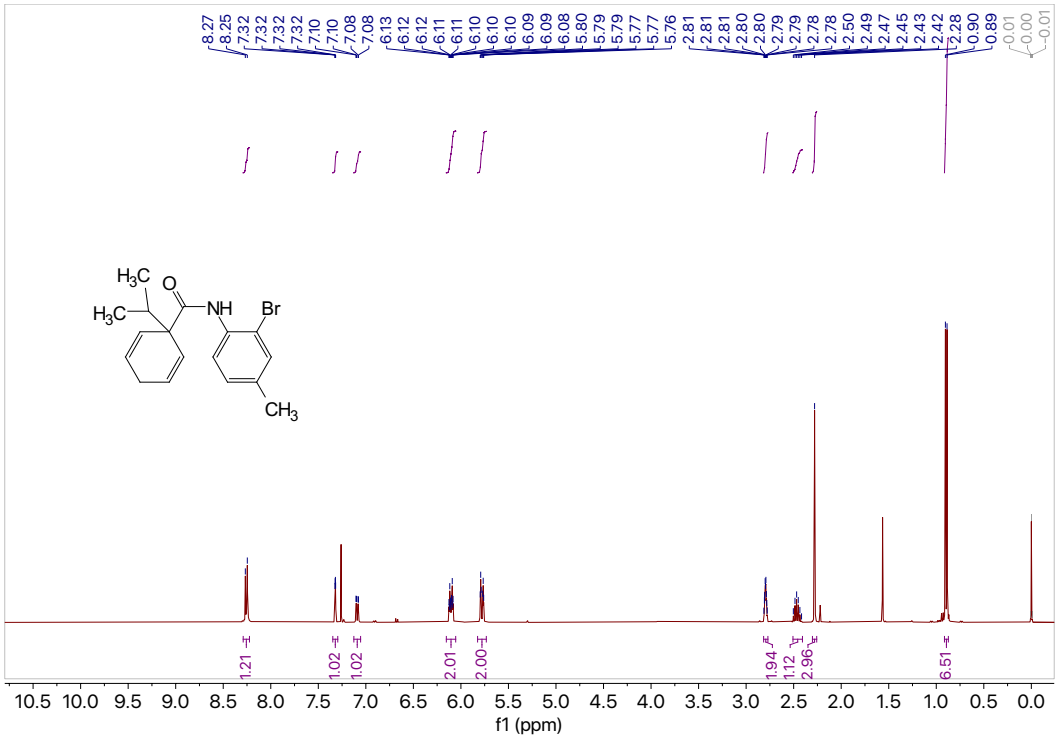

Figure 7.41 ^{1}H NMR (400 MHz, $CDCl_3$) of compound **S2k**.

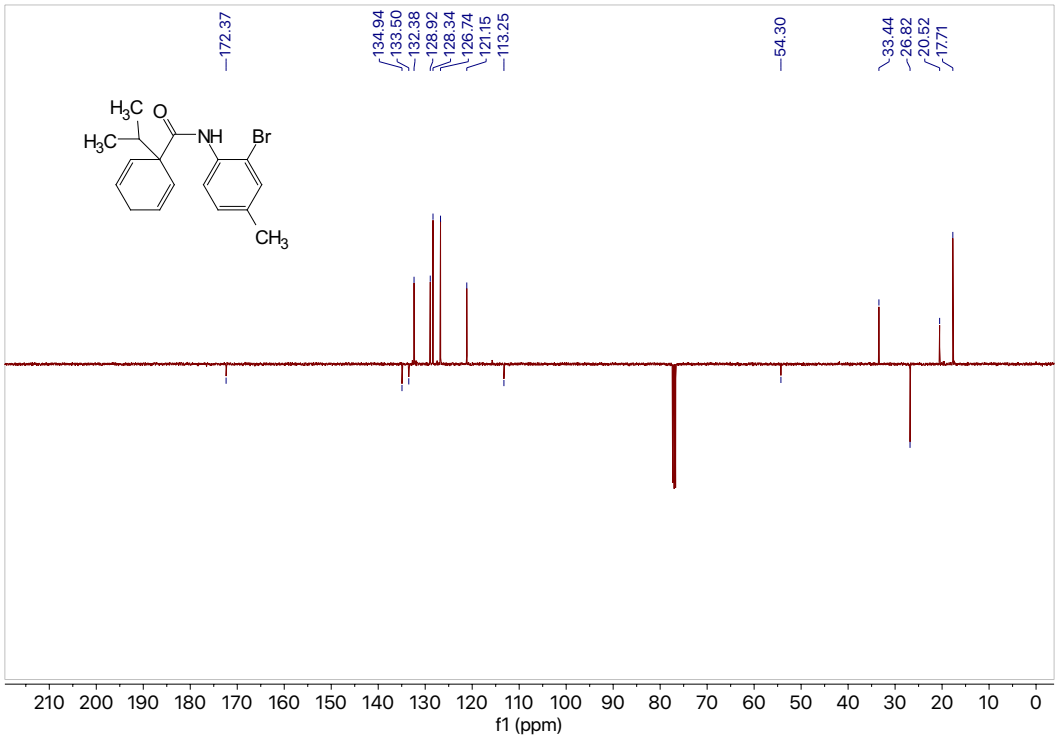

Figure 7.42 ^{13}C NMR (101 MHz, $CDCl_3$) of compound **S2k**.

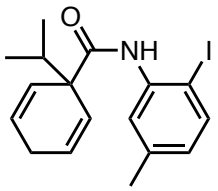

S2l-I

***N*-(2-Iodo-5-methylphenyl)-1-isopropylcyclohexa-2,5-diene-1-carboxamide (S2l-I).** Using the general benzamide synthesis procedure, diene acid **S1c** (0.501 g, 3.00 mmol, 1.0 equiv) in DCM (7.5 mL, 0.4 M) reacted with 2-iodo-5-methylaniline (0.735 g, 3.15 mmol, 1.05 equiv) in DCM (7.9 mL, 0.4 M) to afford the crude product which was purified by column chromatography (silica, 10:1 hexanes: EtOAc) to afford pure **S2l-I** (1.13 g, 2.96 mmol) in 99% yield as a white solid, m.p. = 78.2 – 79.1°C.

^{1}H NMR (400 MHz, $CDCl_3$) δ 8.11 (d, *J* = 2.1 Hz, 1H), 8.01 (s, 1H), 7.52 (d, *J* = 8.1 Hz, 1H), 6.57 (dd, *J* = 8.1, 1.5 Hz, 1H), 6.05 (dt, *J* = 10.3, 3.3 Hz, 2H), 5.72 (dt, *J* = 10.5, 2.0 Hz, 2H), 2.85 – 2.64 (m, 2H), 2.40 (hept, *J* = 6.9 Hz, 1H), 2.24 (s, 3H), 0.84 (d, *J* = 6.9 Hz, 6H).

^{13}C NMR (101 MHz, $CDCl_3$) δ_u 138.3, 129.50, 128.5, 126.7, 126.7, 122.0, 33.4, 21.3, 17.8; δ_d 172.8, 139.6, 138.3, 54.3, 26.9.

GC (Method B) t_R = 3.659 min. EI-MS m/z (%): 381.1 (M^+, 26), 338.0 (196), 260.9 (60), 232.9 (50), 211.0 (18), 134.0 (99), 121.0 (81), 105.0 (76), 85 (18), 79.0 (100), 65.0 (5), 51.0 (10).

HRMS (ESI) calculated for $C_{17}H_{21}ONI$ $[M+H]^+$: 382.0668, found 382.0658.

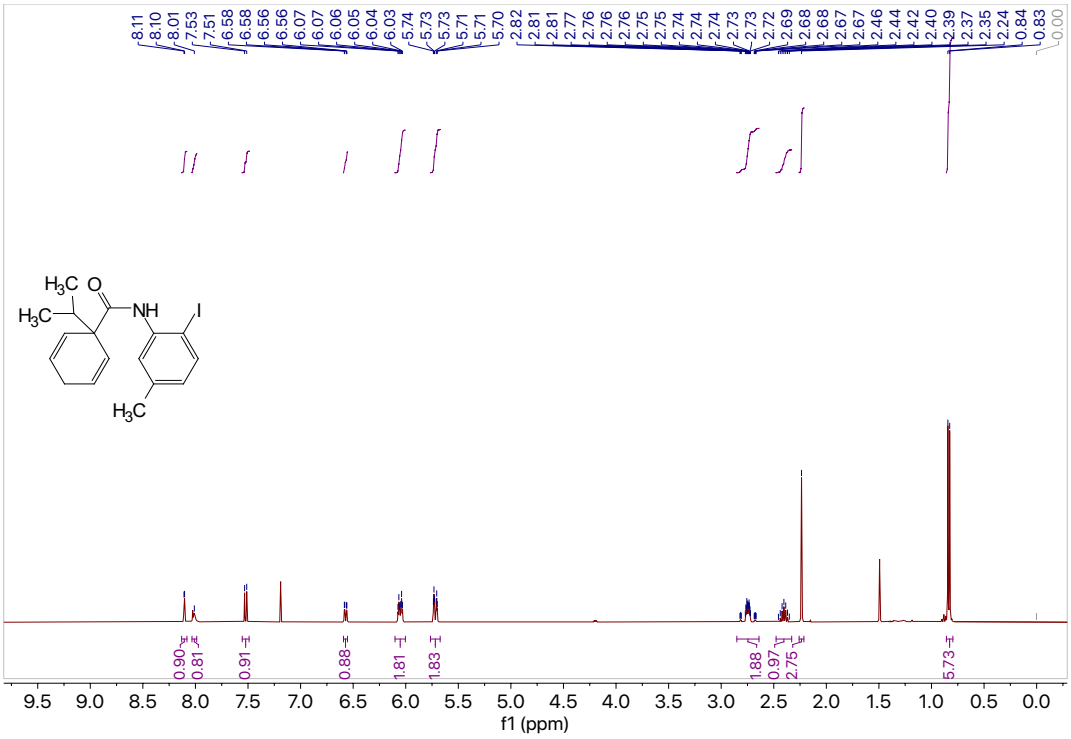

Figure 7.43 ^{1}H NMR (400 MHz, $CDCl_3$) of compound **S2l-I**.

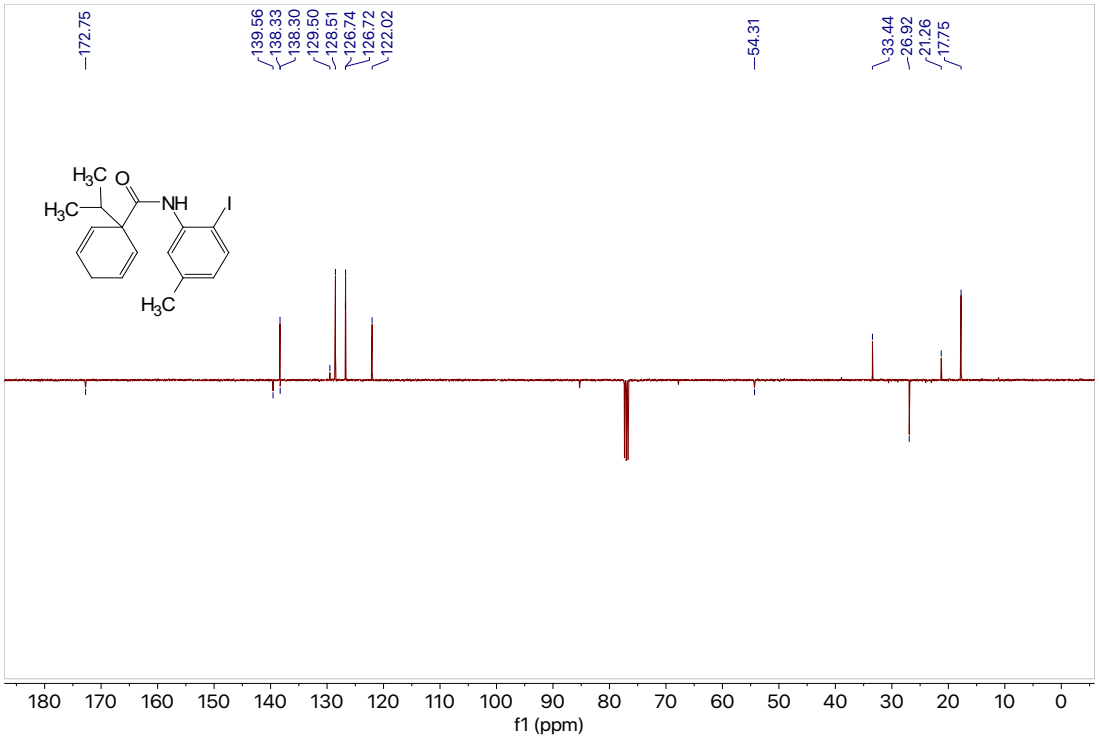

Figure 7.44 ^{13}C NMR (101 MHz, $CDCl_3$) of compound **S2l-I**.

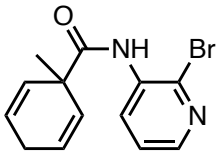

S2m

***N*-(2-Bromopyridin-3-yl)-1-methylcyclohexa-2,5-diene-1-carboxamide (S2m).** Using the general benzamide synthesis procedure, diene acid **S1a** (0.501 g, 3.62 mmol, 1.0 equiv) in DCM (9.1 mL, 0.4 M) reacted with 2-bromopyridin-3-amine (0.814 g, 4.71 mmol, 1.3 equiv) in DCM (11.8 mL, 0.4 M) to afford the crude product which was purified by column chromatography (silica, 4:1 hexanes: EtOAc) to afford pure **S2m** (0.899 g, 3.07 mmol) in 85% yield as a white-tan solid, m.p. = 96.0 – 97.8°C.

^{1}H NMR (400 MHz, $CDCl_3$) δ 8.69 (dd, *J* = 8.1, 1.8 Hz, 1H), 8.40 (s, 1H), 8.05 (dd, *J* = 4.6, 1.8 Hz, 1H), 7.25 (dd, *J* = 8.2, 4.7 Hz, 1H), 6.05 (dt, *J* = 10.2, 3.4 Hz, 2H), 5.78 (dt, *J* = 10.3, 2.1 Hz, 2H), 2.96 – 2.75 (m, 2H), 1.42 (s, 3H).

^{13}C NMR (101 MHz, $CDCl_3$) δ_u 144.2, 129.3, 127.8, 126.5, 123.6, 24.5; δ_d 173.4, 133.9, 132.9, 46.5, 26.0.

GC (Method B) t_R = 2.454 min. EI-MS m/z (%): 292.0 (M-1$^+$, 1), 199.0 (8), 171.9 (5), 119.0 (6), 93.0 (100), 77.0 (31), 65.0 (8), 51.0 (4).

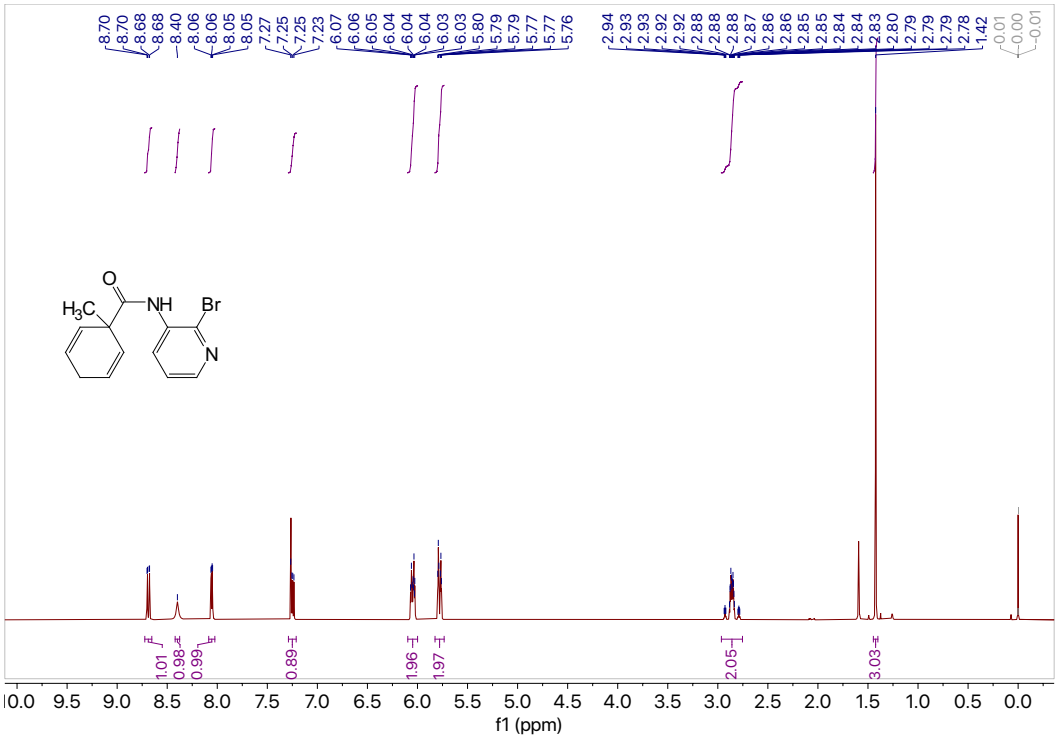

Figure 7.45 ^{1}H NMR (400 MHz, $CDCl_3$) of compound **S2m**.

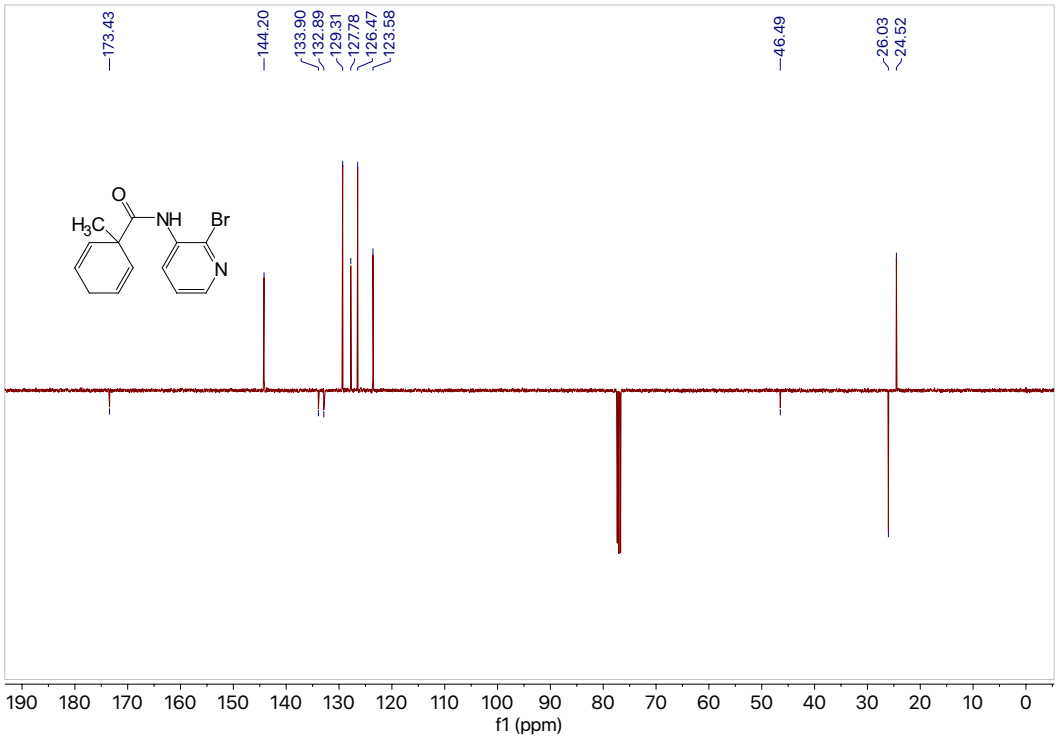

Figure 7.46 ^{13}C NMR (101 MHz, $CDCl_3$) of compound **S2m**.

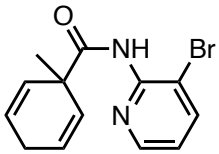

S2n

***N*-(3-Bromopyridin-2-yl)-1-methylcyclohexa-2,5-diene-1-carboxamide (S2n).** Using the general benzamide synthesis procedure, diene acid **S1a** (0.501 g, 3.62 mmol, 1.0 equiv) in DCM (9.1 mL, 0.4 M) reacted with 2-amino-3-bromopyridine (0.814 g, 4.71 mmol, 1.3 equiv) in DCM (11.8 mL, 0.4 M) to afford the crude product which was purified by column chromatography (silica, 4:1 hexanes: EtOAc) to afford pure **S2n** (0.858 g, 2.93 mmol) in 81% yield as a white solid, m.p. = 96.0 – 97.8°C

^{1}H NMR (400 MHz, $CDCl_3$) δ 8.47 (s, 1H), 8.43 (dd, J = 4.8, 1.6 Hz, 1H), 7.83 (dd, J = 7.9, 1.6 Hz, 1H), 6.94 (dd, J = 7.9, 4.7 Hz, 1H), 6.06 – 5.96 (m, 2H), 5.82 (dt, J = 10.4, 2.0 Hz, 2H), 2.94 – 2.75 (m, 2H), 1.43 (s, 3H).

^{13}C NMR (101 MHz, $CDCl_3$) δ_u 147.6, 141.1, 129.7, 126.1, 120.8, 24.6; δ_d 171.7, 148.6, 111.0, 46.6, 26.0.

GC (Method B) t_R = 2.695 min. EI-MS m/z (%): 293.0 (M^+, 12), 200.9 (42), 171.9 (83), 157.9 (16), 119.0 (6), 93.1 (100), 77.0 (54), 65.0 (14), 51.0 (7).

HRMS (ESI) calculated for $C_{13}H_{14}ON_2Br$ $[M+H]^+$: 293.0289, found 293.0287.

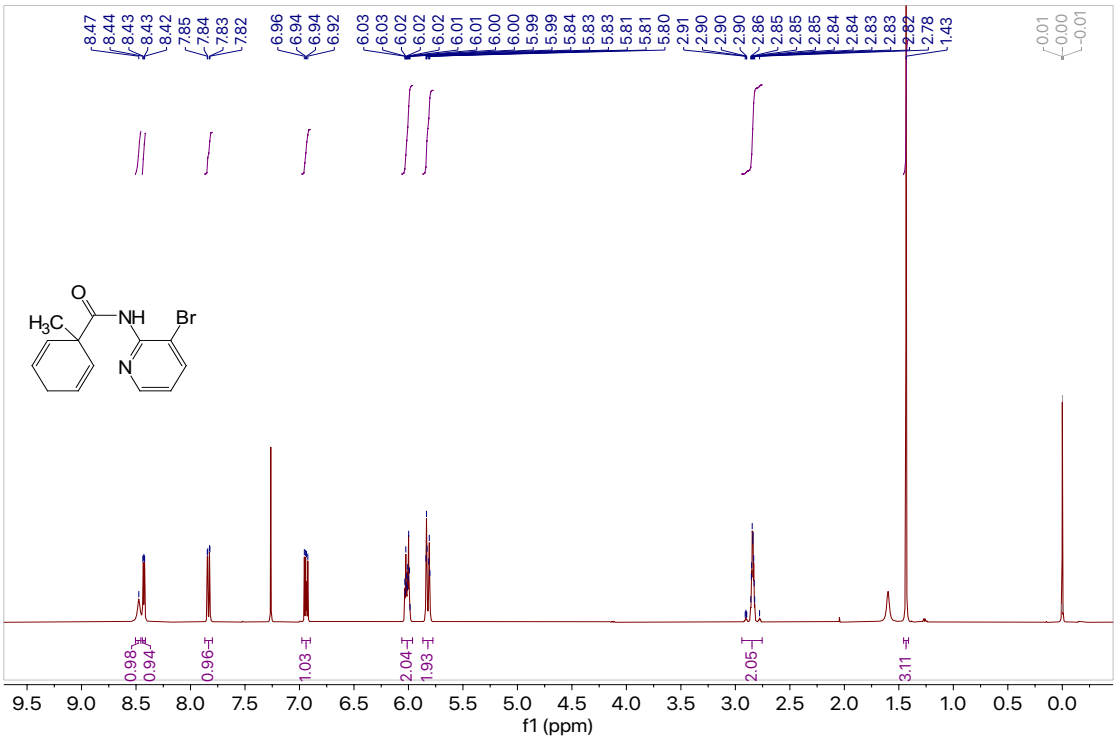

Figure 7.47 ^{1}H NMR (400 MHz, $CDCl_3$) of compound **S2n**.

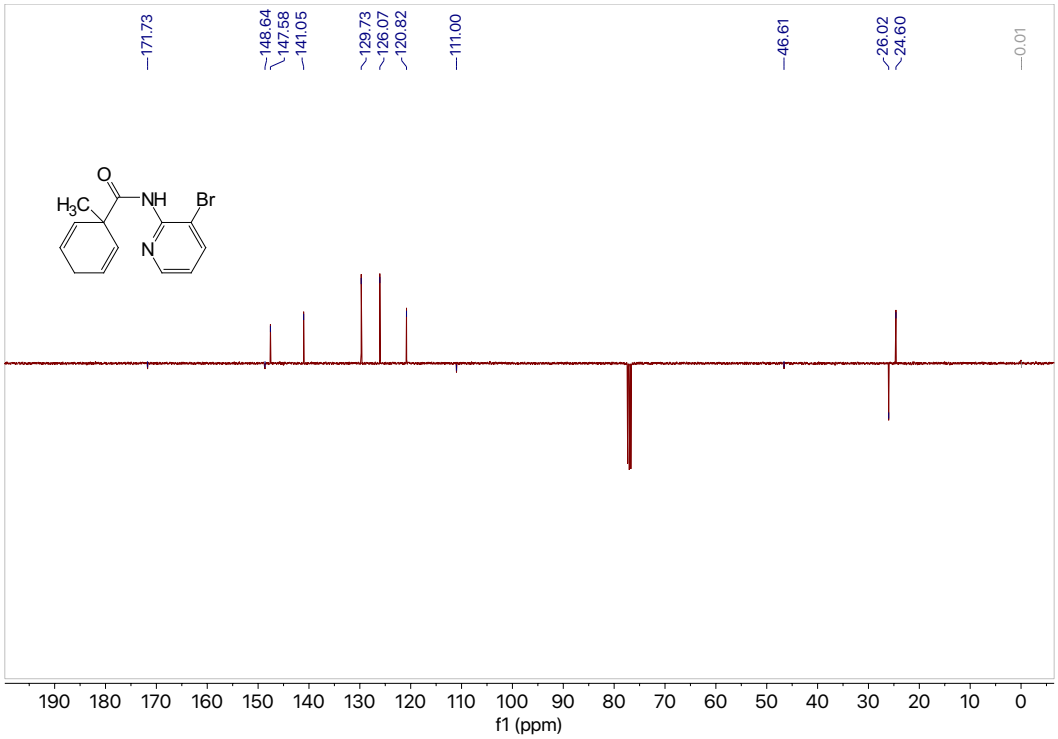

Figure 7.48 ^{13}C NMR (101 MHz, $CDCl_3$) of compound **S2n**.

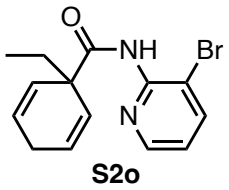

S2o

***N*-(3-Bromopyridin-2-yl)-1-ethylcyclohexa-2,5-diene-1-carboxamide (S2o).** Using the general benzamide synthesis procedure, diene acid **S1b** (1.11 g, 6.50 mmol, 1.0 equiv) in DCM (16.3 mL, 0.4 M) reacted with 2-amino-3-bromopyridine (1.71 g, 9.88 mmol, 1.5 equiv) in DCM (24.7 mL, 0.4 M) to afford the crude product which was purified by column chromatography (silica, 3:2 hexanes: EtOAc) to afford pure **S2o** (1.575 g, 5.13 mmol) in 78% yield as a white solid, m.p. = 81.3 – 84.5°C.

^{1}H NMR (400 MHz, $CDCl_3$) δ 8.48 (s, 1H), 8.43 (dd, J = 4.7, 1.6 Hz, 1H), 7.83 (dd, J = 7.9, 1.6 Hz, 1H), 6.94 (dd, J = 7.9, 4.7 Hz, 1H), 6.11 (dt, J = 10.3, 3.4 Hz, 2H), 5.74 (dt, J = 10.4, 2.1 Hz, 2H), 2.87 – 2.79 (m, 2H), 1.91 (q, J = 7.5 Hz, 2H), 0.86 (t, J = 7.5 Hz, 3H).

^{13}C NMR (101 MHz, $CDCl_3$) δ_u 147.6, 141.1, 128.0, 127.8, 120.8, 8.8; δ_d 171.6, 148.6, 111.1, 51.1, 29.3, 26.3.

GC (Method B) t_R = 3.072 min. EI-MS m/z (%): 307.0 (M^+, 5), 200.9 (18), 171.9 (49), 157.9 (8), 108.1 (40), 91.1 (30), 79.1 (100), 65.1 (7), 51.1 (5).

HRMS (ESI) calculated for $C_{14}H_{16}ON_2Br$ $[M+H]^+$: 307.0446, found 307.0447.

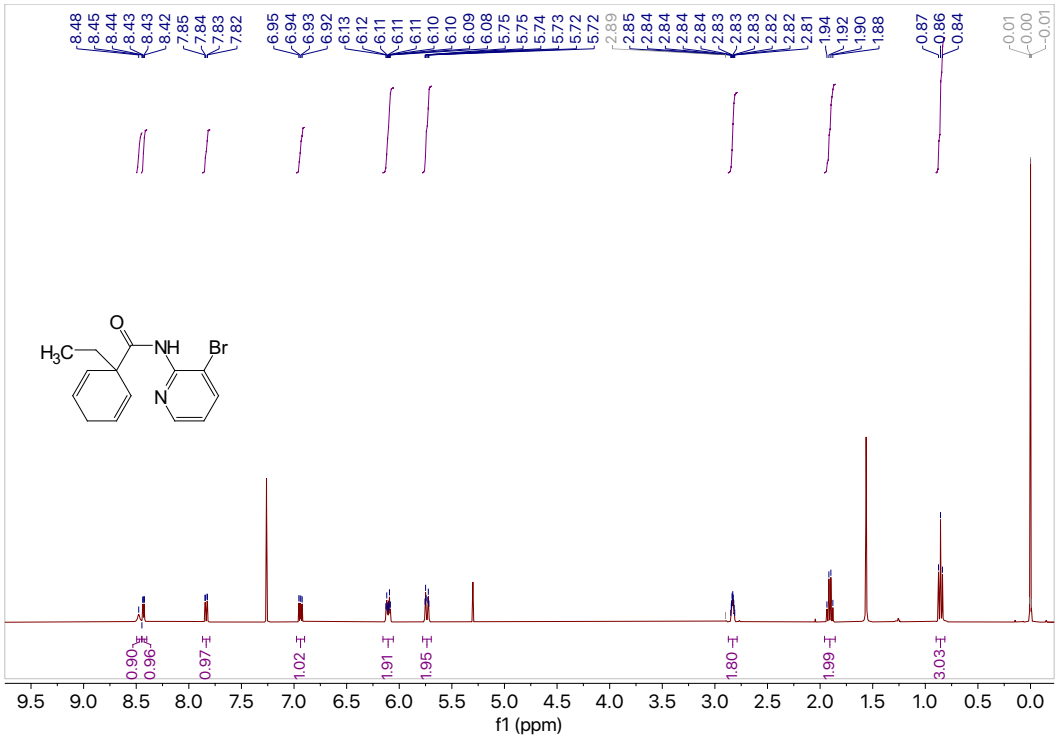

Figure 7.49 ^{1}H NMR (400 MHz, $CDCl_3$) of compound **S2o**.

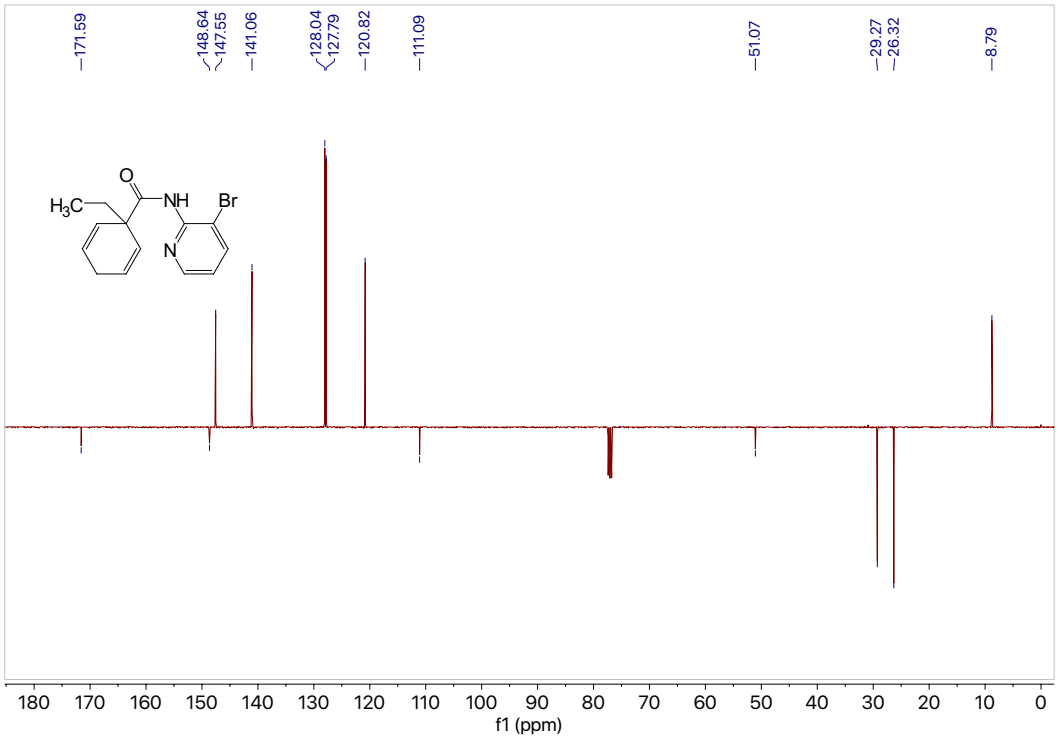

Figure 7.50 ^{13}C NMR (101 MHz, $CDCl_3$) of compound **S2o**.

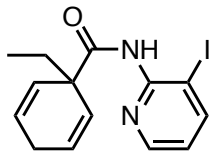

S2o-I

***N*-(3-Iodopyridin-2-yl)-1-ethylcyclohexa-2,5-diene-1-carboxamide (S2o-I).** Using the general benzamide synthesis procedure, diene acid **S1b** (0.561 g, 3.29 mmol, 1.0 equiv) in DCM (8.2 mL, 0.4 M) reacted with 2-amino-3-iodopyridine (0.759 g, 3.45 mmol, 1.05 equiv) in DCM (8.6 mL, 0.4 M) to afford the crude product which was purified by column chromatography (silica, 3:2 hexanes: EtOAc) to afford pure **S2o-I** (1.04 g, 2.94 mmol) in 89% yield as a white solid, m.p. = 101.3 – 101.9°C.

^{1}H NMR (400 MHz, $CDCl_3$) δ 8.38 (dd, J = 4.7, 1.7 Hz, 1H), 8.26 (s, 1H), 7.99 (dd, J = 7.9, 1.6 Hz, 1H), 6.72 (dd, J = 7.9, 4.7 Hz, 1H), 6.09 – 5.99 (m, 2H), 5.72 – 5.63 (m, 2H), 2.88 – 2.67 (m, 2H), 1.84 (q, J = 7.5 Hz, 2H), 0.79 (t, J = 7.5 Hz, 3H).

^{13}C NMR (101 MHz, $CDCl_3$) δ_u 148.4, 147.8, 128.1, 127.8, 121.3, 8.8; δ_d 171.8, 150.9, 86.0, 51.0, 29.3, 26.4.

GC (Method B) t_R = 3.444 min. EI-MS m/z (%): 353.1 ($M\text{-}1^+$, 9), 246.9 (39), 219.9 (100), 203.9 (12), 108.0 (33), 93.0 (21), 79.0 (60), 65.0 (5), 51.0 (4).

HRMS (ESI) calculated for $C_{14}H_{16}ON_2I$ $[M+H]^+$: 355.0307, found 355.0299.

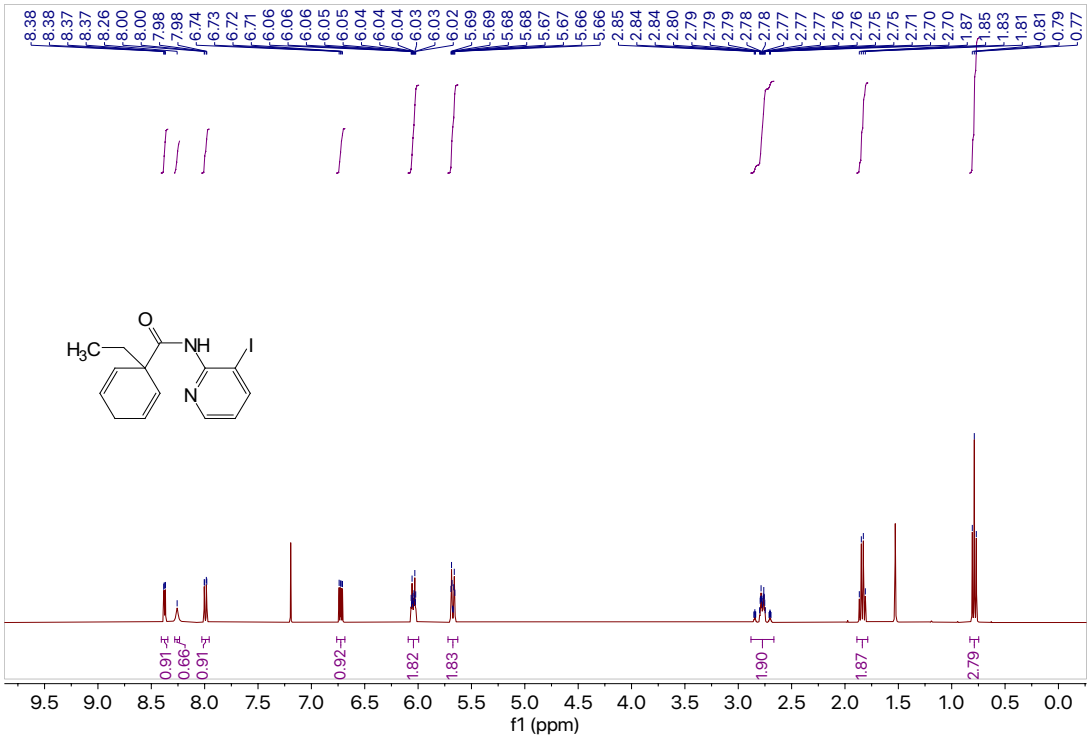

Figure 7.51 ^{1}H NMR (400 MHz, $CDCl_3$) of compound **S2o-I**.

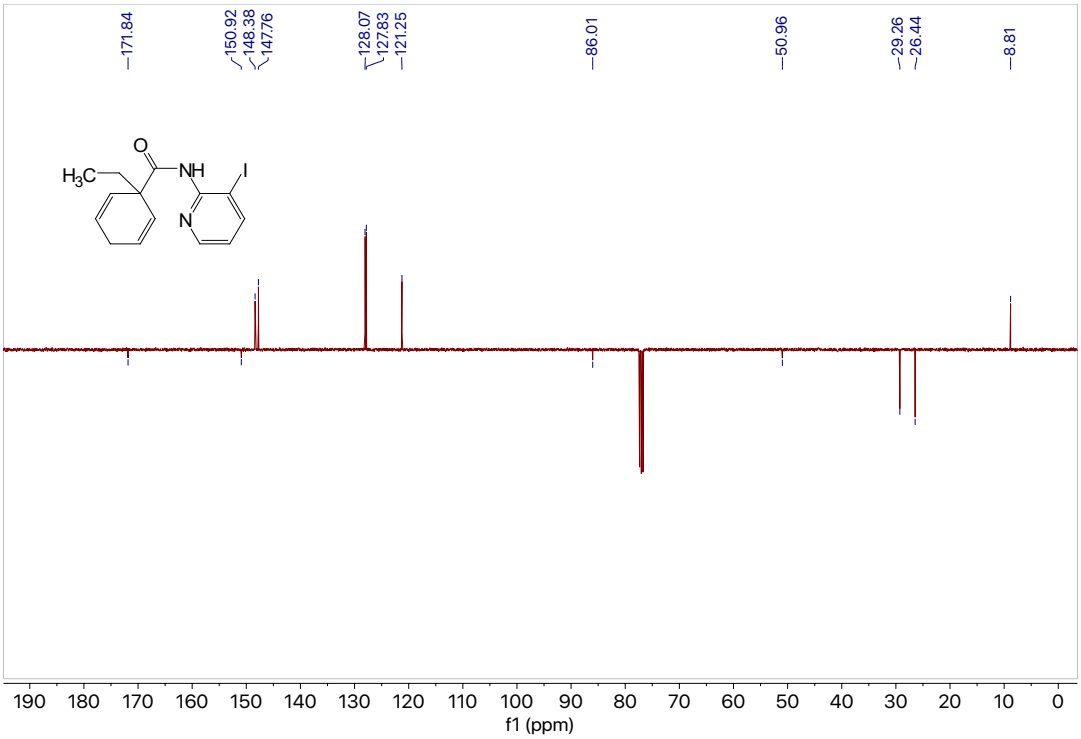

Figure 7.52 ^{13}C NMR (101 MHz, $CDCl_3$) of compound **S2o-I**.

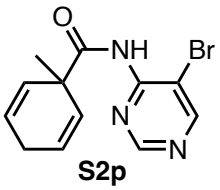

***N*-(5-Bromopyrimidin-4-yl)-1-methylcyclohexa-2,5-diene-1-carboxamide (S2p).** Using the general benzamide synthesis procedure B, diene acid **S1b** (0.501 g, 3.69 mmol, 1.1 equiv) reacted in DCM (9.2 mL, 0.4 M) with 4-amino-5-bromopyrimidine (0.584 g, 3.35 mmol, 1.0 equiv) in DCM (8.4 mL, 0.4 M) to afford the crude product which was purified by column chromatography (silica, 3:2 hexanes: EtOAc) to afford pure **S2p** (0.50 g, 1.69 mmol) in 51% yield as a white-tan solid.

^{1}H NMR (400 MHz, $CDCl_3$) δ 8.92 (s, 1H), 8.75 (s, 1H), 8.67 (s, 1H), 6.11 – 6.01 (m, 2H), 5.78 (dt, J = 10.4, 2.1 Hz, 2H), 2.91 – 2.83 (m, 2H), 1.44 (s, 3H).

^{13}C NMR (101 MHz, $CDCl_3$) δ_u 158.5, 157.3, 129.2, 126.7, 24.2; δ_d 171.2, 154.6, 108.1, 47.3, 26.0

GC (Method B) t_R = 2.603 min. EI-MS m/z (%): 292.0 (M-2$^+$, 1), 200.8 (9), 172.9 (35), 93.0 (100), 77.0 (40), 65.0 (8), 51.0 (6).

HRMS (ESI) calculated for $C_{12}H_{13}ON_3Br$ $[M+H]^+$: 294.0242, found 294.0245.

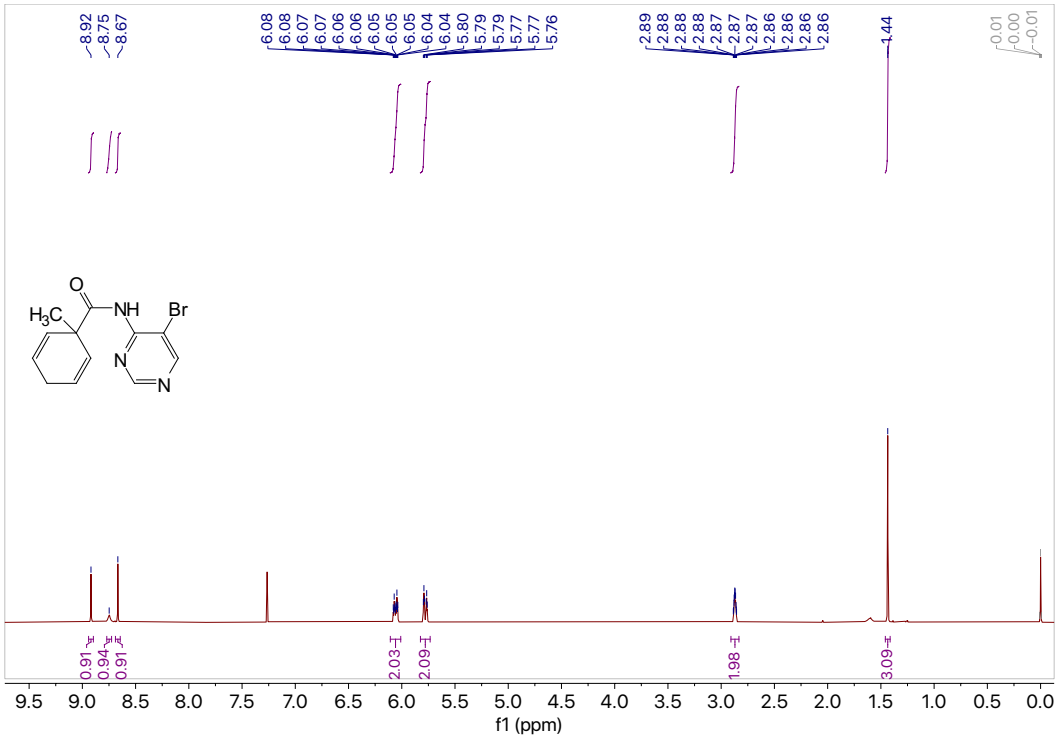

Figure 7.53 ^{1}H NMR (400 MHz, $CDCl_3$) of compound **S2p**.

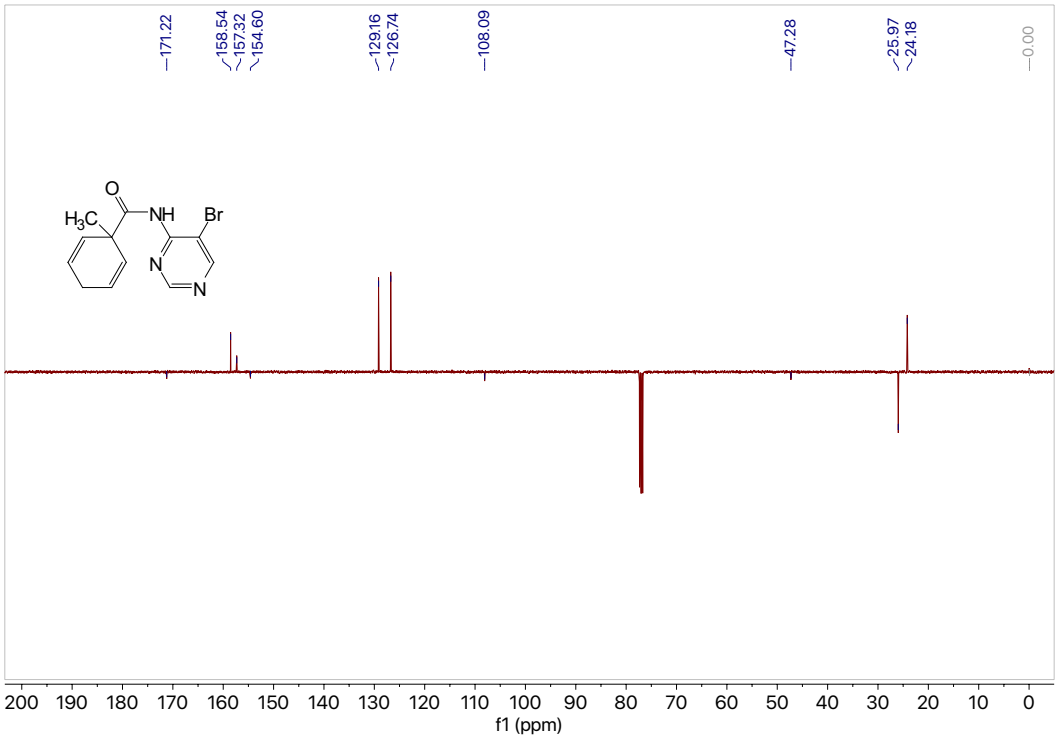

Figure 7.54 ^{13}C NMR (101 MHz, $CDCl_3$) of compound **S2p**.

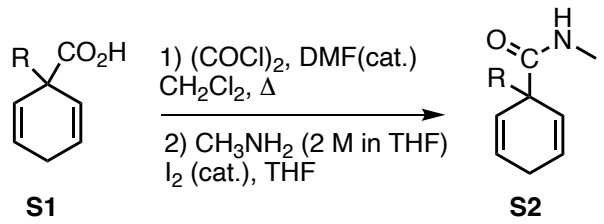

Scheme 7.6 N-acylation of methylamine reaction.

General procedure and data

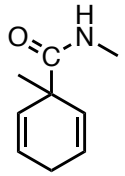

S2q

***N*,1-dimethylcyclohexa-2,5-diene-1-carboxamide (S2q).** To a round bottom flask with a stir bar were added iodine (0.053 g, 0.207 mmol, 0.1 equiv) and methylamine (2 M in THF, 2.1 mL, 4.14 mmol, 2.0 equiv) and the mixture was cooled to 0°C. Another round bottom flask was charged with the acid chloride intermediate of **S1a** (0.34 g, 2.17 mmol, 1.05 equiv) in THF (6.1 mL, 0.4 M) and cooled to 0°C. The solution of acid chloride in THF was added the mixture of methylamine and iodine. Upon completion, the reaction mixture was diluted with diethyl ether, washed with $Na_2S_2O_3$, saturated $NaHCO_3$, brine and then dried with $MgSO_4$, and concentrated in vacuo. The crude product (0.205 g, 1.36 mmol) was obtained in 63% yield as a yellow oil and was used without further purification.

^{1}H NMR (400 MHz, $CDCl_3$) δ 5.88 – 5.82 (m, 2H), 5.69 (dp, *J* = 10.5, 2.0 Hz, 2H), 2.77 (d, *J* = 4.8 Hz, 3H), 2.71 (ttd, *J* = 3.2, 2.1, 1.0 Hz, 2H), 1.92 (s, 1H), 1.32 (s, 3H).

^{13}C NMR (101 MHz, $CDCl_3$) δ_u 130.2, 125.0, 26.7, 25.5; δ_d 175.4, 44.8, 25.9.

GC (Method B) t_R = 5.245 min. EI-MS m/z (%): 150.0 (M^+, 7), 136.0 (15), 93.0 (100), 79.0 (73), 65.0 (13), 58.0 (20), 51.0 (7).

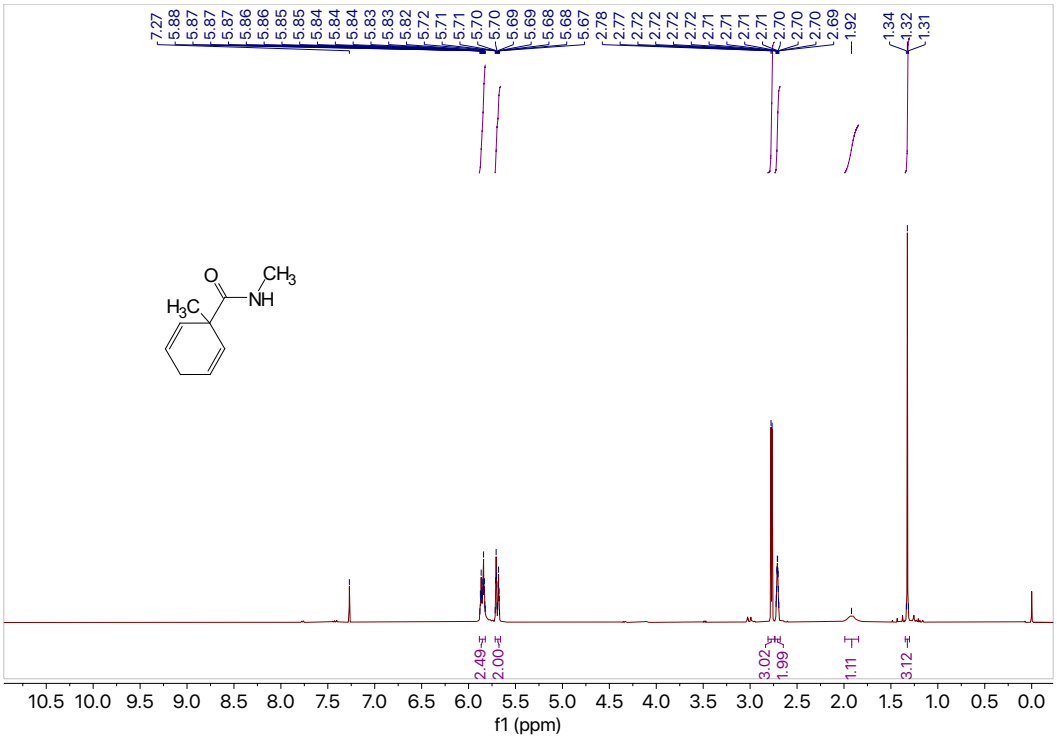

Figure 7.55 ^{1}H NMR (400 MHz, $CDCl_3$) of compound **S2q**.

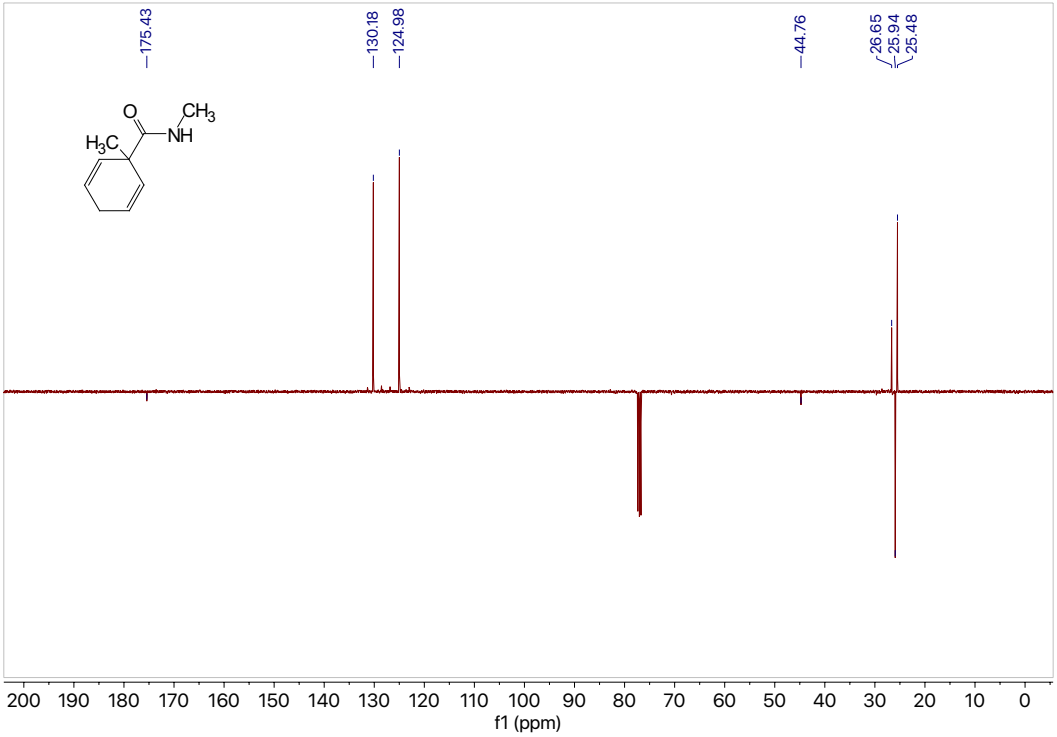

Figure 7.56 ^{13}C NMR (101 MHz, $CDCl_3$) of compound **S2q**.

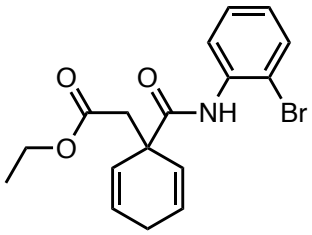

S2r

Ethyl 2-(1-((2-bromophenyl)carbamoyl)cyclohexa-2,5-dien-1-yl)acetate (S2r). Using the general benzamide synthesis procedure, diene acid **S1e** (0.501 g, 2.38 mmol, 1.0 equiv) in DCM (6.0 mL, 0.4 M) reacted with 2-bromoaniline (0.532 g, 3.09 mmol, 1.3 equiv) in DCM (7.7 mL, 0.4 M) to afford the crude product which was purified by column chromatography (silica, 9:1 hexanes: EtOAc) to afford pure **S2r** (0.805g, 2.21 mmol) in 93% yield as an yellow oil.

^{1}H NMR (400 MHz, $CDCl_3$) δ 8.40 (s, 1H), 8.38 (dd, J = 8.3, 1.6 Hz, 1H), 7.49 (dd, J = 8.0, 1.5 Hz, 1H), 7.32 – 7.27 (m, 1H), 6.94 (td, J = 7.7, 1.6 Hz, 1H), 6.13 – 6.06 (m, 2H), 5.96 (dt, J = 10.4, 2.0 Hz, 2H), 4.13 (q, J = 7.1 Hz, 2H), 2.88 (s, 2H), 2.84 (tp, J = 3.7, 2.0 Hz, 2H), 1.23 (t, J = 7.1 Hz, 3H).

^{13}C NMR (101 MHz, $CDCl_3$) δ_u 132.1, 128.4, 128.0, 127.3, 125.0, 121.1, 14.8; δ_d 170.9, 136.0, 113.2, 60.5, 48.0, 42.3, 26.3.

GC (Method B) t_R = 3.875 min. EI-MS m/z (%): 365.0 ($M+1^+$, 1), 318.0 (4), 166.1 (52), 137.0 (6), 119.0 (14), 105.0 (5), 91.1 (100), 77.1 (5), 63.1 (5).

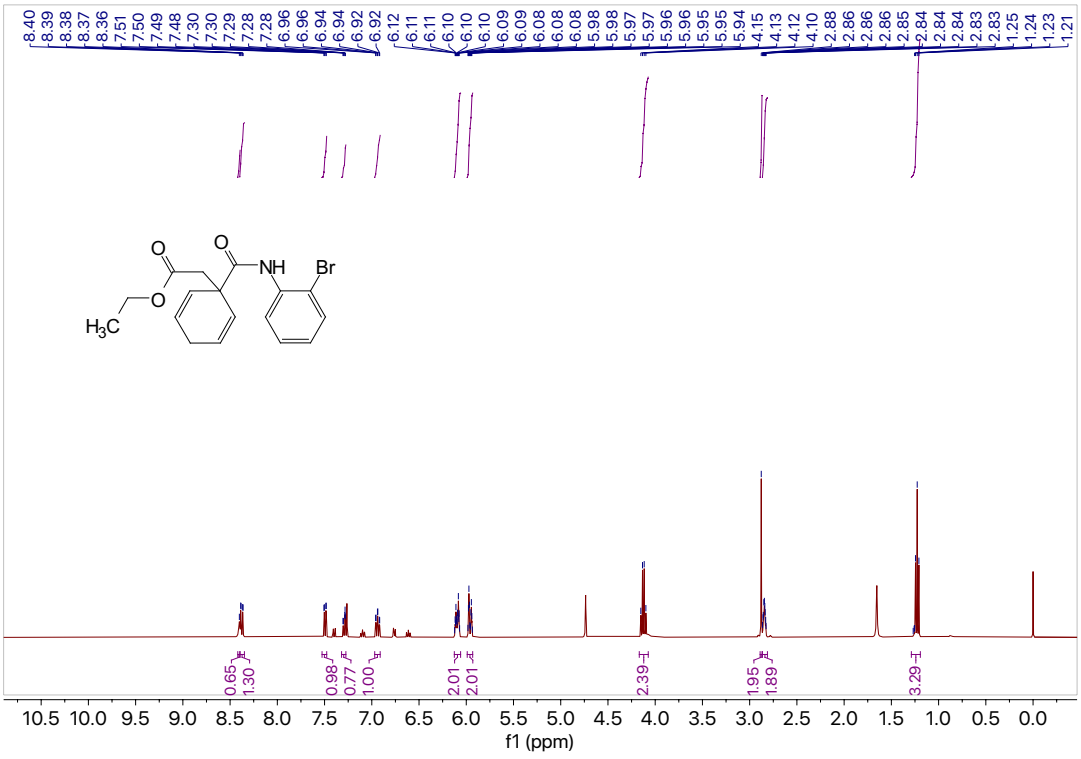

Figure 7.57 ^{1}H NMR (400 MHz, $CDCl_3$) of compound **S2r**.

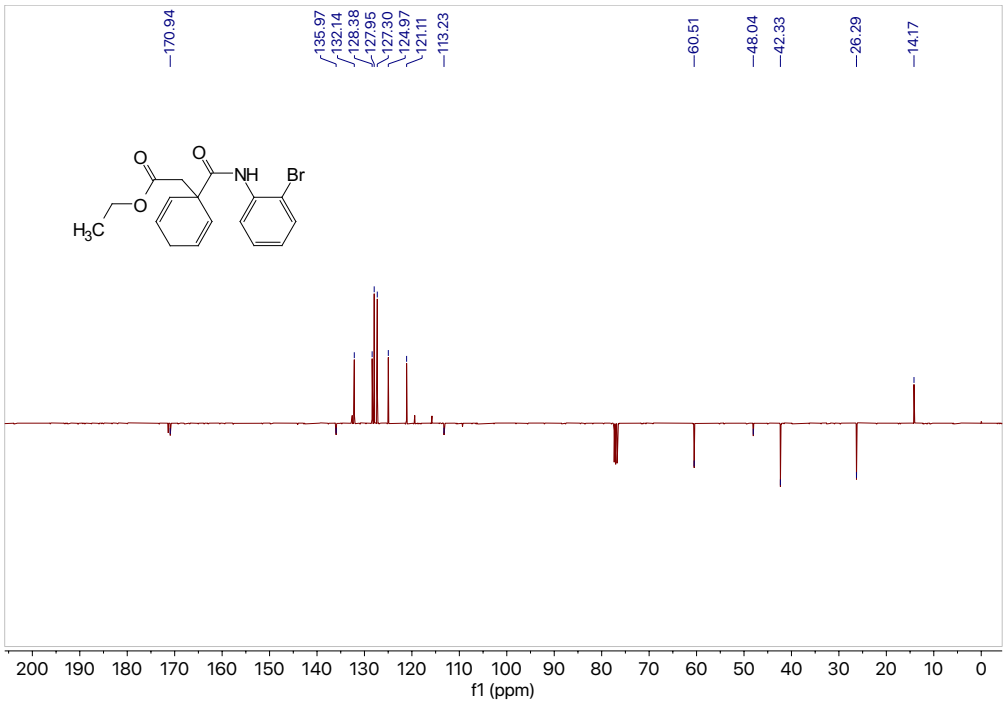

Figure 7.58 ^{13}C NMR (101 MHz, $CDCl_3$) of compound **S2r**.

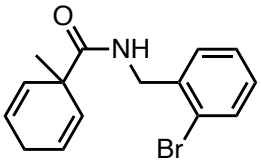

S2u

***N*-(2-bromobenzyl)-1-methylcyclohexa-2,5-diene-1-carboxamide (S2u).** Using the general benzamide synthesis procedure, diene acid **S1a** (0.502 g, 3.62 mmol, 1.0 equiv) in DCM (9.1 mL, 0.4 M) reacted with 2-bromobenzylamine (0.875 g, 4.71 mmol, 1.3 equiv) in DCM (11.8 mL, 0.4 M) to afford the crude product which was purified by column chromatography (silica, 9:1 hexanes: EtOAc) to afford pure **S2u** (0.893 g, 2.92 mmol) in 81% yield as a white solid.

^{1}H NMR (400 MHz, $CDCl_3$) δ 7.54 (d, J = 1.1 Hz, 1H), 7.32 – 7.26 (m, 2H), 7.13 (ddd, J = 9.0, 7.1, 2.1 Hz, 1H), 6.36 (s, 1H), 5.87 (dtd, J = 10.5, 3.3, 1.7 Hz, 2H), 5.71 (dt, J = 10.4, 2.0 Hz, 2H), 4.45 (d, J = 6.1 Hz, 2H), 2.72 (tt, J = 3.5, 2.1 Hz, 2H), 1.34 (s, 3H).

^{13}C NMR (101 MHz, $CDCl_3$) δ_u 132.8, 130.1, 129.0, 127.7, 125.3, 25.3; δ_d 174.6, 137.5, 123.6, 45.0, 44.0, 26.0.

GC (Method B) t_R = 2.677 min. EI-MS m/z (%): 306.0 (M^+, 4), 290.0 (10), 213.9 (10), 168.9 (30), 134.0 (12), 94.1 (100), 77.1 (40), 65.1 (5), 51.0 (5).

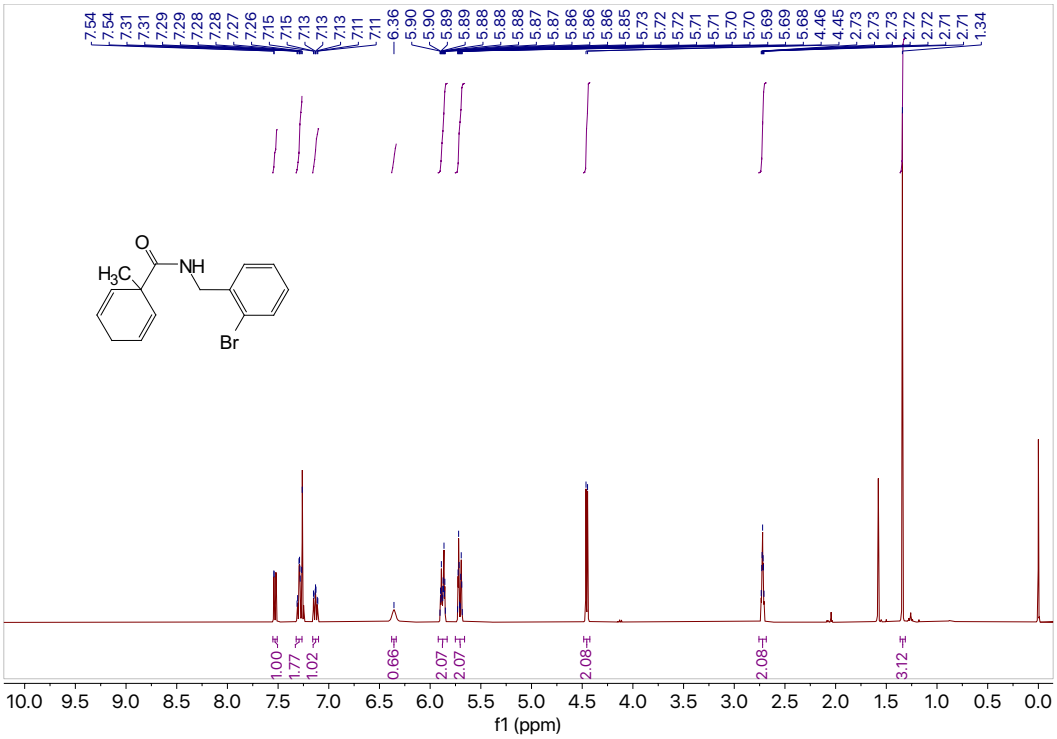

Figure 7.59 ^{1}H NMR (400 MHz, $CDCl_3$) of compound **S2u**.

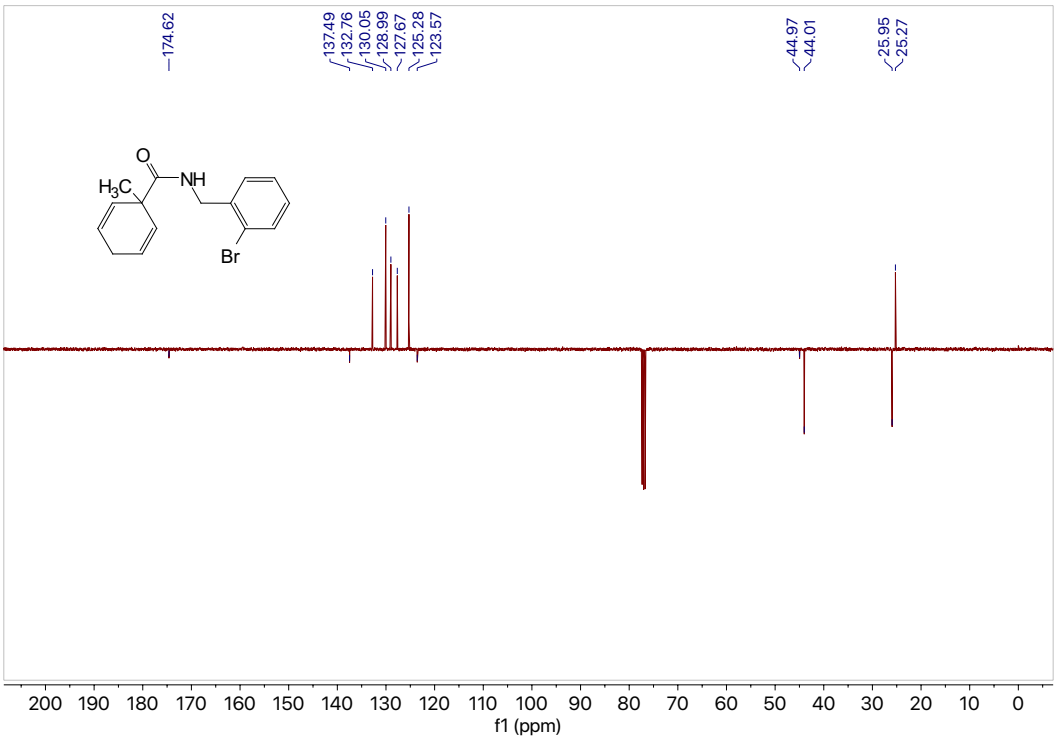

Figure 7.60 ^{13}C NMR (101 MHz, $CDCl_3$) of compound **S2u**.

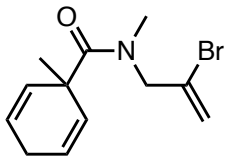

1v

***N*-(2-bromoallyl)-*N*,1-dimethylcyclohexa-2,5-diene-1-carboxamide (1v).** Using the general benzamide synthesis procedure, diene acid **S1a** (0.301 g, 2.17 mmol, 1.0 equiv) in DCM (5.4 mL, 0.4 M) reacted with 2-bromo-*N*-methylprop-2-en-1-amine (0.675 g, 4.50 mmol, 2.1 equiv) in DCM (11.3 mL, 0.4 M) to afford the crude product which was purified by column chromatography (silica, 4:1 hexanes: EtOAc) to afford pure **1v** (0.471 g, 2.17 mmol) in 80% yield as a clear colorless oil.

^{1}H NMR (400 MHz, $CDCl_3$) δ 5.82 – 5.66 (m, 4H), 5.63 (s, 1H), 5.59 – 5.53 (m, 1H), 4.24 (s, 2H), 2.99 (d, J = 34.3 Hz, 3H), 2.80 – 2.65 (m, 2H), 1.33 (s, 3H).

^{13}C NMR (101 MHz, DMSO) δ_u 130.0, 123.9, 35.7, 29.1; δ_d 172.8, 129.7, 117.9, 56.7, 44.9, 25.9.

GC (Method B) t_R = 1.470 min. EI-MS m/z (%): 270.0 (M^+, 1), 190.1 (7), 147.9 (15), 119.0 (10), 93.1 (100), 77.0 (40), 65.1 (7), 51.1 (5)

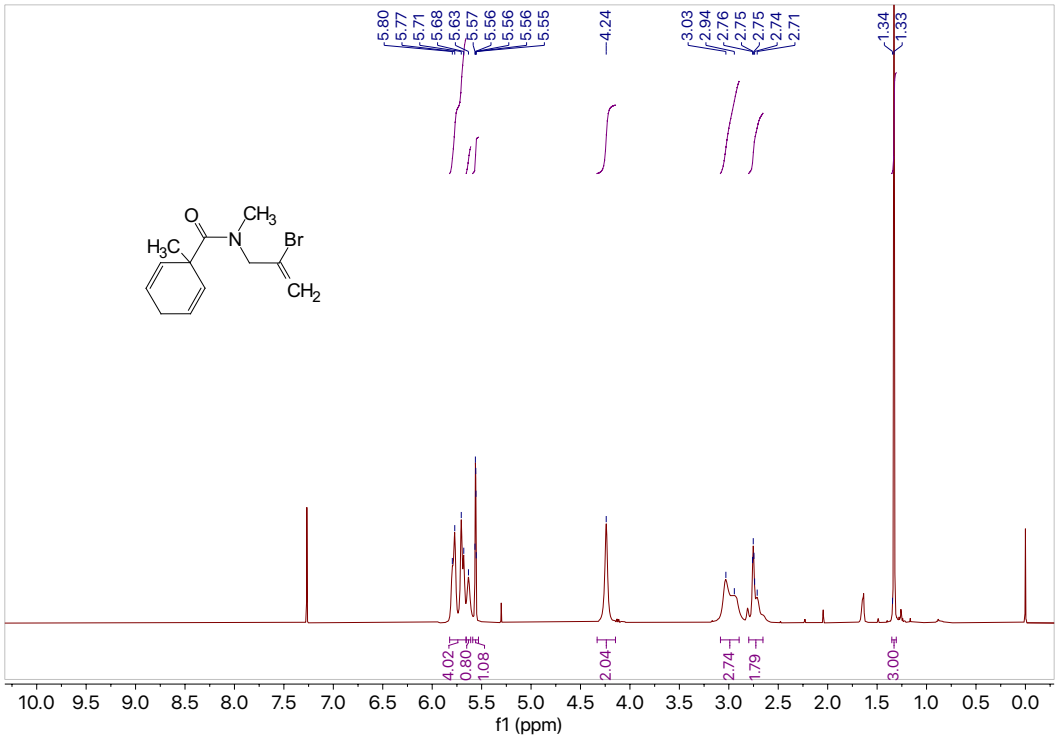

Figure 7.61 ^{1}H NMR (400 MHz, $CDCl_3$) of compound **1v**.

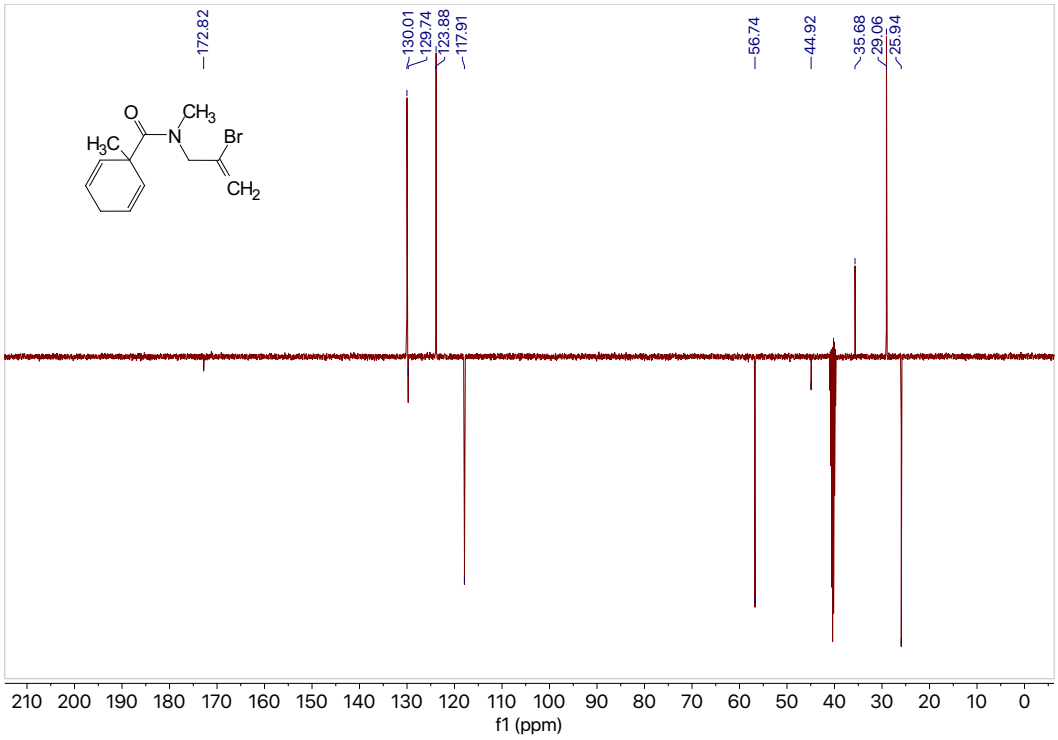

Figure 7.62 ^{13}C NMR (101 MHz, DMSO-d_6) of compound **1v**.

7.6 Secondary amide protection general procedure and data

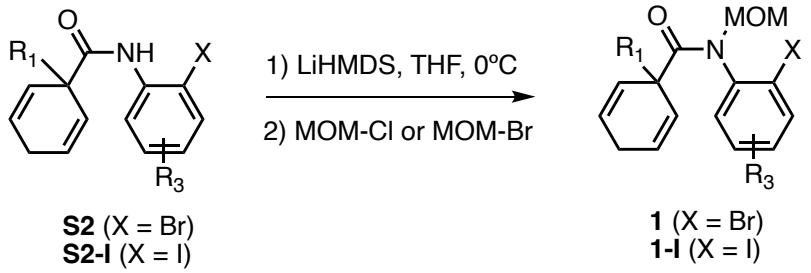

S2 (X = Br)
S2-I (X = I)

1 (X = Br)
1-I (X = I)

Scheme 7.7 MOM protection general reaction.

General procedure

Secondary amide (1.0 mmol, 1.0 equiv) was dissolved in THF (7 mL, 0.14 M) and cooled to 0ºC. LiHMDS (1.0 M in hexanes, 1.2 mmol, 1.2 equiv) was added dropwise and the solution was stirred for 10 min. Chloro- or bromomethyl methyl ether (2.0-5.0 mmol, 2.0-5.0 equiv) was added dropwise to the reaction solution and the reaction was left stirring while slowly warming to r.t. Upon completion, the reaction was quenched with saturated NH_4Cl and diluted with EtOAc. The aqueous layer was extracted with EtOAc (2 x). The combined organic layers were washed with brine, dried with $MgSO_4$, filtered, and concentrated. The crude product was purified by column chromatography.

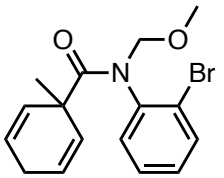

1b

***N*-(2-Bromophenyl)-*N*-(methoxymethyl)-1-methylcyclohexa-2,5-diene-1-carboxamide (1b).** Using the general procedure for MOM group protection, secondary amide **S2b** (0.444 g, 1.52 mmol, 1.0 equiv) in THF (10.6 mL, 0.14 M) was alkylated with chloromethyl methyl ether (0.248 mL, 3.04 mmol, 2.0 equiv). The crude product was purified by column chromatography (silica, 9:1 hexanes: EtOAc) to afford **1b** (0.389 g, 1.16 mmol) in 76% yield as a clear colorless oil.

^{1}H NMR (400 MHz, DMSO-d_6) δ 7.62 (d, J = 7.6 Hz, 1H), 7.34 – 7.21 (m, 3H), 5.58 (s, 2H), 5.46 (s, 1H), 5.25 (s, 1H), 4.25 (s, 1H), 3.25 (s, 3H), 2.45 – 2.05 (m, 2H), 1.22 (s, 3H).

^{13}C NMR (101 MHz, DMSO-d_6) δ_u 133.2, 130.5, 130.1, 128.3, 124.4, 122.7, 56.4, 29.4; δ_d 174.1, 140.6, 121.4, 80.2, 46.0, 25.9.

GC (Method B) t_R = 2.578 min. EI-MS m/z (%): 335.1 ($M+1^+$, 1), 305.1 (5), 244.0 (4), 224.1 (19), 211.9 (8), 198.9 (8), 184.9 (70), 164.0 (58), 152.0 (5), 134.0 (6), 105.0 (7), 93.0 (100), 77.0 (39), 65.0 (7), 51.0 (5).

HRMS (ESI) calculated for $C_{16}H_{19}O_2NBr$ $[M+H]^+$: 336.0599, found 336.0590.

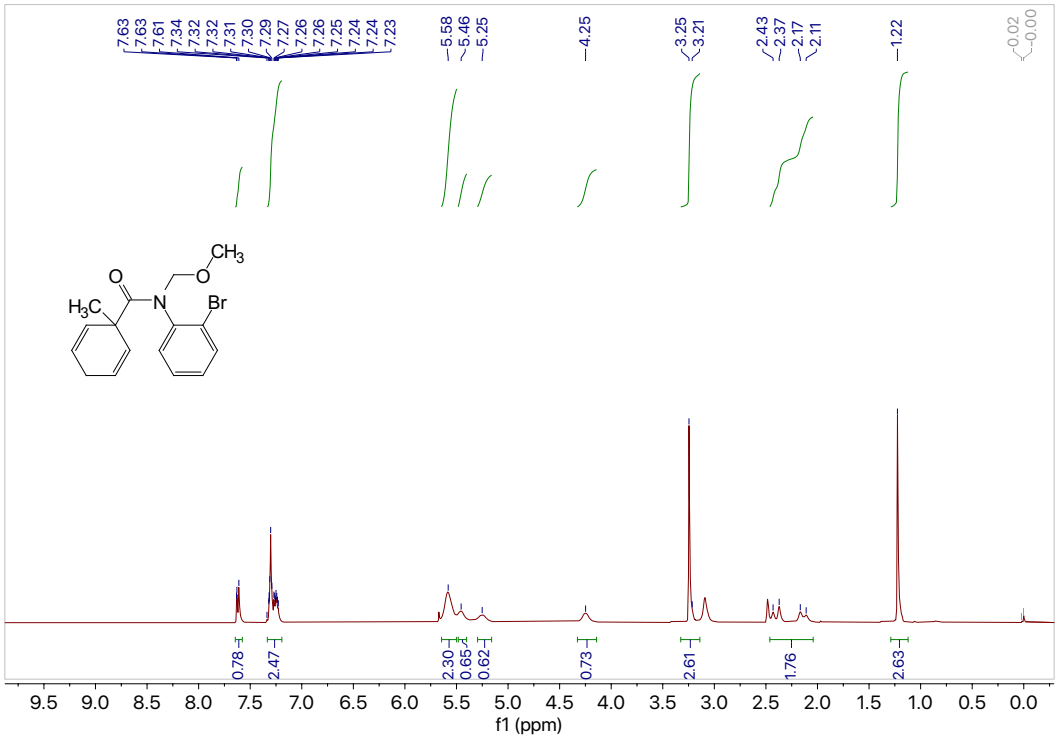

Figure 7.63 ^{1}H NMR (400 MHz, DMSO-d_6) of compound **1b**.

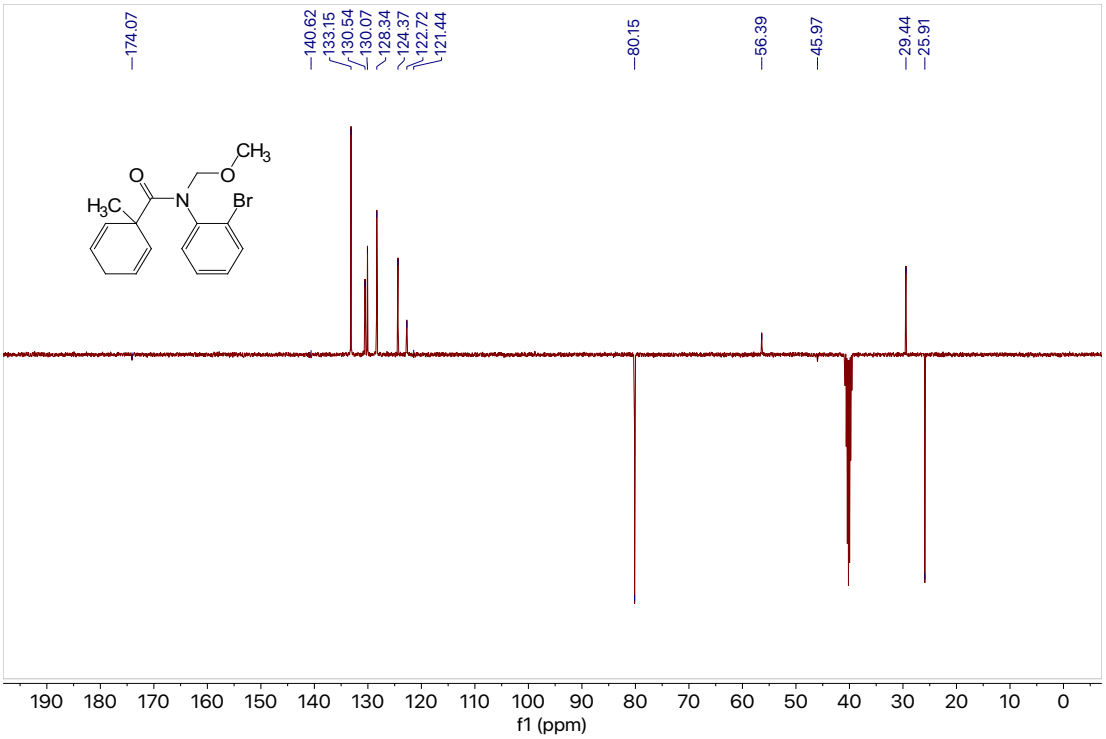

Figure 7.64 ^{13}C NMR (101 MHz, DMSO-d$_6$) of compound **1b**.

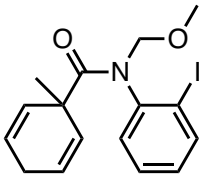

1b-I

***N*-(2-Iodophenyl)-*N*-(methoxymethyl)-1-methylcyclohexa-2,5-diene-1-carboxamide (1b-I).** Using the general procedure for MOM group protection, secondary amide **S2b-I** (0.998 g, 2.95 mmol, 1.0 equiv) in THF (20.7 mL, 0.14 M) was alkylated with chloromethyl methyl ether (0.90 mL, 11.8 mmol, 4.0 equiv). The crude product was purified by column chromatography (silica, 9:1 hexanes: EtOAc) to afford **1b-I** (0.990 g, 2.58 mmol) in 88% yield as a yellow oil.

^{1}H NMR (400 MHz, DMSO-*d*$_6$) δ 7.90 – 7.86 (m, 1H), 7.36 (td, *J* = 7.6, 1.6 Hz, 1H), 7.28 (dd, *J* = 7.8, 1.8 Hz, 1H), 7.09 (td, *J* = 7.5, 1.8 Hz, 1H), 5.72 – 5.55 (m, 3H), 5.50 (d, *J* = 9.9 Hz, 1H), 5.27 (s, 1H), 4.22 (d, *J* = 10.1 Hz, 1H), 3.26 (s, 3H), 2.48 – 2.14 (m, 2H), 1.26 (s, 3H).

^{13}C NMR (101 MHz, DMSO-*d*$_6$) δ$_u$ 139. 9, 139.5, 132.4, 130.8, 129.9, 129.0, 124.2, 122.5, 56.5, 29.5, 26.8; δ$_d$ 174.1, 150.7, 144.0, 80.6, 46.1, 25.9.

GC (Method B) t_R = 2.935 min. EI-MS m/z (%): 383.1 (M^+, 1), 292.0 (4), 259.9 (6), 244.9 (11), 230.9 (100), 224.1 (18), 202.9 (5), 164.0 (28), 134.0 (4), 93.0 (50), 77.0 (24), 65.0 (5), 51.0 (5).

HRMS (ESI) calculated for $C_{16}H_{19}O_2NI$ $[M+H]^+$: 384.0461, found 384.0447.

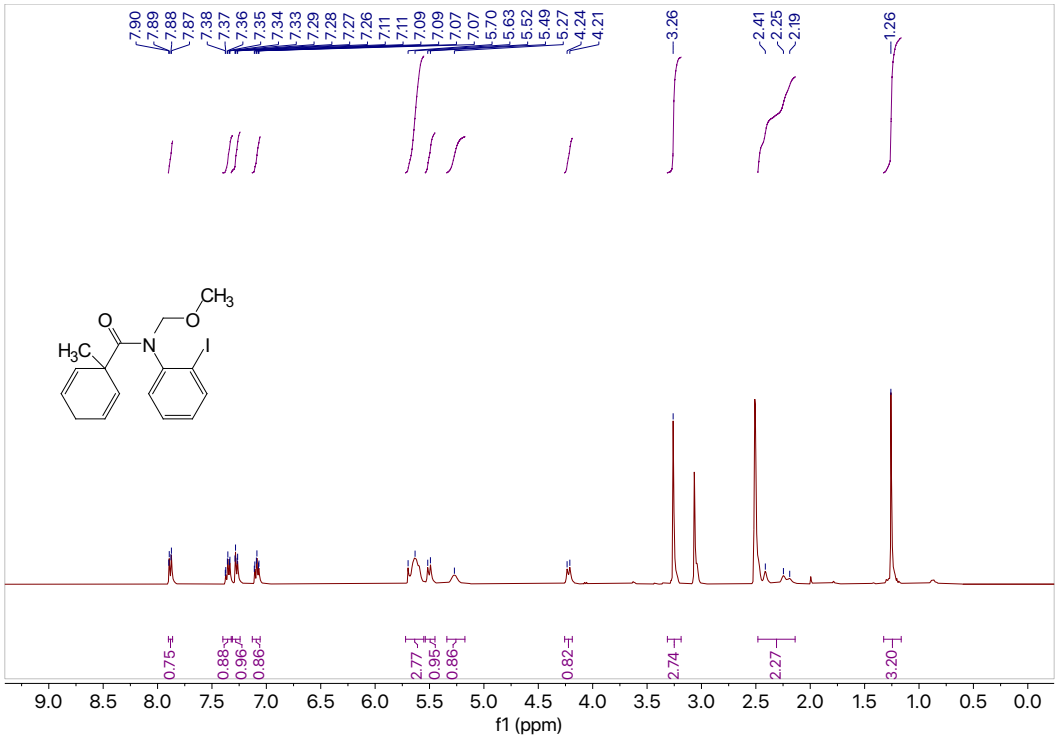

Figure 7.65 ^{1}H NMR (400 MHz, DMSO-d_6) of compound **1b-I**.

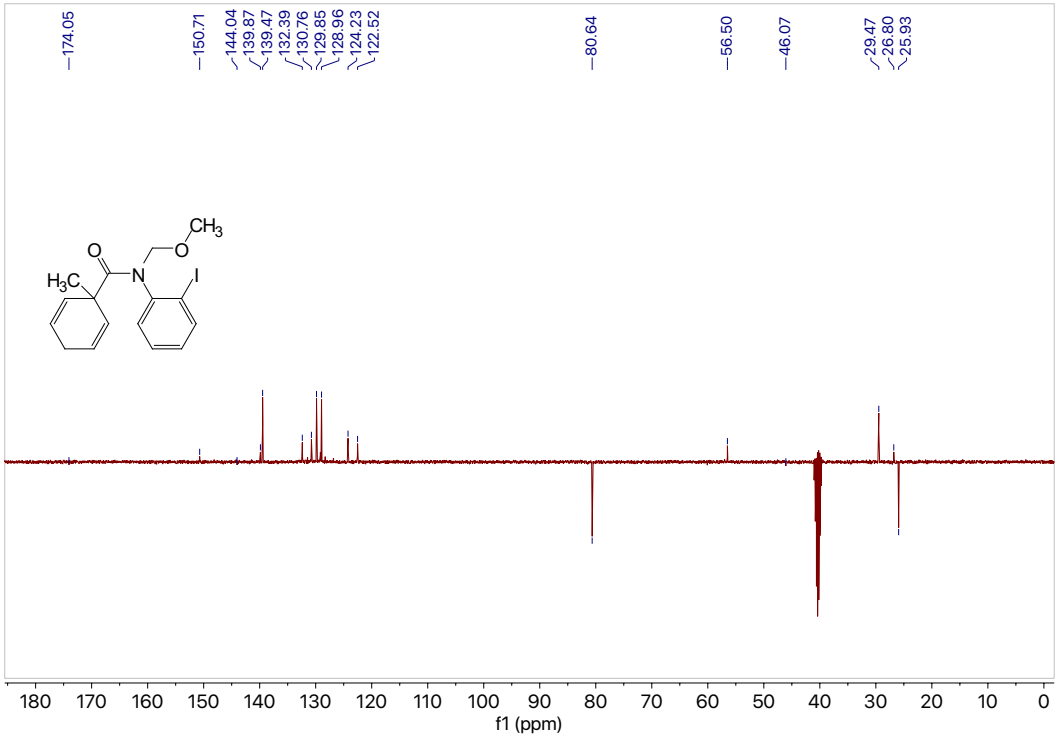

Figure 7.66 ^{13}C NMR (101 MHz, DMSO-d_6) of compound **1b-I**.

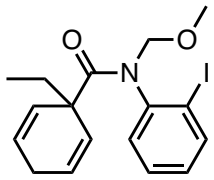

1c-I

1-Ethyl-*N*-(2-iodophenyl)-*N*-(methoxymethyl)cyclohexa-2,5-diene-1-carboxamide (1c-I). Using the general procedure for MOM group protection, secondary amide **S2c-I** (1.10 g, 3.12 mmol, 1.0 equiv) in THF (21.8 mL, 0.14 M) was alkylated with chloromethyl methyl ether (0.47 mL, 6.24 mmol, 2.0 equiv). The crude product was purified by column chromatography (silica, 9:1 hexanes: EtOAc) to afford **1c-I** (0.978 g, 2.46 mmol) in 79% yield as an orange solid, m.p. = 64.9 – 66.0°C.

^{1}H NMR (400 MHz, DMSO-d_6) δ 7.84 (dd, J = 7.8, 2.3 Hz, 1H), 7.30 (t, J = 7.6 Hz, 1H), 7.21 (d, J = 7.7 Hz, 1H), 7.09 – 7.00 (m, 1H), 5.66 (d, J = 10.0 Hz, 1H), 5.52 – 5.39 (m, 3H), 5.27 (s, 1H), 4.17 (d, J = 9.8 Hz, 1H), 3.22 (s, 3H), 2.37 (d, J = 23.2 Hz, 1H), 2.18 (d, J = 23.3 Hz, 1H), 1.69 (q, J = 6.9 Hz, 2H), 0.70 (q, J = 0.7 Hz, 3H).

^{13}C NMR (101 MHz, DMSO-d_6) δ_u 139.5, 132.4, 129.8, 129.2, 128.9, 127.2, 125.6, 123.9, 56.6, 8.7; δ_d 174.0, 144.1, 117.5, 80.5, 50.4, 33.2, 26.3.

GC (Method B) t_R = 3.233 min. EI-MS m/z (%): 397.1 (M^+, 1), 365.0 (5), 292.0 (7), 259.9 (13), 239.0 (16), 230.9 (100), 202.9 (4), 164.0 (25), 134.0 (4), 107.0 (26), 90.0 (17), 79.0 (43).

HRMS (ESI) calculated for $C_{17}H_{21}O_2NI$ $[M+H]^+$: 398.0617, found 398.0611.

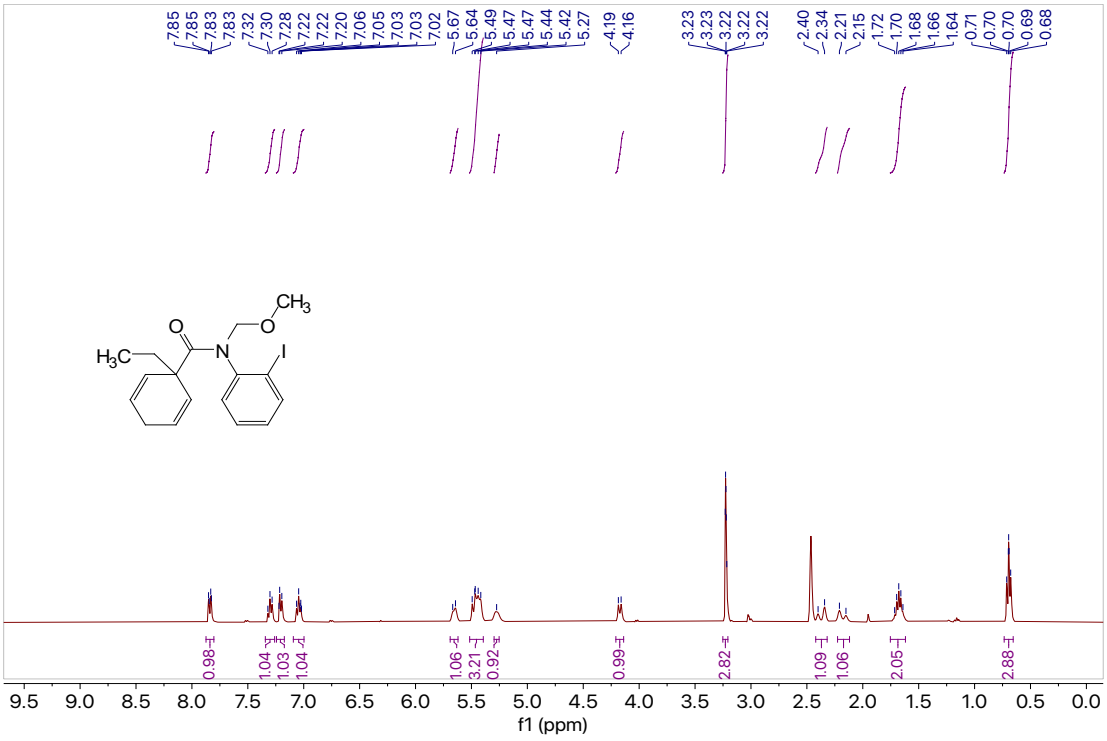

Figure 7.67 ^{1}H NMR (400 MHz, DMSO-d_6) of compound **1c-I**.

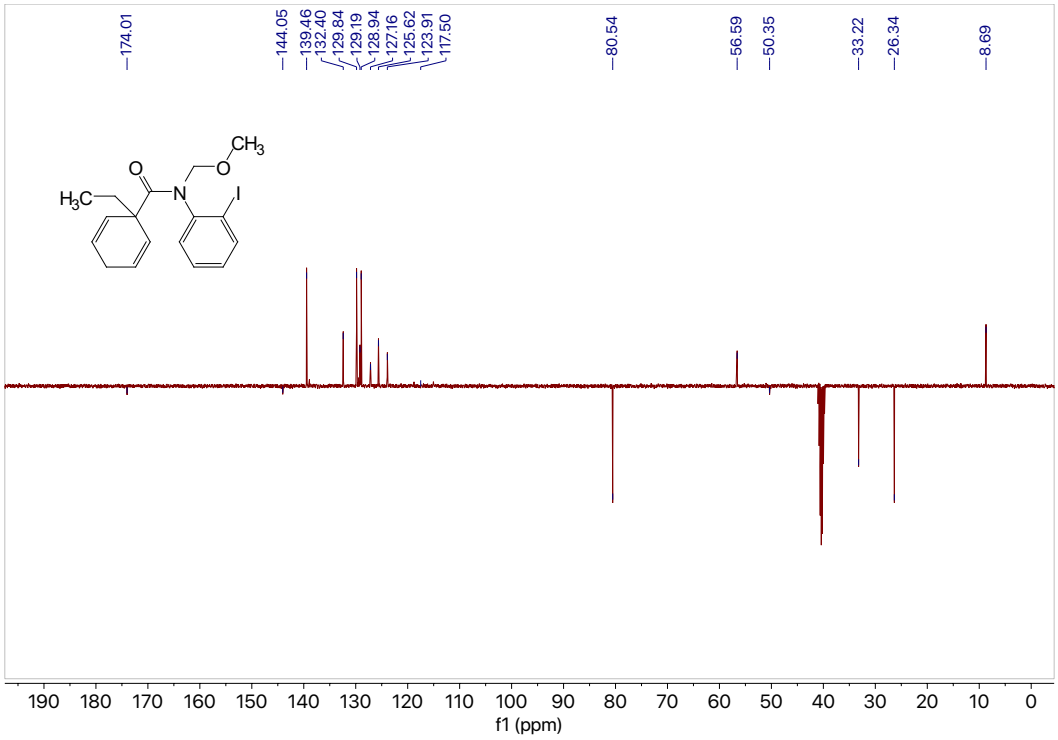

Figure 7.68 ^{13}C NMR (101 MHz, DMSO-d$_6$) of compound **1c-I**.

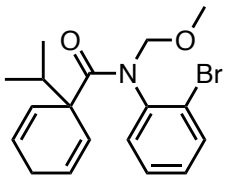

1e

***N*-(2-Bromophenyl)-1-isopropyl-*N*-(methoxymethyl)cyclohexa-2,5-diene-1-carboxamide (1e).** Using the general procedure for MOM group protection, secondary amide **S2e** (1.10 g, 3.43 mmol, 1.0 equiv) in THF (24 mL, 0.14 M) was alkylated with chloromethyl methyl ether (0.51 mL, 6.86 mmol, 2.0 equiv). The crude product was purified by column chromatography (silica, 9:1 hexanes: EtOAc) to afford **1e** (1.01 g, 2.77 mmol) in 81% yield as an orange solid, m.p. = 70.2 – 71.5°C.

^{1}H NMR (400 MHz, DMSO-d_6) δ 7.61 (dd, J = 7.6, 1.8 Hz, 1H), 7.33 – 7.19 (m, 3H), 5.62 (s, 1H), 5.46 (s, 1H), 5.40 – 5.20 (m, 3H), 4.27 (s, 1H), 3.28 (s, 3H), 2.44 – 2.34 (m, 1H), 2.33 – 2.12 (m, 2H), 0.75 (s, 6H).

^{13}C NMR (101 MHz, DMSO-d_6) δ_u 133.2, 133.1, 130.0, 128.3, 124.5, 56.8, 35.09, 17.8; δ_d 174.4, 141.1, 124.5, 80.6, 54.4, 26.7.

GC (Method B) t_R = 3.046 min. EI-MS m/z (%): 363.1 (M-1$^+$, 1), 331.1 (7), 252.1 (10), 213.9 (15), 183.0 (68), 164.1 (64), 121.1 (21), 105.1 (100), 91.0 (15), 79.1 (47), 51.1 (6).

HRMS (ESI) calculated for $C_{18}H_{23}O_2NBr$ $[M+H]^+$: 364.0912, found 364.0907.

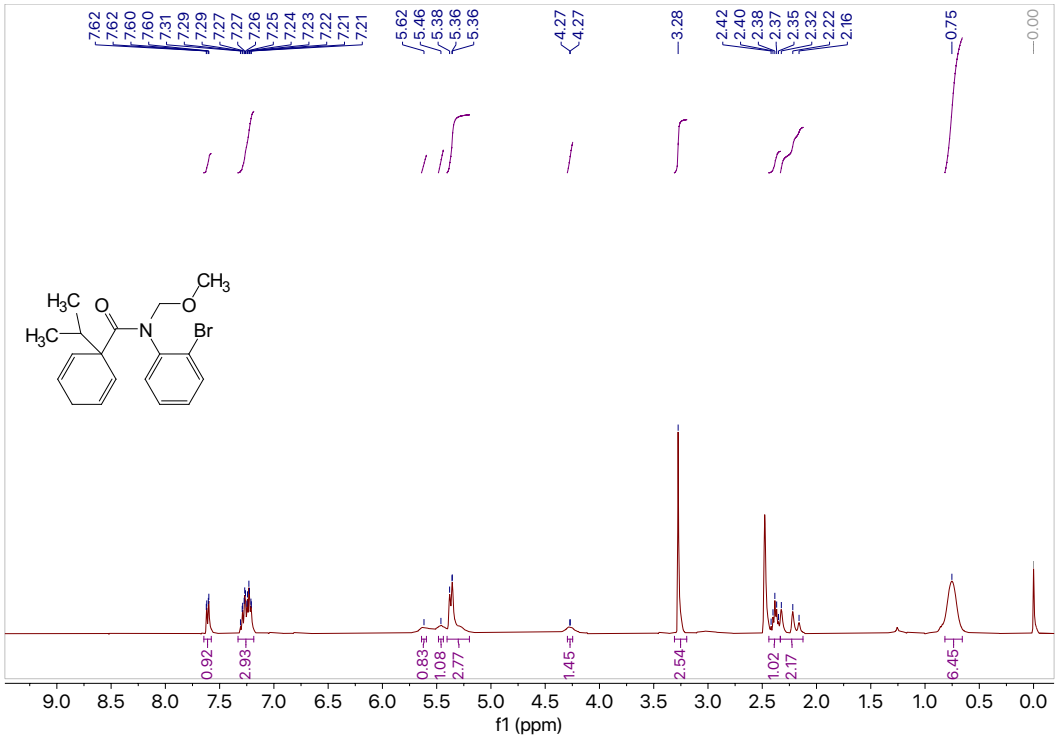

Figure 7.69 ^{1}H NMR (400 MHz, DMSO-d_6) of compound **1e**.

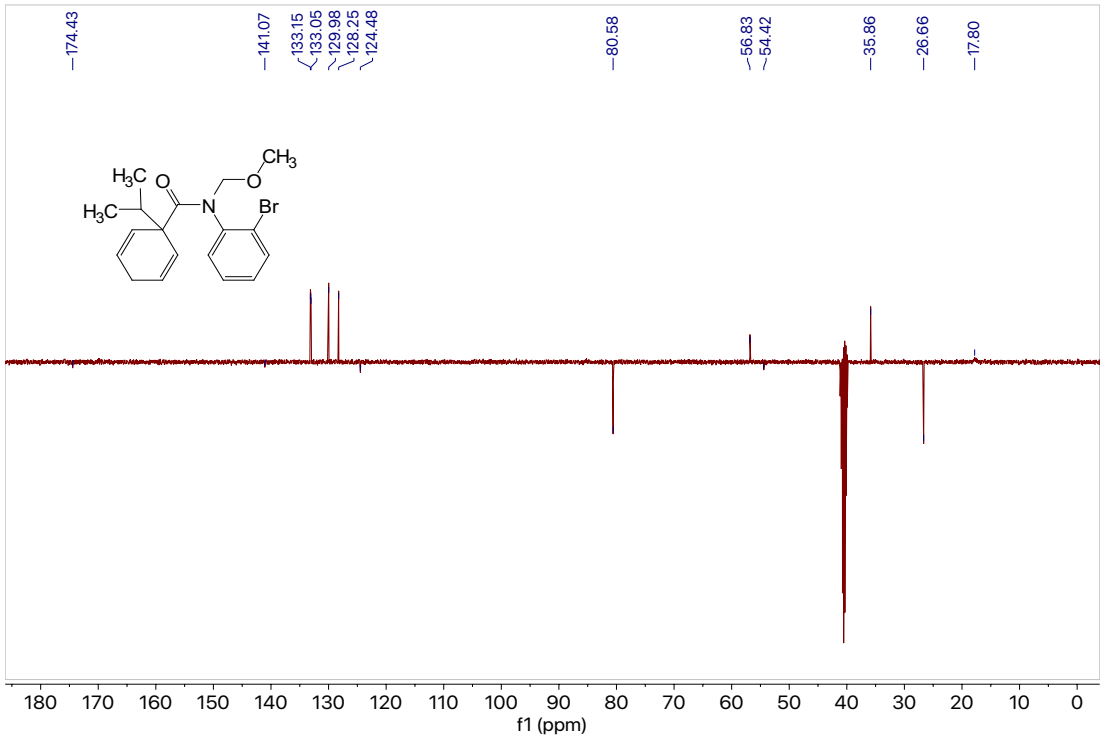

Figure 7.70 ^{13}C NMR (101 MHz, DMSO-d_6) of compound **1e**.

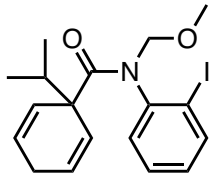

1e-I

***N*-(2-Iodophenyl)-1-isopropyl-*N*-(methoxymethyl)cyclohexa-2,5-diene-1-carboxamide**

(1e-I). Using the general procedure for MOM group protection, secondary amide **S2e-I** (0.359 g, 0.978 mmol, 1.0 equiv) in THF (6.8 mL, 0.14 M) was alkylated with bromomethyl methyl ether (0.16 mL, 1.96 mmol, 2.0 equiv). The crude product was purified by column chromatography (silica, 9:1 hexanes: EtOAc) to afford **1e-I** (0.289 g, 0.703 mmol) in 72% yield as a light orange solid, m.p. = 76.9 – 79.8°C.

^{1}H NMR (400 MHz, DMSO-d_6) δ 7.90 (d, J = 7.9 Hz, 1H), 7.35 (t, J = 7.6 Hz, 1H), 7.24 – 7.18 (m, 1H), 7.11 (td, J = 7.7, 1.7 Hz, 1H), 5.70 (d, J = 10.2 Hz, 1H), 5.56 (d, J = 9.8 Hz, 1H), 5.41 (m, J, 2H), 5.27 (d, J = 10.3 Hz, 1H), 4.23 (d, J = 9.9 Hz, 1H), 3.31 (s, 3H), 2.43 (hept, J = 6.7 Hz, 1H), 2.38 – 2.18 (m, 2H), 0.88 (d, J = 6.6 Hz, 3H), 0.73 (d, J = 6.6 Hz, 3H).

^{13}C NMR (101 MHz, DMSO-d_6) δ_u 139.5, 132.3, 129.9, 129.6, 129.1, 128.9, 125.9, 124.7, 124.6, 56.8, 35.8, 26.7, 18.3, 17.6; δ_d 174.3, 144.1, 102.7, 80.6, 54.3, 26.7.

GC (Method B) t_R = 3.451 min. EI-MS m/z (%): 411.1 (M^+, 1), 379.1 (4), 292.0 (10), 260.1 (10), 252.1 (12), 230.9 (100), 202.9 (5), 164.0 (34), 121.1 (15), 105.0 (55), 90.0 (10), 79.0 (26), 51.0 (4).

HRMS (ESI) calculated for $C_{18}H_{23}O_2NI$ $[M+H]^+$: 412.0773, found 412.0767.

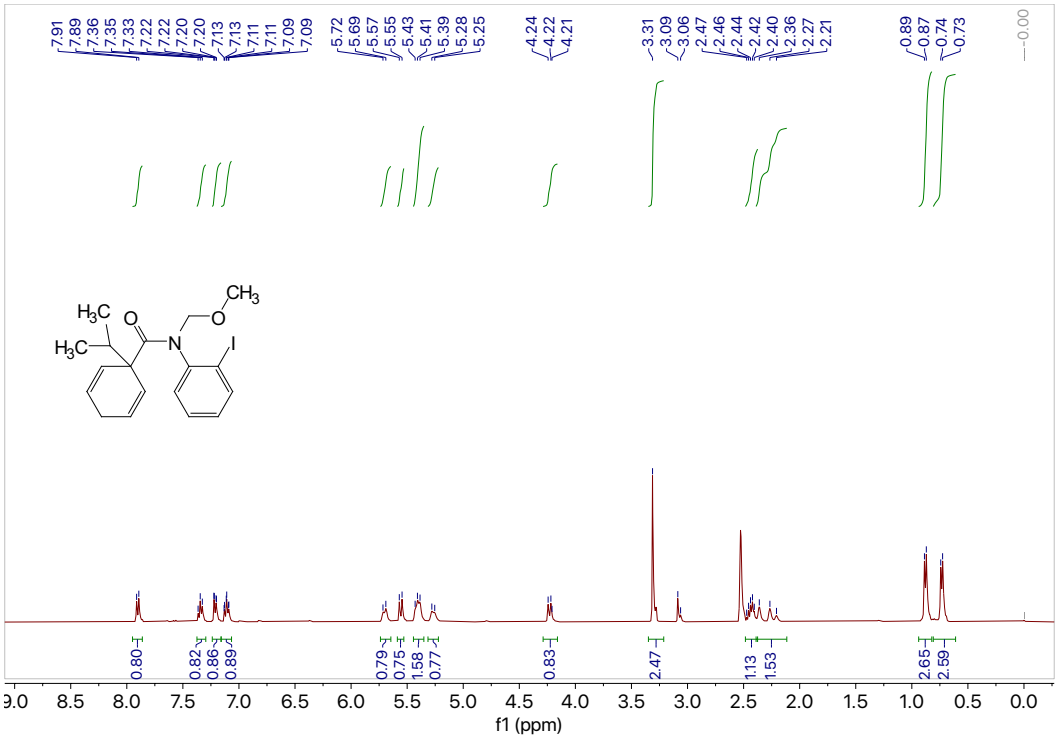

Figure 7.71 ^{1}H NMR (400 MHz, DMSO-d_6) of compound **1e-I**.

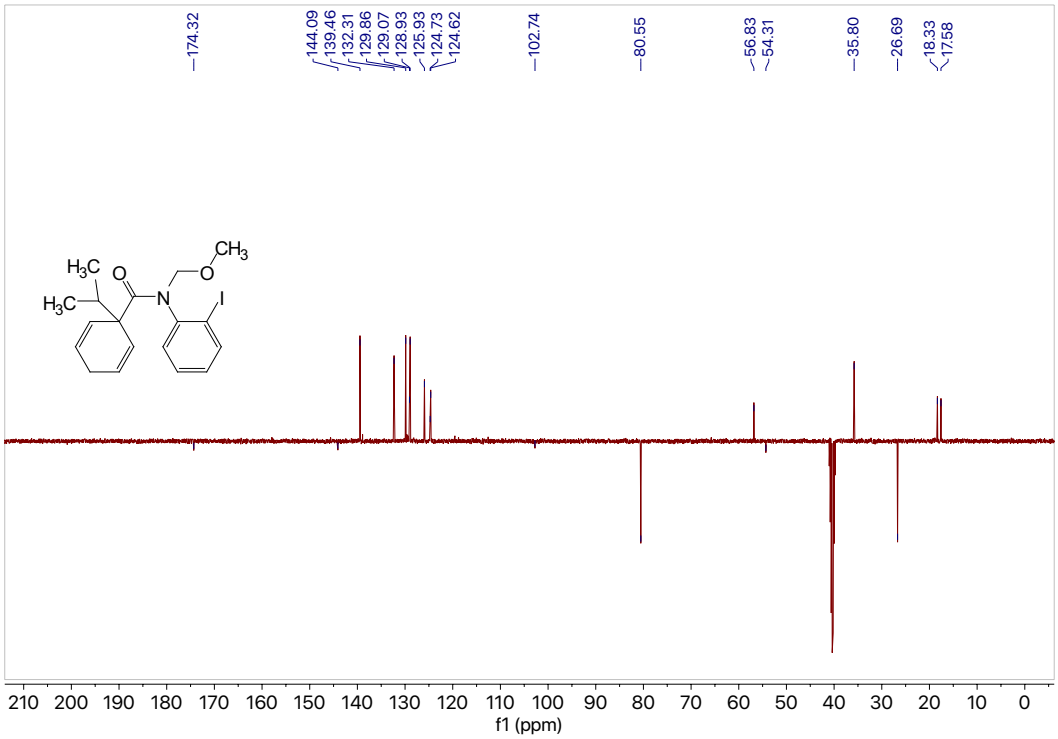

Figure 7.72 ^{13}C NMR (101 MHz, DMSO-d_6) of compound **1e-I**.

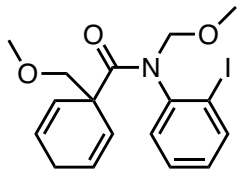

1f-I

***N*-(2-Iodophenyl)-*N*,1-bis(methoxymethyl)cyclohexa-2,5-diene-1-carboxamide (1f-I).** Using the general procedure for MOM group protection, secondary amide **S2f-I** (0.503 g, 1.36 mmol, 1.0 equiv) in THF (9.5 mL, 0.14 M) was alkylated with chloromethyl methyl ether (0.41 mL, 5.45 mmol, 4.0 equiv). The crude product was purified by column chromatography (silica, 7:1 hexanes: EtOAc) to afford **1f-I** (0.506 g, 1.22 mmol) in 90% yield as a dark yellow oil.

^{1}H NMR (400 MHz, DMSO-d_6) δ 7.88 (dt, J = 8.2, 2.0 Hz, 1H), 7.37 – 7.31 (m, 1H), 7.27 – 7.20 (m, 1H), 7.12 – 7.05 (m, 1H), 5.66 – 5.57 (m, 2H), 5.56 – 5.42 (m, 2H), 5.32 (s, 1H), 4.21 (d, J = 9.9 Hz, 1H), 3.60 (d, J = 8.7 Hz, 1H), 3.35 (d, J = 8.8 Hz, 1H), 3.28 (s, 3H), 3.24 (s, 3H), 2.49 – 2.19 (m, 2H).

^{13}C NMR (101 MHz, DMSO-d_6) δ_u 139.5, 132.6, 129.9, 128.9, 126.9, 126.5, 126.3, 124.3, 59.3, 56.6; δ_d 172.6, 143.6, 102.6, 80.3, 80.0, 51.3, 26.4.

GC (Method B) t_R = 3.399 min. EI-MS m/z (%): 413.1 (M^+, 1), 337.0 (7), 289.9 (9), 259.9 (6), 245.1 (9), 231.9 (100), 202.9 (4), 180.0 (4), 164.0 (9), 121.0 (6), 105.0 (44), 90.0 (34), 77.0 (16), 65.0 (4), 51.0 (4).

HRMS (ESI) calculated for $C_{17}H_{21}O_3NI$ $[M+H]^+$: 414.0566, found 414.0557.

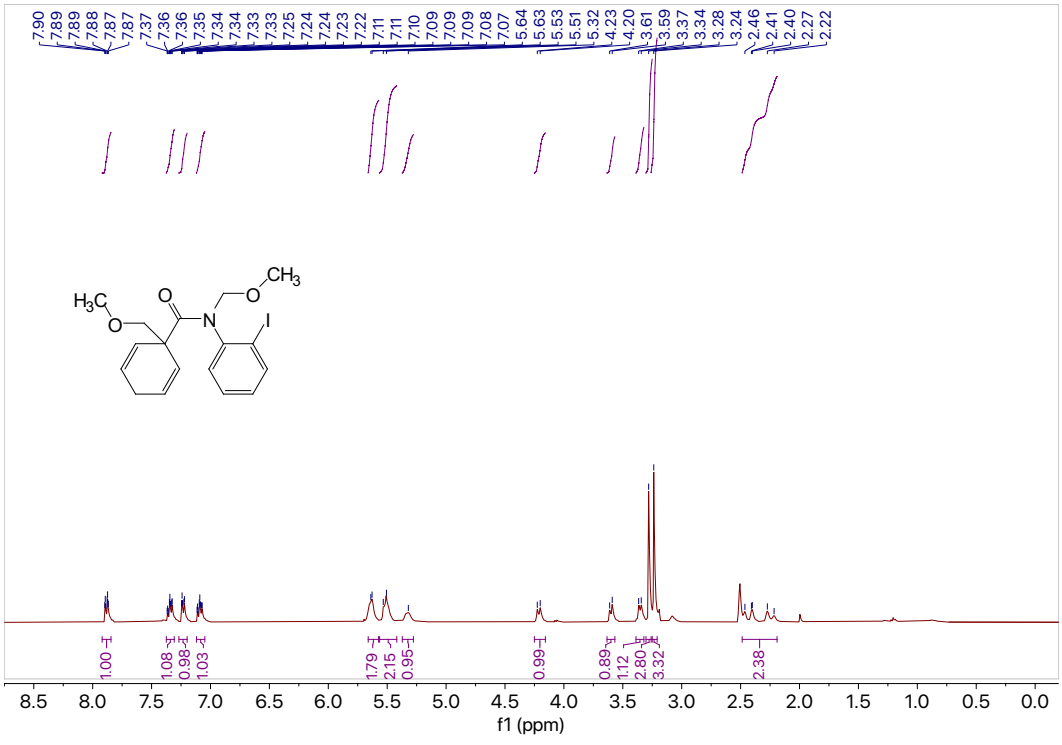

Figure 7.73 ^{1}H NMR (400 MHz, DMSO-d_6) of compound **1f-I**.

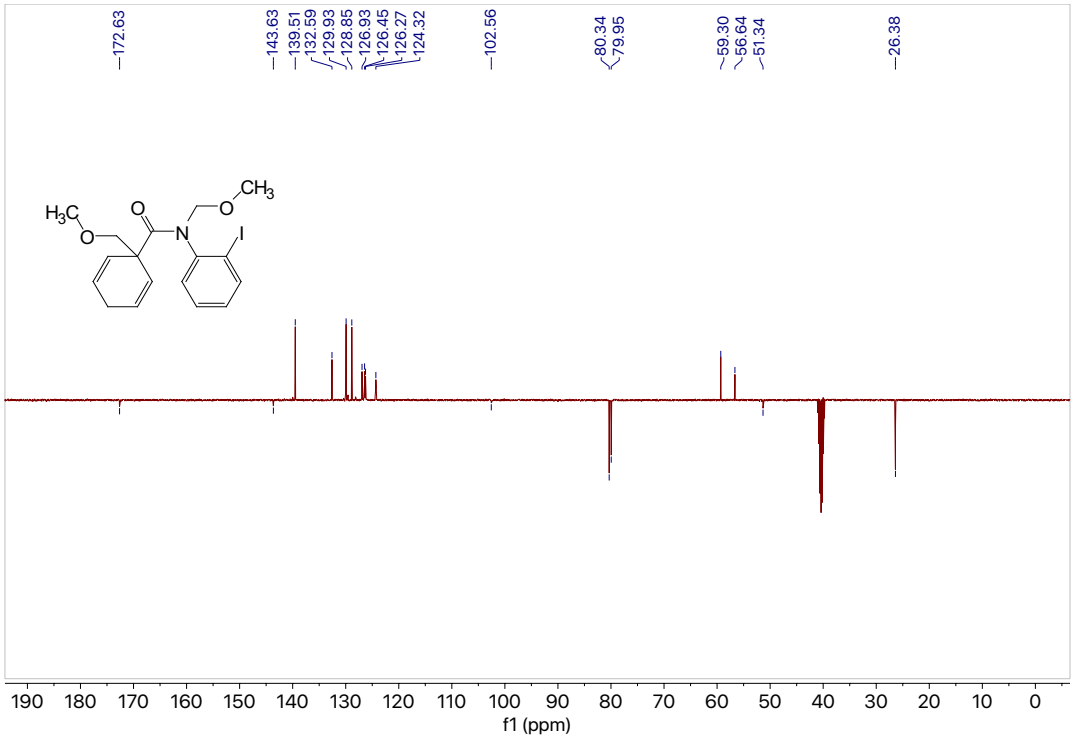

Figure 7.74 ^{13}C NMR (101 MHz, DMSO-d$_6$) of compound **1f-I**.

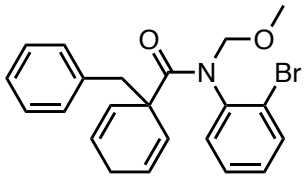

1h

1-Benzyl-*N*-(2-bromophenyl)-*N*-(methoxymethyl)cyclohexa-2,5-diene-1-carboxamide (1h). Using the general procedure for MOM group protection, secondary amide **S2h** (0.996 g, 2.71 mmol, 1.0 equiv) in THF (19 mL, 0.14 M) was alkylated with bromomethyl methyl ether (0.44 mL, 5.41 mmol, 2.0 equiv). The crude product was purified by column chromatography (silica, 9:1 hexanes: EtOAc) to afford **1h** (1.03 g, 2.49 mmol) in 92% yield as a yellow oil.

^{1}H NMR (400 MHz, $CDCl_3$) δ 7.48 (s, 1H), 7.23 – 7.16 (m, 1H), 7.17 – 7.11 (m, 3H), 7.11 – 7.05 (m, 4H), 5.69 (d, *J* = 10.2 Hz, 1H), 5.63 (s, 1H), 5.52 (s, 1H), 5.41 (s, 1H), 5.01 (s, 1H), 4.28 (d, *J* = 10.0 Hz, 1H), 3.43 (s, 3H), 3.19 (d, *J* = 13.1 Hz, 1H), 3.07 (d, *J* = 13.2 Hz, 1H), 1.93 (s, 2H).

^{13}C NMR (101 MHz, $CDCl_3$) δ_u 132.8, 131.4, 129.3, 129.1, 127.3, 126.3, 125.9, 125.5, 123.4, 57.05; δ_d 174.7, 140.3, 137.4, 124.0, 80.2, 51.4, 46.6, 26.0.

GC (Method A) t_R = 18.724 min. EI-MS m/z (%): 413.2 ($M+1^+$, 1), 379.1 (4), 288.0 (9), 240.1 (26), 213.9 (8), 184.9 (30), 168.0 (32), 152.0 (6), 105.0 (99), 91.0 (100), 79.0 (16), 65.0 (7).

HRMS (ESI) calculated for $C_{22}H_{23}O_2NBr$ $[M+H]^+$: 412.0774, found 412.0767.

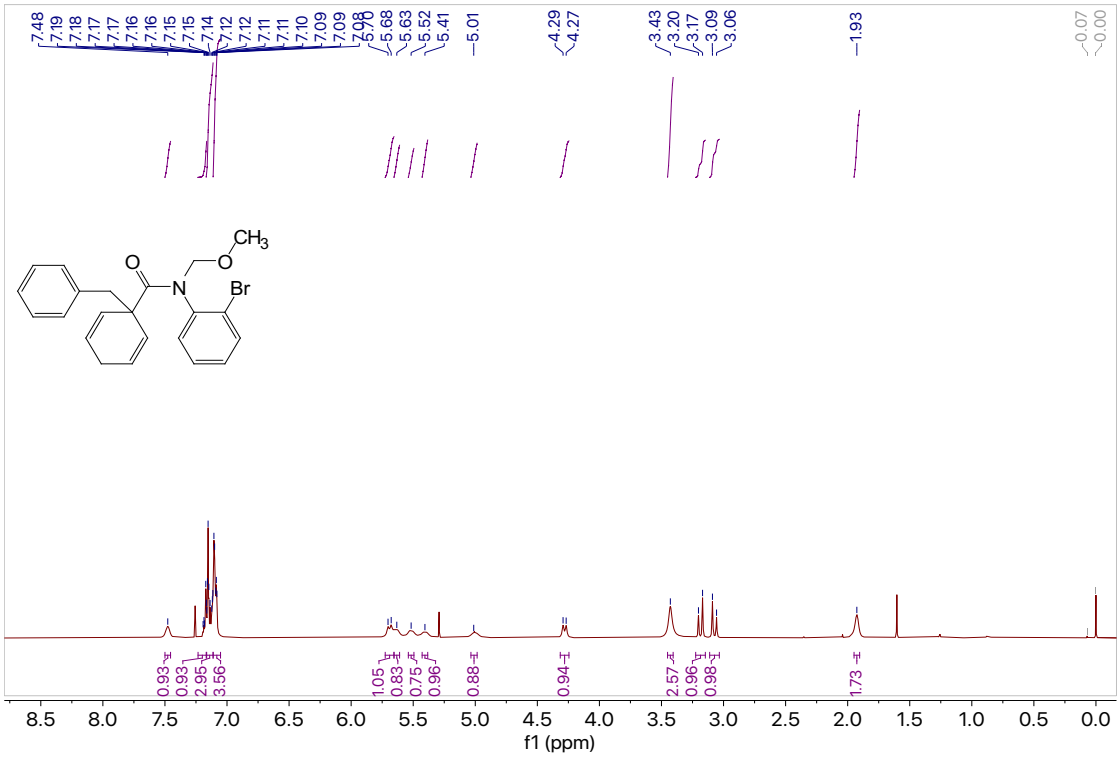

Figure 7.75 ^{1}H NMR (400 MHz, $CDCl_3$) of compound **1h**.

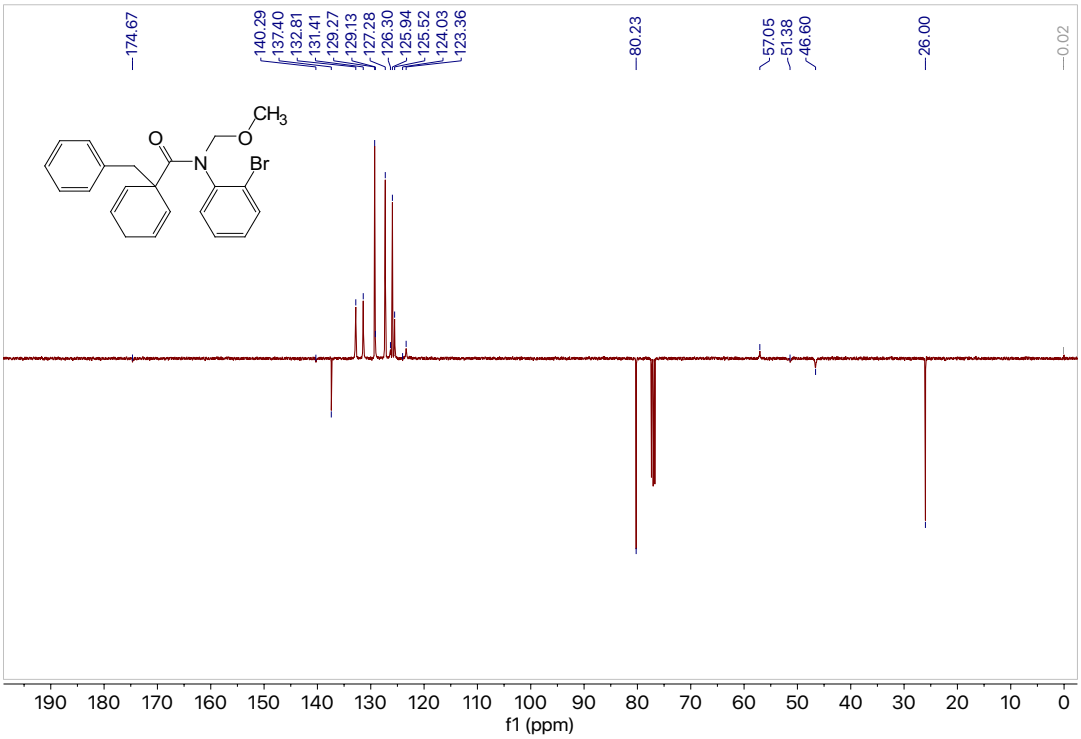

Figure 7.76 ^{13}C NMR (101 MHz, $CDCl_3$) of compound **1h**.

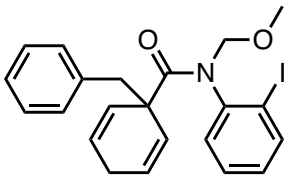

1h-I

1-Benzyl-*N*-(2-iodophenyl)-*N*-(methoxymethyl)cyclohexa-2,5-diene-1-carboxamide (1h-I).

Using the general procedure for MOM group protection, secondary amide **S2h-I** (0. 501 g, 1.204 mmol, 1.0 equiv) in THF (8.4 mL, 0.14 M) was alkylated with chloromethyl methyl ether (0.37 mL, 4.82 mmol, 4.0 equiv). The crude product was purified by column chromatography (silica, 9:1 hexanes: EtOAc) to afford **1h-I** (0.470 g, 1.02 mmol) in 85% yield as a yellow oil.

^{1}H NMR (400 MHz, DMSO-d_6) δ 7.80 (d, J = 8.2 Hz, 1H), 7.24 (t, J = 7.6 Hz, 1H), 7.19 – 6.97 (m, 7H), 5.59 – 5.40 (m, 4H), 5.13 (s, 1H), 4.19 (d, J = 9.9 Hz, 1H), 3.24 (s, 3H), 3.02 – 2.90 (m, 2H), 2.10 – 1.93 (m, 2H).

^{13}C NMR (101 MHz, DMSO-d_6) δ_u 139.5, 132.4, 131.5, 129.9, 129.2, 128.8, 127.7, 127.6, 126.3, 125.5, 123.8, 56.7; δ_d 173.8, 143.9, 137.6, 115.1, 80.7, 60.1, 51.3, 46.8, 26.1.

GC (Method A) t_R = 19.957 min. EI-MS m/z (%): 459 (M^+, 1), 427.1 (6), 336.0 (15), 300.0 (6), 292.0 (10), 259.9 (10), 259.9 (20), 240.1 (42), 230.9 (70), 213.1 (4), 196.0 (5), 168.0 (31), 150.9 (7), 105.0 (98), 91.0 (100), 79.0 (18), 65.0 (8).

HRMS (ESI) calculated for $C_{22}H_{23}O_2NI$ $[M+H]^+$: 459.0695, found 459.0696.

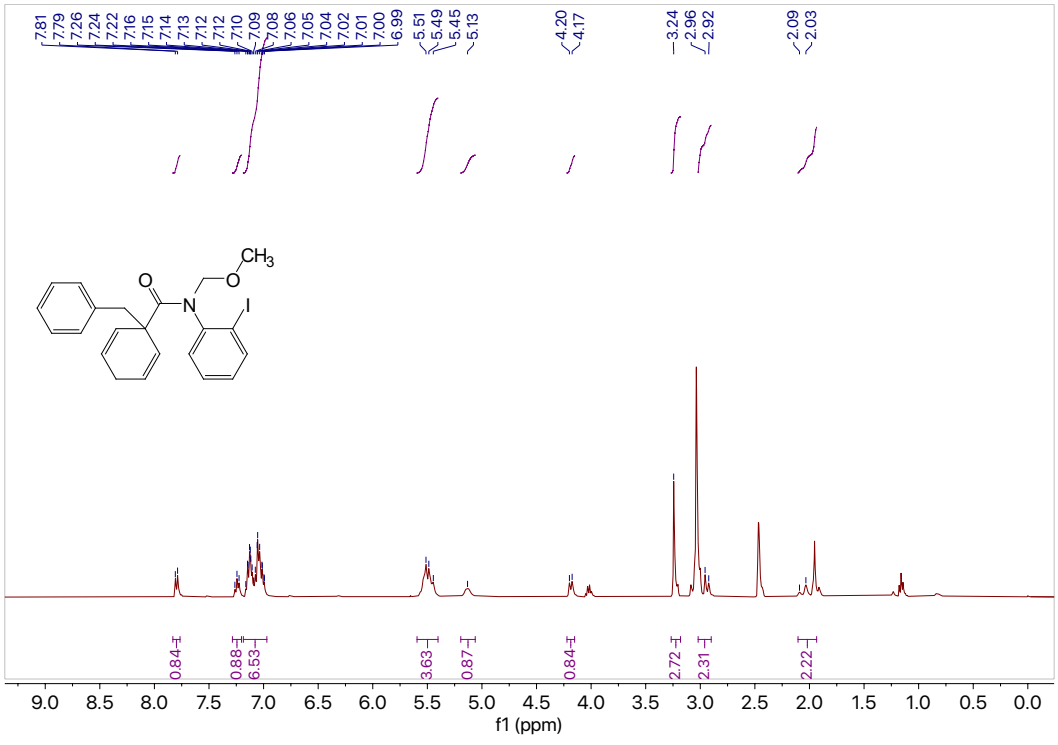

Figure 7.77 ^{1}H NMR (400 MHz, DMSO-d_6) of compound **1h-I**.

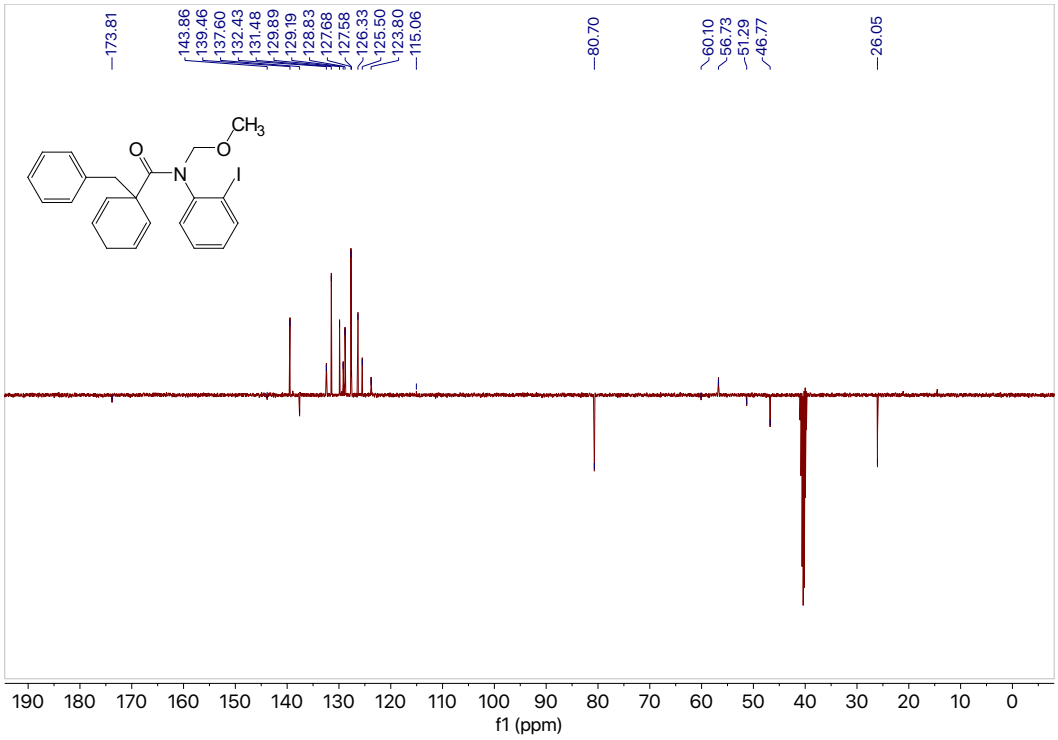

Figure 7.78 ^{13}C NMR (101 MHz, DMSO-d$_6$) of compound **1h-I**.

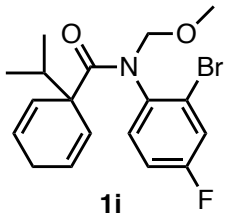

1i

***N*-(2-Bromo-4-fluorophenyl)-1-isopropyl-*N*-(methoxymethyl)cyclohexa-2,5-diene-1-carboxamide (1i).** Using the general procedure for MOM group protection, secondary amide **S2i** (0.8434 g, 2.49 mmol, 1.0 equiv) in THF (17.4 mL, 0.14 M) was alkylated with chloromethyl methyl ether (0.38 mL, 4.98 mmol, 2.0 equiv). The crude product was purified by column chromatography (silica, 9:1 hexanes: EtOAc) to afford **1i** (0.828 g, 2.17 mmol) in 87% yield as a white solid, m.p.= 66.8 – 69.9°C.

^{1}H NMR (400 MHz, DMSO-*d*$_6$) δ 7.58 (dd, *J* = 8.3, 2.9 Hz, 1H), 7.26 (dd, *J* = 8.9, 5.7 Hz, 1H), 7.19 (td, *J* = 8.4, 2.9 Hz, 1H), 5.69 (s, 1H), 5.49 (d, *J* = 9.7 Hz, 1H), 5.43 – 5.35 (m, 3H), 4.26 (d, *J* = 9.9 Hz, 1H), 3.30 (s, 3H), 2.47 – 2.35 (m, 2H), 2.24 (d, *J* = 23.5 Hz, 1H), 0.82 (d, *J* = 7.1 Hz, 3H), 0.72 (d, *J* = 6.9 Hz, 3H).

^{13}C NMR (101 MHz, DMSO-*d*$_6$) δ$_u$ 134.0 (d, $^3J_{C\text{-}F}$ = 9.4 Hz), 128.8, 126.0, 125.0, 124.6, 120.2 (d, $^2J_{C\text{-}F}$ = 25.7 Hz), 115.3 (d, $^2J_{C\text{-}F}$ = 22.1 Hz), 56.8, 35.8, 18.1, 17.5; δ$_d$ 174.4, 161.7 (d, $^1J_{C\text{-}F}$=250 Hz), 137.6, 125.1, 80.3, 54.3, 26.7.

^{19}F NMR (376 MHz, DMSO-*d*$_6$) δ -111.69.

GC (Method B**)** t_R = 2.815 min. EI-MS m/z (%): 381.1 (M+1$^+$, 1), 349.1 (5), 262.0 (6), 246.0 (4), 232.0 (10), 201.0 (57), 182.1 (37), 121.1 (26), 105.1 (100), 90.0 (12), 105.1 (100), 51.1 (4).

HRMS (ESI) calculated for $C_{18}H_{22}O_2NBrF$ [M+H]$^+$: 382.0818, found 382.0813.

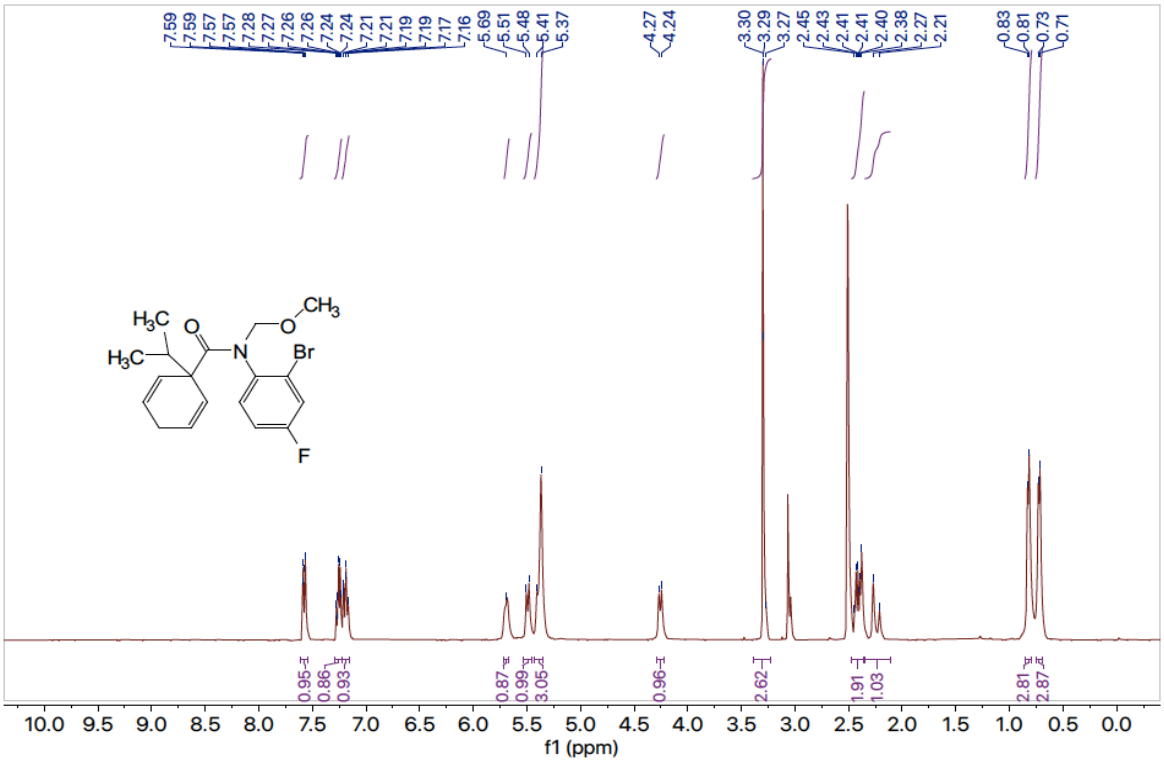

Figure 7.79 ^{1}H NMR (400 MHz, DMSO-d_6) of compound **1i**.

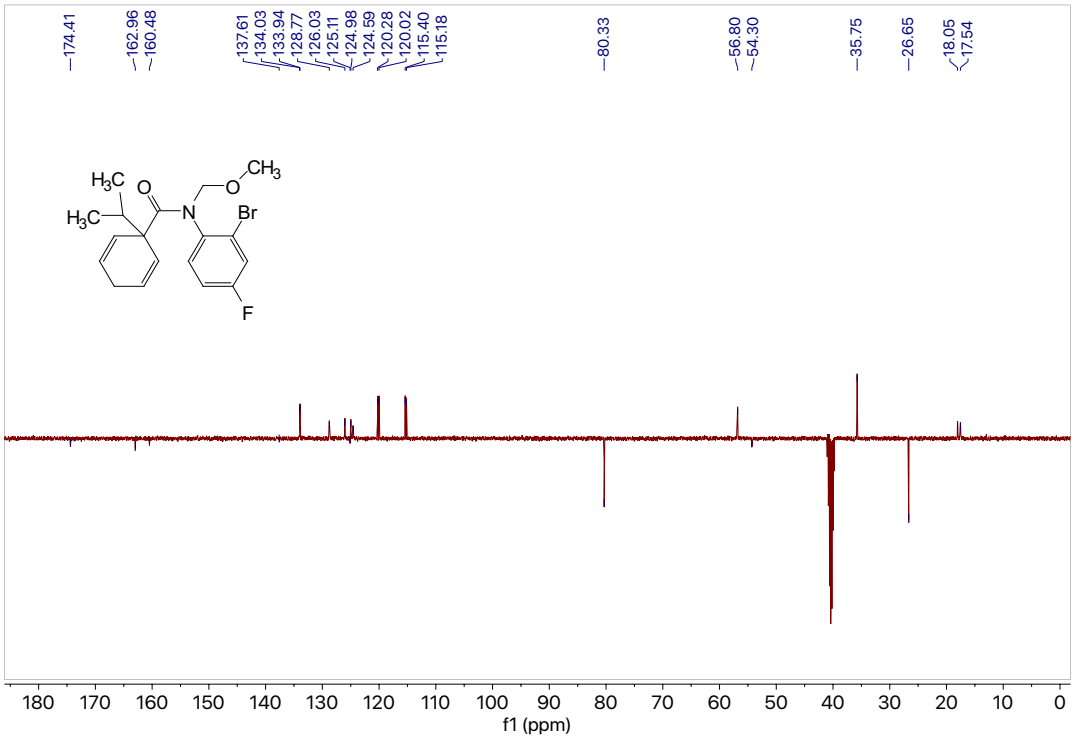

Figure 7.80 ^{13}C NMR (101 MHz, DMSO-d_6) of compound **1i**.

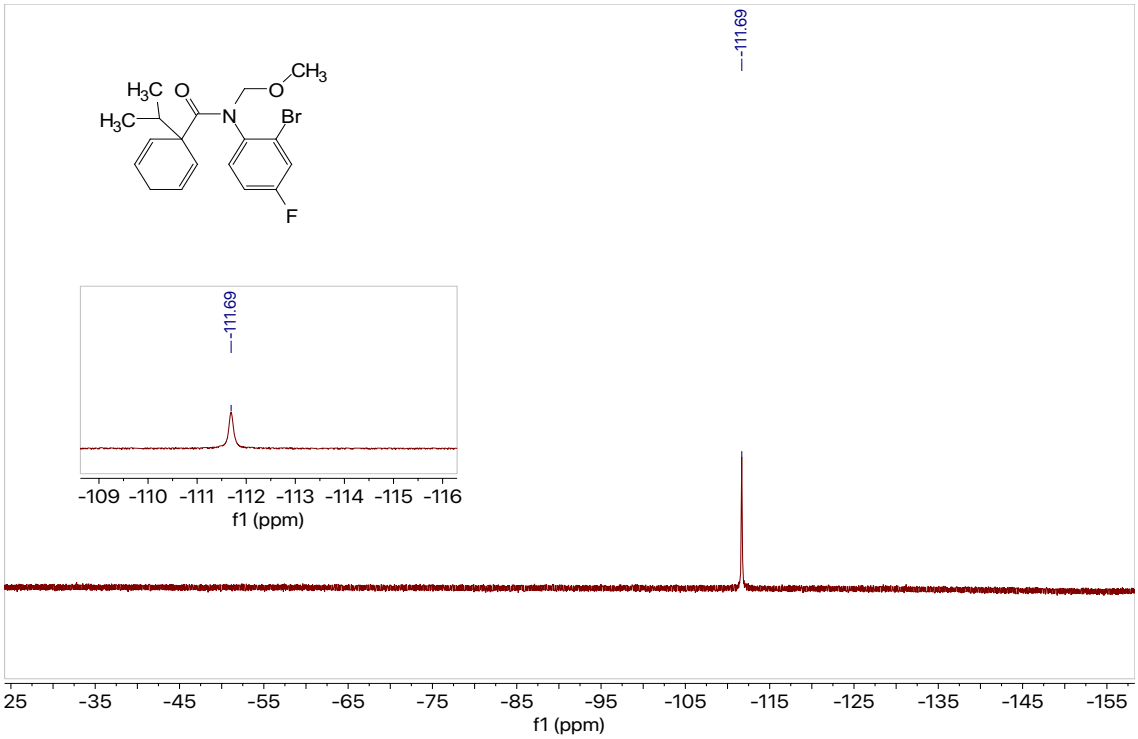

Figure 7.81 ^{19}F NMR (376 MHz, DMSO-d$_6$) of compound **1i**.

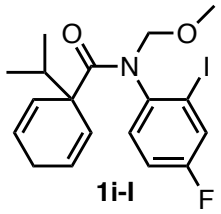

1i-I

***N*-(4-Fluoro-2-iodophenyl)-1-isopropyl-*N*-(methoxymethyl)cyclohexa-2,5-diene-1-carboxamide (1i-I).** Using the general procedure for MOM group protection, secondary amide **S2i-I** (0.201 g, 0.519 mmol, 1.0 equiv) in THF (3.6 mL, 0.14 M) was alkylated with chloromethyl methyl ether (0.16 mL, 2.08 mmol, 4.0 equiv). The crude product was purified by column chromatography (silica, 9:1 hexanes: EtOAc) to afford **1i-I** (0.214 g, 0.499 mmol) in 96% yield solid, m.p.= 65.1 – 66.6°C.

^{1}H NMR (400 MHz, DMSO-d_6) δ 7.73 (dd, J = 8.2, 1.9 Hz, 1H), 7.22 – 7.15 (m, 2H), 5.71 (d, J = 9.7 Hz, 1H), 5.53 (d, J = 9.6 Hz, 1H), 5.38 (dd, J = 19.5, 10.4 Hz, 2H), 4.19 (d, J = 9.6 Hz, 1H), 3.29 (s, 3H), 2.46 – 2.40 (m, 1H), 2.39 – 2.19 (m, 2H), 0.86 (d, J = 6.7 Hz, 3H), 0.72 (d, J = 6.9 Hz, 3H).

^{13}C NMR (101 MHz, DMSO-d_6) δ$_u$ 133.0 (d, $^3J_{C\text{-}F}$ = 9.0 Hz), 129.0, 125.9 (d, $^2J_{C\text{-}F}$ = 24.9 Hz), 124.8, 124.7, 115.8 (d, $^2J_{C\text{-}F}$ = 22.3 Hz), 56.8, 35.8, 18.3, 17.5; δ$_d$ 174.3, 161.3 (d, $^1J_{C\text{-}F}$=251 Hz), 140.8, 100.0, 80.5, 54.3, 26.7.

^{19}F NMR (376 MHz, DMSO-d_6) δ -113.19.

GC (Method B**)** t_R = 3.193 min. EI-MS m/z (%): 429.1 (M^+, 1), 397.1 (7), 310.0 (9), 278.0 (12), 265.0 (7), 262.0 (4), 248.9 (100), 182.0 (27), 121.1 (18), 105.0 (55), 79.0 (28).

HRMS (ESI) calculated for $C_{18}H_{22}O_2NFI$ $[M+H]^+$: 430.0679, found 430.0675.

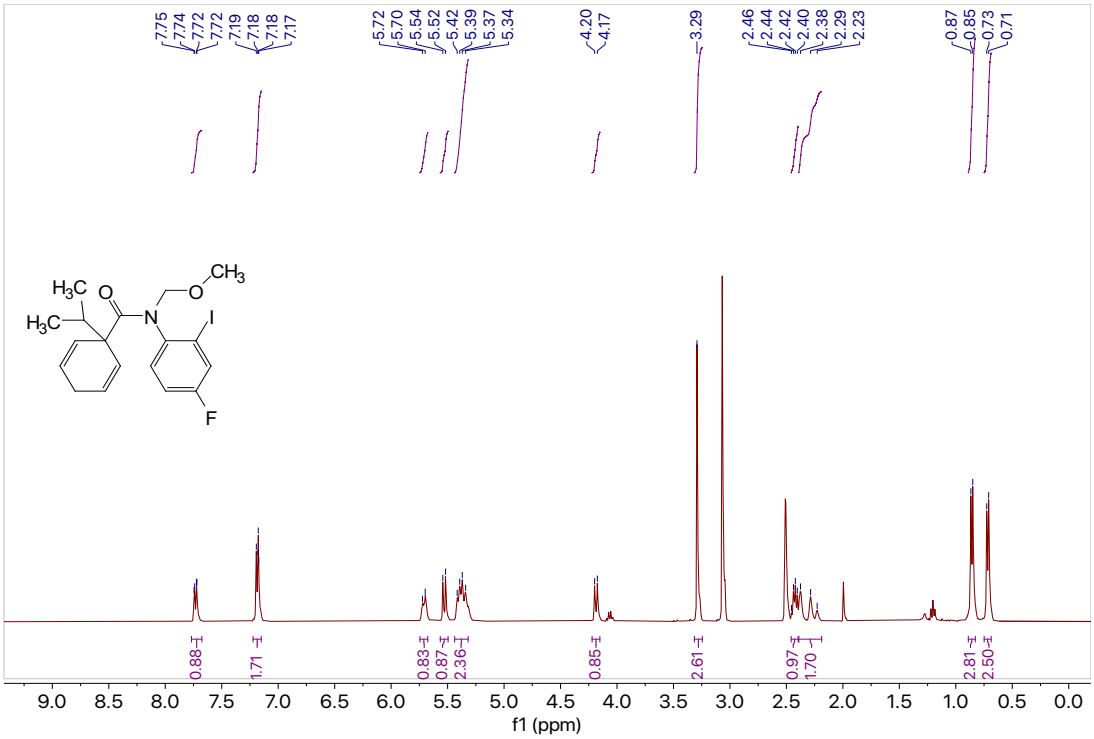

Figure 7.82 ^{1}H NMR (400 MHz, DMSO-d$_6$) of compound **1i-I**.

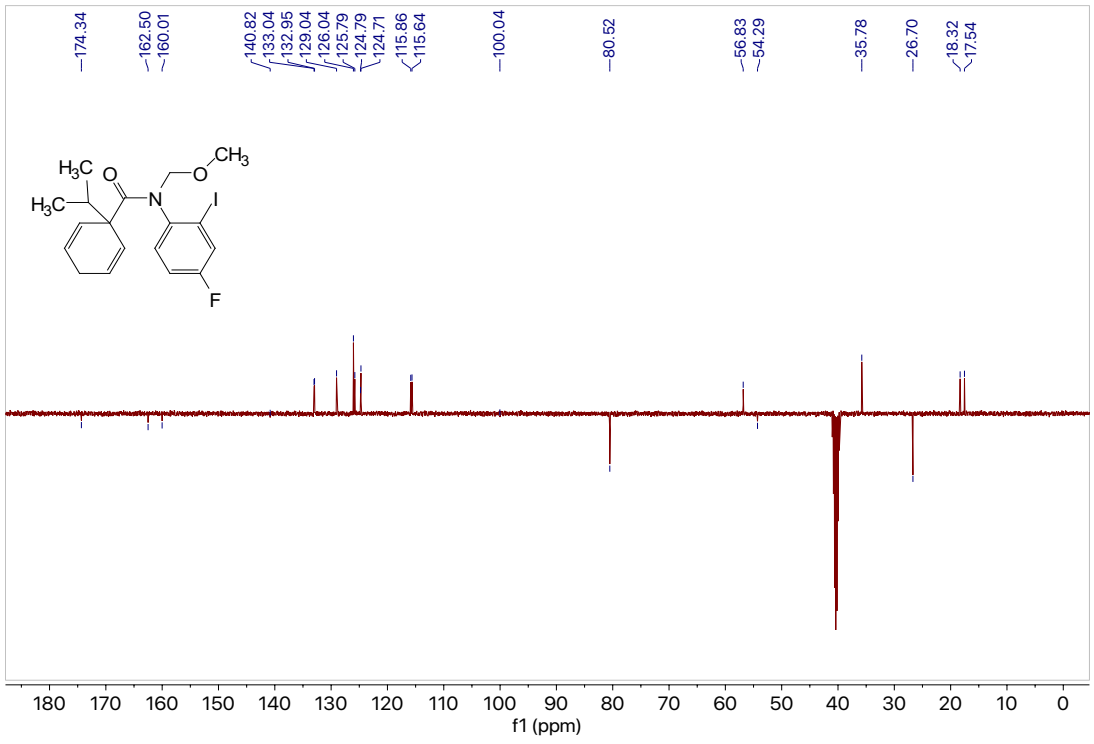

Figure 7.83 ^{13}C NMR (101 MHz, DMSO-d$_6$) of compound **1i-I**.

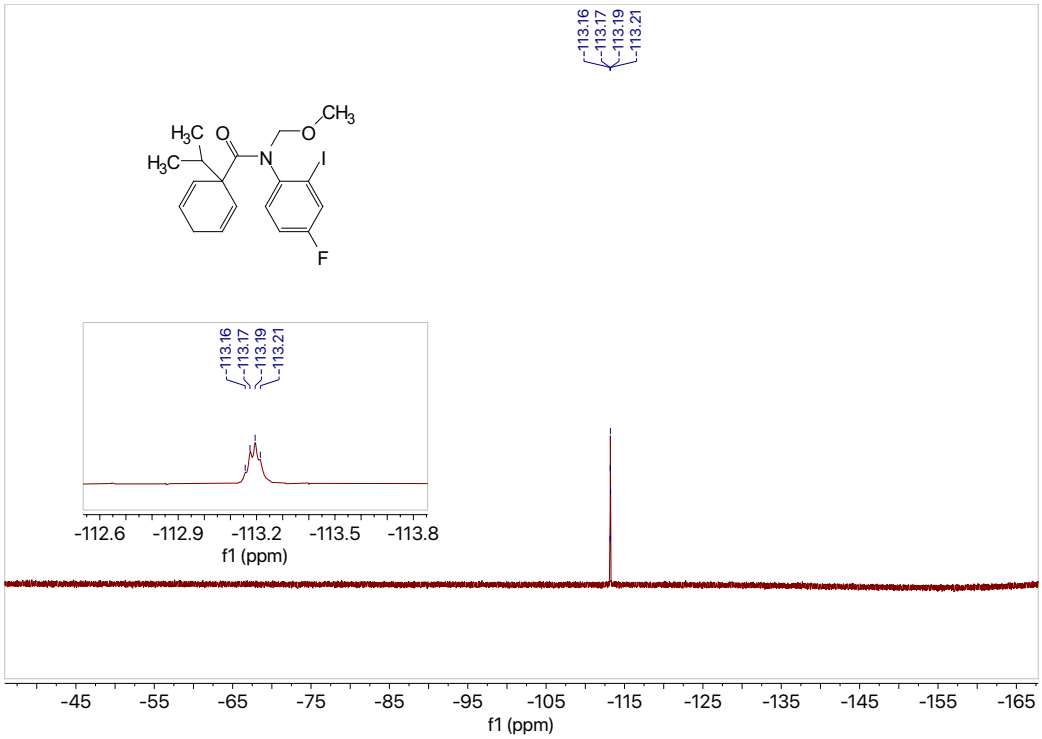

Figure 7.84 ^{19}F NMR (376 MHz, DMSO-d$_6$) of compound **1i-I**.

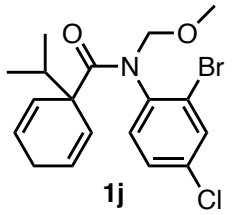

***N*-(2-Bromo-4-chlorophenyl)-1-isopropyl-*N*-(methoxymethyl)cyclohexa-2,5-diene-1-carboxamide (1j).** Using the general procedure for MOM group protection, secondary amide **S2j** (0.969 g, 2.73 mmol, 1.0 equiv) in THF (19.1 mL, 0.14 M) was alkylated with chloromethyl methyl ether (0.42 mL, 5.50 mmol, 2.0 equiv). The crude product was purified by column chromatography (silica, 9:1 hexanes: EtOAc) to afford **1j** (0.855 g, 2.14 mmol) in 79% yield as a low-melting orange solid.

^{1}H NMR (400 MHz, $CDCl_3$) δ 7.57 (t, *J* = 1.3 Hz, 1H), 7.16 (d, *J* = 1.3 Hz, 2H), 5.70 – 5.62 (m, 2H), 5.49 (d, *J* = 10.2 Hz, 1H), 5.38 (d, *J* = 10.4 Hz, 1H), 5.25 (s, 1H), 4.24 (d, *J* = 10.0 Hz, 1H), 3.40 (s, 3H), 2.51 (hept, *J* = 6.8 Hz, 1H), 2.40 (d, *J* = 23.4 Hz, 1H), 2.16 (d, *J* = 23.6 Hz, 1H), 0.87 (d, *J* = 6.8 Hz, 3H), 0.71 (d, *J* = 6.9 Hz, 3H).

^{13}C NMR (101 MHz, $CDCl_3$) δ_u 133.1, 132.4, 129.6, 127.7, 125.7, 124.9, 79.9, 57.1, 35.7, 17.8, 17.1; δ_d 175.2, 139.5, 134.4, 124.9, 79.9, 54.4, 26.7.

GC (Method B) t_R = 3.480 min. EI-MS m/z (%): 399.1 ($M+1^+$, 1), 367.1 (4), 280.0 (5), 263.9 (4), 247.9 (8), 218.9 (65), 198.0 (42), 121.1 (28), 105.1 (100), 90.0 (12), 79.1 (50), 51.1 (4).

HRMS (ESI) calculated for $C_{18}H_{22}O_2NBrCl$ $[M+H]^+$: 398.0522, found 398.0515.

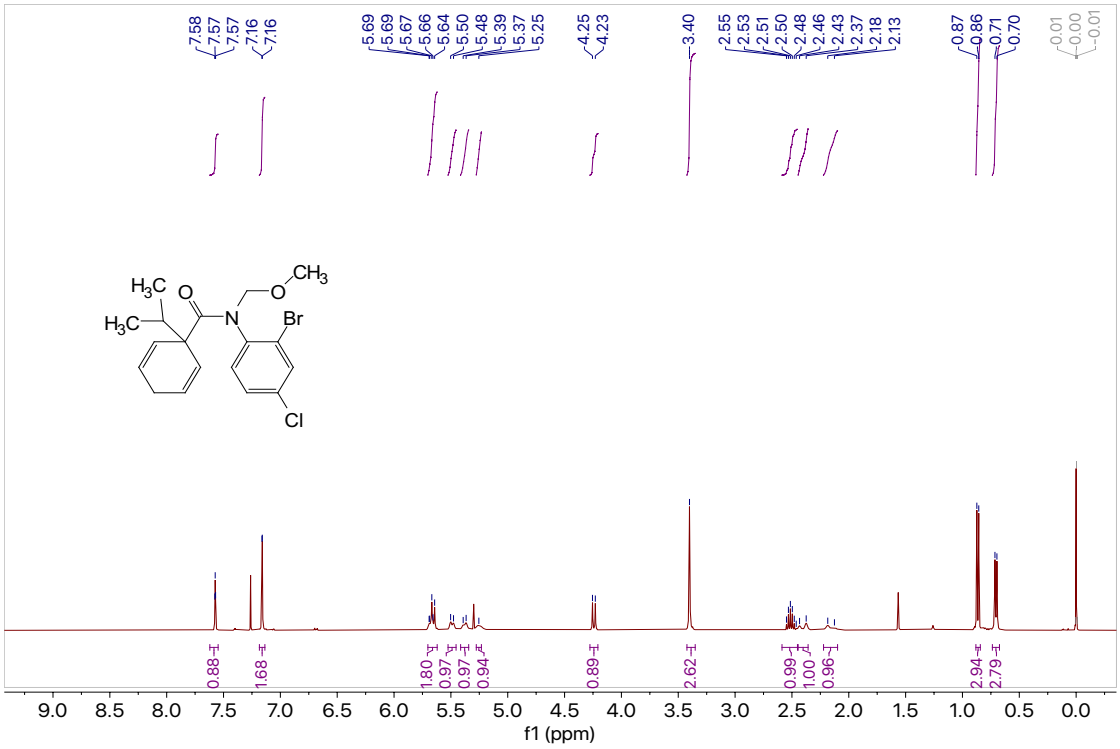

Figure 7.85 ^{1}H NMR (400 MHz, $CDCl_3$) of compound **1j**.

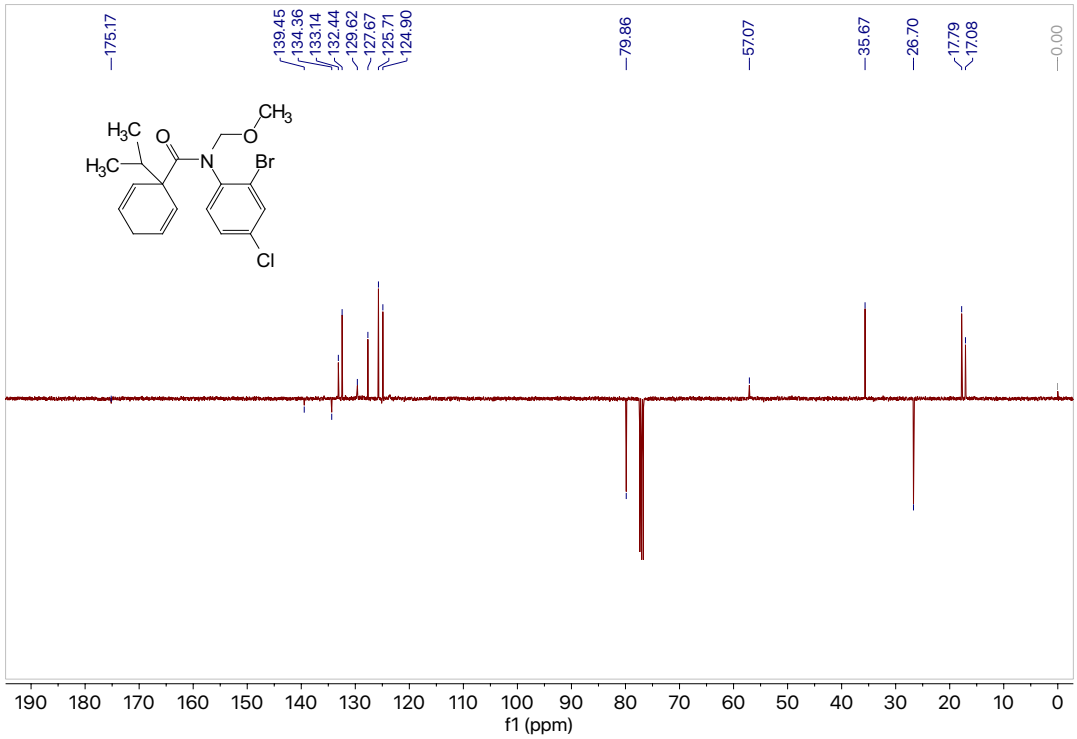

Figure 7.86 ^{13}C NMR (101 MHz, $CDCl_3$) of compound **1j**.

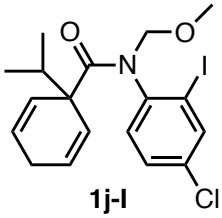

1j-I

***N*-(4-Chloro-2-iodophenyl)-1-isopropyl-*N*-(methoxymethyl)cyclohexa-2,5-diene-1-carboxamide (1j-I).** Using the general procedure for MOM group protection, secondary amide **S2j-I** (0.500 g, 1.25 mmol, 1.0 equiv) in THF (8.8 mL, 0.14 M) was alkylated with chloromethyl methyl ether (0.38 mL, 4.98 mmol, 4.0 equiv). The crude product was purified by column chromatography (silica, 10:1 hexanes: EtOAc) to afford **1j-I** (0.483 g, 1.08 mmol) in 87% yield as a low-melting tan solid.

^{1}H NMR (400 MHz, DMSO-d_6) δ 7.92 (d, J = 2.4 Hz, 1H), 7.40 (dd, J = 8.4, 2.4 Hz, 1H), 7.17 (dd, J = 8.4, 2.0 Hz, 1H), 5.72 – 5.65 (m, 1H), 5.51 (d, J = 9.8 Hz, 1H), 5.45 – 5.30 (m, 3H), 4.23 (d, J = 9.8 Hz, 1H), 3.29 (s, 3H), 2.49 – 2.36 (m, 2H), 2.27 (d, J = 23.4 Hz, 1H), 0.86 (d, J = 6.9 Hz, 3H), 0.74 (d, J = 7.1 Hz, 2H).

^{13}C NMR (101 MHz, DMSO-d_6) δ_u 138.3, 133.0, 129.0, 128.9, 126.2, 125.2, 124.8, 56.9, 35.8, 18.3, 17.6; δ_d 174.2, 143.3, 133.4, 103.7, 80.4, 54.3, 26.8.

GC (Method B) t_R = 4.011 min. EI-MS m/z (%): 445.0 (M^+, 1), 413.1 (5), 326.0 (6), 293.9 (8), 290.1 (7), 264.9 (100), 198.0 (34), 121.1 (25), 105.1 (80), 90.0 (10), 79.1 (45), 51.0 (4).

HRMS (ESI) calculated for $C_{18}H_{22}O_2NClI$ $[M+H]^+$: 446.0384, found 446.0373.

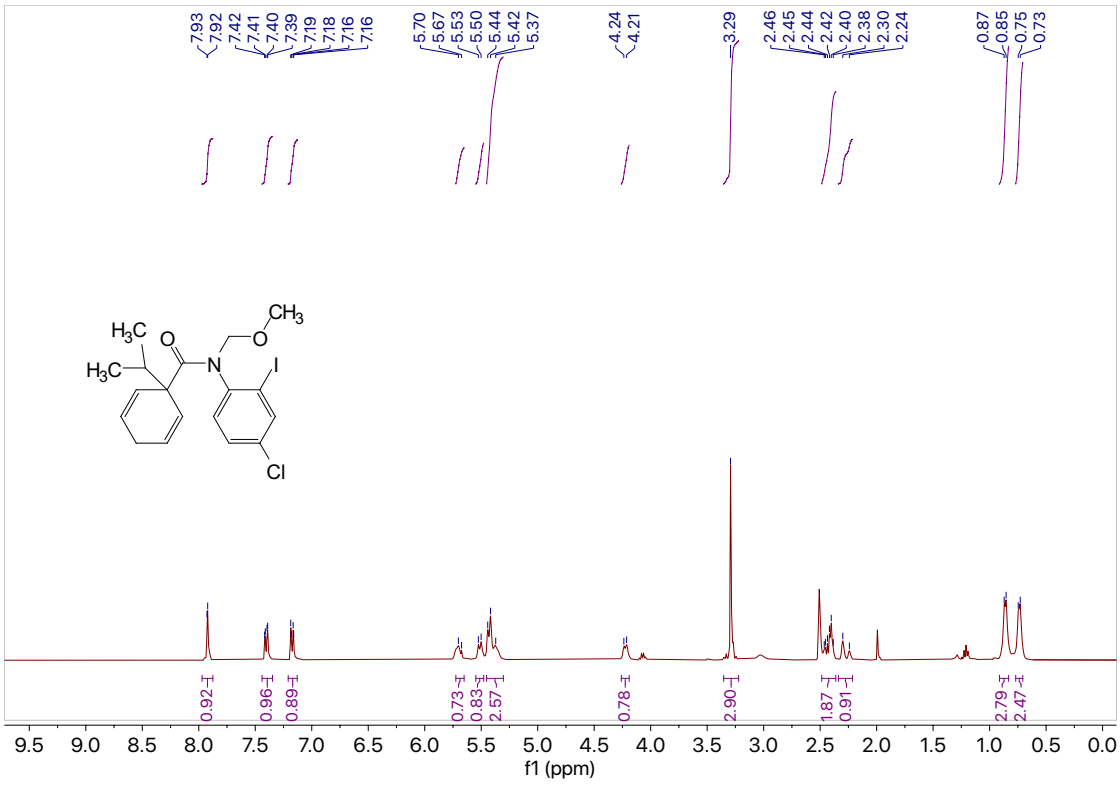

Figure 7.87 ^{1}H NMR (400 MHz, DMSO-d_6) of compound **1j-I**.

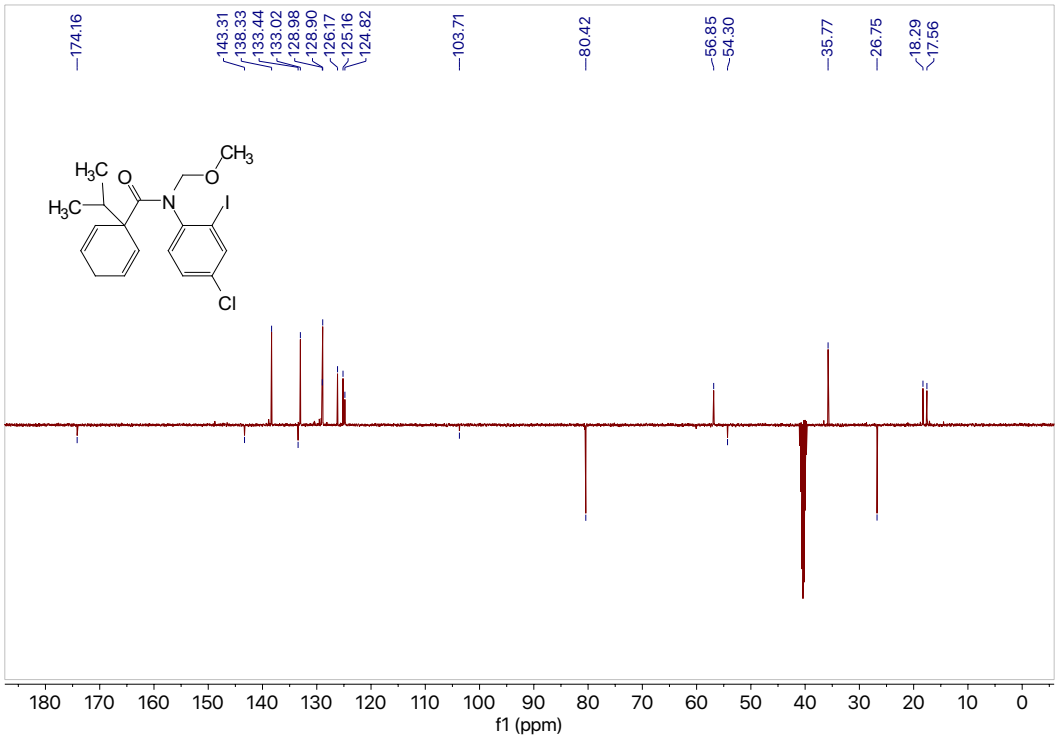

Figure 7.88 ^{13}C NMR (101 MHz, DMSO-d_6) of compound **1j-I**.

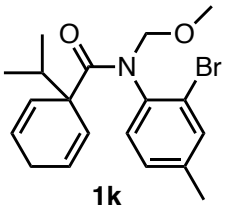

1k

***N*-(2-Bromo-4-methylphenyl)-1-isopropyl-*N*-(methoxymethyl)cyclohexa-2,5-diene-1-carboxamide (1k).** Using the general procedure for MOM group protection, secondary amide **S2k** (0.99 g, 2.96 mmol, 1.0 equiv) in THF (20.7 mL, 0.14 M) was alkylated with chloromethyl methyl ether (0.45 mL, 5.92 mmol, 2.0 equiv). The crude product was purified by column chromatography (silica, 9:1 hexanes: EtOAc) to afford **1k** (0.857 g, 2.2 mmol) in 77% yield as a tan solid, m.p.= 66.2 – 68.8°C.

^{1}H NMR (400 MHz, DMSO-d_6) δ 7.48 (s, 1H), 7.11 (s, 2H), 5.67 (d, J = 19.2 Hz, 1H), 5.49 (d, J = 9.9 Hz, 1H), 5.37 (d, J = 10.5 Hz, 2H), 5.30 (s, 1H), 4.24 (d, J = 9.8 Hz, 1H), 3.29 (s, 3H), 2.45 – 2.36 (m, 1H), 2.36 – 2.32 (m, 4H), 2.23 (d, J = 23.0 Hz, 1H), 0.82 (d, J = 7.0 Hz, 3H), 0.72 (d, J = 7.0 Hz, 3H).

^{13}C NMR (101 MHz, DMSO-d_6) δ_u 133.3, 132.6, 130.3, 128.8, 128.0, 126.4, 125.0, 56.8, 35.8, 20.6, 17.9; δ_d 174.5, 140.2, 138.4, 124.1, 80.6, 54.4, 26.7.

GC (Method B) t_R = 3.480 min. EI-MS m/z (%): 399.1 (M+1$^+$, 1), 367.1 (4), 280.0 (5), 263.9 (4), 247.9 (8), 218.9 (65), 198.0 (42), 121.1 (28), 105.1 (100), 90.0 (12), 79.1 (50), 51.1 (4).

HRMS (ESI) calculated for $C_{19}H_{25}O_2NBr$ [M+H]$^+$: 378.1069, found 378.1063.

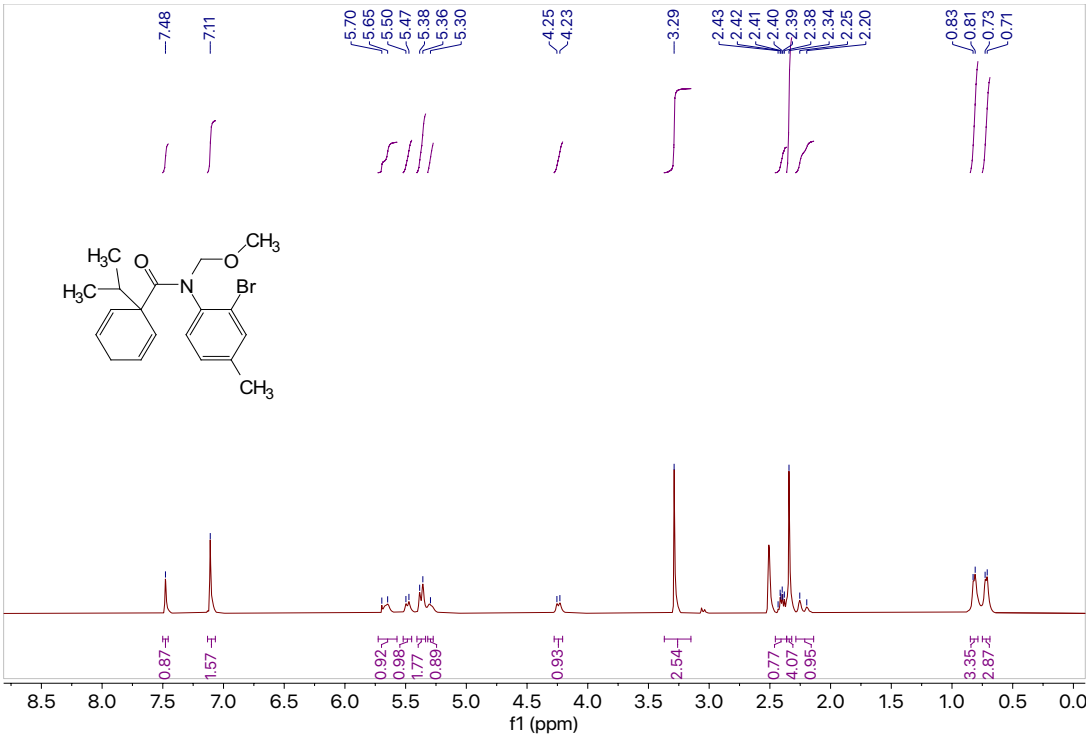

Figure 7.89 ^{1}H NMR (400 MHz, DMSO-d_6) of compound **1k**.

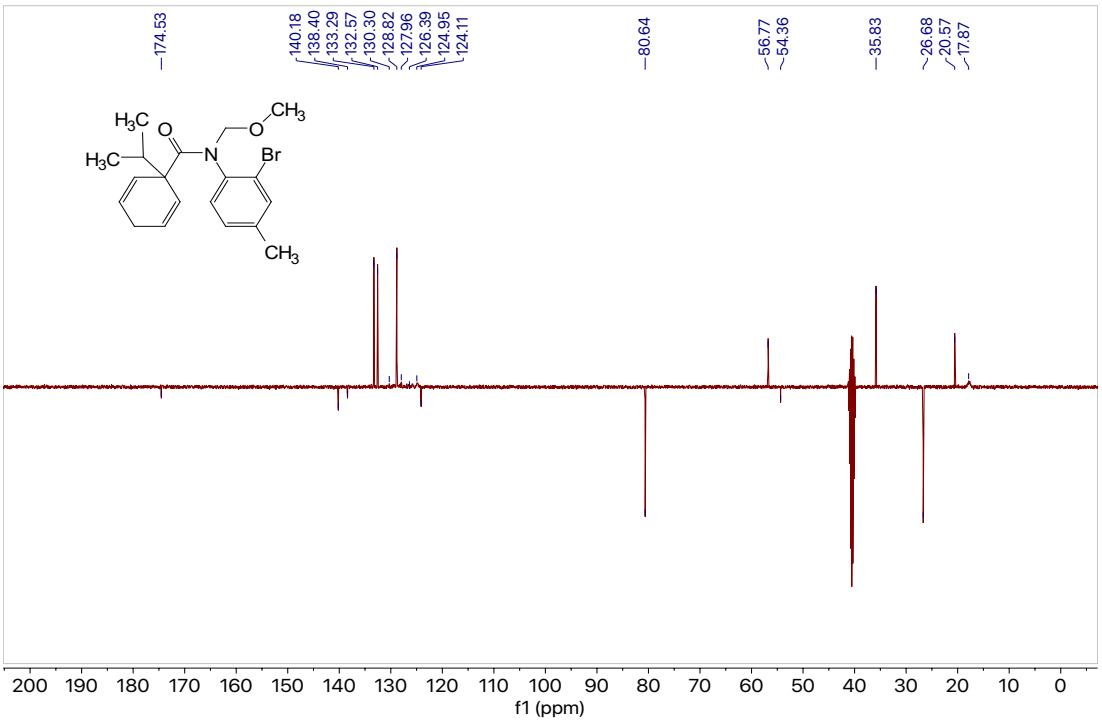

Figure 7.90 ^{13}C NMR (101 MHz, DMSO-d$_6$) of compound **1k**.

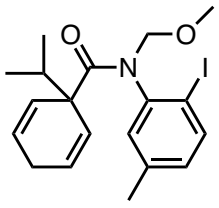

1l-I

***N*-(2-Iodo-5-methylphenyl)-1-isopropyl-*N*-(methoxymethyl)cyclohexa-2,5-diene-1-carboxamide (1l-I).** Using the general procedure for MOM group protection, secondary amide **S2l-I** (0.883 g, 2.32 mmol, 1.0 equiv) in THF (16.2 mL, 0.14 M) was alkylated with chloromethyl methyl ether (0.53 mL, 6.95 mmol, 3.0 equiv). The crude product was purified by column chromatography (silica, 9:1 hexanes: EtOAc) to afford **1l-I** (0.832 g, 1.95 mmol) in 84% yield as a yellow oil that solidified to yellow crystals on cooling, m.p. = 71.6 – 72.3 °C.

^{1}H NMR (400 MHz, DMSO-*d*$_6$) δ 7.73 (d, *J* = 8.0 Hz, 1H), 7.00 (d, *J* = 2.2 Hz, 1H), 6.92 (dd, *J* = 8.1, 2.3 Hz, 1H), 5.72 (d, *J* = 10.1 Hz, 1H), 5.49 (d, *J* = 9.6 Hz, 1H), 5.47 – 5.36 (m, 2H), 5.25 (d, *J* = 10.1 Hz, 1H), 4.24 (d, *J* = 9.8 Hz, 1H), 3.30 (s, 3H), 2.47 – 2.39 (m, 1H), 2.37 (s, 1H), 2.24 (s, 3H), 2.16 (d, *J* = 23.5 Hz, 1H), 0.87 (d, *J* = 6.7 Hz, 3H), 0.73 (d, *J* = 6.7 Hz, 3H).

^{13}C NMR (101 MHz, DMSO-*d*$_6$) δ$_u$ 139.1, 133.1, 130.8, 129.5, 125.7, 124.2, 124.1, 56.9, 35.8, 20.5, 18.3, 17.5; δ$_d$ 174.4, 143.8, 138.6, 98.6, 80.5, 54.3, 26.7.

GC (Method B) t_R = 3.610 min. EI-MS m/z (%): 425.1 (M^+, 1), 266.1 (22), 259.1 (7), 245.0 (100), 178.0 (55), 148.0 (6), 121.1 (11), 105.0 (40), 90.0 (12), 79.0 (22).

HRMS (ESI) calculated for $C_{19}H_{25}O_2NI$ $[M+H]^+$: 426.0930, found 426.0919.

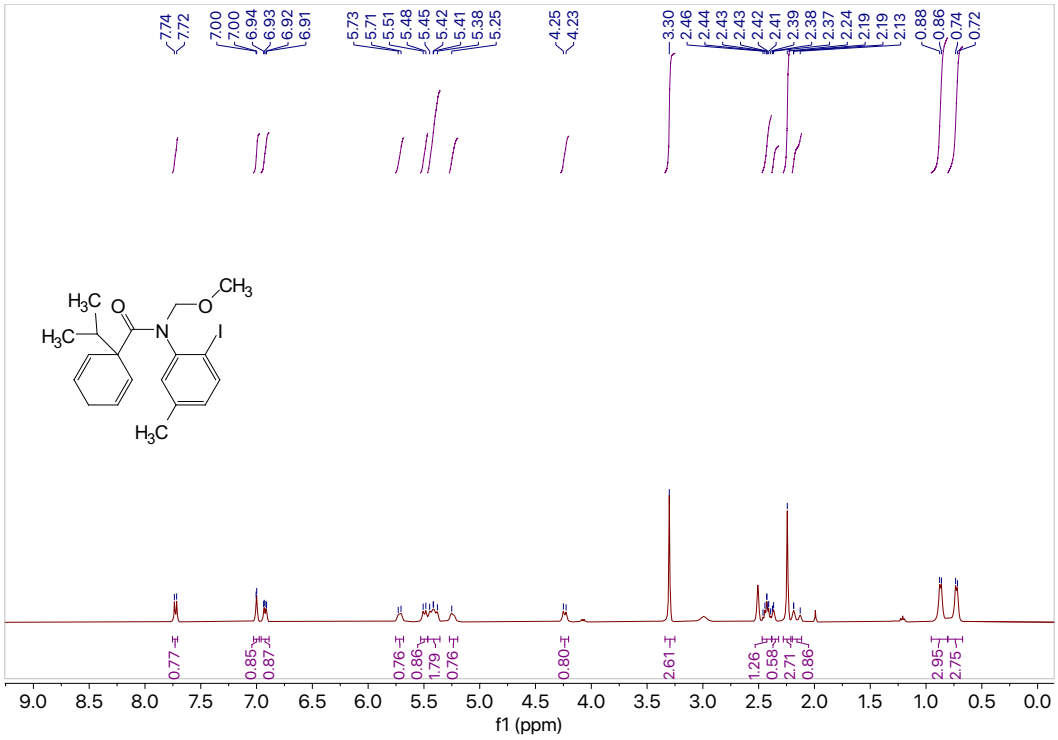

Figure 7.91 ^{1}H NMR (400 MHz, DMSO-d_6) of compound **1l-I**.

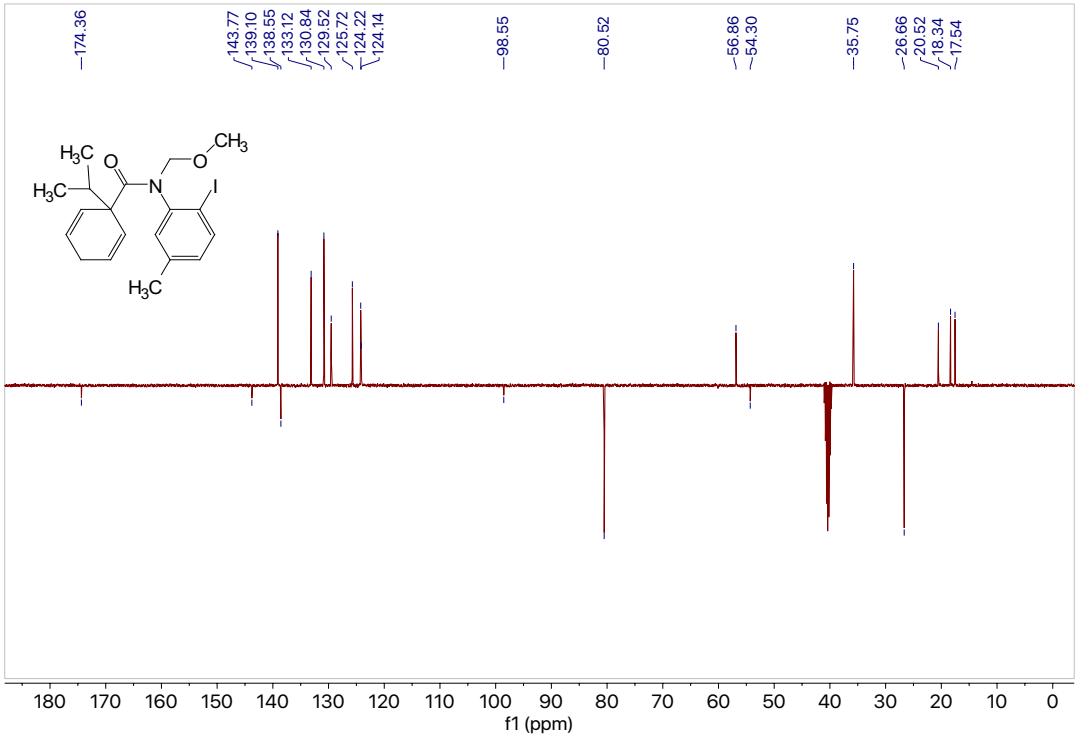

Figure 7.92 ^{13}C NMR (101 MHz, DMSO-d_6) of compound **1l-I**.

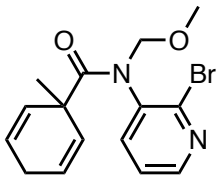

1m

***N*-(2-Bromopyridin-3-yl)-*N*-(methoxymethyl)-1-methylcyclohexa-2,5-diene-1-carboxamide (1m).** Using the general procedure for MOM group protection, secondary amide **S2m** (0.856 g, 2.92 mmol, 1.0 equiv) in THF (20.4 mL, 0.14 M) was alkylated with chloromethyl methyl ether (0.44 mL, 5.84 mmol, 2.0 equiv). The crude product was purified by column chromatography (silica, 4:1 hexanes: EtOAc) to afford **1m** (0.822 g, 2.45 mmol) in 84% yield as a yellow solid, m.p.= 59.0 – 61.3°C.

^{1}H NMR (400 MHz, DMSO-d_6) δ 8.29 (dd, J = 4.7, 1.9 Hz, 1H), 7.68 (dd, J = 7.7, 1.9 Hz, 1H), 7.38 (dd, J = 7.8, 4.7 Hz, 1H), 5.60 (s, 2H), 5.47 (s, 1H), 5.32 (s, 1H), 4.30 (s, 1H), 3.25 (s, 3H), 2.41 (d, J = 24.3 Hz, 1H), 2.07 (d, J = 23.3 Hz, 1H), 1.21 (s, 3H).

^{13}C NMR (101 MHz, DMSO-d_6) δ_u 149.2, 141.2, 123.8, 56.6, 29.1; δ_d 173.9, 144.3, 138.0, 80.2, 46.1, 25.9.

GC (Method B) t_R = 2.786 min. EI-MS m/z (%): 339.1 ($M+2^+$, 1), 306.0 (4), 245.0 (9), 216.0 (32), 200.9 (26), 184.9 (44), 165.0 (25), 137.0 (8), 119.0 (11), 106.0 (8), 93.1 (100), 77.1 (50), 64.0 (10), 51.0 (7).

HRMS (ESI) calculated for $C_{15}H_{18}O_2N_2Br$ $[M+H]^+$: 337.0552, found 337.0555.

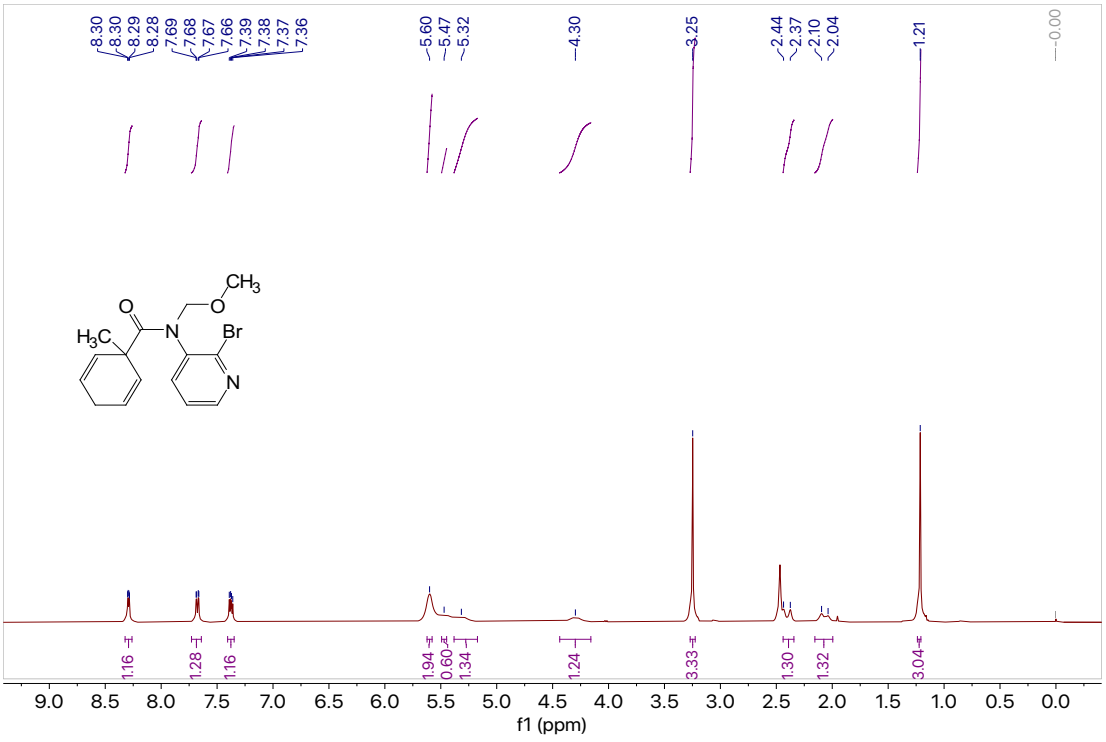

Figure 7.93 ^{1}H NMR (400 MHz, DMSO-d_6) of compound **1m**.

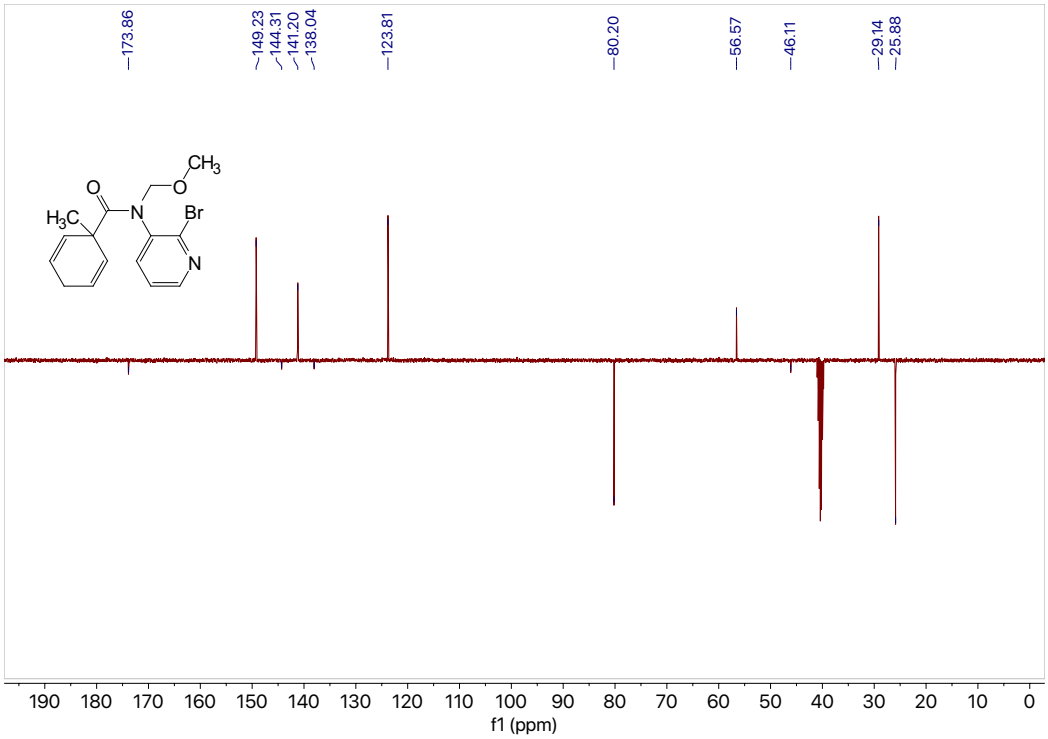

Figure 7.94 ^{13}C NMR (101 MHz, DMSO-d_6) of compound **1m**.

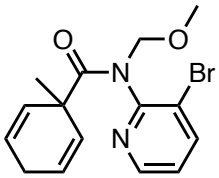

1n

***N*-(3-Bromopyridin-2-yl)-*N*-(methoxymethyl)-1-methylcyclohexa-2,5-diene-1-carboxamide (1n).** Using the general procedure for MOM group protection, secondary amide **S2n** (0.737 g, 2.51 mmol, 1.0 equiv) in THF (17.6 mL, 0.14 M) was alkylated with bromomethyl methyl ether (0.82 mL, 10.0 mmol, 4.0 equiv). The crude product was purified by column chromatography (silica, 4:1 hexanes: EtOAc) to afford **1n** (0.547 g, 1.62 mmol) in 65% yield as a yellow oil.

^{1}H NMR (400 MHz, DMSO-d_6) δ 8.43 (dd, J = 4.6, 1.7 Hz, 1H), 8.11 (dd, J = 8.0, 1.7 Hz, 1H), 7.33 (dd, J = 7.9, 4.6 Hz, 1H), 5.60 – 5.42 (m, 4H), 5.05 (s, 1H), 3.27 (s, 3H), 2.49 – 2.30 (m, 2H), 1.28 (s, 3H).

^{13}C NMR (101 MHz, DMSO-d_6) δ_u 148.1, 142.5, 129.8, 125.4, 123.5, 56.7, 29.4; δ_d 175.0, 153.0, 121.0, 79.6, 46.3, 25.9.

GC (Method B) t_R = 2.740 min. EI-MS m/z (%): 338.1 ($M+1^+$, 1), 304.0 (6), 245.0 (20), 214.9 (21), 200.9 (41), 185.9 (66), 156.0 (33), 135.0 (3), 120.0 (9), 106.0 (6), 93.1 (100), 77.1 (50), 65.1 (11), 51.1 (8).

HRMS (ESI) calculated for $C_{15}H_{18}O_2N_2Br$ $[M+H]^+$: 337.0552, found 337.0547.

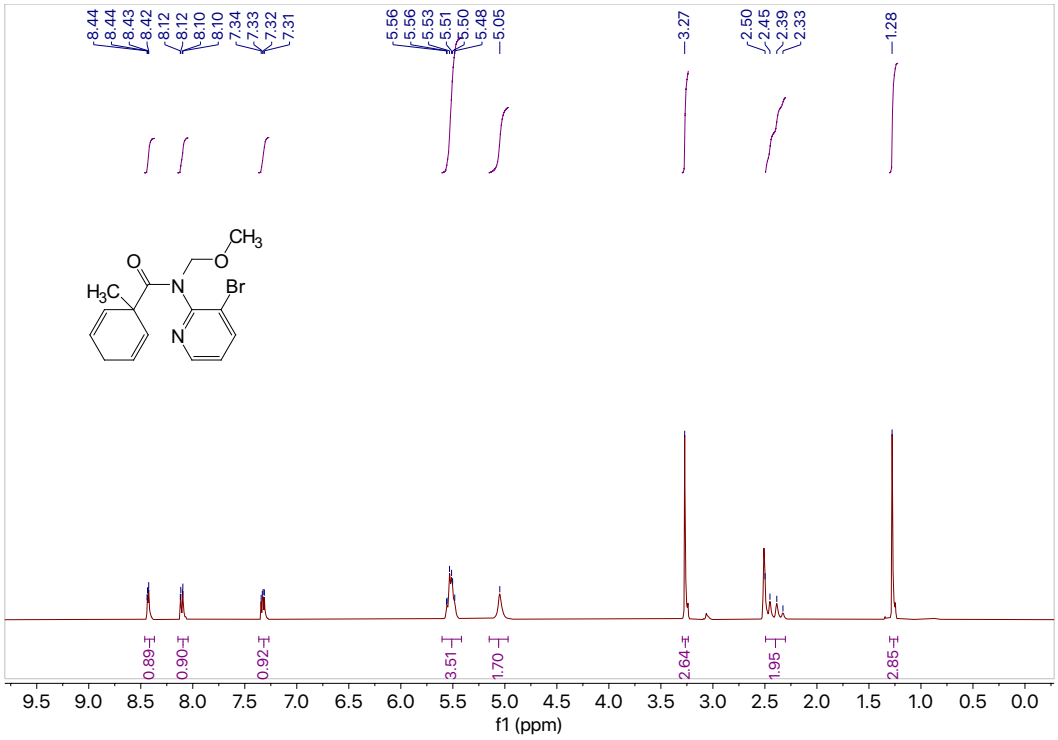

Figure 7.95 ^{1}H NMR (400 MHz, DMSO-d_6) of compound **1n**.

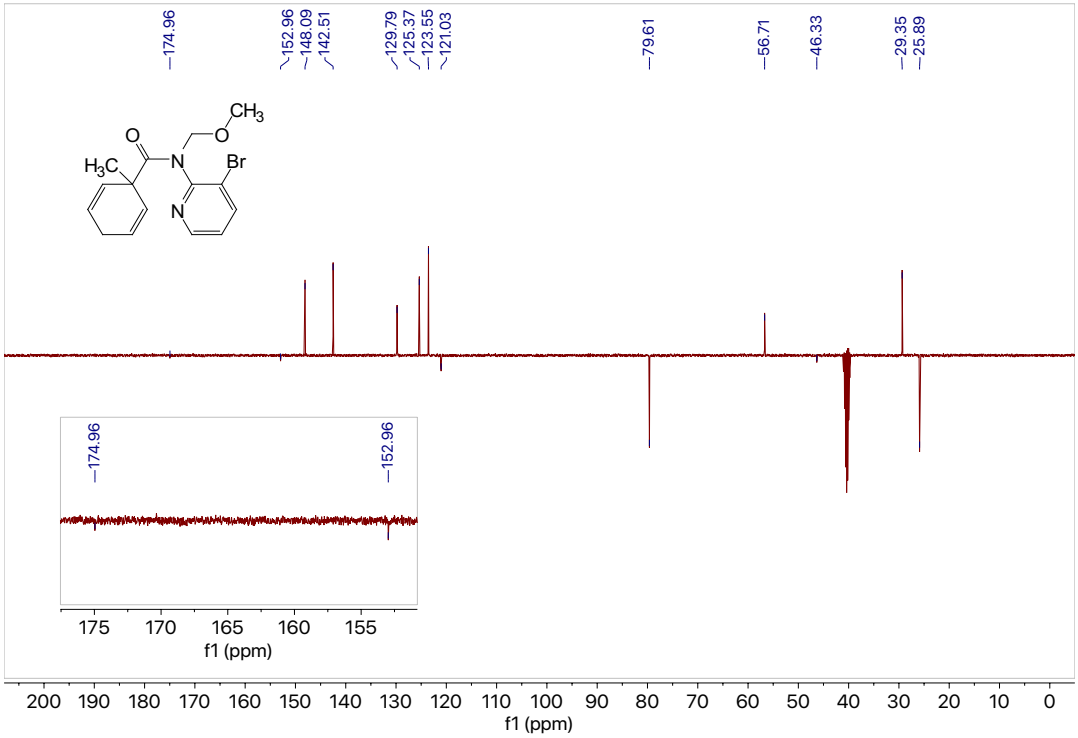

Figure 7.96 ^{13}C NMR (101 MHz, DMSO-d_6) of compound **1n**.

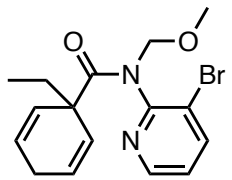

1o

***N*-(3-Bromopyridin-2-yl)-1-ethyl-*N*-(methoxymethyl)cyclohexa-2,5-diene-1-carboxamide (1o).** Using the general procedure for MOM group protection, secondary amide **S2o** (1.43 g, 4.66 mmol, 1.0 equiv) in THF (32.6 mL, 0.14 M) was alkylated with bromomethyl methyl ether (2.3 mL, 27.9 mmol, 6.0 equiv). The crude product was purified by column chromatography (silica, 3:2 hexanes: EtOAc) to afford **1o** (1.28 g, 3.64 mmol) in 78% yield as a yellow solid, m.p.= 41.9 – 44.4°C.

^{1}H NMR (400 MHz, DMSO-d_6) δ 8.42 (d, J = 4.6 Hz, 1H), 8.10 (d, J = 8.0 Hz, 1H), 7.32 (dd, J = 8.0, 4.7 Hz, 1H), 5.56 (d, J = 10.2 Hz, 2H), 5.39 (d, J = 10.3 Hz, 2H), 5.05 (s, 2H), 3.28 (s, 3H), 2.45 – 2.36 (m, 2H), 1.74 (q, J = 7.5 Hz, 2H), 0.74 (t, J = 7.5 Hz, 3H).

^{13}C NMR (101 MHz, DMSO-d_6) δ_u 148.1, 142.5, 128.0, 125.4, 125.0, 56.8, 8.6; δ_d 176.1, 153.0, 121.1, 79.5, 50.7, 33.4, 26.3.

GC (Method B) t_R = 3.027 min. EI-MS m/z (%): 350.1 (M-1$^+$, 1), 320.1 (6), 245.0 (15), 215.0 (19), 200.9 (33), 186.0 (61), 156.9 (29), 134.0 (12), 107.1 (39), 91.1 (50), 79.1 (100), 65.1 (5), 51.1 (6).

HRMS (ESI) calculated for $C_{16}H_{20}O_2N_2Br$ $[M+H]^+$: 351.0708, found 351.0706.

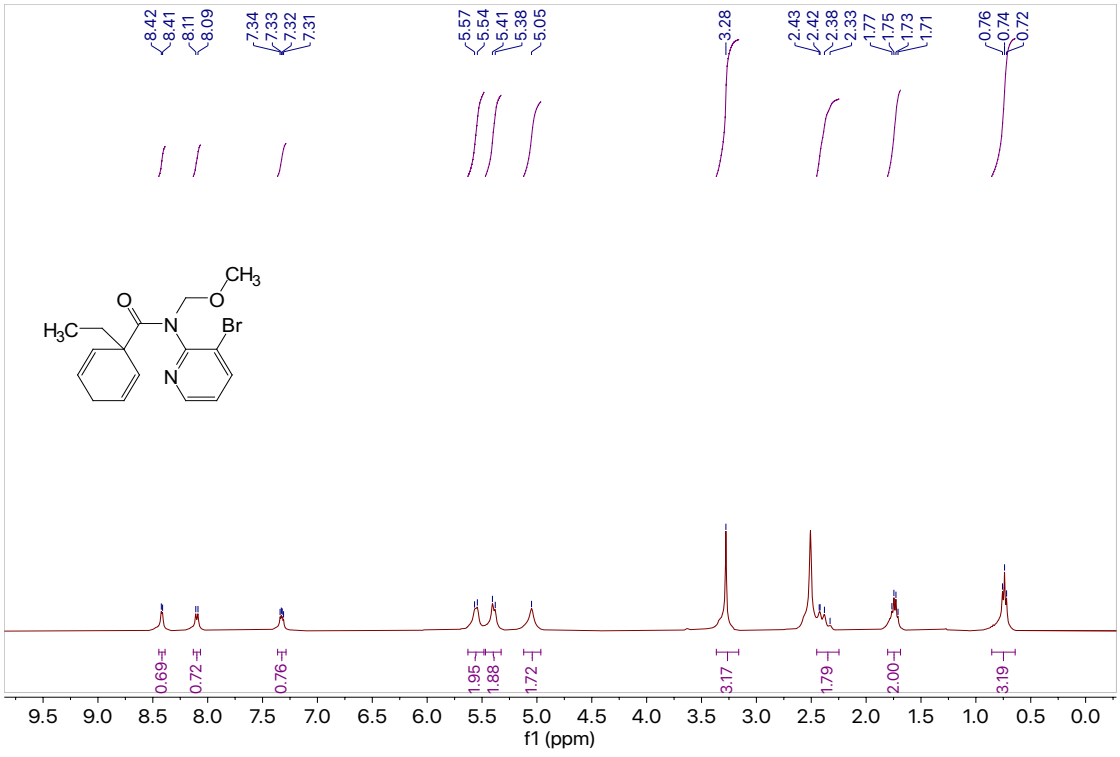

Figure 7.97 ^{1}H NMR (400 MHz, DMSO-d_6) of compound **1o**.

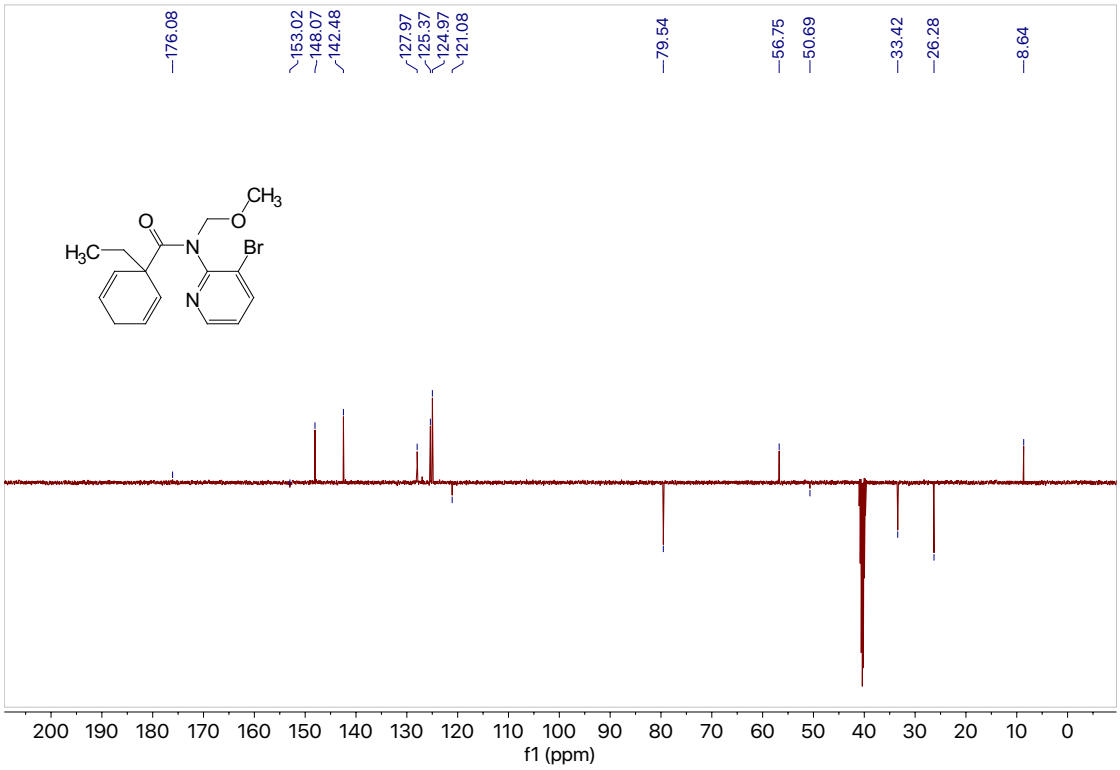

Figure 7.98 ^{13}C NMR (101 MHz, DMSO-d$_6$) of compound **1o**.

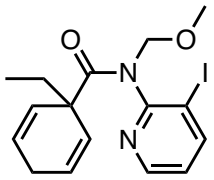

1o-I

1-Ethyl-*N*-(2-iodopyridin-3-yl)cyclohexa-2,5-diene-1-carboxamide (1o-I). Using the general procedure for MOM group protection, secondary amide **S2o-I** (0.497 g, 1.41 mmol, 1.0 equiv) in THF (9.9 mL, 0.14 M) was alkylated with bromomethyl methyl ether (0.46 mL, 5.65 mmol, 4.0 equiv). The crude product was purified by column chromatography (silica, 4:1 hexanes: EtOAc) to afford **1o-I** (0.283 g, 0.711 mmol) in 50% yield as a tan solid, m.p.= 71.3 – 72.1°C.

^{1}H NMR (400 MHz, DMSO-*d*$_6$) δ 8.45 – 8.38 (m, 1H), 8.28 (dd, *J* = 7.8, 1.7 Hz, 1H), 7.12 (dd, *J* = 7.9, 4.6 Hz, 1H), 5.56 (d, *J* = 10.7 Hz, 2H), 5.42 (d, *J* = 10.0 Hz, 2H), 5.04 (s, 2H), 3.28 (s, 3H), 2.43 (s, 2H), 1.76 (q, *J* = 7.7 Hz, 2H), 0.76 (t, *J* = 7.4 Hz, 3H).

^{13}C NMR (101 MHz, DMSO-*d*$_6$) δ$_u$ 148.8, 148.6, 128.1, 124.9, 56.8, 8.7; δ$_d$ 176.2, 155.9, 97.9, 79.9, 50.7, 33.5, 26.3.

GC (Method B) t_R = 3.496 min. EI-MS m/z (%): 398.1 (M^+, 1), 366.1 (5), 291.0 (20), 264.0 (30), 246.9 (36), 231.9 (100), 204.9 (37), 165 (6), 134.0 (10), 107.1 (25), 91.1 (25), 79.0 (58), 51.0 (4).

HRMS (ESI) calculated for $C_{16}H_{20}O_2N_2I$ $[M+H]^+$: 399.0570, found 399.0567.

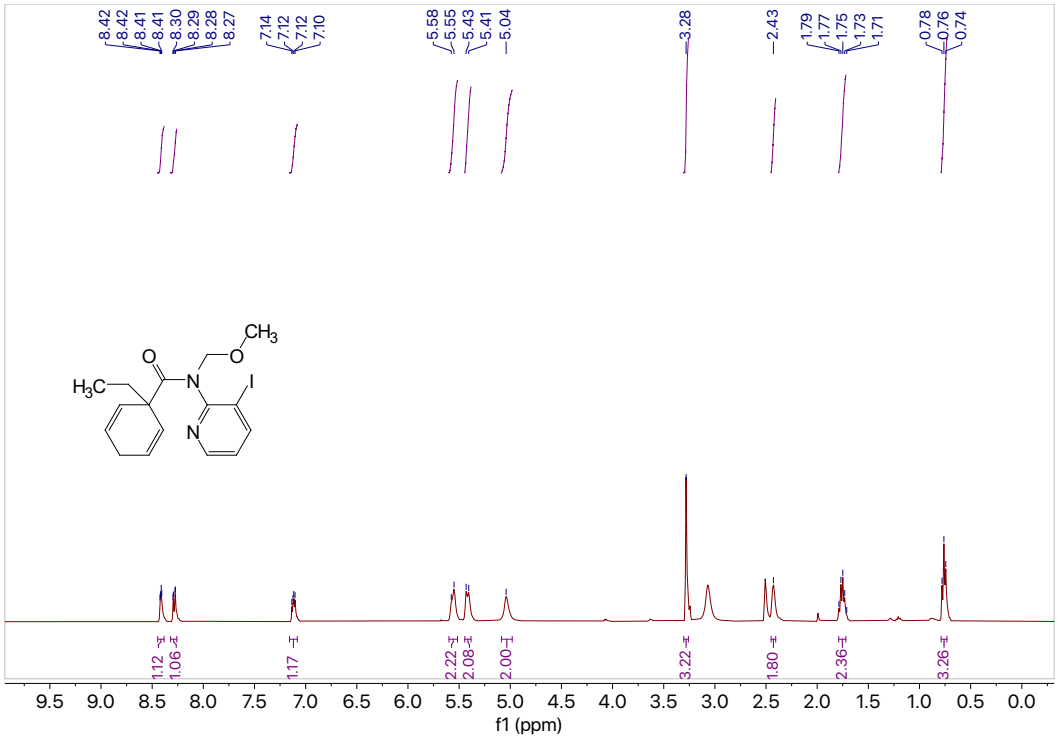

Figure 7.99 ^{1}H NMR (400 MHz, DMSO-d_6) of compound **1o-I**.

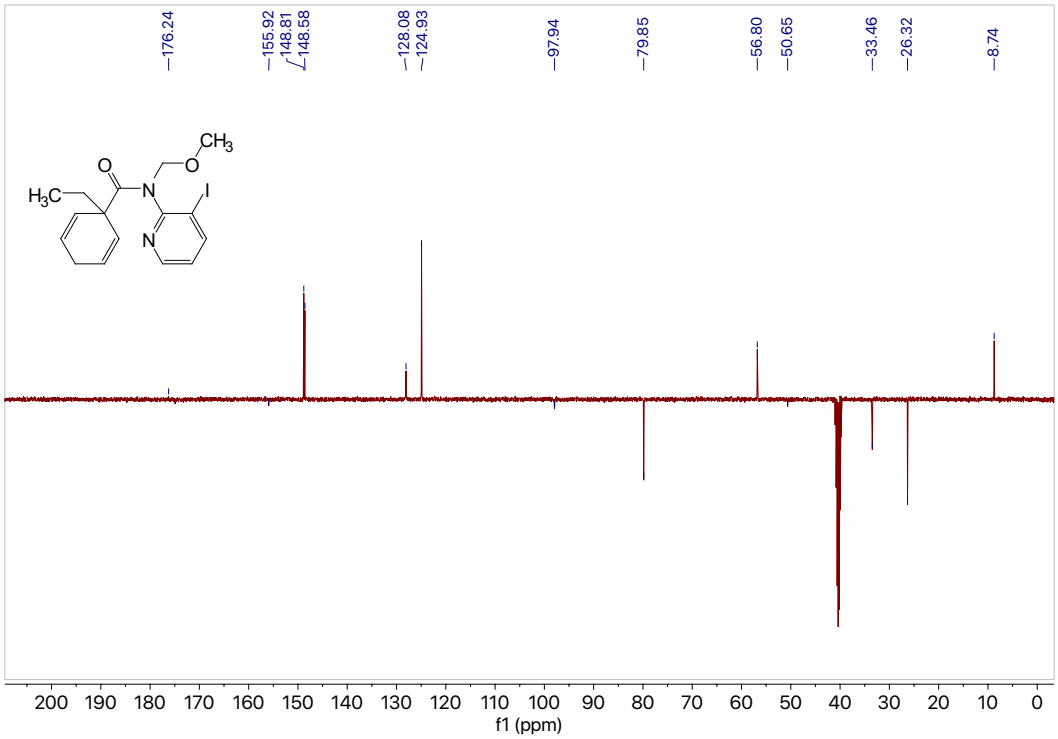

Figure 7.100 ^{13}C NMR (101 MHz, DMSO-d_6) of compound **1o-I**.

7.7 Amide reduction general procedures and data

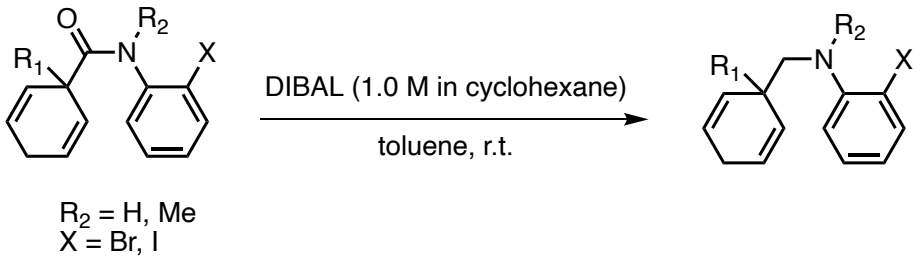

Scheme 7.8 Amide reduction with DIBAL general reaction.

General procedure A

A flame dried round bottom flask with a stir bar, under argon, was charged with tertiary amide (1.0 mmol, 1.0 equiv) in toluene (20 mL, 0.05 M). DIBAL (1 M in cyclohexane, 3 mL, 3.0 mmol, 3 equiv) was added dropwise and the reaction mixture was stirred for 2-3 h. The reaction was quenched with water and extracted with Et_2O (3 x 5 mL/mmol). The organic layers were combined and washed with brine, dried over $MgSO_4$, and concentrated in vacuo. The crude products were purified by column chromatography.

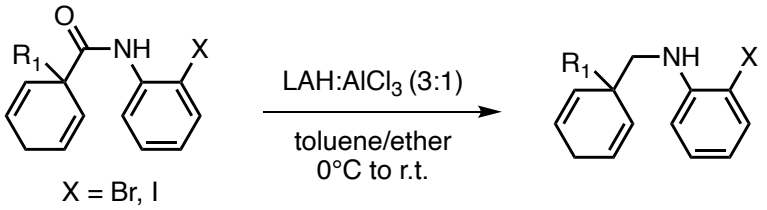

Scheme 7.9 Amide reduction with alane (AlH_3), general reaction.

General procedure B

A flame dried round bottom flask with a stir bar, under argon, was charged with $AlCl_3$ (1.5 mmol, 1.5 equiv) in ether (2.8 mL, 0.36 M) and cooled to 0°C. Then LAH (4.5 mmol, 4.5 equiv) was added and the mixture was stirred on ice for 10 minutes. To a separate flame dried round bottom flask with a stir bar, amide (1.0 mmol, 1 equiv) was added, dissolved in THF (2 mL, 0.5 M), and then transferred to the in situ generated alane (AlH_3). Upon completion, the reaction was cooled 0°C, quenched with 1 M NaOH, and filtered. The filtrate solution was extracted with EtOAc, washed with brine, dried over $MgSO_4$, and concentrated in vacuo. The crude products were purified by column chromatography.

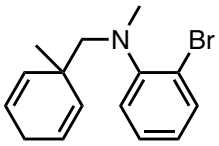

1w

2-bromo-*N*-methyl-*N*-((1-methylcyclohexa-2,5-dien-1-yl)methyl)aniline (1w). Using the general procedure A for amide reduction, tertiary amide **1a** (0.101 g, 0.327 mmol, 1.0 equiv) in toluene (6.5 mL, 0.05 M) was reacted with DIBAL (1 M in cyclohexane, 0.98 mL, 0.98 mmol, 3.0 equiv). The crude product was purified by column chromatography (silica, 9:1 hexanes: EtOAc) to afford **1w** (0.0592 g, 0.203 mmol) in 62% yield as a clear colorless oil.

^{1}H NMR (400 MHz, $CDCl_3$) δ 7.44 (dd, *J* = 7.9, 1.5 Hz, 1H), 7.13 (ddd, *J* = 8.5, 7.1, 1.5 Hz, 1H), 7.07 (dd, *J* = 8.1, 1.8 Hz, 1H), 6.78 (ddd, *J* = 7.9, 7.1, 1.7 Hz, 1H), 5.55 (dt, *J* = 10.5, 3.1 Hz, 2H), 5.48 (dt, *J* = 10.4, 1.9 Hz, 2H), 3.03 (s, 2H), 2.74 (s, 3H), 2.53 (qt, *J* = 3.4, 1.9 Hz, 2H), 0.94 (s, 3H).

^{13}C NMR (101 MHz, $CDCl_3$) δ_u 133.7, 133.5, 127.8, 124.5, 124.1, 123.0, 45.2, 27.7; δ_d 152.7, 121.1, 66.4, 39.1, 26.5.

GC (Method B) t_R = 1.791 min. EI-MS m/z (%): 290.0 (M^+, 1), 197.9 (100), 183.9 (4), 118.0 (16), 91.0 (10), 77.0 (5).

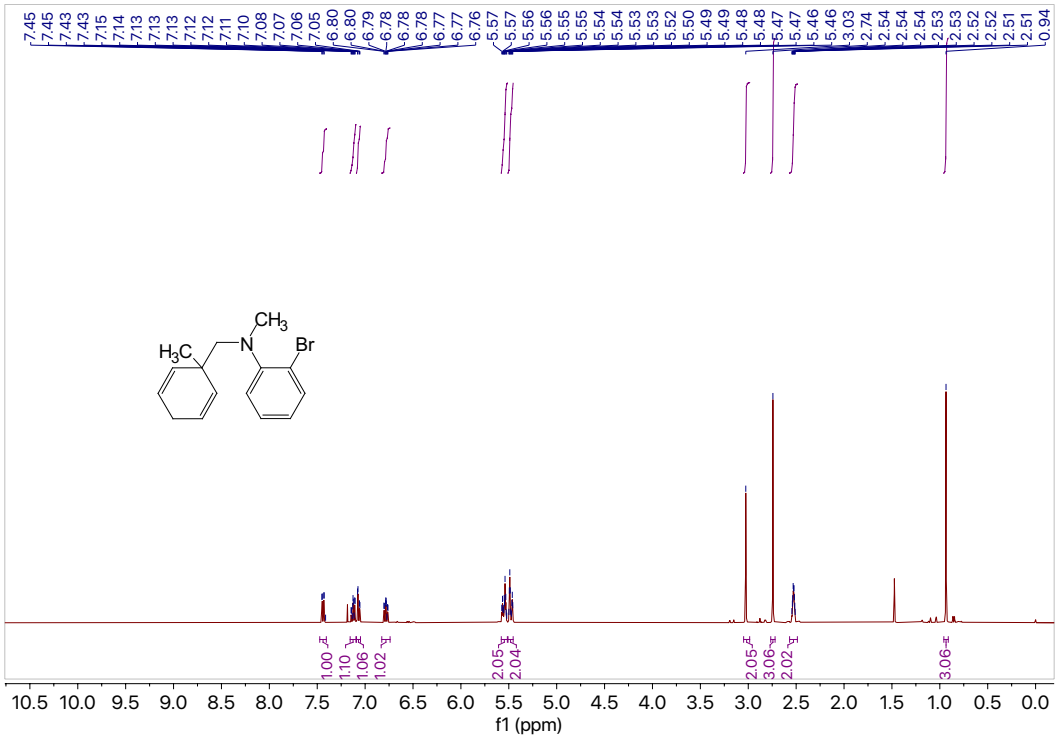

Figure 7.101 ^{1}H NMR (400 MHz, $CDCl_3$) of compound **1w**.

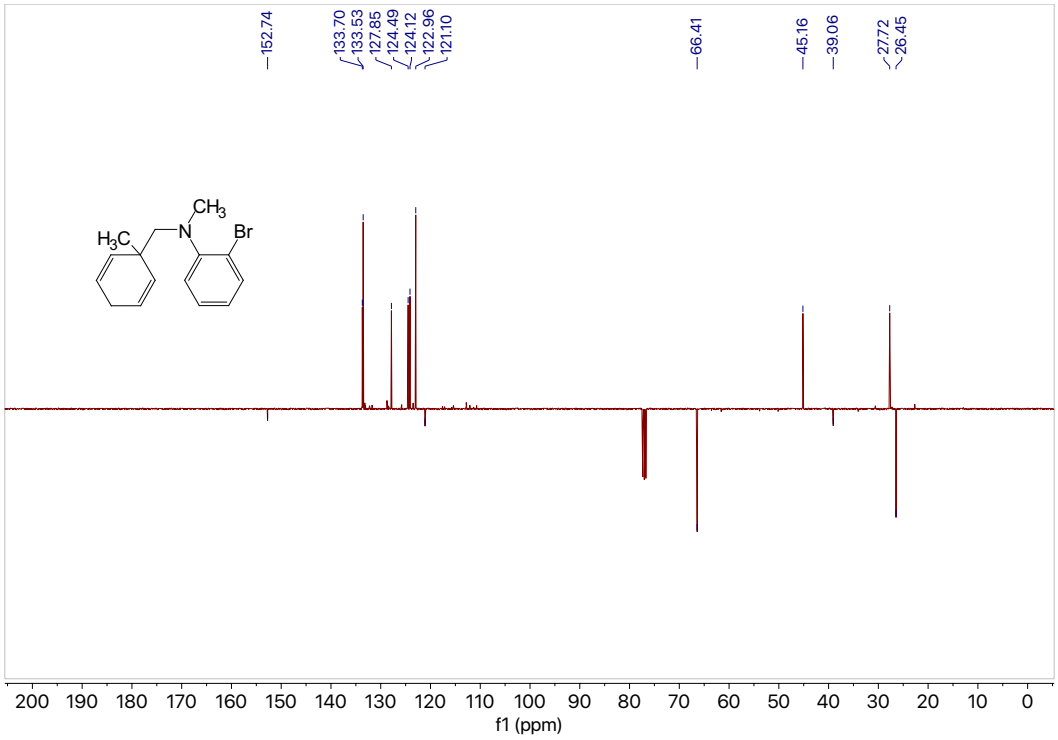

Figure 7.102 ^{13}C NMR (101 MHz, $CDCl_3$) of compound **1w**.

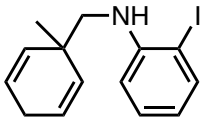

S2x-I

2-iodo-*N*-((1-methylcyclohexa-2,5-dien-1-yl)methyl)aniline (S2x-I). Using the general procedure A for amide reduction, secondary amide **S2b-I** (0.807 g, 2.38 mmol, 1.0 equiv) in toluene (6.9 mL, 0.05 M) was reacted with DIBAL (1 M in cyclohexane, 23.8 mL, 23.8 mmol, 10 equiv). The crude product was purified by column chromatography (silica, 9:1 hexanes: EtOAc) to afford **S2x-I** (0.459 g, 1.14 mmol) in 59% yield as a clear colorless oil.

^{1}H NMR (400 MHz, $CDCl_3$) δ 7.53 (dd, J = 7.8, 1.5 Hz, 1H), 7.09 (ddd, J = 8.1, 7.3, 1.5 Hz, 1H), 6.41 (dd, J = 8.1, 1.5 Hz, 1H), 6.31 (td, J = 7.5, 1.5 Hz, 1H), 5.86 (dt, J = 10.3, 3.3 Hz, 2H), 5.42 (dp, J = 10.6, 2.1 Hz, 2H), 4.21 (s, 1H), 2.86 (s, 2H), 2.83 – 2.57 (m, 2H), 1.10 (s, 3H).

^{13}C NMR (101 MHz, $CDCl_3$) δ_u 138.9, 131.8, 129.3, 125.9, 118.1, 110.6, 27.2; δ_d 147.5, 85.1, 54.2, 37.2, 26.5.

GC (Method B) t_R = 2.304 min. EI-MS m/z (%): 325.0 (M^+, 4), 231.9 (100), 104.0 (14), 91.0 (6), 77.0 (7).

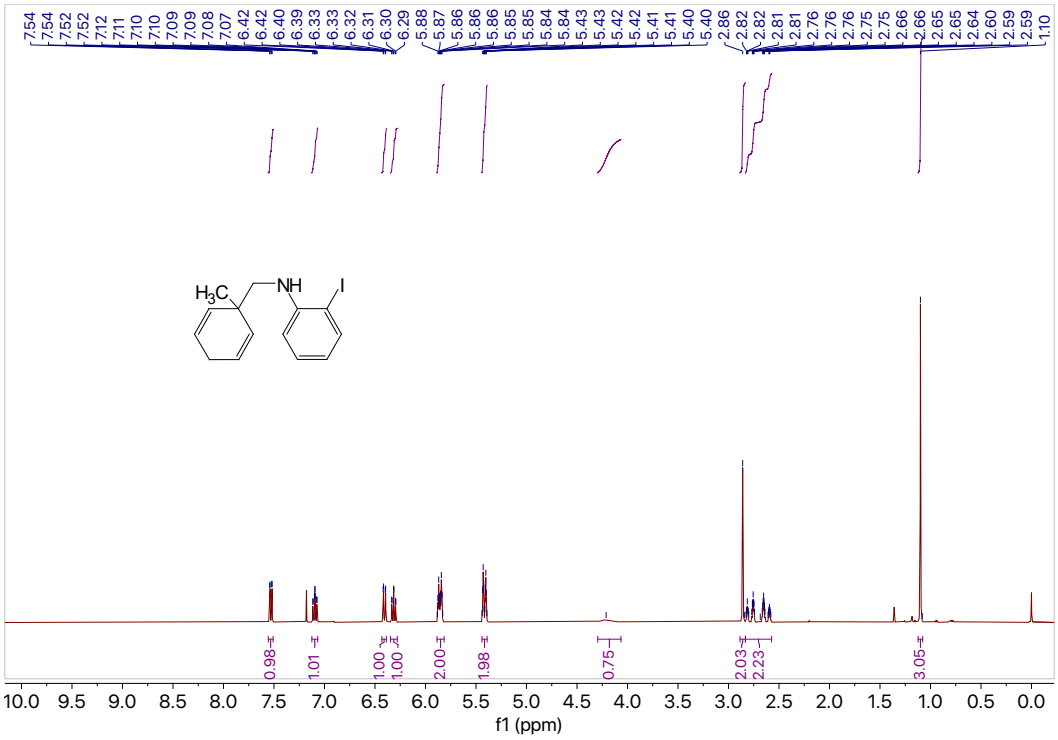

Figure 7.103 ^{1}H NMR (400 MHz, $CDCl_3$) of compound **S2x-I**.

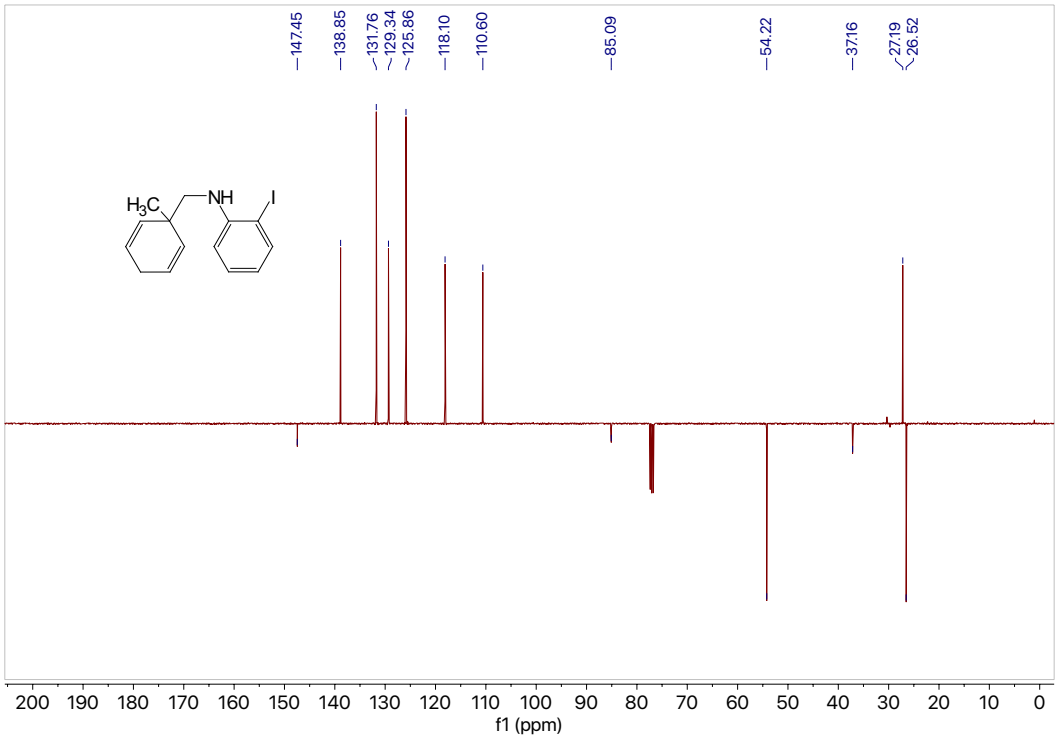

Figure 7.104 ^{13}C NMR (101 MHz, $CDCl_3$) of compound **S2x-I**.

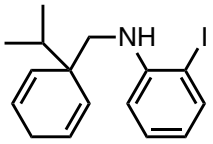

S2y-I

2-iodo-*N*-((1-isopropylcyclohexa-2,5-dien-1-yl)methyl)aniline (S2y-I). Using the general procedure B for amide reduction, secondary amide **S2e-I** (0.500 g, 1.36 mmol, 1.0 equiv) in THF (2.72 mL, 0.5 M) was reacted with a mixture of $AlCl_3$ (0.272 g, 2.04 mmol, 1.5 equiv) and LAH (0.232 g, 6.12 mmol, 4.5 equiv) in ether (5.7 mL, 0.36 M) The crude product was purified by column chromatography (silica, 9:1 hexanes: EtOAc) to afford **S2y-I** (0.343 g, 0.971 mmol) in 71% yield as an orange oil.
^{1}H NMR (400 MHz, $CDCl_3$) δ 7.53 (dd, *J* = 7.8, 1.5 Hz, 1H), 7.10 (ddd, *J* = 8.2, 7.3, 1.5 Hz, 1H), 6.43 – 6.40 (m, 1H), 6.32 (td, *J* = 7.5, 1.5 Hz, 1H), 5.97 (dt, *J* = 10.4, 3.3 Hz, 2H), 5.38 (dt, *J* = 10.6, 2.1 Hz, 2H), 2.94 (s, 2H), 2.86 – 2.73 (m, 1H), 2.68 – 2.55 (m, 1H), 1.61 (hept, *J* = 6.9 Hz, 1H), 0.86 (d, *J* = 6.9 Hz, 6H).
^{13}C NMR (101 MHz, $CDCl_3$) δ_u 138.8, 129.3, 129.1, 127.7, 118.1, 110.6, 35.5, 17.8; δ_d 147.6, 85.2, 51.7, 44.0, 27.1.
GC (Method B) t_R = 2.918 min. EI-MS m/z (%): 353.0 (M^+, 1), 231.9 (100), 104.0 (10), 91.0 (9), 77.0 (5).

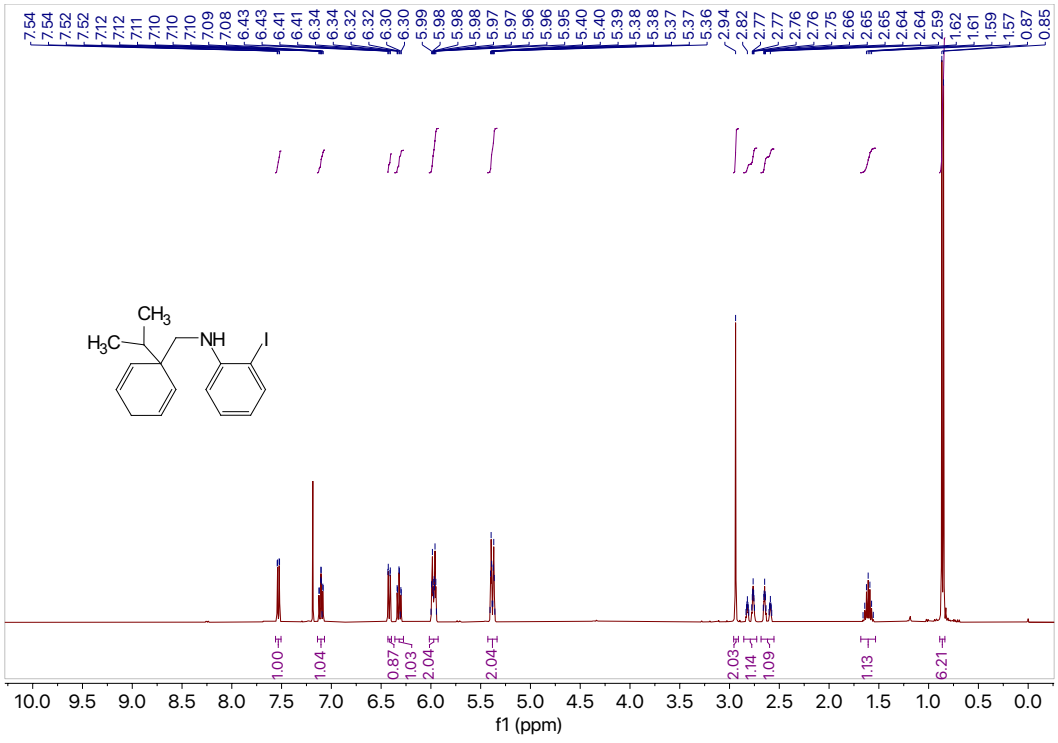

Figure 7.105 ^{1}H NMR (400 MHz, $CDCl_3$) of compound **S2y-I**.

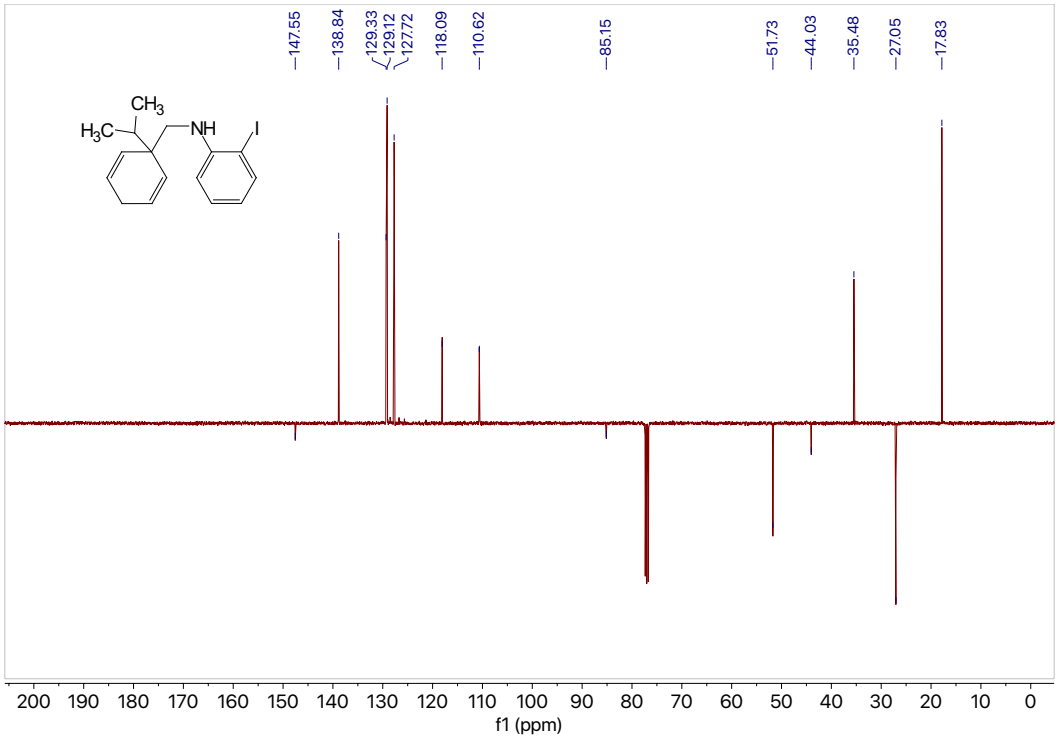

Figure 7.106 ^{13}C NMR (101 MHz, $CDCl_3$) of compound **S2y-I**.

7.8 Secondary amine protection general procedures and data

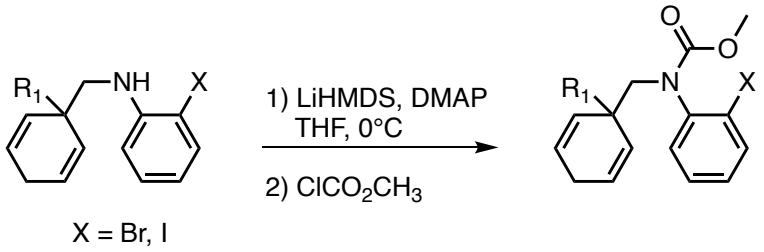

Scheme 7.10 Methyl carbamate amine N protection general reaction.

General procedure A

A flame dried round bottom flask with a stir bar, under argon, was charged with secondary amine (1.0 mmol, 1.0 equiv) and DMAP (0.25 mmol, 0.25 equiv) in THF (30 mL, 0.03 M) and cooled to 0°C. LiHMDS (1.0 M in hexanes, 3.0 mmol, 3.0 equiv) was added dropwise and the solution was stirred for 10 min. Methyl chloroformate (4.0 mmol, 4.0 equiv) was added dropwise to the reaction solution and the reaction was left stirring while slowly warming to r.t. Upon completion, the reaction was quenched with saturated NH_4Cl and diluted with EtOAc. The aqueous layer was extracted with EtOAc (2 x). The combined organic layers were washed with brine, dried with $MgSO_4$, filtered, and concentrated. The crude product was purified by column chromatography.

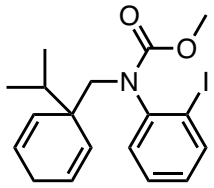

1ye-I

Methyl (2-iodophenyl)((1-isopropylcyclohexa-2,5-dien-1-yl)methyl)carbamate (1ye-I). Using the general procedure A for methyl carbamate group protection, secondary amine **S2y-I** (0.0317 g, 0.0897 mmol, 1.0 equiv) in THF (3 mL, 0.03 M) was acylated with methyl chloroformate (0.0339 g, 0.3589 mmol, 4.0 equiv). The crude product was purified by column chromatography (silica, 9:1 hexanes: EtOAc) to afford **1ye-I** (0.0338 g, 0.0822 mmol) in 91% yield as a yellow oil.

^{1}H NMR (400 MHz, $CDCl_3$) δ 7.63 – 7.56 (m, 1H), 7.03 – 6.96 (m, 2H), 6.72 (ddd, *J* = 7.9, 6.1, 2.8 Hz, 1H), 5.66 (dtd, *J* = 10.4, 3.3, 1.6 Hz, 1H), 5.46 (d, *J* = 10.4 Hz, 1H), 5.40 (d, *J* = 10.6 Hz, 1H), 4.85 (dd, *J* = 10.5, 2.3 Hz, 1H), 4.07 (d, *J* = 14.2 Hz, 1H), 3.38 (s, 3H), 2.94 (d, *J* = 14.2 Hz, 1H), 2.50 – 2.33 (m, 2H), 1.37 (h, *J* = 7.0 Hz, 1H), 0.61 (dd, *J* = 15.3, 6.8 Hz, 6H).

^{13}C NMR (101 MHz, $CDCl_3$) δ_u 139.3, 132.6, 130.3, 130.0, 128.7, 127.8, 126.1, 125.5, 53.2, 36.4, 17.8, 17.1; δ_d 156.7, 144.8, 99.5, 57.9, 45.4, 26.9.

GC (Method B) t_R = 3.227 min. EI-MS m/z (%): 412.0 ($M+1^+$, 1), 289.0 (52), 279.0 (31), 230.9 (20), 164.1 (100), 149.0 (25), 118 (33), 91.0 (46), 79.0 (13), 65.0 (5).

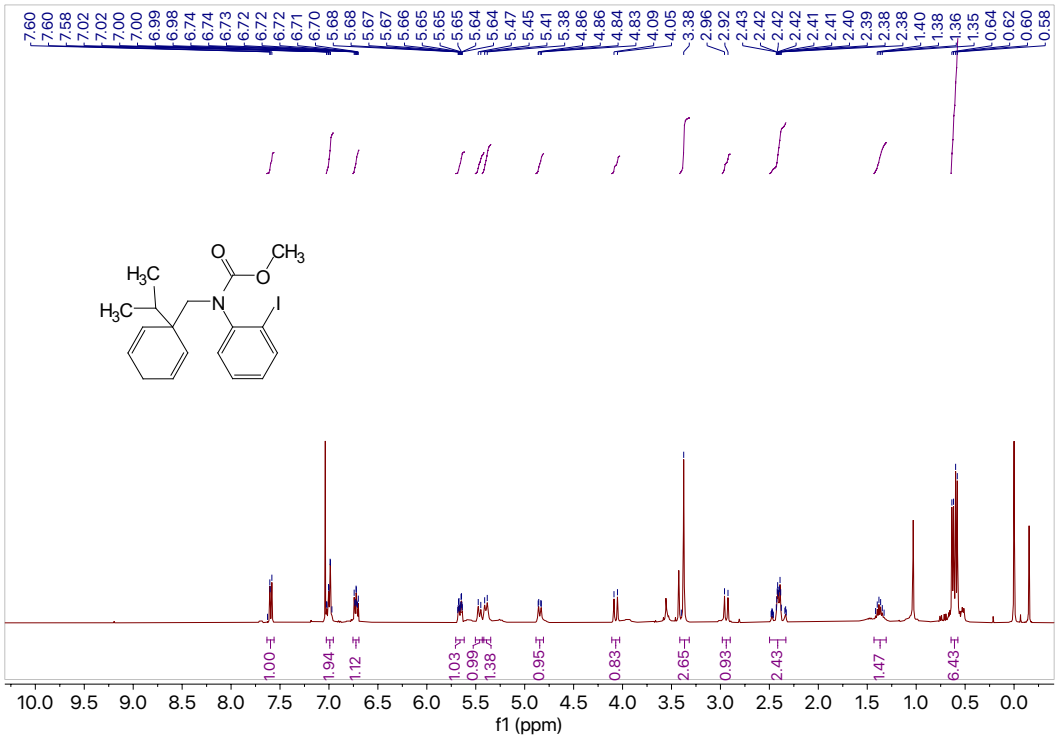

Figure 7.107 ^{1}H NMR (400 MHz, $CDCl_3$) of compound **1ye-I**.

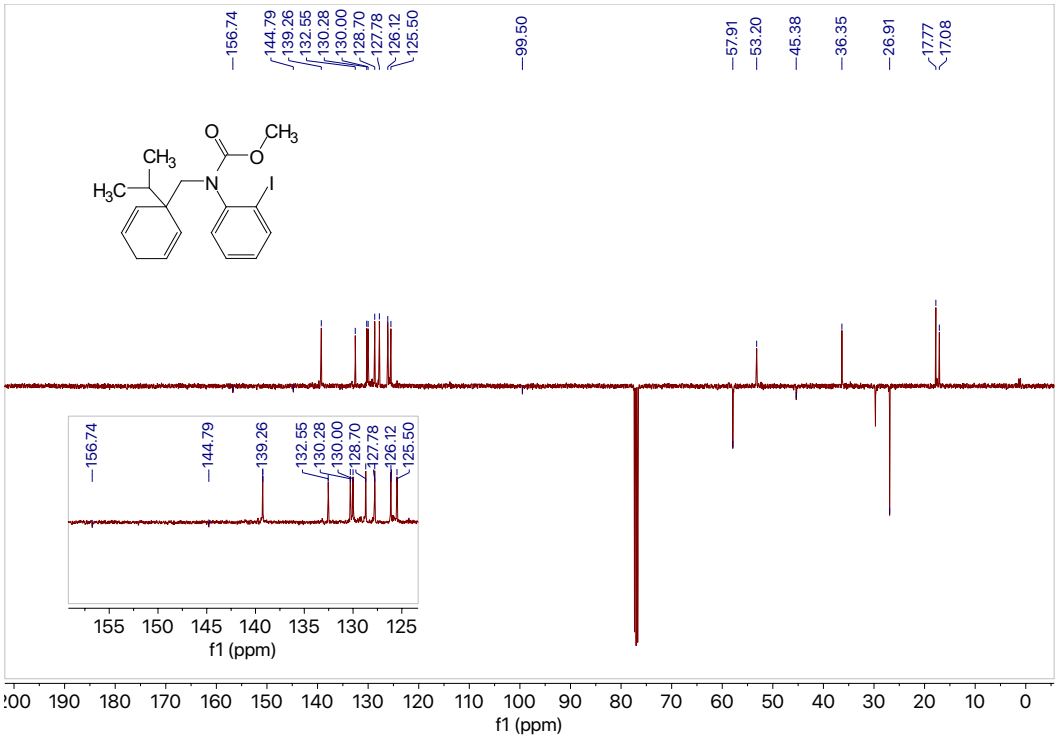

Figure 7.108 ^{13}C NMR (101 MHz, $CDCl_3$) of compound **1ye-I**.

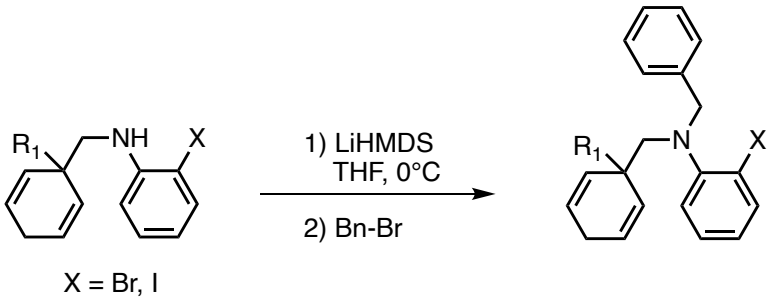

Scheme 7.11 Benzyl amine N protection general reaction.

General procedure B

A flame dried round bottom flask with a stir bar, under argon, was charged with secondary amine (1.0 mmol, 1.0 equiv) in THF (10 mL, 0.1 M) and cooled to 0°C. LiHMDS (1.0 M in hexanes, 1.3 mmol, 1.3 equiv) was added dropwise and the solution was stirred for 10 min. Benzyl bromide (2.0 mmol, 2.0 equiv) was added dropwise to the reaction solution and the reaction was left stirring while slowly warming to r.t. Upon completion, the reaction was quenched with saturated NH_4Cl and diluted with EtOAc. The aqueous layer was extracted with EtOAc (2 x). The combined organic layers were washed with brine, dried with $MgSO_4$, filtered, and concentrated. The crude product was purified by column chromatography.

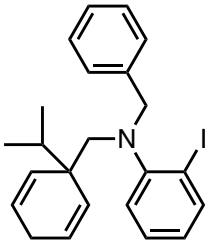

1yf-I

***N*-benzyl-2-iodo-*N*-((1-isopropylcyclohexa-2,5-dien-1-yl)methyl)aniline (1yf-I).** Using the general procedure B for benzyl group protection, secondary amine **S2y-I** (0.0747 g, 0.211 mmol, 1.0 equiv) in THF (2.1 mL, 0.1 M) was benzylated with benzyl bromide (0.072 g, 0.422 mmol, 2.0 equiv). The crude product was purified by column chromatography (silica, 9:1 hexanes: EtOAc) to afford **1yf-I** (0.0725 g, 0.164 mmol) in 77% yield as a clear colorless oil.

^{1}H NMR (400 MHz, $CDCl_3$) δ 7.75 (dd, J = 7.8, 1.5 Hz, 1H), 7.17 – 7.11 (m, 5H), 7.11 (s, 1H), 6.91 (d, J = 7.8 Hz, 1H), 6.71 – 6.63 (m, 1H), 5.67 – 5.55 (m, 2H), 5.30 (d, J = 10.1 Hz, 2H), 4.14 (s, 2H), 3.11 (s, 2H), 2.58 – 2.39 (m, 2H), 1.69 – 1.54 (m, 1H), 0.65 (d, J = 6.8 Hz, 6H).

GC (Method A) t_R = 18.253 min. EI-MS m/z (%): 443.1 (M^+, 1), 322.0 (100), 194.1 (12), 91.0 (81), 79.1 (4), 65.1 (5).

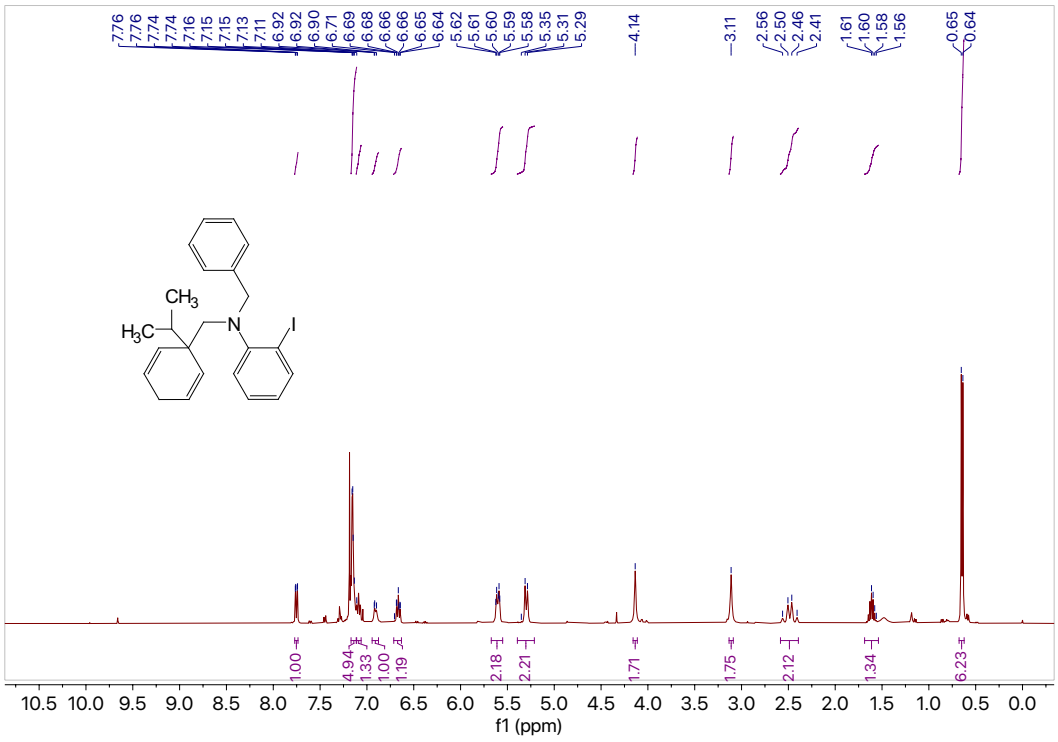

Figure 7.109 ^{13}C NMR (101 MHz, $CDCl_3$) of compound **1yf-I**.

7.9 Ni-catalyzed Mizoroki-Heck general procedure and data

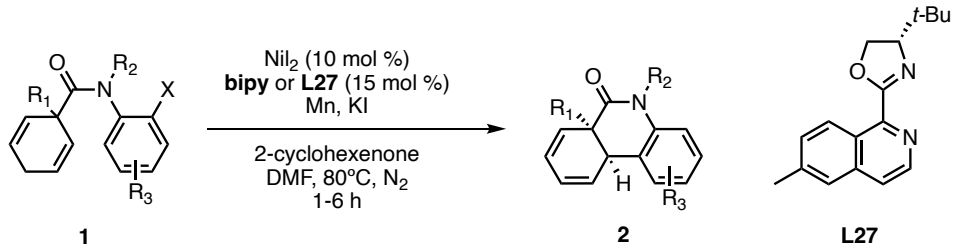

Scheme 7.12 Ni-catalyzed Heck reaction general reaction.

General procedure

A vial with a stir bar was either flame dried under argon or oven-dried, charged with the aryl halide diene (0.1 mmol, 1.0 equiv) and then brought into a glovebox. Anhydrous nickel salt (0.01 mmol, 10 mol %), ligand (bipy or **L27**) (0.015 mmol, 15 mol %) Mn (0.3 mmol, 3.0 equiv), KI (0.1 mmol, 1.0 equiv), 2-cyclohexenone (0.3 mmol, 3.0 equiv), and DMF (1.2 mL, 0.08 M) were added, and the vial was sealed with a pressure relief cap and removed from the glovebox. The vial was stirred at 80˚C in a pie reactor until the reaction was determined to be complete by GC-MS analysis (typically 1-6 h). GC-MS analysis was optimal because the reactant and the product have quite similar thin-layer chromatography properties. Upon completion, the reaction mixture was filtered through an aluminum oxide plug to remove Ni and Mn metals and the plug was washed with EtOAc. The resulting organic solution was washed with 1 N HCl (twice) or water (for pyridine and pyrimidine containing substrates) and brine, dried with $MgSO_4$, and filtered. The crude product was concentrated *in vacuo* and purified by column chromatography.

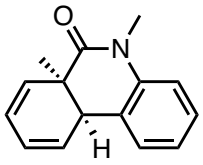

2a

(6aR,10aR)-5,6a-Dimethyl-6a,10a-dihydrophenanthridin-6(5H)-one (2a).

Racemic procedure:

Using the general procedure detailed above, diene bromide **1a** (0.0995 g, 0.327 mmol, 1.0 equiv) in DMF (3.9 mL, 0.08M) or diene iodide **1a-I** (0.101 g, 0.283 mmol, 1.0 equiv) in DMF (3.4 mL, 0.08 M) was subjected to the Heck reaction conditions with 10 mol% NiI_2/15 mol% 2,2'-bipyridine for 1.5 h (**1a**) and 3 h (**1a-I**) respectively. The crude products were purified by column chromatography (silica, 4:1 hexanes: EtOAc) to afford **2a** (0.0626 g, 0.278 mmol) in 85% yield from **1a** or in 98% yield (0.0631 g, 0.280 mmol) from **1a-I** as a yellow oil.

Enantioselective procedure:

Using the general procedure detailed above, diene iodide **1a-I** (0.0449 g, 0.127 mmol, 1.0 equiv) in DMF (1.5 mL, 0.08 M) was subjected to the Heck reaction conditions with 10 mol% NiI_2/15 mol% *t*Bu-^{6}CH$_3$*i*Quinox (**L27**) for 1.5 h. The crude products were purified

by column chromatography (silica, 4:1 hexanes: EtOAc) to afford **2a** (0.0226 g, 0.100 mmol) with an enantiomeric ratio of 10:1 (82% e.e.) in 79% yield as a yellow oil. Spectral data were in accordance with a prior literature report.[10]
$[\alpha]_D^{20}$= +146 (*c* 0.95, $CHCl_3$).
^{1}H NMR (400 MHz, $CDCl_3$) δ 7.30 (td, *J* = 8.0, 1.6 Hz, 1H), 7.23 (dd, *J* = 7.5, 1.6 Hz, 1H), 7.08 (td, *J* = 7.5, 1.1 Hz, 1H), 6.99 (dd, *J* = 8.2, 1.1 Hz, 1H), 6.12 – 6.07 (m, 1H), 6.05 – 5.99 (m, 1H), 5.91 – 5.87 (m, 1H), 5.58 (ddt, *J* = 9.3, 3.0, 1.0 Hz, 1H), 3.52 – 3.45 (m, 1H), 3.35 (s, 3H), 1.23 (s, 3H).
^{13}C NMR (101 MHz, $CDCl_3$) δ_u 131. 8, 128. 6, 127.8, 125.2, 124.2, 123.3, 114.3, 44.3, 29.9, 23.4; δ_d 173.4, 139.0, 126.6, 40.8.
GC (Method B) t_R = 1.940 min. EI-MS m/z (%): 224.1 (M-1$^+$, 79), 210.1 (100), 195.1 (23), 182.1 (28), 167.1 (30), 152.1 (9), 139.0 (5), 128.0 (5), 115.0 (8), 105.0 (4), 90.9 (7), 77.0 (9), 63.0 (6), 51.1 (6).
HPLC: Chiralcel OD-H, n-hexane/isopropanol=97.5:2.5, flow rate=1 mL/min, I=254 nm, t_{R1} =11.39 min. (major), t_{R2} = 12.87 min. (minor).

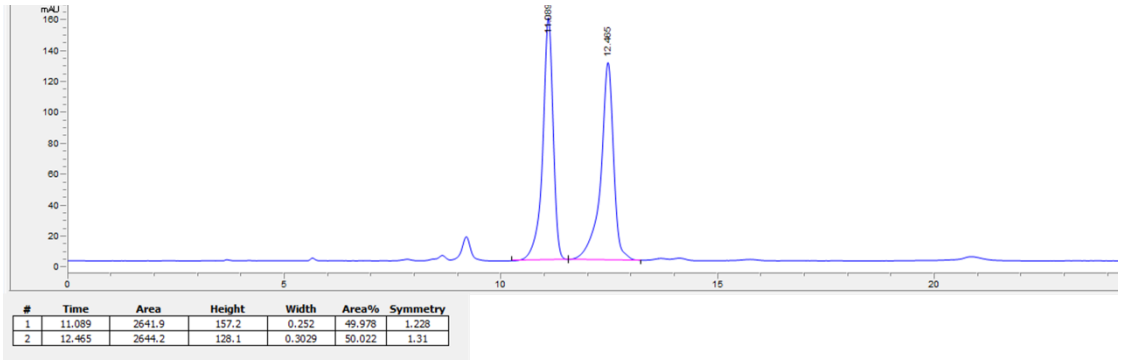

#	Time	Area	Height	Width	Area%	Symmetry
1	11.089	2641.9	157.2	0.252	49.978	1.228
2	12.465	2644.2	128.1	0.3029	50.022	1.31

Figure 7.110 Chiral LC for racemic **2a** sample.

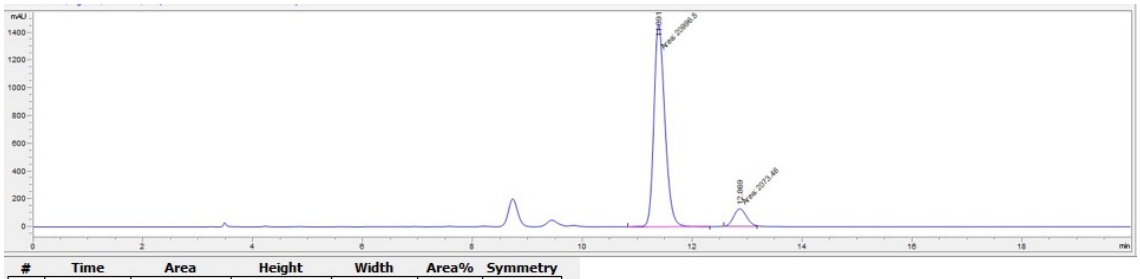

#	Time	Area	Height	Width	Area%	Symmetry
1	11.391	20996.5	1477.7	0.2368	91.012	0.733
2	12.869	2073.5	127.8	0.2704	8.988	0.872

Figure 7.111 Chiral LC for enantioselective **2a** reaction.

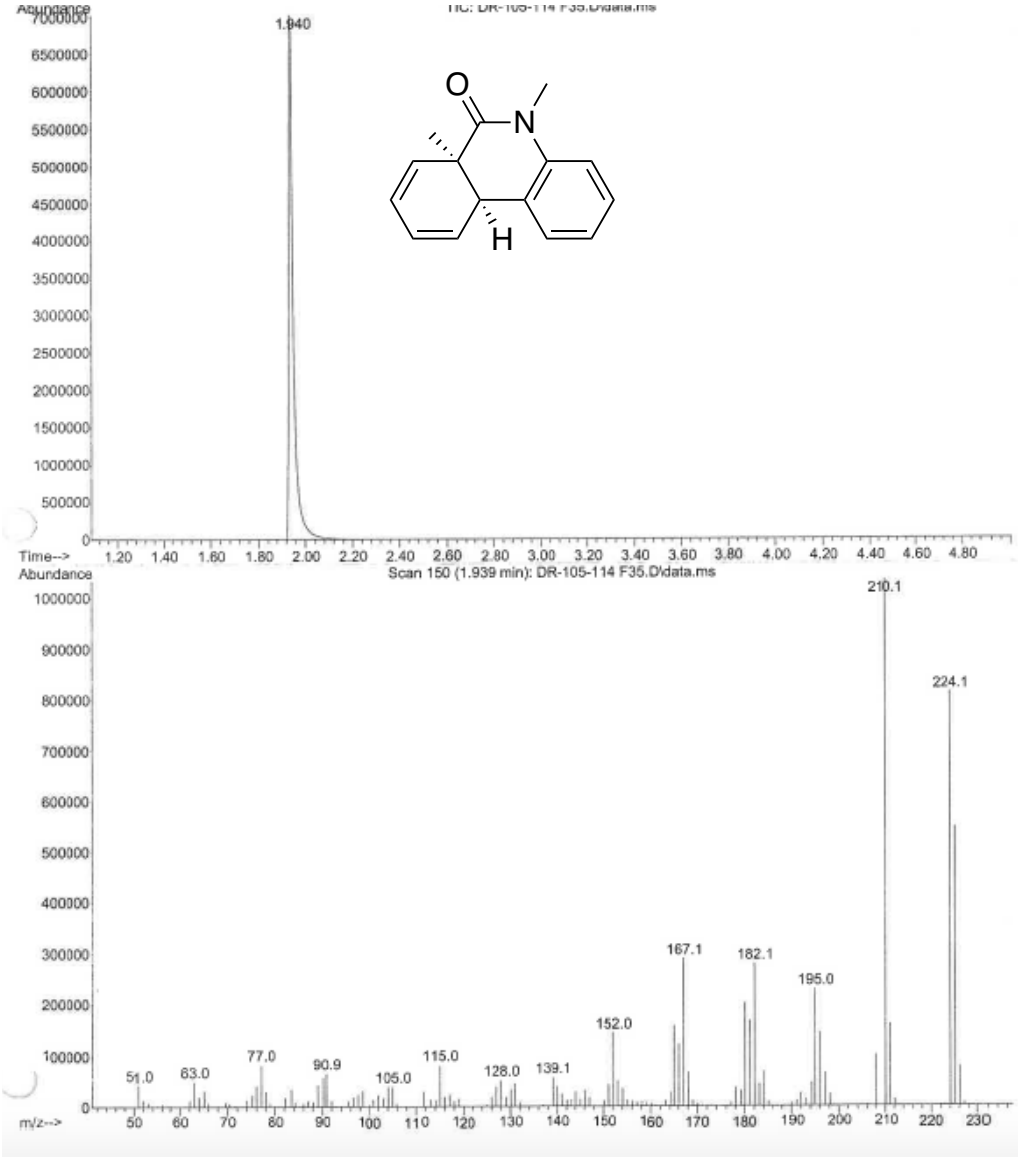

Figure 7.112 GCMS data of compound **2a**.

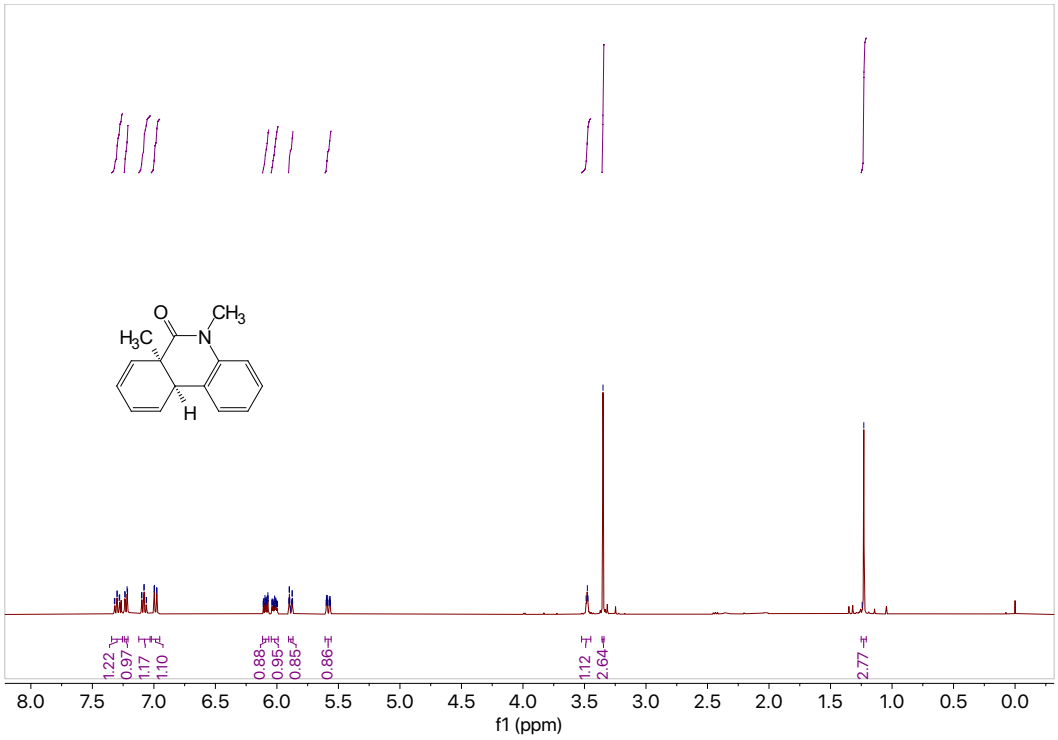

Figure 7.113 ^{1}H NMR (400 MHz, $CDCl_3$) of compound **2a**.

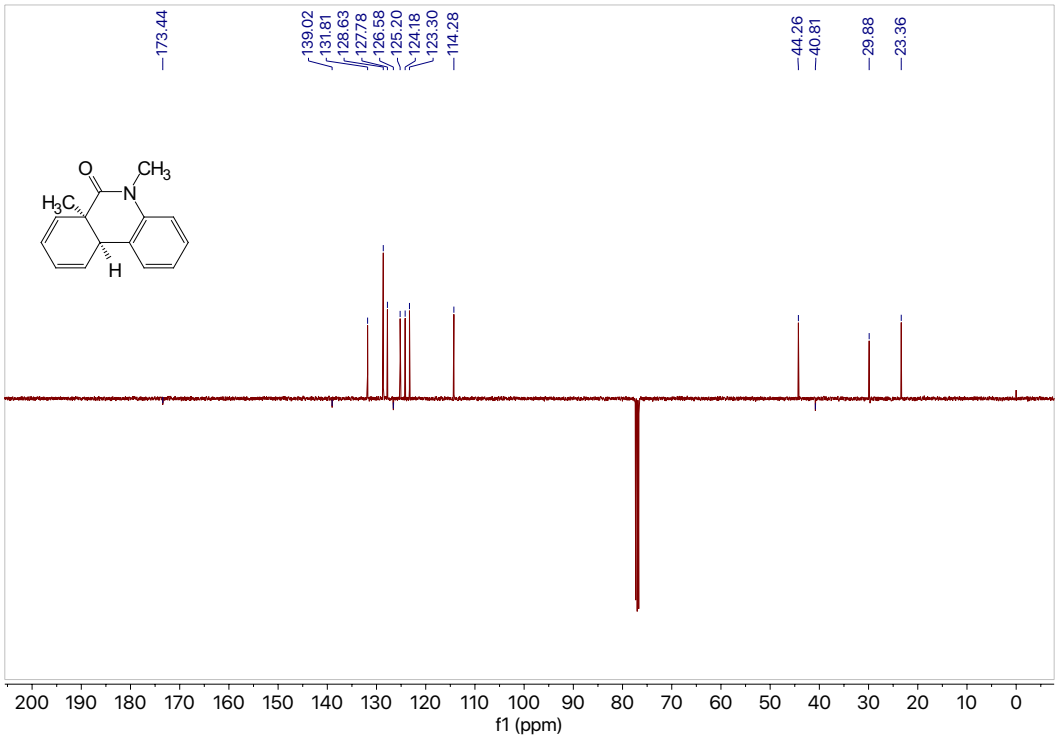

Figure 7.114 ^{13}C NMR (101 MHz, $CDCl_3$) of compound **2a**.

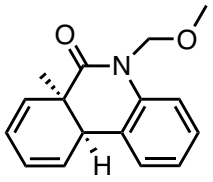

2b

6aR,10aR)-5-(Methoxymethyl)-6a-methyl-6a,10a-dihydrophenanthridin-6(5H)-one (2b).

Racemic procedure:

Using the general procedure detailed above, diene bromide **1b** (0.0797 g, 0.237 mmol, 1.0 equiv) in DMF (2.8 mL, 0.08 M) or diene iodide **1b-I** (0.0404 g, 0.104 mmol, 1.0 equiv) in DMF (1.2 mL, 0.08 M)was subjected to the Heck reaction conditions with 10 mol% NiI_2/15 mol% 2,2'-bipyridine for 2 h (**1b**) and 4 h (**1b-I**) respectively. The crude product was purified by column chromatography (silica, 10:1 hexanes: EtOAc) to afford **2b** (0.0459 g, 0.179 mmol) in 76% yield from **1b** or in 75% yield (0.0201 g, 0.0787 mmol) from **1b-I** as a white solid, m.p.= 136.5-138.3°C.

Enantioselective procedure:

Using the general procedure detailed above, diene iodide **1b-I** (0.0504 g, 0.130 mmol, 1.0 equiv) in DMF (1.6 mL, 0.08 M) was subjected to the Heck reaction conditions with 10 mol% NiI_2/15 mol% *t*Bu-^{6}CH$_3$*i*Quinox (**L27**) for 2.5 h. The crude product was purified by column chromatography (silica, 10:1 hexanes: EtOAc) to afford **2b** (0.0281 g, 0.110 mmol) with an enantiomeric ratio of 10:1 (82% e.e.) in 85% yield as a white solid. Spectral data were in accordance with a prior literature report.[10]

$[\alpha]_D^{20}$= +312 (*c* 0.74, $CHCl_3$).

^{1}H NMR (400 MHz, $CDCl_3$) δ 7.23 – 7.19 (m, 2H), 7.15 (dd, *J* = 7.4, 1.3 Hz, 1H), 7.07 – 7.01 (m, 1H), 6.09 – 6.02 (m, 1H), 5.99 – 5.92 (m, 1H), 5.86 – 5.81 (m, 1H), 5.55 – 5.49 (m, 2H), 5.03 (d, *J* = 10.7 Hz, 1H), 3.46 – 3.39 (m, 1H), 3.27 (s, 3H), 1.21 (s, 3H).

GC (Method B) t_R = 2.128. EI-MS m/z (%): 255.1 (35, M^+), 240.0 (5), 223.0 (23), 210.0 (100), 192.0 (92), 180.0 (43), 165.0 (41), 152.0 (24), 139.0 (5), 128.0 (6), 115.0 (8), 91.0 (10), 77.0 (8).

^{13}C NMR (101 MHz, $CDCl_3$) δ_u 131.6, 128.8, 128.7, 128.0, 125.3, 124.5, 124.0, 115.6, 56.1, 44.5, 23.3. δ_d 174.8, 137.6, 126.3, 73.7, 40.9.

HPLC: Chiralcel OD-H, n-hexane/isopropanol=97.5:2.5, flow rate=1 mL/min, I=254 nm, t_{R1} =9.54 min. (major), t_{R2} = 14.52 min. (minor).

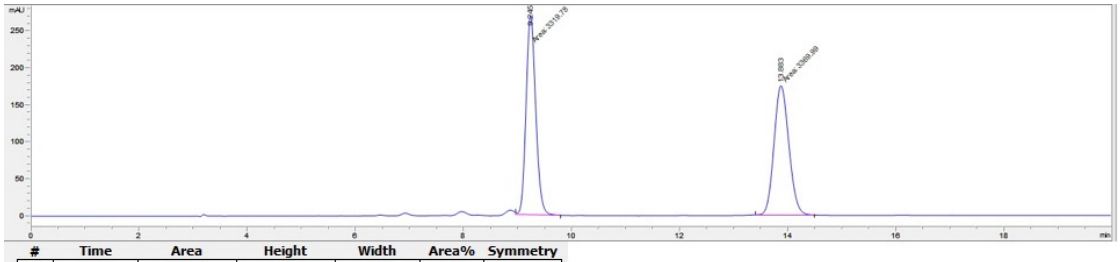

#	Time	Area	Height	Width	Area%	Symmetry
1	9.245	3319.8	268.6	0.206	49.625	0.843
2	13.883	3370	175.1	0.3209	50.375	0.874

Figure 7.115 Chiral LC for racemic **2b** sample.

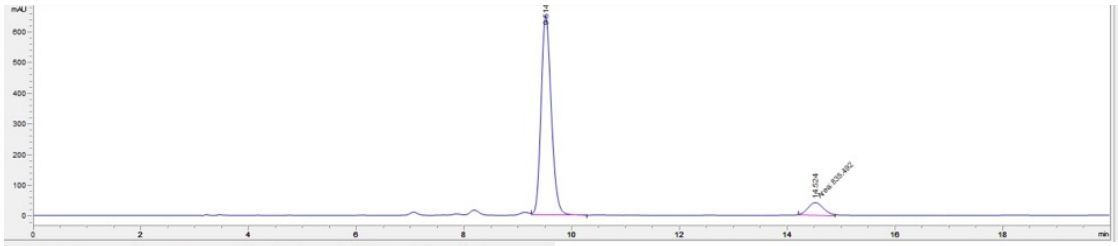

#	Time	Area	Height	Width	Area%	Symmetry
1	9.514	8599.8	651.5	0.204	91.145	0.78
2	14.524	835.5	41.3	0.337	8.855	0.857

Figure 7.116 Chiral LC for enantioselective **2b** reaction.

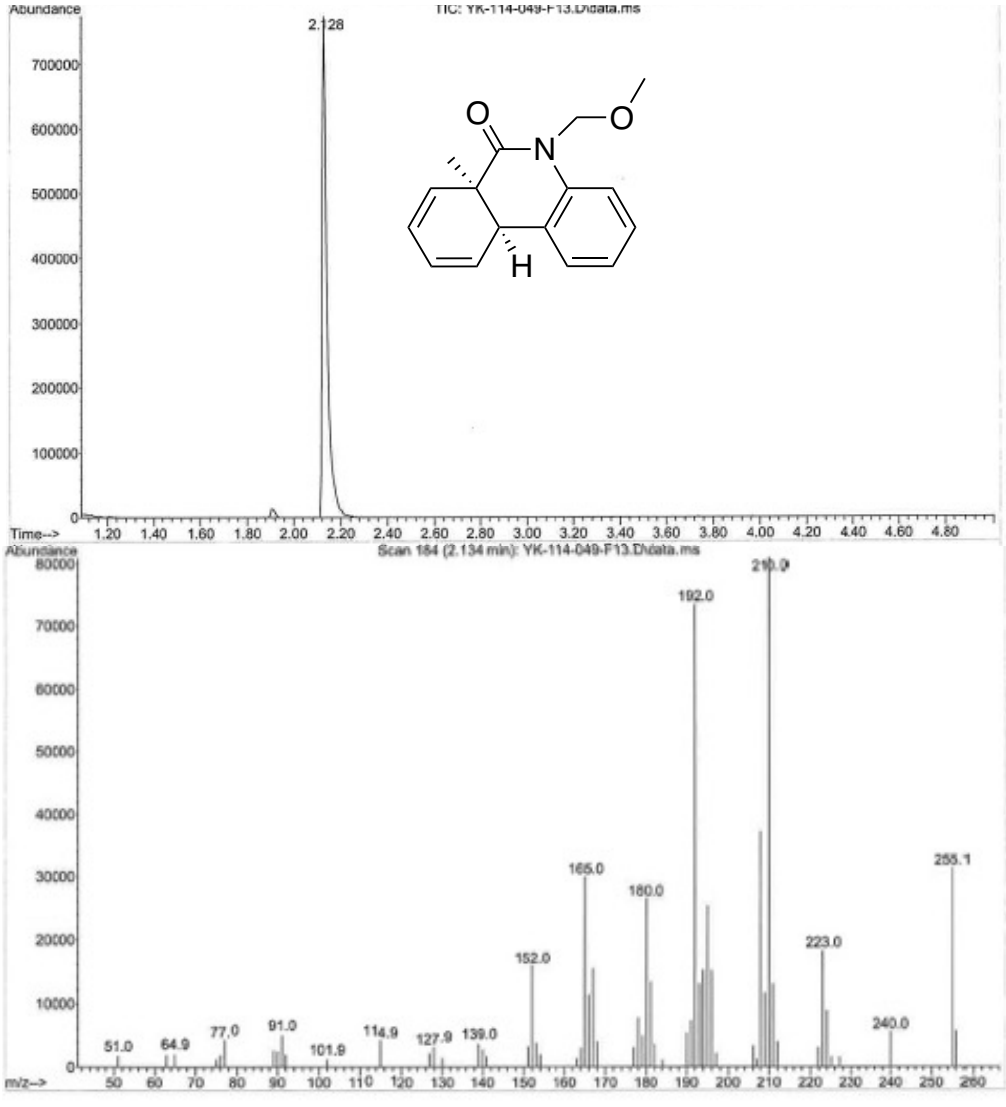

Figure 7.117 GCMS data of compound **2b**.

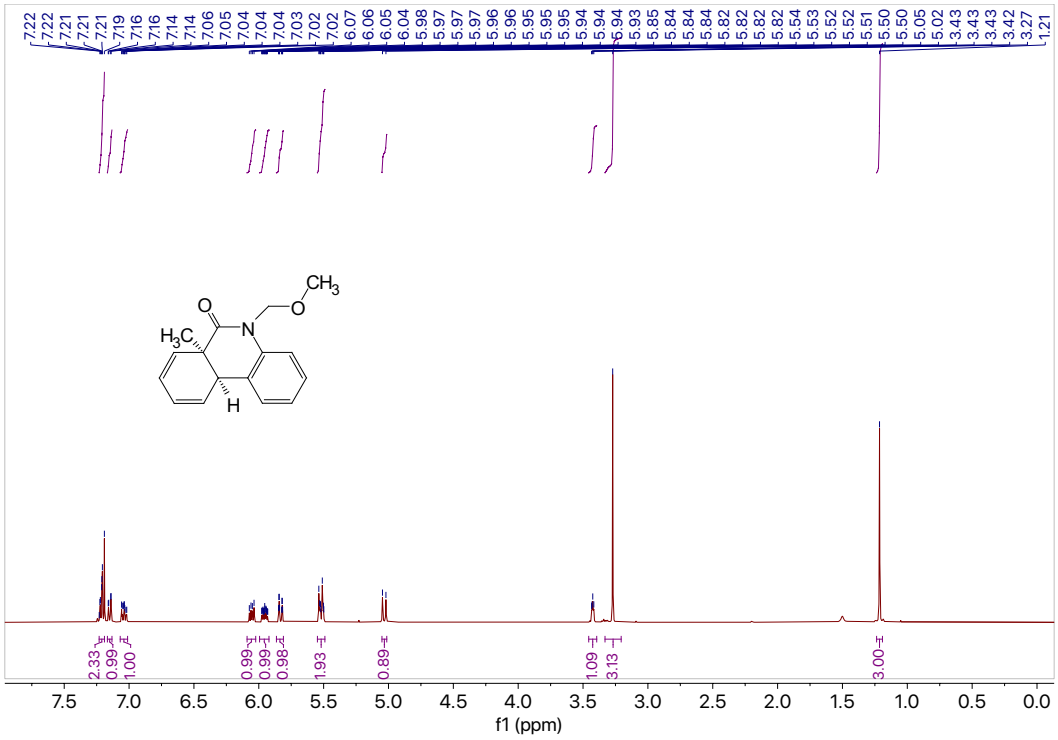

Figure 7.118 ^{1}H NMR (400 MHz, $CDCl_3$) of compound **2b**.

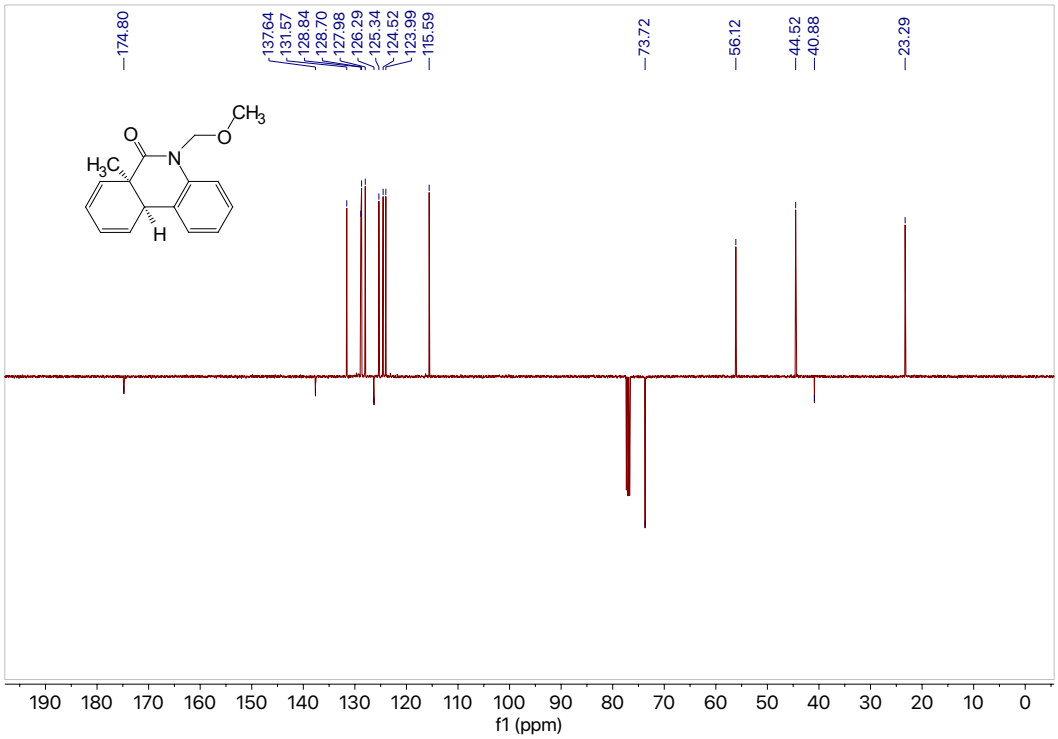

Figure 7.119 ^{13}C NMR (101 MHz, $CDCl_3$) of compound **2b**.

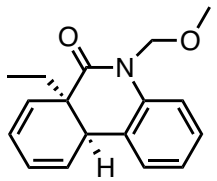

2c

(6aR,10aR)-6a-Ethyl-5-(methoxymethyl)-6a,10a-dihydrophenanthridin-6(5H)-one (2c).

Racemic procedure:

Using the general procedure detailed above, diene iodide **1c-I** (0.135 g, 0.336 mmol, 1.0 equiv) in DMF (4 mL, 0.08 M) was subjected to the Heck reaction conditions with 10 mol% NiI_2/15 mol% 2,2'-bipyridine for 2 h. The crude product was purified by column chromatography (silica, 10:1 hexanes: EtOAc) to afford **2c** (0.0786 g, 0.292 mmol) in 87% yield as a clear colorless oil.

Enantioselective procedure:

Using the general procedure detailed above, diene iodide **1c-I** (0.100 g, 0.252 mmol, 1.0 equiv) in DMF (3 mL, 0.08 M) was subjected to the Heck reaction conditions with 10 mol% NiI_2/15 mol% *t*Bu-$^6CH_3$*i*Quinox (**L27**) for 3 h. The crude product was purified by column chromatography (silica, 10:1 hexanes: EtOAc) to afford **2c** (0.0559 g, 0.208 mmol) with an enantiomeric ratio of 12:1 (84% e.e.) in 82% yield as a clear colorless oil.

1 mmol-scale enantioselective procedure:

Using the general procedure detailed above, diene iodide **1c-I** (0.397 g, 1.0 mmol, 1.0 equiv) in DMF (12 mL, 0.08 M) was subjected to the Heck reaction conditions with 10 mol% NiI_2/15 mol% *t*Bu-$^6CH_3$*i*Quinox (**L27**) for 6 h. The crude product was purified by column chromatography (silica, 10:1 hexanes: EtOAc) to afford **2c** (0.142 g, 0.527 mmol) with an enantiomeric ratio of 9:1 (80% e.e.) in 53% yield as a clear colorless oil. Spectral data were in accordance with a prior literature report.[10]

$[\boldsymbol{\alpha}]_{\boldsymbol{D}}^{\boldsymbol{20}}$**=** +157 (*c* 0.35, $CHCl_3$).

^{1}H NMR (400 MHz, $CDCl_3$) δ 7.31 – 7.24 (m, 2H), 7.21 (d, 1H), 7.10 (td, *J* = 6.9, 2.0 Hz, 1H), 6.22 – 6.14 (m, 1H), 6.04 – 5.99 (m, 1H), 5.95 (d, *J* = 9.1 Hz, 1H), 5.63 (d, *J* = 10.6 Hz, 1H), 5.55 (dd, *J* = 9.4, 2.5 Hz, 1H), 5.05 (d, *J* = 10.6 Hz, 1H), 3.70 – 3.64 (m, 1H), 3.34 (s, 3H), 1.75 – 1.64 (m, 1H), 1.59 – 1.46 (m, 1H), 0.91 (t, *J* = 7.4 Hz, 3H).

^{13}C NMR (101 MHz, $CDCl_3$) δ_u 129.8, 128.9, 128.6, 128.0, 125.2, 125.2, 124.0, 115.5, 56.2, 41.3, 9.1; δ_d 174.4, 137.8, 126.2, 73.8, 45.2, 27.9.

GC (Method B) t_R = 2.380. EI-MS m/z (%): 269.1 (36, M^+), 237.0 (28), 224.0 (100), 208.0 (91), 196.0 (64), 178.0 (82), 167.0 (28), 152.0 (26), 139.0 (5), 115.0 (5), 91.0 (8), 77.0 (8).

HPLC: Chiralcel OD-H, n-hexane/isopropanol=97.5:2.5, flow rate=1 mL/min, I=254 nm, t_{R1} =8.27 min. (major), t_{R2} = 14.30 min. (minor).

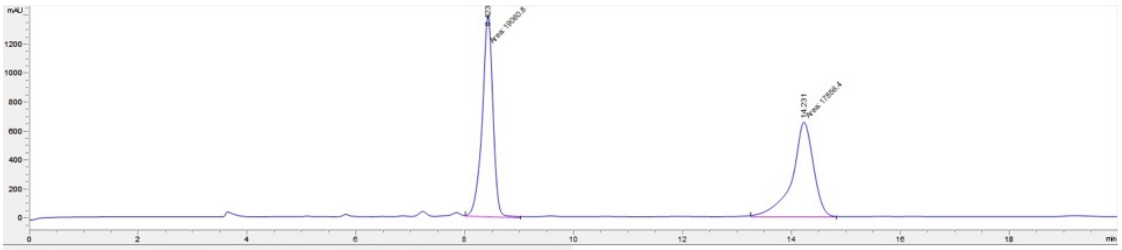

#	Time	Area	Height	Width	Area%	Symmetry
1	8.423	19060.8	1384	0.2295	51.631	1.13
2	14.231	17856.4	653.2	0.4556	48.369	1.25

Figure 7.120 Chiral LC for racemic **2c** sample.

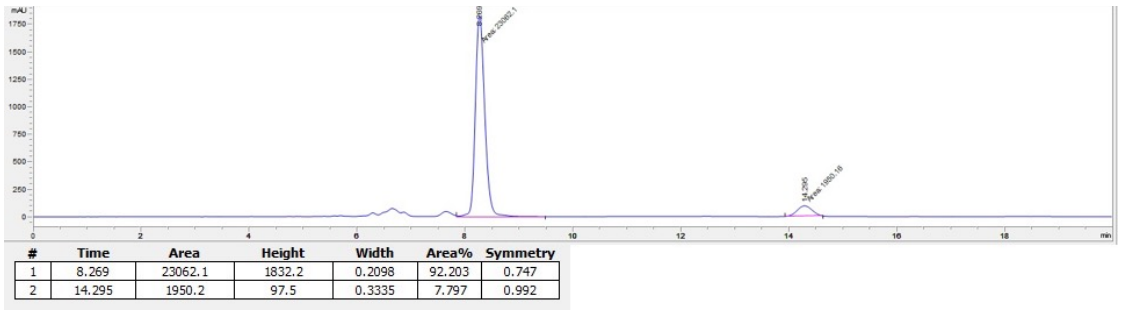

#	Time	Area	Height	Width	Area%	Symmetry
1	8.269	23062.1	1832.2	0.2098	92.203	0.747
2	14.295	1950.2	97.5	0.3335	7.797	0.992

Figure 7.121 Chiral LC for enantioselective **2c** reaction.

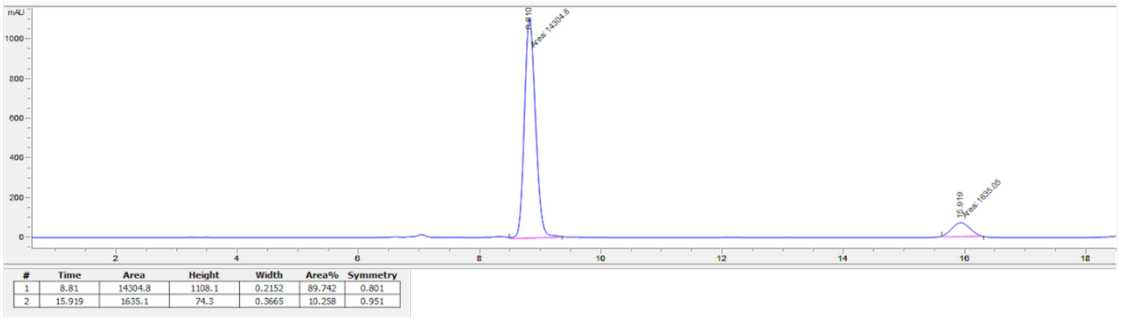

#	Time	Area	Height	Width	Area%	Symmetry
1	8.81	14304.8	1108.1	0.2152	89.742	0.801
2	15.919	1635.1	74.3	0.3665	10.258	0.951

Figure 7.122 Chiral LC for enantioselective 1mmol-scale **2c** reaction.

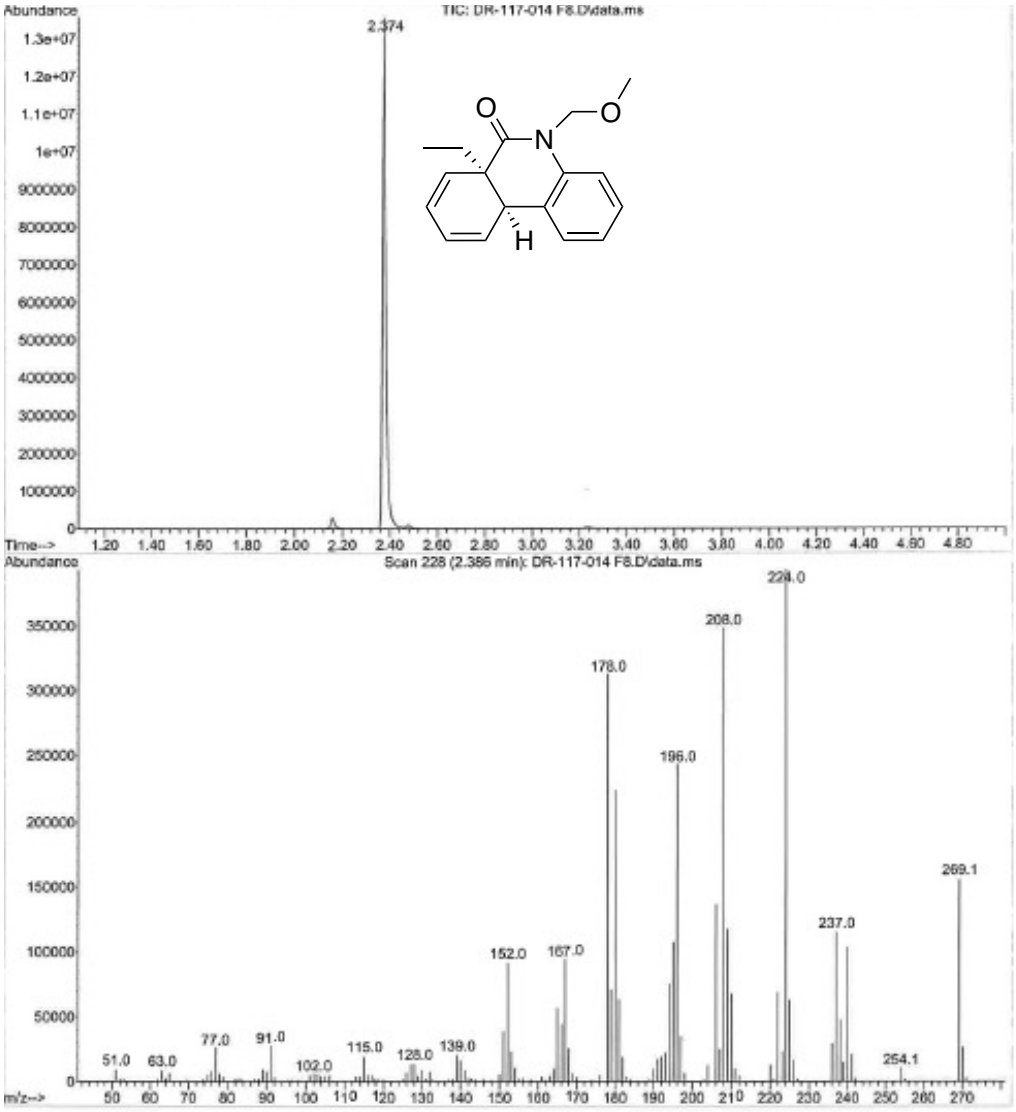

Figure 7.123 GCMS data of compound **2c**.

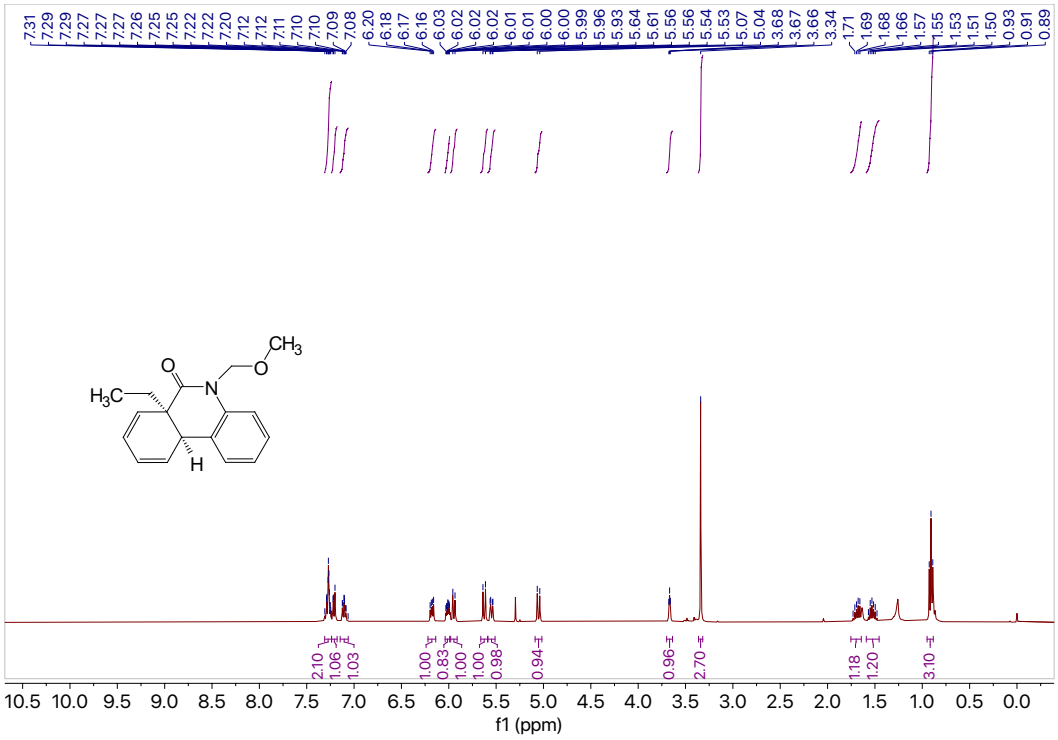

Figure 7.124 ^{1}H NMR (400 MHz, $CDCl_3$) of compound **2c**.

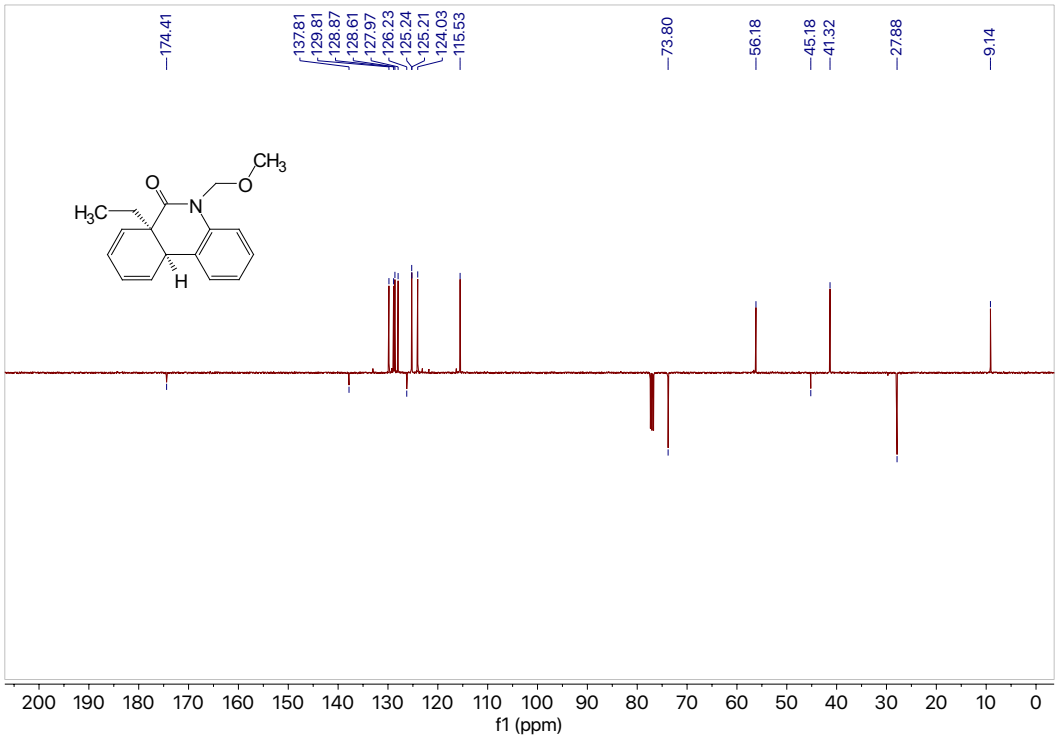

Figure 7.125 ^{13}C NMR (101 MHz, $CDCl_3$) of compound **2c**.

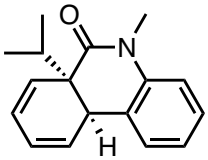

2d

(6aR,10aR)-6a-Isopropyl-5-methyl-6a,10a-dihydrophenanthridin-6(5H)-one (2d).

Racemic procedure:

Using the general procedure detailed above, diene bromide **1d** (0.0954 g, 0.285 mmol, 1.0 equiv) in DMF (3.4 mL, 0.08M) or diene iodide **1d-I** (0.0993 g, 0.262 mmol, 1.0 equiv) in DMF (3.1 mL, 0.08 M) was subjected to the Heck reaction conditions with 10 mol% NiI_2/15 mol% 2,2'-bipyridine for 1.5 h (**1d**) and 3 h (**1d-I**) respectively. The crude products were purified by column chromatography (silica, 10:1 hexanes: EtOAc) to afford **2d** (0.0613 g, 0.242 mmol) in 85% yield from **1d** or in 90% yield (0.0595 g, 0.235 mmol) from **1d-I** as a clear colorless oil.

Enantioselective procedure:

Using the general procedure detailed above, diene iodide **1d-I** (0.0499 g, 0.131 mmol, 1.0 equiv) in DMF (1.6 mL, 0.08 M) was subjected to the Heck reaction conditions with 10 mol% NiI_2/15 mol% *t*Bu-$^6CH_3$*i*Quinox (**L27**) for 2.5 h. The crude product was purified by column chromatography (silica, 10:1 hexanes: EtOAc) to afford **2d** (0.0273 g, 0.108 mmol) with an enantiomeric ratio of 9:1 (79% e.e.) in 83% yield as a clear colorless oil. Spectral data were in accordance with a prior literature report.[10]

$[\boldsymbol{\alpha}]_{\boldsymbol{D}}^{\boldsymbol{20}}$= +270 (*c* 0.5, $CHCl_3$).

^{1}H NMR (400 MHz, $CDCl_3$) δ 7.23 (ddd, *J* = 8.1, 7.5, 1.6 Hz, 1H), 7.13 (dd, *J* = 7.3, 1.6 Hz, 1H), 7.00 (td, *J* = 7.4, 1.1 Hz, 1H), 6.90 (dd, *J* = 8.2, 1.1 Hz, 1H), 6.17 – 6.08 (m, 1H), 6.00 – 5.86 (m, 2H), 5.48 – 5.40 (m, 1H), 3.74 (s, 1H), 3.29 (s, 3H), 1.73 – 1.58 (m, 1H), 0.86 (d, *J* = 6.9 Hz, 3H), 0.74 (d, *J* = 6.8 Hz, 3H).

^{13}C NMR (101 MHz, $CDCl_3$) δ_u 129.2, 128.5, 127.8, 127.2, 125.4, 125.2, 123.3, 114.2, 41.09, 29.9, 29.8, 18.5, 18.0; δ_d 172.6, 139.3, 126.9, 48.5.

GC (Method B) t_R = 2.294. EI-MS m/z (%): 253.1 (12, M^+), 210.1 (100), 195.0 (23), 180.0 (7), 167.0 (10), 152.0 (7).

HPLC: Chiralcel OD-H, n-hexane/isopropanol=97.5:2.5, flow rate=1 mL/min, I=254 nm, t_{R1} =9.96 min. (major), t_{R2} = 11.76 min. (minor).

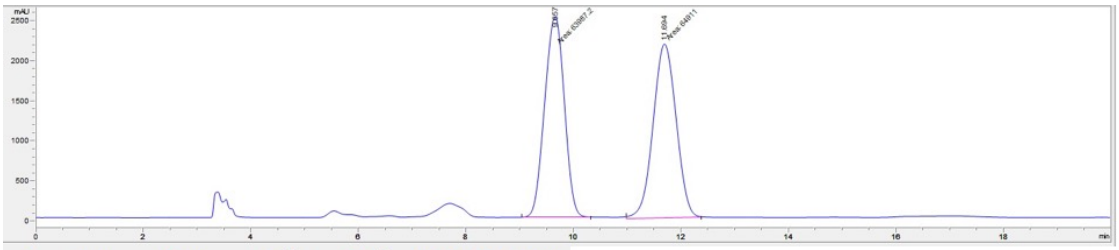

#	Time	Area	Height	Width	Area%	Symmetry
1	9.657	63987.2	2496.4	0.4272	49.642	1.083
2	11.694	64911	2165.8	0.4995	50.358	0.965

Figure 7.126 Chiral LC for racemic **2d** sample.

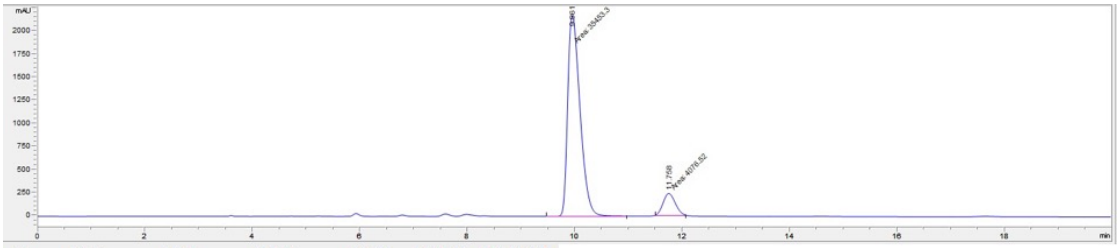

#	Time	Area	Height	Width	Area%	Symmetry
1	9.961	35453.3	2170	0.2723	89.687	0.572
2	11.758	4076.5	246.4	0.2757	10.313	0.845

Figure 7.127 Chiral LC for enantioselective **2d** reaction.

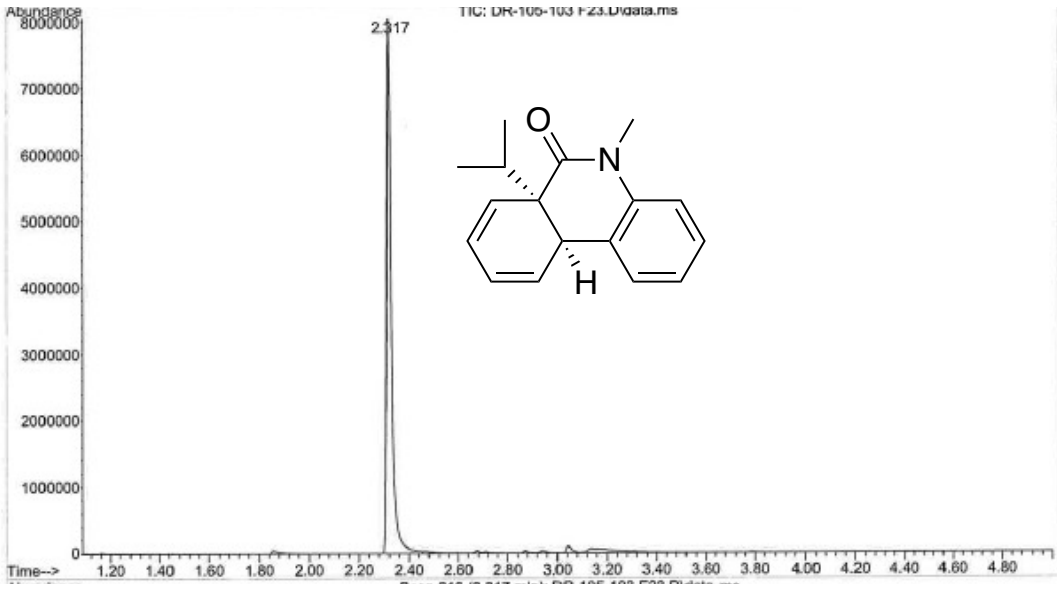

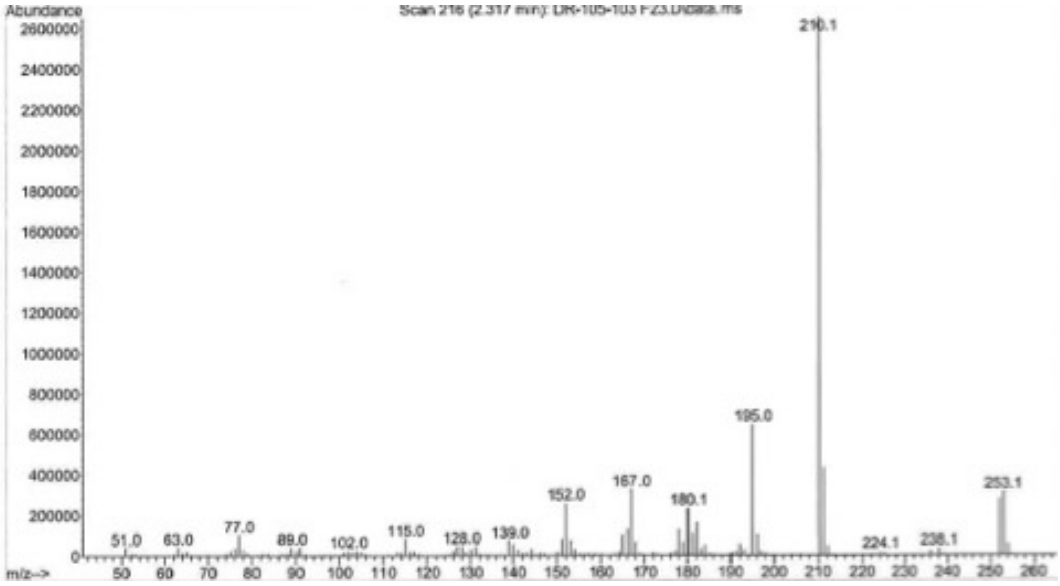

Figure 7.128 GCMS data of compound **2d**.

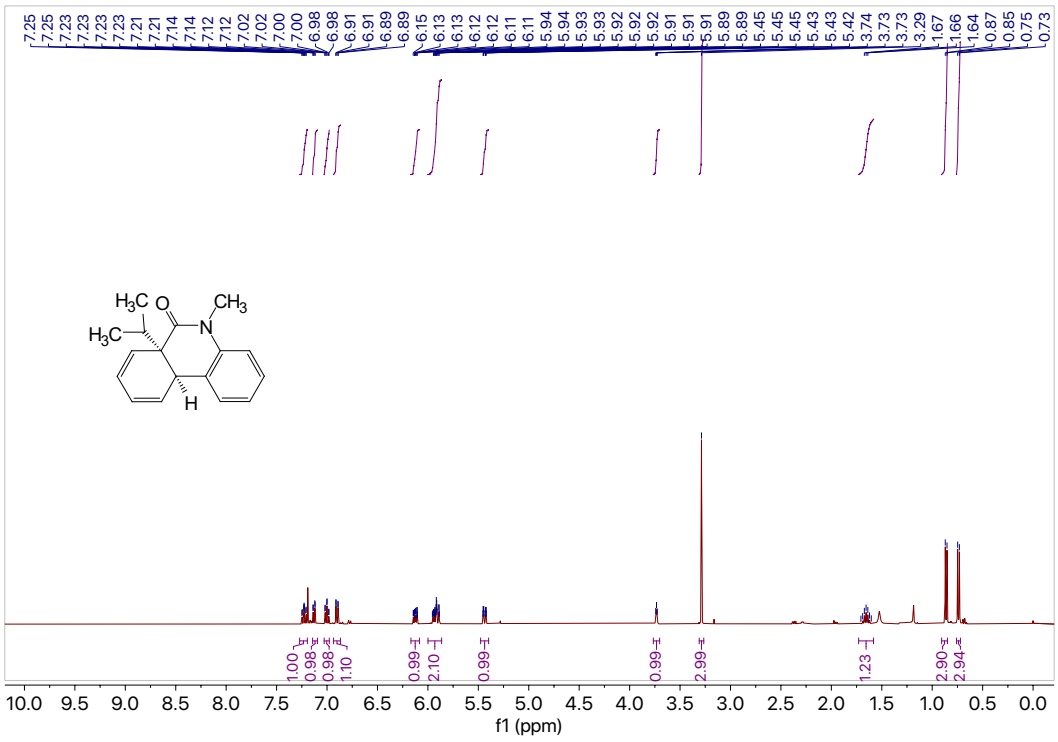

Figure 7.129 ^{1}H NMR (400 MHz, $CDCl_3$) of compound **2d**.

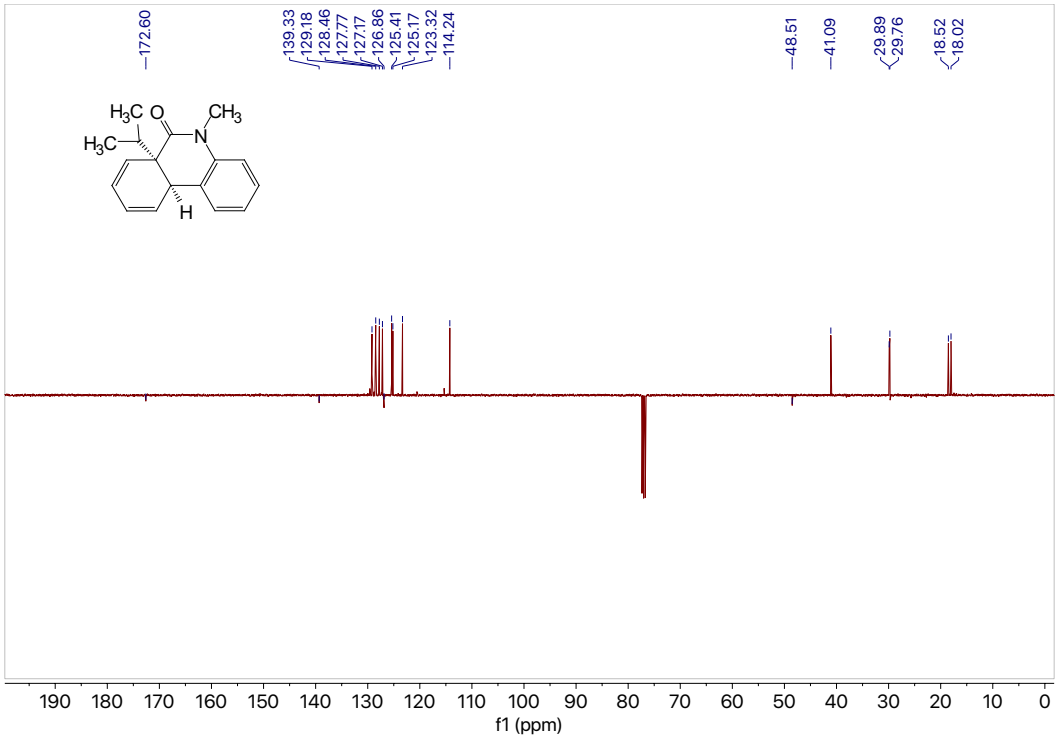

Figure 7.130 ^{13}C NMR (101 MHz, $CDCl_3$) of compound **2d**.

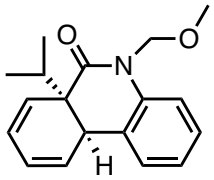

2e

(6aR,10aR)-6a-Isopropyl-5-(methoxymethyl)-6a,10a-dihydrophenanthridin-6(5H)-one (2e).

Racemic procedure:

Using the general procedure detailed above, diene bromide **1e** (0.0988 g, 0.275 mmol, 1.0 equiv) in DMF (3.3 mL, 0.08 M) or diene iodide **1e-I** (0.103 g, 0.243 mmol, 1.0 equiv) in DMF (2.9 mL, 0.08 M) was subjected to the Heck reaction conditions with 10 mol% NiI_2/15 mol% 2,2'-bipyridine for 2 h (**1e**) and 2.5 h (**1e-I**) respectively. The crude products were purified by column chromatography (silica, 10:1 hexanes: EtOAc) to afford **2e** (0.0708 g, 0.24 mmol) in 90% yield from **1e** or in 91% yield (0.0625 g, 0.221 mmol) from **1e-I** as a white solid, m.p.= 104.4 – 106.5°C.

Chiral procedure:

Using the general procedure detailed above, diene iodide **1e-I** (0.103 g, 0.243 mmol, 1.0 equiv) in DMF (2.9 mL, 0.08 M) was subjected to the Heck reaction conditions with 10 mol% NiI_2/15 mol% *t*Bu-^{6}CH$_3$*i*Quinox (**L27**) for 3 h. The crude product was purified by column chromatography (silica, 10:1 hexanes: EtOAc) to afford **2e** (0.0460 g, 0.162

mmol) with an enantiomeric ratio of 11:1 (84% e.e.) in 67% yield as a tan oil that solidified to white crystals on cooling.
$[\alpha]_D^{20}$= +160 (*c* 0.65, $CHCl_3$).
^{1}H NMR (400 MHz, $CDCl_3$) δ 7.32 – 7.22 (m, 2H), 7.19 (dd, *J* = 7.4, 1.5 Hz, 1H), 7.10 (td, *J* = 7.2, 1.8 Hz, 1H), 6.22 (ddd, *J* = 9.6, 5.2, 1.0 Hz, 1H), 6.07 – 5.95 (m, 2H), 5.66 (d, *J* = 10.6 Hz, 1H), 5.53 (ddt, *J* = 9.3, 2.2, 1.0 Hz, 1H), 5.02 (d, *J* = 10.5 Hz, 1H), 3.81 (t, *J* = 3.2 Hz, 1H), 3.36 (s, 3H), 1.79 (hept, *J* = 6.9 Hz, 1H), 0.98 (d, *J* = 6.9 Hz, 3H), 0.84 (d, *J* = 6.8 Hz, 3H).
^{13}C NMR (101 MHz, $CDCl_3$) δ_u 129.2, 128.4, 128.0, 126.7, 125.8, 125.4, 124.0, 115.5, 74.1, 56.3, 48.7, 41.3, 40.7, 29.3, 18.5, 17.7; δ_d 173.8, 138.2, 126.6, 74.1, 48.7.
GC (Method B) t_R = 2.560 min. EI-MS m/z (%): 283.1 (M^+, 17), 251.0 (12), 240.0 (17), 224 (10), 208.0 (100), 196.0 (99), 178 (67), 167 (14), 152.0 (17), 139 (4), 115.0 (4), 105.0 (4), 77.0 (5).
HRMS (ESI) calculated for $C_{18}H_{22}O_2N$ $[M+H]^+$: 284.1651, found 284.1646.
HPLC: Chiralcel OD-H, n-hexane/isopropanol=97.5:2.5, flow rate=1 mL/min, I=254 nm, t_{R1} = 7.80 min. (major), t_{R2} = 13.46 min. (minor).

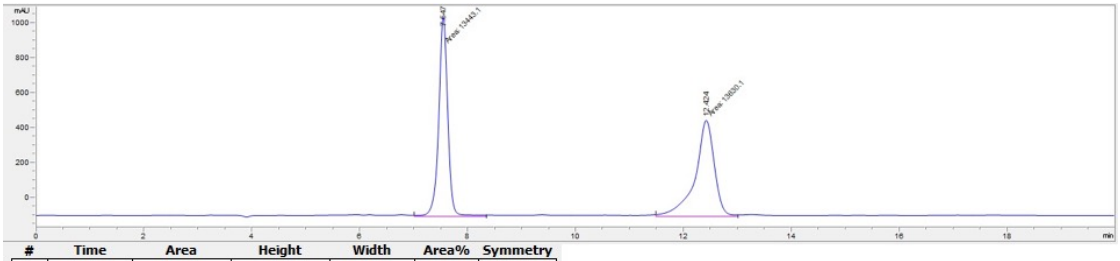

#	Time	Area	Height	Width	Area%	Symmetry
1	7.547	13443.1	1141.5	0.1963	49.655	0.994
2	12.424	13630.1	549.3	0.4136	50.345	1.357

Figure 7.131 Chiral LC for racemic **2e** sample.

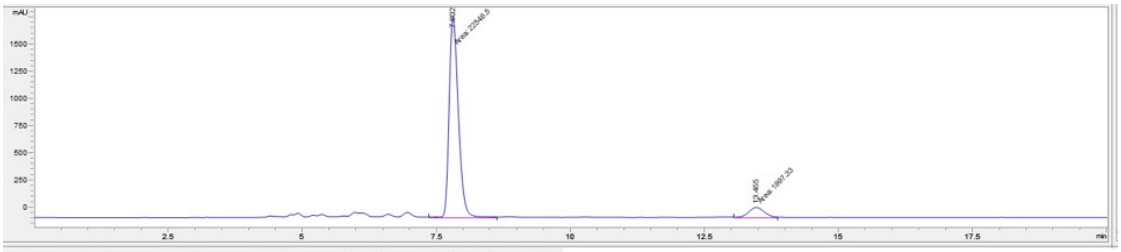

#	Time	Area	Height	Width	Area%	Symmetry
1	7.802	22546.5	1837.9	0.2045	91.862	0.671
2	13.455	1997.3	94.7	0.3517	8.138	0.913

Figure 7.132 Chiral LC for enantioselective **2e** reaction (at 80 ˚C).

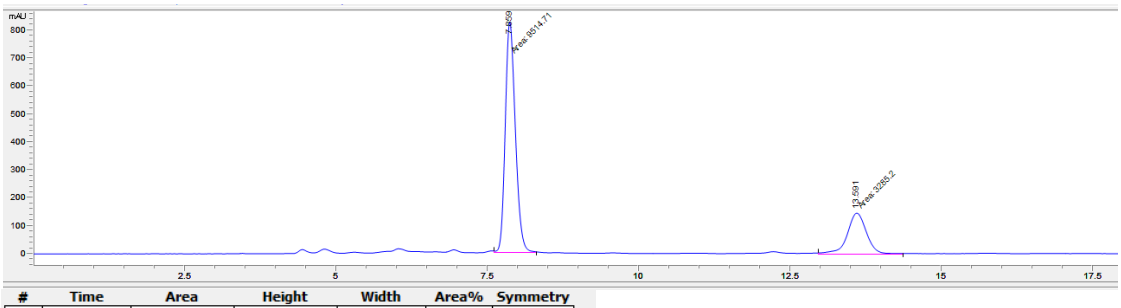

#	Time	Area	Height	Width	Area%	Symmetry
1	7.859	9514.7	821.5	0.193	74.334	0.776
2	13.591	3285.2	146.5	0.3737	25.666	0.969

Figure 7.133 Chiral LC for enantioselective **2e** reaction (at 60 ˚C).

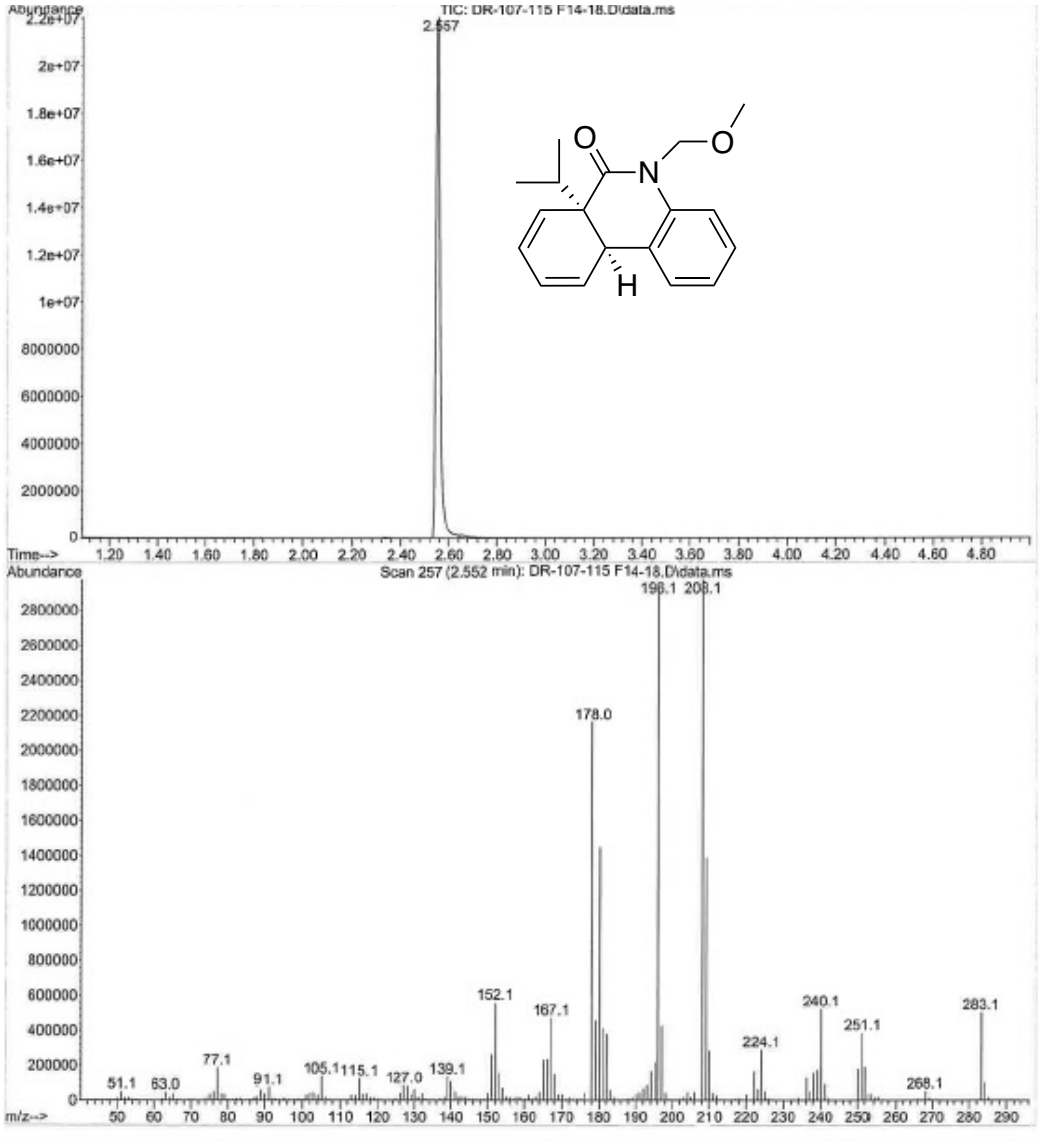

Figure 7.134 GCMS data of compound **2e**.

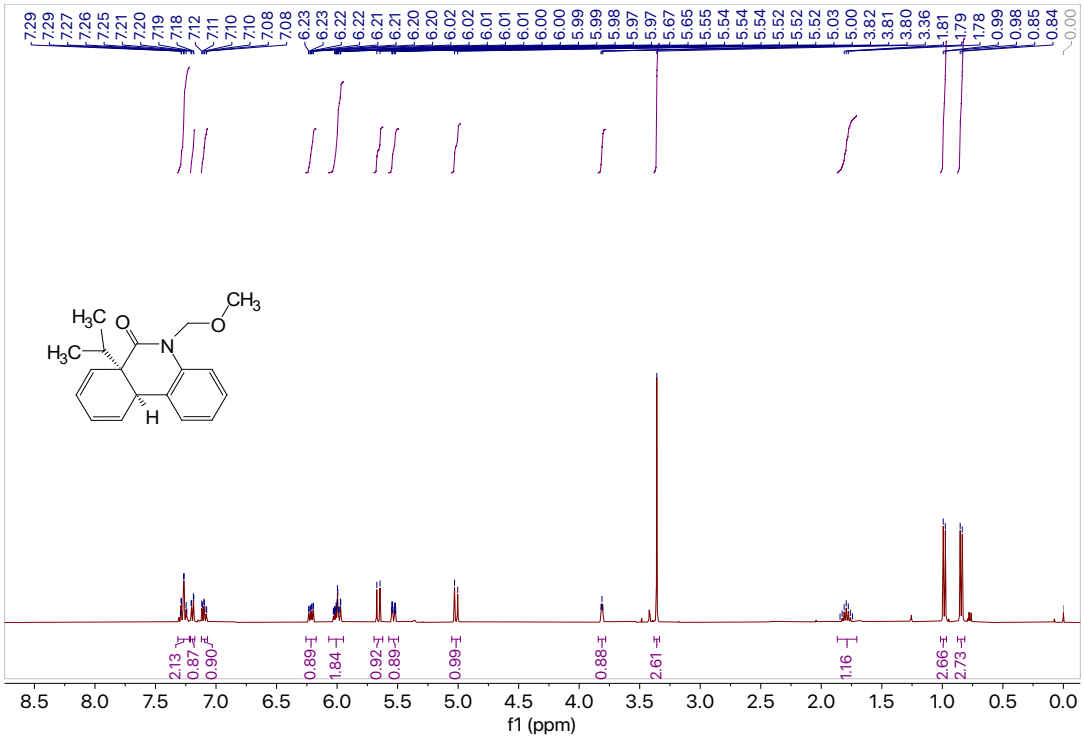

Figure 7.135 ^{1}H NMR (400 MHz, $CDCl_3$) of compound **2e**.

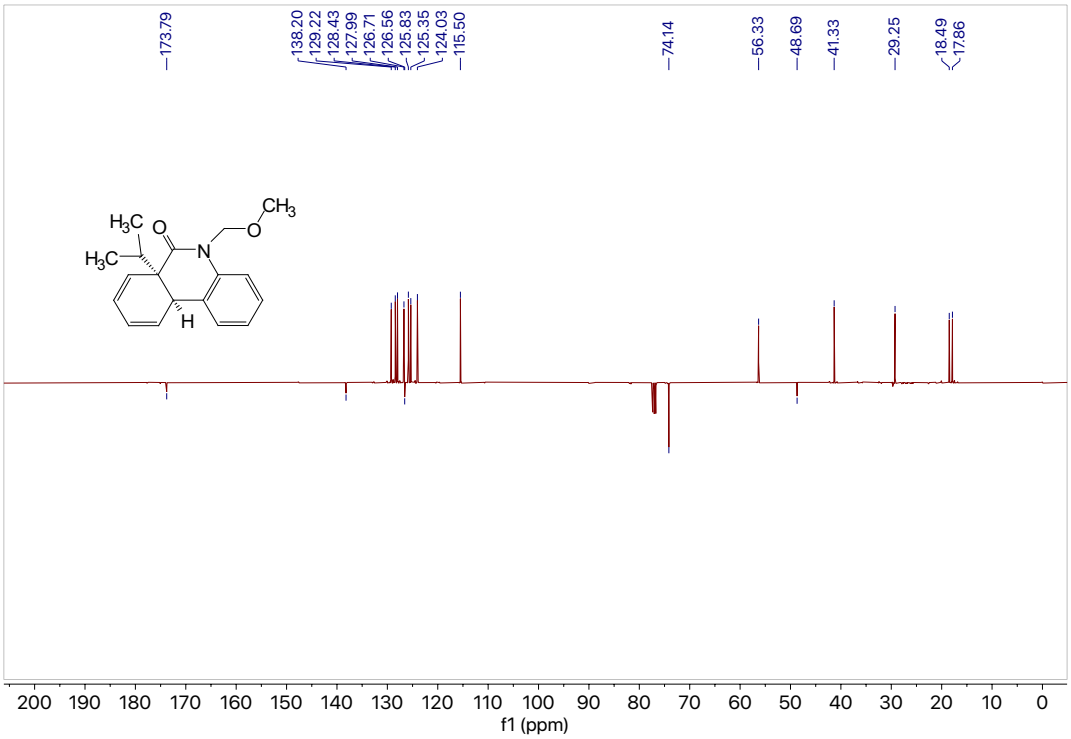

Figure 7.136 ^{13}C NMR (101 MHz, $CDCl_3$) of compound **2e**.

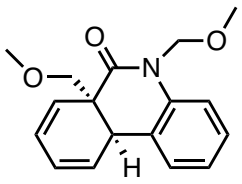

2f

(6aR,10aR)-5,6a-Bis(methoxymethyl)-6a,10a-dihydrophenanthridin-6(5H)-one (2f).

Racemic procedure:

Using the general procedure detailed above, diene iodide **1f-I** (0.100 g, 0.242 mmol, 1.0 equiv) in DMF (2.9 mL, 0.08 M) was subjected to the Heck reaction conditions with 10 mol% NiI_2/15 mol% 2,2'-bipyridine for 3 h. The crude product was purified by column chromatography (silica, 7:1 hexanes: EtOAc) to afford **2f** (0.0630 g, 0.221 mmol) in 91% yield as a yellow oil.

Enantioselective procedure:

Using the general procedure detailed above, diene iodide **1f-I** (0.0500 g, 0.121 mmol, 1.0 equiv) in DMF (1.5 mL, 0.08 M) was subjected to the Heck reaction conditions with 10 mol% NiI_2/15 mol% *t*Bu-$^6CH_3$*i*Quinox (**L27**) for 4 h. The crude product was purified by column chromatography (silica, 7:1 hexanes: EtOAc) to afford **2f** (0.0313 g, 0.110 mmol) with an enantiomeric ratio of 12:1 (85% e.e.) in 91% yield as a yellow oil.

$[\alpha]_D^{20}$= +126 (*c* 0.21, $CHCl_3$).

^{1}H NMR (400 MHz, $CDCl_3$) δ 7.22 – 7.18 (m, 2H), 7.18 – 7.14 (m, 1H), 7.06 – 7.00 (m, 1H), 6.12 – 6.04 (m, 1H), 6.02 – 5.92 (m, 1H), 5.86 – 5.79 (m, 1H), 5.71 – 5.63 (m, 1H), 5.40 (d, *J* = 10.6 Hz, 1H), 5.17 (d, *J* = 10.6 Hz, 1H), 3.88 – 3.82 (m, 1H), 3.46 – 3.36 (m, 2H), 3.29 (s, 3H), 3.23 (s, 3H).

^{13}C NMR (101 MHz, $CDCl_3$) δ_u 128.2, 127.9, 127.9, 127.5, 125.8, 124.8, 124.0, 115.5, 59.5, 56.2, 37.6; δ_d 171.9, 137.8, 125.8, 74.1, 73.5, 47.1.

GC (Method B) t_R = 2.597 min. EI-MS m/z (%): 285.1 (M^+, 1), 240.0 (5), 221.0 (5), 209.0 (100), 195.0 (11), 180.0 (45), 165.0 (10), 152.0 (10).

HRMS (ESI) calculated for $C_{17}H_{20}O_3N$ $[M+H]^+$: 286.1443, found 286.1442.

HPLC: Chiralcel OD-H, n-hexane/isopropanol=97.5:2.5, flow rate=1 mL/min, I=254 nm, t_{R1} =18.33 min. (major), t_{R2} = 24.17 min. (minor).

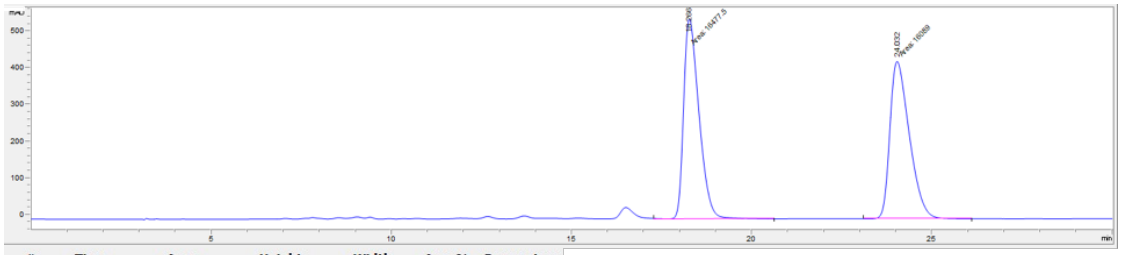

#	Time	Area	Height	Width	Area%	Symmetry
1	18.266	16477.5	547.6	0.5015	50.596	0.576
2	24.032	16089	429.5	0.6244	49.404	0.579

Figure 7.137 Chiral LC for racemic **2f** sample.

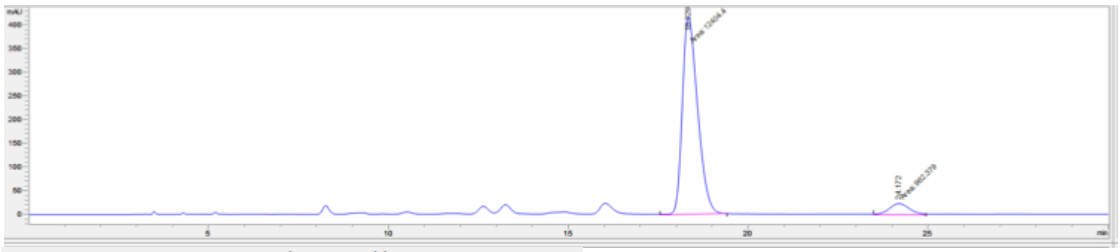

#	Time	Area	Height	Width	Area%	Symmetry
1	18.329	12404.4	416.4	0.4965	92.800	0.638
2	24.172	962.4	24	0.6672	7.200	0.861

Figure 7.138 Chiral LC for enantioselective **2f** reaction.

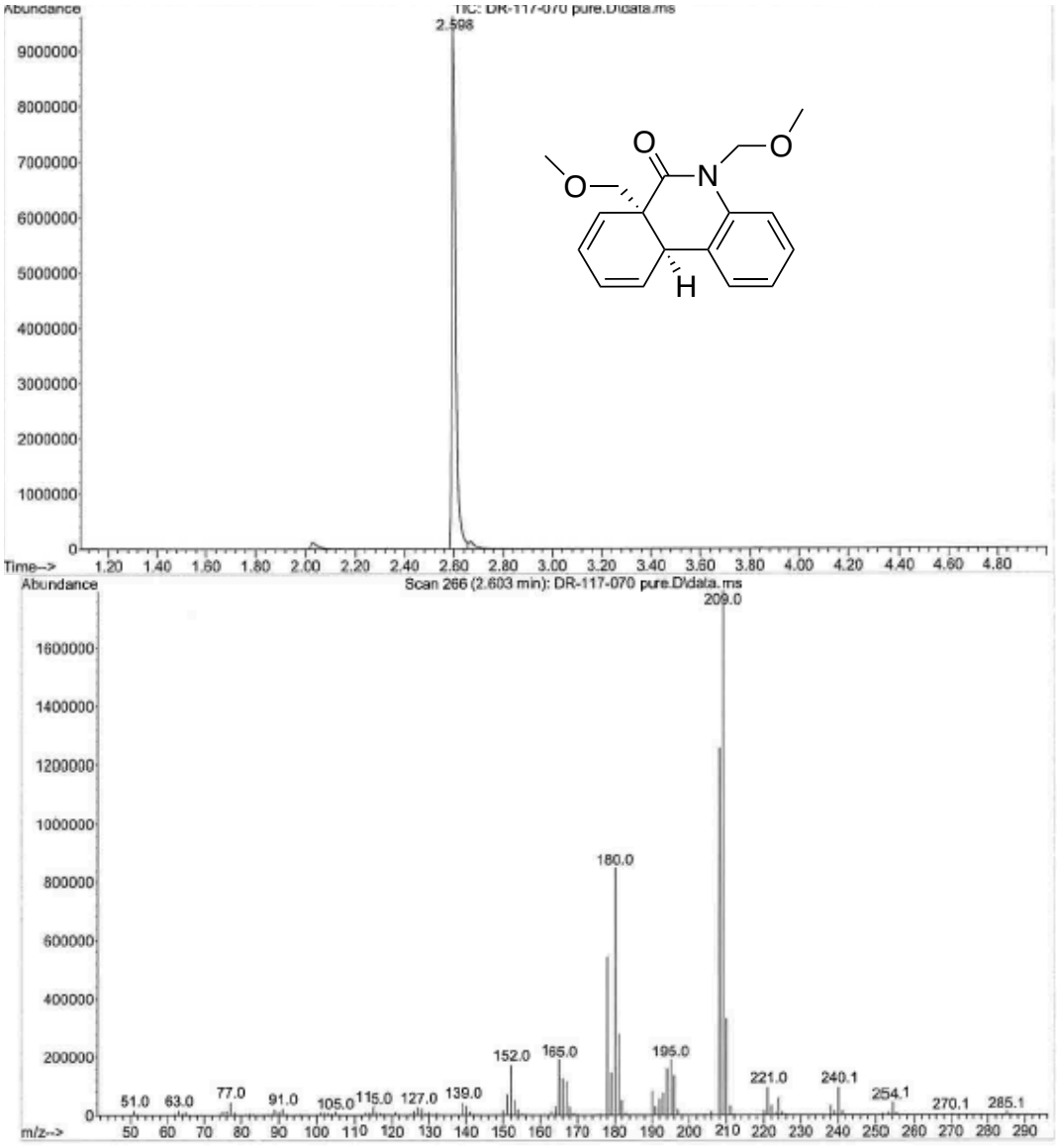

Figure 7.139 GCMS data of compound **2f**.

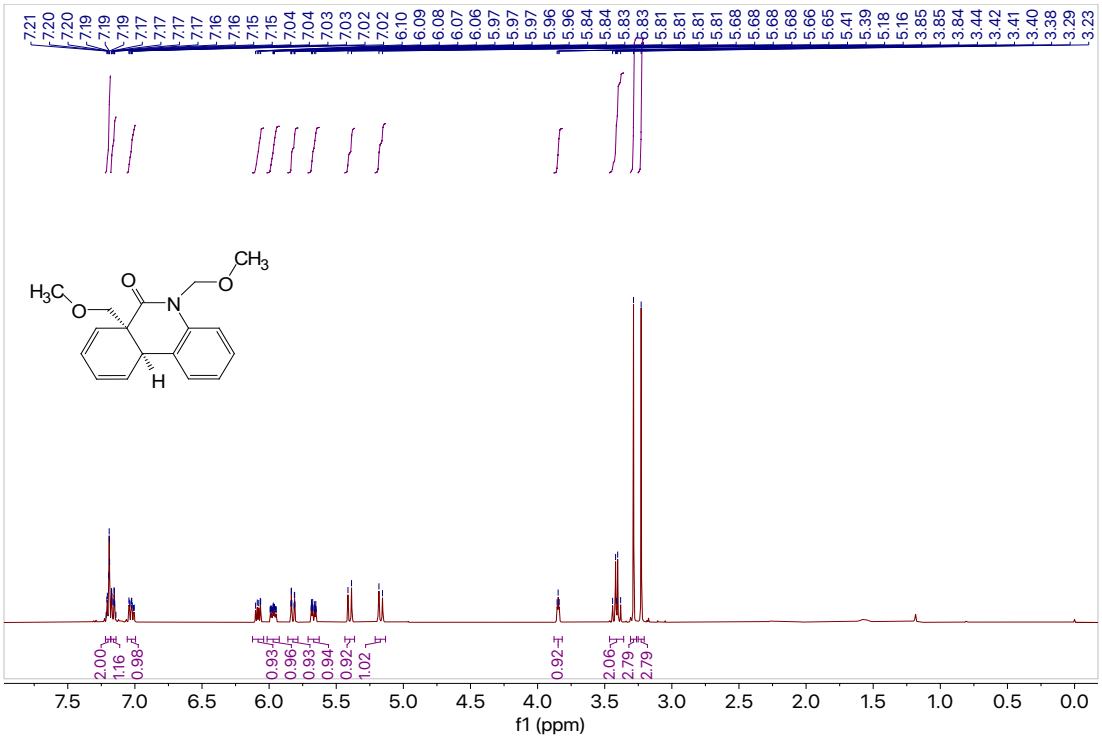

Figure 7.140 ^{1}H NMR (400 MHz, $CDCl_3$) of compound **2f**.

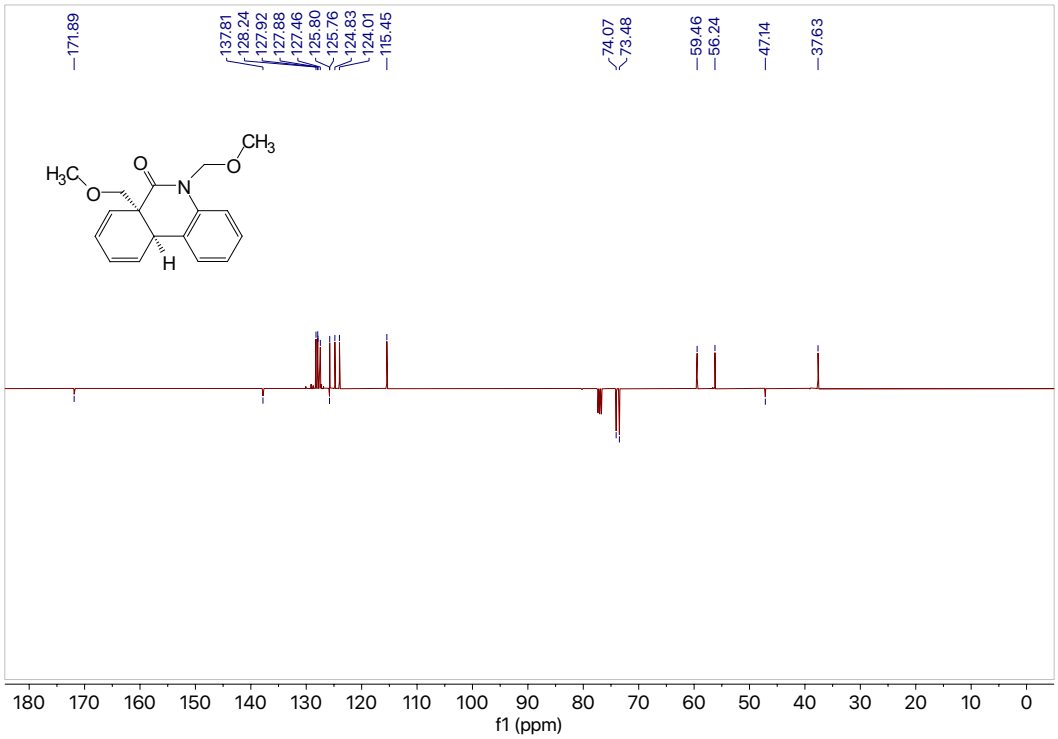

Figure 7.141 ^{13}C NMR (101 MHz, $CDCl_3$) of compound **2f**.

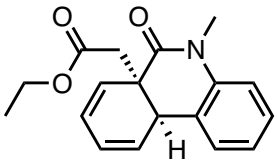

2g

Ethyl 2-((6aR,10aR)-5-methyl-6-oxo-5,10a-dihydrophenanthridin-6a(6H)-yl)acetate (2g).

Racemic procedure:

Using the general procedure detailed above, diene iodide **1g-I** (0.202 g, 0.475 mmol, 1.0 equiv) in DMF (5.7 mL, 0.08 M) was subjected to the Heck reaction conditions with 10 mol% NiI_2/15 mol% 2,2'-bipyridine for 2 h. The crude product was purified by column chromatography (silica, 10:1 hexanes: EtOAc) to afford **2g** (0.104 g, 0.349 mmol) in 74% yield as a clear colorless oil.

Enantioselective procedure:

Using the general procedure detailed above, diene iodide **1g-I** (0.0501 g, 0.118 mmol, 1.0 equiv) in DMF (1.4 mL, 0.08 M) was subjected to the Heck reaction conditions with 10 mol% NiI_2/15 mol% *t*Bu-$^6CH_3$*i*Quinox (**L27**) for 2 h. The crude product was purified by column chromatography (silica, 10:1 hexanes: EtOAc) to afford **2g** (0.0249 g, 0.0837 mmol) with an enantiomeric ratio of 3:1 (49% e.e.) in 71% yield as a clear colorless oil. Spectral data were in accordance with a prior literature report.[10]

$[\alpha]_D^{20}$= +209 (*c* 0.86, $CHCl_3$).

^{1}H NMR (400 MHz, $CDCl_3$) δ 7.31 – 7.21 (m, 2H), 7.05 (td, *J* = 7.5, 1.1 Hz, 1H), 6.97 (dd, *J* = 8.1, 1.1 Hz, 1H), 6.14 – 5.99 (m, 2H), 5.95 – 5.85 (m, 1H), 5.85 – 5.75 (m, 1H), 4.17 – 4.01 (m, 3H), 3.38 (s, 3H), 2.70 (q, 2H), 1.23 (t, *J* = 7.1 Hz, 3H).

^{13}C NMR (101 MHz, $CDCl_3$) δ_u 128.5, 127.9, 127.8, 127.7, 125.2, 125.0, 123.3, 114.2, 38.5, 30.2, 14.2 δ_d 171.4, 170.9, 139.4, 125.8, 60.6, 44.3, 37.8.

GC (Method B) t_R = 3.162 min. EI-MS m/z (%): 296.1 (1, M^+), 252.1 (5), 210.0 (100), 195.0 (10), 180.0 (15), 165.0 (7), 152.0 (8).

HPLC: Chiralcel OD-H, n-hexane/isopropanol=60:40, flow rate=1 mL/min, I=254 nm, t_{R1} = 18.93 min. (major), t_{R2} = 24.37 min. (minor).

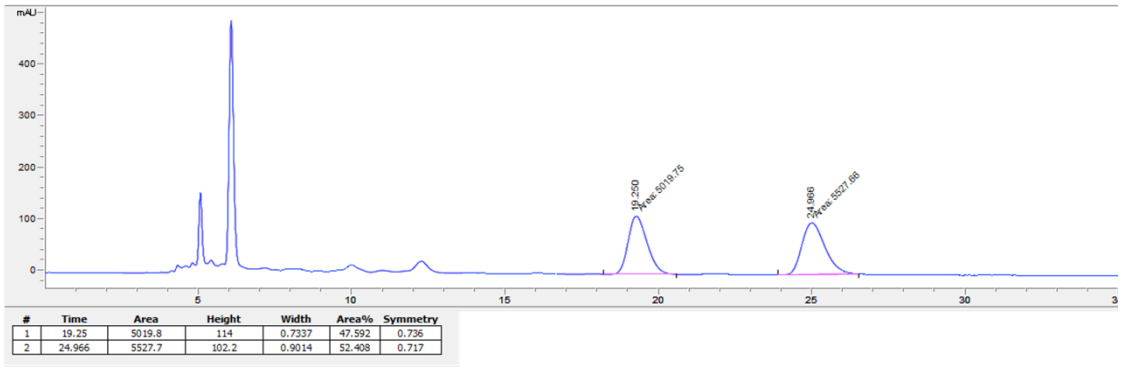

#	Time	Area	Height	Width	Area%	Symmetry
1	19.25	5019.8	114	0.7337	47.592	0.736
2	24.966	5527.7	102.2	0.9014	52.408	0.717

Figure 7.142 Chiral LC for racemic **2g** sample.

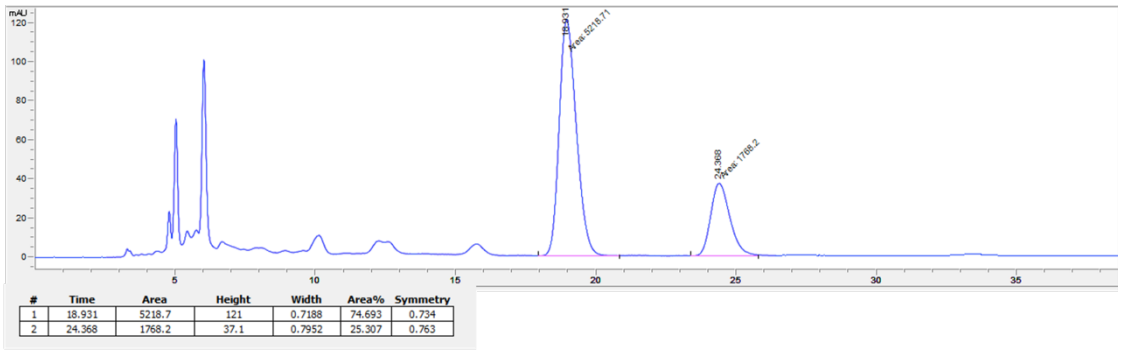

Figure 7.143 Chiral LC for enantioselective **2g** reaction.

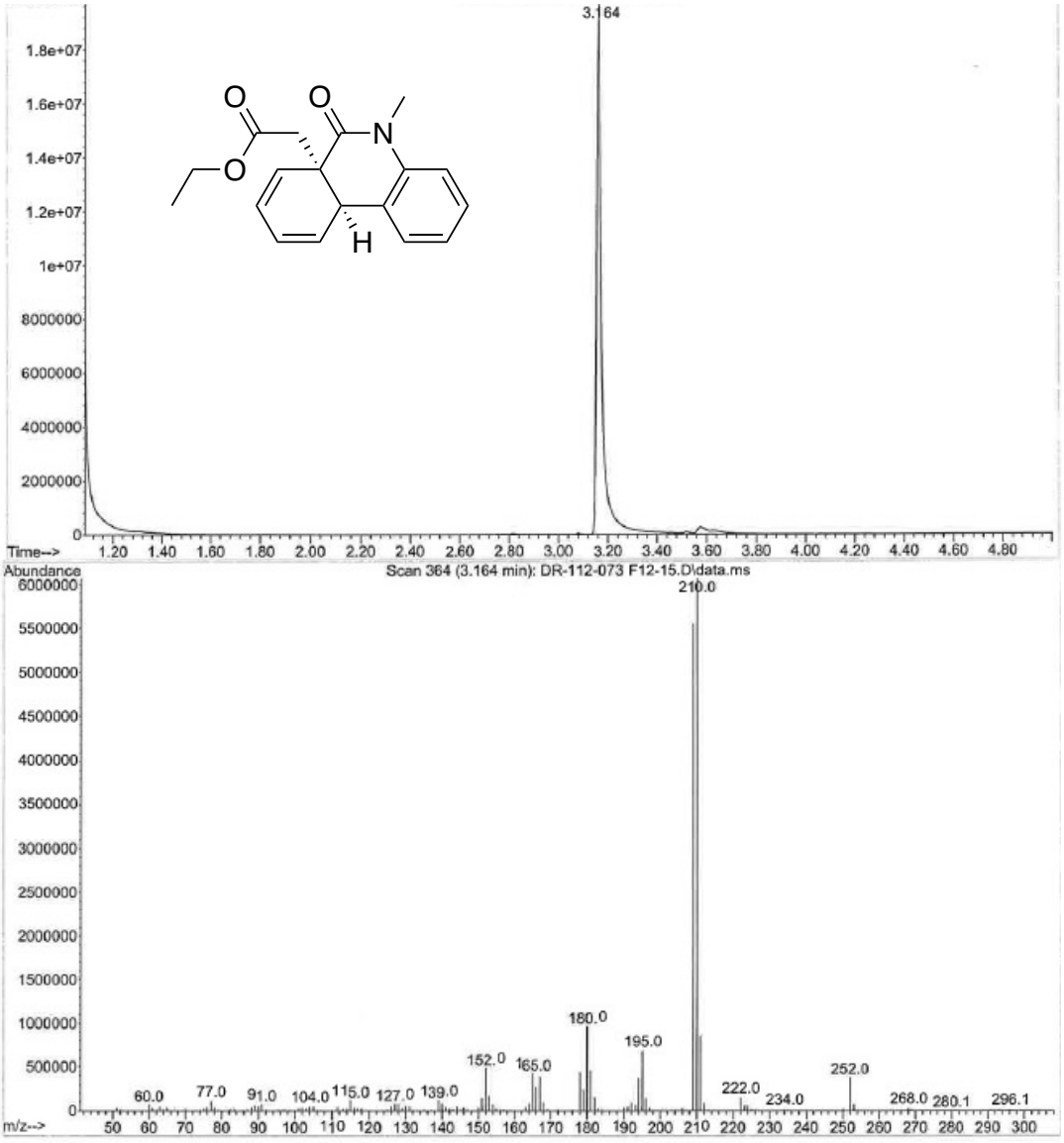

Figure 7.144 GCMS data of compound **2g**.

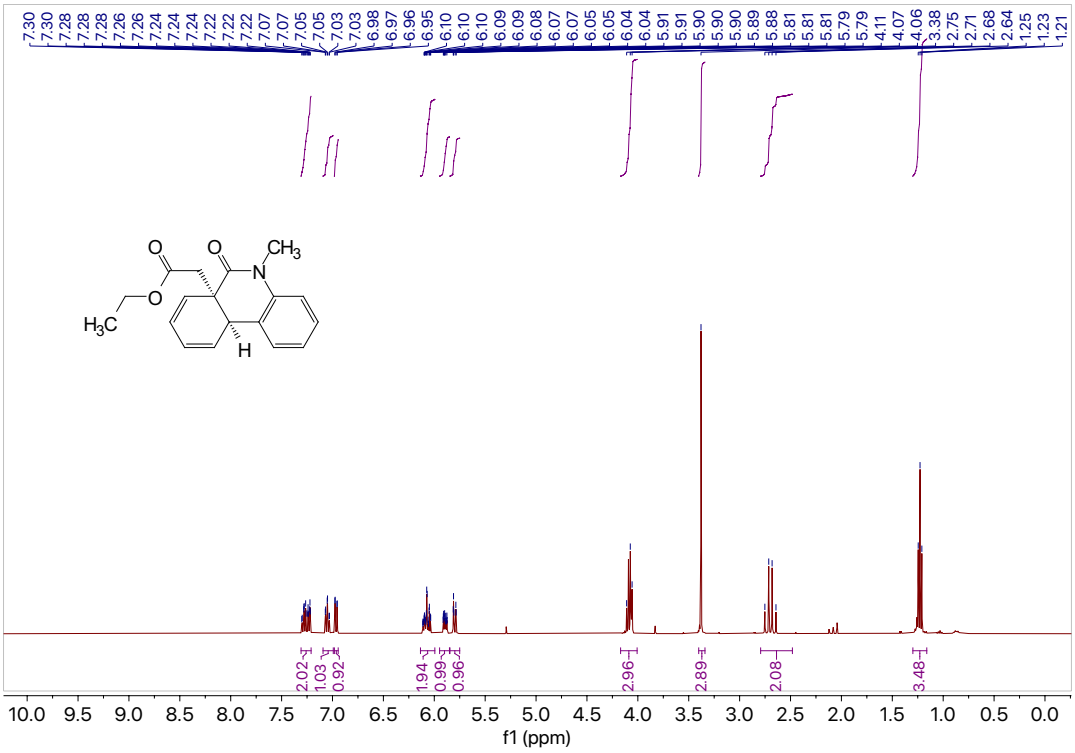

Figure 7.145 ^{1}H NMR (400 MHz, $CDCl_3$) of compound **2g**.

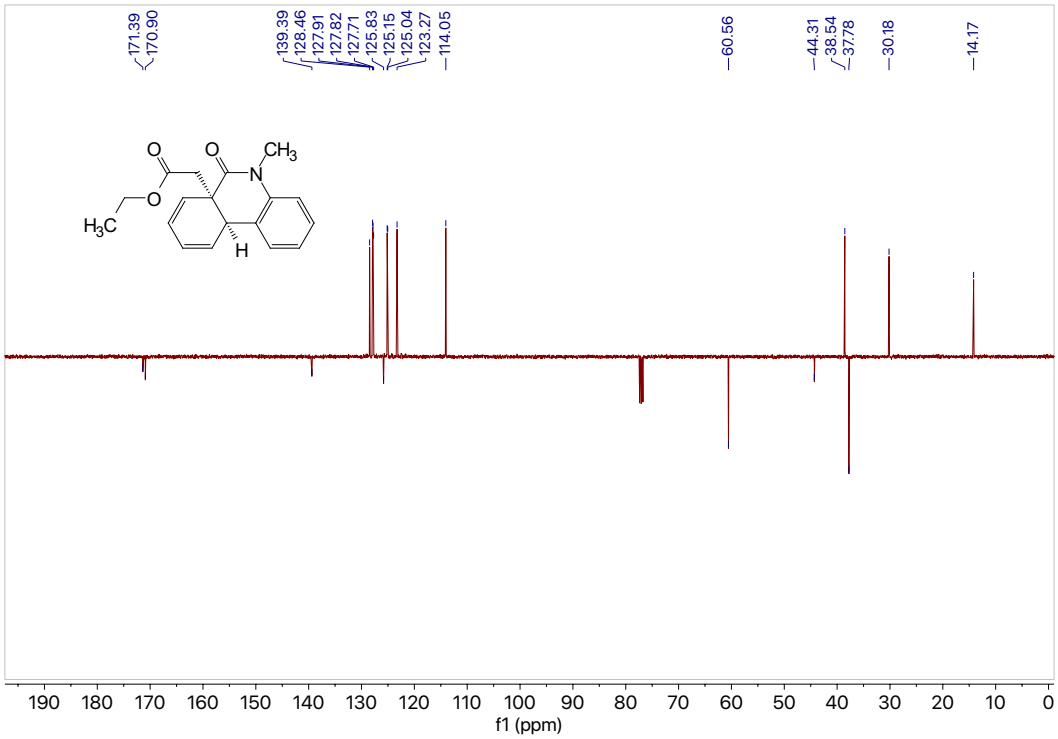

Figure 7.146 ^{13}C NMR (101 MHz, $CDCl_3$) of compound **2g**.

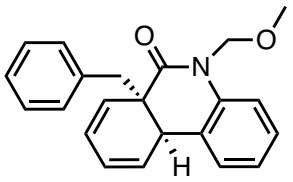

2h

(6aR,10aR)-6a-Benzyl-5-(methoxymethyl)-6a,10a-dihydrophenanthridin-6(5H)-one (2h).

Racemic procedure:

Using the general procedure detailed above, diene bromide **1h** (0.0990 g, 0.241 mmol, 1.0 equiv) in DMF (2.9 mL, 0.08 M) or diene iodide **1h-I** (0.0504 g, 0.109 mmol, 1.0 equiv) in DMF (1.3 mL, 0.08M) was subjected to the Heck reaction conditions with 10 mol% NiI_2/15 mol% 2,2'-bipyridine for 2 h (**1h**) and 4 h (**1h-I**) respectively. The crude product was purified by column chromatography (silica, 10:1 hexanes: EtOAc) to afford **2h** (0.0721 g, 0.218 mmol) in 90% yield from **1h** or in 97% yield (0.0625 g, 0.105 mmol) from **1h-I** as a yellow oil.

Chiral procedure:

Using the general procedure detailed above, diene iodide **1h-I** (0.0503 g, 0.109 mmol, 1.0 equiv) in DMF (1.3 mL, 0.08M) was subjected to the Heck reaction conditions with 10 mol% NiI_2/15 mol% *t*Bu-$^6CH_3$*i*Quinox (**L27**) for 3 h. The crude product was purified by column chromatography (silica, 10:1 hexanes: EtOAc) to afford **2h** (0.0237 g, 0.0715 mmol) with an enantiomeric ratio of 11:1 (83% e.e.) in 66% yield as a tan oil. Spectral data were in accordance with a prior literature report.[10]

$[\alpha]_D^{20}$= +50 (*c* 0.23, $CHCl_3$).

^{1}H NMR (400 MHz, $CDCl_3$) δ 7.33 – 7.30 (m, 2H), 7.30 – 7.26 (m, 1H), 7.25 – 7.19 (m, 2H), 7.18 – 7.14 (m, 2H), 7.04 – 6.99 (m, 2H), 6.10 – 6.04 (m, 2H), 5.98 – 5.89 (m, 1H), 5.59 (d, *J* = 10.6 Hz, 1H), 5.55 (dd, *J* = 9.4, 2.9 Hz, 1H), 5.18 (d, *J* = 10.6 Hz, 1H), 3.62 – 3.58 (m, 1H), 3.39 (s, 3H), 3.01 (d, *J* = 13.3 Hz, 1H), 2.86 (d, *J* = 13.3 Hz, 1H).

^{13}C NMR (101 MHz, $CDCl_3$) δ_u 130.7, 130.2, 128.7, 128.4, 128.3, 128.1, 126.8, 125.3, 124.7, 124.2, 115.7, 56.4, 40.2 δ_d 174.1, 137.9, 136.3, 125.9, 74.0, 46.8, 40.9.

GC (Method A) t_R = 17.679 min. EI-MS m/z (%): 331.1 (1, M^+), 239.0 (10), 224.0 (19), 208.0 (100), 196.0 (15), 178.0 (26), 165.0 (6), 152.0 (7), 91.0 (40).

HPLC: Chiralcel OD-H, n-hexane/isopropanol=97.5:2.5, flow rate=1 mL/min, I=254 nm, t_{R1} =9.21 min. (major), t_{R2} = 15.29 min. (minor).

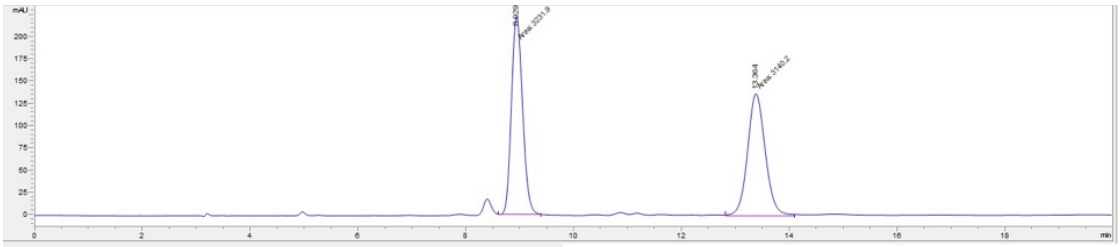

#	Time	Area	Height	Width	Area%	Symmetry
1	8.929	3231.9	223.7	0.2407	50.720	0.833
2	13.364	3140.2	137.6	0.3804	49.280	0.878

Figure 7.147 Chiral LC for racemic **2h** sample.

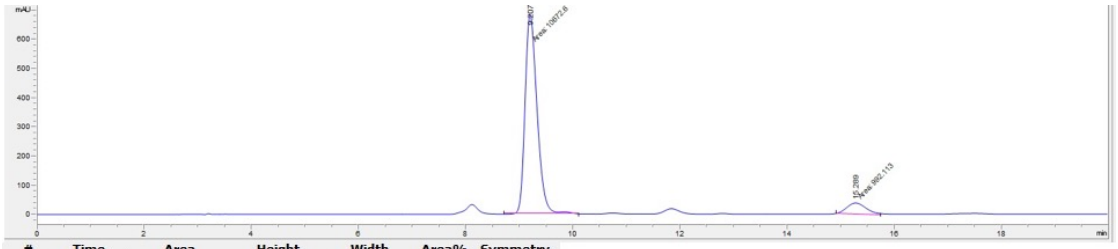

#	Time	Area	Height	Width	Area%	Symmetry
1	9.207	10672.6	680.1	0.2615	91.495	0.692
2	15.289	992.1	38.7	0.4271	8.505	0.814

Figure 7.148 Chiral LC for enantioselective **2h** reaction.

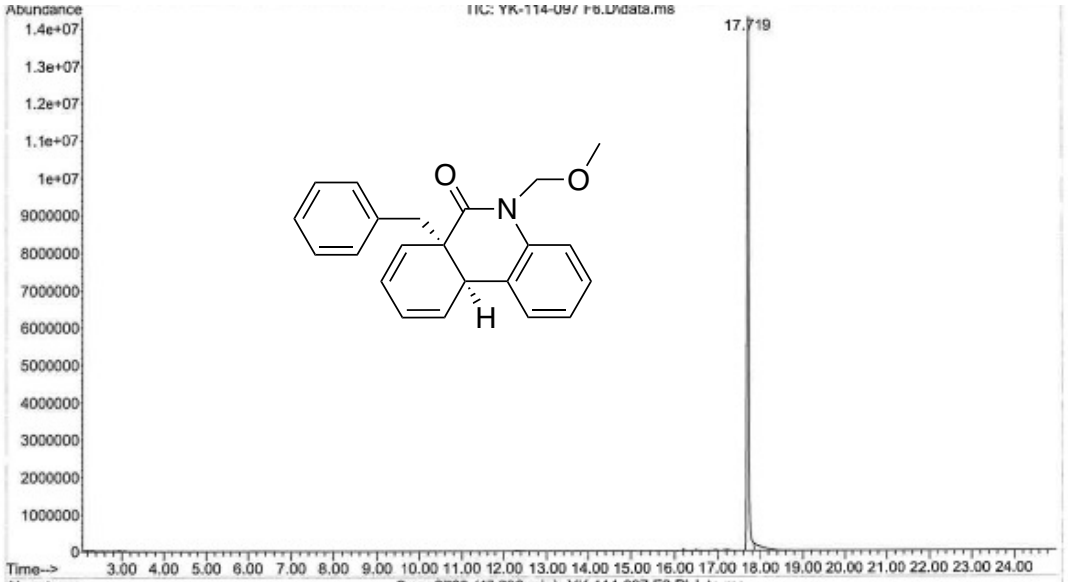

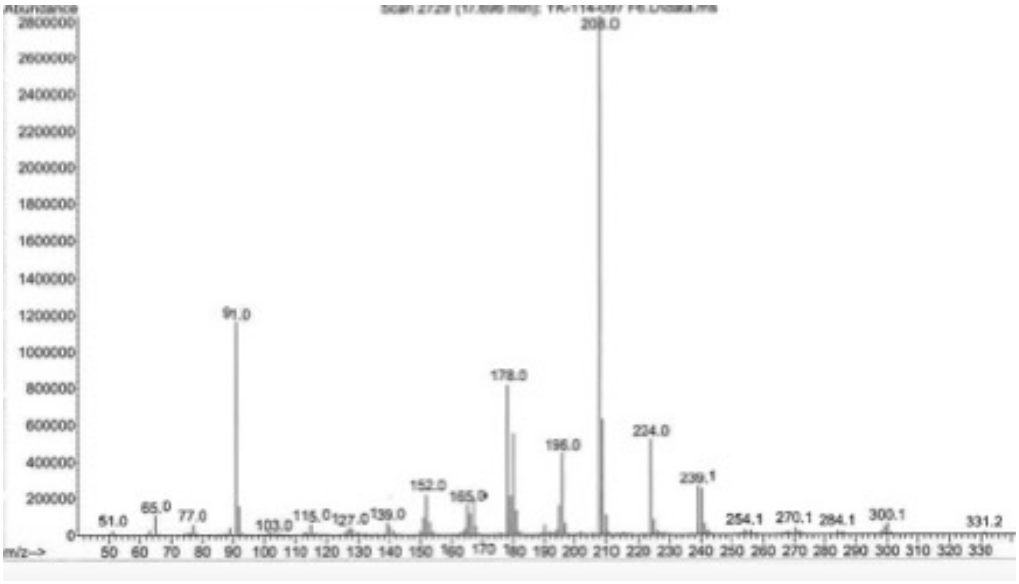

Figure 7.149. GCMS data of compound **2h**.

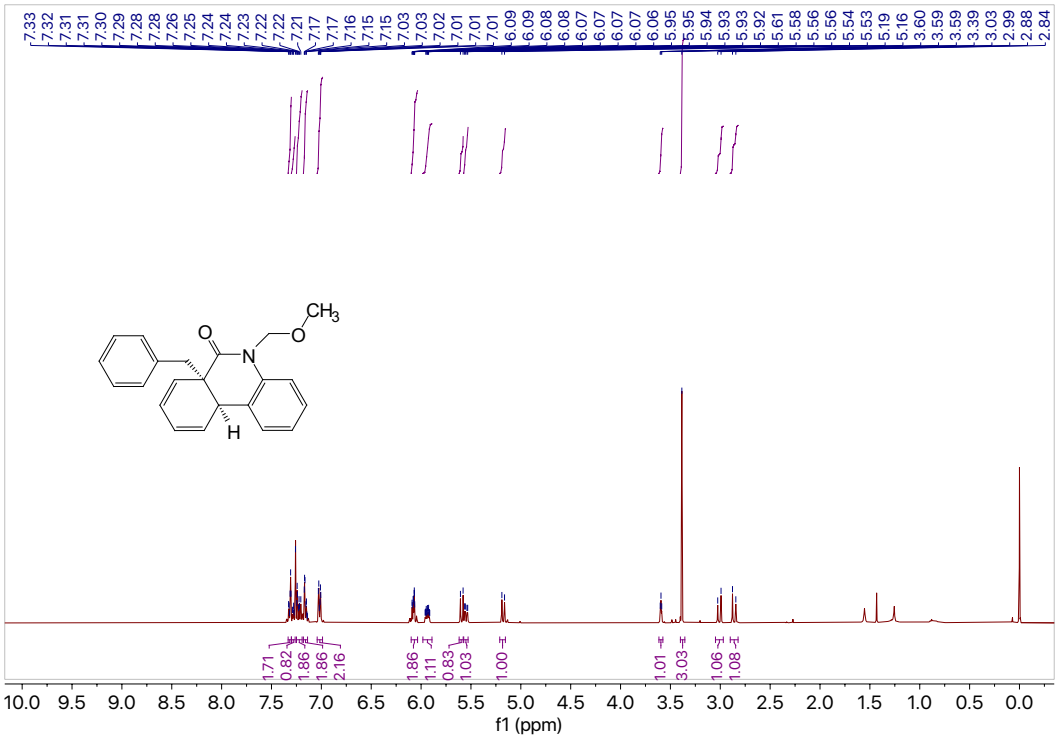

Figure 7.150 ^{1}H NMR (400 MHz, $CDCl_3$) of compound **2h**.

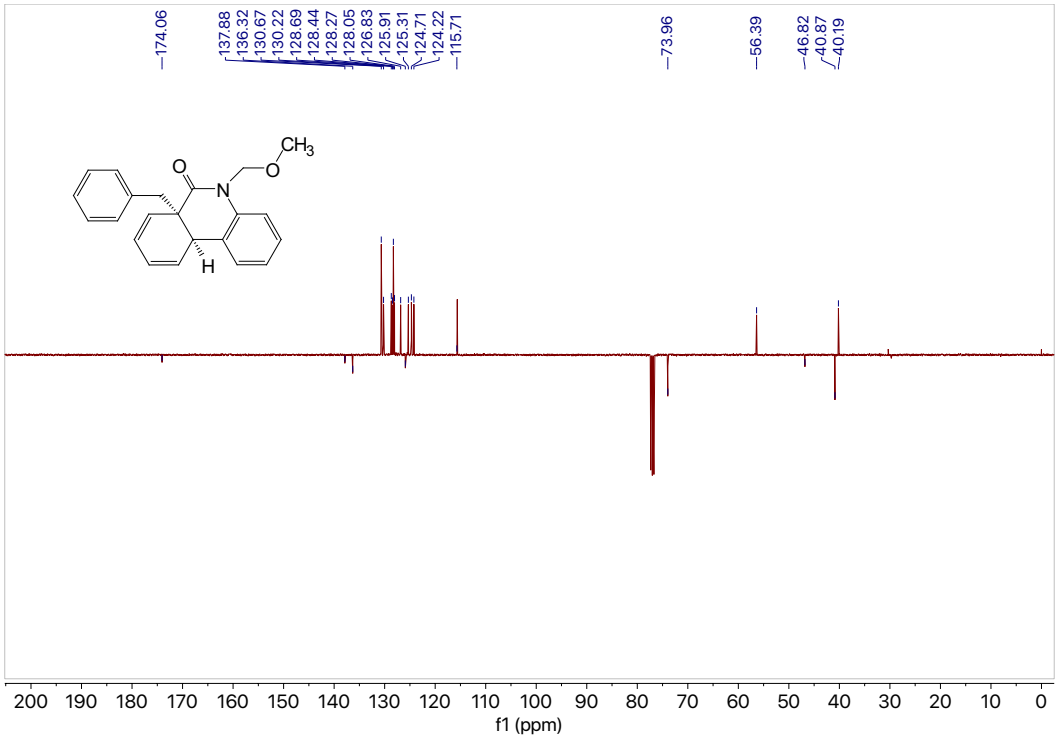

Figure 7.151 ^{13}C NMR (101 MHz, $CDCl_3$) of compound **2h**.

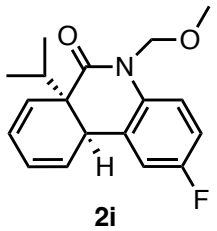

2i

(6a*R*,10a*R*)-2-Fluoro-6a-isopropyl-5-(methoxymethyl)-6a,10a-dihydrophenanthridin-6(5*H*)-one (2i).

Racemic procedure:

Using the general procedure detailed above, diene bromide **1i** (0.101 g, 0.262 mmol, 1.0 equiv) in DMF (3.1 mL, 0.08 M) or diene iodide **1i-I** (0.0501 g, 0.117 mmol, 1.0 equiv) in DMF (1.4 mL, 0.08 M) was subjected to the Heck reaction conditions with 10 mol% NiI_2/15 mol% 2,2'-bipyridine for 4 h. The crude product was purified by column chromatography (silica, 10:1 hexanes: EtOAc) to afford **2i** (0.0669 g, 0.222 mmol) in 85% yield from **1i** or in 61% yield (0.0214 g, 0.0710 mmol) from **1i-I** as a white solid, m.p.= 130.3 – 132.0°C.

Enantioselective procedure:

Using the general procedure detailed above, diene iodide **1i-I** (0.0502 g, 0.117 mmol, 1.0 equiv) in DMF (1.4 mL, 0.08M) was subjected to the Heck reaction conditions with 10 mol% NiI_2/15 mol% *t*Bu-^{6}CH$_3$*i*Quinox (**L27**) for 6 h. The crude product was purified by column chromatography (silica, 10:1 hexanes: EtOAc) to afford **2i** (0.0307 g, 0.102

mmol) with an enantiomeric ratio of 10:1 (81% e.e.) in 87% yield as a white oil that solidified to white crystals on cooling.

$[\alpha]_D^{20}$= +152 (*c* 0.21, $CHCl_3$).

^{1}H NMR (400 MHz, $CDCl_3$) δ 7.23 (dd, *J* = 8.9, 4.8 Hz, 1H), 6.97 (td, *J* = 8.6, 3.0 Hz, 1H), 6.92 (dd, *J* = 8.2, 2.9 Hz, 1H), 6.26 – 6.17 (m, 1H), 6.07 – 5.94 (m, 2H), 5.64 (d, *J* = 10.7 Hz, 1H), 5.51 (ddt, *J* = 9.4, 2.2, 1.0 Hz, 1H), 4.97 (d, *J* = 10.8 Hz, 1H), 3.78 (s, 1H), 3.35 (s, 3H), 1.77 (hept, *J* = 6.9 Hz, 1H), 0.99 (d, *J* = 6.9 Hz, 3H), 0.85 (d, *J* = 6.8 Hz, 3H).

^{13}C NMR (101 MHz, $CDCl_3$) δ_u 128.2, 126.7, 125.8 (d, $^3J_{C\text{-}F}$ = 12.1 Hz), 117.0, 116.9, 115.2 (d, $^2J_{C\text{-}F}$ = 23.2 Hz), 114.4 (d, $^2J_{C\text{-}F}$ = 23.2 Hz), 56.3, 41.4, 29.3, 18.5, 17.9; δ_d 173.3, 160.5 (d, $^1J_{C\text{-}F}$ = 245.5 Hz), 134.4, 128.6, 74.4, 48.5.

^{19}F NMR (376 MHz, $CDCl_3$) δ -119.34.

GC (Method B) t_R = 2.490 min. EI-MS m/z (%): 301.1 (M^+, 32), 269 (14), 258.0 (7), 242.0 (9), 226.0 (77), 214.0 (100), 196.0 (58), 185.0 (14), 170.0 (10), 105.0 (5).

HRMS (ESI) calculated for $C_{18}H_{21}O_2NF$ $[M+H]^+$: 302.1556, found 302.1550.

HPLC: Chiralcel OD-H, n-hexane/isopropanol=97.5:2.5, flow rate=1 mL/min, I=254 nm, t_{R1} = 9.53 min. (major), t_{R2} = 16.15 min. (minor).

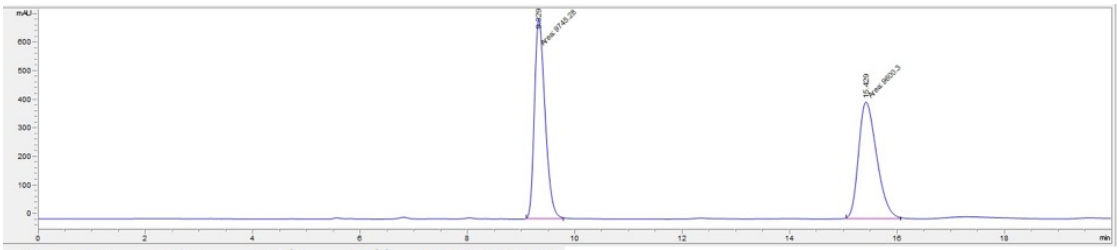

#	Time	Area	Height	Width	Area%	Symmetry
1	9.329	9745.3	701.2	0.2316	50.375	0.685
2	15.429	9600.3	408.4	0.3918	49.625	0.681

Figure 7.152 Chiral LC for racemic **2i** sample.

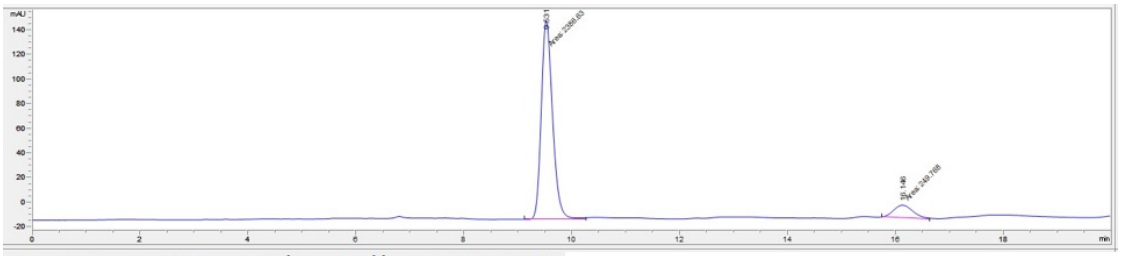

#	Time	Area	Height	Width	Area%	Symmetry
1	9.531	2386.6	162.2	0.2453	90.526	0.755
2	16.146	249.8	10.1	0.4121	9.474	0.772

Figure 7.153 Chiral LC for enantioselective **2i** reaction.

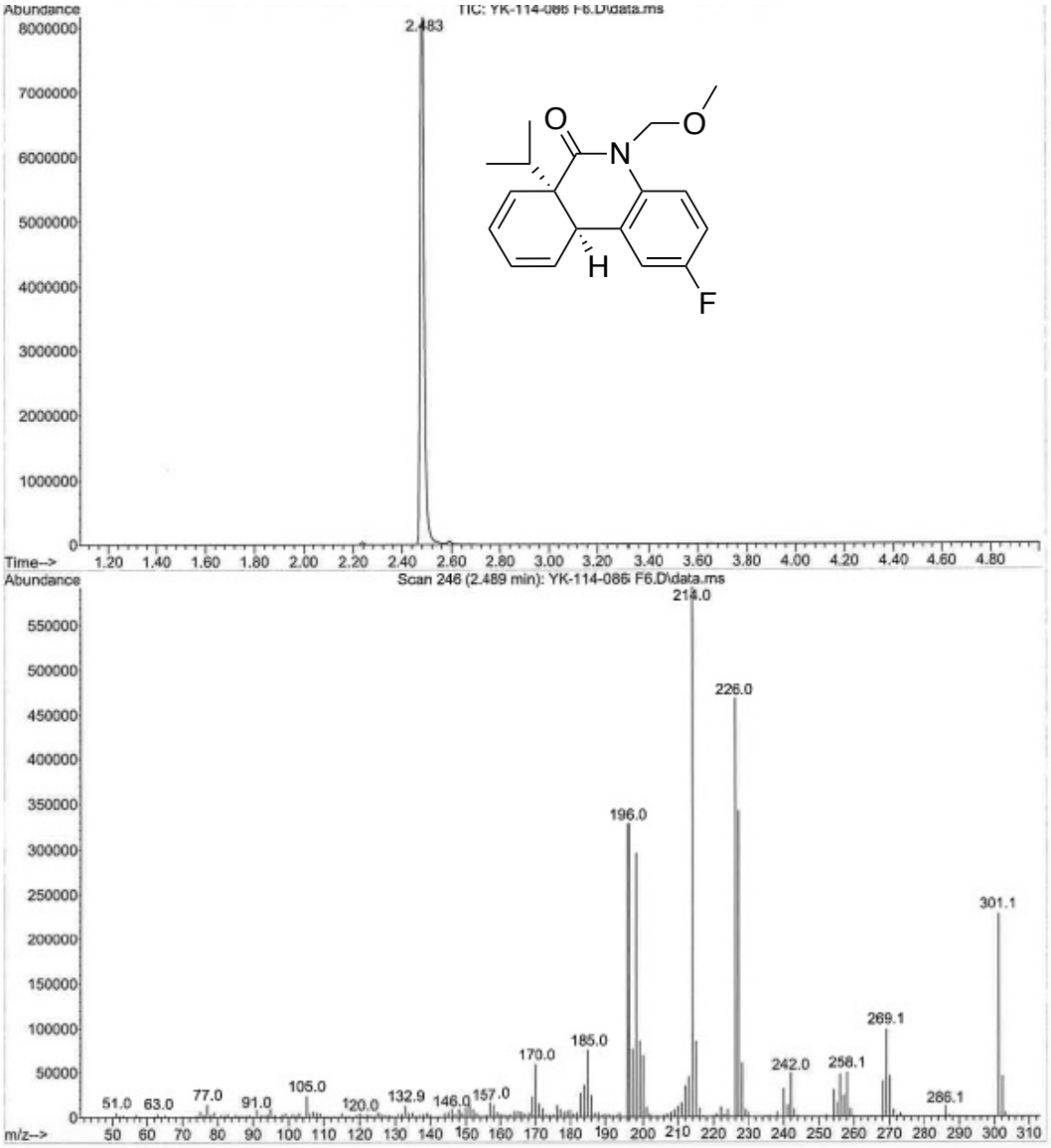

Figure 7.154 GCMS data of compound **2i**.

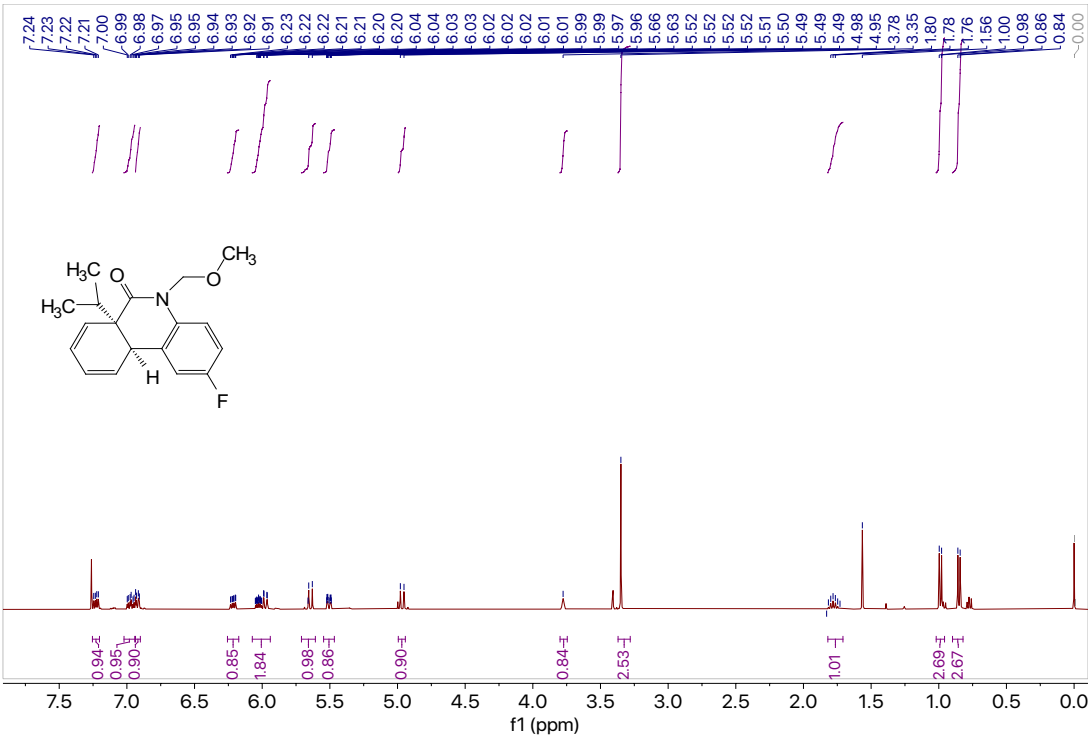

Figure 7.155 ^{1}H NMR (400 MHz, $CDCl_3$) of compound **2i**.

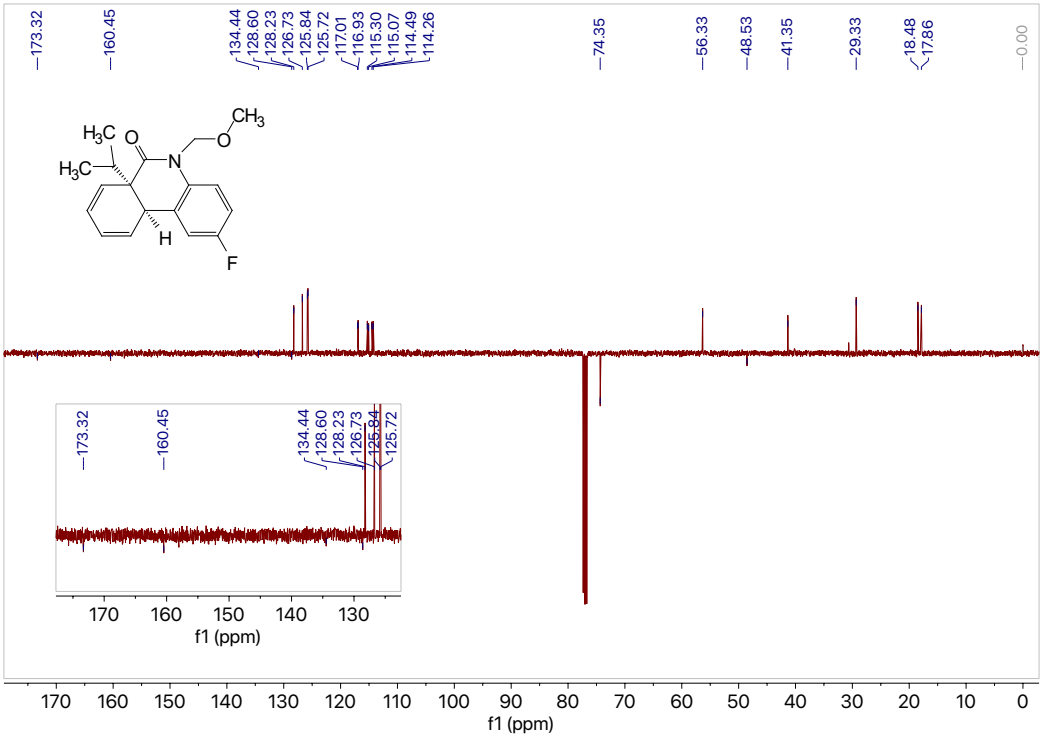

Figure 7.156 ^{13}C NMR (101 MHz, $CDCl_3$) of compound **2i**.

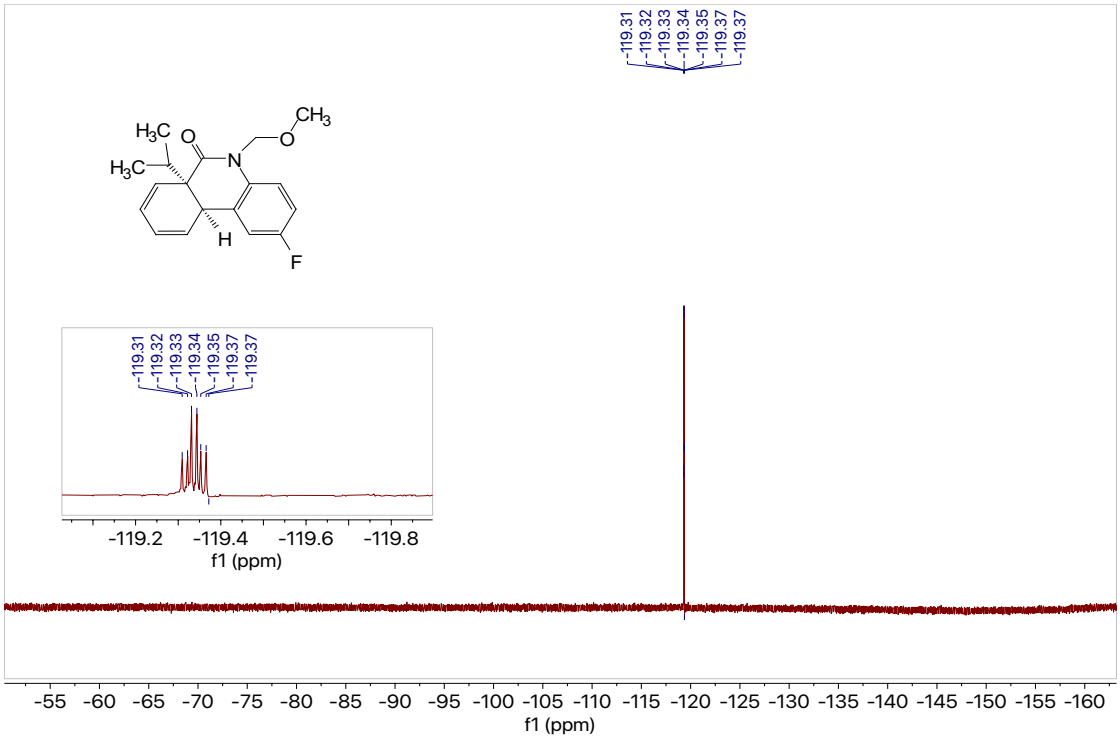

Figure 7.157 ^{19}F NMR (376 MHz, $CDCl_3$) of compound **2i**.

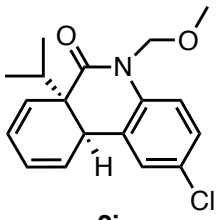

2j

(6aR,10aR)-2-Chloro-6a-isopropyl-5-(methoxymethyl)-6a,10a-dihydrophenanthridin-6(5H)-one (2j).

Racemic procedure:

Using the general procedure detailed above, diene bromide **1j** (0.0999 g, 0.251 mmol, 1.0 equiv) in DMF (3 mL, 0.08 M) or diene iodide **1j-I** (0.0502 g, 0.112 mmol, 1.0 equiv) in DMF (1.3 mL, 0.08 M) was subjected to the Heck reaction conditions with 10 mol% NiI_2/15 mol% 2,2'-bipyridine for 6 h at 65˚C. The crude product was purified by column chromatography (silica, 10:1 hexanes: EtOAc) to afford **2j** (0.0531 g, 0.167 mmol) in 67% yield from **1j** or in 91% yield (0.0324 g, 0.102 mmol) from **1j-I** as a tan solid, m.p.= 101.1 – 102.9°C.

Enantioselective procedure:

Using the general procedure detailed above, diene iodide **1j-I** (0.0508 g, 0.114 mmol, 1.0 equiv) in DMF (1.4 mL, 0.08 M) was subjected to the Heck reaction conditions with 10 mol% NiI_2/15 mol% *t*Bu-^{6}CH$_3$*i*Quinox (**L27**) for 6 h at 65˚C. The crude product was purified by column chromatography (silica, 10:1 hexanes: EtOAc) to afford **2j** (0.0242 g,

0.0761 mmol) with an enantiomeric ratio of 7:1 (74% e.e.) in 68% yield as a clear oil that solidified to tan crystals on cooling.
$[\alpha]_D^{20}$= +99 (*c* 0.22, $CHCl_3$).
^{1}H NMR (400 MHz, $CDCl_3$) δ 7.20 – 7.16 (m, 1H), 7.14 (s, 1H), 7.11 (d, *J* = 2.3 Hz, 1H), 6.19 – 6.10 (m, 1H), 5.99 – 5.93 (m, 1H), 5.90 (d, *J* = 10.7 Hz, 1H), 5.56 (d, *J* = 10.7 Hz, 1H), 5.47 – 5.39 (m, 1H), 4.91 (d, *J* = 10.6 Hz, 1H), 3.74 – 3.68 (m, 1H), 3.27 (s, 3H), 1.70 (hept, *J* = 6.7 Hz, 1H), 0.91 (d, *J* = 6.9 Hz, 3H), 0.79 (d, *J* = 6.8 Hz, 3H).
^{13}C NMR (101 MHz, $CDCl_3$) δ_u 128.3, 128.2, 127.9, 126.6, 125.9, 125.8, 116.9, 56.3, 41.2, 29.3, 18.5, 17.8; δ_d 173.4, 136.9, 129.0, 128.5, 74.2, 48.6.
GC (Method B) t_R = 3.135 min. EI-MS m/z (%): 317.1 (M^+, 29), 285.1 (10), 272.0 (9), 258.0 (10), 242.0 (86), 230.0 (100), 214.0 (61), 195.0 (12), 180.0 (13), 166.0 (13), 152.0 (14), 139.0 (6), 105.0 (7), 77.0 (5).
HRMS (ESI) calculated for $C_{18}H_{21}O_2NCl$ $[M+H]^+$: 318.1261, found 318.1260.
HPLC: Chiralcel OD-H, n-hexane/isopropanol=97.5:2.5, flow rate=1 mL/min, I=254 nm, t_{R1} = 8.98 min. (major), t_{R2} = 13.42 min. (minor).

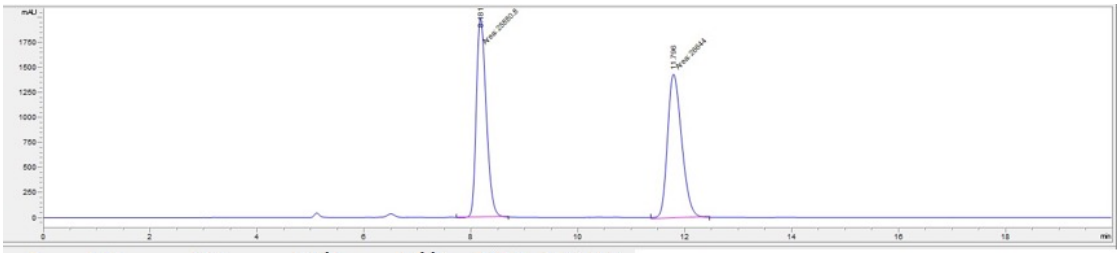

#	Time	Area	Height	Width	Area%	Symmetry
1	8.181	25880.8	1992.4	0.2165	49.274	0.704
2	11.796	26644	1439.7	0.3084	50.726	0.727

Figure 7.158 Chiral LC for racemic **2j** sample.

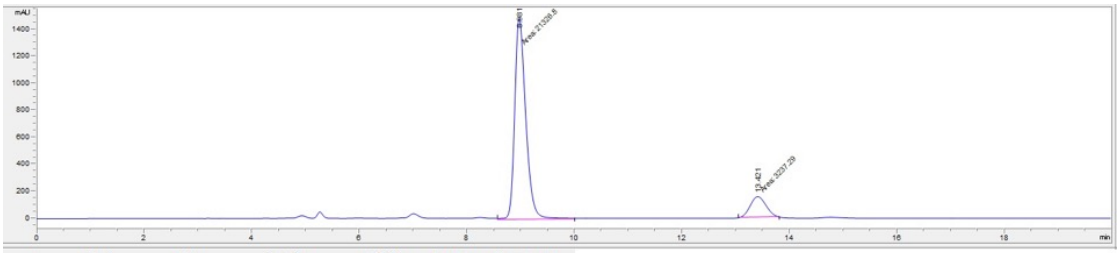

#	Time	Area	Height	Width	Area%	Symmetry
1	8.981	21326.8	1486.7	0.2391	86.821	0.675
2	13.421	3237.3	155.6	0.3467	13.179	0.894

Figure 7.159 Chiral LC for enantioselective **2j** reaction.

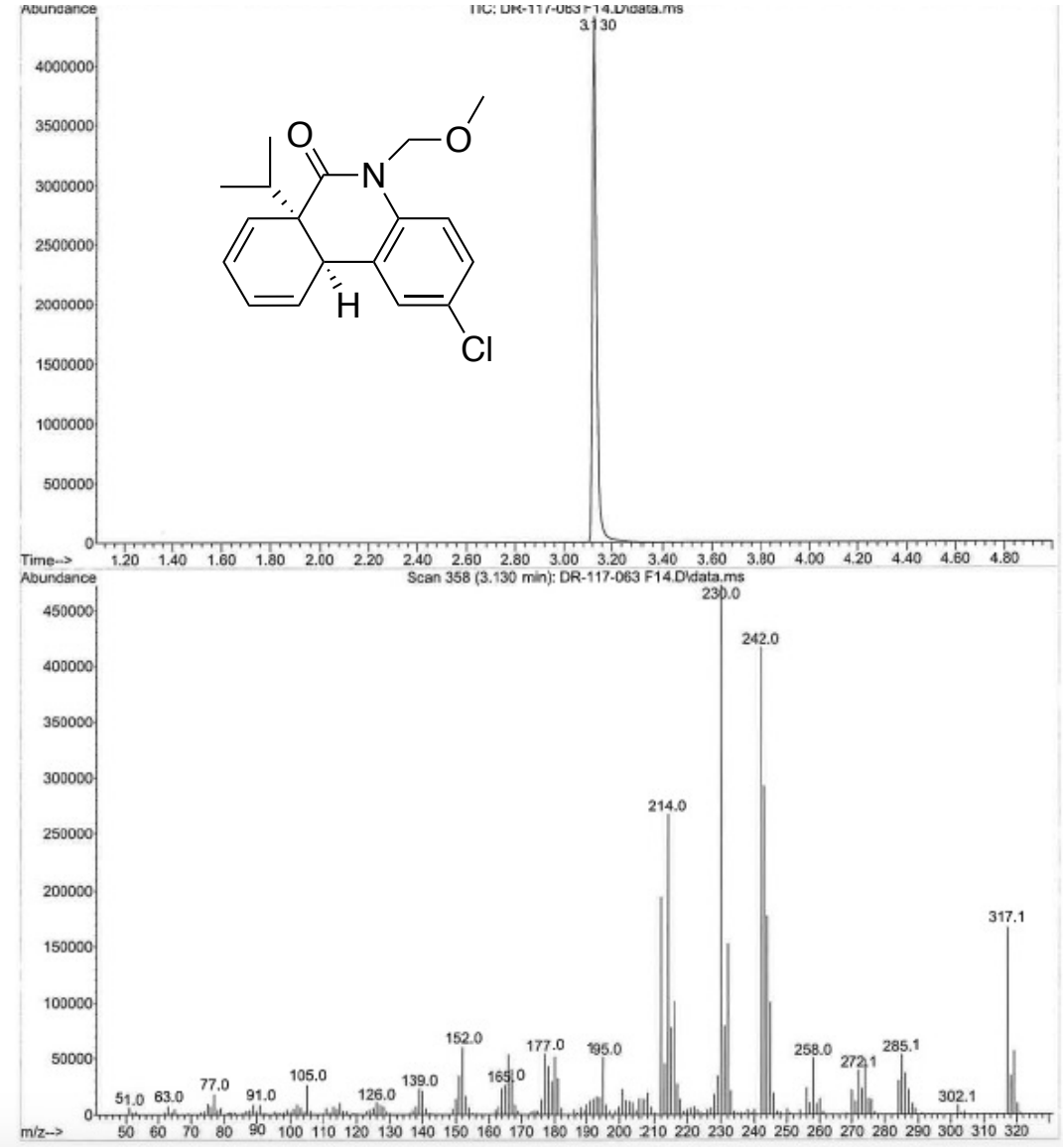

Figure 7.160 GCMS data of compound **2j**.

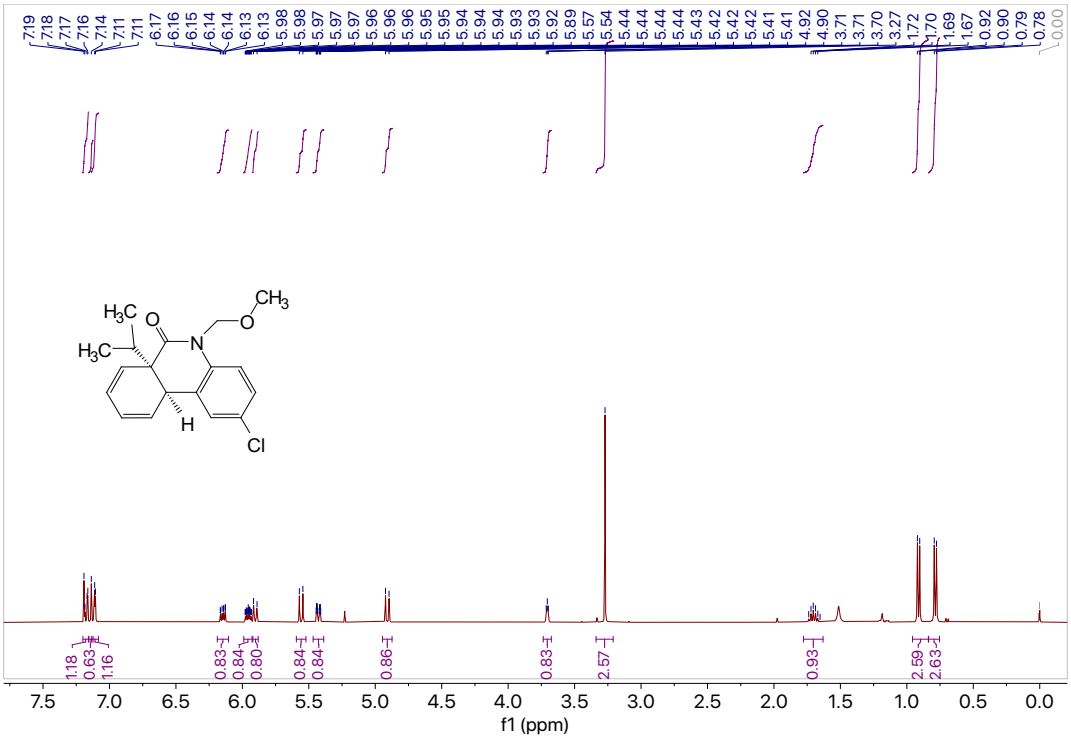

Figure 7.161 ^{1}H NMR (400 MHz, $CDCl_3$) of compound **2j**.

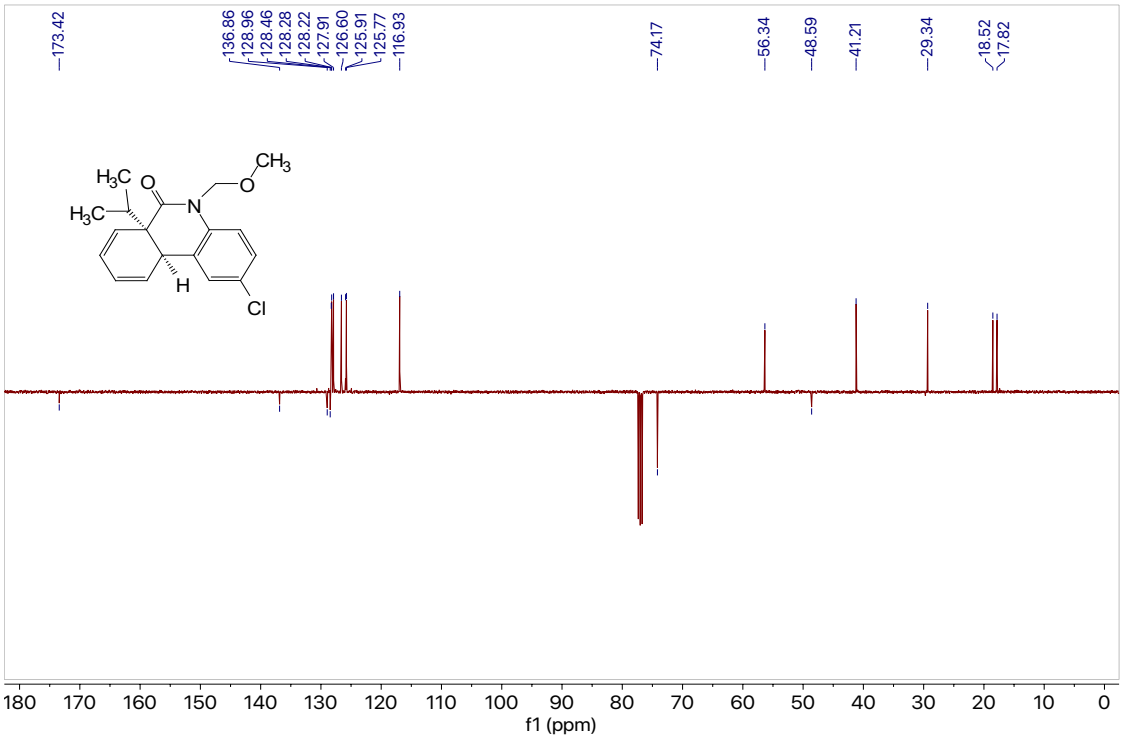

Figure 7.162 ^{13}C NMR (101 MHz, $CDCl_3$) of compound **2j**.

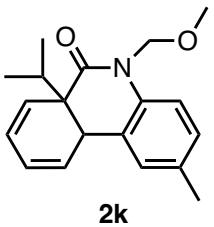

2k

6a-Isopropyl-5-(methoxymethyl)-2-methyl-6a,10a-dihydrophenanthridin-6(5*H*)-one (2k).

Using the general procedure detailed above, diene bromide **1k** (0.101 g, 0.264 mmol, 1.0 equiv) in DMF (3.2 mL, 0.08 M) was subjected to the Heck reaction conditions with 10 mol% NiI_2/15 mol% 2,2'-bipyridine for 3 h. The crude product was purified by column chromatography (silica, 10:1 hexanes: EtOAc) to afford **2k** (0.0684 g, 0.229 mmol) in 87% yield as a clear colorless oil.

^{1}H NMR (400 MHz, $CDCl_3$) δ 7.14 (d, J = 8.3 Hz, 1H), 7.08 (dd, J = 8.1, 2.3 Hz, 1H), 6.99 (d, J = 2.1 Hz, 1H), 6.25 – 6.16 (m, 1H), 6.06 – 5.94 (m, 2H), 5.63 (d, J = 10.6 Hz, 1H), 5.52 (ddt, J = 9.3, 2.2, 1.1 Hz, 1H), 5.01 (d, J = 10.6 Hz, 1H), 3.76 (d, J = 3.3 Hz, 1H), 3.34 (s, 3H), 2.34 (s, 3H), 1.78 (hept, J = 7.0 Hz, 1H), 0.98 (d, J = 6.9 Hz, 3H), 0.84 (d, J = 6.8 Hz, 3H).

^{13}C NMR (101 MHz, $CDCl_3$) δ_u 129.3, 129.1, 128.4, 126.8, 125.8, 125.3, 115.4, 56.3, 41.3, 29.2, 20.7, 18.5, 17.9; δ_d 173.7, 135.7, 133.6, 126.4, 74.1, 48.7.

GC (Method B) t_R = 2.836 min. EI-MS m/z (%): 297.1 (M^+, 28), 265.1 (5), 254.1 (8), 238.0 (6), 222.0 (98), 210.0 (100), 192.0 (53), 180.0 (14), 165.0 (16), 152.0 (11), 77.0 (4).

HRMS (ESI) calculated for $C_{19}H_{24}O_2N$ $[M+H]^+$: 298.1807, found 298.1803.

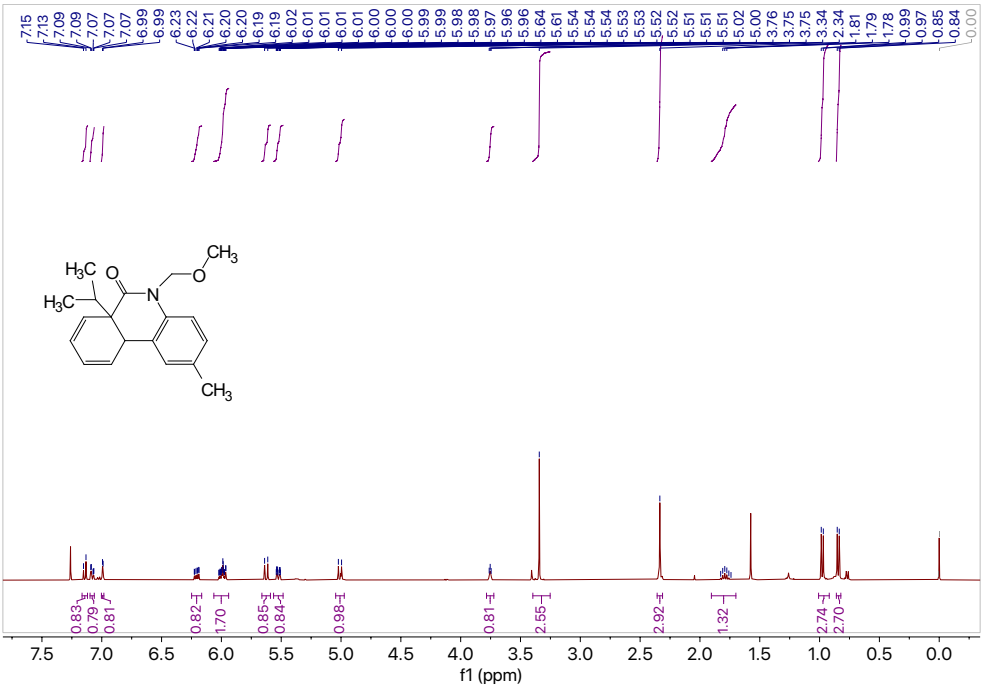

Figure 7.163 ^{1}H NMR (400 MHz, $CDCl_3$) of compound **2k**.

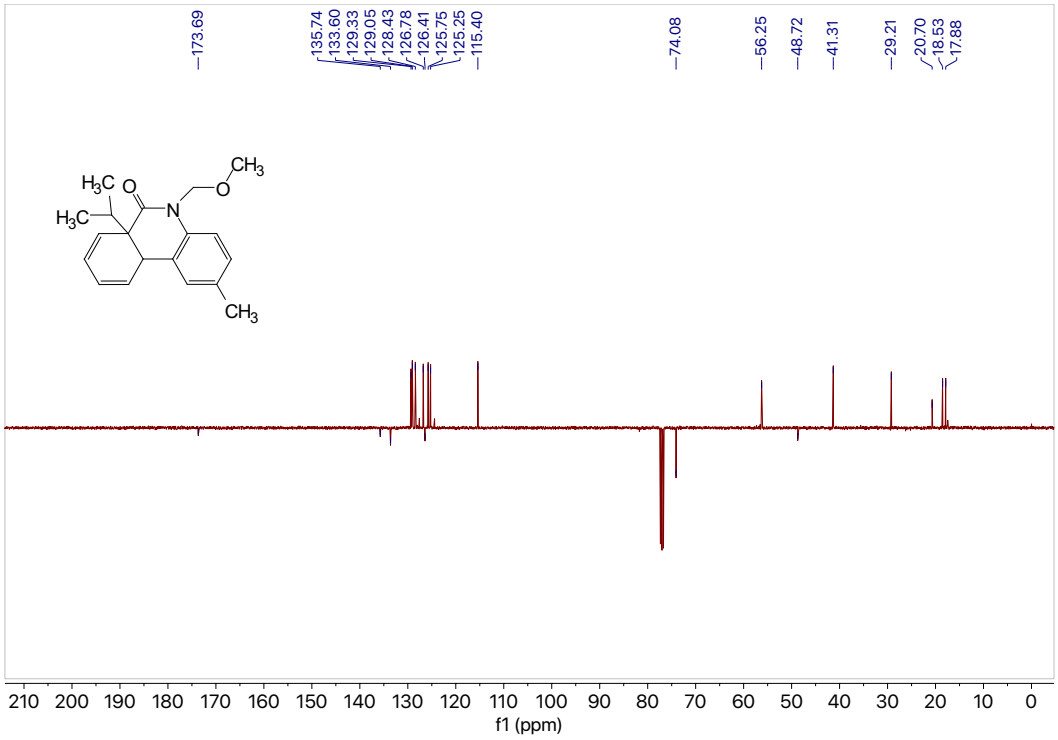

Figure 7.164 ^{13}C NMR (101 MHz, $CDCl_3$) of compound **2k**.

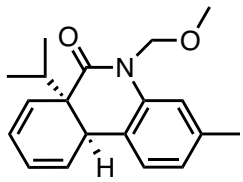

2l

(6aR,10aR)-6a-Isopropyl-5-(methoxymethyl)-3-methyl-6a,10a-dihydrophenanthridin-6(5H)-one (2l).

Racemic procedure:

Using the general procedure detailed above, diene iodide **1l-I** (0.101 g, 0.235 mmol, 1.0 equiv) in DMF (2.8 mL, 0.08 M) was subjected to the Heck reaction conditions with 10 mol% NiI_2/15 mol% 2,2'-bipyridine for 2 h. The crude product was purified by column chromatography (silica, 10:1 hexanes: EtOAc) to afford **2l** (0.0562 g, 0.189 mmol) in 81% yield as a white cloudy oil.

Enantioselective procedure:

Using the general procedure detailed above, diene iodide **1l-I** (0.0501 g, 0.118 mmol, 1.0 equiv) in DMF (1.4 mL, 0.08 M) was subjected to the Heck reaction conditions with 10 mol% NiI_2/15 mol% *t*Bu-^{6}CH_3*i*Quinox (**L27**) for 1.5 h. The crude product was purified by column chromatography (silica, 10:1 hexanes: EtOAc) to afford **2l** (0.0222 g, 0.0746 mmol) with an enantiomeric ratio of 10:1 (81% e.e.) in 63% yield as a white cloudy oil.

$[\alpha]_D^{20}$= +130 (*c* 0.39, $CHCl_3$).

^{1}H NMR (400 MHz, $CDCl_3$) δ 7.03 – 6.97 (m, 2H), 6.88 – 6.81 (m, 1H), 6.17 – 6.09 (m, 1H), 5.96 – 5.88 (m, 2H), 5.58 (d, *J* = 10.6 Hz, 1H), 5.47 – 5.43 (m, 1H), 4.93 (d, *J* = 10.6 Hz, 1H), 3.73 – 3.65 (m, 1H), 3.30 (s, 3H), 2.30 (s, 3H), 1.72 (hept, *J* = 6.9 Hz, 1H), 0.90 (d, *J* = 6.9 Hz, 3H), 0.76 (d, *J* = 6.8 Hz, 3H).
^{13}C NMR (101 MHz, $CDCl_3$) δ_u 129.6, 128.3, 126.7, 125.8, 125.2, 124.7, 116.2, 56.4, 40.9, 29.2, 21.6, 18.5, 17.9; δ_d 174.0, 138.1, 137.9, 123.6, 74.1, 48.6.
GC (Method B) t_R = 2.775 min. EI-MS m/z (%): 297.1 (M^+, 18), 266.1 (4), 254.1 (22), 238.0 (6), 222.0 (100), 210.0 (68), 192.0 (45), 180.0 (10), 165.0 (12), 152.0 (8), 105.0 (5).
HRMS (ESI) calculated for $C_{19}H_{24}O_2N$ $[M+H]^+$: 298.1807, found 298.1800.
HPLC: Chiralcel OD-H, n-hexane/isopropanol=97.5:2.5, flow rate=1 mL/min, I=254 nm, t_{R1} = 7.32 min. (major), t_{R2} = 12.13 min. (minor).

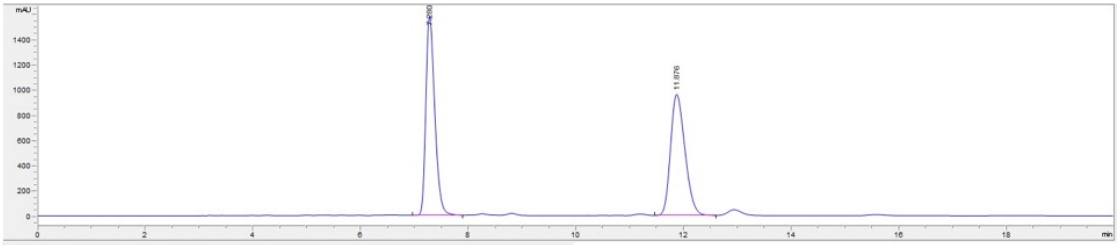

#	Time	Area	Height	Width	Area%	Symmetry
1	7.28	18318.5	1582.2	0.1771	50.433	0.661
2	11.876	18004.1	962.8	0.2902	49.567	0.718

Figure 7.165 Chiral LC for racemic **2l** sample.

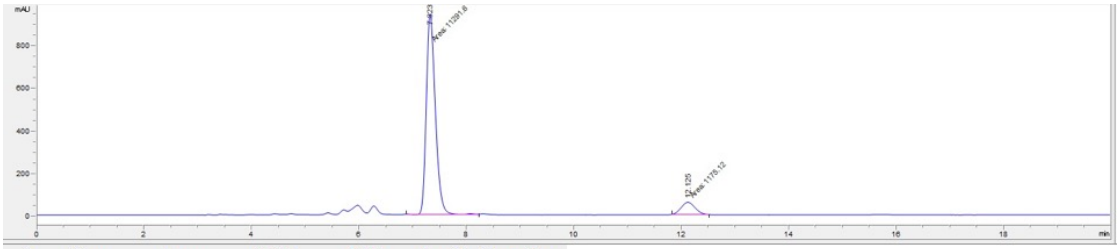

#	Time	Area	Height	Width	Area%	Symmetry
1	7.323	11291.6	938.3	0.2006	90.574	0.714
2	12.125	1175.1	60.6	0.323	9.426	0.891

Figure 7.166 Chiral LC for enantioselective **2l** reaction.

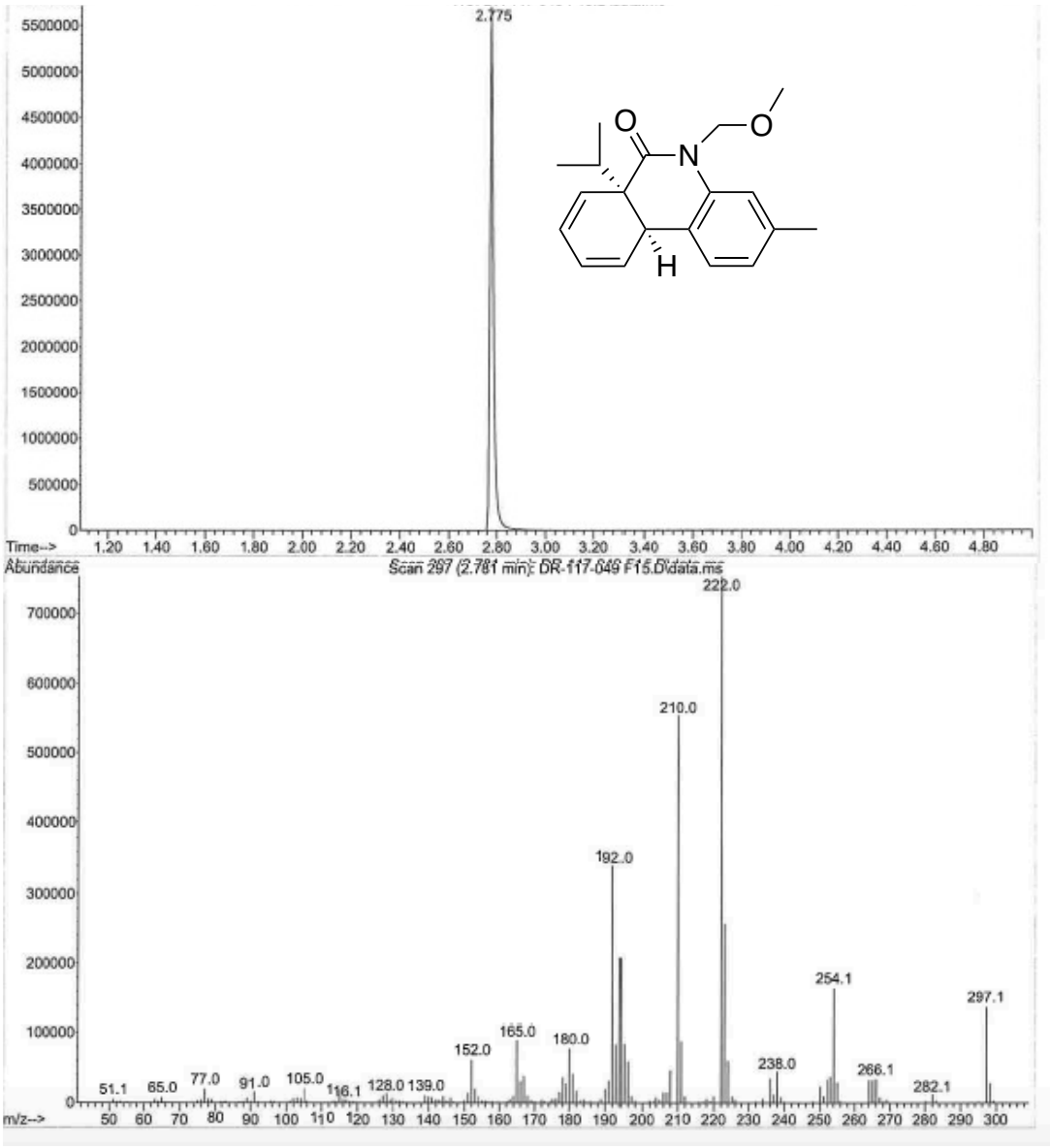

Figure 7.167 GCMS data of compound **2l**.

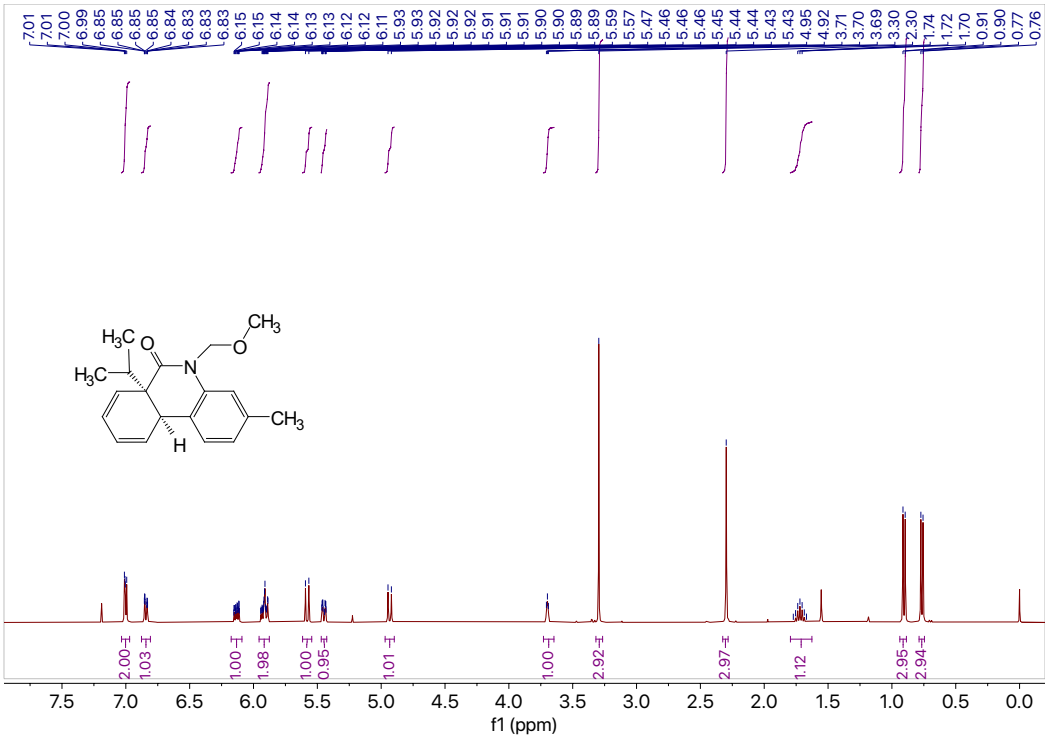

Figure 7.168 ^{1}H NMR (400 MHz, $CDCl_3$) of compound **2l**.

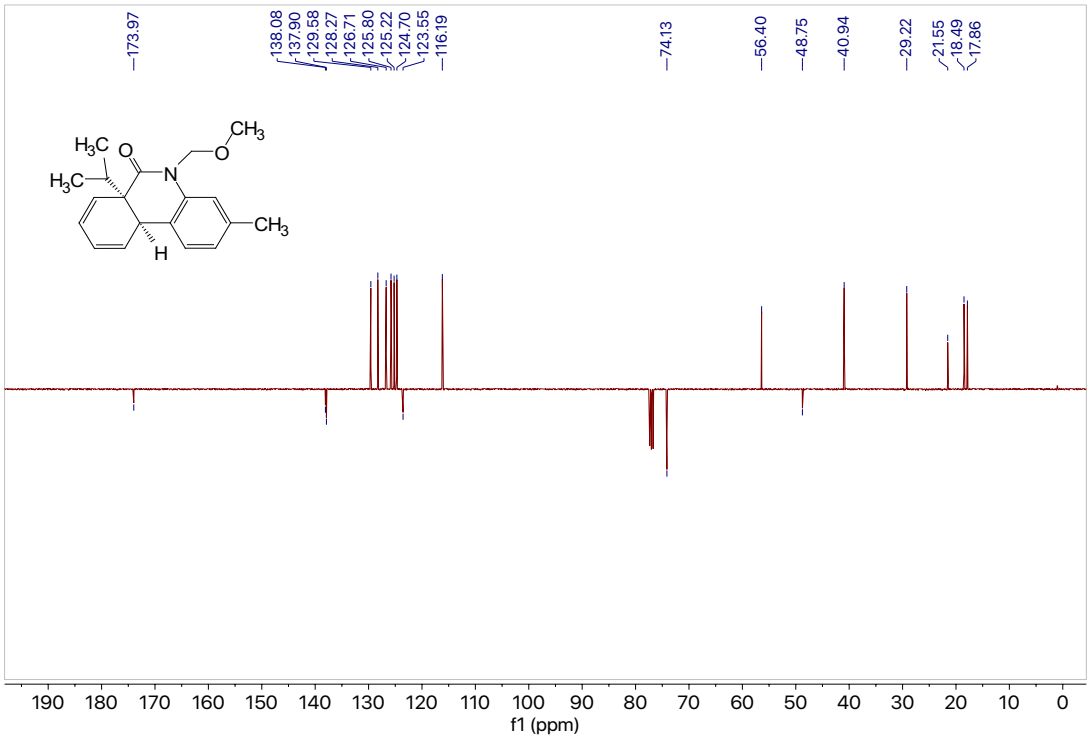

Figure 7.169 ^{13}C NMR (101 MHz, $CDCl_3$) of compound **2l**.

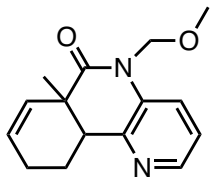

2m-2

5-(Methoxymethyl)-6a-methyl-6a,9,10,10a-tetrahydrobenzo[*c*][1,5]naphthyridin-6(5*H*)-one (2m-2). Using the general procedure detailed above, diene bromide **1m** (0.100 g, 0.297 mmol, 1.0 equiv) in DMF (3.6 mL, 0.08 M) was subjected to the Heck reaction conditions with 10 mol% NiI_2/15 mol% 2,2'-bipyridine for 6 h. The crude product was purified by column chromatography (silica, 10:1 hexanes: EtOAc) to afford **2m-2** (0.0635 g, 0.246 mmol) in 85% yield as a yellow oil.

^{1}H NMR (400 MHz, $CDCl_3$) δ 8.30 (dd, *J* = 4.8, 1.4 Hz, 1H), 7.54 (dd, *J* = 8.3, 1.4 Hz, 1H), 7.19 (dd, *J* = 8.3, 4.8 Hz, 1H), 5.91 (d, *J* = 1.5 Hz, 2H), 5.62 (d, *J* = 10.8 Hz, 1H), 5.04 (d, *J* = 10.8 Hz, 1H), 3.37 (s, 3H), 2.91 (dd, *J* = 12.9, 3.0 Hz, 1H), 2.26 – 2.20 (m, 1H), 2.19 – 2.14 (m, 1H), 1.98 – 1.91 (m, 1H), 1.69 – 1.62 (m, 1H), 1.27 (s, 3H).

^{13}C NMR (101 MHz, $CDCl_3$) δ_u 144.4, 129.8, 128.0, 122.4, 56.3, 47.0, 24.9; δ_d 174.8, 148.5, 133.5, 73.6, 42.5, 26.0, 24.7.

GC (Method B) t_R = 2.260 min. EI-MS m/z (%): 258.1 (M^+, 100), 243.0 (99), 227.0 (6), 211.0 (21), 205.0 (13), 197.0 (23), 185.0 (85), 171.0 (25), 156.0 (5), 144.0 (4), 131.0 (5), 91.0 (6), 77.0 (6).

HRMS (ESI) calculated for $C_{15}H_{19}O_2N_2$ $[M+H]^+$: 259.1447, found 259.1447.

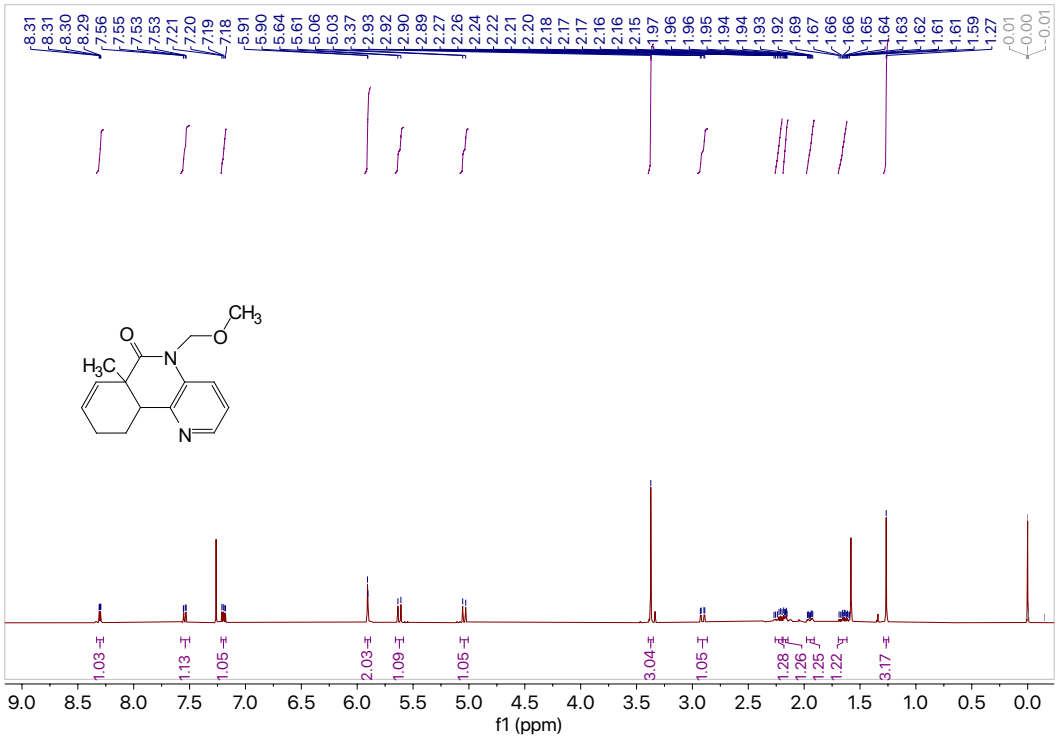

Figure 7.170 ^{1}H NMR (400 MHz, $CDCl_3$) of compound **2m-2**.

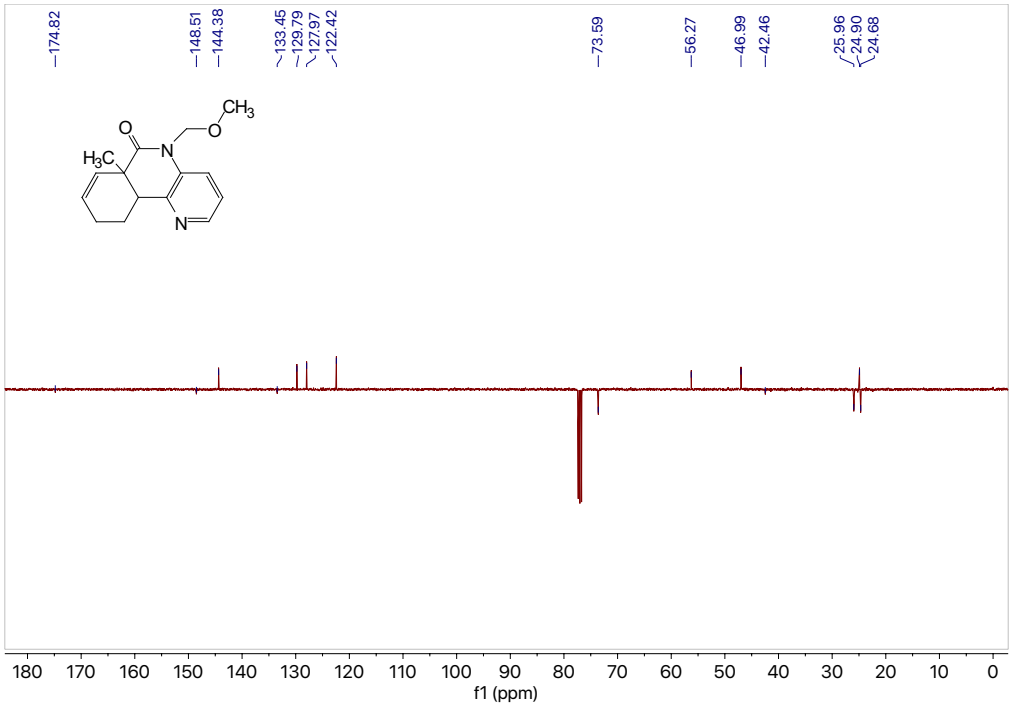

Figure 7.171 ^{13}C NMR (101 MHz, $CDCl_3$) of compound **2m-2**.

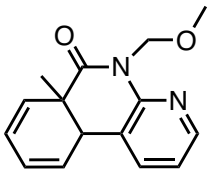

2n

5-(Methoxymethyl)-6a-methyl-6a,10a-dihydrobenzo[*c*][1,8]naphthyridin-6(5*H*)-one (2n).

Using the general procedure detailed above, diene bromide **1n** (0.0895 g, 0.267 mmol, 1.0 equiv) in DMF (3.2 mL, 0.08 M) was subjected to the Heck reaction conditions with 10 mol% NiI_2/15 mol% 2,2'-bipyridine for 5 h. The crude product was purified by column chromatography (silica, 4:1 hexanes: EtOAc) to afford **2n** (0.0542 g, 0.211 mmol) in 80% yield as a tan solid, m.p.= 124.9 – 126.0°C.

^{1}H NMR (400 MHz, $CDCl_3$) δ 8.37 (dd, *J* = 5.0, 1.8 Hz, 1H), 7.60 – 7.57 (m, 1H), 7.05 (dd, *J* = 7.4, 4.9 Hz, 1H), 6.17 – 6.07 (m, 2H), 5.92 – 5.88 (m, 1H), 5.73 (d, *J* = 9.6 Hz, 1H), 5.65 – 5.58 (m, 1H), 5.56 (d, *J* = 9.7 Hz, 1H), 3.51 (t, *J* = 3.1 Hz, 1H), 3.41 (s, 3H), 1.33 (s, 3H).

^{13}C NMR (101 MHz, $CDCl_3$) δ_u 147.0, 136.9, 131.3, 127.4, 125.9, 124.6, 119.3, 57.1, 42.7, 23.3; δ_d 175.1, 150.0, 121.3, 71.4, 41.2.

GC (Method B) t_R = 2.290 min. EI-MS m/z (%): 256.1 (M^+, 13), 241.0 (46), 224.0 (82), 211.0 (71), 195.0 (25), 181.0 (24), 167.0 (100), 153.0 (8), 142.0 (10), 133.0 (18), 129.1 (7), 121.0 (11), 115.0 (12), 109.0 (4), 91.0 (15), 79.0 (6), 65.0 (4).

HRMS (ESI) calculated for $C_{15}H_{17}O_2N_2$ $[M+H]^+$: 257.1290, found 257.1289.

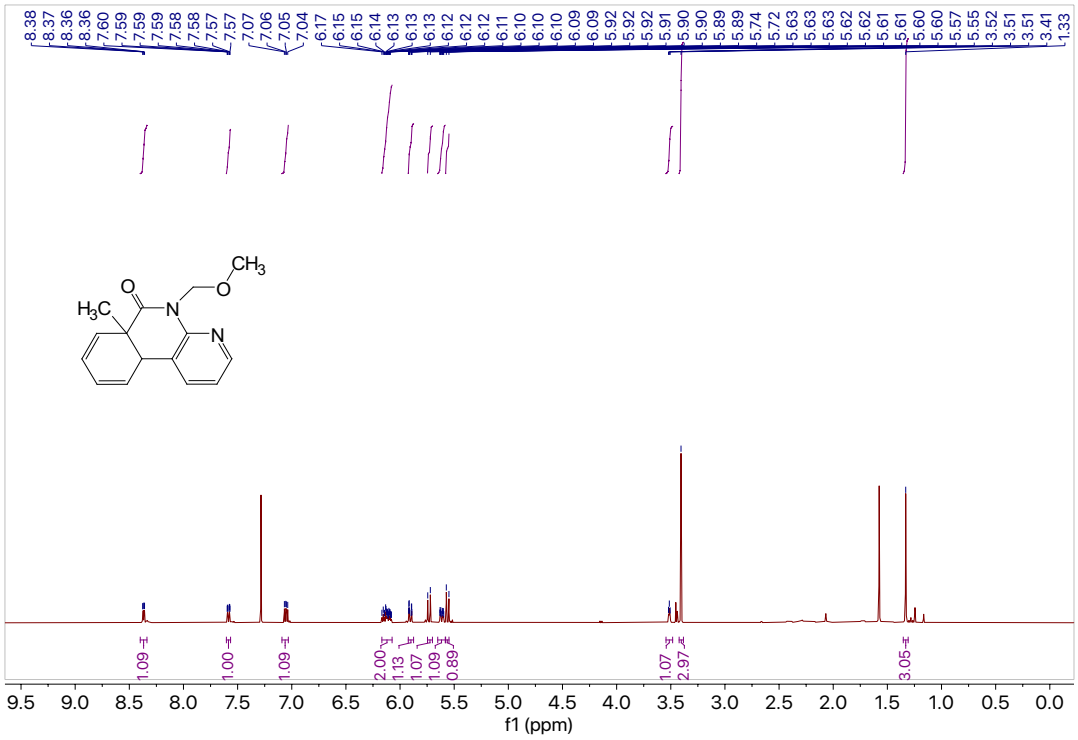

Figure 7.172 ^{1}H NMR (400 MHz, $CDCl_3$) of compound **2n**.

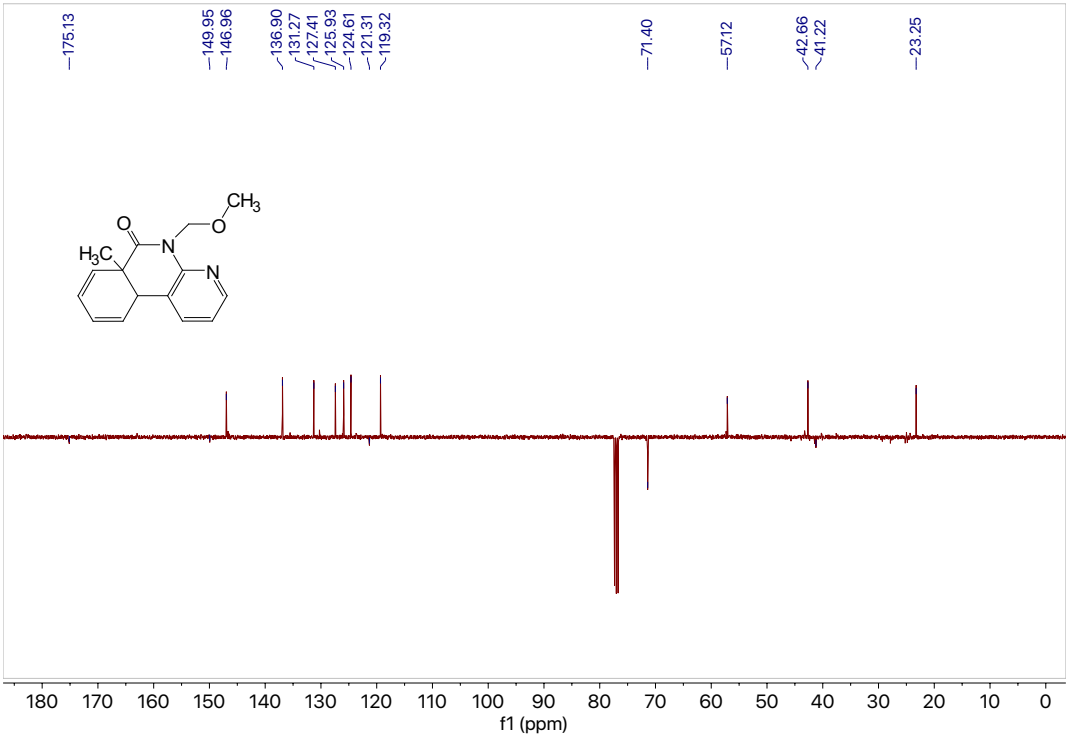

Figure 7.173 ^{13}C NMR (101 MHz, $CDCl_3$) of compound **2n**.

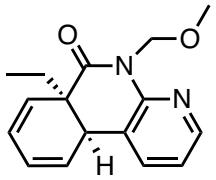

2o

(6aR,10aR)-6a-Ethyl-5-(methoxymethyl)-6a,10a-dihydrobenzo[c][1,8]naphthyridin-6(5H)-one (2o).

Racemic procedure:

Using the general procedure detailed above, diene bromide **1o** (0.151 g, 0.427 mmol, 1.0 equiv) in DMF (5.1 mL, 0.08 M) or diene iodide **1o-I** (0.100 g, 0.251 mmol, 1.0 equiv) in DMF (3 mL, 0.08 M) was subjected to the Heck reaction conditions with 10 mol% NiI_2/15 mol% 2,2'-bipyridine for 3h (**1o**) and 4 h (**1o-I**) respectively. The crude product was purified by column chromatography (silica, 4:1 hexanes: EtOAc) to afford **2o** (0.0873 g, 0.323 mmol) in 76% yield from **1o** or in 82% yield (0.0557 g, 0.206 mmol) from **1o-I** as a clear colorless oil.

Enantioselective procedure:

Using the general procedure detailed above, diene iodide **1o-I** (0.0198 g, 0.0502 mmol, 1.0 equiv) in DMF (0.6 mL, 0.08 M) was subjected to the Heck reaction conditions with 10 mol% NiI_2/15 mol% *t*Bu-^{6}F*i*Quinox (**L26**) for 2.5 h. The crude product was purified by column chromatography (silica, 10:1 hexanes: EtOAc) to afford **2o** (0.0103 g, 0.0381 mmol) with an enantiomeric ratio of 7:1 (76% e.e.) in 76% yield as a clear colorless oil.

$[\boldsymbol{\alpha}]_{\boldsymbol{D}}^{\boldsymbol{20}}$**=** +73 (*c* 0.16, $CHCl_3$).

^{1}H NMR (400 MHz, $CDCl_3$) δ 8.27 (dd, *J* = 4.9, 1.8 Hz, 1H), 7.48 (dd, *J* = 7.3, 0.6 Hz, 1H), 6.96 (dd, *J* = 7.4, 4.9 Hz, 1H), 6.16 – 6.08 (m, 1H), 6.05 – 5.95 (m, 1H), 5.91 – 5.83 (m, 1H), 5.65 (d, *J* = 9.7 Hz, 1H), 5.49 – 5.40 (m, 2H), 3.62 – 3.56 (m, 1H), 3.31 (s, 3H), 1.65 – 1.59 (m, 1H), 1.49 – 1.43 (m, 1H), 0.85 (t, *J* = 7.5 Hz, 3H).

^{13}C NMR (101 MHz, $CDCl_3$) δ_u 146.9, 136.9, 129.6, 127.6, 125.9, 125.3, 119.3, 57.1, 39.7, 9.1; δ_d 174.8, 150.1, 121.3, 71.4, 45.4, 28.1.

GC (Method B) t_R = 2.626 min. EI-MS m/z (%): 270.1 (M^+, 10), 255.1 (24), 238.1 (100), 225.1 (53), 209.1 (25), 197.0 (52), 181.1 (36), 167.1 (50), 154.0 (16), 140.0 (8), 132.0 (14), 127.0 (19), 121.0 (19), 115.0 (6), 91.0 (10), 77.0 (7).

HRMS (ESI) calculated for $C_{16}H_{19}O_2N_2$ $[M+H]^+$: 271.1447, found 271.1445.

HPLC: Chiralcel OD-H, n-hexane/isopropanol=85:15, flow rate=1 mL/min, I=254 nm, t_{R1} = 11.17 min. (minor), t_{R2} = 12.18 min. (major).

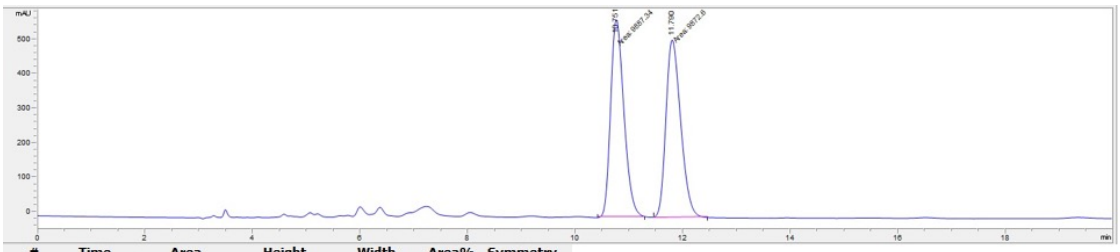

#	Time	Area	Height	Width	Area%	Symmetry
1	10.751	9887.3	573.2	0.2875	50.037	0.723
2	11.79	9872.6	516	0.3189	49.963	0.718

Figure 7.174 Chiral LC for racemic **2o** sample.

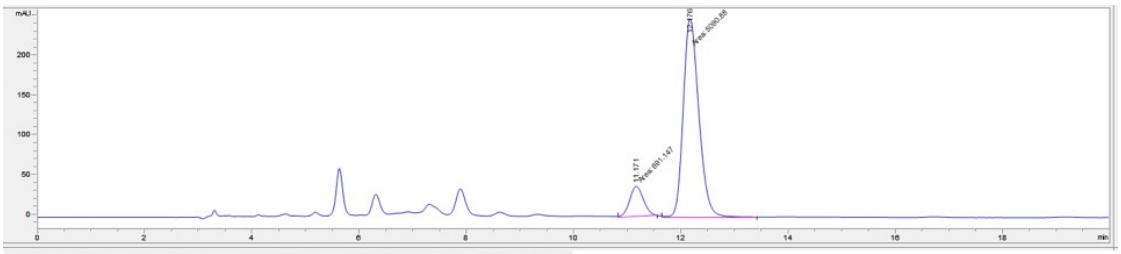

#	Time	Area	Height	Width	Area%	Symmetry
1	11.171	691.1	37.8	0.3044	11.953	0.897
2	12.176	5090.9	249.3	0.3403	88.047	0.757

Figure 7.175 Chiral LC for enantioselective **2o** crude reaction (with **L26**).

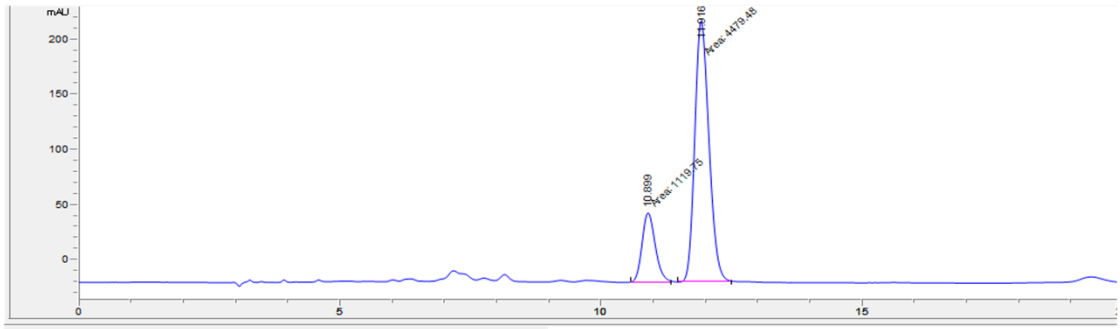

#	Time	Area	Height	Width	Area%	Symmetry
1	10.899	1119.7	63.3	0.2947	19.998	0.815
2	11.916	4479.5	237.1	0.3149	80.002	0.787

Figure 7.176 Chiral LC for enantioselective **2o** reaction (with **L27**).

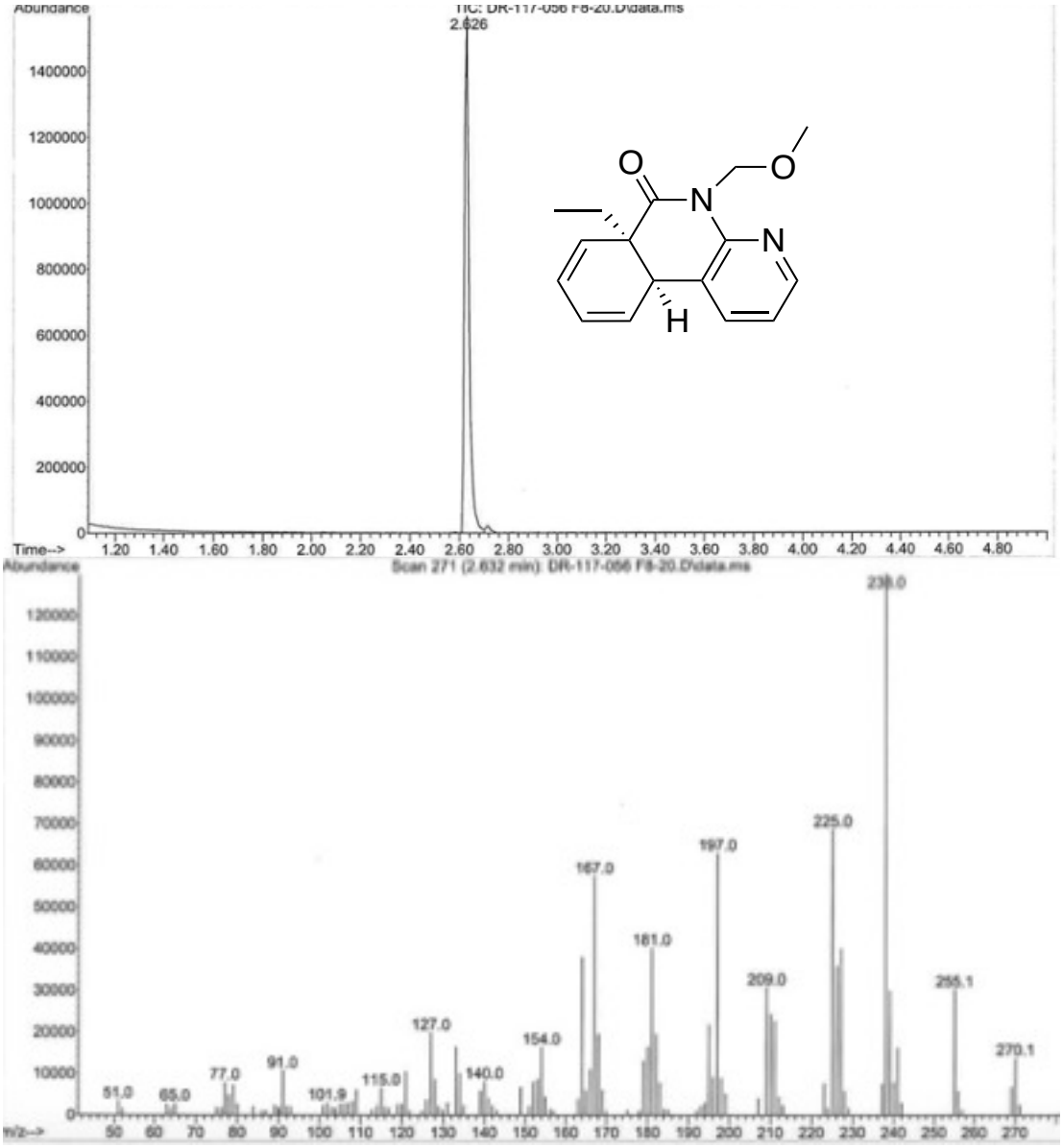

Figure 7.177 GCMS data of compound **2o**.

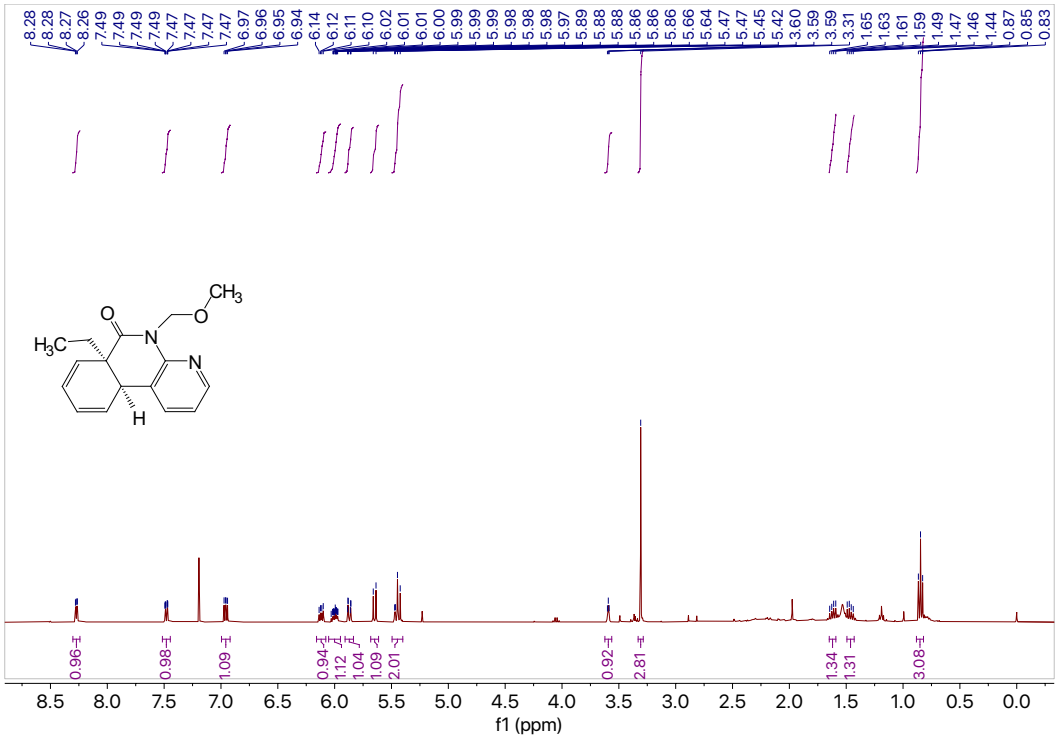

Figure 7.178 ^{1}H NMR (400 MHz, $CDCl_3$) of compound **2o**.

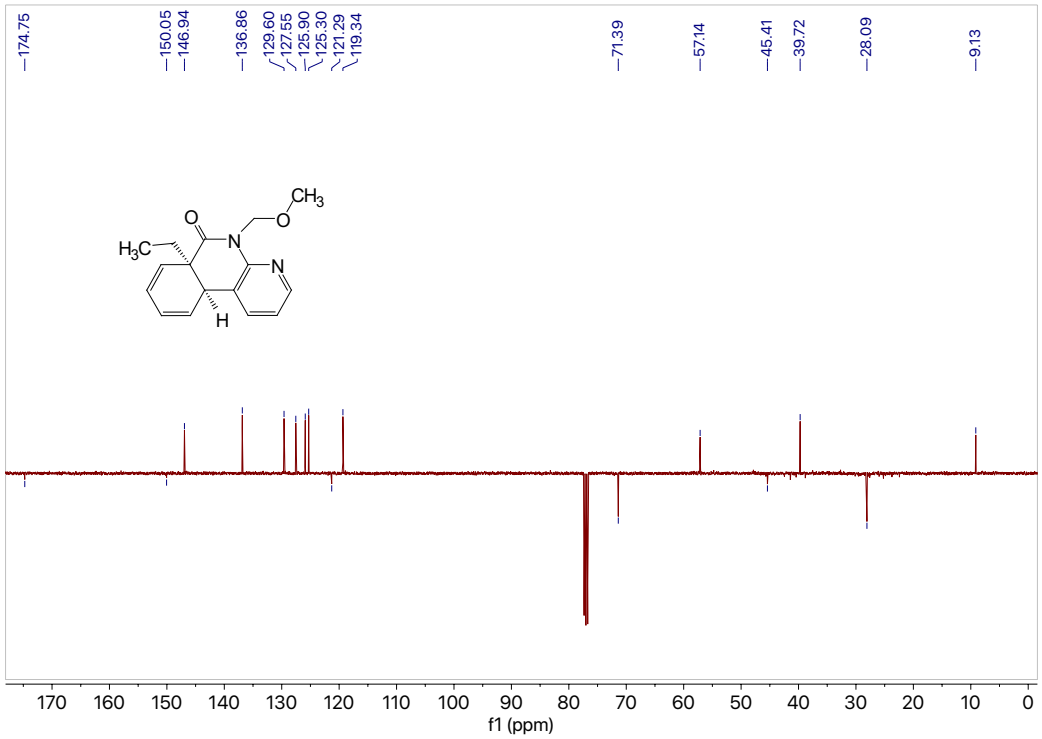

Figure 7.179 ^{13}C NMR (101 MHz, $CDCl_3$) of compound **2o**.

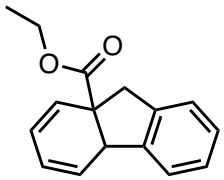

2s

Ethyl 4b,9-dihydro-8a*H*-fluorene-8a-carboxylate (2s). Using the general procedure detailed above, diene iodide **S1g** (0.199 g, 0.543 mmol, 1.0 equiv) in DMF (6.5 mL, 0.08 M) was subjected to the Heck reaction conditions with 10 mol% NiI_2/15 mol% 2,2'-bipyridine for 3 h. The crude product was purified by column chromatography (silica, 4:1 hexanes: EtOAc) to afford **2s** (0.0947 g, 0.394 mmol) in 73% yield as a clear colorless oil. Spectral data were in accordance with a prior literature report.[11]

^{1}H NMR (400 MHz, $CDCl_3$) δ 7.24 – 7.15 (m, 4H), 6.07 – 5.98 (m, 1H), 5.95 – 5.86 (m, 2H), 5.80 – 5.72 (m, 1H), 4.48 (d, J = 4.9 Hz, 1H), 4.18 (q, J = 7.1 Hz, 2H), 3.58 (d, J = 15.9 Hz, 1H), 3.15 (d, J = 15.9 Hz, 1H), 1.26 (t, J = 7.1 Hz, 4H).

^{13}C NMR (101 MHz, $CDCl_3$) δ_u 128.2, 127.1, 127.0, 126.8, 124.0, 123.7, 123.2, 121.1, 46.2, 14.2. δ_d 175.2, 144.3, 139.8, 61.2, 46.0.

GC (Method B) t_R = 1.676 min. EI-MS m/z (%): 240.1 (12, M+), 167.1 (100), 152.0 (13), 139.0 (4), 115.0 (4).

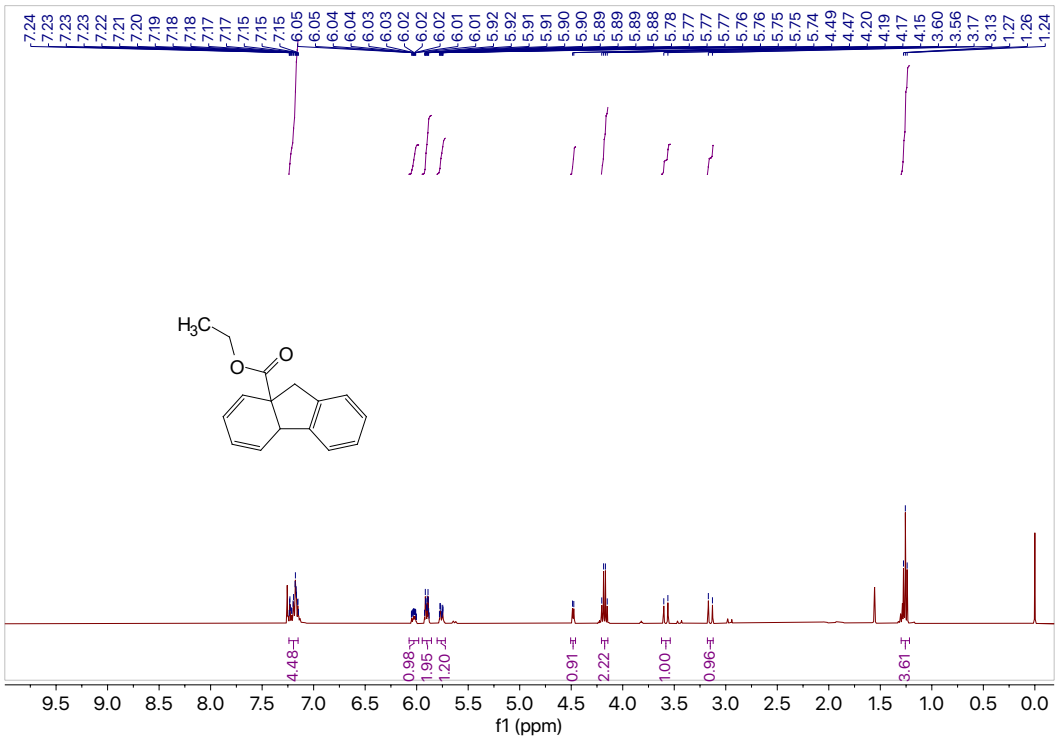

Figure 7.180 ^{1}H NMR (400 MHz, $CDCl_3$) of compound **2s**.

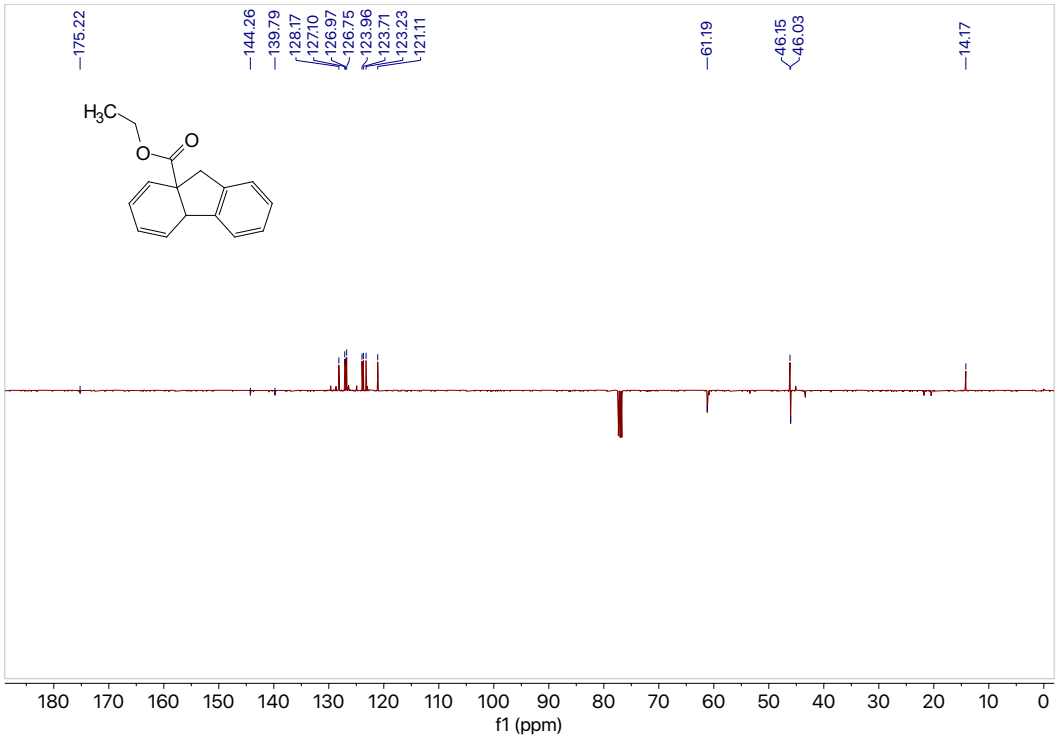

Figure 7.181 ^{13}C NMR (101 MHz, $CDCl_3$) of compound **2s**.

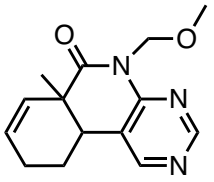

2p-2

5-(methoxymethyl)-6a-methyl-6a,9,10,10a-tetrahydropyrimido[4,5-*c*]isoquinolin-6(5*H*)-one (2p-2). Using the general procedure detailed above, diene bromide **S2p** (0.033 g, 0.0975 mmol, 1.0 equiv) in DMF (1.17 mL, 0.08 M) was subjected to the Heck reaction conditions with 10 mol% Ni/15 mol% 2,2'-bipyridine for 6 h. The crude product was purified by column chromatography (silica, 4:1 hexanes: EtOAc) to afford **2p-2** (0.0175 g, 0.0675 mmol) in 70% yield (66% purity by GCMS) as a yellow oil.

^{1}H NMR (400 MHz, $CDCl_3$) δ 8.89 (s, 1H), 8.48 (s, 1H), 5.91 (s, 2H), 5.67 (d, J = 9.7 Hz, 1H), 5.48 – 5.45 (m, 1H), 3.43 (s, 3H), 2.74 (dd, J = 12.6, 3.3 Hz, 1H), 2.20 – 2.16 (m, 2H), 1.79 – 1.75 (m, 2H), 1.25 (s, 3H).
GC (Method B) t_R = 2.483 min. EI-MS m/z (%): 259.1 (M^+, 2), 244.1 (55), 229.1 (7), 216.0 (100), 198.0 (10), 186.0 (17), 172.0 (7), 160.0 (3), 148.0 (6), 134.0 (4), 115.0 (5), 91.0 (4), 77.0 (4).

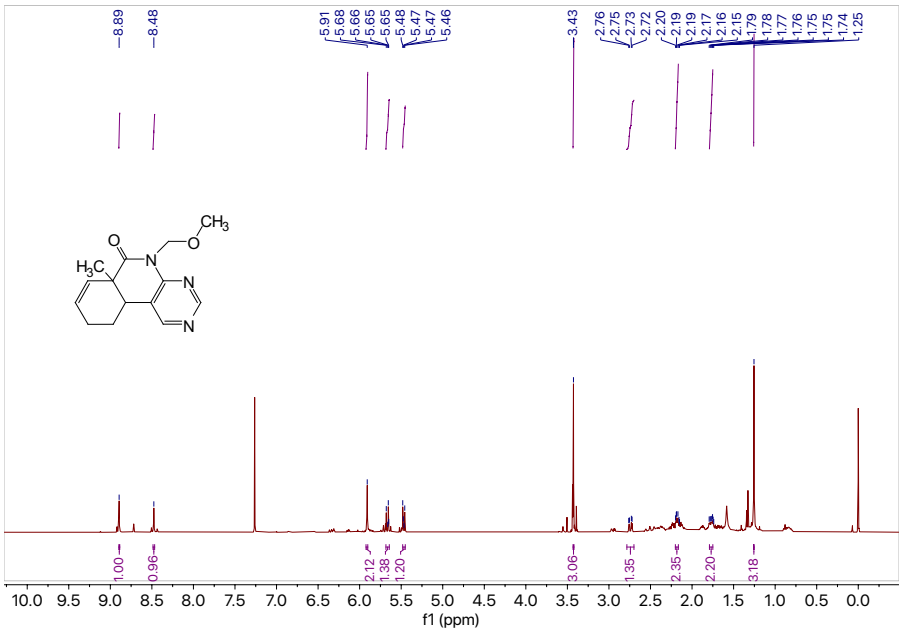

Figure 7.182 ^{1}H NMR (400 MHz, $CDCl_3$) of compound **2p-2**.

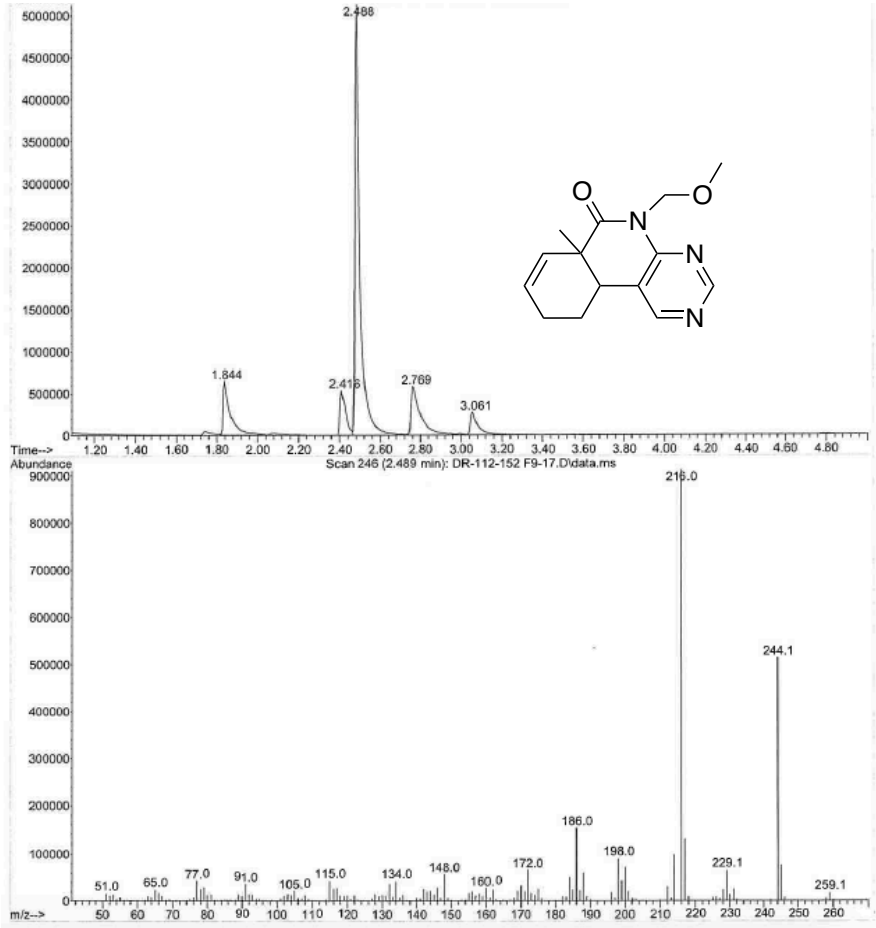

Figure 7.183 GCMS data of compound **2p-2**.

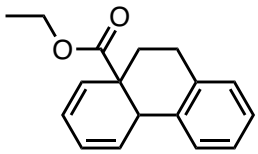

2t

Ethyl 9,10-dihydrophenanthrene-8a(4b*H*)-carboxylate (2t): Using the general procedure detailed above, diene iodide **S1h** (0.101 g, 0.262 mmol, 1.0 equiv) in DMF (3.3 mL, 0.08 M) was subjected to the Heck reaction conditions with 10 mol% Ni/15 mol% 2,2'-bipyridine for 6 h. The crude product was purified by column chromatography (silica, 4:1 hexanes: EtOAc) to afford **2t** (0.0479 g, 0.188 mmol) in 72% yield (80% purity by GCMS) as a clear colorless oil.

^{1}H NMR (400 MHz, $CDCl_3$) δ 8.04 (dd, *J* = 7.9, 1.5 Hz, 1H), 7.48 (td, *J* = 7.5, 1.5 Hz, 1H), 7.19 – 7.14 (m, 2H), 6.01 – 5.95 (m, 2H), 5.84 – 5.81 (m, 1H), 5.78 – 5.75 (m, 1H), 4.14 (dd, *J* = 7.1, 2.4 Hz, 2H), 3.09 (t, *J* = 6.4 Hz, 1H), 2.78 – 2.72 (m, 2H), 2.14 (t, *J* = 6.4 Hz, 2H), 1.20 (t, *J* = 7.1 Hz, 3H).
^{13}C NMR (101 MHz, $CDCl_3$) δ_u 133.3, 128.8, 128.4, 127.1, 126.8, 126.5, 126.3, 123.7, 39.4, 14.1; δ_d 175.2, 137.9, 134.8, 61.0, 36.5, 26.6, 24.9.
GC (Method B) t_R = 2.002 min. EI-MS m/z (%): 254.1 (M^+, 1), 210 (36), 192.0 (45), 178.0 (10), 165.0 (20), 152.0 (10), 133.0 (32), 118.0 (48), 103.0 (14), 91.0 (100), 77.0 (14), 65.0 (10), 51.0 (6).
HRMS (ESI) calculated for $C_{17}H_{19}O_2$ $[M+H]^+$: 255.1385, found 255.1384.

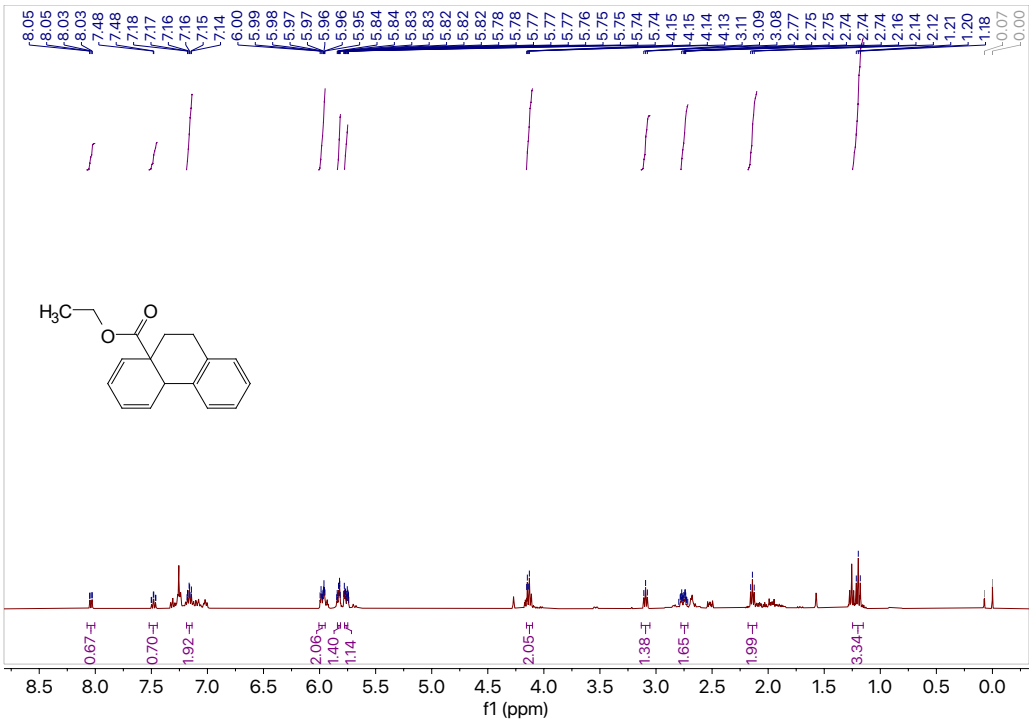

Figure 7.184 ^{1}H NMR (400 MHz, $CDCl_3$) of compound **2t**.

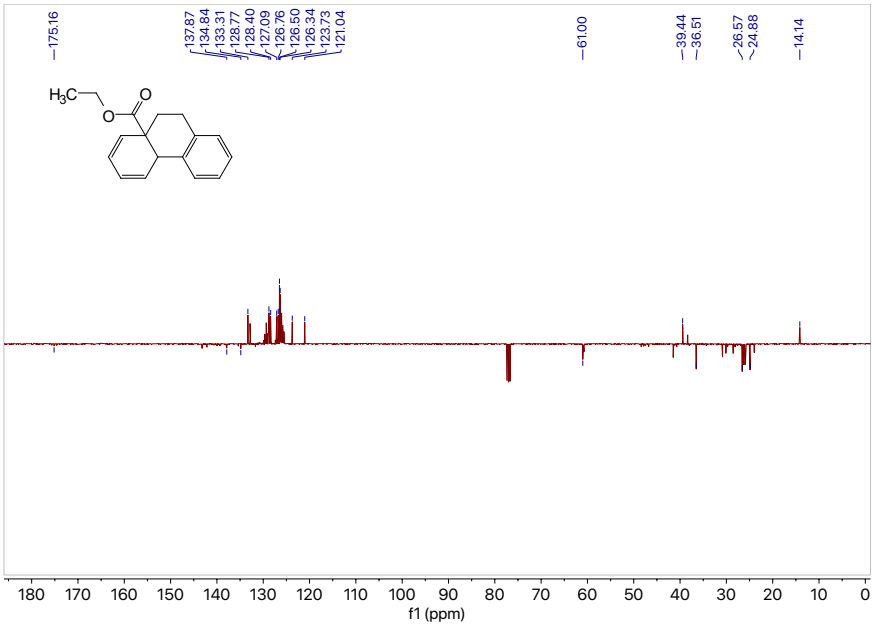

Figure 7.185 ^{13}C NMR (101 MHz, $CDCl_3$) of compound **2t**.

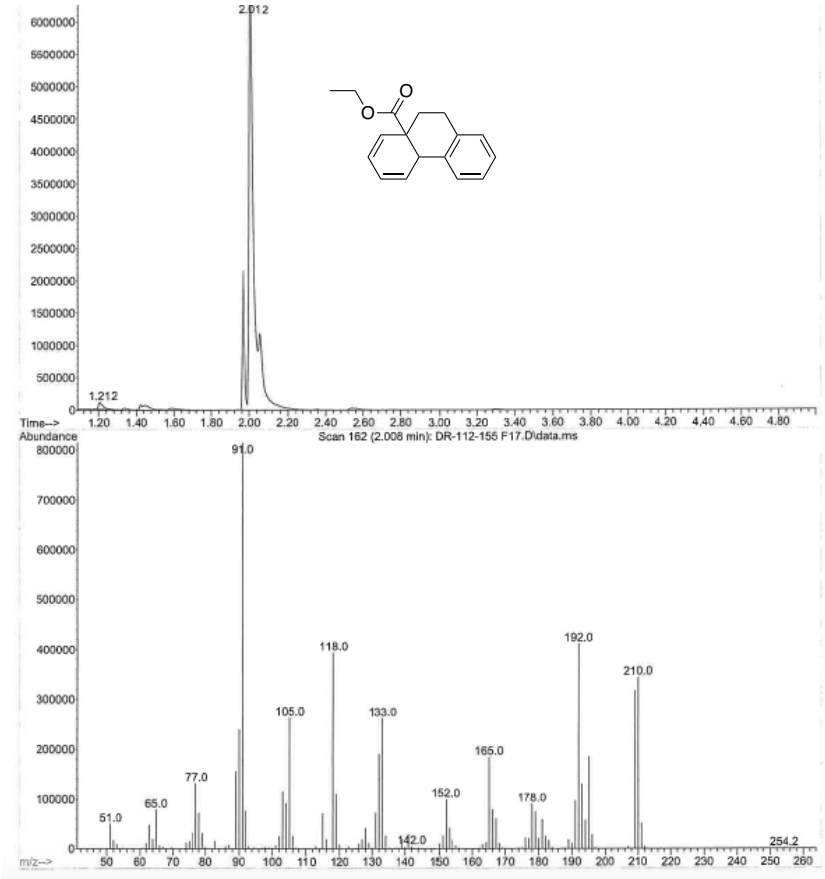

Figure 7.186 GCMS data of compound **2t**.

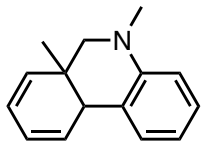

2w

5,6a-dimethyl-5,6,6a,10a-tetrahydrophenanthridine (2w). Using the general procedure detailed above, diene bromide **1w** (0.0331 g, 0.113 mmol, 1.0 equiv) in DMF (1.4 mL, 0.08 M) was subjected to the Heck reaction conditions with 10 mol% Ni/15 mol% 2,2'-bipyridine for 6 h. The crude product was purified by column chromatography (silica, 9:1 hexanes: EtOAc) to afford **2w** (0.0202 g, 0.0956 mmol) in 85% yield (76% purity by GCMS) as a light green oil.

^{1}H NMR (400 MHz, $CDCl_3$) δ 7.05 (ddd, *J* = 8.5, 7.1, 1.7 Hz, 1H), 6.99 (dd, *J* = 8.0, 1.6 Hz, 1H), 6.62 (td, *J* = 7.4, 1.2 Hz, 1H), 6.55 (d, *J* = 8.2 Hz, 1H), 5.87 – 5.81 (m, 1H), 5.65 (dp, *J* = 2.8, 1.0 Hz, 2H), 5.41 (dq, *J* = 9.5, 1.0 Hz, 1H), 3.30 (s, 1H), 3.19 (d, *J* = 11.0 Hz, 1H), 2.83 (s, 3H), 2.49 (dd, *J* = 11.2, 1.3 Hz, 1H), 1.03 (s, 3H).
^{13}C NMR (101 MHz, $CDCl_3$) δ_u 134.2, 129.6, 127.3, 124.0, 121.0, 116.9, 111.1, 43.9, 39.3, 25.0; δ_d 145.51, 123.72, 55.3.
GC (Method B) t_R = 1.499 min. EI-MS m/z (%): 211.0 (M^+, 100), 196.0 (40), 180.0 (18), 165.9 (16), 151.9 (7), 143.9 (5), 131.0 (5), 117.9 (12), 104.1 (3), 90.9 (45), 76.9 (7).

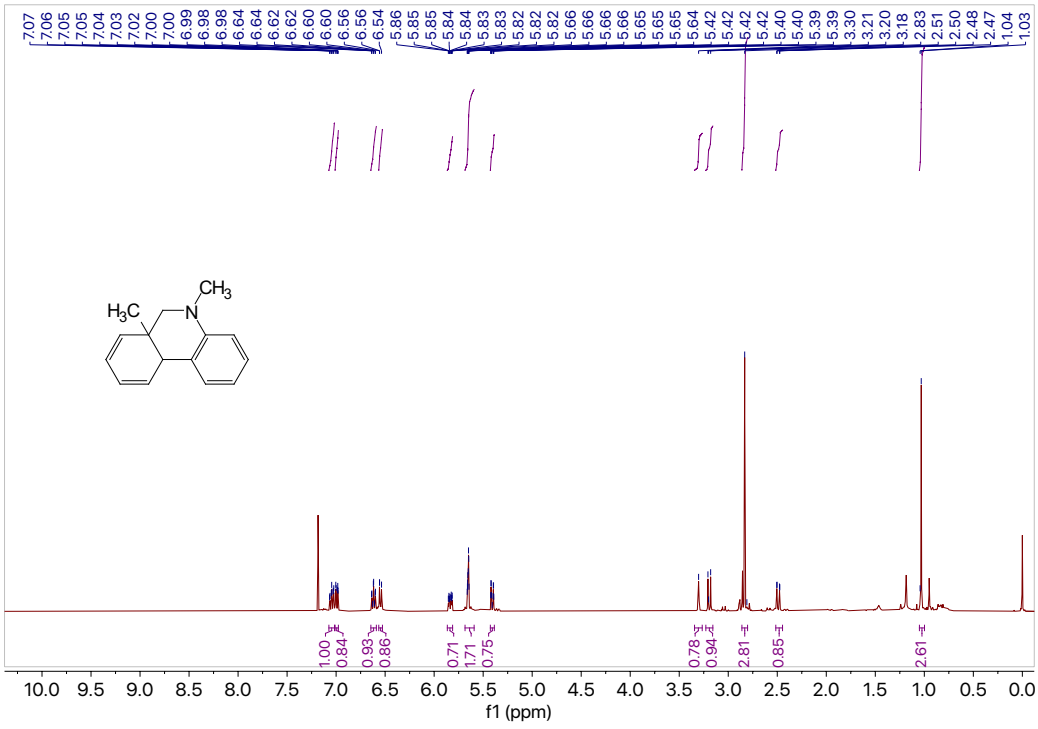

Figure 7.187 ^{1}H NMR (400 MHz, $CDCl_3$) of compound **2w**.

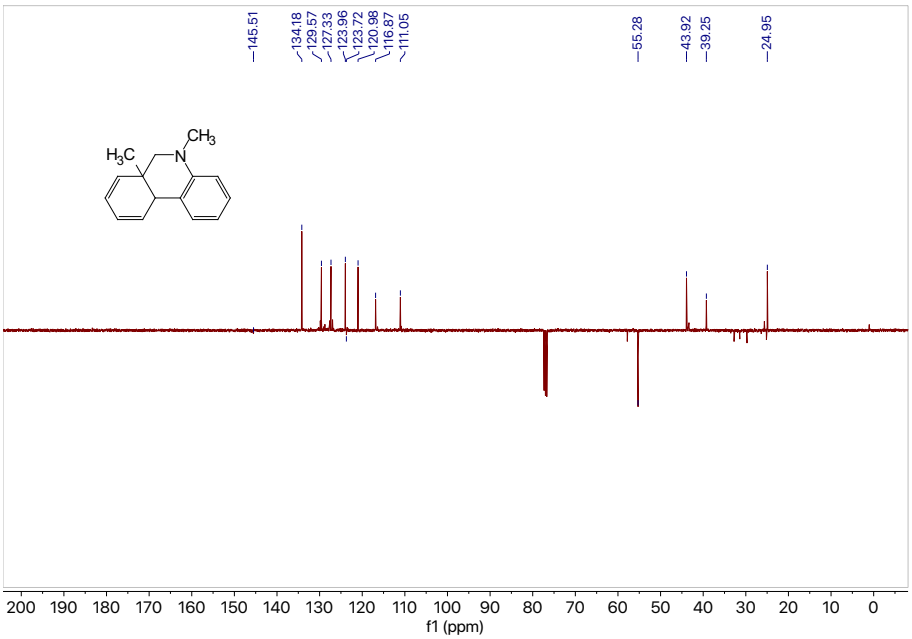

Figure 7.188 ^{13}C NMR (101 MHz, $CDCl_3$) of compound **2w**.

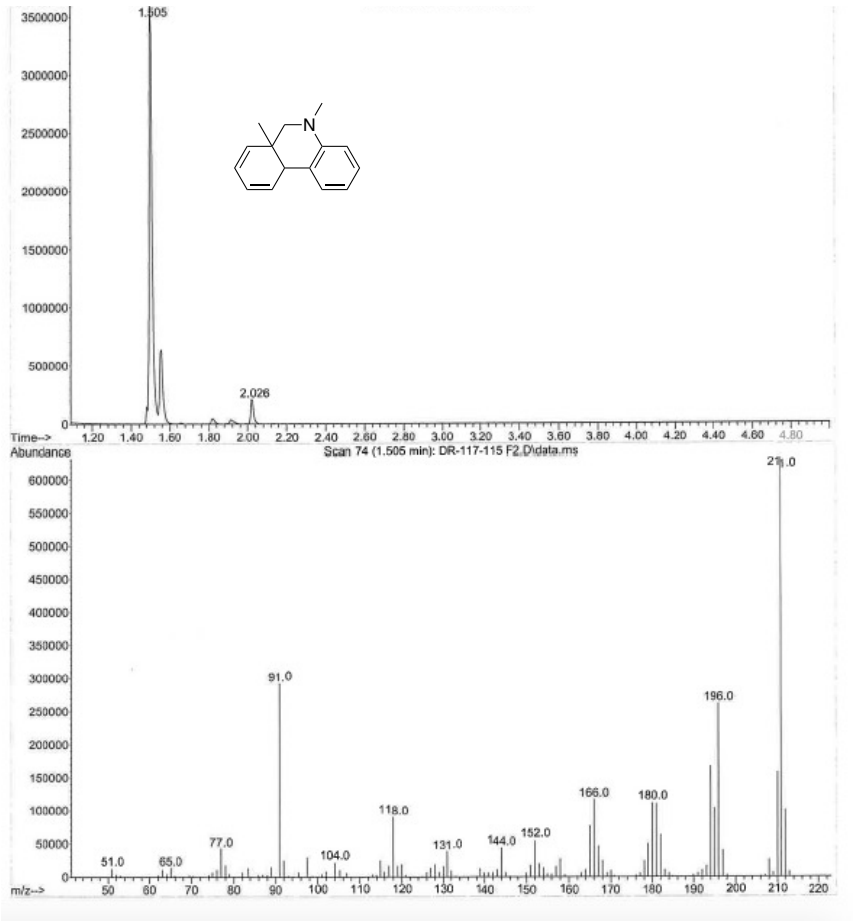

Figure 7.189 GCMS data of compound **2w**.

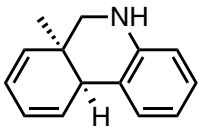

2x

(6a*R*,10a*S*)-6a-methyl-5,6,6a,10a-tetrahydrophenanthridine (2x).

Racemic procedure:

Using the general procedure detailed above, diene iodide **S2x-I** (0.0302 g, 0.0923 mmol, 1.0 equiv) in DMF (1.9 mL, 0.08 M) was subjected to the Heck reaction conditions with 10 mol% Ni/15 mol% 2,2'-bipyridine for 2 h. The crude product **2x** was delivered in 70% purity by GCMS as a yellow oil.

Enantioselective procedure:

Using the general procedure detailed above, diene iodide **S2x-I** (0.0998 g, 0.308 mmol, 1.0 equiv) in DMF (3.7 mL, 0.08 M) was subjected to the Heck reaction conditions with 10 mol% NiI_2/15 mol% *t*Bu-$^6CH_3$*i*Quinox (**L27**) for 2 h. The crude product was purified by column chromatography (silica, 9:1 hexanes: EtOAc) to afford **2x** (0.0316 g, 0.160 mmol) with an enantiomeric ratio of 49:1 (96% e.e.) in 52% yield (65% purity by GCMS) as a yellow oil

^{1}H NMR (400 MHz, $CDCl_3$) δ 6.99 (dt, *J* = 7.6, 1.1 Hz, 1H), 6.95 – 6.89 (m, 1H), 6.62 (td, *J* = 7.4, 1.2 Hz, 1H), 6.43 (dd, *J* = 8.0, 1.2 Hz, 1H), 5.86 – 5.80 (m, 1H), 5.68 (dd, *J* = 3.0, 1.0 Hz, 2H), 5.45 – 5.41 (m, 1H), 3.29 (s, 1H), 3.20 (d, *J* = 11.1 Hz, 1H), 2.63 – 2.56 (m, 1H), 1.04 (s, 3H).

^{13}C NMR (101 MHz, $CDCl_3$) δ_u 133.4, 132.9, 128.9, 126.0, 122.9, 120.1, 116.8, 113.3, 44.9, 40.1, 23.6; δ_d 142.5, 121.6, 42.2.

GC (Method B) t_R = 1.537 min. EI-MS m/z (%): 197.0 (M^+, 100), 182.0 (38), 167.0 (19), 151.9 (8), 130.0 (5), 115.0 (4), 103.9 (31), 90.2 (5), 77.9 (10).

HPLC: Chiralcel OD-H, n-hexane/isopropanol=97.5:2.5, flow rate=1 mL/min, I=254 nm, t_{R1} = 6.73 min. (major), t_{R2} = 7.59 min. (minor).

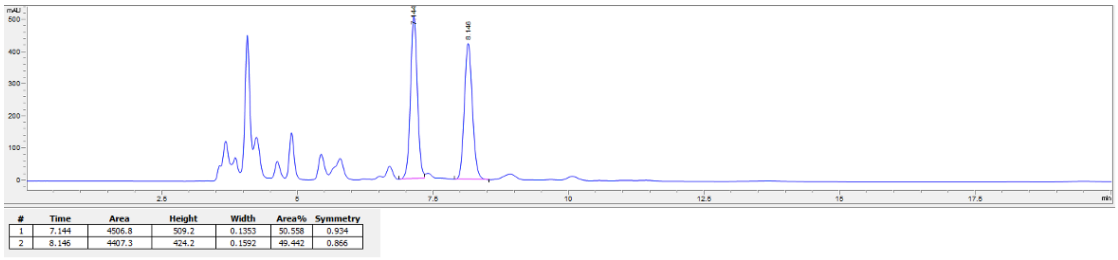

#	Time	Area	Height	Width	Area%	Symmetry
1	7.144	4506.8	509.2	0.1353	50.558	0.934
2	8.146	4407.3	424.2	0.1592	49.442	0.866

Figure 7.190 Chiral LC for crude racemic **2x** sample.

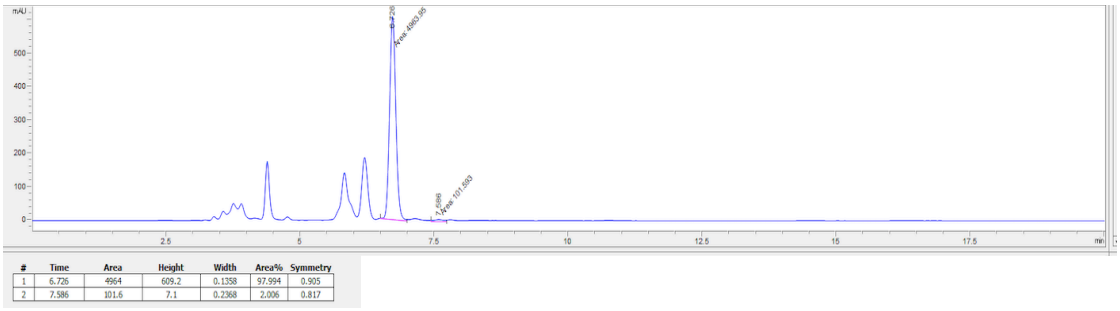

#	Time	Area	Height	Width	Area%	Symmetry
1	6.726	4964	609.2	0.1358	97.994	0.905
2	7.586	101.6	7.1	0.2368	2.006	0.817

Figure 7.191 Chiral LC for enantioselective **2x** reaction.

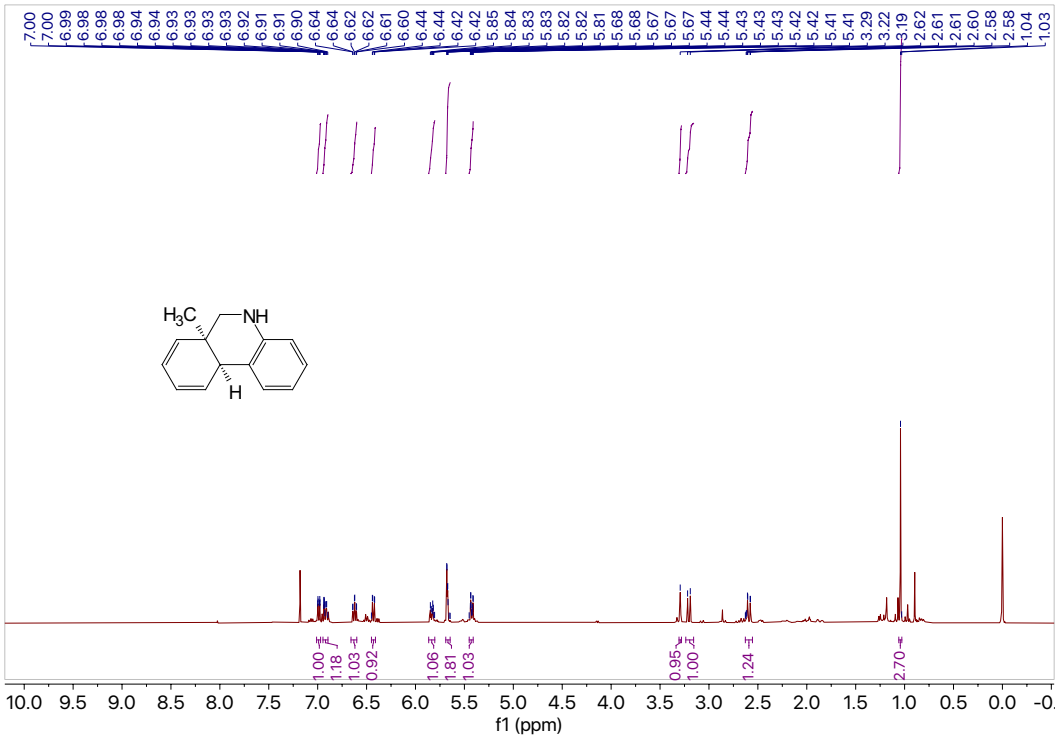

Figure 7.192 ^{1}H NMR (400 MHz, $CDCl_3$) of compound **2x**.

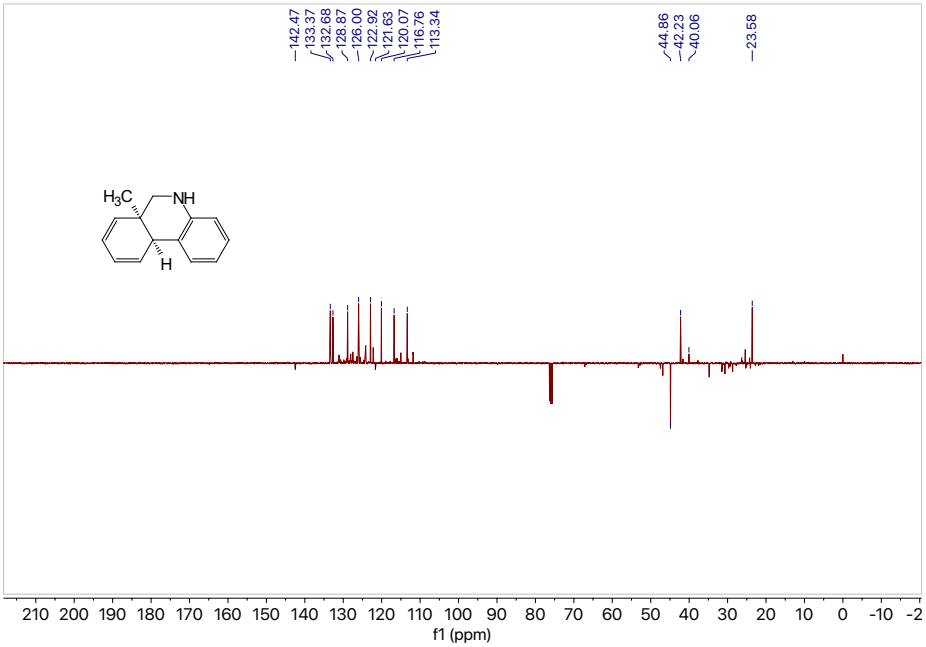

Figure 7.193 ^{13}C NMR (101 MHz, $CDCl_3$) of compound **2x**.

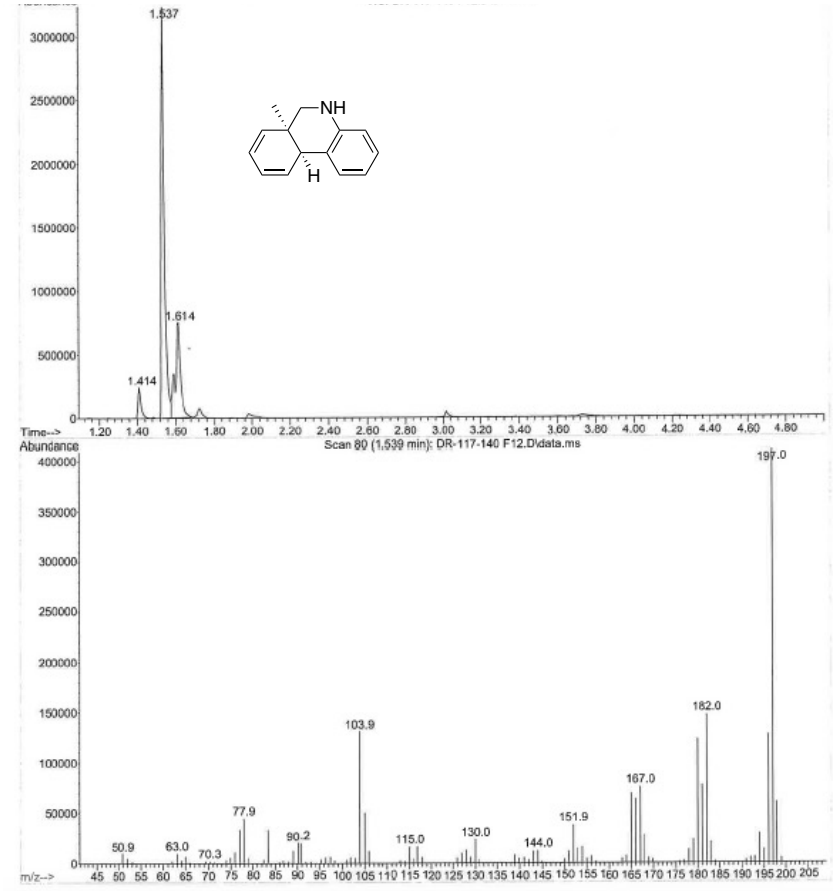

Figure 7.194 GCMS data of compound **2x**.

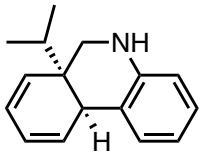

2y

(6a*R*,10a*S*)-6a-isopropyl-5,6,6a,10a-tetrahydrophenanthridine (2y).

Racemic procedure:

Using the general procedure detailed above, diene iodide **S2y-I** (0.0501 g, 0.142 mmol, 1.0 equiv) in DMF (1.7 mL, 0.08 M) was subjected to the Heck reaction conditions with 10 mol% Ni/15 mol% 2,2'-bipyridine for 3 h. The crude product was purified by column chromatography (silica, 9:1 hexanes: EtOAc) to afford **2y** (0.0210 g, 0.0932 mmol) in 66% yield as a yellow oil.

Enantioselective procedure:

Using the general procedure detailed above, diene iodide **S2y-I** (0.0806 g, 0.226 mmol, 1.0 equiv) in DMF (2.7 mL, 0.08 M) was subjected to the Heck reaction conditions with 10 mol% NiI_2/15 mol% *t*Bu-$^6CH_3$*i*Quinox (**L27**) for 3 h. The crude product was purified by column chromatography (silica, 9:1 hexanes: EtOAc) to afford **2y** (0.0428 g, 0.190 mmol) with an enantiomeric ratio of 39:1 (95% e.e.) in 84% yield (75% purity by GCMS) as a yellow oil.

^{1}H NMR (400 MHz, $CDCl_3$) δ 7.02 – 6.98 (m, 1H), 6.94 (td, *J* = 7.6, 1.6 Hz, 1H), 6.63 (dd, *J* = 7.4, 1.2 Hz, 1H), 6.45 (dd, *J* = 8.0, 1.2 Hz, 1H), 5.92 – 5.85 (m, 1H), 5.64 (ddt, *J* = 4.5, 2.3, 1.2 Hz, 2H), 5.50 (dd, *J* = 9.8, 1.1 Hz, 1H), 3.69 (s, 1H), 3.24 (d, *J* = 11.6 Hz, 1H), 2.81 (dd, *J* = 11.6, 1.5 Hz, 1H), 1.69 (dq, *J* = 13.8, 6.8 Hz, 1H), 0.92 (d, *J* = 6.8 Hz, 3H), 0.83 (d, *J* = 6.9 Hz, 3H).

^{13}C NMR (101 MHz, $CDCl_3$) δ_u 135.0, 130.2, 128.4, 127.0, 124.9, 120.6, 117.9, 114.3, 40.3, 29.4, 19.4, 16.7; δ_d 144.2, 123.0, 41.6, 38.8.

GC (Method B) t_R = 2.030 min. EI-MS m/z (%): 225.0 (M^+, 100), 210.0 (18), 194.0 (7), 182.0 (63), 165.0 (19), 152.0 (17), 143.0 (4), 130.0 (7), 117.0 (4), 104.0 (34), 78.0 (10).

HPLC: Chiralcel OD-H, n-hexane/isopropanol=97.5:2.5, flow rate=1 mL/min, I=254 nm, t_{R1} = 7.12 min. (minor), t_{R2} = 8.77 min. (major).

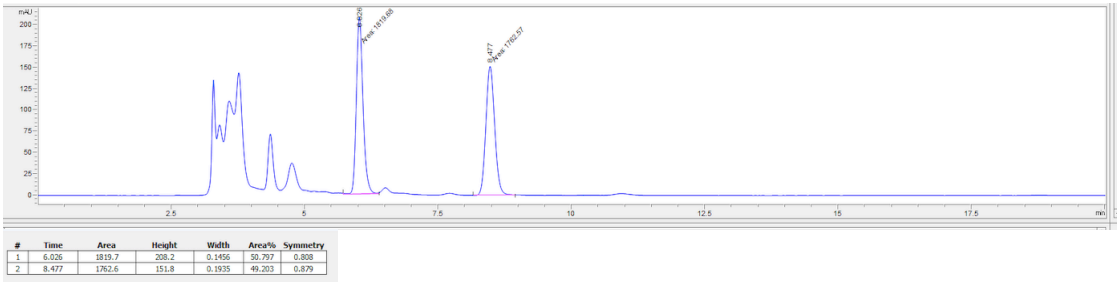

#	Time	Area	Height	Width	Area%	Symmetry
1	6.026	1819.7	208.2	0.1456	50.797	0.808
2	8.477	1762.6	151.8	0.1935	49.203	0.879

Figure 7.195 Chiral LC for crude racemic **2y** sample.

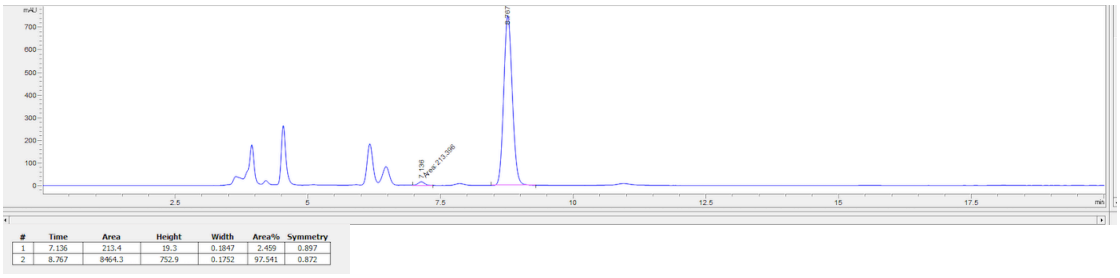

#	Time	Area	Height	Width	Area%	Symmetry
1	7.136	213.4	19.3	0.1847	2.459	0.897
2	8.767	8464.3	752.9	0.1752	97.541	0.872

Figure 7.196 Chiral LC for enantioselective **2y** reaction.

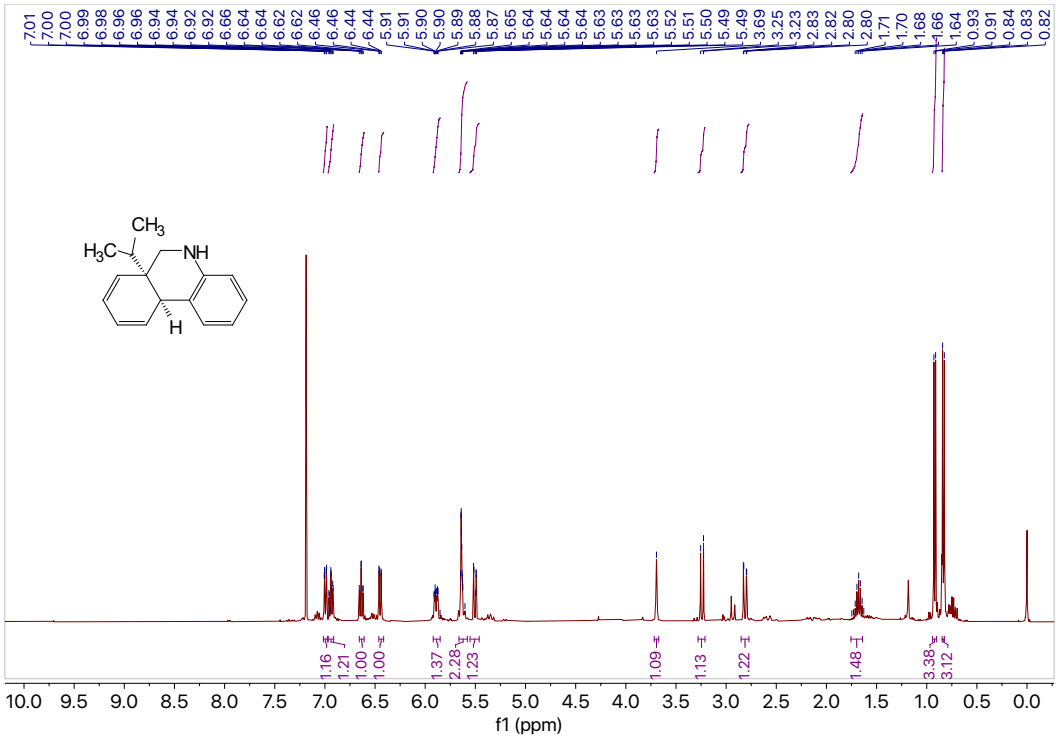

Figure 7.197 ^{1}H NMR (400 MHz, $CDCl_3$) of compound **2y**.

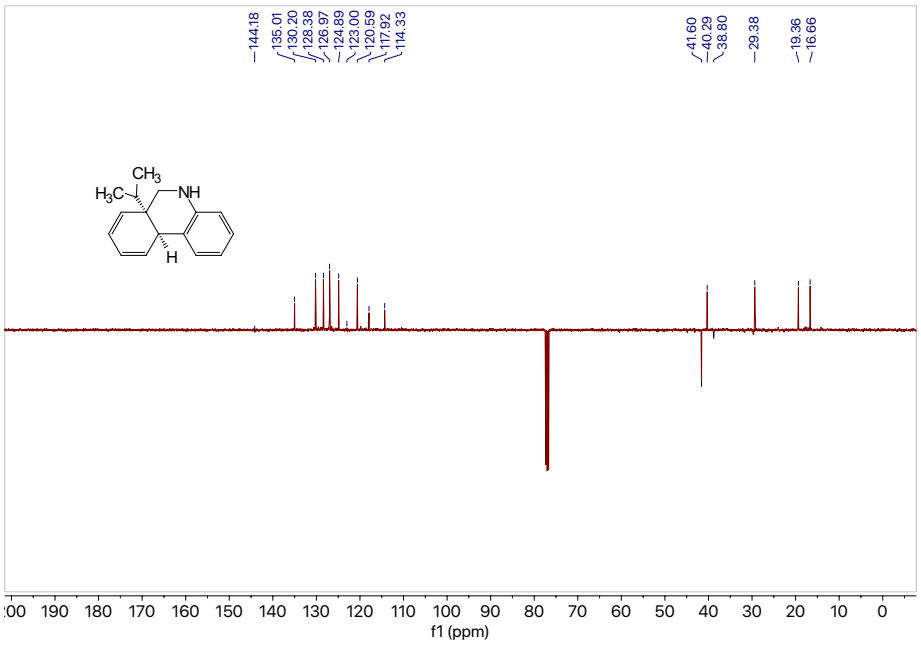

Figure 7.198 ^{13}C NMR (101 MHz, $CDCl_3$) of compound **2y**.

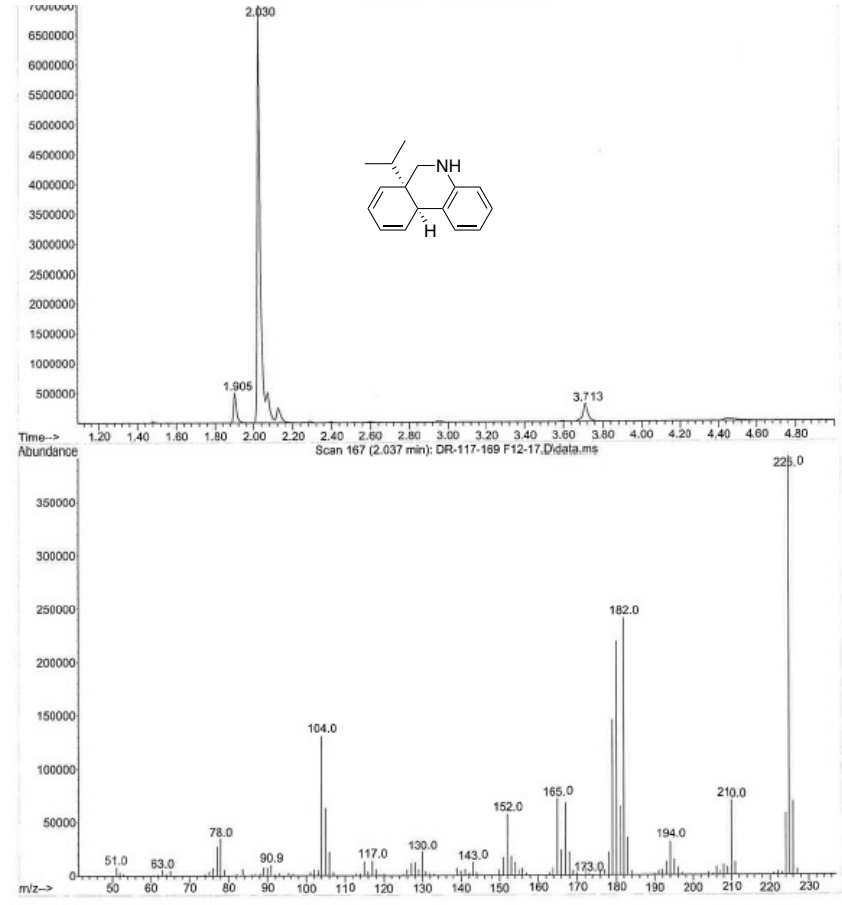

Figure 7.199 GCMS data of compound **2y**.

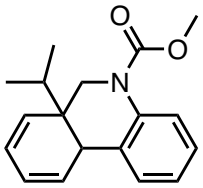

2ye

Methyl 6a-isopropyl-6a,10a-dihydrophenanthridine-5(6*H*)-carboxylate (2ye). Using the general procedure detailed above, diene iodide **1ye-I** (0.0323 g, 0.0914 mmol, 1.0 equiv) in DMF (1.1 mL, 0.08 M) was subjected to the Heck reaction conditions with 10 mol% Ni/15 mol% 2,2'-bipyridine for 4 h. The crude product **2ye** was delivered in 40% purity by GCMS as a yellow oil.

GC (Method B) t_R = 2.809 min. EI-MS m/z (%): 283.1 (M^+, 70), 268.0 (16), 250.1 (15), 240.0 (21), 224.0 (13), 208.0 (100), 190.0 (24), 180.0 (80), 165.0 (21), 152.0 (23), 132.0 (4), 115.0 (4), 105.0 (3), 91.0 (10), 77.0 (12), 59.0 (5).

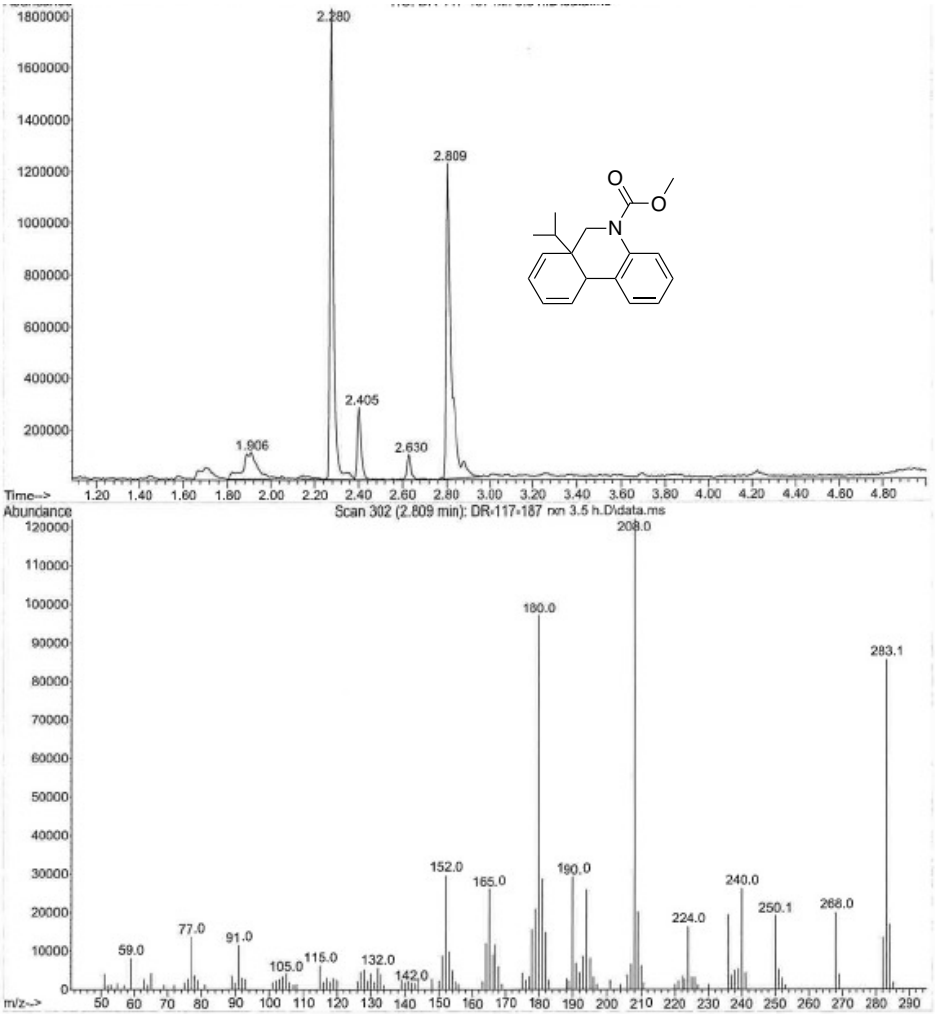

Figure 7.200 GCMS data of compound **2ye**.

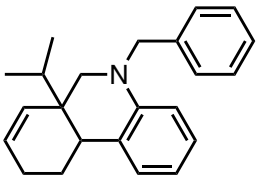

2yf-2

5-benzyl-6a-isopropyl-5,6,6a,9,10,10a-hexahydrophenanthridine (2yf-2). Using the general procedure detailed above, diene iodide **1yf-I** (0.0175 g, 0.0395 mmol, 1.0 equiv) in DMF (0.5 mL, 0.08 M) was subjected to the Heck reaction conditions with 10 mol% Ni/15 mol% 2,2'-bipyridine for 2 h. The crude product **2yf-2** was delivered in 59% purity by GCMS as a yellow oil.

GC (Method A) t_R = 17.285 min. EI-MS m/z (%): 317.2 (M^+, 100), 274.1 (33), 262.1 (12), 226.1 (24), 196.0 (10), 182.0 (31), 167.0 (12), 152.0 (5), 130.0 (7), 115.0 (5), 91.0 (81), 77.0 (5), 65.0 (8).

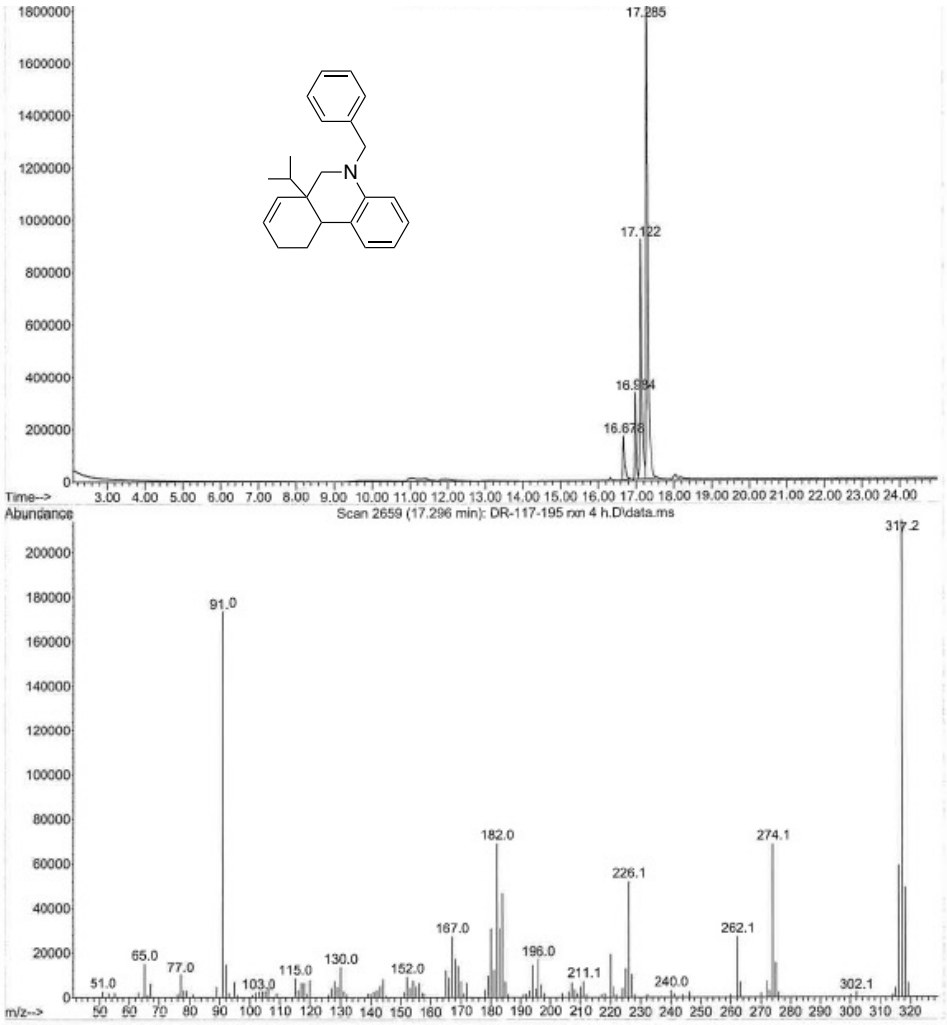

Figure 7.201 GCMS data of compound **2yf-2**.

7.10 Chiral ligand screening – HPLC data

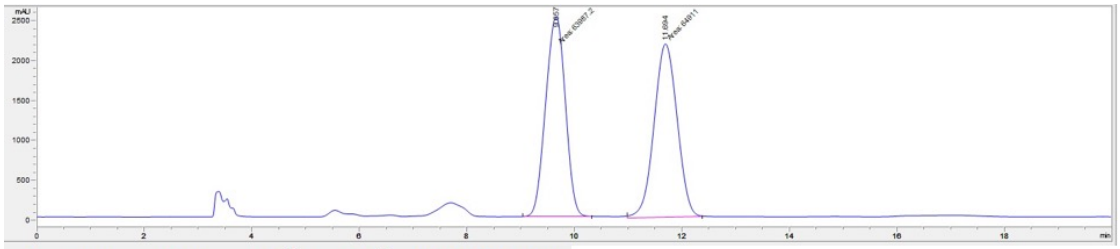

#	Time	Area	Height	Width	Area%	Symmetry
1	9.657	63987.2	2496.4	0.4272	49.642	1.083
2	11.694	64911	2165.8	0.4995	50.358	0.965

Figure 7.202 Chiral LC for racemic **2d** sample with bipy (reference).

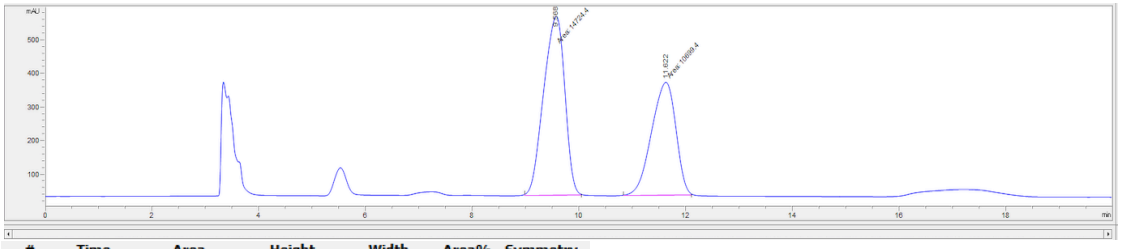

#	Time	Area	Height	Width	Area%	Symmetry
1	9.568	14724.4	533.5	0.46	57.916	1.433
2	11.622	10699.4	336.7	0.5296	42.084	1.38

Figure 7.203 Chiral LC for enantioselective **2d** reaction with **L1**.

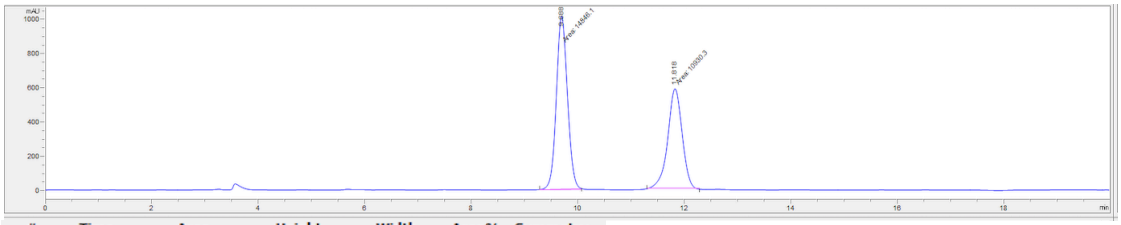

#	Time	Area	Height	Width	Area%	Symmetry
1	9.688	14846.1	1016.1	0.2435	57.596	0.92
2	11.818	10930.3	583.8	0.312	42.404	1.046

Figure 7.204 Chiral LC for enantioselective **2d** reaction with **L1** reaction (at 60 ˚C).

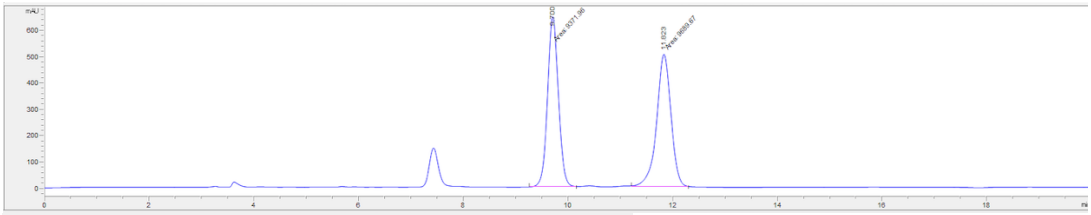

#	Time	Area	Height	Width	Area%	Symmetry
1	9.7	9372	649.7	0.2404	49.167	0.889
2	11.823	9689.7	506.1	0.3191	50.833	1.014

Figure 7.205 Chiral LC for enantioselective **2d** reaction with **L3**.

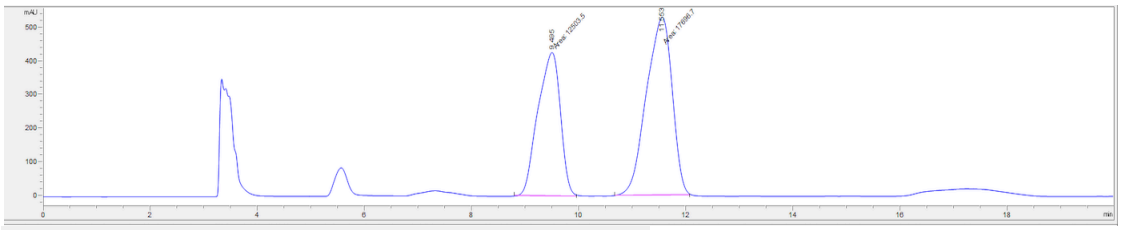

#	Time	Area	Height	Width	Area%	Symmetry
1	9.495	12503.5	427.5	0.4874	41.402	1.579
2	11.553	17696.7	529.1	0.5575	58.598	1.533

Figure 7.206 Chiral LC for enantioselective **2d** reaction with **L4**.

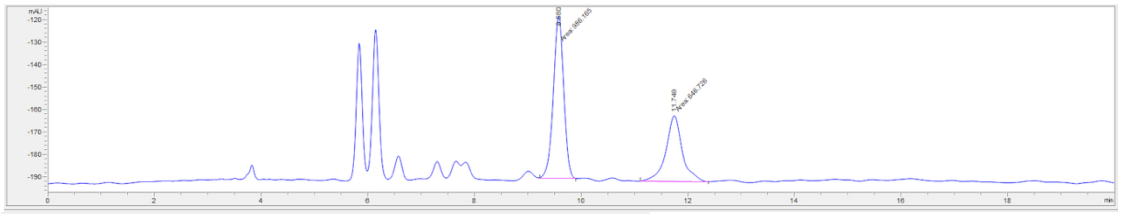

#	Time	Area	Height	Width	Area%	Symmetry
1	9.58	986.2	72.3	0.2274	60.394	1.007
2	11.749	646.7	29.5	0.3653	39.606	0.997

Figure 7.207 Chiral LC for enantioselective crude **2d** reaction with **L5**.

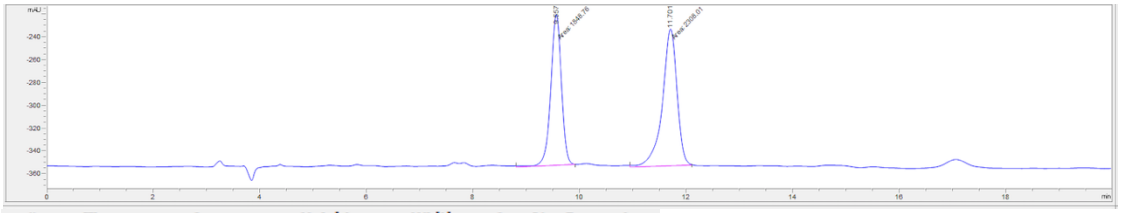

#	Time	Area	Height	Width	Area%	Symmetry
1	9.557	1848.8	132.3	0.2329	44.476	1.072
2	11.701	2308	120	0.3206	55.524	1.256

Figure 7.208 Chiral LC for enantioselective **2d** reaction with **L6**.

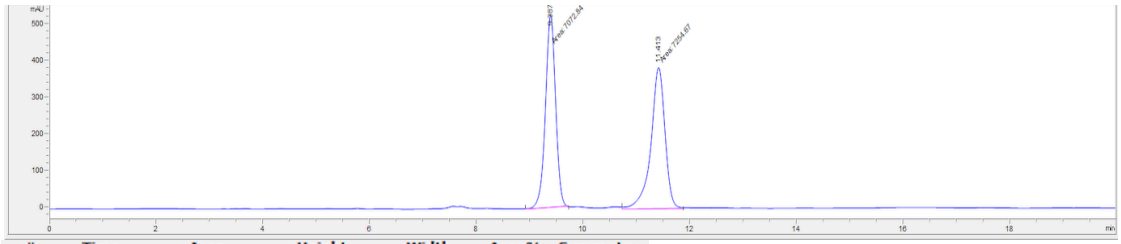

#	Time	Area	Height	Width	Area%	Symmetry
1	9.387	7072.8	528.3	0.2231	49.365	1.065
2	11.413	7254.7	388.4	0.3113	50.635	1.194

Figure 7.209 Chiral LC for enantioselective **2d** reaction with **L7**.

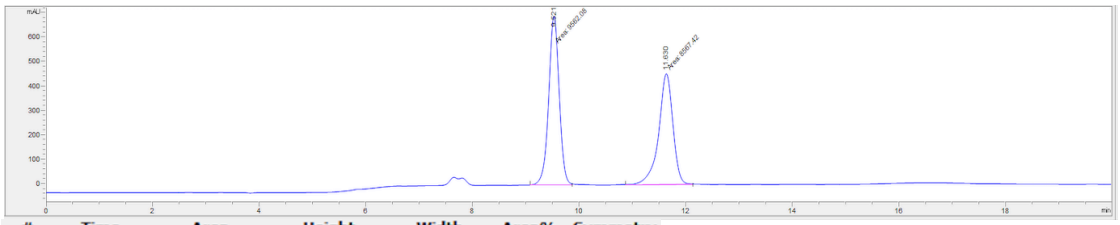

#	Time	Area	Height	Width	Area%	Symmetry
1	9.521	9562.1	692	0.2303	52.743	0.962
2	11.63	8567.4	453.9	0.3146	47.257	1.176

Figure 7.210 Chiral LC for enantioselective **2d** reaction with **L8**.

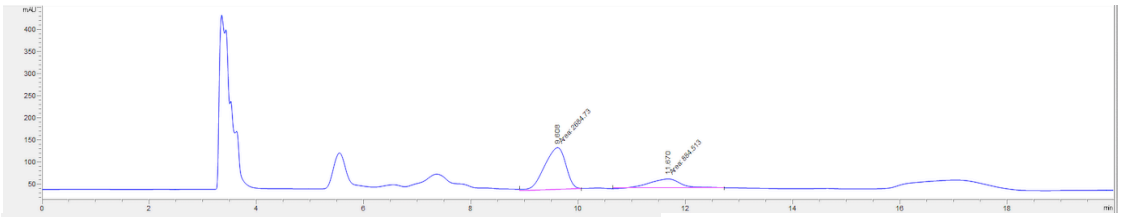

#	Time	Area	Height	Width	Area%	Symmetry
1	9.584	8941.4	322.1	0.4626	50.138	1.418
2	11.638	8892.1	278.8	0.5315	49.862	1.373

Figure 7.211 Chiral LC for enantioselective crude **2d** reaction with **L9**.

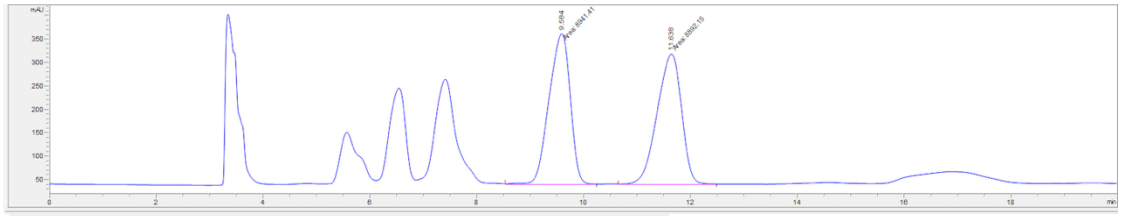

#	Time	Area	Height	Width	Area%	Symmetry
1	9.584	8941.4	322.1	0.4626	50.138	1.418
2	11.638	8892.1	278.8	0.5315	49.862	1.373

Figure 7.212 Chiral LC for enantioselective crude **2d** reaction with **L10**.

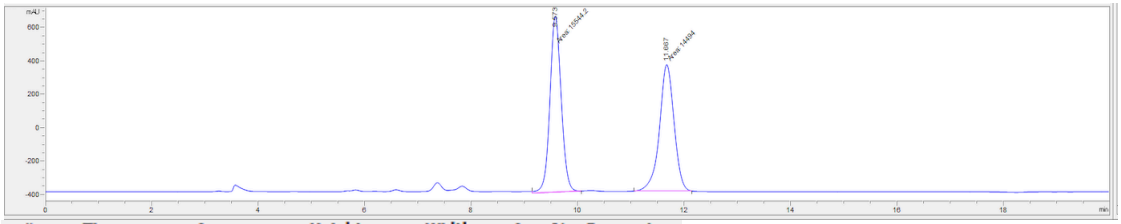

#	Time	Area	Height	Width	Area%	Symmetry
1	9.573	15544.2	1052	0.2463	51.748	0.881
2	11.667	14494	755.7	0.3196	48.252	0.968

Figure 7.213 Chiral LC for enantioselective **2d** reaction with **L11**.

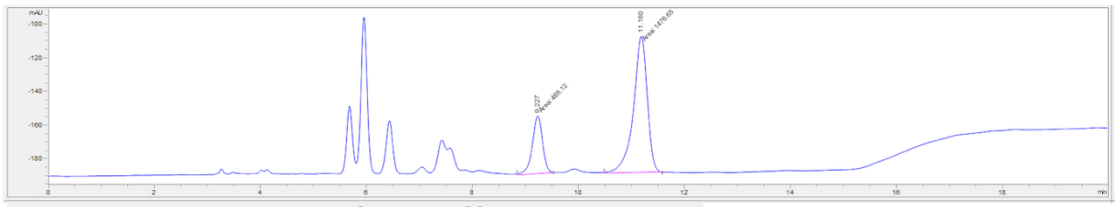

#	Time	Area	Height	Width	Area%	Symmetry
1	9.227	468.1	34.4	0.227	24.071	1.122
2	11.18	1476.7	80.8	0.3047	75.929	1.289

Figure 7.214 Chiral LC for enantioselective crude **2d** reaction with **L12**.

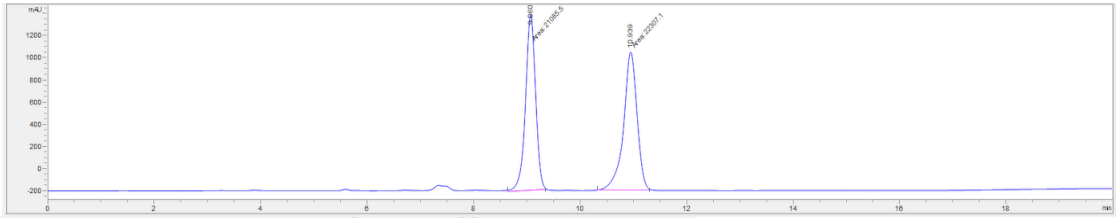

#	Time	Area	Height	Width	Area%	Symmetry
1	9.06	21085.5	1588.7	0.2212	48.592	0.999
2	10.939	22307.1	1252.1	0.2969	51.408	1.097

Figure 7.215 Chiral LC for enantioselective crude **2d** reaction with **L13**.

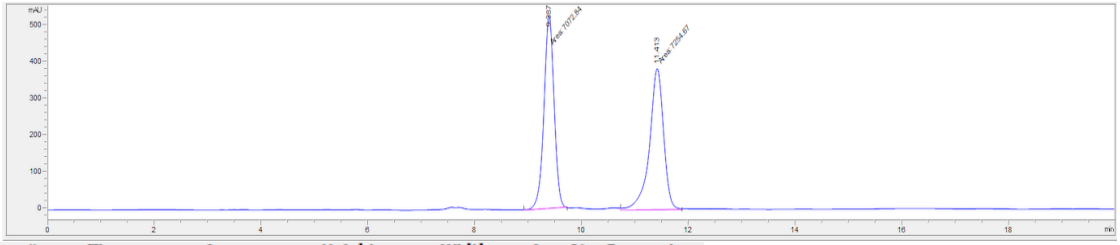

#	Time	Area	Height	Width	Area%	Symmetry
1	9.387	7072.8	528.3	0.2231	49.365	1.065
2	11.413	7254.7	388.4	0.3113	50.635	1.194

Figure 7.216 Chiral LC for enantioselective **2d** reaction with **L16**.

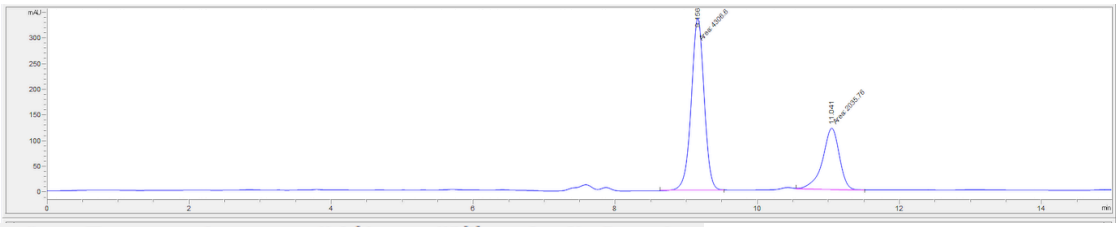

#	Time	Area	Height	Width	Area%	Symmetry
1	9.156	4306.6	338	0.2124	67.902	1.033
2	11.041	2035.8	120.7	0.2811	32.098	1.123

Figure 7.217 Chiral LC for enantioselective **2d** reaction with **L18**.

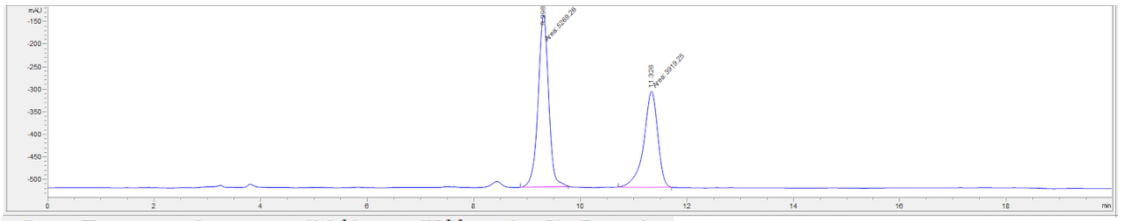

#	Time	Area	Height	Width	Area%	Symmetry
1	9.298	5269.3	381.1	0.2304	57.346	1.02
2	11.326	3919.2	212.8	0.307	42.654	1.269

Figure 7.218 Chiral LC for enantioselective **2d** reaction with **L19**.

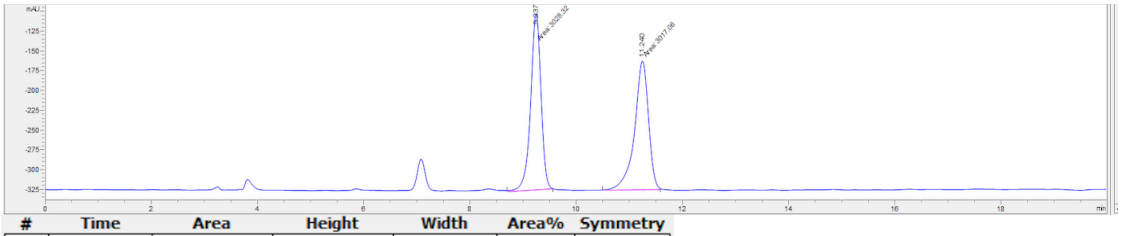

#	Time	Area	Height	Width	Area%	Symmetry
1	9.237	3028.3	222.6	0.2267	50.093	1.102
2	11.24	3017.1	162.8	0.3088	49.907	1.314

Figure 7.219 Chiral LC for enantioselective **2d** reaction with **L20**.

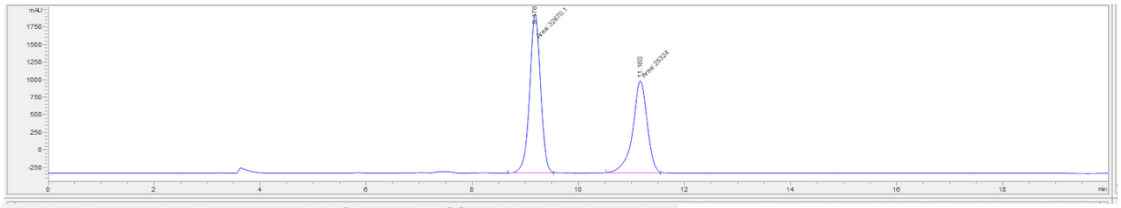

#	Time	Area	Height	Width	Area%	Symmetry
1	9.176	32670.1	2262.8	0.2406	56.333	0.992
2	11.16	25324	1313	0.3214	43.667	1.128

Figure 7.220 Chiral LC for enantioselective **2d** reaction with **L21**.

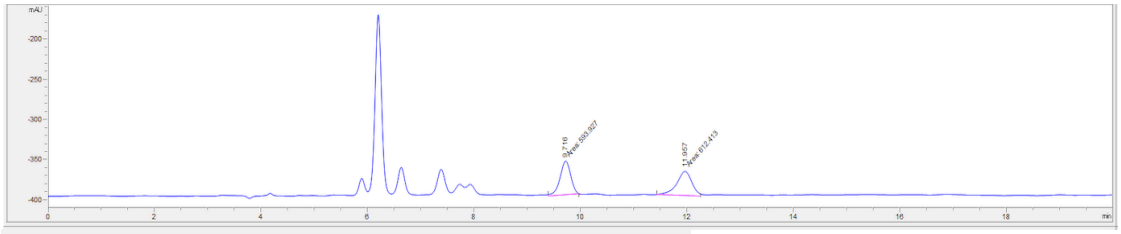

#	Time	Area	Height	Width	Area%	Symmetry
1	9.716	593.9	42.1	0.235	49.234	1.07
2	11.957	612.4	30.3	0.3373	50.766	1.224

Figure 7.221 Chiral LC for enantioselective **2d** reaction with **L22**.

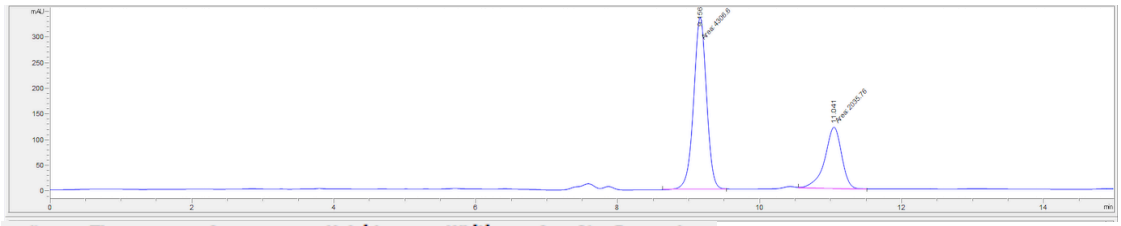

#	Time	Area	Height	Width	Area%	Symmetry
1	9.156	4306.6	338	0.2124	67.902	1.033
2	11.041	2035.8	120.7	0.2811	32.098	1.123

Figure 7.222 Chiral LC for enantioselective **2d** reaction with **L23**.

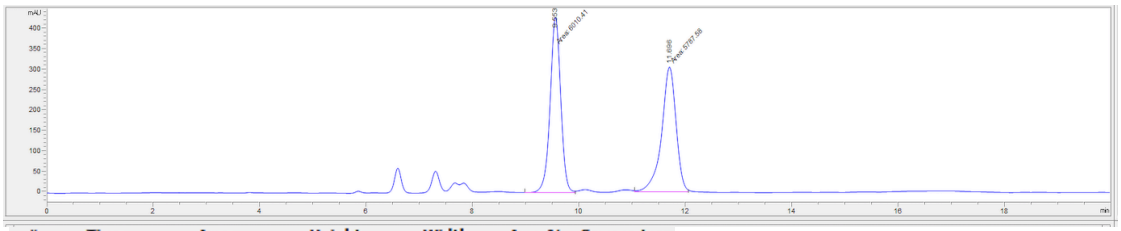

#	Time	Area	Height	Width	Area%	Symmetry
1	9.553	6010.4	429.6	0.2332	50.944	0.996
2	11.696	5787.6	305.6	0.3156	49.056	1.194

Figure 7.223 Chiral LC for enantioselective **2d** reaction with **L24**.

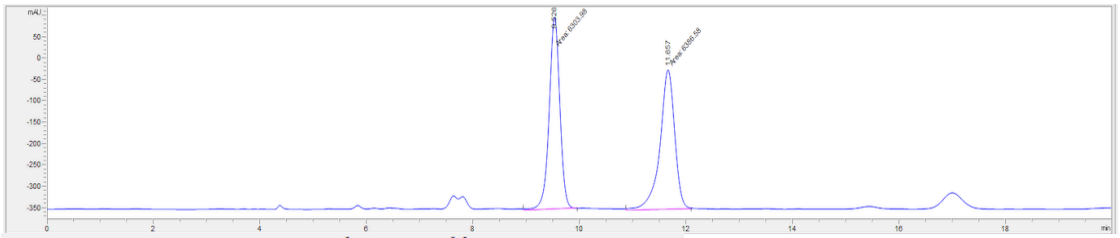

#	Time	Area	Height	Width	Area%	Symmetry
1	9.526	6304	449.2	0.2339	49.675	1.041
2	11.657	6386.6	327.5	0.3251	50.325	1.224

Figure 7.224 Chiral LC for enantioselective **2d** reaction with **L25**.

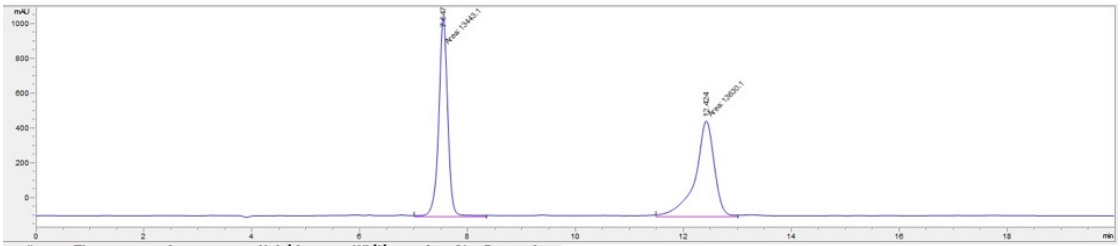

#	Time	Area	Height	Width	Area%	Symmetry
1	7.547	13443.1	1141.5	0.1963	49.655	0.994
2	12.424	13630.1	549.3	0.4136	50.345	1.357

Figure 7.225 Chiral LC for racemic **2e** sample with bipy (reference).

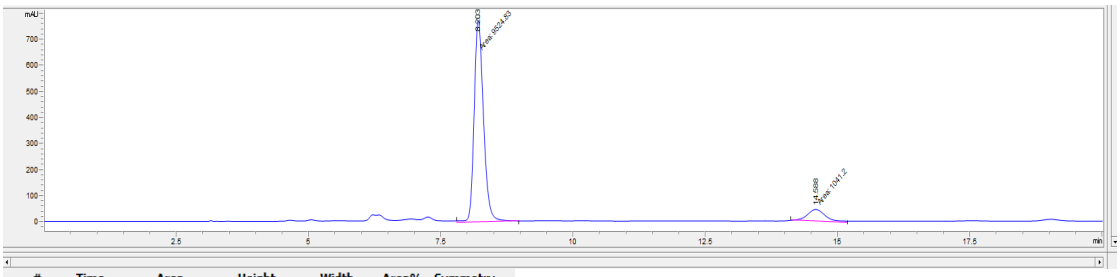

#	Time	Area	Height	Width	Area%	Symmetry
1	8.203	9524.8	774.8	0.2049	90.146	0.765
2	14.588	1041.2	44.1	0.3933	9.854	0.777

Figure 7.226 Chiral LC for enantioselective **2e** reaction with **L26**.

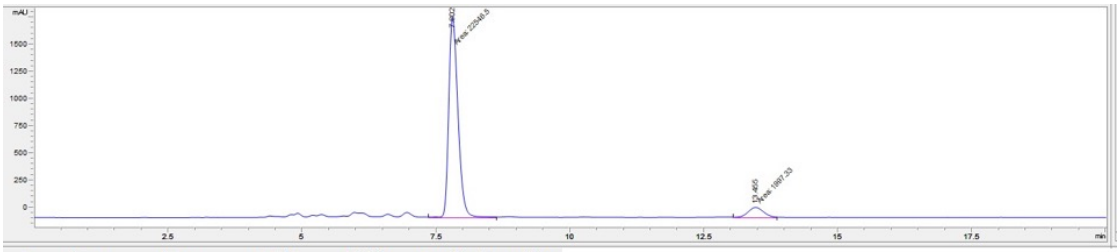

#	Time	Area	Height	Width	Area%	Symmetry
1	7.802	22546.5	1837.9	0.2045	91.862	0.671
2	13.455	1997.3	94.7	0.3517	8.138	0.913

Figure 7.227 Chiral LC for enantioselective **2e** reaction with **L27**.

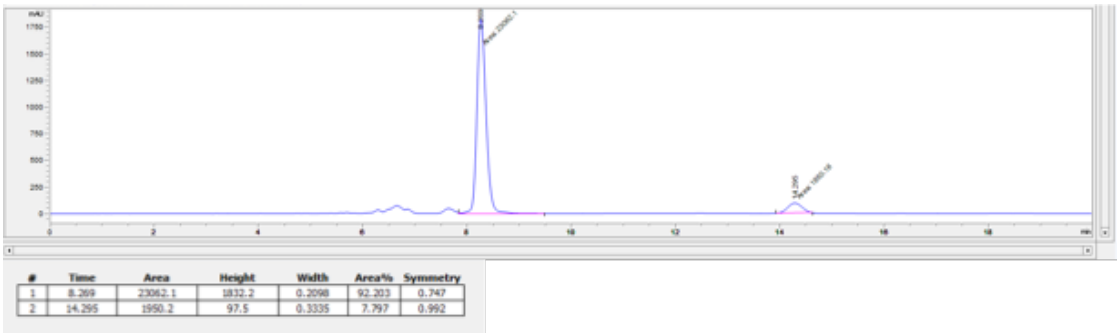

#	Time	Area	Height	Width	Area%	Symmetry
1	8.269	23062.1	1832.2	0.2098	92.203	0.747
2	14.295	1950.2	97.5	0.3335	7.797	0.992

Figure 7.228 Chiral LC for enantioselective **2e** reaction with **L28**.

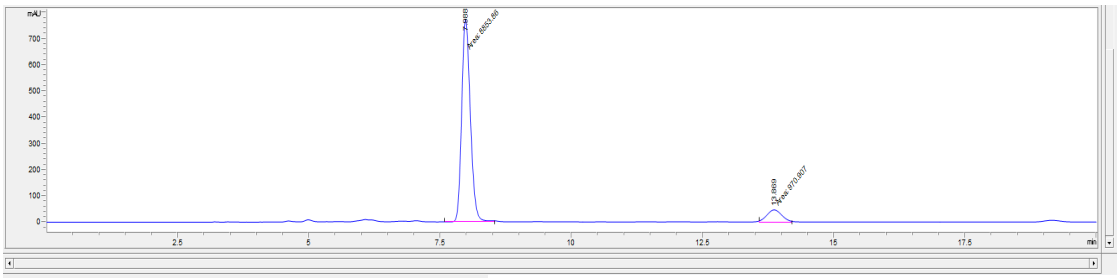

#	Time	Area	Height	Width	Area%	Symmetry
1	7.988	8853.9	771.7	0.1912	90.118	0.787
2	13.869	970.9	47.9	0.3381	9.882	0.926

Figure 7.229 Chiral LC for enantioselective **2e** reaction with **L29**.

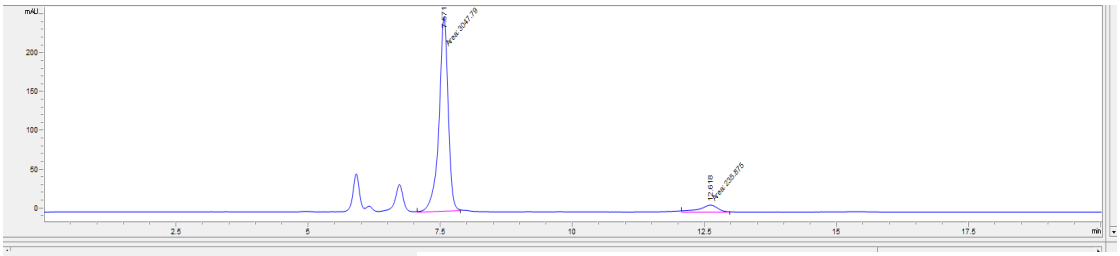

#	Time	Area	Height	Width	Area%	Symmetry
1	7.571	3047.8	250.7	0.2026	92.817	1.182
2	12.618	235.9	9.3	0.425	7.183	1.593

Figure 7.230 Chiral LC for enantioselective **2e** reaction with **L30**.

7.11 Synthesis of chiral *t*Bu-Pyox ligands general procedures and data

7.11.1 Synthesis (*S*)-*N*-(l-Hydroxy-3,3-dimethylbutan-2-yl)picolinamide

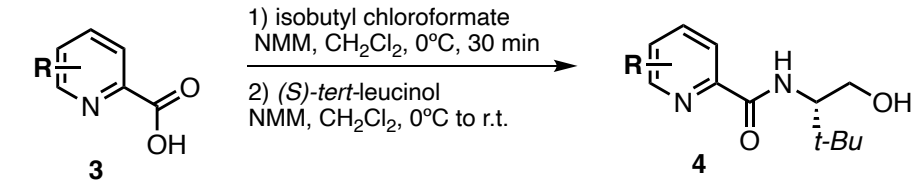

3

R = CH_3, OMe, F

4

Scheme 7.13 Synthesis of picolinamide general reaction.

General procedure[16]

A flame dried round bottom flask with a stir bar, under argon, was charged with 2-picolinic acid (1.0 mmol, 1.0 equiv) in DCM (5.9 mL, 0.17 M). *N*-methylmorpholine (1.5 mmol, 1.5 equiv) was added and the flask was cooled to 0ºC. Isobutylchloroformate (1.05 mmol, 1.05 equiv) was added slowly dropwise and the reaction mixture was stirred for additional 30 minutes. A separate flame dried round bottom flask was charged with *(S)-tert*-leucinol (1.1 mmol, 1.1 equiv), DCM (7.8 mL, 0.14 M), and *N*-methylmorpholine (1.1 mmol, 1.1 equiv) and the mixture was added to the first flask cooled to 0ºC and

stirred overnight. Upon completion, the reaction mixture was quenched with a saturated NH_4Cl solution and diluted with H_2O. The aqueous layer was extracted with DCM. The combined organic layers were washed with saturated $NaHCO_3$ and brine, dried over $MgSO_4$, and filtered. The crude product was concentrated *in vacuo* and purified by column chromatography.

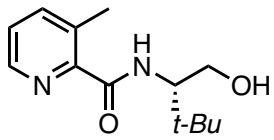

4a

(*S*)-*N*-(1-hydroxy-3,3-dimethylbutan-2-yl)-3-methylpicolinamide (4a). Using the general procedure for picolinamide synthesis, 3-methylpicolinic acid **3a** (0.201 g, 1.46 mmol, 1.0 equiv) in DCM (8.6 mL, 0.17 M) reacted with isobutyl chloroformate (0.20 mL, 1.53 mmol, 1.05 equiv) and *(S)-tert*-leucinol (0.188 g, 1.60 mmol, 1.1 equiv) in DCM (9.4 mL, 0.17 M) to afford the crude product which was purified by column chromatography (silica, 4:1 hexanes: EtOAc) to afford pure **4a** (0.291 g, 1.23 mmol) in 84% yield as a white solid.

^{1}H NMR (400 MHz, $CDCl_3$) δ 8.24 (d, J = 9.7 Hz, 1H), 8.17 (dd, J = 4.6, 1.6 Hz, 1H), 7.36 (dd, J = 7.9, 1.7 Hz, 1H), 7.06 (dd, J = 7.7, 4.6 Hz, 1H), 4.28 (s, 1H), 3.91 (ddd, J = 9.6, 8.1, 3.2 Hz, 1H), 3.84 (d, J = 11.6 Hz, 1H), 3.62 (dd, J = 11.4, 8.2 Hz, 1H), 2.49 (s, 3H), 0.93 (s, 9H).

GC t_R = 1.956 min (Method B). EI-MS m/z (%): 236.1 (M^+, 1), 205.1 (99), 179.0 (75), 161.0 (21), 149.0 (4), 137.0 (18), 120.0 (70), 92.0 (100), 65.0 (21).

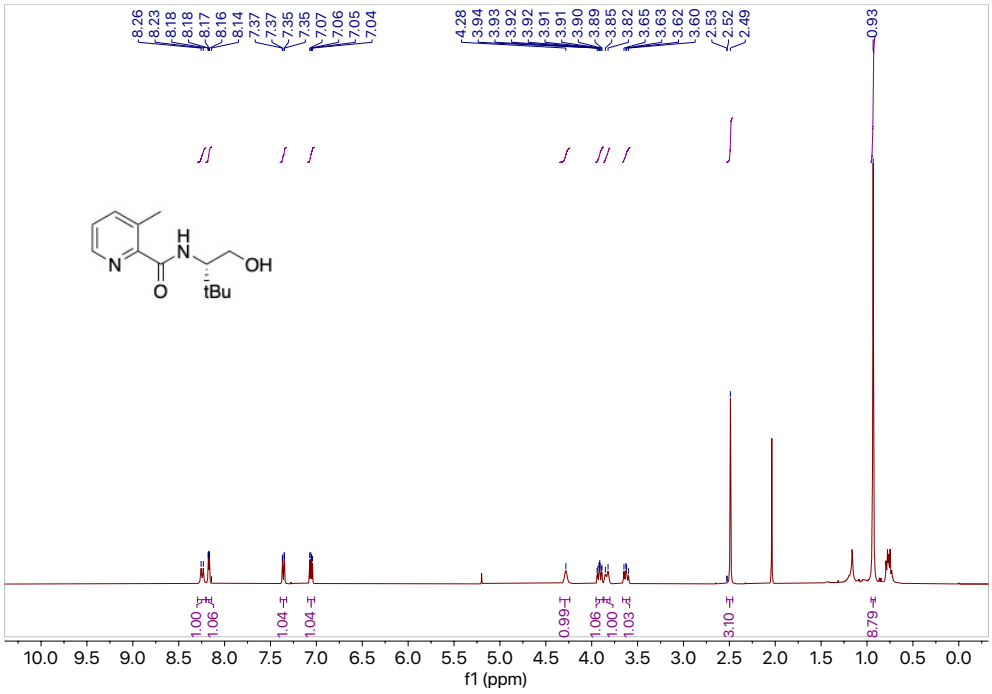

Figure 7.231 ^{1}H NMR (400 MHz, $CDCl_3$) of compound **4a**.

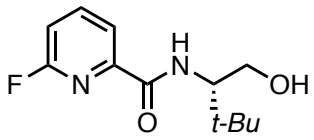

4b

(*S*)-6-fluoro-*N*-(1-hydroxy-3,3-dimethylbutan-2-yl)picolinamide (4b). Using the general procedure for picolinamide synthesis, 6-fluoropicolinic acid **3b** (0.200 g, 1.42 mmol, 1.0 equiv) in DCM (8.4 mL, 0.17 M) reacted with isobutyl chloroformate (0.20 mL, 1.49 mmol, 1.05 equiv) and *(S)-tert*-leucinol (0.188, 1.60 mmol, 1.1 equiv) in DCM (9.4 mL, 0.17 M) to afford the crude product which was purified by column chromatography (silica, 4:1 hexanes: EtOAc) to afford pure **4b** (0.241 g, 1.0 mmol) in 71% yield as a white solid.

^{1}H NMR (400 MHz, $CDCl_3$) δ 8.05 (dd, *J* = 7.4, 2.4 Hz, 1H), 7.93 (dt, *J* = 13.3, 6.7 Hz, 2H), 7.07 (dd, *J* = 8.2, 2.5 Hz, 1H), 4.06 – 3.93 (m, 2H), 3.68 (dd, *J* = 11.1, 7.9 Hz, 1H), 2.99 (s, 1H), 1.03 (s, 9H).

GC t_R = 1.671 min (Method B). EI-MS m/z (%): 241.0 (M+, 1), 209.1 (100), 195.0 (5), 183.0 (57), 165.0 (55), 141.0 (79), 123.9 .0 (88), 111.0 (4), 96.0 (99), 86.0 (7), 69.0 (18), 57.0 (6).

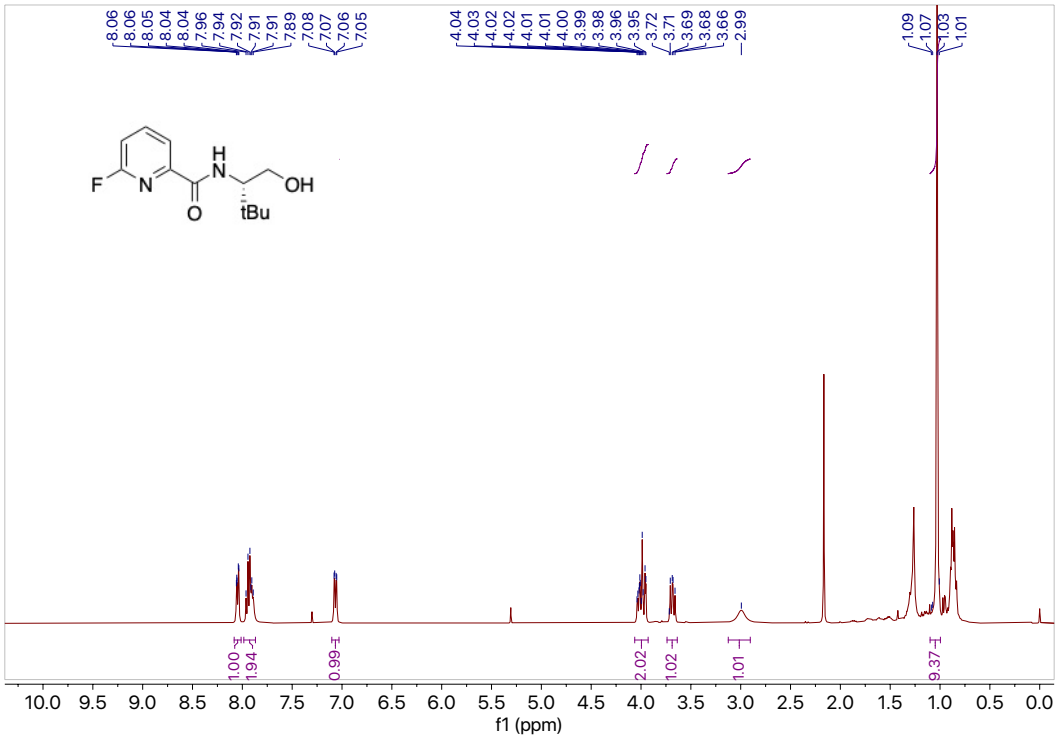

Figure 7.232 ^{1}H NMR (400 MHz, $CDCl_3$) of compound **4b**.

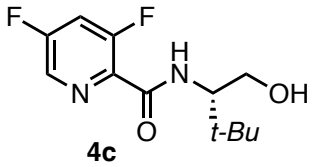

4c

(*S*)-3,5-difluoro-*N*-(1-hydroxy-3,3-dimethylbutan-2-yl)picolinamide (4c). Using the general procedure for picolinamide synthesis, 3,5-difluoropicolinic acid **3c** (0.201 g, 1.26 mmol, 1.0 equiv), in DCM (7.4 mL, 0.17 M) reacted with isobutyl chloroformate (0.17 mL, 1.32 mmol, 1.05 equiv) and *(S)-tert*-leucinol (0.169 g, 1.44 mmol, 1.1 equiv), in DCM (7.9 mL, 0.17 M) to afford the crude product which was purified by column chromatography (silica, 3:2 hexanes: EtOAc) to afford pure **4c** (0.223 g, 0.862 mmol) in 70% yield as a white solid.

^{1}H NMR (400 MHz, $CDCl_3$) δ 8.29 (d, J = 2.3 Hz, 1H), 7.90 (d, J = 9.3 Hz, 1H), 7.38 – 7.28 (m, 1H), 4.06 – 3.92 (m, 2H), 3.68 (ddt, J = 11.6, 7.6, 4.1 Hz, 1H), 2.81 (t, J = 5.4 Hz, 1H), 1.03 (s, 9H).

GC t_R = 1.671 min (Method B). EI-MS m/z (%): 243.0 (M-15+, 1), 227 (69), 200.9 (36), 182.9 (48), 158.9 (48), 141.9 (100), 128.9 (8), 113.9 (78), 86.0 (5), 69.0 (10), 57.0 (8).

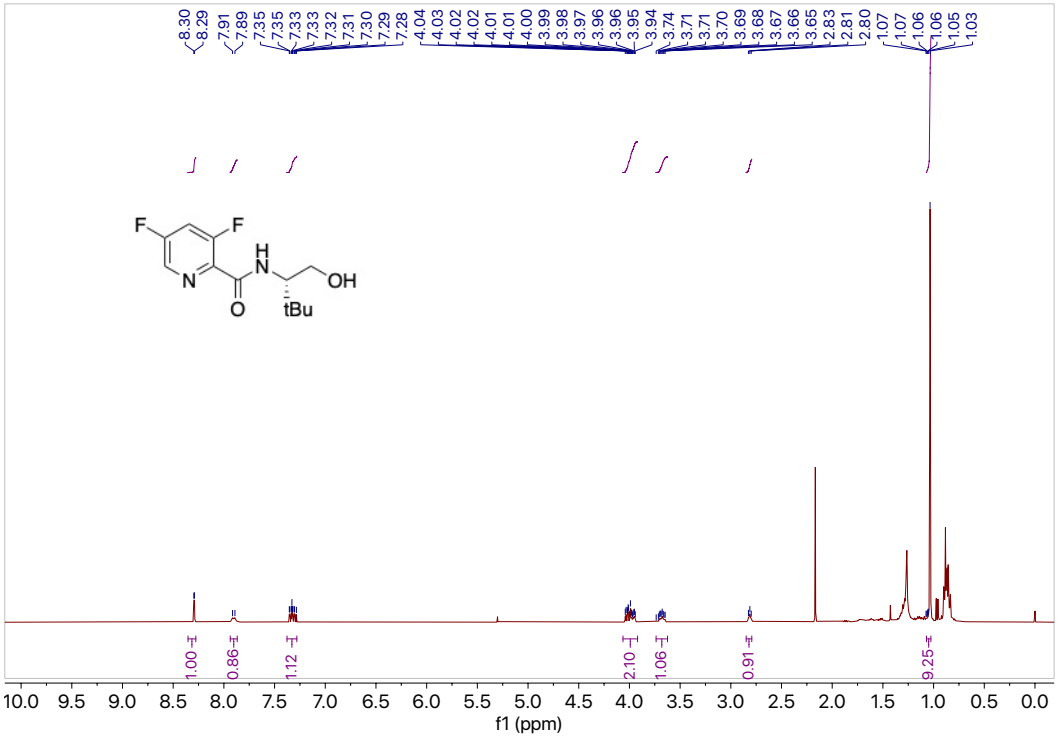

Figure 7.233 ^{1}H NMR (400 MHz, $CDCl_3$) of compound **4c**.

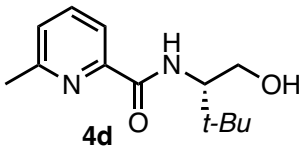

4d

(*S*)-*N*-(1-hydroxy-3,3-dimethylbutan-2-yl)-6-methylpicolinamide (4d). Using the general procedure for picolinamide synthesis, 3,5-difluoropicolinic acid **3d** (0.201 g, 1.46 mmol, 1.0 equiv), in DCM (8.6 mL, 0.17 M) reacted with isobutyl chloroformate (0.209 g, 0.2 mL, 1.53 mmol, 1.05 equiv) and *(S)-tert*-leucinol (0.189 g, 1.61 mmol, 1.1 equiv) in DCM (9.5 mL, 0.17 M) to afford the crude product which was purified by column chromatography (silica, 4:1 hexanes: EtOAc) to afford pure **4d** (0.340 g, 1.44 mmol) in 99% yield as a tan oil.

^{1}H NMR (400 MHz, $CDCl_3$) δ 8.41 (d, *J* = 8.6 Hz, 1H), 8.00 (dt, *J* = 7.5, 0.9 Hz, 1H), 7.73 (t, *J* = 7.7 Hz, 1H), 7.29 (dd, *J* = 7.5, 1.1 Hz, 1H), 4.04 – 3.93 (m, 2H), 3.69 (ddd, *J* = 9.0, 7.4, 4.8 Hz, 1H), 2.68 (t, *J* = 5.7 Hz, 1H), 2.59 (s, 3H), 1.05 (s, 9H).

^{13}C NMR (101 MHz, $CDCl_3$) δ_u 137.6, 126.0, 119.4, 60.6, 27.0, 24.4; δ_d 165.9, 157.2, 148.9, 63.7, 33.7.

GC t_R = 1.963 min (Method B). EI-MS m/z (%): 237.1 (M+, 1), 205.1 (96), 179.0 (70), 161.0 (30), 137.0 (34), 120.0 (52), 92.0 (100), 65.0 (20).

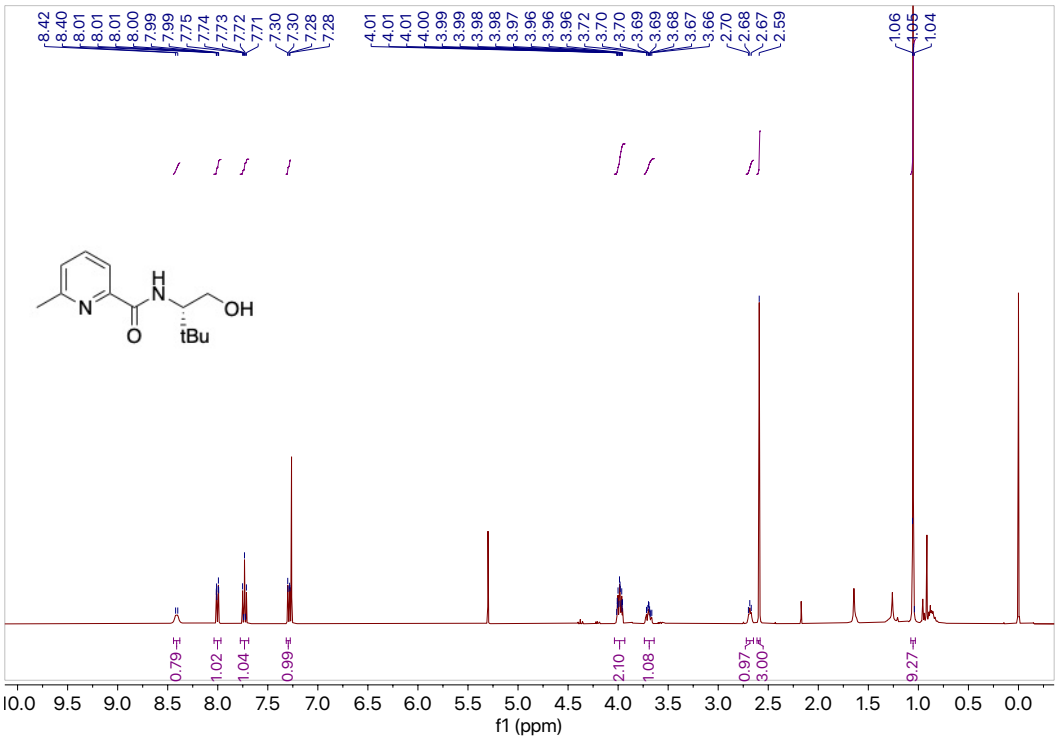

Figure 7.234 ^{1}H NMR (400 MHz, $CDCl_3$) of compound **4d**.

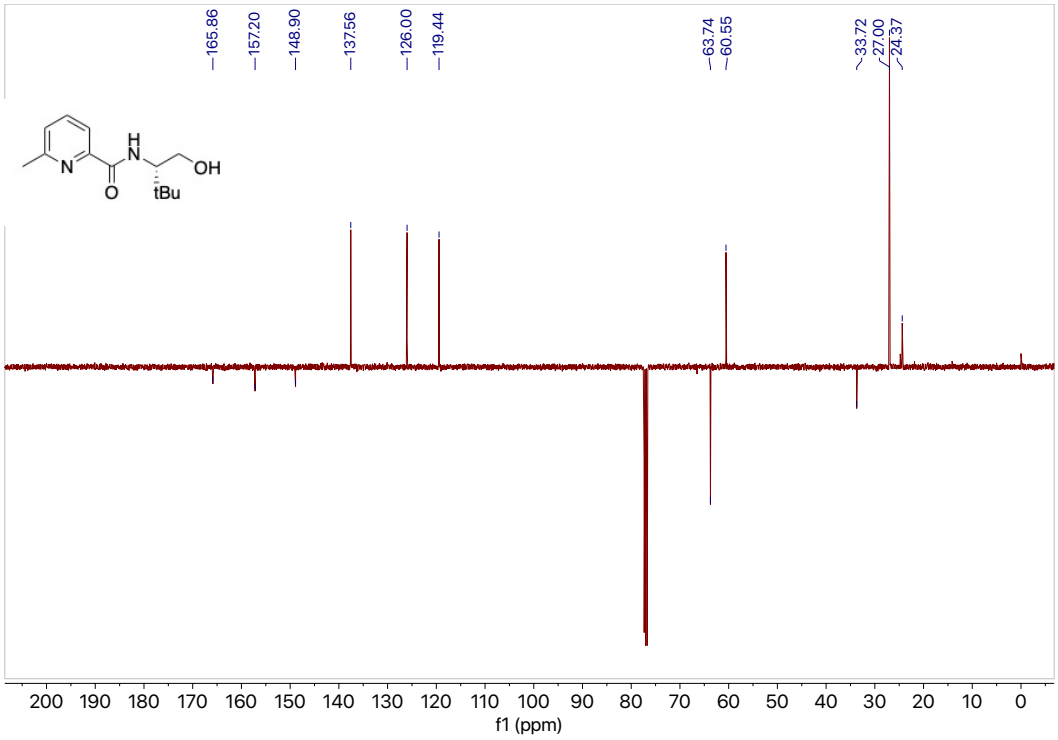

Figure 7.235 ^{13}C NMR (101 MHz, $CDCl_3$) of compound **4d**.

7.11.2 (*S*)-4-(*tert*-butyl)-2-(pyridin-2-yl)-4,5-dihydrooxazoles (L19-24).

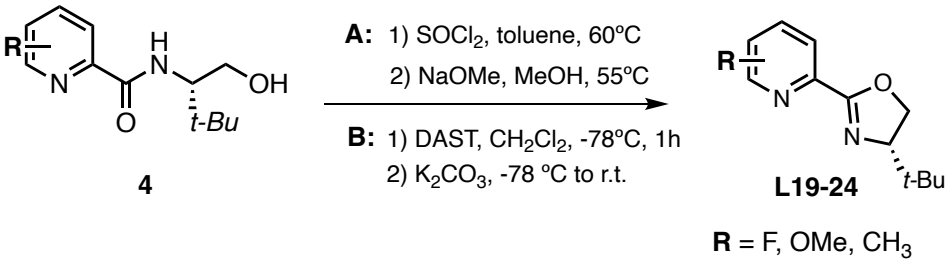

Scheme 7.14 Synthesis of chiral tBu-Pyox ligand general reaction.

General procedure A[16]

To a flame dried round bottom flask with a stir bar, under argon, was added (*S*)-*N*-(l-hydroxy-3,3-dimethylbutan-2-yl)picolinamide (1.0 mmol, 1.0 equiv) and dissolved in toluene (3.5 mL, 0.285 M). The reaction mixture was heated at 60 °C in a mineral oil bath. In a separate flame dried round bottom flask with a stir bar, under argon, $SOCl_2$ (2.0 mmol, 2.0 equiv) was added and dissolved in toluene (4 mL, 0.5 M). The $SOCl_2$ solution was added slowly dropwise to the vigorously stirring reaction mixture. Upon completion, the reaction mixture was cooled down to room temperature, concentrated in vacuo to afford (*S*)-*N*-(l-chloro-3,3-dimethylbutan-2-yl)picolinamide hydrochloride salt. The crude material was used in the next step without purification.

A flame dried round bottom flask with a stir bar, under argon, was charged with (*S*)-*N*-(1-chloro-3,3-dimethylbutan-2-yl)picolinamide hydrochloride salt (1.0 mmol, 1.0 equiv) in methanol (2.7 mL, 0.37 M). Sodium methoxide (5.0 mmol, 5.0 equiv) was added in one portion and the reaction mixture was heated at 55 °C in the mineral oil bath until completion. After cooling the reaction to room temperature, the mixture was diluted with toluene (5 mL, 0.2 M) and partially concentrated to remove methanol. The resulting slurry was transferred to a separatory funnel, washed with water, and extracted with toluene. The combined organic layers were washed with brine, dried over $MgSO_4$, and filtered. The crude product was concentrated in vacuo and purified by column chromatography.

General procedure B[17]

To a flame dried round bottom flask with a stir bar, under argon, was added (*S*)-*N*-(1-hydroxy-3,3-dimethylbutan-2-yl)picolinamide (1.0 mmol, 1.0 equiv) and dissolved in DCM (7 mL, 0.14 M). After the solution was cooled to -78°C, DAST (1.4 mmol, 1.4 equiv) was added, and the mixture was stirred at -78°C for 1 h. Then, K_2CO_3 (2.0 mmol, 2.0 equiv) was added and the reaction mixture was warmed to room temperature while stirring overnight. Upon completion, the reaction was quenched with H_2O and extracted with DCM. The combined organic layers were washed with brine, dried over $MgSO_4$, and filtered. The crude product was concentrated in vacuo and purified by column chromatography.

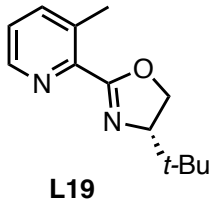

L19

(*S*)-4-(*tert*-butyl)-2-(3-methylpyridin-2-yl)-4,5-dihydrooxazole (L19). Using the general procedure A with **4a** (0.291 g, 1.15 mmol, 1.0 equiv) afforded the crude product which was purified by column chromatography (silica, 4:1 hexanes: acetone) to afford pure **L19** (0.108 g, 0.50 mmol) in 45% yield as a white solid.

^{1}H NMR (400 MHz, $CDCl_3$) δ 8.56 – 8.50 (m, 1H), 7.59 (ddt, J = 7.8, 1.7, 0.8 Hz, 1H), 7.27 – 7.25 (m, 1H), 4.41 (dd, J = 9.9, 8.3 Hz, 1H), 4.28 – 4.12 (m, 2H), 2.64 (s, 3H), 0.99 (s, 9H).

^{13}C NMR (101 MHz, $CDCl_3$) δ_u 146.8, 139.2, 124.7, 77.2, 26.0, 20.6; δ_d 162.2, 145.9, 135.1, 68.2, 33.9.

GC t_R = 1.473 min (Method B). EI-MS m/z (%): 218.0 (M+, 43), 203.0 (4), 173.0 (4), 161.0 (100), 133.0 (41), 119.0 (53), 106.0 (50), 92.0 (53), 79.0 (5), 57.0 (7).

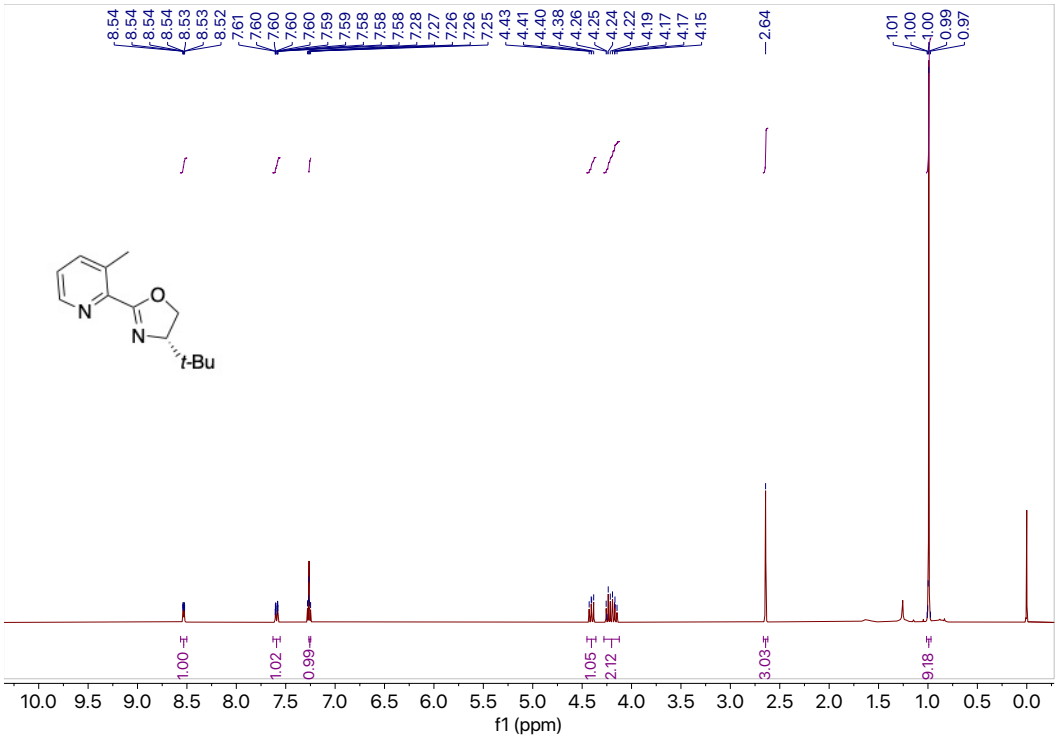

Figure 7.236 ^{1}H NMR (400 MHz, $CDCl_3$) of compound **L19**.

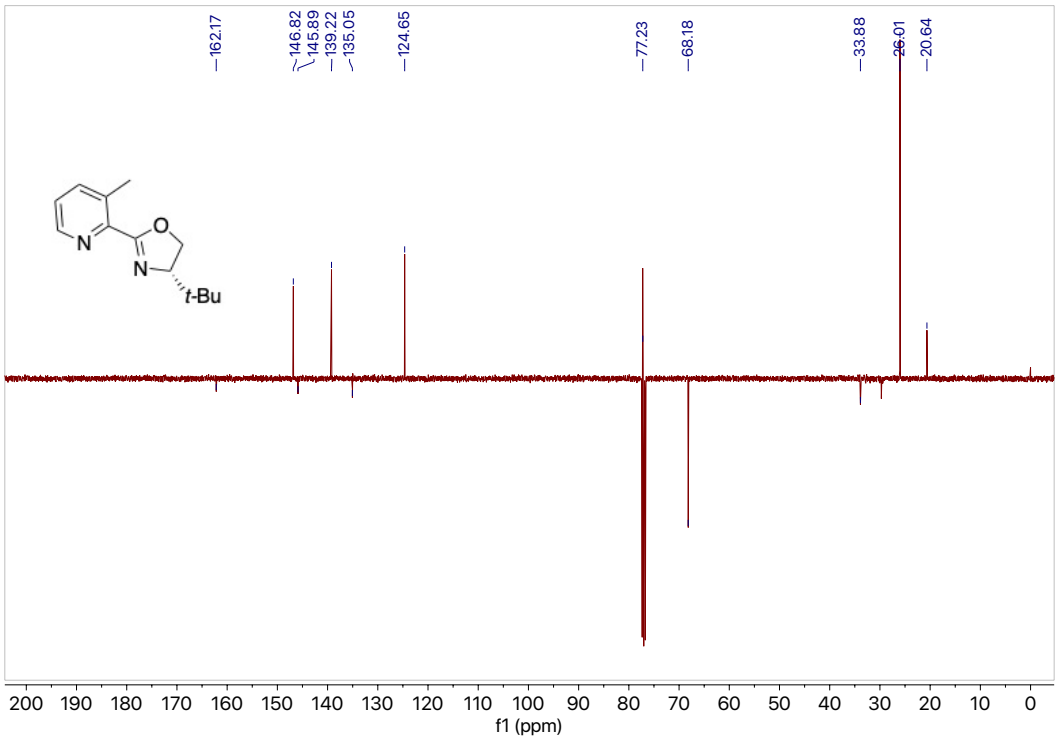

Figure 7.237 ^{13}C NMR (101 MHz, $CDCl_3$) of compound **L19**.

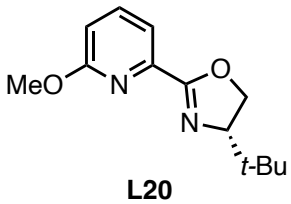

L20

(*S*)-4-(*tert*-butyl)-2-(6-methoxypyridin-2-yl)-4,5-dihydrooxazole (L20). Using the general procedure A with **4b** (0.241 g, 1.10 mmol, 1.0 equiv) afforded the crude product which was purified by column chromatography (silica, 3:2 hexanes: acetone) to afford pure **L20** (0.0307 g, 0.13 mmol) in 15% yield as a white solid.

^{1}H NMR (400 MHz, $CDCl_3$) δ 7.70 (dd, *J* = 7.3, 1.0 Hz, 1H), 7.64 (dd, *J* = 8.2, 7.3 Hz, 1H), 6.85 (dd, *J* = 8.2, 1.1 Hz, 1H), 4.44 (dd, *J* = 10.2, 8.7 Hz, 1H), 4.31 (dd, *J* = 8.7, 8.2 Hz, 1H), 4.12 (dd, *J* = 10.2, 8.2 Hz, 1H), 4.03 (s, 3H), 0.99 (s, 9H).

^{13}C NMR (101 MHz, $CDCl_3$) δ_u 138.8, 117.4, 113.4, 76.3, 53.6, 25.9; δ_d 163.8, 162.6, 144.5, 69.3, 34.0.

GC t_R = 1.447 min (Method B). EI-MS m/z (%): 234.1 (M+, 6), 117.0 (100), 173.0 (4), 163.0 (9), 149.0 (18), 134.0 (41), 123.0 (6) 108.0 (26), 93.0 (11), 79.0 (5), 57.0 (5).

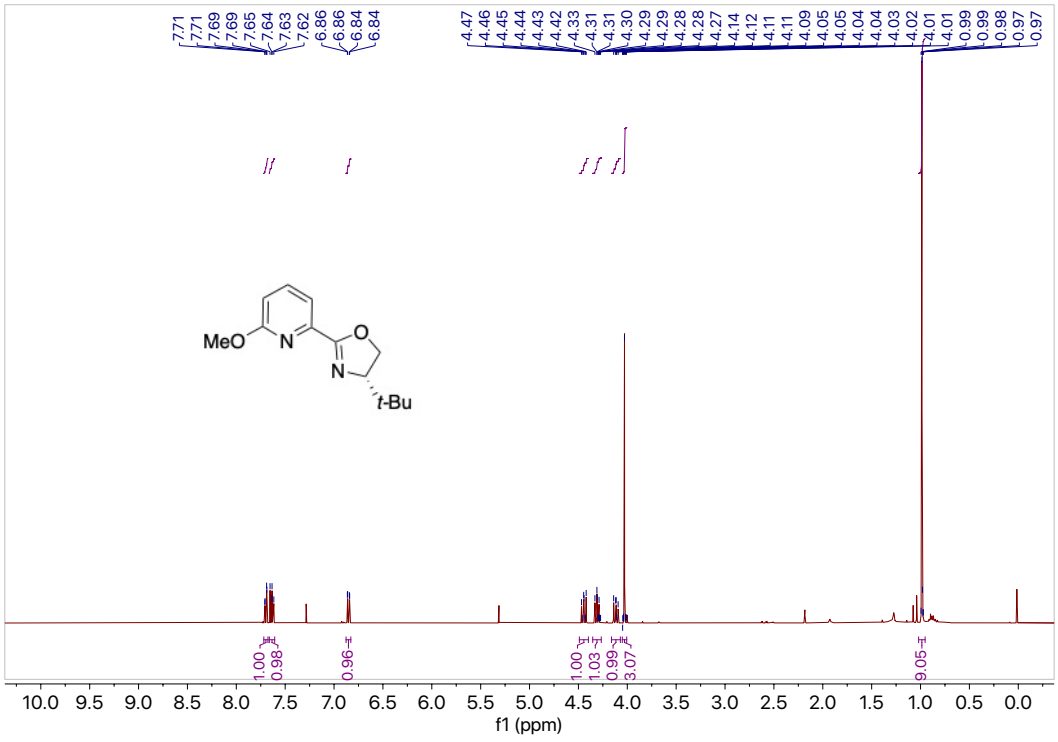

Figure 7.238 ^{1}H NMR (400 MHz, $CDCl_3$) of compound **L20**.

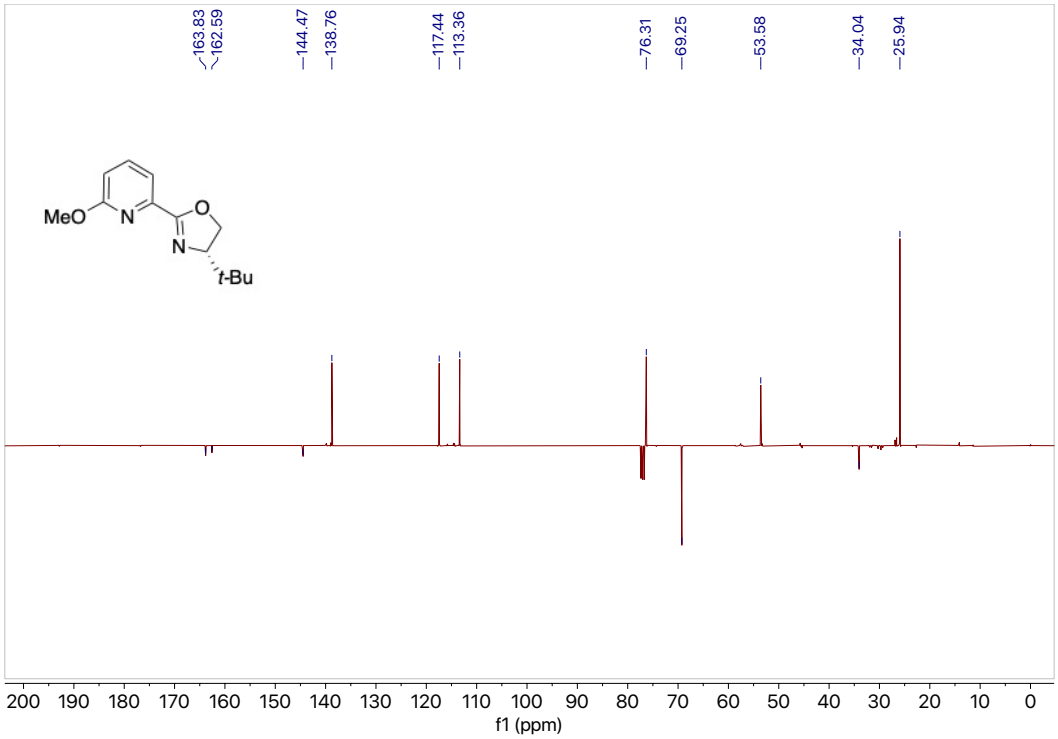

Figure 7.239 ^{13}C NMR (101 MHz, $CDCl_3$) of compound **L20**.

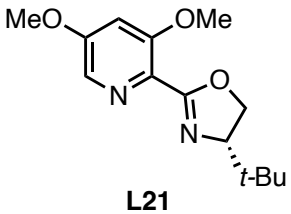

L21

(*S*)-4-(*tert*-butyl)-2-(3,5-dimethoxypyridin-2-yl)-4,5-dihydrooxazole (L21). Using the general procedure A with **4c** (0.223 g, 0.86 mmol, 1.0 equiv) afforded the crude product which was purified by column chromatography (silica, 4:1 hexanes: acetone) to afford pure **L21** (0.0741 g, 0.28 mmol) in 37% yield as a yellow oil.

^{1}H NMR (400 MHz, $CDCl_3$) δ 7.99 (d, J = 2.4 Hz, 1H), 6.82 (d, J = 2.3 Hz, 1H), 4.40 – 4.29 (m, 1H), 4.29 – 4.11 (m, 2H), 3.91 (d, J = 3.1 Hz, 6H), 0.98 (s, 9H).

GC t_R = 2.624 min (Method B). EI-MS m/z (%): 264.1 (M+, 3), 249.1 (3), 207.0 (100), 179.0 (37), 164.0 (15), 152.0 (18), 135.0 (3), 122.0 (15) 108.0 (15), 93.0 (5), 57.0 (5).

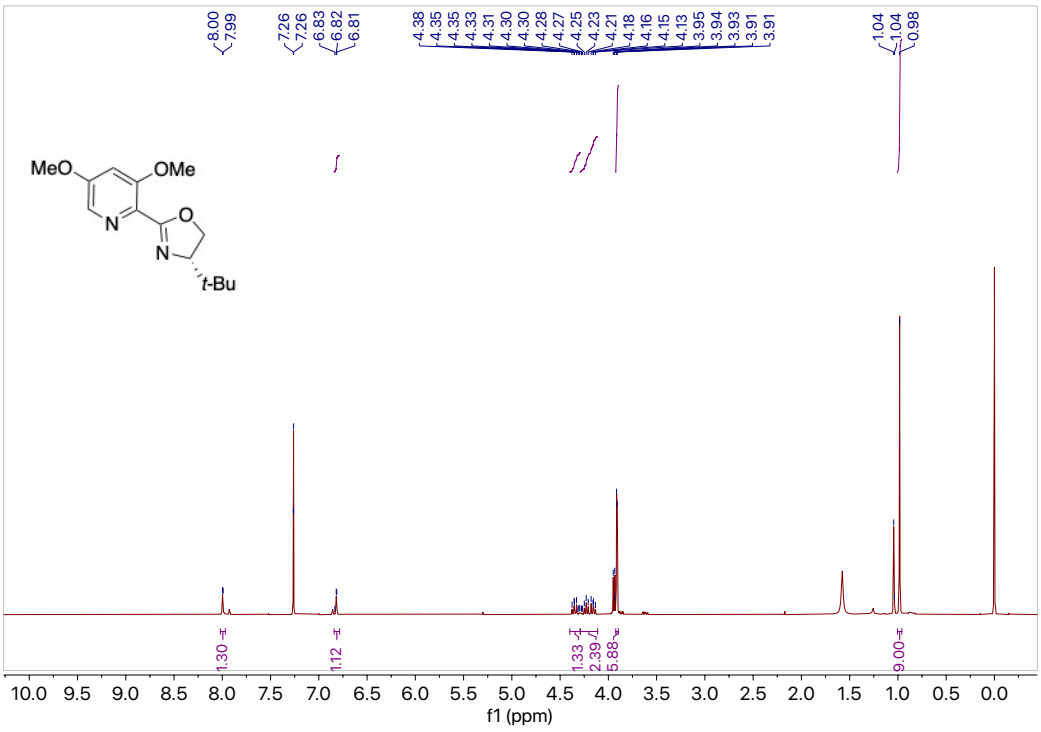

Figure 7.240 ^{1}H NMR (400 MHz, $CDCl_3$) of compound **L21**.

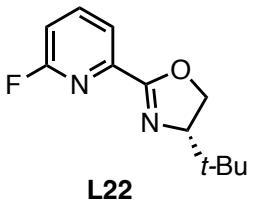

L22

(*S*)-4-(*tert*-butyl)-2-(6-fluoropyridin-2-yl)-4,5-dihydrooxazole (L22). Using the general procedure B with **4b** (0.2202 g, 0.92 mmol, 1.0 equiv) afforded the crude product which was purified by column chromatography (silica, 3:2 hexanes: acetone) to afford pure **L22** (0.0978 g, 0.440 mmol) in 48% yield as a white solid.
^{1}H NMR (400 MHz, $CDCl_3$) δ 7.99 (ddd, J = 7.6, 2.2, 0.8 Hz, 1H), 7.87 (q, J = 7.8 Hz, 1H), 7.05 (ddd, J = 8.2, 2.8, 0.8 Hz, 1H), 4.45 (dd, J = 10.3, 8.7 Hz, 1H), 4.31 (t, J = 8.6 Hz, 1H), 4.12 (dd, J = 10.3, 8.3 Hz, 1H), 0.97 (s, 9H).
^{13}C NMR (101 MHz, $CDCl_3$) δ_u 141.6 (d, $^{3}J_{C\text{-}F}$ = 8.1 Hz), 121.4 (d, $^{4}J_{C\text{-}F}$ = 4.0 Hz), 111.9 (d, ^{2}J = 36.7 Hz), 76.1, 25.9; δ_d 163.0 (d, $^{1}J_{C\text{-}F}$ = 242.1 Hz), 145.3, 114.8, 69.5, 34.0.
^{19}F NMR (376 MHz, $CDCl_3$) δ -65.38.
GC t_R = 1.269 min (Method B). EI-MS m/z (%): 222.0 (M+, 1), 177.0 (4), 166.0 (100), 136.9 (17), 123.9 (30) 109.9 (19), 95.9 (36), 75.9 (6), 57.0 (11).

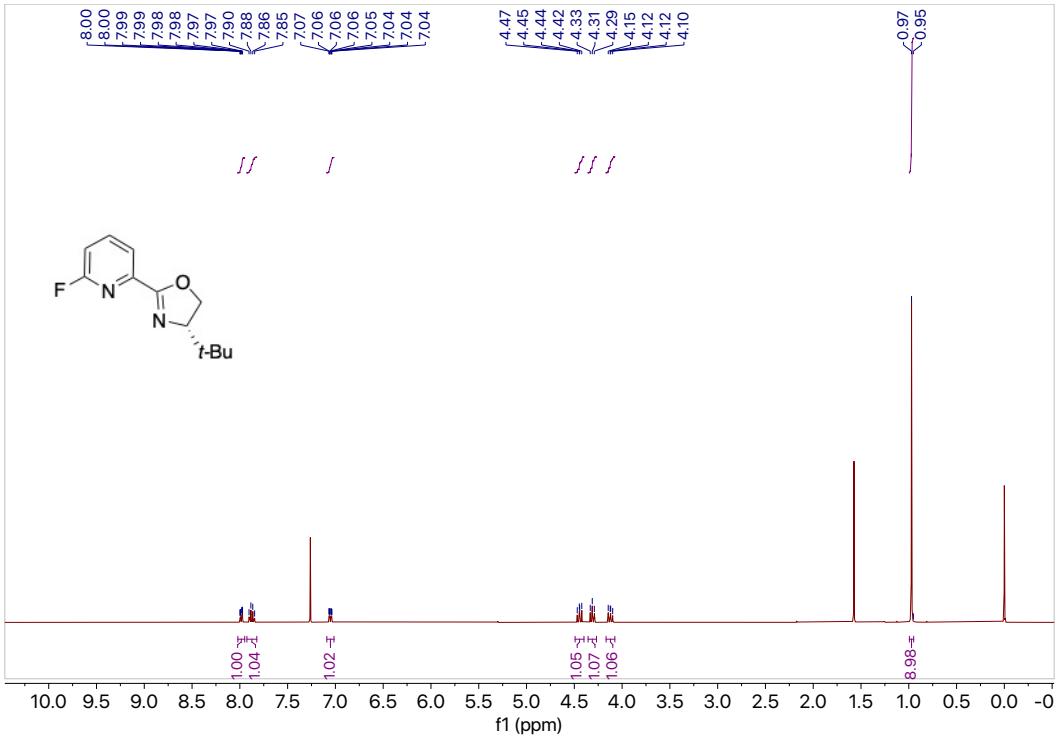

Figure 7.241 ^{1}H NMR (400 MHz, $CDCl_3$) of compound **L22**.

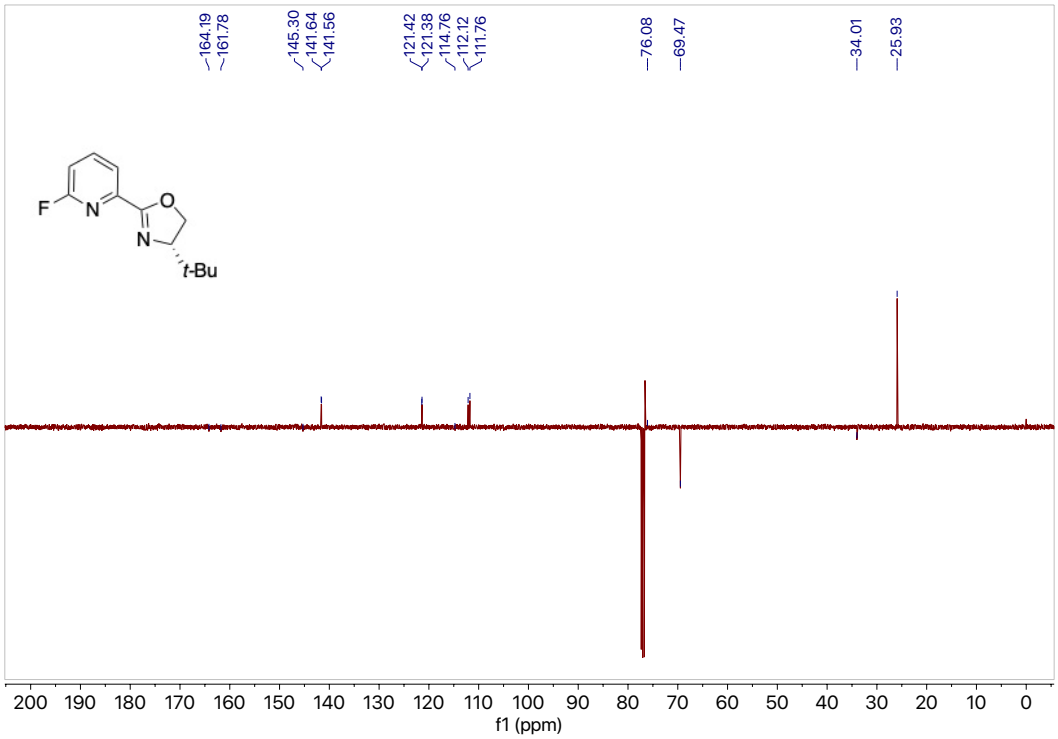

Figure 7.242 ^{13}C NMR (101 MHz, $CDCl_3$) of compound **L22**.

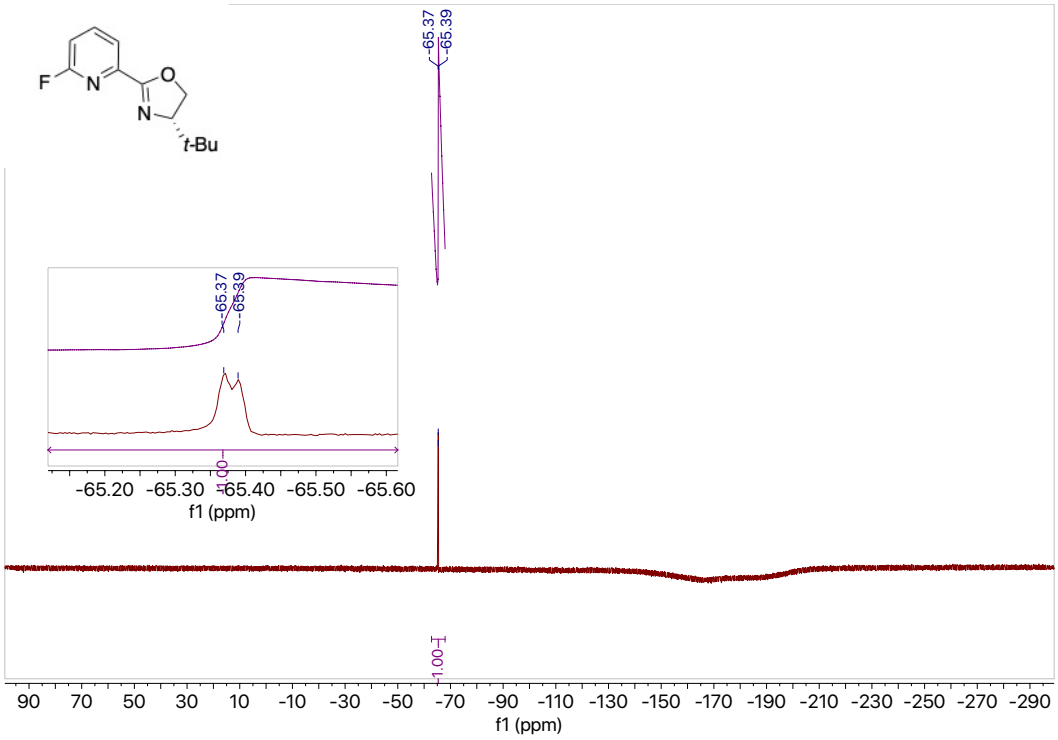

Figure 7.243 ^{19}F NMR (376 MHz, $CDCl_3$) of compound **L22**.

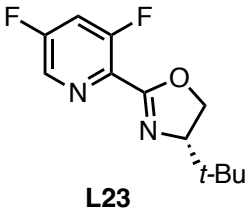

L23

(*S*)-4-(*tert*-butyl)-2-(3,5-difluoropyridin-2-yl)-4,5-dihydrooxazole (L23). Using the general procedure B with **4c** (0.325 g, 1.26 mmol, 1.0 equiv) afforded the crude product which was purified by column chromatography (silica, 3:2 hexanes: acetone) to afford pure **L23** (0.1312 g, 0.546 mmol) in 43% yield as a white solid.

^{1}H NMR (400 MHz, $CDCl_3$) δ 8.44 (d, *J* = 2.4 Hz, 1H), 7.33 (ddd, *J* = 9.6, 8.0, 2.3 Hz, 1H), 4.42 (dd, *J* = 10.2, 8.6 Hz, 1H), 4.29 (t, *J* = 8.4 Hz, 1H), 4.19 (dd, *J* = 10.2, 8.1 Hz, 1H), 0.99 (s, 9H).

^{19}F NMR (376 MHz, $CDCl_3$) δ -111.17, -118.58.

GC t_R = 8.118 min (Method A). EI-MS m/z (%): 240.0 (M+, 1), 195.0 (4), 184.0 (100), 155.0 (20), 141.9 (53), 129.0 (53), 113.9 (39), 57.0 (15).

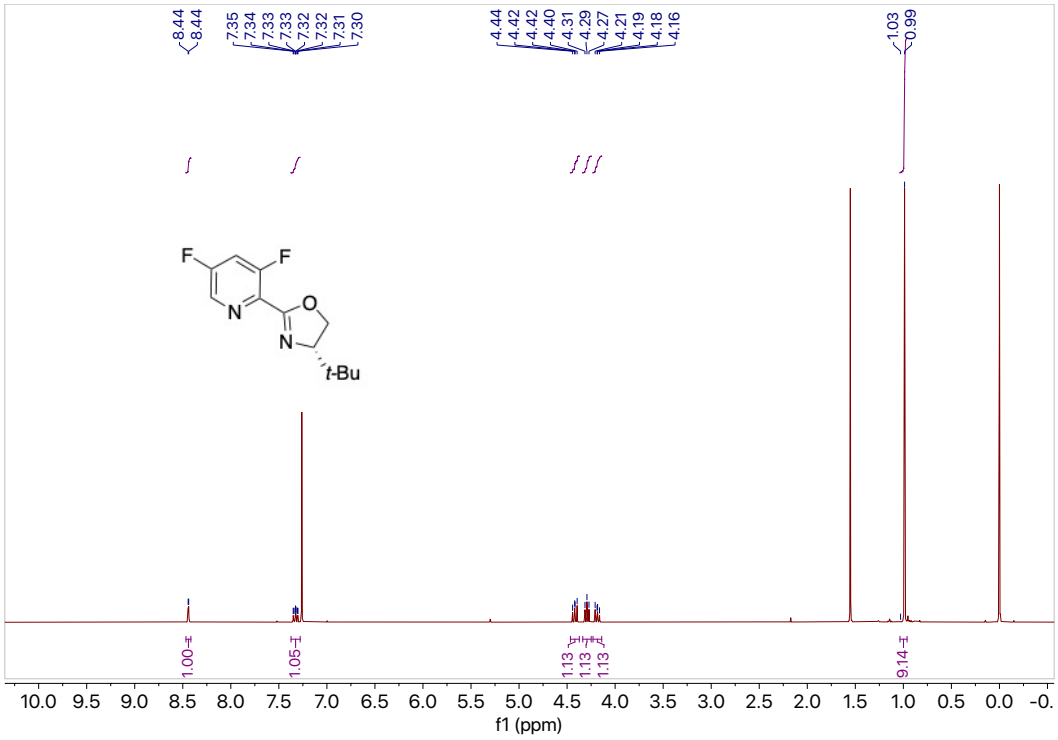

Figure 7.244 ^{1}H NMR (400 MHz, $CDCl_3$) of compound **L23**.

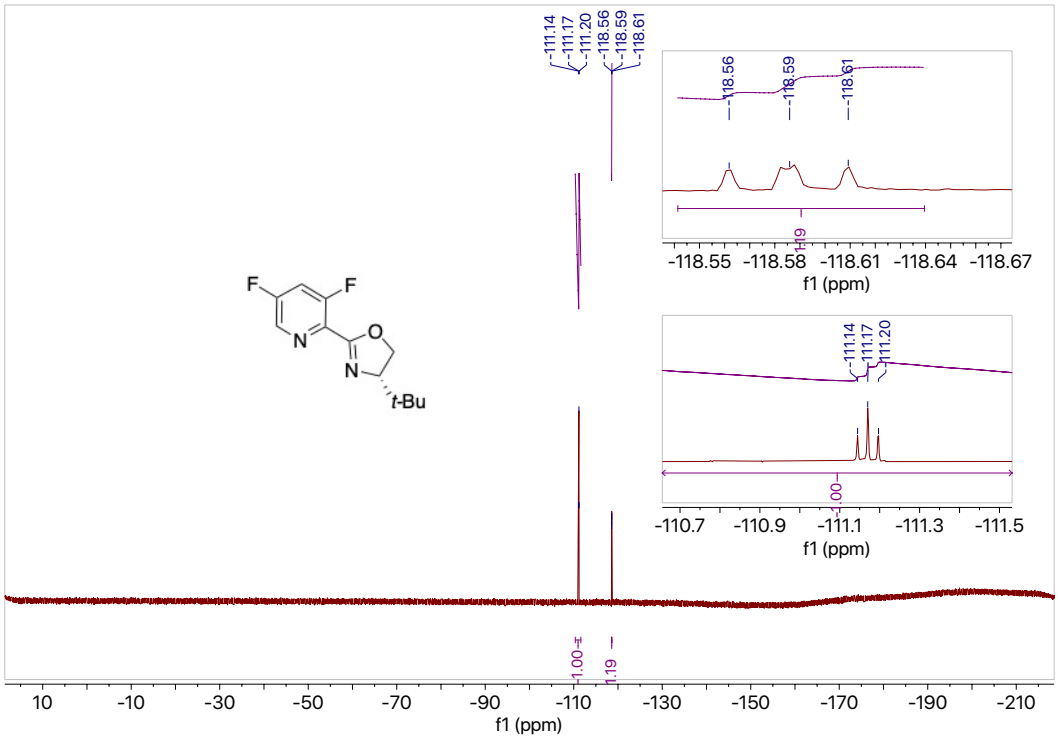

Figure 7.245 ^{19}F NMR (376 MHz, $CDCl_3$) of compound **L23**.

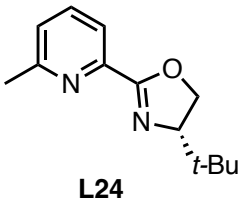

L24

(*S*)-4-(*tert*-butyl)-2-(6-methylpyridin-2-yl)-4,5-dihydrooxazole (L24). Using the general procedure A with **4d** (0.345 g, 1.46 mmol, 1.0 equiv) afforded the crude product which was purified by column chromatography (silica, 4:1 hexanes: acetone) to afford pure **L24** (0.1805 g, 0.827 mmol) in 68% yield as a white solid.

^{1}H NMR (400 MHz, $CDCl_3$) δ 7.94 (d, J = 7.8 Hz, 1H), 7.65 (t, J = 7.8 Hz, 1H), 7.24 (s, 1H), 4.45 (dd, J = 10.2, 8.8 Hz, 1H), 4.32 (t, J = 8.5 Hz, 1H), 4.11 (dd, J = 10.3, 8.2 Hz, 1H), 2.64 (s, 3H), 0.97 (s, 9H).

^{13}C NMR (101 MHz, $CDCl_3$) δ_u136.7, 125.2, 121.3, 76.4, 26.0, 24.7; 158.6, 135.5, 122.9, 69.4, 34.0.

GC t_R = 1.417 min (Method B). EI-MS m/z (%): 218.0 (M+, 1), 203.0 (3), 173.0 (4), 161.0 (100), 133.0 (25), 119.0 (16), 106.0 (43), 92.0 (42), 79.0 (5), 65.0 (16), 57.0 (6).

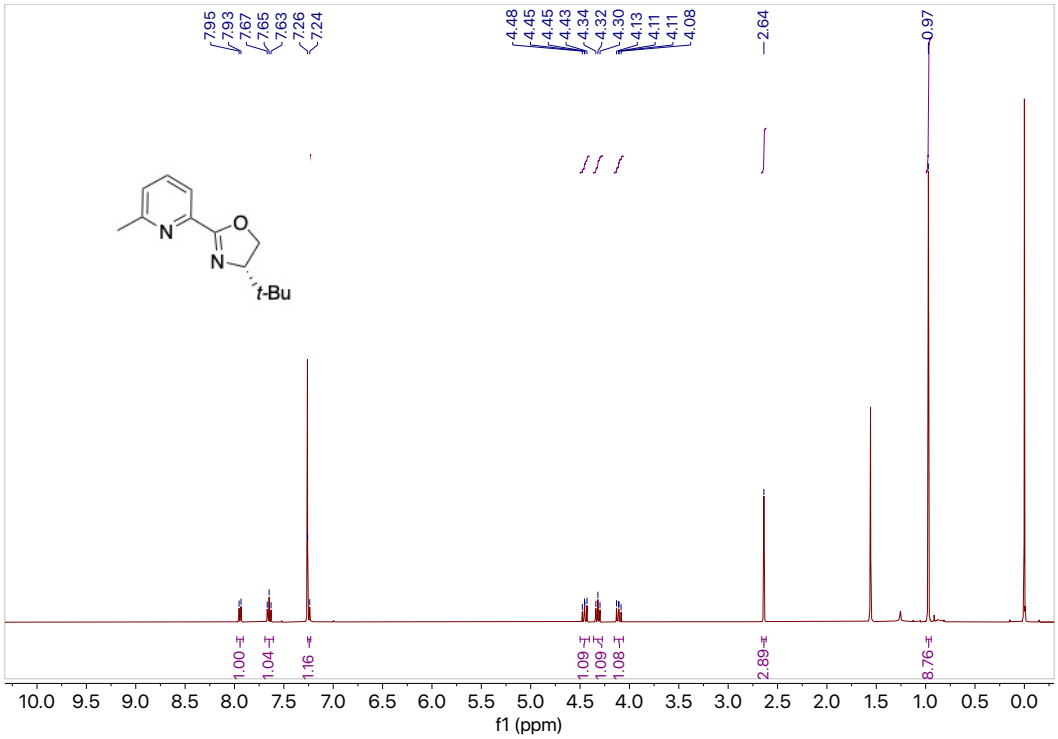

Figure 7.246 ^{1}H NMR (400 MHz, $CDCl_3$) of compound **L24**.

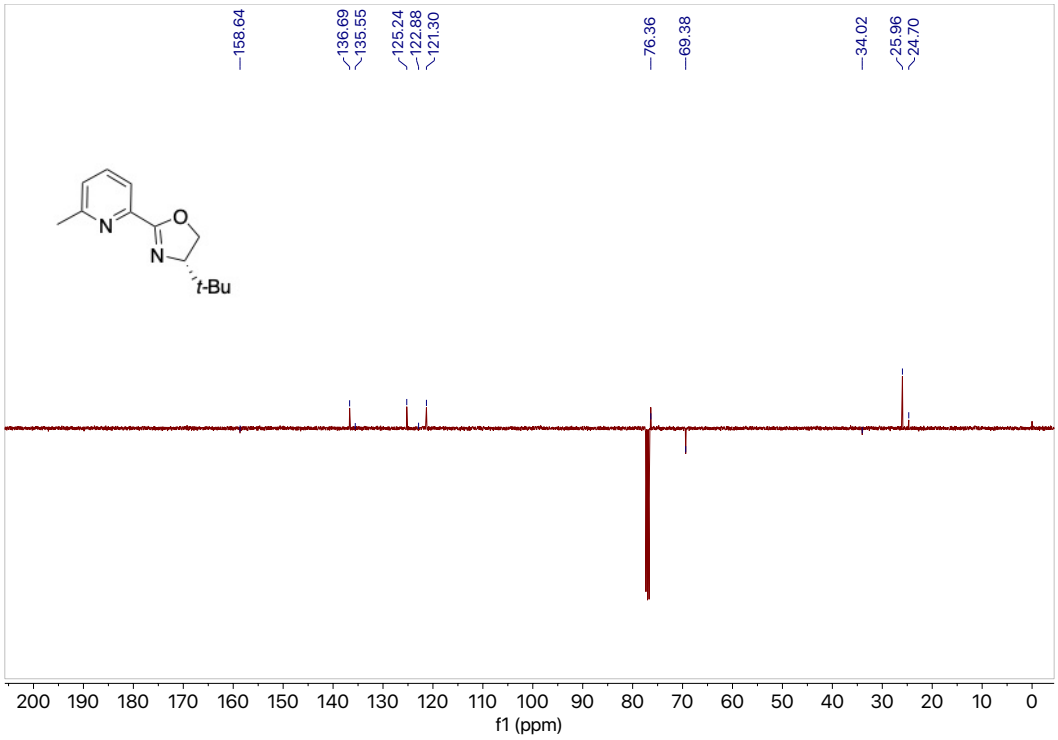

Figure 7.247 ^{13}C NMR (101 MHz, $CDCl_3$) of compound **L24**.

7.12 Synthesis of chiral *t*Bu-*i*Quinox ligands general procedures and data

7.12.1 Synthesis of isoquinoline *N*-oxides (6a-d).

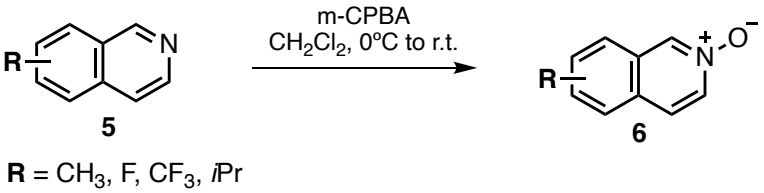

Scheme 7.15 Synthesis of isoquinoline N-oxides general reaction.

General procedure[18]

In a round bottom flask with a stir bar, isoquinoline (1.0 mmol, 1.0 equiv) was dissolved in DCM (0.55 mL, 1.8 M) and cooled to 0°C. Meta-chloroperbenzoic acid (mCPBA) (2.0 mmol, 2.0 equiv) was dissolved in DCM (1.1 mL, 1.8 M) and added dropwise to the reaction mixture. The mixture was allowed to warm to room temperature and react overnight. The reaction mixture was diluted with DCM, washed with 3 N NaOH, brine and then dried with $MgSO_4$. The crude product was concentrated under vacuum and purified by column chromatography.

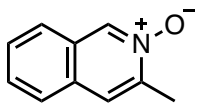

6a

3-methylisoquinoline 2-oxide (6a). Using the general procedure for synthesis of isoquinoline *N*-oxides, 3-methylisoquinoline **5a** (0.201 g, 1.40 mmol, 1.0 equiv) in DCM (0.8 mL, 1.8 M) reacted with mCPBA (0.482 g, 2.79 mmol, 2.0 equiv) in DCM (1.6 mL, 1.8 M) to afford the crude product which was purified by column chromatography (silica, 10:1 EtOAc: MeOH) to afford pure **6a** (0.203 g, 1.28 mmol) in 92% yield as a tan solid.
^{1}H NMR (400 MHz, $CDCl_3$) δ 8.86 (s, 1H), 7.71 (ddd, *J* = 9.4, 5.7, 3.1 Hz, 2H), 7.64 (s, 1H), 7.59 – 7.51 (m, 2H), 2.65 (s, 3H).
^{13}C NMR (101 MHz, $CDCl_3$) δ_u 136.4, 128.7, 128.3, 125.9, 124.5, 123.1, 17.7; δ_d 146.0, 129.2, 128.5.

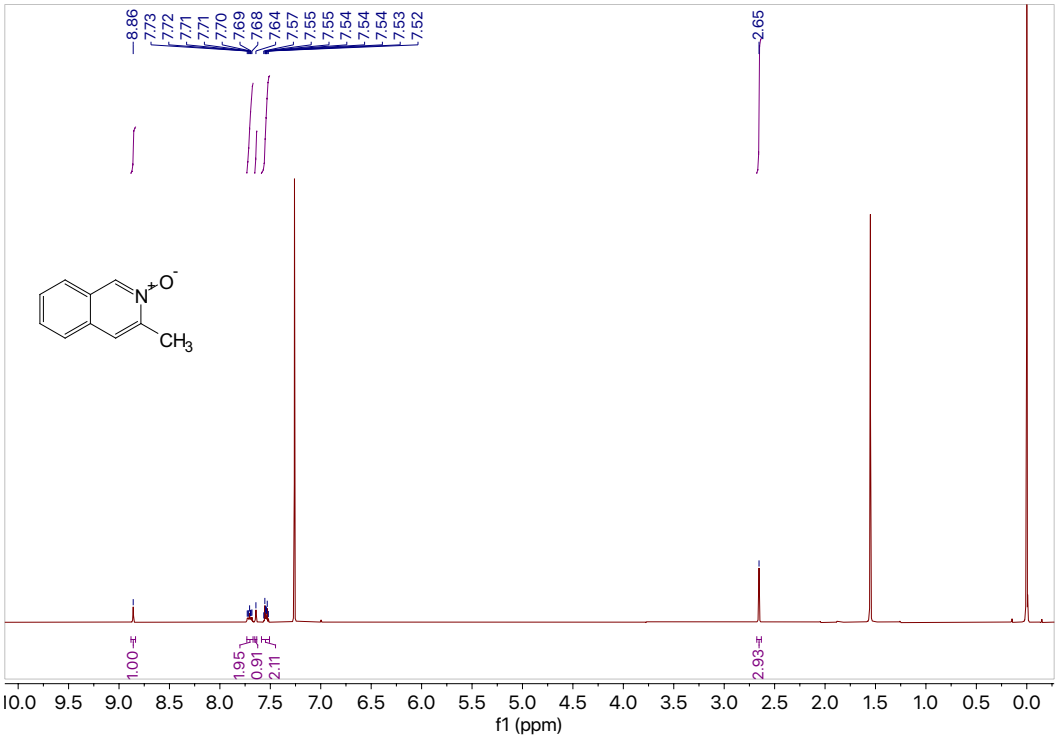

Figure 7.248 ^{1}H NMR (400 MHz, $CDCl_3$) of compound **6a**.

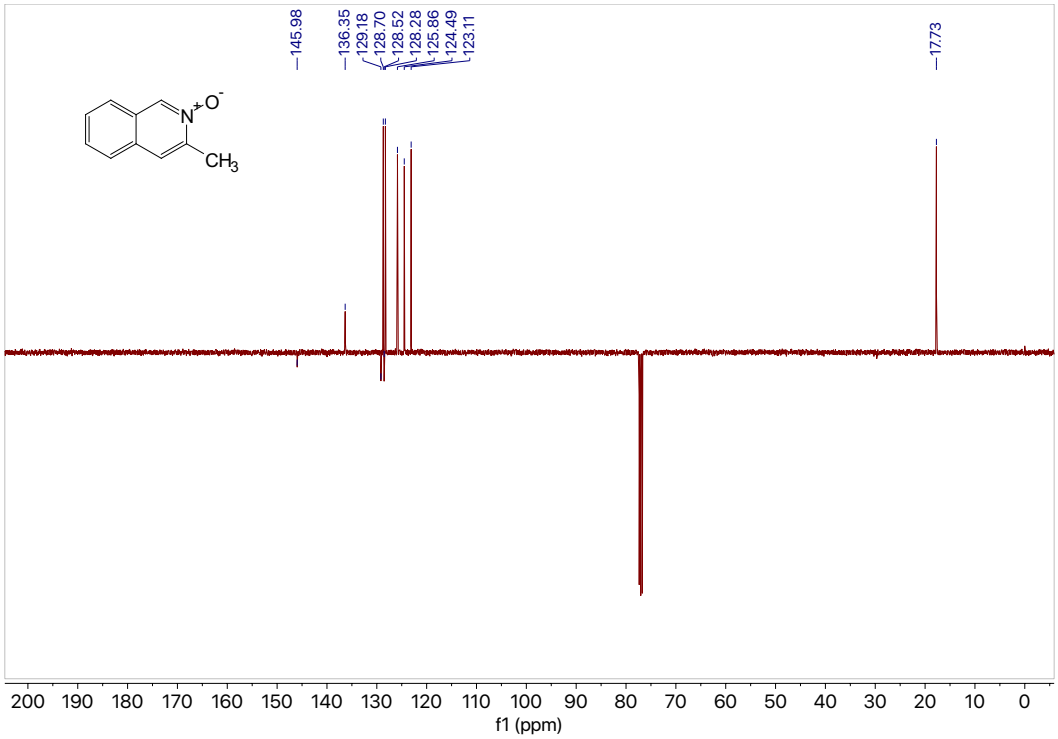

Figure 7.249 ^{13}C NMR (101 MHz, $CDCl_3$) of compound **6a**.

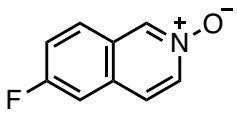

6b

6-fluoroisoquinoline 2-oxide (6b). Using the general procedure for synthesis of isoquinoline *N*-oxides, 6-fluoroisoquinoline **5b** (0.300 g, 2.04 mmol, 1.0 equiv) in DCM (1.13 mL, 1.8 M) reacted with mCPBA (1.01 g, 4.08 mmol, 2.0 equiv) in DCM (2.3 mL, 1.8 M) to afford the crude product which was purified by column chromatography (silica, 10:1 EtOAc: MeOH) to afford pure **6b** (0.288 g, 1.76 mmol) in 86% yield as a tan solid, m.p. = 225.1-225.6°C.

^{1}H NMR (400 MHz, $CDCl_3$) δ 8.76 (d, J = 4.0 Hz, 1H), 8.20 – 8.13 (m, 1H), 7.75 (dd, J = 9.0, 5.2 Hz, 1H), 7.64 (d, J = 7.2 Hz, 1H), 7.48 – 7.37 (m, 2H).

^{13}C NMR (101 MHz, $CDCl_3$) δ_u 137.8, 136.1, 127.7 (d, $^{3}J_{C\text{-}F}$ = 9.2 Hz), 123.6 (d, $^{4}J_{C\text{-}F}$ = 5.5 Hz), 120.2 (d, $^{2}J_{C\text{-}F}$ = 25.7 Hz), 110.9 (d, $^{2}J_{C\text{-}F}$ = 22.1 Hz); δ_d 162.3 (d, $^{1}J_{C\text{-}F}$ = 253.1 Hz), 130.0 (d, $^{3}J_{C\text{-}F}$ = 9.9 Hz), 126.7.

^{19}F NMR (376 MHz, $CDCl_3$) δ -108.08.

HRMS (ESI) calculated for C_9H_7ONF $[M+H]^+$: 164.0512, found 164.0504.

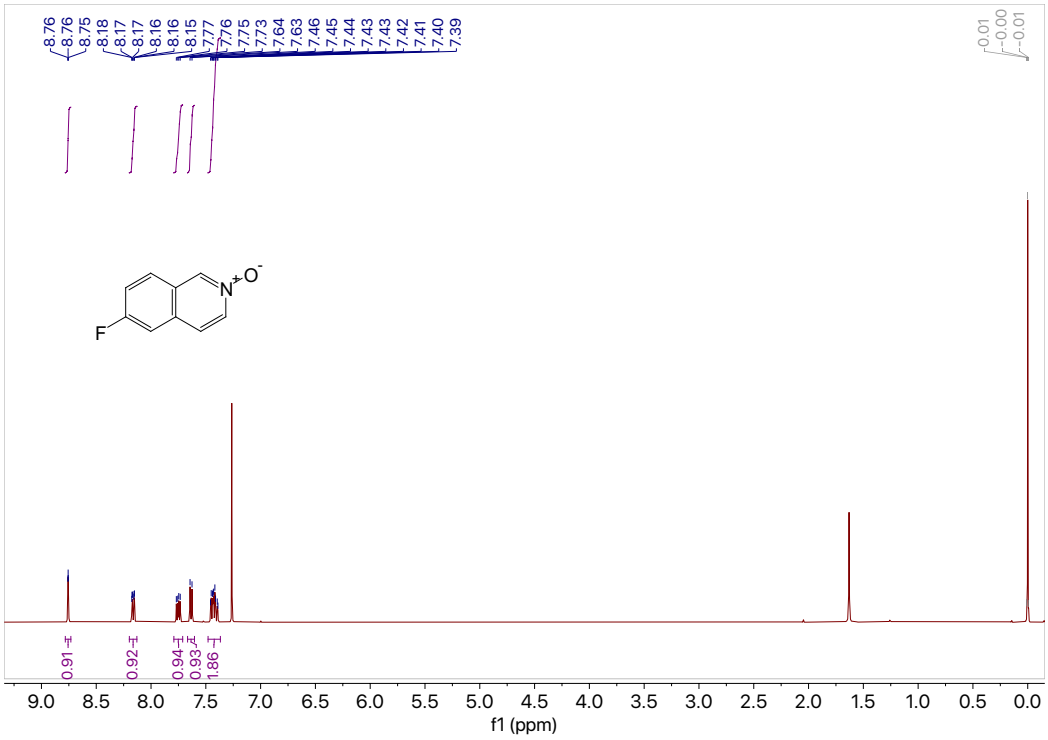

Figure 7.250 ^{1}H NMR (400 MHz, $CDCl_3$) of compound **6b**.

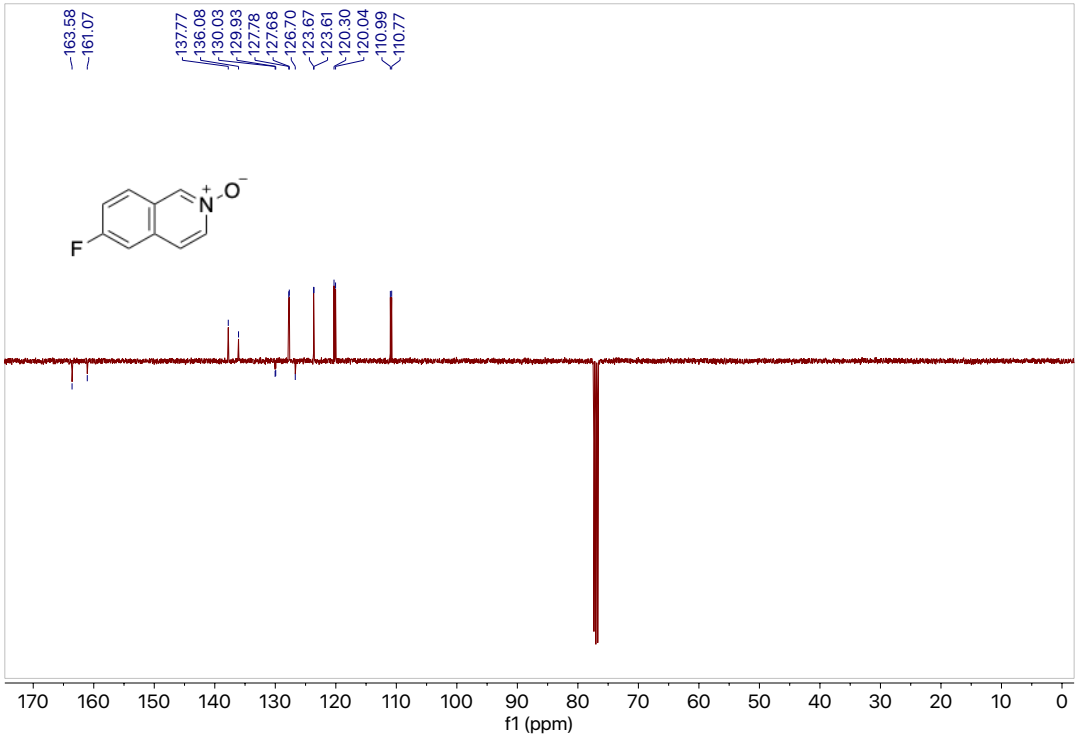

Figure 7.251 ^{13}C NMR (101 MHz, $CDCl_3$) of compound **6b**.

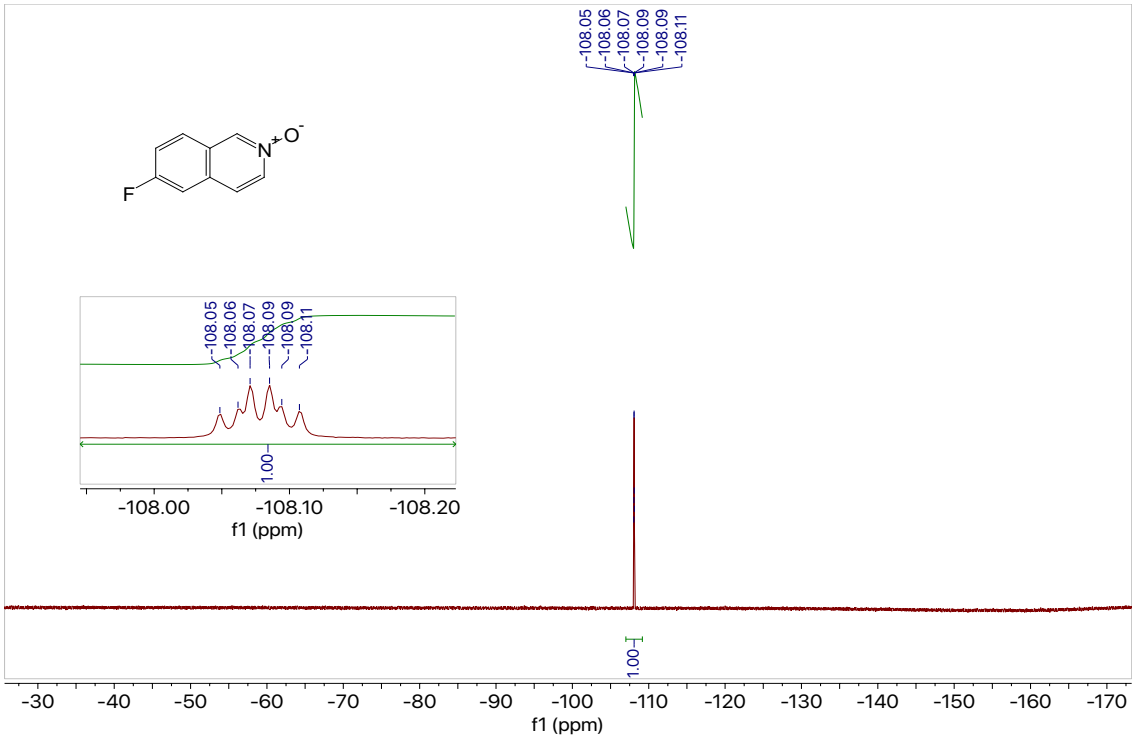

Figure 7.252 ^{19}F NMR (376 MHz, $CDCl_3$) of compound **6b**.

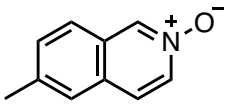

6c

6-methylisoquinoline 2-oxide (6c). Using the general procedure for synthesis of isoquinoline *N*-oxides, 6-methylisoquinoline **5c** (0.200 g, 1.40 mmol, 1.0 equiv) in DCM (0.8 mL, 1.8 M) reacted with mCPBA (0.688 g, 2.79 mmol, 2.0 equiv) in DCM (1.6 mL, 1.8 M) to afford the crude product which was purified by column chromatography (silica, 10:1 EtOAc: MeOH) to afford pure **6c** (0.180 g, 1.13 mmol) in 81% yield as a white solid, m.p. = 135.5 – 135.8°C.

^{1}H NMR (400 MHz, $CDCl_3$) δ 8.72 (d, *J* = 1.8 Hz, 1H), 8.11 (dd, *J* = 7.1, 1.8 Hz, 1H), 7.63 (d, *J* = 8.5 Hz, 1H), 7.61 – 7.54 (m, 2H), 7.46 (dd, *J* = 8.4, 1.6 Hz, 1H), 2.52 (s, 3H).

^{13}C NMR (101 MHz, $CDCl_3$) δ_u 136.7, 136.0, 131.8, 125.8, 124.8, 123.6; 21.8; δ_d 139.6, 129.1, 127.7.

HRMS (ESI) calculated for $C_{10}H_{10}ON$ $[M+H]^+$: 160.0762, found 160.0757.

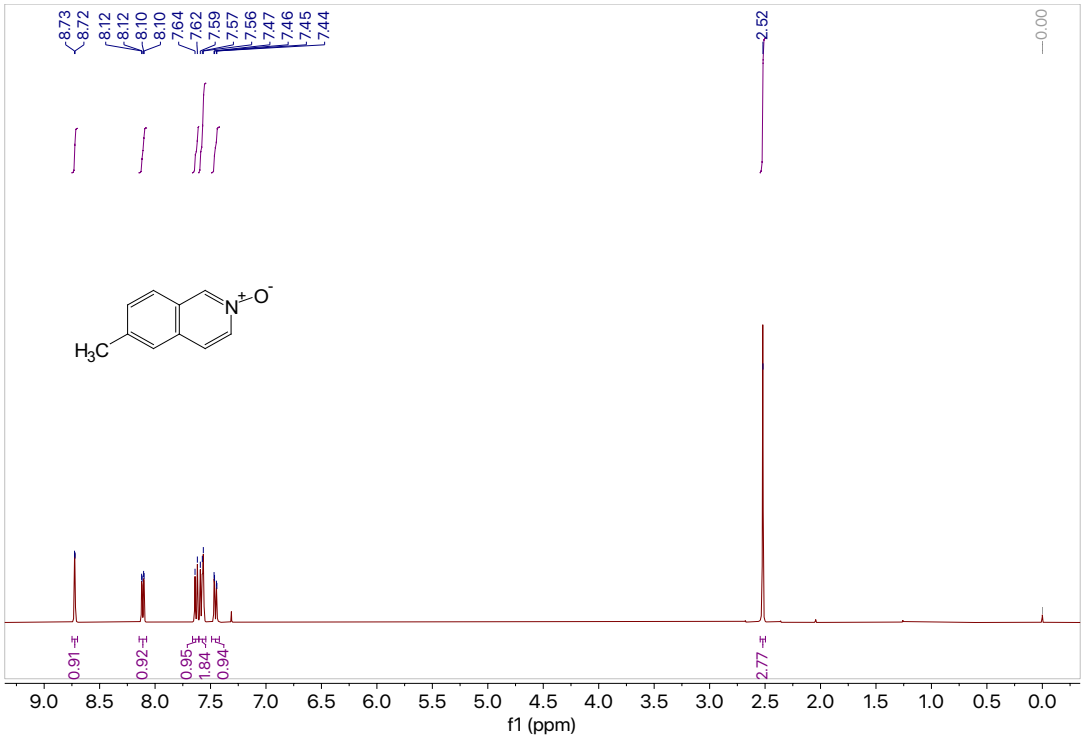

Figure 7.253 ^{1}H NMR (400 MHz, $CDCl_3$) of compound **6c**.

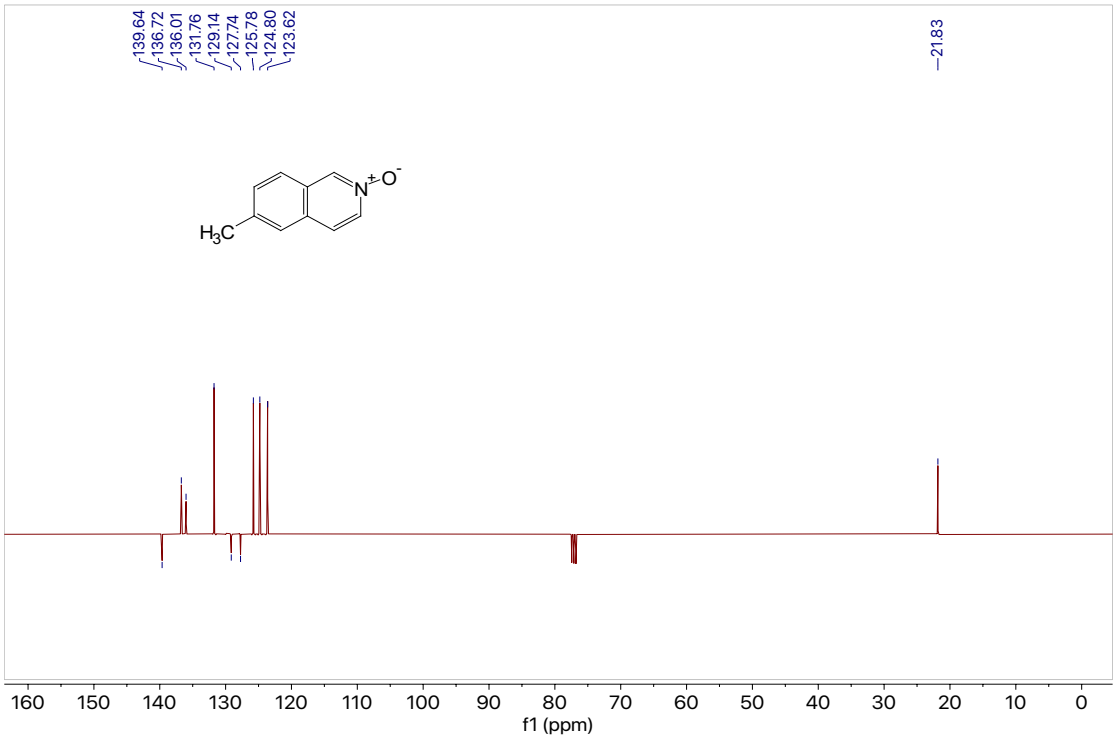

Figure 7.254 ^{13}C NMR (101 MHz, $CDCl_3$) of compound **6c**.

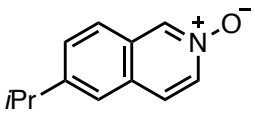

6d

6-isopropylisoquinoline 2-oxide (6d). Using the general procedure for synthesis of isoquinoline *N*-oxides, 6-isopropylisoquinoline **5d** (0.300 g, 1.75 mmol, 1.0 equiv) in DCM (1 mL, 1.8 M) reacted with mCPBA (0.319 g, 1.846 mmol, 2.0 equiv) in DCM (1.1 mL, 1.8 M) to afford the crude product which was purified by column chromatography (silica, 10:1 EtOAc: MeOH) to afford pure **6d** (0.300 g, 1.60 mmol) in 91% yield as a clear colorless oil.

^{1}H NMR (400 MHz, $CDCl_3$) δ 8.65 – 8.60 (m, 1H), 8.00 (dd, J = 7.1, 1.8 Hz, 1H), 7.55 (d, J = 8.6 Hz, 1H), 7.50 (d, J = 7.1 Hz, 1H), 7.46 (d, J = 1.6 Hz, 1H), 7.40 (dd, J = 8.5, 1.7 Hz, 1H), 2.94 (hept, J = 6.9 Hz, 1H), 1.20 (d, J = 6.9 Hz, 6H).

^{13}C NMR (101 MHz, $CDCl_3$) δ_u 136.5, 136.1, 129.9, 125.2, 124.0, 123.1, 34.3, 23.5; δ_d 150.6, 129.5, 128.0.

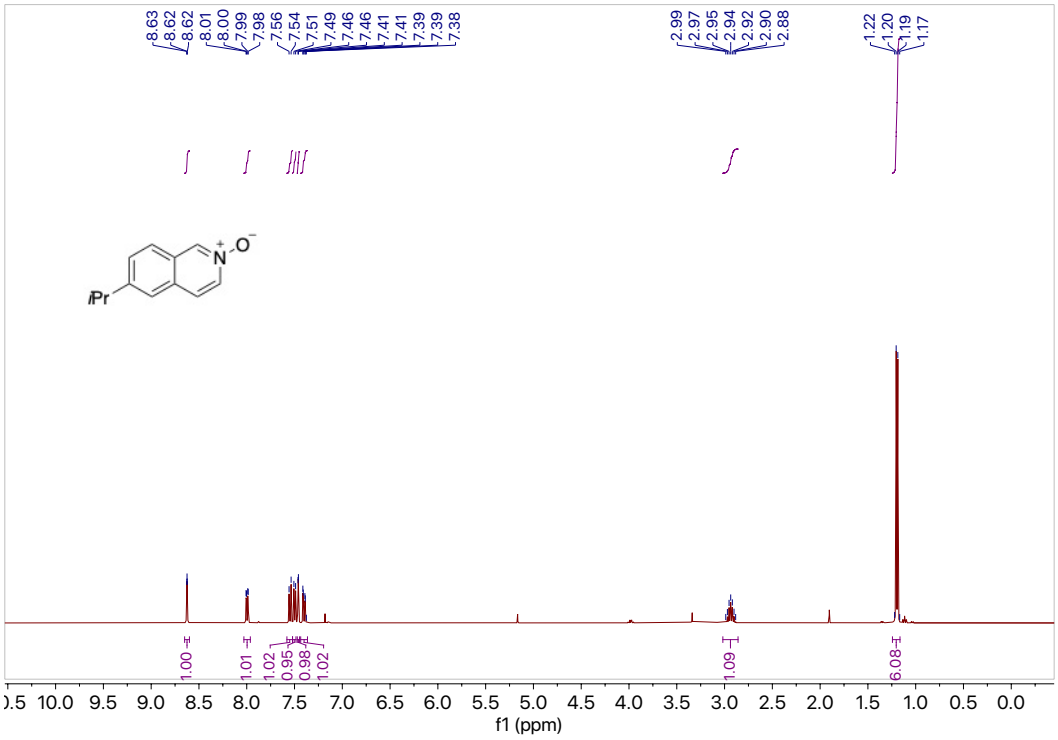

Figure 7.255 ^{1}H NMR (400 MHz, $CDCl_3$) of compound **6d**.

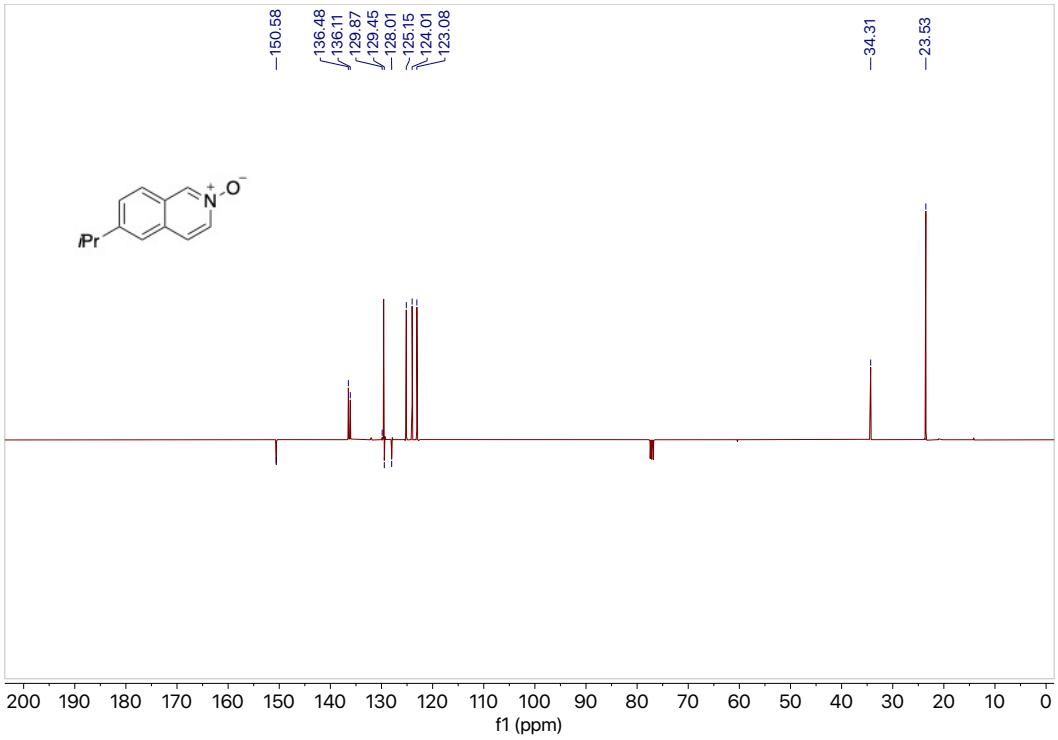

Figure 7.256 ^{13}C NMR (101 MHz, $CDCl_3$) of compound **6d**.

7.12.2 Synthesis of 6-(trifluoromethyl)isoquinoline 2-oxide (6e).

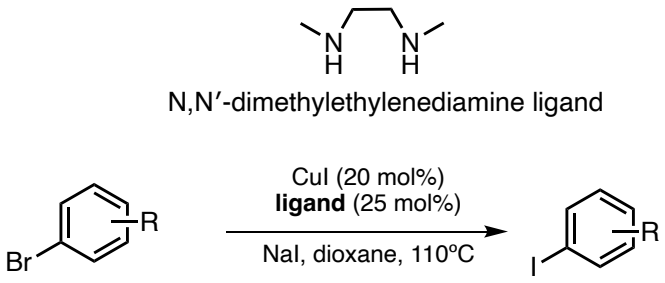

Scheme 7.16 Copper-catalyzed halogen exchange in aryl halides.

General procedure[19]

A vial with a stir bar was either flame dried under argon or oven-dried, brought into a glovebox, and charged with the aryl bromide (1 mmol, 1.0 equiv). Copper(I) iodide (0.2 mmol, 20 mol %), 1,2-diamine ligand (0.25 mmol, 25 mol %), NaI (2.0 mmol, 2.0 equiv), and dioxane (3 mL, 0.3 M) were added. The vial was sealed with a pressure relief cap and removed from the glovebox. The vial was stirred at 110˚C in a pie reactor for 12-15 hrs. Upon completion, the reaction mixture quenched with ammonia solution (25% aq.), diluted with water, and extracted with diethyl ether. The resulting organic solution was

washed with brine, dried with $MgSO_4$, and filtered. The crude product was concentrated *in vacuo* and purified by column chromatography.

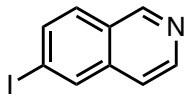

9e

6-iodoisoquinoline (9e). Using the general procedure for the copper-catalyzed halogen exchange, 6-bromoisoquinoline **8e** (0.501 g, 2.40 mmol, 1.0 equiv) in dioxane (8 mL, 0.3 M) afforded the crude product which was purified by column chromatography (silica, 4:1 hexanes: EtOAc) to afford pure **9e** (0.540 g, 2.12 mmol) in 88% yield as a white solid.
^{1}H NMR (400 MHz, $CDCl_3$) δ 9.23 (s, 1H), 8.56 (d, J = 5.8 Hz, 1H), 8.27 – 8.22 (m, 1H), 7.87 (dd, J = 8.6, 1.6 Hz, 1H), 7.68 (d, J = 8.6 Hz, 1H), 7.53 (d, J = 5.7 Hz, 1H).
^{13}C NMR (101 MHz, $CDCl_3$) δ_u 152.51, 143.87, 136.12, 135.44, 128.92, 119.08; δ_u 136.98, 97.65.
GC (Method B) t_R = 1.314 min. EI-MS m/z (%): 253.9 ($M\text{-}1^+$, 100), 127 (75), 101.0 (5), 77.0 (6).

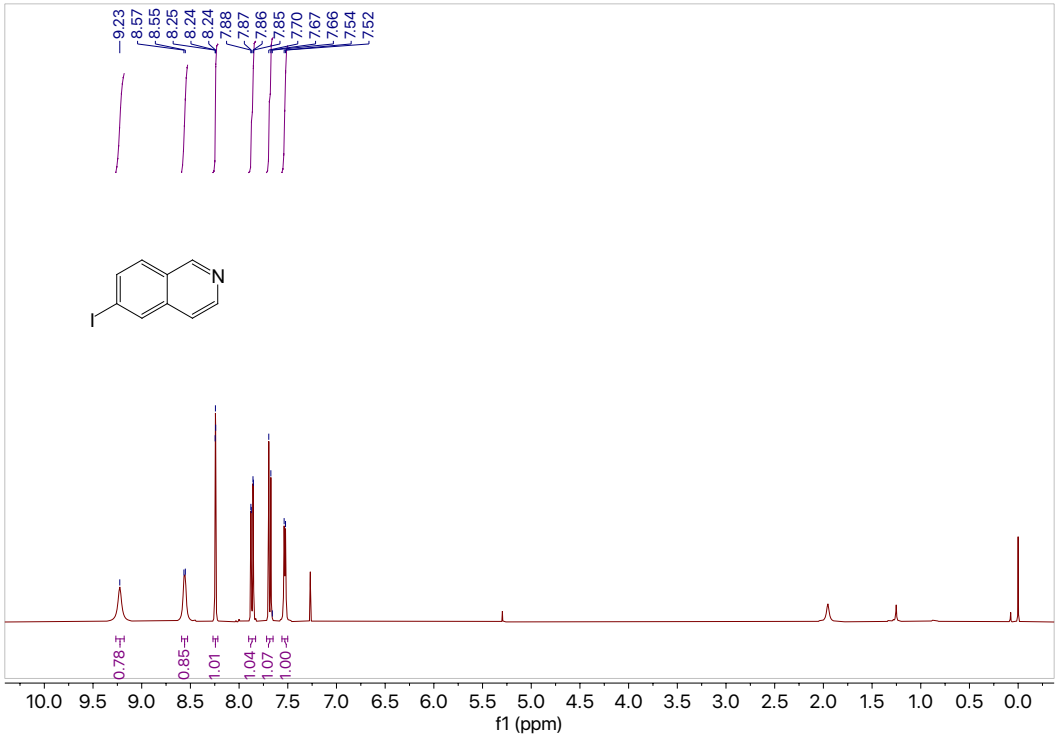

Figure 7.257 ^{1}H NMR (400 MHz, $CDCl_3$) of compound **9e**.

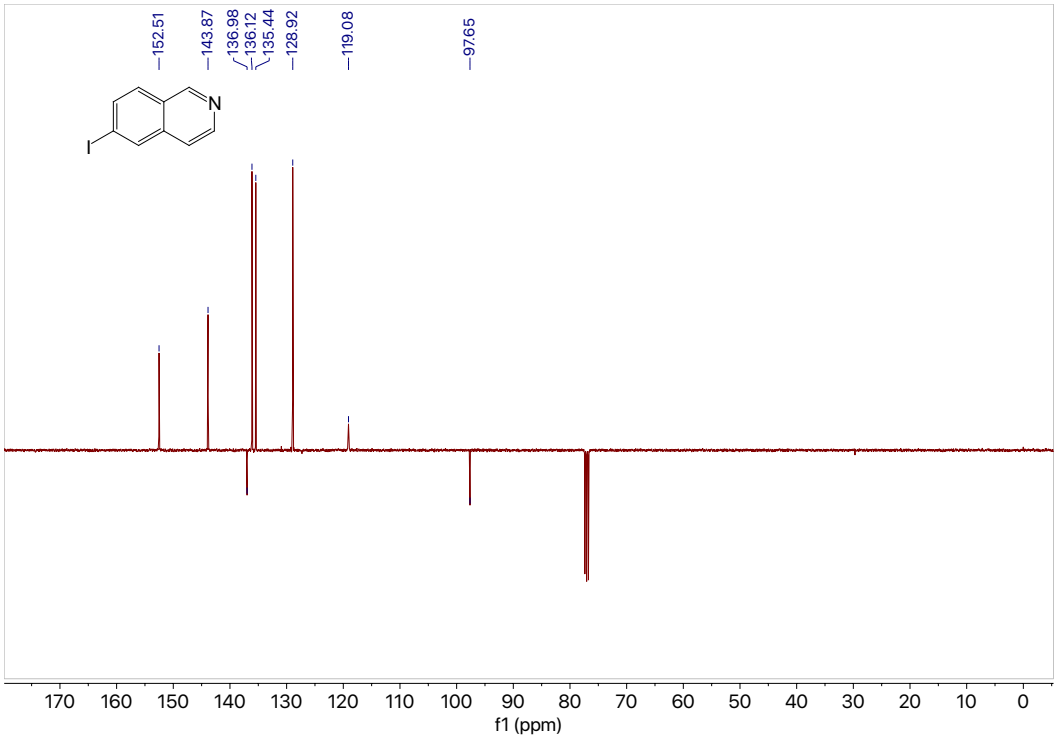

Figure 7.258 ^{13}C NMR (101 MHz, $CDCl_3$) of compound **9e**.

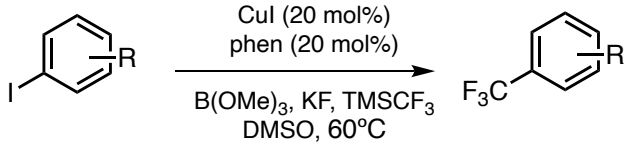

Scheme 7.17 Copper-catalyzed trifluoromethylation of aryl iodides.

General procedure[20]

A vial with a stir bar was either flame dried under argon or oven-dried, brought into a glovebox, and charged with the aryl iodide (1 mmol, 1.0 equiv). Copper(I) iodide (0.2 mmol, 20 mol %), 1,10-phenanthroline (0.2 mmol, 20 mol %), $B(OMe)_3$ (3.0 mmol, 3.0 equiv), $TMSCF_3$ (3.,0 mmol, 3.0 equiv), KF (2.0 mmol, 2.0 equiv), and DMSO (3 mL, 0.35 M) were added. The vial was sealed with a pressure relief cap and removed from the glovebox. The vial was stirred at 60˚C in a pie reactor for 24 hrs. Upon completion, the reaction mixture quenched with ammonia solution (25% aq.), diluted with water, and extracted with diethyl ether. The resulting organic solution was washed with brine, dried with $MgSO_4$, and filtered. The crude product was concentrated *in vacuo* and purified by column chromatography.

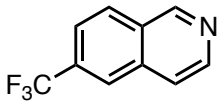

5e

6-(trifluoromethyl)isoquinoline (5e). Using the general procedure for the copper-catalyzed trifluoromethylation of aryl iodides, 6-iodoisoquinoline **9e** (0.444 g, 1.742 mmol, 1.0 equiv) in DMSO (5 mL, 0.35 M) afforded the crude product which was purified by column chromatography (silica, 3:2 hexanes: EtOAc) to afford pure **5e** (0.317 g, 1.61 mmol) in 92% yield as a clear colorless oil.

^{1}H NMR (400 MHz, $CDCl_3$) δ 9.36 (s, 1H), 8.66 (d, J = 5.7 Hz, 1H), 8.20 – 8.14 (m, 1H), 8.14 – 8.08 (m, 1H), 7.82 – 7.71 (m, 2H).

^{13}C NMR (101 MHz, $CDCl_3$) δ_u 152.4, 144.3, 128.9, 124.5 (q, $^{4}J_{C\text{-}F}$ = 4.4 Hz), 123.8 (q, $^{1}J_{C\text{-}F}$ = 272.7 Hz), 121.0; δ_d 134.9, 132.2 (q, $^{2}J_{C\text{-}F}$ = 32.6 Hz), 129.3, 122.4.

^{19}F NMR (376 MHz, $CDCl_3$) δ -62.97.

GC (Method A) t_R = 4.146 min. EI-MS m/z (%): 196.0 ($M\text{-}1^+$, 100), 177 (14), 146.0 (31), 126.0 (5), 98.0 (5).

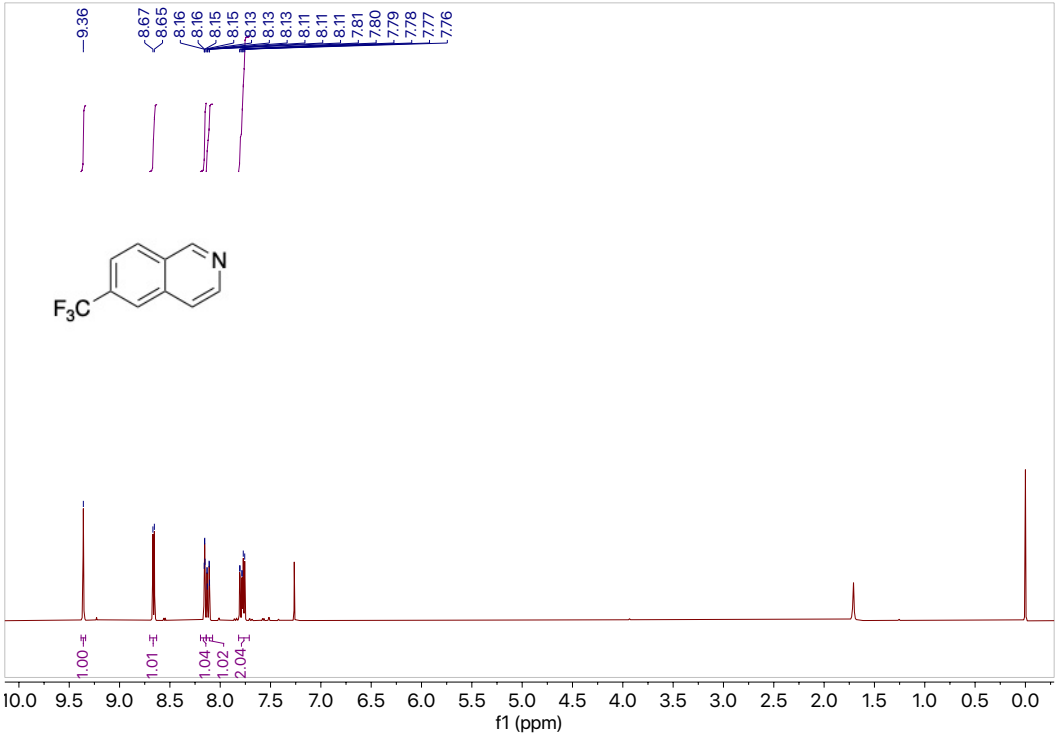

Figure 7.259 ^{1}H NMR (400 MHz, $CDCl_3$) of compound **5e**.

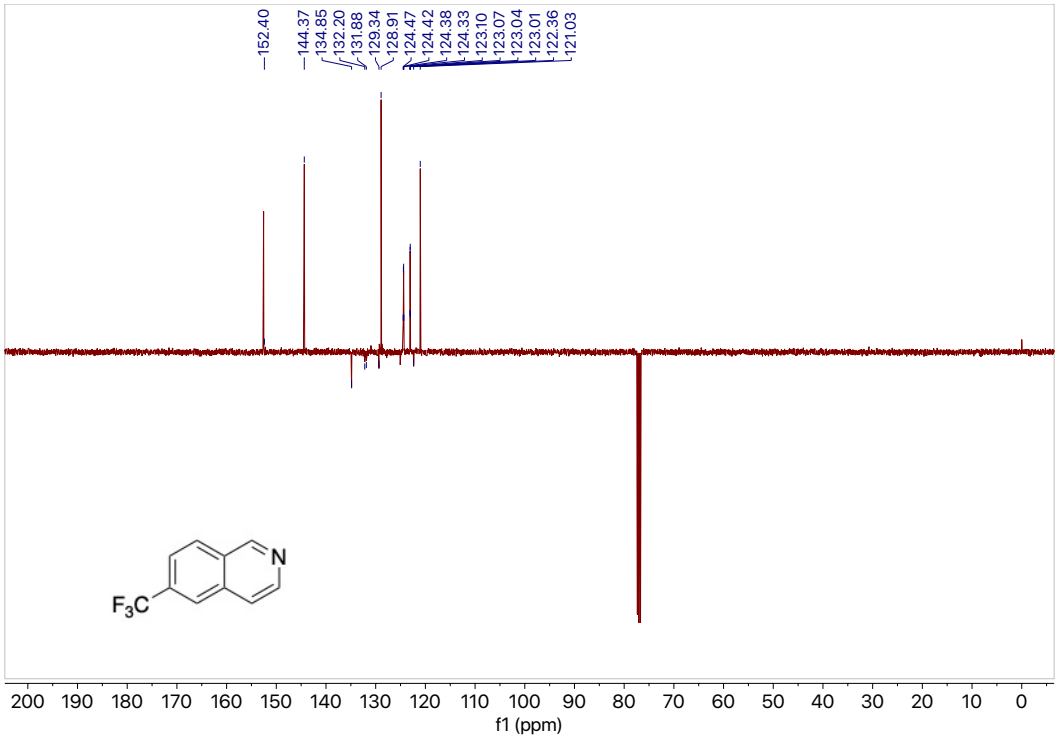

Figure 7.260 ^{13}C NMR (101 MHz, $CDCl_3$) of compound **5e**.

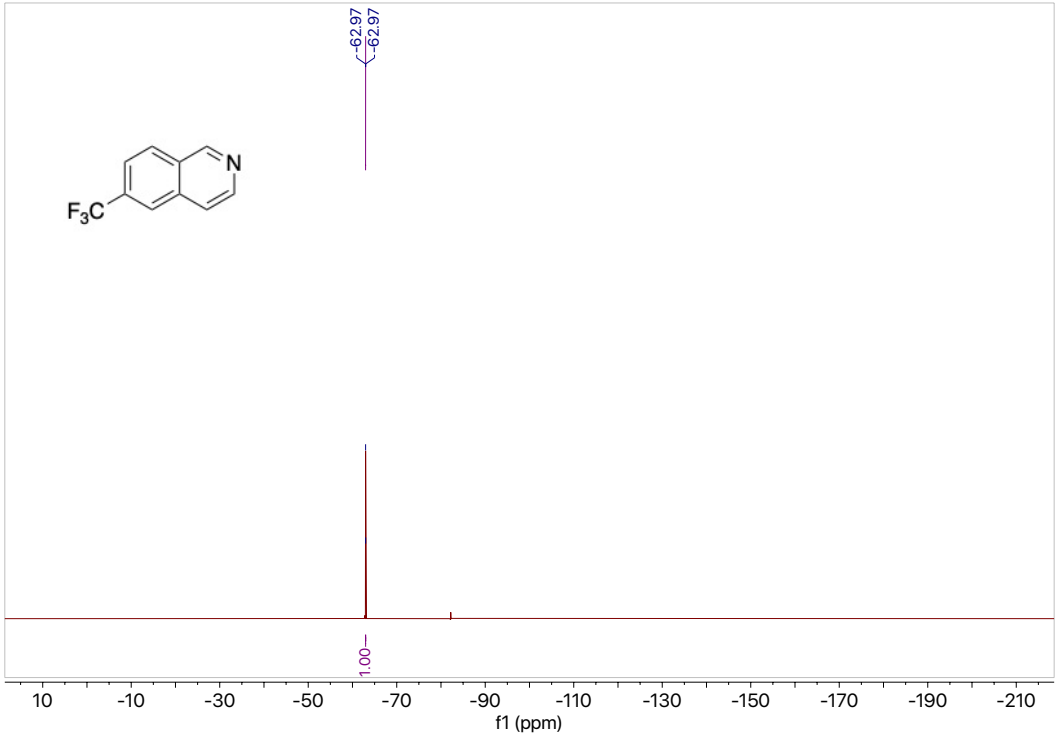

Figure 7.261 ^{19}F NMR (376 MHz, $CDCl_3$) of compound **5e**.

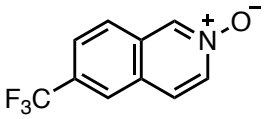

6e

6-(trifluoromethyl)isoquinoline 2-oxide (6e). Using the general procedure for synthesis of isoquinoline *N*-oxides, 6-trifluoromethylisoquinoline **5e** (0.182 g, 0.923 mmol, 1.0 equiv) in DCM (0.5 mL, 1.8 M) reacted with mCPBA (0.319 g, 1.846 mmol, 2.0 equiv) in DCM (1 mL, 1.8 M) to afford the crude product which was purified by column chromatography (silica, 10:1 EtOAc: MeOH) to afford pure **6e** (0.144 g, 0.674 mmol) in 73% yield as a white solid.

^{1}H NMR (400 MHz, $CDCl_3$) δ 8.83 (d, J = 1.8 Hz, 1H), 8.23 (dd, J = 7.2, 1.8 Hz, 1H), 8.10 (s, 1H), 7.86 (d, J = 8.7 Hz, 1H), 7.81 – 7.77 (m, 2H).

^{13}C NMR (101 MHz, $CDCl_3$) δ_u 138.4, 135.9, 125.9, 125.4 (q, $^{4}J_{C\text{-}F}$ = 3.2 Hz), 124.8, 124.4 (q, $^{4}J_{C\text{-}F}$ = 4.5 Hz); δ_d 131.1 – 129.9 (m), 127.5, 122.1, 119.4.

^{19}F NMR (376 MHz, $CDCl_3$) δ -62.95.

GC (Method A) t_R = 10.101 min. EI-MS m/z (%): 213.0 (M-1^{+}, 33), 197 (100), 186.0 (15), 178.0 (8), 169.0 (10), 158.0 (11), 147.0 (10), 138.0 (5), 128.0 (6), 98.9 (4), 75.0 (6).

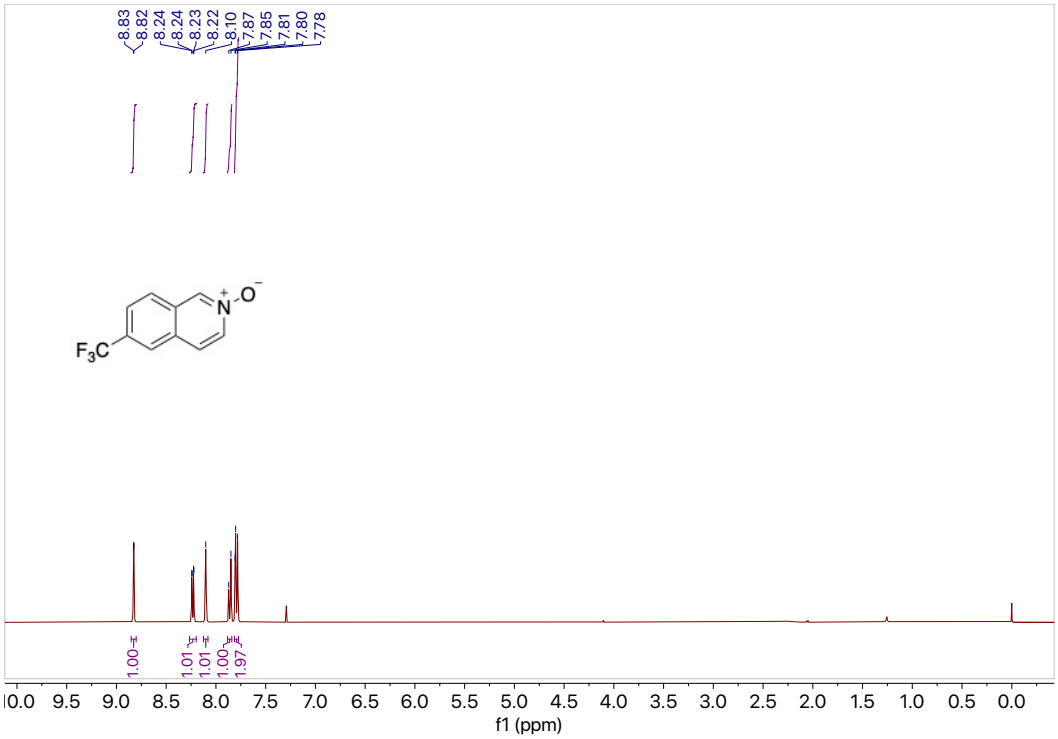

Figure 7.262 ^{1}H NMR (400 MHz, $CDCl_3$) of compound **6e**.

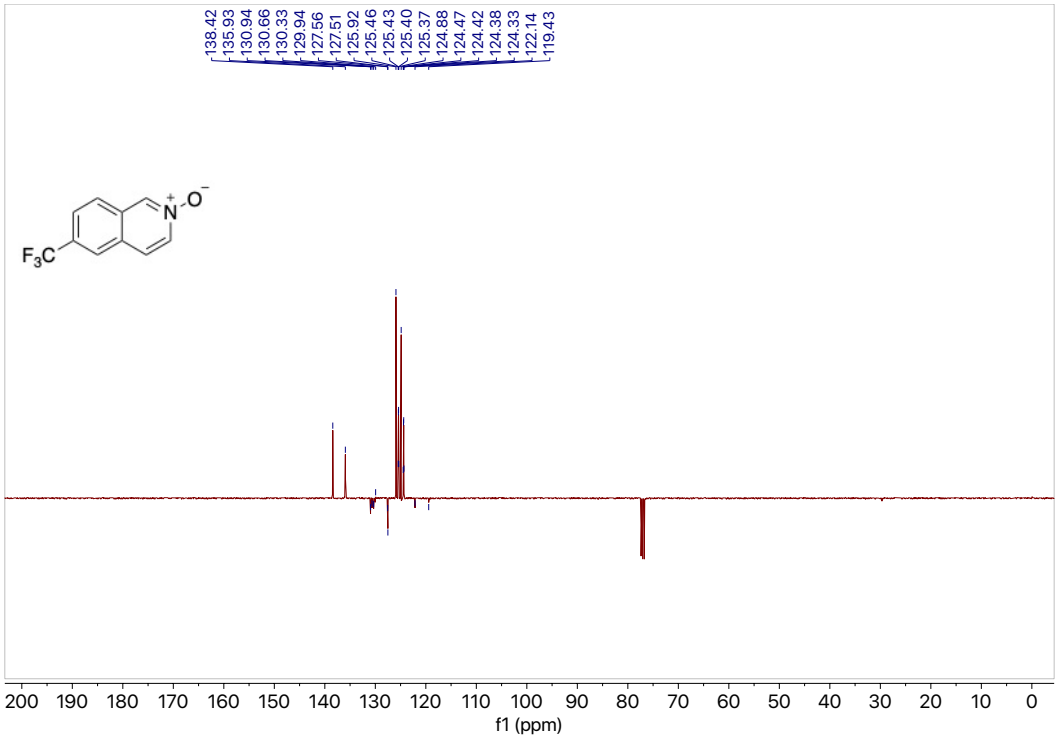

Figure 7.263 ^{13}C NMR (101 MHz, $CDCl_3$) of compound **6e**.

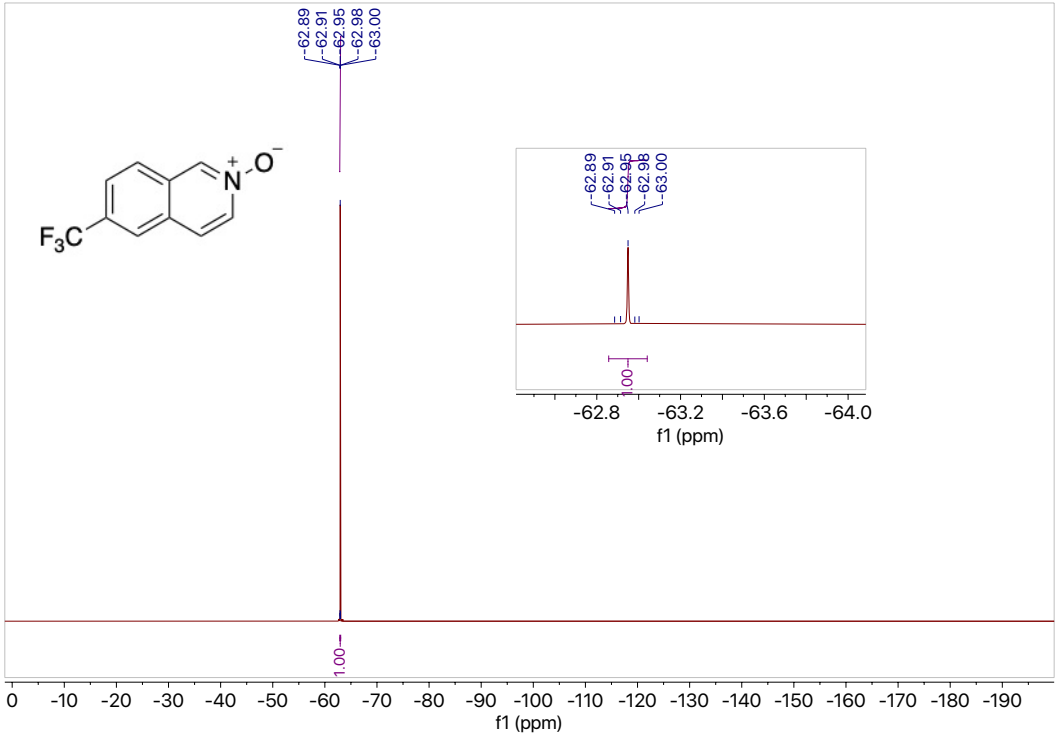

Figure 7.264 ^{19}F NMR (376 MHz, $CDCl_3$) of compound **6e**.

7.12.3 Cyanation of isoquinoline *N*-oxides.

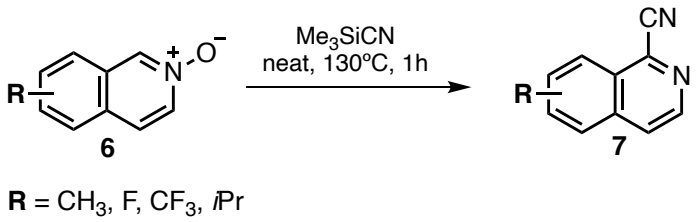

Scheme 7.18 Cyanation of isoquinoline N-oxides general reaction.

General procedure

A vial with a stir bar was either flame dried under argon or oven-dried and charged with isoquinoline *N*-oxide (1.0 mmol, 1.0 equiv) and trimethylsilyl cyanide (2.2 mmol, 2.2 equiv). The vial was sealed with a pressure relief cap and was stirred at 130˚C in a pie reactor for 1 h. Upon completion, the crude reaction mixture was concentrated under vacuum and purified by column chromatography.

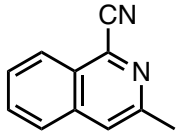

7a

3-methylisoquinoline-1-carbonitrile (7a). Using the general procedure for cyanation of isoquinoline *N*-oxides, the *N*-oxide **6a** (0.2034 g, 1.28 mmol, 1.0 equiv) reacted with trimethylsilyl cyanide (0.278 g, 3.75 mL, 2.81 mmol, 2.2 equiv) to afford the crude product which was purified by column chromatography (silica, 10:1 hexanes: EtOAc) to afford pure **7a** (0.153 g, 0.91 mmol) in 72% yield as a white solid.
^{1}H NMR (400 MHz, $CDCl_3$) δ 8.34 – 8.26 (m, 1H), 7.88 – 7.81 (m, 1H), 7.79 – 7.75 (m, 1H), 7.73 (d, J = 1.3 Hz, 1H), 7.72 – 7.69 (m, 1H), 2.75 (d, J = 0.7 Hz, 3H).
GC t_R = 1.304 min (Method B). EI-MS m/z (%): 168.0 (M^+, 100), 139.9 (22), 127.9 (8), 114.9 (9), 88.9 (3), 74.9 (3), 62.9 (5).

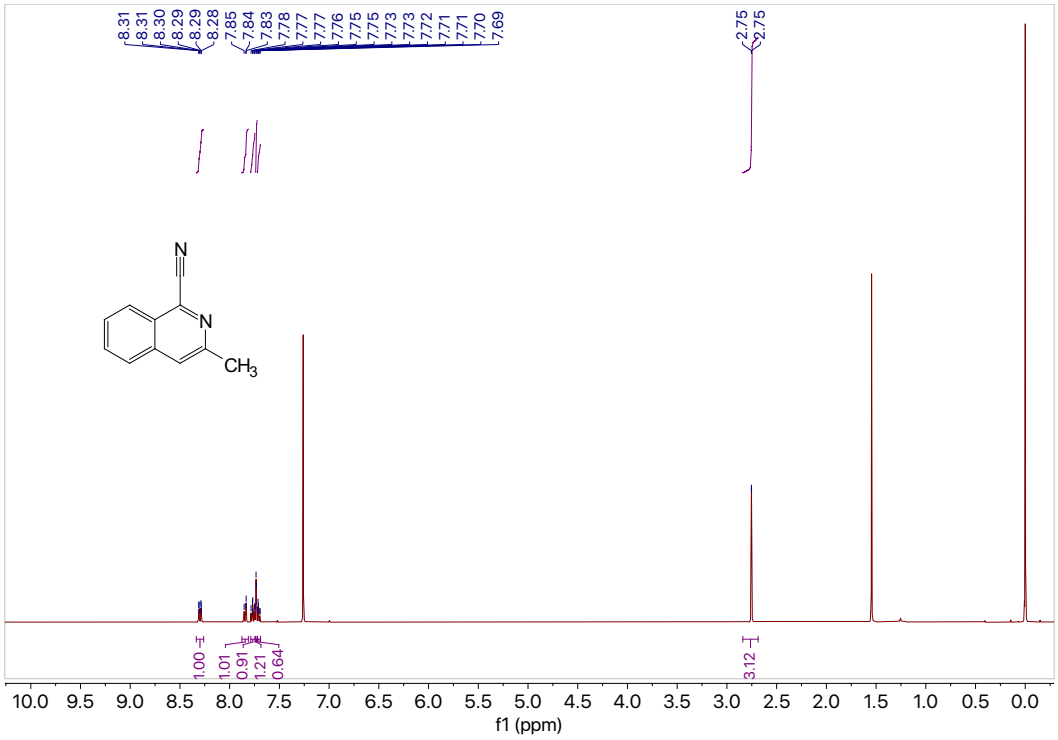

Figure 7.265 ^{1}H NMR (400 MHz, $CDCl_3$) of compound **7a**.

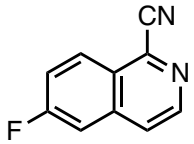

7b

6-fluoroisoquinoline-1-carbonitrile (7b). Using the general procedure for cyanation of isoquinoline *N*-oxides, the *N*-oxide **6b** (0.412 g, 2.53 mmol, 1.0 equiv) reacted with trimethylsilyl cyanide (0.741 mL, 5.56 mmol, 2.2 equiv) to afford the crude product which was purified by column chromatography (silica, 10:1 hexanes: EtOAc) to afford pure **7b** (0.410 g, 2.38 mmol) in 94% yield as a white solid, m.p. = 123.3 – 124.0°C.
^{1}H NMR (400 MHz, $CDCl_3$) δ 8.50 (dd, J = 5.7, 0.8 Hz, 1H), 8.24 (ddt, J = 8.8, 5.2, 0.9 Hz, 1H), 7.71 (dd, J = 5.7, 0.9 Hz, 1H), 7.47 – 7.37 (m, 2H).
^{13}C NMR (101 MHz, $CDCl_3$) δ_u 144.1, 128.8 (d, $^{3}J_{C\text{-}F}$ = 9.9 Hz), 123.9 (d, $^{4}J_{C\text{-}F}$ = 5.6 Hz), 120.8 (d, $^{2}J_{C\text{-}F}$ = 26.2 Hz), 110.8 (d, $^{2}J_{C\text{-}F}$ = 21.4 Hz); δ_d 163.8 (d, $^{1}J_{C\text{-}F}$ = 256.7 Hz), 137.5 (d, $^{3}J_{C\text{-}F}$ = 10.7 Hz), 126.6, 115.6.
^{19}F NMR (376 MHz, $CDCl_3$) δ -103.47.
GC (Method A) t_R = 8.084 min EI-MS m/z (%): 171.9 (M^+, 100), 144.9 (36), 177.8 (4), 99.8 (4), 93.9 (4), 85.8 (4), 73.9 (3).
HRMS (ESI) calculated for $C_{10}H_6N_2F$ $[M+H]^+$: 173.0515, found 173.0509.

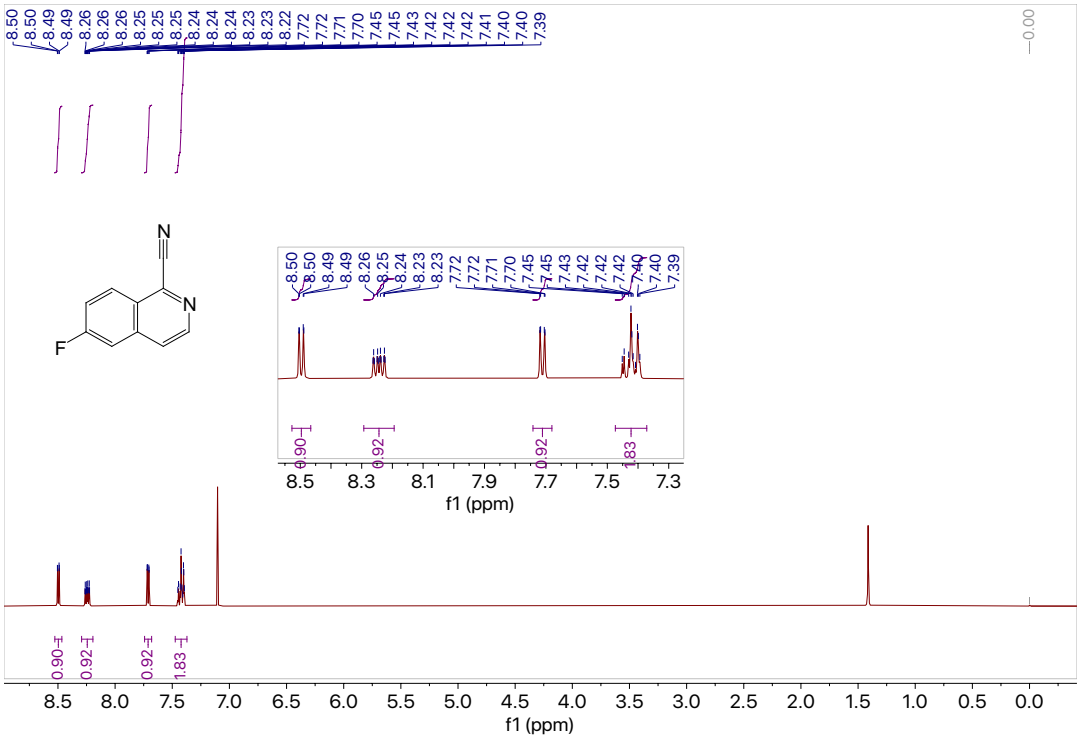

Figure 7.266 ^{1}H NMR (400 MHz, $CDCl_3$) of compound **7b**.

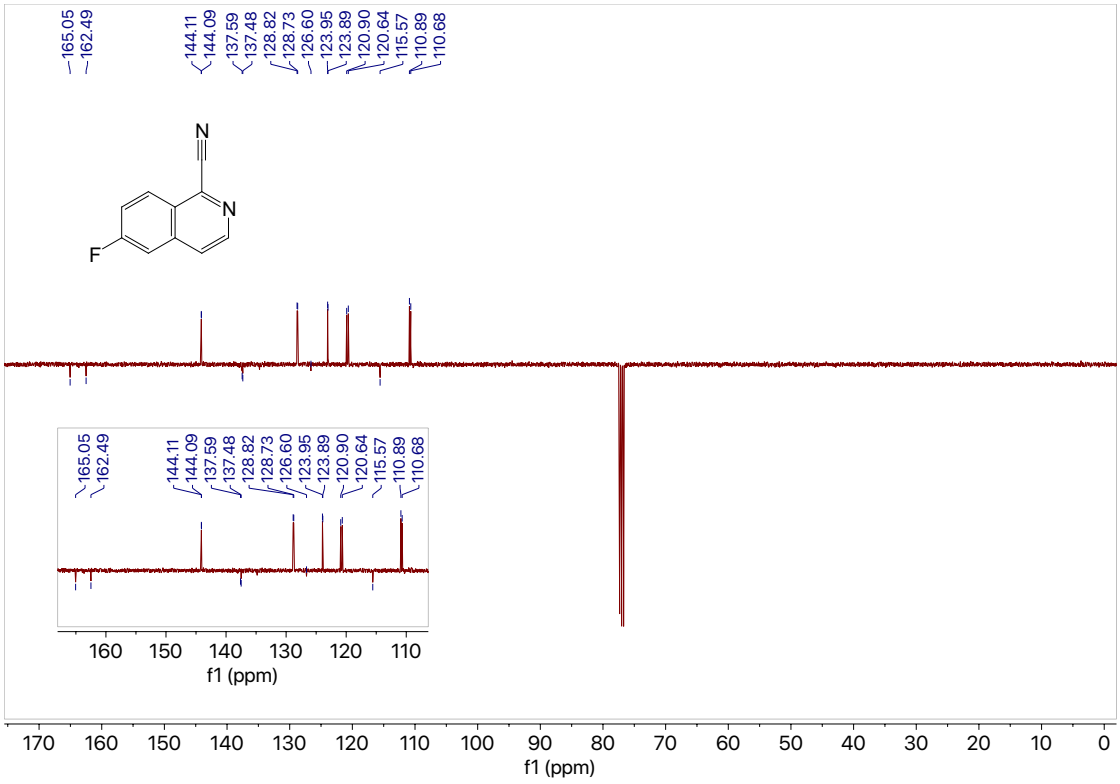

Figure 7.267 ^{13}C NMR (101 MHz, $CDCl_3$) of compound **7b**.

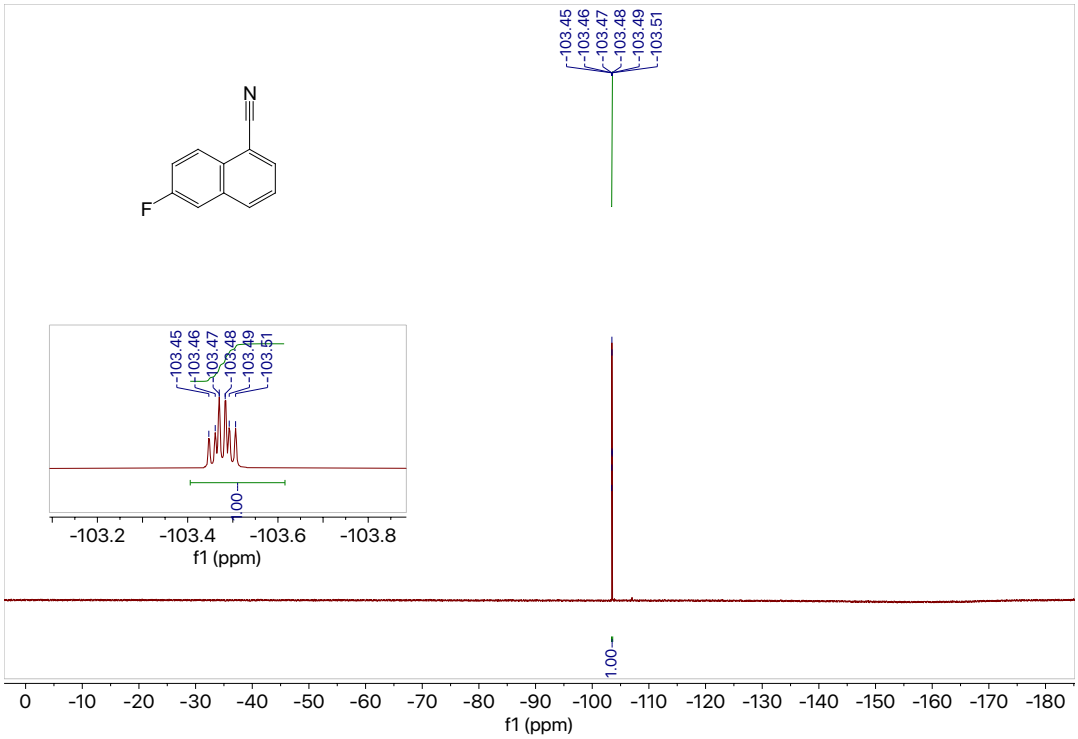

Figure 7.268 ^{19}F NMR (376 MHz, $CDCl_3$) of compound **7b**.

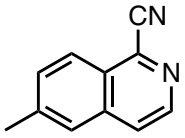

7c

6-methylisoquinoline-1-carbonitrile (7c). Using the general procedure for cyanation of isoquinoline *N*-oxides, the *N*-oxide **6c** (0.159 g, 1.00 mmol, 1.0 equiv) reacted with trimethylsilyl cyanide (0.744 mL, 2.20 mmol, 2.2 equiv) to afford the crude product which was purified by column chromatography (silica, 10:1 hexanes: EtOAc) to afford pure **7c** (0.155 g, 0.922 mmol) in 92% yield as a white solid, m.p. = 103.9 – 104.4 °C.
^{1}H NMR (400 MHz, $CDCl_3$) δ 8.60 (d, J = 5.6 Hz, 1H), 8.24 (d, J = 8.6 Hz, 1H), 7.80 (dd, J = 5.7, 0.9 Hz, 1H), 7.70 (s, 1H), 7.63 (dd, J = 8.5, 1.6 Hz, 1H), 2.60 (s, 3H).
^{13}C NMR (101 MHz, $CDCl_3$) δ_u 143.4, 132.2, 126.1, 125.1, 123.8, 22.1; δ_d 142.6, 136.2, 134.4, 128.0, 116.0.
GC (Method B) t_R = 1.413 min EI-MS m/z (%): 168.0 (M^+, 100), 140.0 (17), 114.0 (9), 63.0 (4).
HRMS (ESI) calculated for $C_{11}H_9N_2$ $[M+H]^+$: 169.0766, found 169.0759.

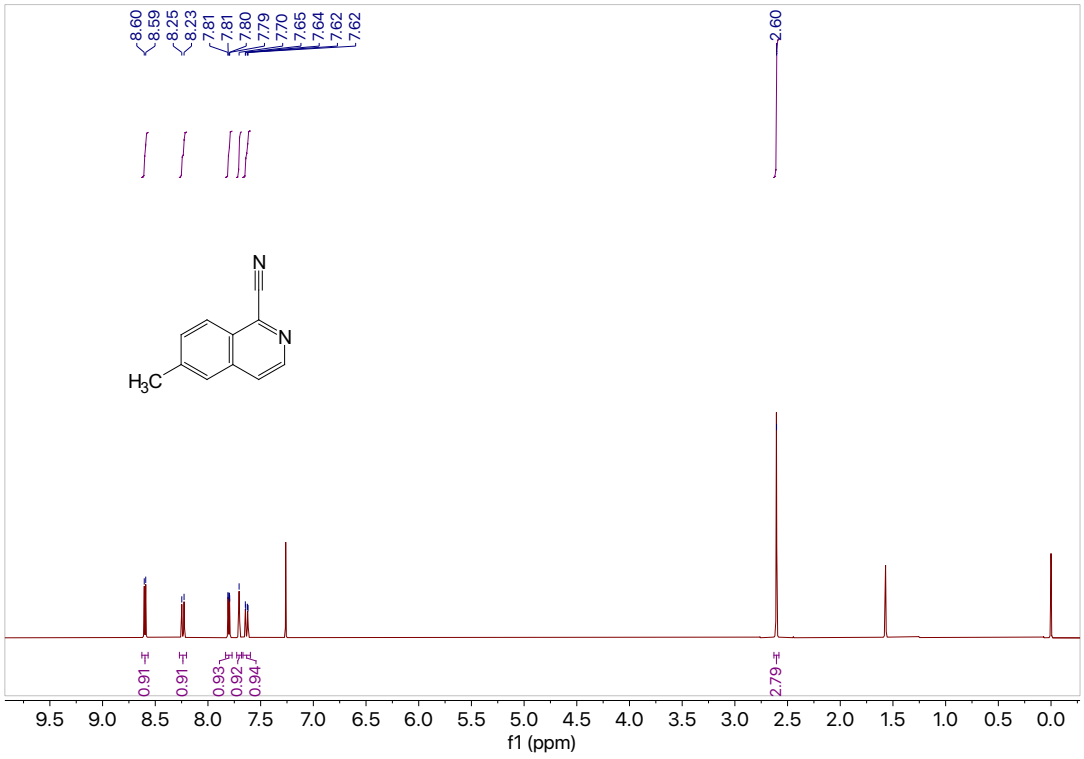

Figure 7.269 ^{1}H NMR (400 MHz, $CDCl_3$) of compound **7c**.

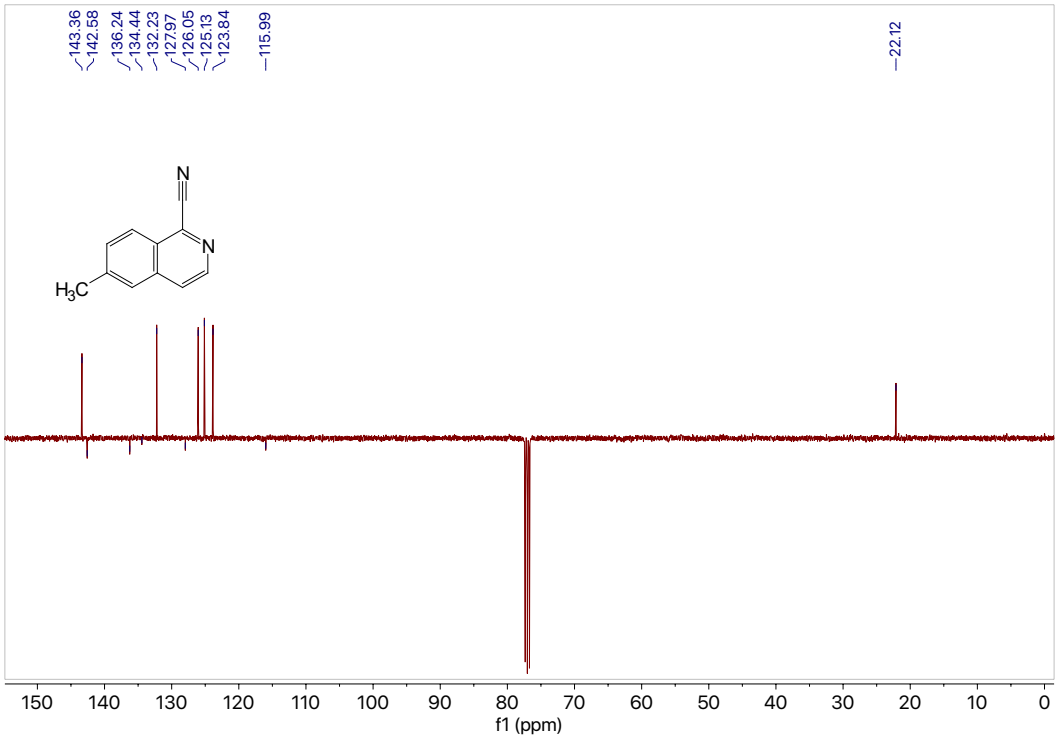

Figure 7.270 ^{13}C NMR (101 MHz, $CDCl_3$) of compound **7c**.

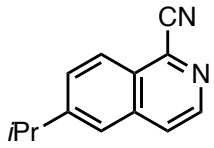

7d

6-isopropylisoquinoline-1-carbonitrile (7d). Using the general procedure for cyanation of isoquinoline *N*-oxides, the *N*-oxide **6d** (0.200 g, 1.07 mmol, 1.0 equiv) reacted with trimethylsilyl cyanide (0.31 mL, 2.35 mmol, 2.2 equiv) to afford the crude product which was purified by column chromatography (silica, 10:1 hexanes: EtOAc) to afford pure **7d** (0.194 g, 0.989 mmol) in 93% yield as a clear colorless oil.

^{1}H NMR (400 MHz, $CDCl_3$) δ 8.53 (d, J = 5.6 Hz, 1H), 8.23 – 8.16 (m, 1H), 7.77 (dd, J = 5.6, 0.9 Hz, 1H), 7.63 (dd, J = 10.4, 1.8 Hz, 2H), 3.08 (hept, J = 6.9 Hz, 1H), 1.30 (d, J = 6.9 Hz, 6H).

^{13}C NMR (101 MHz, $CDCl_3$) δ_u 143.3, 130.01, 125.3, 124.2, 123.3, 34.5, 23.7; δ_d 153.1, 136.4, 134.3, 128.3, 116.0.

GC (Method B) t_R = 1.802 min EI-MS m/z (%): 196.1 (M^+, 57), 181.1 (100), 167.0 (3), 154.0 (21), 140.0 (5), 127.0 (15).

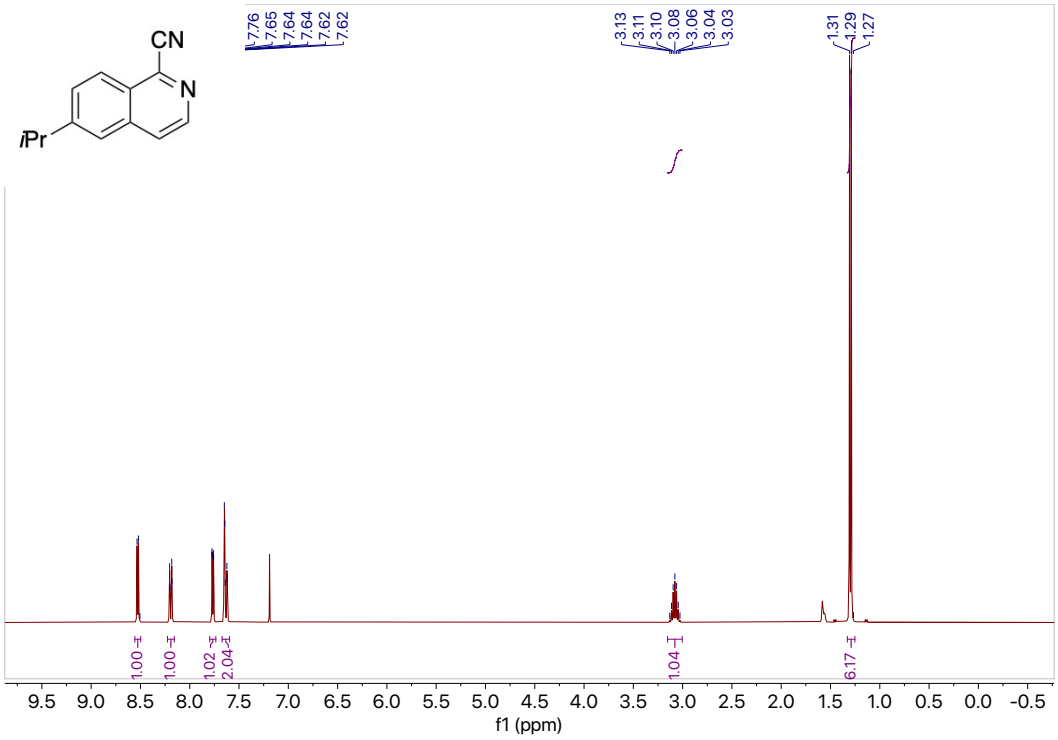

Figure 7.271 ^{1}H NMR (400 MHz, $CDCl_3$) of compound **7d**.

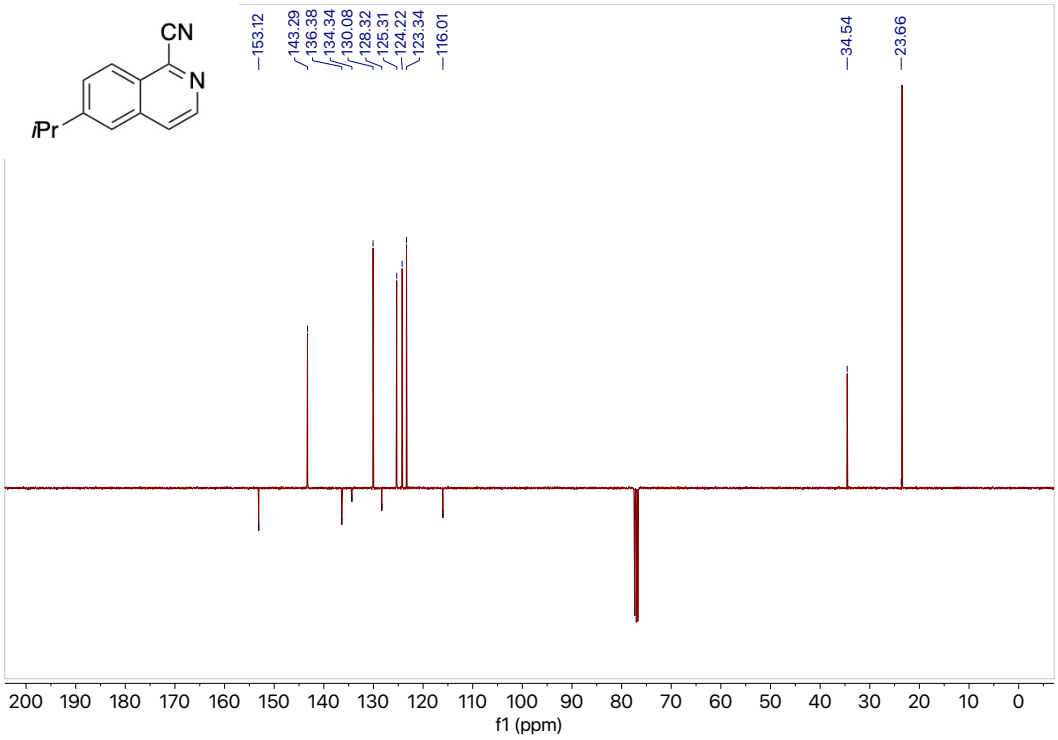

Figure 7.272 ^{13}C NMR (101 MHz, $CDCl_3$) of compound **7d**.

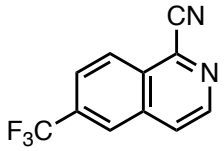

7e

6-(trifluoromethyl)isoquinoline-1-carbonitrile (7e). Using the general procedure for cyanation of isoquinoline *N*-oxides, the *N*-oxide **6e** (0.0872 g, 0.409 mmol, 1.0 equiv) reacted with trimethylsilyl cyanide (0.12 mL, 0.899 mmol, 2.2 equiv) to afford the crude product which was purified by column chromatography (silica, 10:1 hexanes: EtOAc) to afford pure **7e** (0.0863 g, 0.386 mmol) in 95% yield as a white solid.

^{1}H NMR (400 MHz, $CDCl_3$) δ 8.80 (d, J = 5.6 Hz, 1H), 8.51 (d, J = 8.8 Hz, 1H), 8.29 (s, 1H), 8.04 (d, J = 5.6 Hz, 1H), 7.99 (dd, J = 8.8, 1.7 Hz, 1H).

^{13}C NMR (101 MHz, $CDCl_3$) δ_u 144.7, 126.9, 125.6 (q, $^4J_{C\text{-}F}$ = 3.0 Hz), 125.2 (q, $^3J_{C\text{-}F}$ = 4.4 Hz), 125.0; δ_d 135.1 (d, $^4J_{C\text{-}F}$ = 5.5 Hz), 133.5 (q, $^2J_{C\text{-}F}$ = 33.4 Hz), 130.0, 124.5, 121.8, 115.3.

^{19}F NMR (376 MHz, $CDCl_3$) δ -63.28.

GC (Method A) t_R = 7.664 min EI-MS m/z (%): 221.9 (M^+, 100), 203.0 (12), 194.9 (15), 171.9 (12), 144.9 (5), 125.9 (4), 98.9 (3), 75.0 (5).

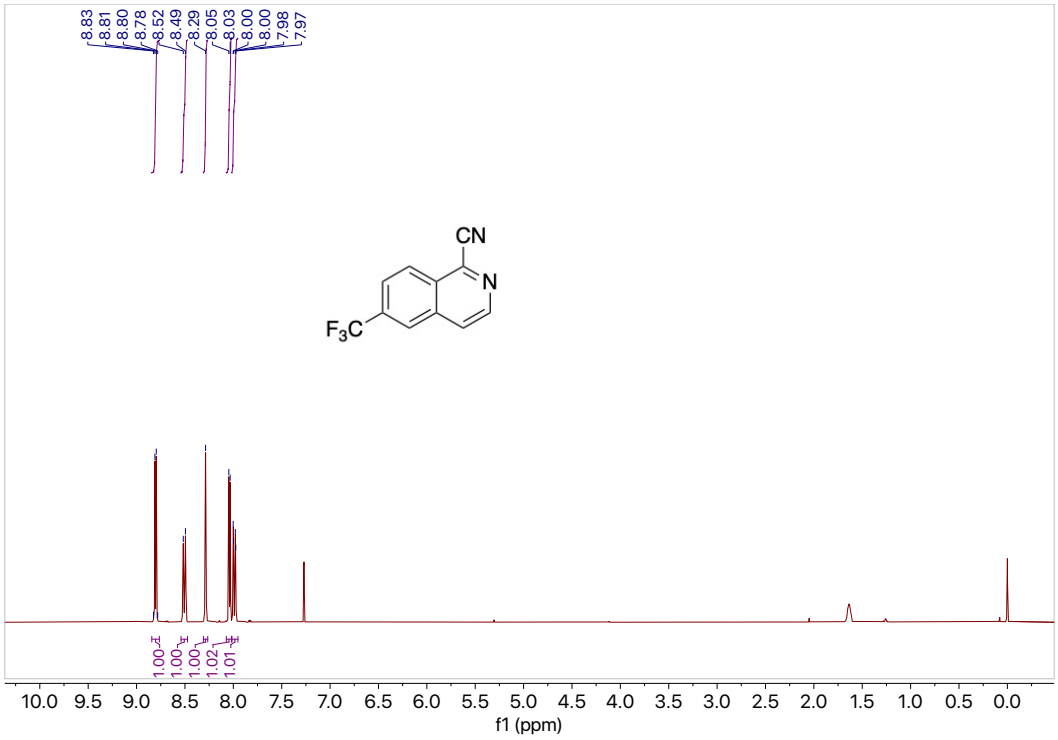

Figure 7.273 ^{1}H NMR (400 MHz, $CDCl_3$) of compound **7e**.

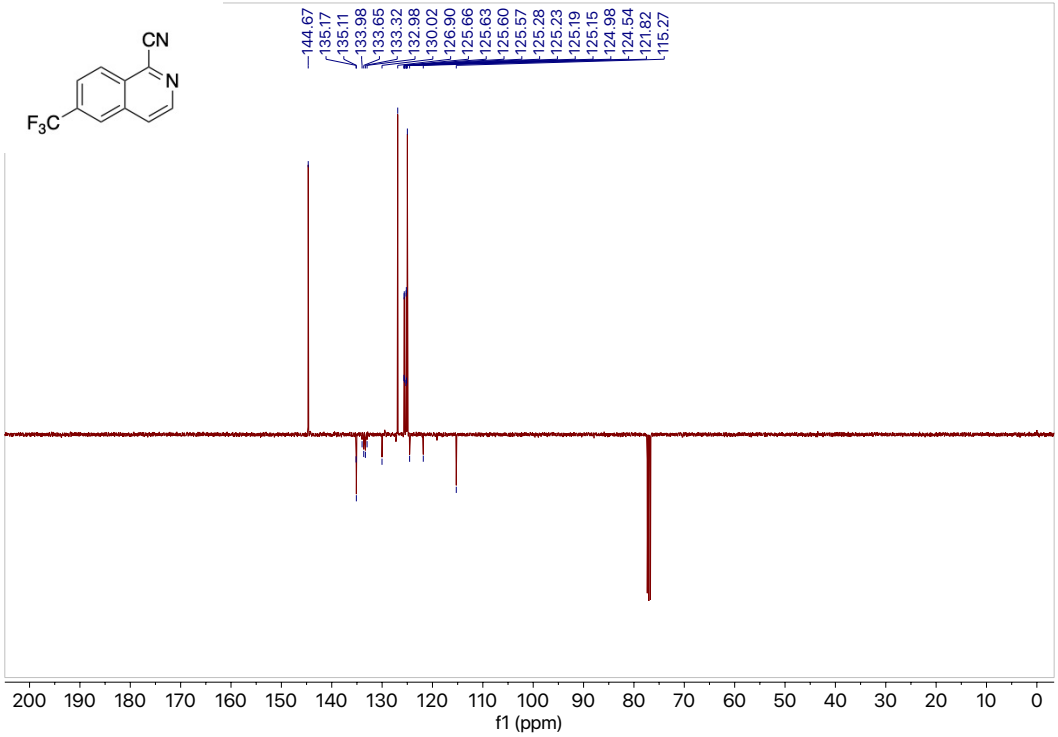

Figure 7.274 ^{13}C NMR (101 MHz, $CDCl_3$) of compound **7e**.

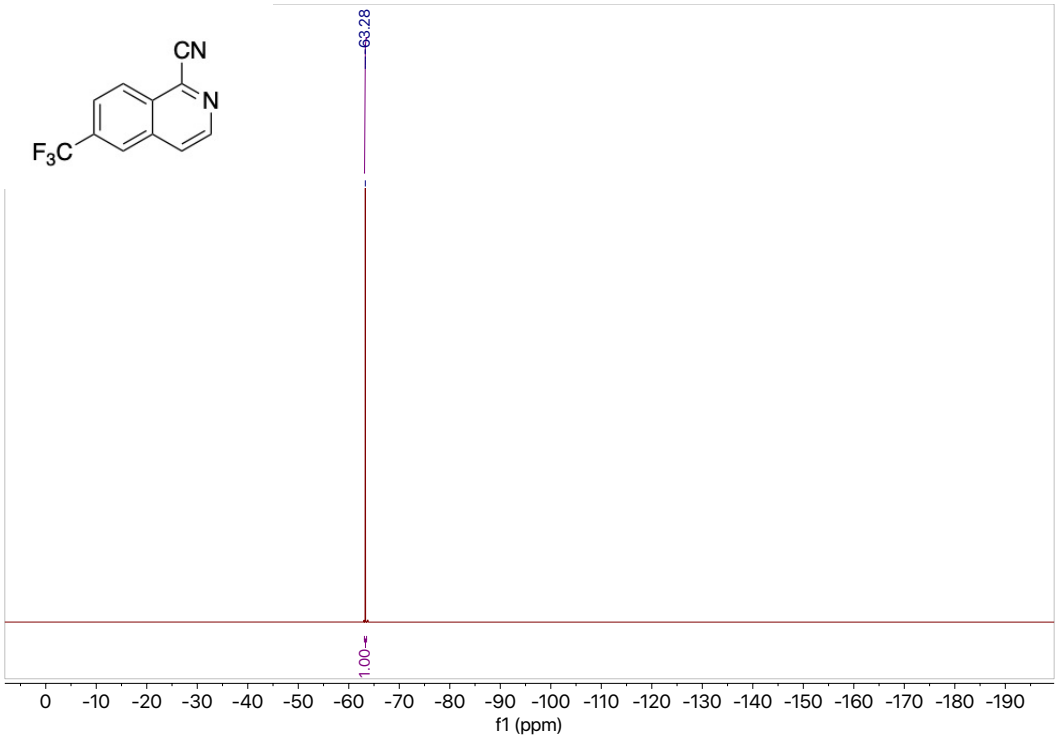

Figure 7.275 ^{19}F NMR (376 MHz, $CDCl_3$) of compound **7e**.

7.12.4 Synthesis of (*S*)-4-(tert-Butyl)-2-(isoquinol-1-yl)-4,5-dihydrooxazoles.

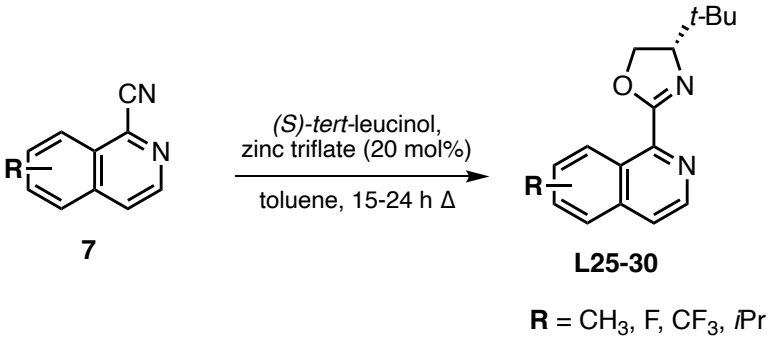

Scheme 7.19 Synthesis of chiral tBu-iQuinox ligand general reaction.

A two-necked round bottom flask with a stir bar was equipped with reflux condenser and charged with zinc triflate (0.2 mmol, 20 mol %). The flask was placed under high vacuum and heated to 90°C for 1 h using a mineral oil bath. In a separate flame-dried round bottom flask with a stir bar, under argon, isoquinoline-1-carbonitrile (1.0 mmol, 1.0 equiv) and (*S*)-tert-leucinol (1.0 mmol, 1.0 equiv) were dissolved in toluene (4 mL, 0.25 M). After cooling the flask with zinc triflate to room temperature, the mixture was added to it and refluxed under argon for 15-24 h. Once completed, as judged by GC-MS or TLC analysis, the reaction mixture was allowed to cool to room temperature, diluted

with EtOAc, washed with saturated $NaHCO_3$, brine and then dried with $MgSO_4$. The crude product was concentrated under vacuum and purified by column chromatography.

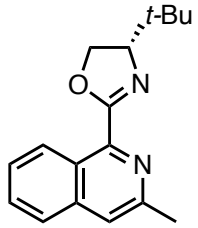

L25

(*S*)-4-(*tert*-butyl)-2-(3-methylisoquinolin-1-yl)-4,5-dihydrooxazole (L25). Using the general procedure for synthesis of (*S*)-tert-Butyl *i*Quinox, **7a** (0.153 g, 0.91 mmol, 1.0 equiv), reacted with (*S*)-tert-leucinol (0.115 g, 0.98 mmol, 1.1 equiv), and zinc triflate (0.0669, 0.18 mmol, 20 mol %) in toluene (3.6 mL, 0.25 M) to afford the crude product which was purified column chromatography (silica, 3:2 hexanes: EtOAc) to afford pure **L25** (0.118 g, 0.439 mmol) in 48% yield as a tan solid.

^{1}H NMR (400 MHz, $CDCl_3$) δ 9.23 – 9.16 (m, 1H), 7.76 (d, *J* = 8.1 Hz, 1H), 7.66 (ddd, *J* = 8.2, 6.8, 1.3 Hz, 1H), 7.62 – 7.56 (m, 2H), 4.52 (dd, *J* = 8.7, 7.0 Hz, 1H), 4.38 – 4.25 (m, 2H), 2.76 (d, *J* = 0.7 Hz, 3H), 1.07 (s, 9H).

GC t_R = 2.907 min (Method B). EI-MS m/z (%): 268.1 (M+, 31), 211.0 (100), 183.0 (45), 169.0 (11), 156.0 (50), 142.0 (41), 129.0 (11), 115.0 (26), 89.0 (4), 57.1 (6).

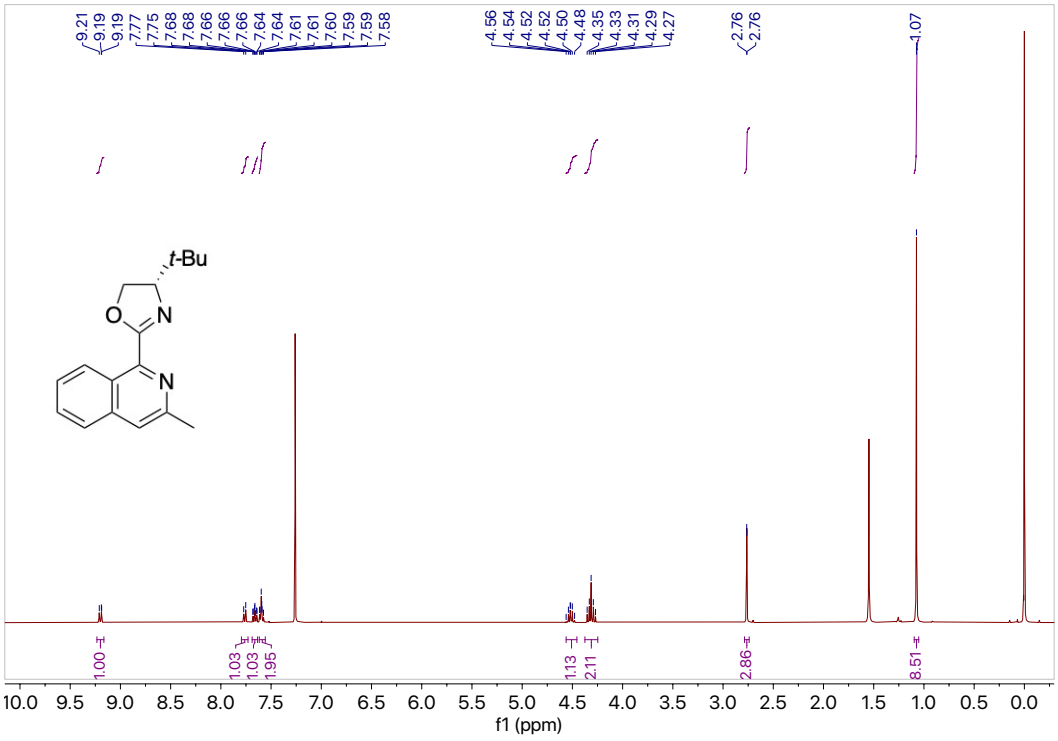

Figure 7.276 ^{1}H NMR (400 MHz, $CDCl_3$) of compound **L25**.

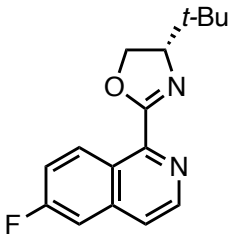

L26

(*S*)-4-(*tert*-Butyl)-2-(6-fluoroisoquinolin-1-yl)-4,5-dihydrooxazole (L26). Using the general procedure for synthesis of (*S*)-tert-Butyl *i*Quinox, **7b** (0.154 g, 0.893 mmol, 1.0 equiv) reacted with (*S*)-tert-leucinol (0.105 g, 0.893 mmol, 1.0 equiv) and zinc triflate (0.065 g, 0.179 mmol, 20 mol %) in toluene (3.6 mL, 0.25 M) to afford the crude product which was purified column chromatography (silica, 3:2 hexanes: EtOAc) to afford pure **L26** (0.154 g, 0.566 mmol) in 63% yield as a white solid, m.p. = 86.9 – 87.2 °C.
$[\alpha]_D^{20}$= -41 (*c* 0.40, $CHCl_3$).
^{1}H NMR (400 MHz, $CDCl_3$) δ 9.41 – 9.32 (m, 1H), 8.54 (d, *J* = 5.6 Hz, 1H), 7.63 (d, *J* = 5.6 Hz, 1H), 7.41 – 7.31 (m, 2H), 4.48 – 4.36 (m, 1H), 4.30 – 4.18 (m, 2H), 0.98 (s, 9H).
^{13}C NMR (101 MHz, $CDCl_3$) δ_u 142.6, 131.2 (d, $^3J_{C\text{-}F}$ = 9.4 Hz), 122.8 (d, $^4J_{C\text{-}F}$ = 5.2 Hz), 119.0 (d, $^2J_{C\text{-}F}$ = 24.7 Hz), 110.2 (d, $^2J_{C\text{-}F}$ = 20.8 Hz), 77.6, 26.1; δ_d 163.0 (d, $^1J_{C\text{-}F}$ = 254.1 Hz), 161.6, 146.3 (d, $^4J_{C\text{-}F}$ = 1.6 Hz), 138.5 (d, $^3J_{C\text{-}F}$ = 10.4 Hz), 124.7, 68.2, 34.1.
^{19}F NMR (376 MHz, $CDCl_3$) δ -107.09.
GC (Method B) t_R = 2.604 min EI-MS m/z (%): 272.0 (M^+, 12), 257.0 (3), 216.0 (100), 186.0 (61), 172.9 (17), 159.9 (49), 145.9 (81), 132.9 (18), 126.0 (17), 118.9 (8), 98.9 (6), 57.0 (12).
HRMS (ESI) calculated for $C_{16}H_{18}ON_2F$ $[M+H]^+$: 273.1403, found 273.1397.

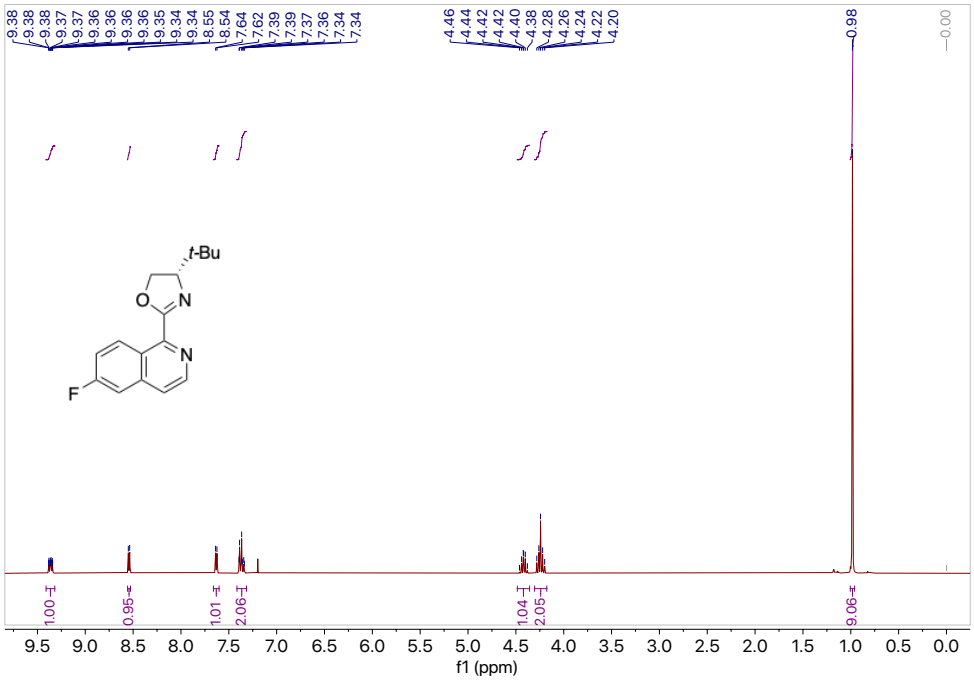

Figure 7.277 ^{1}H NMR (400 MHz, $CDCl_3$) of compound **L26**.

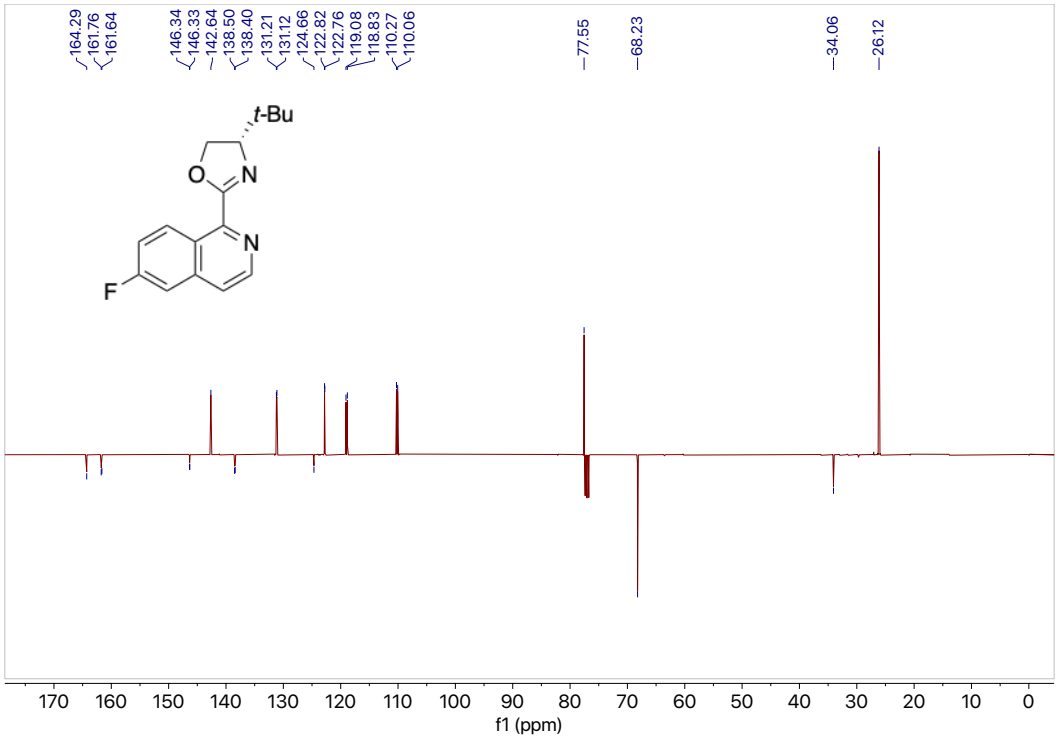

Figure 7.278 ^{13}C NMR (101 MHz, $CDCl_3$) of compound **L26**.

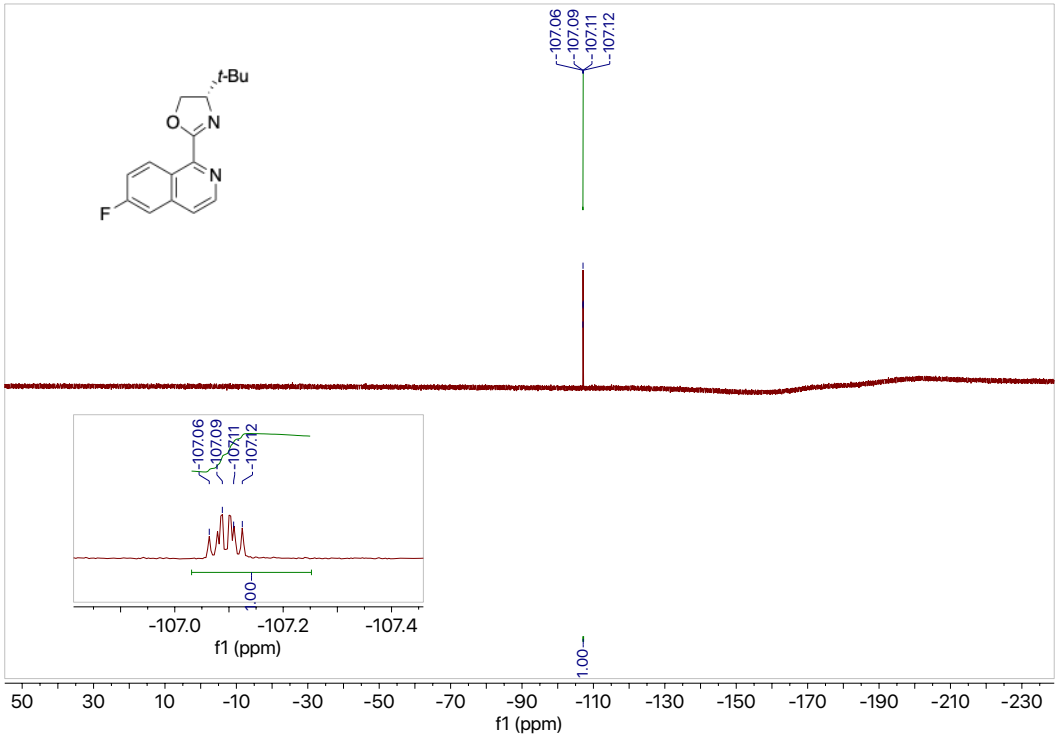

Figure 7.279 ^{19}F NMR (376 MHz, $CDCl_3$) of compound **L26**.

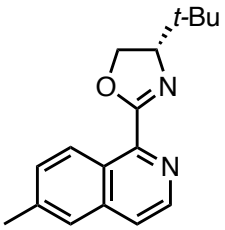

L27

(*S*)-4-(*tert*-Butyl)-2-(6-methylisoquinolin-1-yl)-4,5-dihydrooxazole (L27). Using the general procedure for synthesis of (*S*)-tert-Butyl *i*Quinox, **5c** (0.124 g, 0.737 mmol, 1.0 equiv) reacted with (*S*)-tert-leucinol (0.0860 g, 0.737 mmol, 1.0 equiv) and zinc triflate (0.054 g, 0.147 mmol, 20 mol %) in toluene (2.9 mL, 0.25 M) to afford the crude product which was purified column chromatography (silica, 3:2 hexanes: EtOAc) to afford pure **L27** (0.168 g, 0.626 mmol) in 85% yield as a yellow oil.

$[\alpha]_D^{20}$= -32 (*c* 0.34, $CHCl_3$).

^{1}H NMR (400 MHz, $CDCl_3$) δ 9.19 (d, *J* = 8.8 Hz, 1H), 8.58 (d, *J* = 5.6 Hz, 1H), 7.66 (d, *J* = 5.6 Hz, 1H), 7.62 (s, 1H), 7.51 (dd, *J* = 8.8, 1.8 Hz, 1H), 4.55 – 4.43 (m, 1H), 4.37 – 4.25 (m, 2H), 2.55 (s, 3H), 1.06 (s, 9H).

^{13}C NMR (101 MHz, $CDCl_3$) δ_u 141.9, 130.8, 127.2, 125.9, 122.8, 77.5, 26.1, 21.9; δ_d 161.9, 146.1, 140.7, 137.1, 125.9, 68.1, 34.1.

GC (Method B) t_R = 3.187 min EI-MS m/z (%): 268.1 (M^+, 28), 253.1 (4), 211.1 (100), 197.0 (4), 183.1 (58), 169.0 (13), 156.0 (48), 142.0 (50), 129.0 (12), 115 (17), 89.0 (4), 57.1 (5).

HRMS (ESI) calculated for $C_{17}H_{21}ON_2$ $[M+H]^+$: 269.1654, found 269.1646.

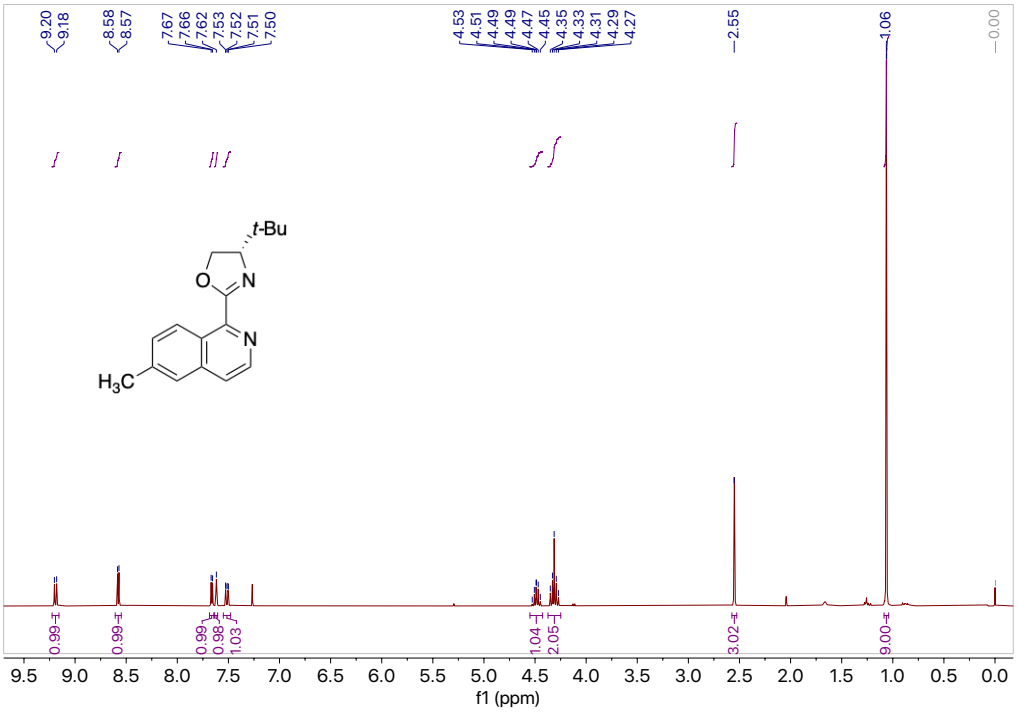

Figure 7.280 ^{1}H NMR (400 MHz, $CDCl_3$) of compound **L27**.

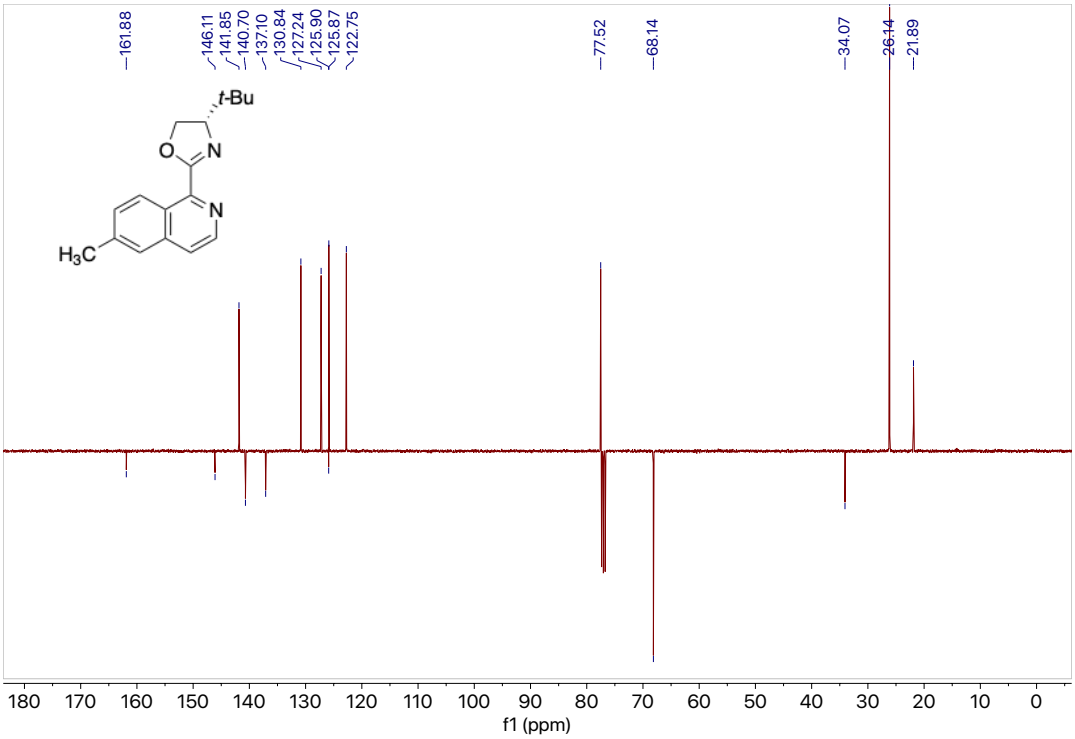

Figure 7.281 ^{13}C NMR (101 MHz, $CDCl_3$) of compound **L27**.

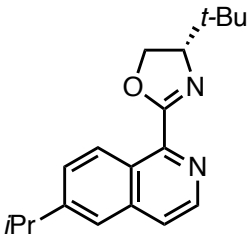

L28

(*S*)-4-(*tert*-butyl)-2-(6-isopropylisoquinolin-1-yl)-4,5-dihydrooxazole (L28). Using the general procedure for synthesis of (*S*)-tert-Butyl *i*Quinox, **7d** (0.100 g, 0.534 mmol, 1.0 equiv) reacted with (*S*)-tert-leucinol (0.063 g, 0.534 mmol, 1.0 equiv) and zinc triflate (0.0388 g, 0.107 mmol, 20 mol%) in toluene (2.2 mL, 0.25 M) to afford the crude product which was purified column chromatography (silica, 4:1 hexanes: EtOAc) to afford pure **L28** (0.149 g, 0.503 mmol) in 94% yield as a clear colorless oil.
GC (Method B) t_R = 3.759 min EI-MS m/z (%): 296.1 (M^+, 24), 239.1 (100), 223.0 (4), 211.0 (60), 195.0 (12), 184.0 (20), 170.0 (40), 154.0 (13), 140.0 (4), 128.0 (11).
^{1}H NMR (400 MHz, $CDCl_3$) δ 9.16 (d, *J* = 8.9 Hz, 1H), 8.51 (d, *J* = 5.5 Hz, 1H), 7.63 (d, *J* = 5.6 Hz, 1H), 7.60 – 7.50 (m, 2H), 4.48 – 4.36 (m, 1H), 4.30 – 4.18 (m, 2H), 3.04 (hept, *J* = 6.9 Hz, 1H), 1.28 (d, *J* = 6.9 Hz, 6H), 0.99 (s, 9H).
^{13}C NMR (101 MHz, $CDCl_3$) δ_u 141.8, 128.6, 127.4, 123.1, 77.5, 34.3, 26.1, 23.54; δ_d 161.9, 151.2, 146.0, 137.2, 126.3, 68.2, 34.1.

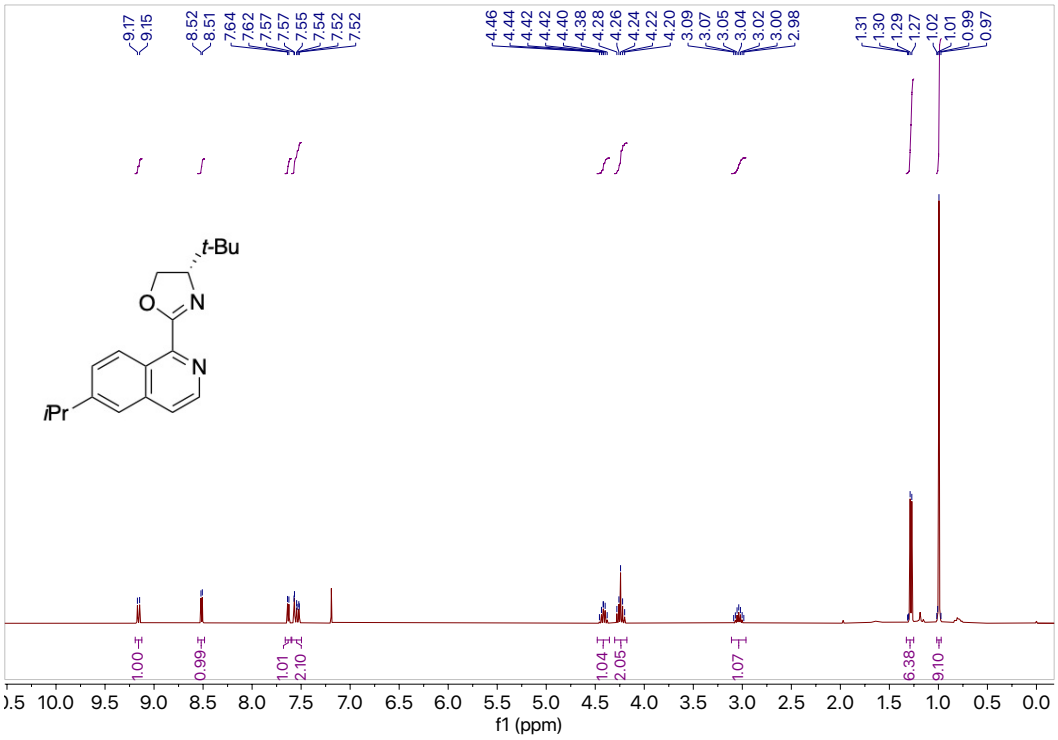

Figure 7.282 ^{1}H NMR (400 MHz, $CDCl_3$) of compound **L28**.

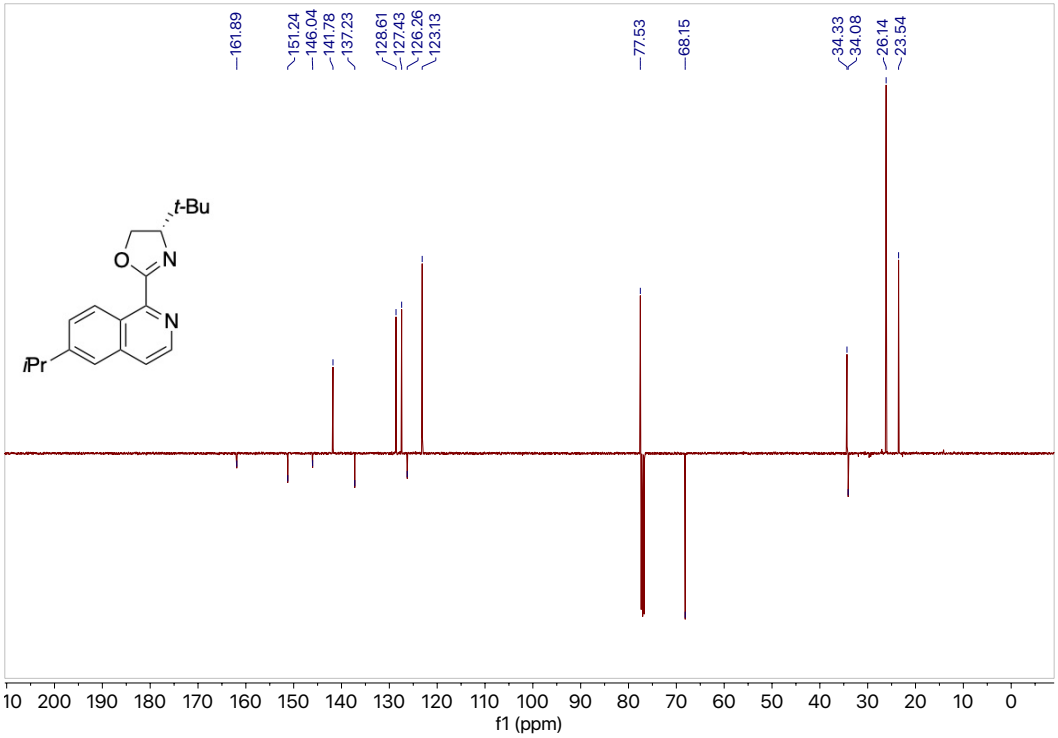

Figure 7.283 ^{13}C NMR (101 MHz, $CDCl_3$) of compound **L28**.

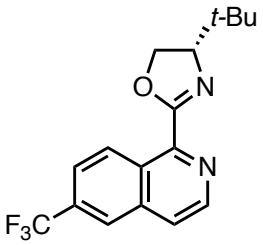

L30

***(S)*-4-(*tert*-butyl)-2-(6-(trifluoromethyl)isoquinolin-1-yl)-4,5-dihydrooxazole (L30).** Using the general procedure for synthesis of (*S*)-tert-Butyl *i*Quinox, **7e** (0.0733 g, 0.329 mmol, 1.0 equiv) reacted with (*S*)-tert-leucinol (0.0386 g, 0.329 mmol, 1.0 equiv) and zinc triflate (0.0239 g, 0.0659 mmol, 20 mol %) in toluene (1.3 mL, 0.25 M) to afford the crude product which was purified column chromatography (silica, 4:1 hexanes: EtOAc) to afford pure **L30** (0.101 g, 0.313 mmol) in 97% yield as a white solid.
^{1}H NMR (400 MHz, $CDCl_3$) δ 9.58 (dd, J = 9.0, 1.2 Hz, 1H), 8.76 (d, J = 5.6 Hz, 1H), 8.18 (s, 1H), 7.91 – 7.83 (m, 2H), 4.58 – 4.46 (m, 1H), 4.40 – 4.28 (m, 2H), 1.07 (s, 9H).
^{13}C NMR (101 MHz, $CDCl_3$) δ_u 143.1, 129.3, 124.7 (q, $^{3}J_{C\text{-}F}$ = 4.8 Hz), 124.1 (q, $^{4}J_{C\text{-}F}$ = 3.0 Hz), 123.8, 77.7, 26.1; δ_d 161.4, 146.6, 135.8, 131.8, 128.3, 68.3, 34.1.
^{19}F NMR (376 MHz, $CDCl_3$) δ -63.25.
GC (Method B) t_R = 2.426 min EI-MS m/z (%): 322.2 (M^+, 7), 303.1 (5), 266.1 (100), 237.1 (60), 223.1 (15), 210.1 (35), 196.1 (78), 176.0 (18), 57.1 (13).

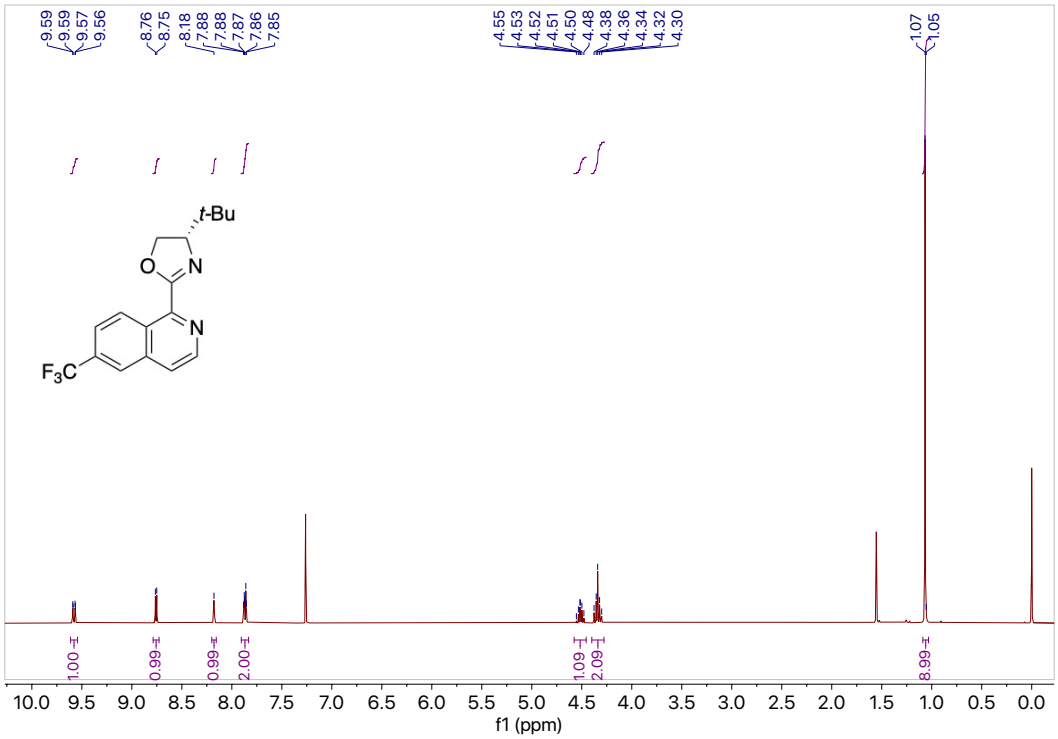

Figure 7.284 ^{1}H NMR (400 MHz, $CDCl_3$) of compound **L30**.

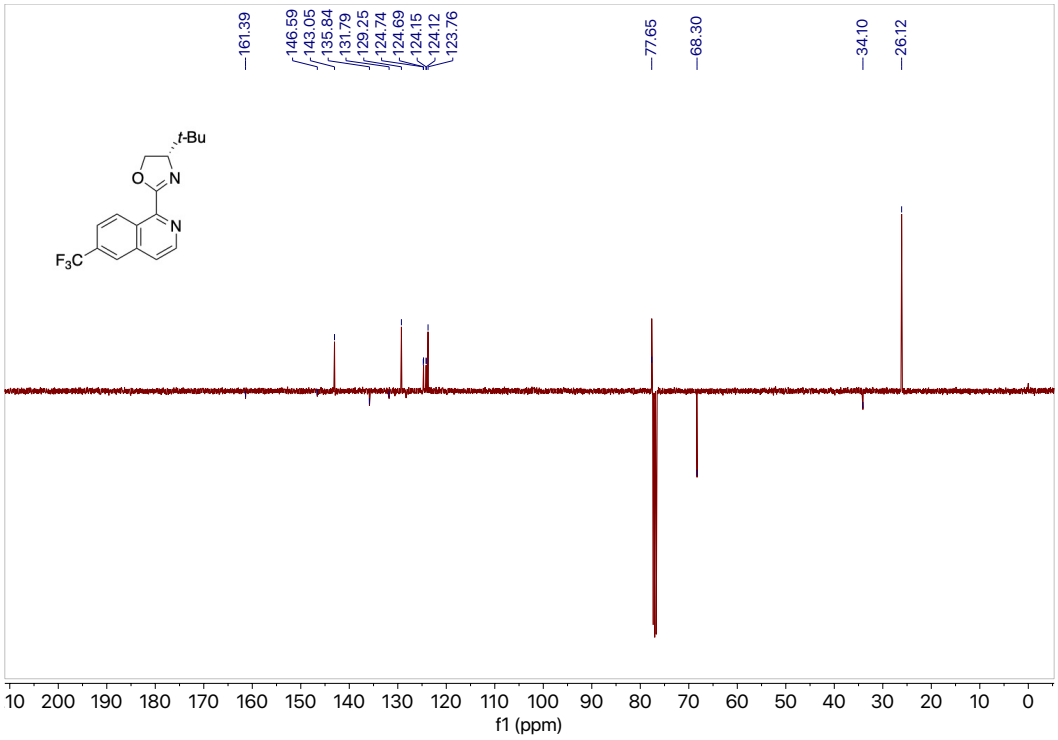

Figure 7.285 ^{13}C NMR (101 MHz, $CDCl_3$) of compound **L30**.

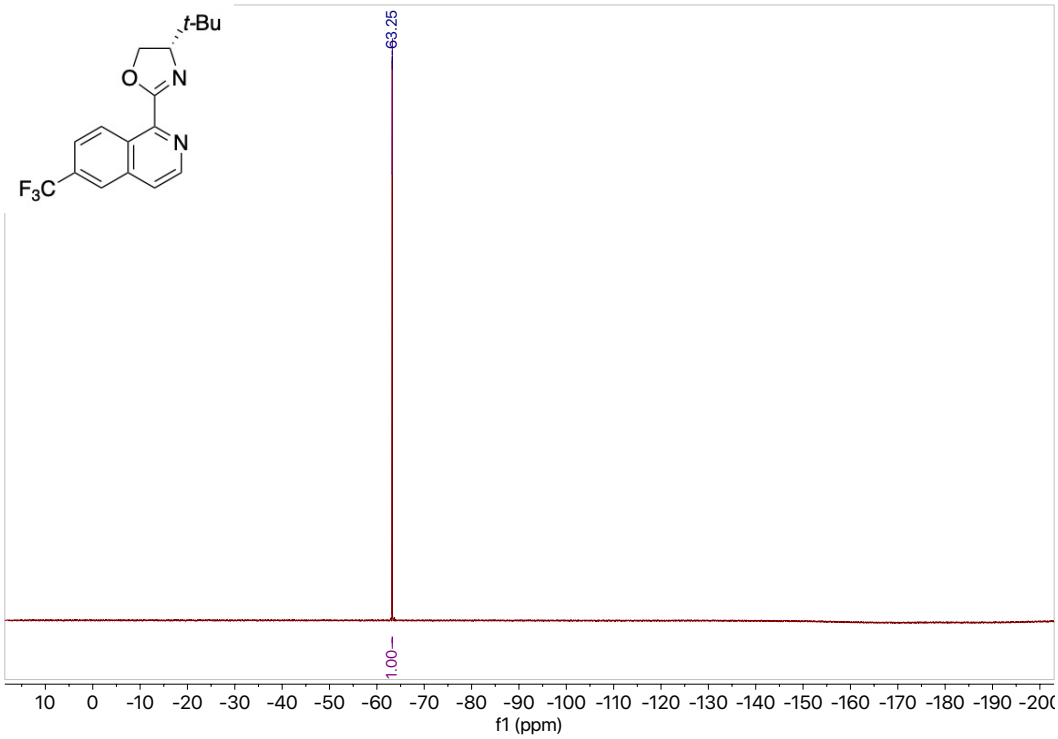

Figure 7.286 ^{19}F NMR (376 MHz, $CDCl_3$) of compound **L30**.

7.13 MOM (methoxymethyl) group deprotection general procedures and data

General procedure A

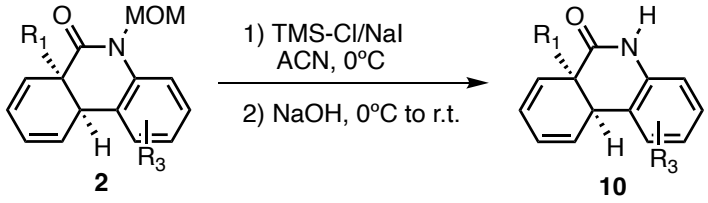

Scheme 7.20 MOM deprotection with TMS-I general reaction.

A flame dried round bottom flask with a stir bar, under argon, was charged with chlorotrimethylsilane (0.45 mmol, 4.5 equiv) and dissolved in CH_3CN (1.7 mL, 0.06 M). After NaI (0.45 mmol, 4.5 equiv) was added, the resulting heterogeneous solution was stirred for 15 min at room temperature. In a second round bottom flask, the MOM-protected Heck product (0.1 mmol, 1.0 equiv) was dissolved in CH_3CN (1.7 mL, 0.06 M) and cooled to 0°C. The TMS-Cl/NaI solution was added to the Heck product by syringe. The resulting mixture was stirred at 0°C for 1 h. The reaction progress was monitored by TLC and GCMS. Upon completion, the reaction mixture was quenched with 1 M NaOH (17 mL/mmol) and stirred overnight. The aqueous layer was extracted with Et_2O (3 x). The combined organic layers were washed with brine, dried over $MgSO_4$, and concentrated under reduced pressure. The crude products were purified by column chromatography.

General procedure B

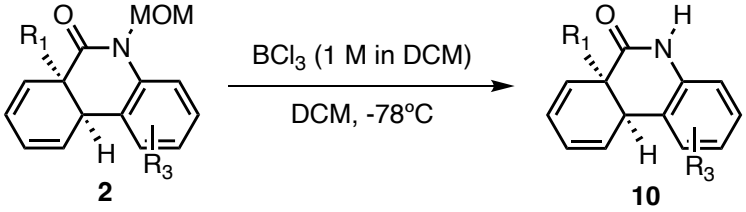

Scheme 7.21 MOM deprotection with boron trichloride general reaction.

A flame dried round bottom flask with a stir bar, under argon, was charged with the MOM-protected Heck product (0.1 mmol, 1.0 equiv) and dissolved in DCM (5 mL, 0.02 M). After the solution was cooled to -78°C, BCl_3 (1.0 M in DCM, 1 mmol, 10 equiv) was added, and the reaction mixture was stirred for 2-3 h. The reaction progress was monitored by TLC and GC-MS. Upon starting material consumption, the reaction mixture was quenched with saturated $NaHCO_3$ (50 mL/mmol) and extracted with DCM (3 x). The combined organic layers were washed with brine, dried over $MgSO_4$, and concentrated under reduced pressure. The crude intermediate was placed in a vial and redissolved in THF (5 mL, 0.02 M). 1 M NaOH (5 mL, 5 mmol, 50 equiv) was added, and the vial was sealed with a pressure relief cap and stirred at 65˚C in a pie reactor until the reaction was determined to be complete by GC-MS analysis (typically 1 h). Upon completion, the reaction was extracted with Et_2O (3 x). The combined organic layers

were washed with brine, dried over $MgSO_4$, and concentrated under reduced pressure. The crude products were purified by column chromatography.

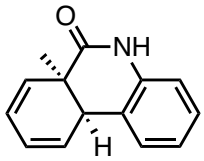

10b

6a-Methyl-6a,10a-dihydrophenanthridin-6(5*H*)-one (10b): Using the general MOM-group deprotection procedure A with the MOM-protected Heck product **2b** (0.0305 g, 0.129 mmol, 1 equiv) in CH_3CN (4.3 mL, 0.03 M) afforded the crude deprotected product which was purified by column chromatography (silica, 3:2 hexanes: EtOAc) to obtain pure **10b** (0.022 g, 0.104 mmol) in 81% yield as a white solid, m.p.= 133.9-136.6.
^{1}H NMR (400 MHz, $CDCl_3$) δ 8.35 – 8.31 (br s, 1H), 7.25 – 7.15 (m, 2H), 7.04 (td, J = 7.5, 1.2 Hz, 1H), 6.76 (dd, J = 7.9, 1.2 Hz, 1H), 6.11 (dd, J = 9.3, 5.1 Hz, 1H), 6.03 (dddd, J = 9.1, 5.2, 2.9, 1.0 Hz, 1H), 5.89 – 5.82 (m, 1H), 5.61 (ddt, J = 9.3, 3.1, 1.0 Hz, 1H), 3.55 (t, J = 3.1 Hz, 1H), 1.32 (s, 3H).
^{13}C NMR (101 MHz, CDCl3) δ_u 130.6, 130.0, 128.6, 128.5, 127.8, 125.0, 124.70, 123.6, 123.5, 115.1, 44.3, 23.4. δ_d 174.9, 135.9, 124.74, 40.9.
GC (method B) t_R = 2.08 min. EI-MS m/z (%): 210.1 (M+, 60), 196.0 (100), 178.0 (41), 167.0 (30), 152.1 (12).
HRMS (ESI) calculated for $C_{14}H_{14}ON$ $[M+H]^+$: 212.1075, found 212.1073.

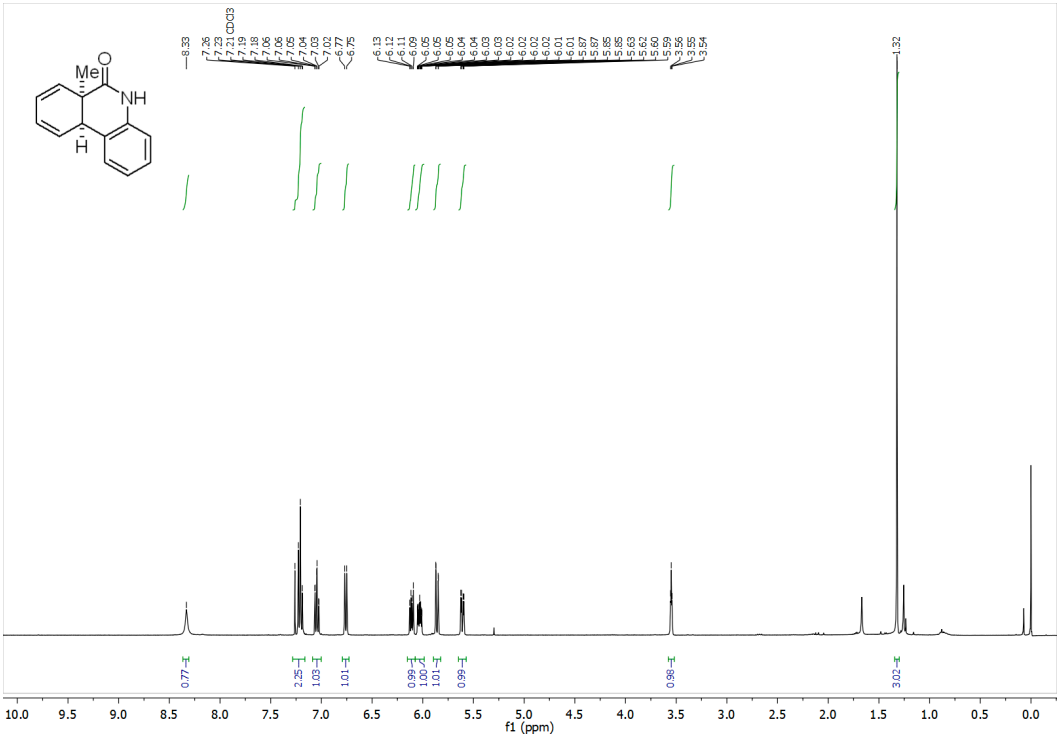

Figure 7.287 ^{1}H NMR (400 MHz, $CDCl_3$) of compound **10b**.

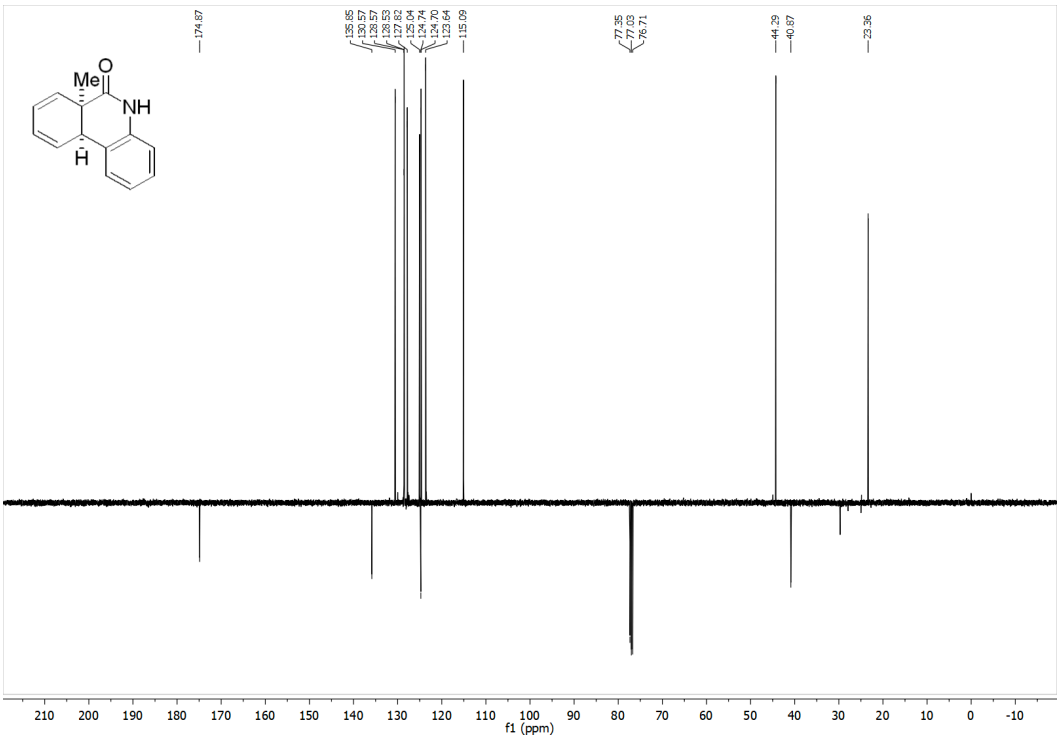

Figure 7.288 ^{13}C NMR (101 MHz, $CDCl_3$) of compound **10b**.

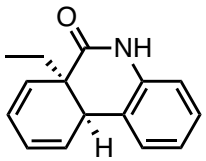

10c

(6aR,10aR)-6a-Ethyl-6a,10a-dihydrophenanthridin-6(5H)-one (10c). Using the general MOM-group deprotection procedure A with the MOM-protected Heck product **2c** (0.0368 g, 0.137 mmol, 1.0 equiv) in CH_3CN (4.7 mL, 0.03 M) afforded the crude deprotected product which was purified by column chromatography (silica, 4:1 hexanes: EtOAc) to obtain pure **10c** (0.0253 g, 0.112 mmol) in 82% yield as a white solid, m.p.= 127.4 – 129.2°C.

^{1}H NMR (400 MHz, $CDCl_3$) δ 8.22 (s, 1H), 7.17 – 7.10 (m, 2H), 6.97 (td, J = 7.4, 1.2 Hz, 1H), 6.67 (dd, J = 7.8, 1.4 Hz, 1H), 6.14 – 6.06 (m, 1H), 5.99 – 5.90 (m, 1H), 5.87 – 5.80 (m, 1H), 5.52 – 5.44 (m, 1H), 3.69 – 3.63 (m, 1H), 1.71 – 1.59 (m, 1H), 1.55 – 1.45 (m, 1H), 0.86 (t, J = 7.5 Hz, 3H).

^{13}C NMR (101 MHz, $CDCl_3$) δ_u 128.9, 128.8, 128.5, 127.8, 125.4, 125.0, 124.0, 115.0, 41.2, 9.2; δ_d 174.5, 135.9, 124.8, 45.2, 28.1.

GC (Method B) t_R = 2.352 min. EI-MS m/z (%): 224.1 (M-1$^+$,14), 196 (100), 178.0 (49), 167 (17), 152.0 (11), 139.0 (4), 115.0 (4), 77.0 (4).

HRMS (ESI) calculated for $C_{15}H_{16}ON$ $[M+H]^+$: 226.1232, found 226.1232.

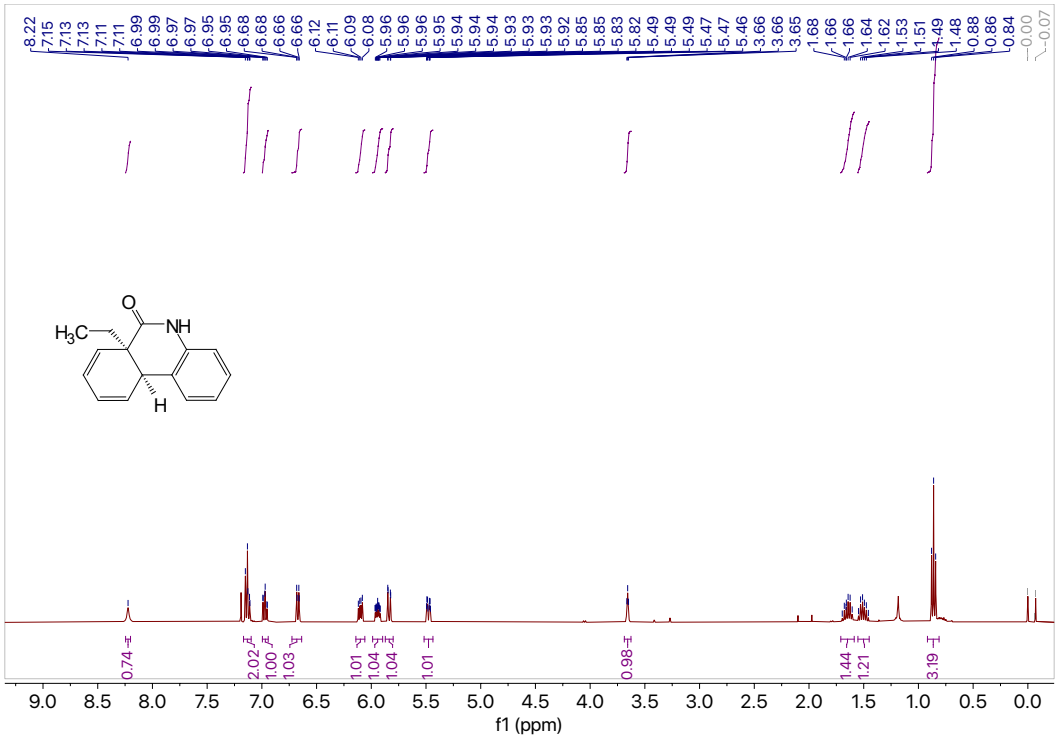

Figure 7.289 ^{1}H NMR (400 MHz, $CDCl_3$) of compound **10c**.

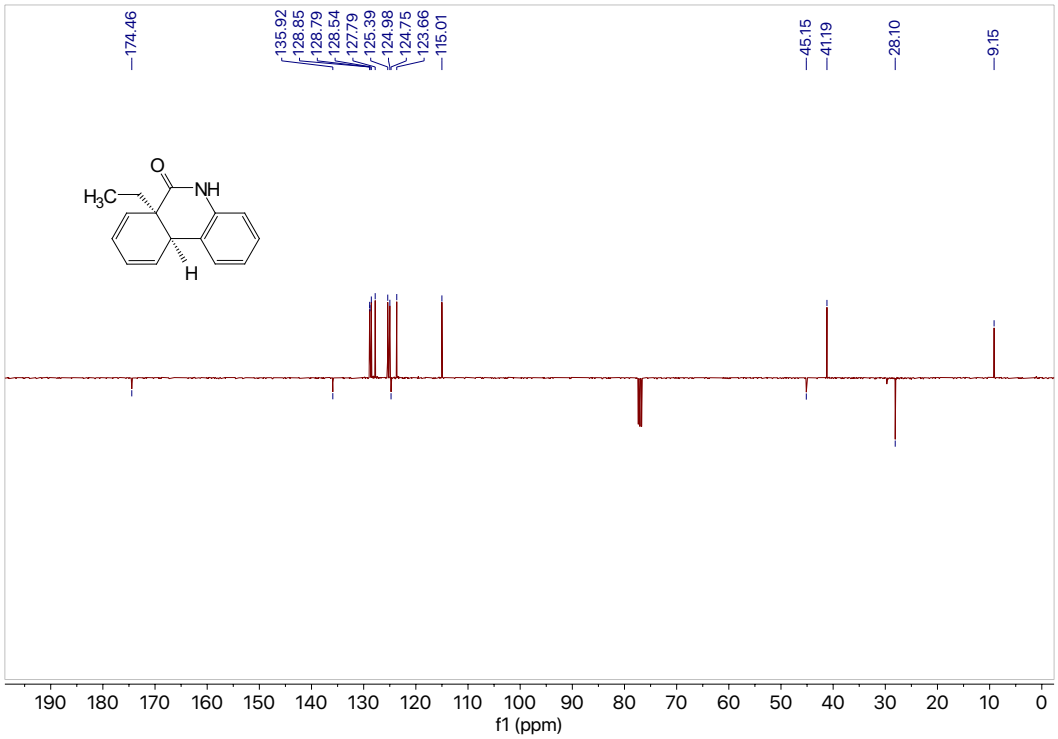

Figure 7.290 ^{13}C NMR (101 MHz, $CDCl_3$) of compound **10c**.

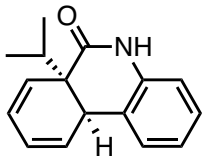

10e

(6aR,10aR)-6a-Isopropyl-6a,10a-dihydrophenanthridin-6(5H)-one (10e). Using the general MOM-group deprotection procedure A with the MOM-protected Heck product **2e** (0.100 g, 0.353 mmol, 1.0 equiv) in CH_3CN (12 mL, 0.03 M) afforded the crude deprotected product which was purified by column chromatography (silica, 3:2 hexanes: EtOAc) to obtain pure **10e** (0.0681 g, 0.284 mmol) in 81% yield as a white solid, m.p.= 169.9 – 172.4°C.

^{1}H NMR (400 MHz, $CDCl_3$) δ 7.45 (s, 1H), 7.25 – 7.16 (m, 2H), 7.05 (td, J = 7.5, 1.2 Hz, 1H), 6.68 (dd, J = 7.9, 1.1 Hz, 1H), 6.22 (dd, J = 9.7, 5.0 Hz, 1H), 6.06 – 5.97 (m, 1H), 5.94 (d, J = 9.2 Hz, 1H), 5.54 – 5.47 (m, 1H), 3.89 (s, 1H), 1.84 (hept, J = 6.8 Hz, 1H), 1.01 (d, J = 6.8 Hz, 3H), 0.86 (s, 3H).

^{13}C NMR (101 MHz, $CDCl_3$) δ_u 129.3, 128.6, 127.8, 126.0, 125.9, 125.2, 123.8, 114.7, 41.3, 29.9, 18.5, 17.9; δ_d 173.6, 136.0, 125.3, 48.7.

GC (Method B) t_R = 2.523 min. EI-MS m/z (%): 239.1 (M^+, 6), 196 (100), 178.0 (42), 167 (12), 152.0 (9), 139.0 (4).

HRMS (ESI) calculated for $C_{16}H_{18}ON$ $[M+H]^+$: 240.1388, found 240.1383.

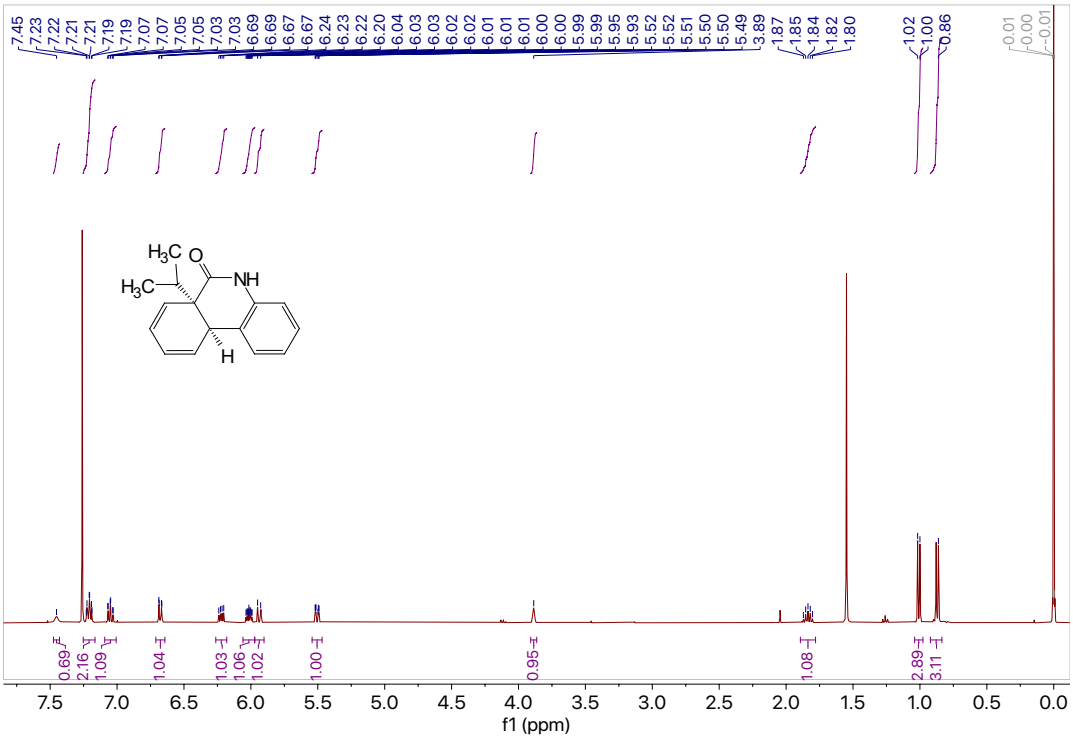

Figure 7.291 ^{1}H NMR (400 MHz, $CDCl_3$) of compound **10e**.

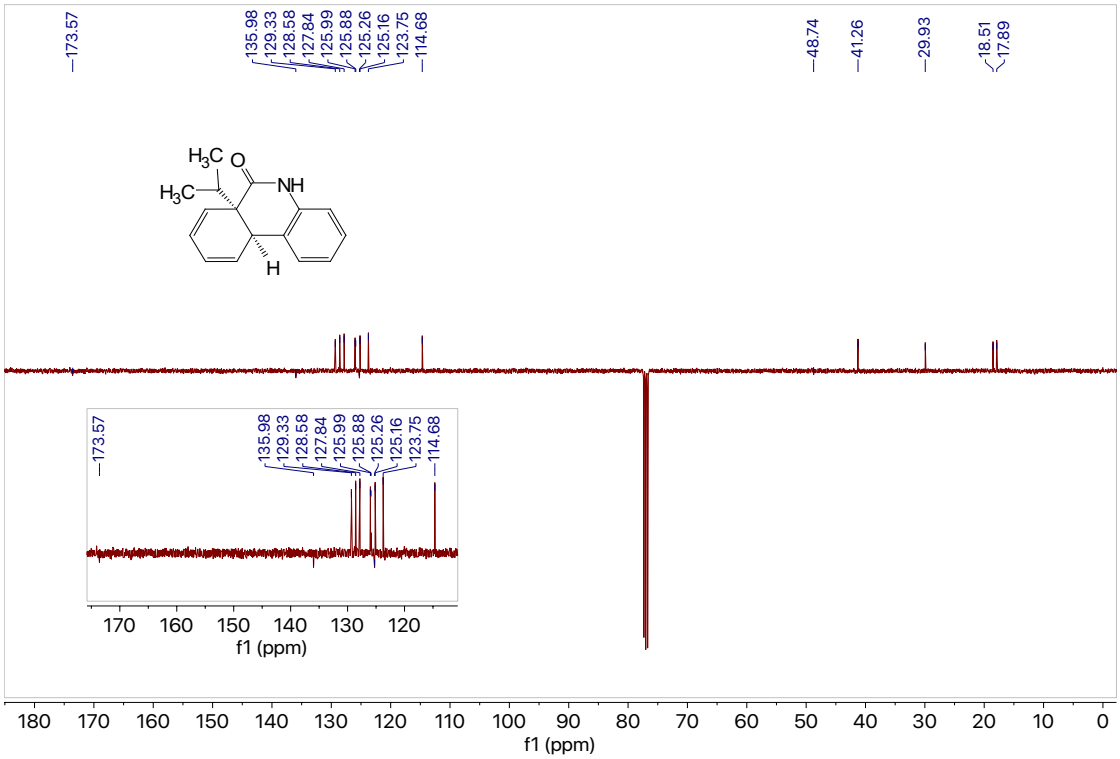

Figure 7.292 ^{13}C NMR (101 MHz, $CDCl_3$) of compound **10e**.

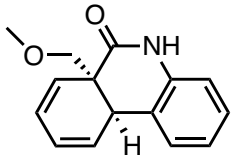

10f

(6aR,10aR)-6a-(Methoxymethyl)-6a,10a-dihydrophenanthridin-6(5*H*)-one (10f). Using the general MOM-group deprotection procedure A with the MOM-protected Heck product **2f** (0.0326 g, 0.114 mmol, 1.0 equiv) in CH_3CN (3.9 mL, 0.03 M) afforded the crude deprotected product which was purified by column chromatography (silica, 4:1 hexanes: EtOAc) to obtain pure **10f** (0.0268 g, 0.111 mmol) in 97% yield as a clear colorless oil.

^{1}H NMR (400 MHz, $CDCl_3$) δ 8.05 (s, 1H), 7.16 (d, J = 7.5 Hz, 1H), 7.12 (td, J = 7.7, 1.5 Hz, 1H), 6.96 (td, J = 7.5, 1.2 Hz, 1H), 6.64 (dd, J = 7.8, 1.2 Hz, 1H), 6.06 (dd, J = 9.5, 5.1 Hz, 1H), 6.03 – 5.95 (m, 1H), 5.78 (dd, J = 9.4, 4.3 Hz, 1H), 5.68 (d, J = 9.4 Hz, 1H), 3.98 (dd, J = 4.6, 2.1 Hz, 1H), 3.55 (d, J = 8.9 Hz, 1H), 3.39 (d, J = 8.9 Hz, 1H), 3.27 (s, 3H).

^{13}C NMR (101 MHz, $CDCl_3$) δ_u 128.0, 127.7, 127.3, 126.2, 126.2, 124.5, 124.5, 123.6, 114.8, 59.5, 36.6; δ_d 171.8, 135.8, 124.5, 72.8, 47.3.

GC (Method B) t_R = 2.603 min. EI-MS m/z (%): 240.1 (M-1$^+$, 21), 210.0 (20), 196.0 (100), 177.9 (64), 167.0 (15), 152.0 (16), 138.9 (6), 76.9 (4).

HRMS (ESI) calculated for $C_{15}H_{16}NO_2$ $[M+H]^+$: 242.1181, found 242.1174.

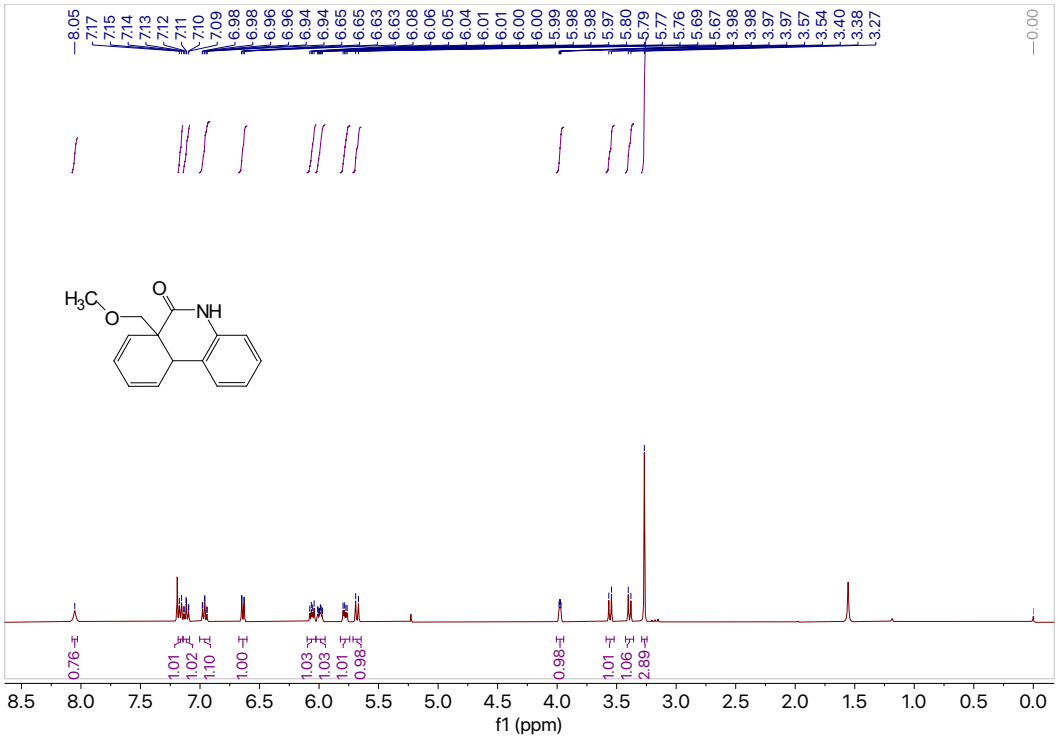

Figure 7.293 ^{1}H NMR (400 MHz, $CDCl_3$) of compound **10f**.

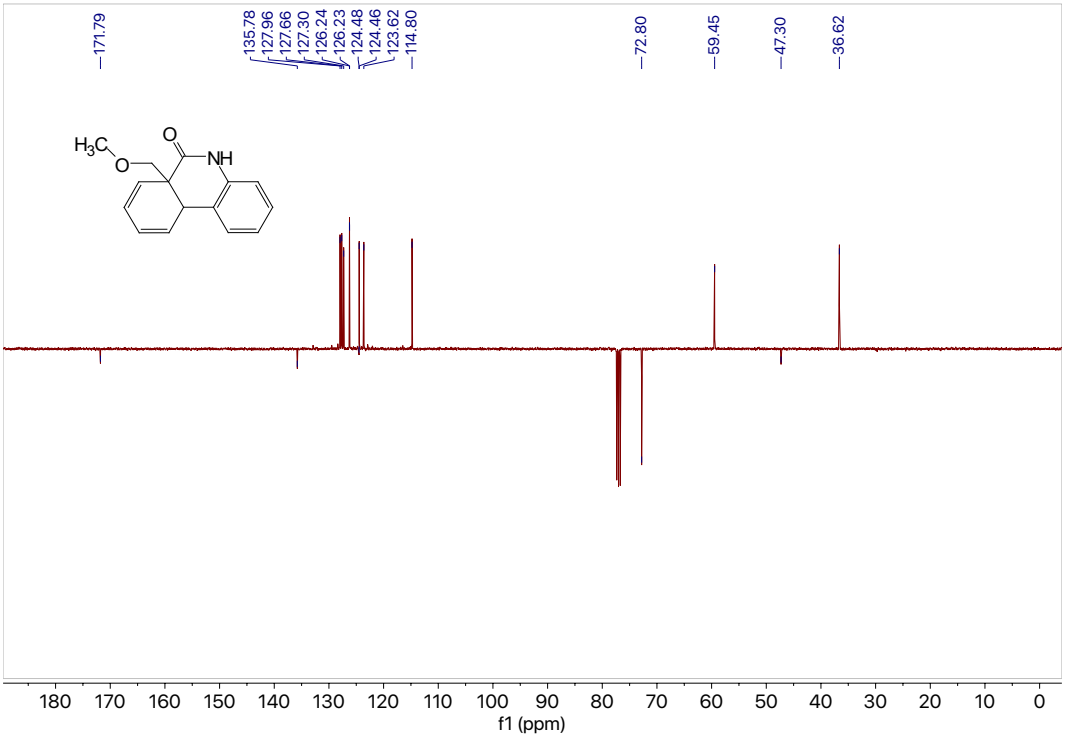

Figure 7.294 ^{13}C NMR (101 MHz, $CDCl_3$) of compound **10f**.

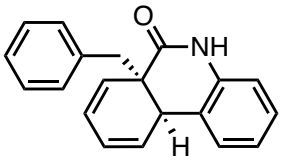

10h

6a-Benzyl-6a,10a-dihydrophenanthridin-6(5*H*)-one (10h): Using the general MOM-group deprotection procedure A with the MOM-protected Heck product **2h** (0.0346 g, 0.104 mmol, 1.0 equiv) in CH_3CN (3.5 mL, 0.03 M) afforded the crude deprotected product which was purified by column chromatography (silica, 4:1 hexanes: EtOAc) to obtain pure **10h** (0.0213 g, 0.0741 mmol) in 71% yield as a white solid, m.p. = 78.9-82.3˚C. Spectral data were in accordance with a prior literature report.[10]

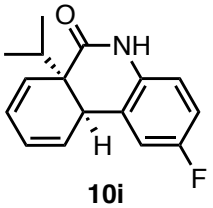

10i

(6aR,10aR)-2-Fluoro-6a-isopropyl-6a,10a-dihydrophenanthridin-6(5H)-one (10i). Using the general MOM-group deprotection procedure A with the MOM-protected Heck product **2i** (0.0793 g, 0.265 mmol, 1.0 equiv) in CH_3CN (9 mL, 0.03 M) afforded the crude deprotected product which was purified by column chromatography (silica, 4:1 hexanes: EtOAc) to obtain pure **10i** 0.0355 g, 0.138 mmol) in 52% yield as a white solid, m.p.= 178.0 – 180.9°C.

^{1}H NMR (400 MHz, $CDCl_3$) δ 8.64 (s, 1H), 6.94 – 6.89 (m, 2H), 6.74 – 6.70 (m, 1H), 6.26 – 6.17 (m, 1H), 6.06 – 5.97 (m, 1H), 5.97 – 5.90 (m, 1H), 5.51 – 5.43 (m, 1H), 3.87 – 3.81 (m, 1H), 1.83 (hept, J = 6.9 Hz, 1H), 1.00 (d, J = 6.9 Hz, 3H), 0.87 (d, J = 6.8 Hz, 3H).

^{13}C NMR (101 MHz, $CDCl_3$) δ_u 128.4, 125.9 (d, $^3J_{C\text{-}F}$ = 8.6 Hz), 125.4, 116.2, 116.1, 115.3 (d, $^2J_{C\text{-}F}$ = 23.0 Hz), 114.4 (d, $^2J_{C\text{-}F}$ = 22.8 Hz), 41.2, 30.0, 18.5, 17.9; δ_d 173.9, 159.0 (d, $^1J_{C\text{-}F}$ = 242.2 Hz) 132.3, 126.9 (d, $^3J_{C\text{-}F}$ = 7.3 Hz), 48.3.

^{19}F NMR (376 MHz, $CDCl_3$) δ -119.38.

GC (Method B) t_R = 2.527 min. EI-MS m/z (%): 257.1 (M^+,10), 214.0 (100), 196.0 (43), 185.0 (12), 169.9 (10).

HRMS (ESI) calculated for $C_{16}H_{17}ONF$ $[M+H]^+$: 258.1294, found 258.1298.

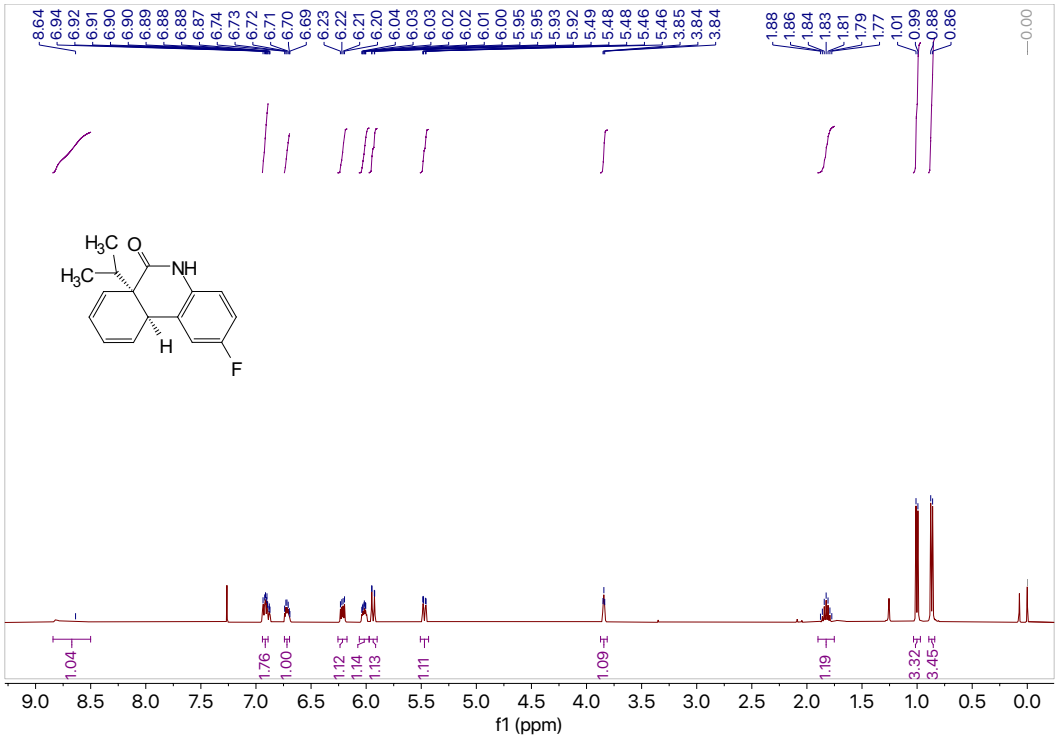

Figure 7.295 ^{1}H NMR (400 MHz, $CDCl_3$) of compound **10i**.

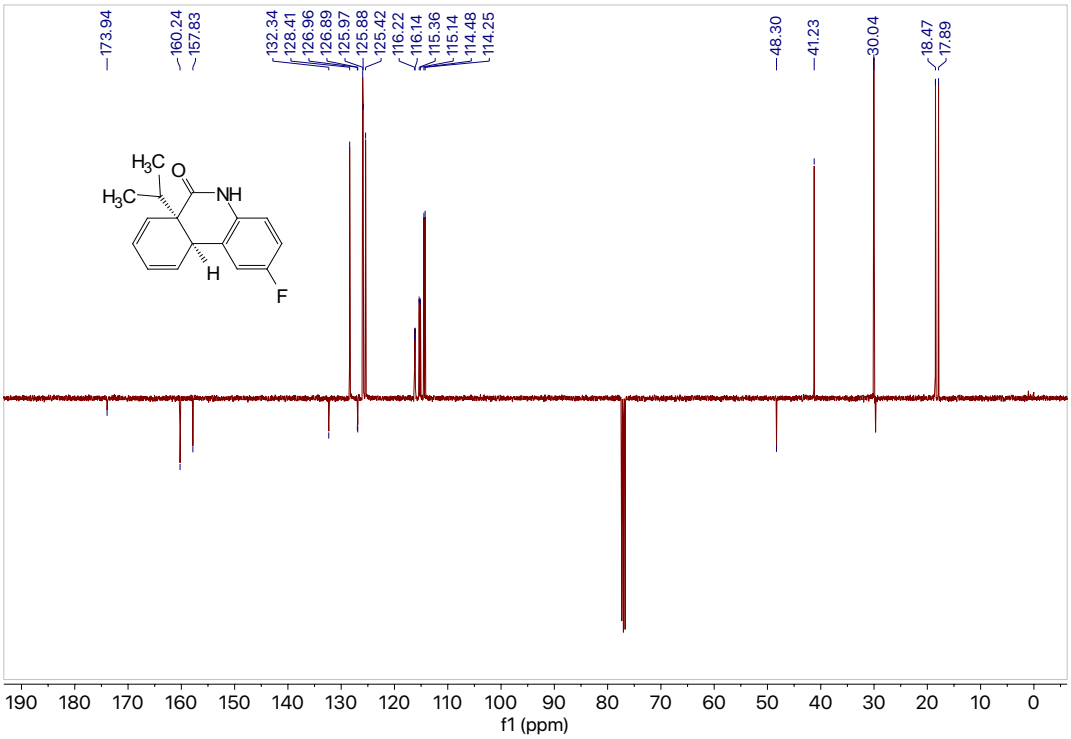

Figure 7.296 ^{13}C NMR (101 MHz, $CDCl_3$) of compound **10i**.

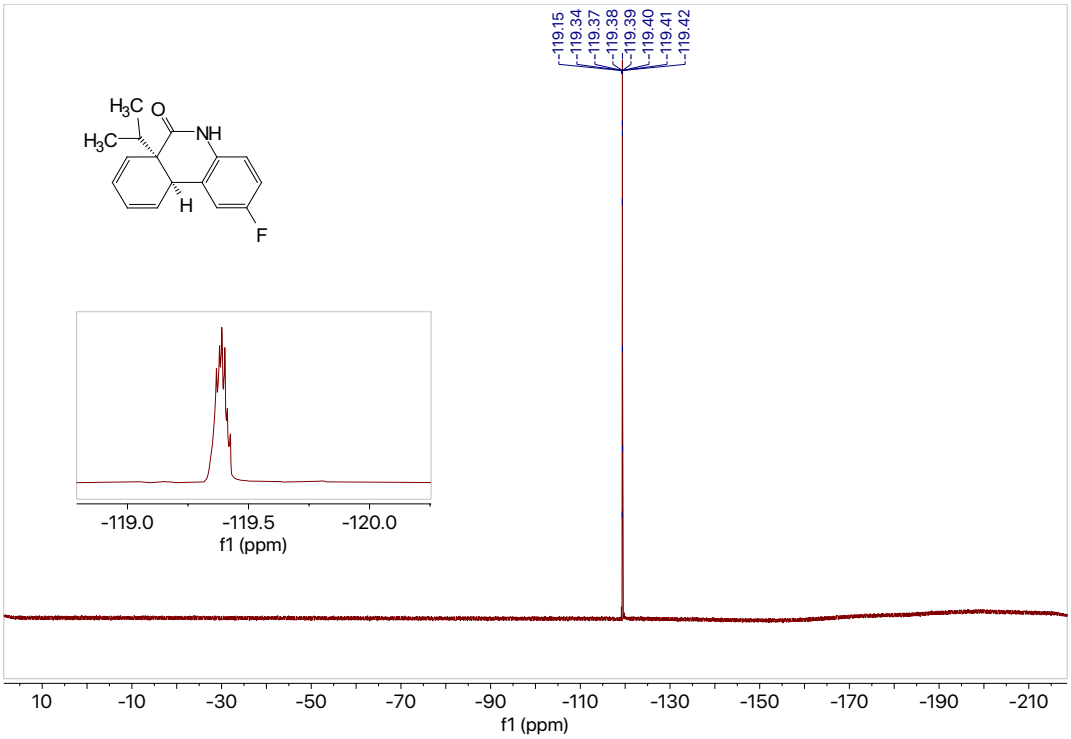

Figure 7.297 ^{19}F NMR (376 MHz, $CDCl_3$) of compound **10i**.

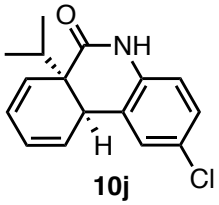

10j

(6aR,10aR)-2-Chloro-6a-isopropyl-6a,10a-dihydrophenanthridin-6(5H)-oneone (10j). Using the general MOM-group deprotection procedure A with the MOM-protected Heck product **2j** (0.0161 g, 0.0507 mmol, 1.0 equiv) in CH_3CN (1.7 mL, 0.03 M) afforded the crude deprotected product which was purified by column chromatography (silica, 4:1 hexanes: EtOAc) to obtain pure **10j** (0.0130 g, 0.0475 mmol) in 94% yield as a white solid, m.p.= 182.5 – 184.4°C.

^{1}H NMR (400 MHz, $CDCl_3$) δ 8.18 (s, 1H), 7.20 – 7.15 (m, 2H), 6.67 (d, J = 8.2 Hz, 1H), 6.22 (m, 1H), 6.07 – 5.98 (m, 1H), 5.93 (m, 1H), 5.51 – 5.43 (m, 1H), 3.87 – 3.82 (m, 1H), 1.81 (hept, J = 6.9 Hz, 1H), 1.00 (d, J = 6.9 Hz, 3H), 0.87 (d, J = 6.8 Hz, 3H).

^{13}C NMR (101 MHz, $CDCl_3$) δ_u 128.4, 128.4, 127.8, 127.0, 126.0, 125.8, 125.5, 116.1, 41.1, 30.0, 18.5, 17.9; δ_d 173.7, 134.8, 128.4, 127.0, 48.5.

GC (Method B) t_R = 3.215 min. EI-MS m/z (%): 273.0 (M^+,10), 230.0 (100), 211.9 (26), 194.9 (12), 177.0 (12), 167.0 (14), 151.9 (6), 138.9 (6).

HRMS (ESI) calculated for $C_{16}H_{17}ONCl$ $[M+H]^+$: 274.0999, found 274.0995.

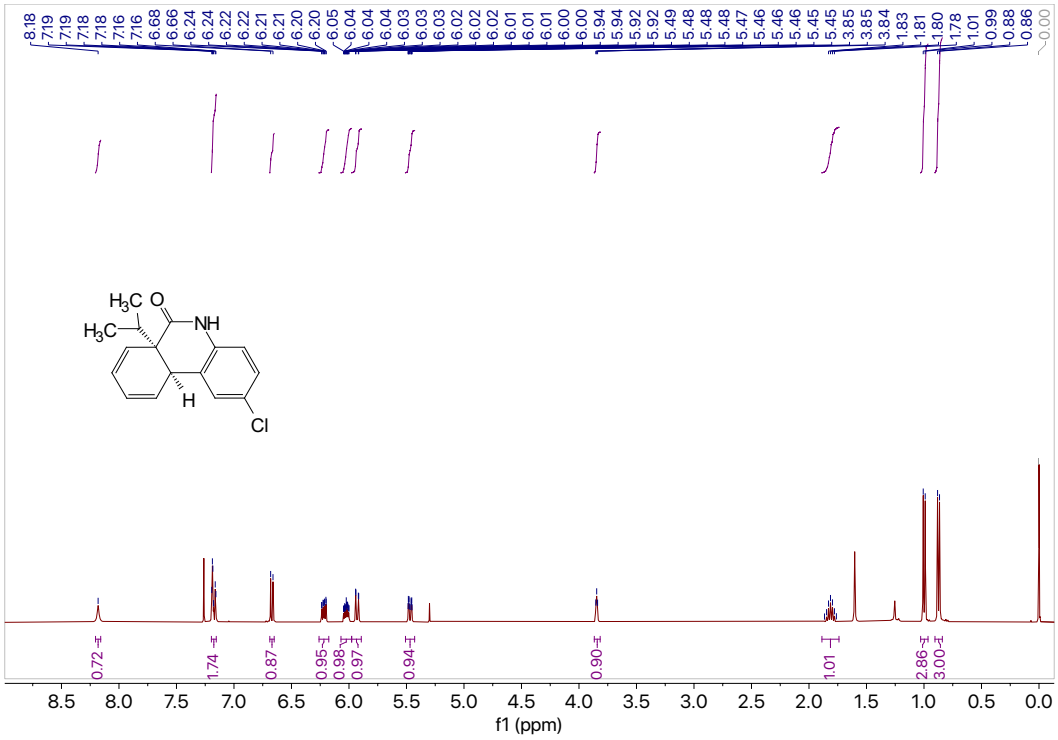

Figure 7.298 ^{1}H NMR (400 MHz, $CDCl_3$) of compound **10j**.

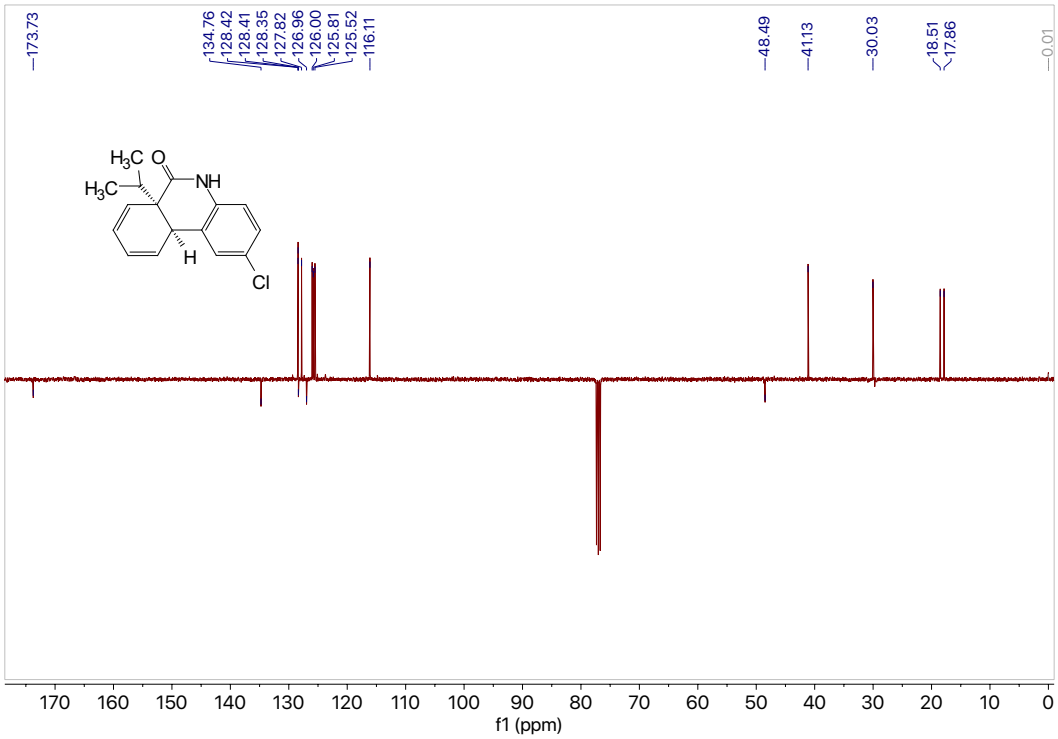

Figure 7.299 ^{13}C NMR (101 MHz, $CDCl_3$) of compound **10j**.

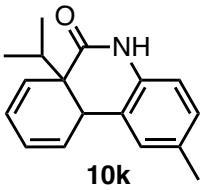

10k

6a-Isopropyl-2-methyl-6a,10a-dihydrophenanthridin-6(5*H*)-one (10k). Using the general MOM-group deprotection procedure A with the MOM-protected Heck product **2k** (0.100 g, 0.336 mmol, 1.0 equiv) in CH_3CN (11.4 mL, 0.03 M) afforded the crude deprotected product which was purified by column chromatography (silica, 3:2 hexanes: EtOAc) to obtain pure **10k** (0.0724 g, 0.285 mmol) in 85% yield as a white solid, m.p.= 193.3 – 194.4°C.

^{1}H NMR (400 MHz, $CDCl_3$) δ 7.41 (s, 1H), 7.02 – 6.98 (m, 2H), 6.57 (d, J = 8.5 Hz, 1H), 6.21 (dd, J = 9.7, 5.1 Hz, 1H), 6.05 – 5.96 (m, 1H), 5.93 (d, J = 9.1 Hz, 1H), 5.50 (ddt, J = 9.3, 1.9, 0.9 Hz, 1H), 3.83 (s, 1H), 2.32 (s, 3H), 1.83 (hept, J = 6.9 Hz, 1H), 1.00 (d, J = 6.9 Hz, 3H), 0.87 (d, J = 6.8 Hz, 3H).

^{13}C NMR (101 MHz, $CDCl_3$) δ_u 129.4, 129.2, 128.3, 126.0, 125.9, 125.1, 114.6, 41.3, 29.9, 20.9, 18.5, 17.9; δ_d 173.5, 133.5, 133.3, 125.1, 48.7.

GC (Method B) t_R = 2.844 min. EI-MS m/z (%): 253.2 (M^+,18), 210.1 (100), 192.1 (46), 180.1 (10), 165.1 (15), 152.1 (10), 77.1 (4).

HRMS (ESI) calculated for $C_{17}H_{20}ON$ $[M+H]^+$: 254.1545, found 254.1545.

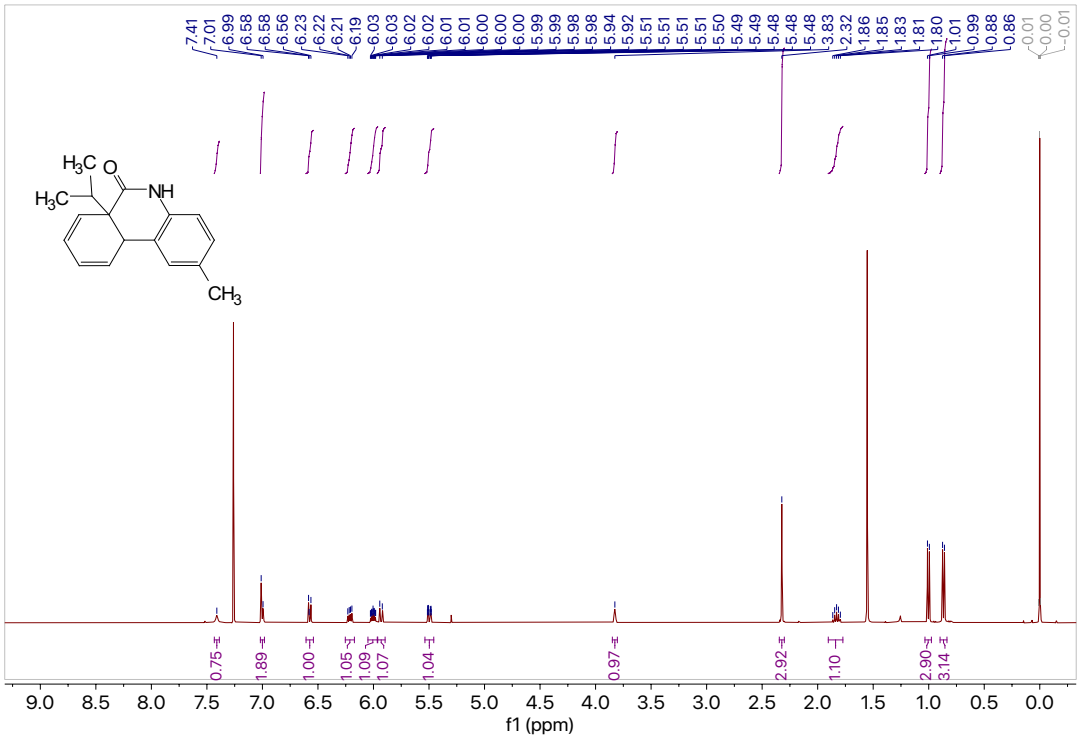

Figure 7.300 ^{1}H NMR (400 MHz, $CDCl_3$) of compound **10k**.

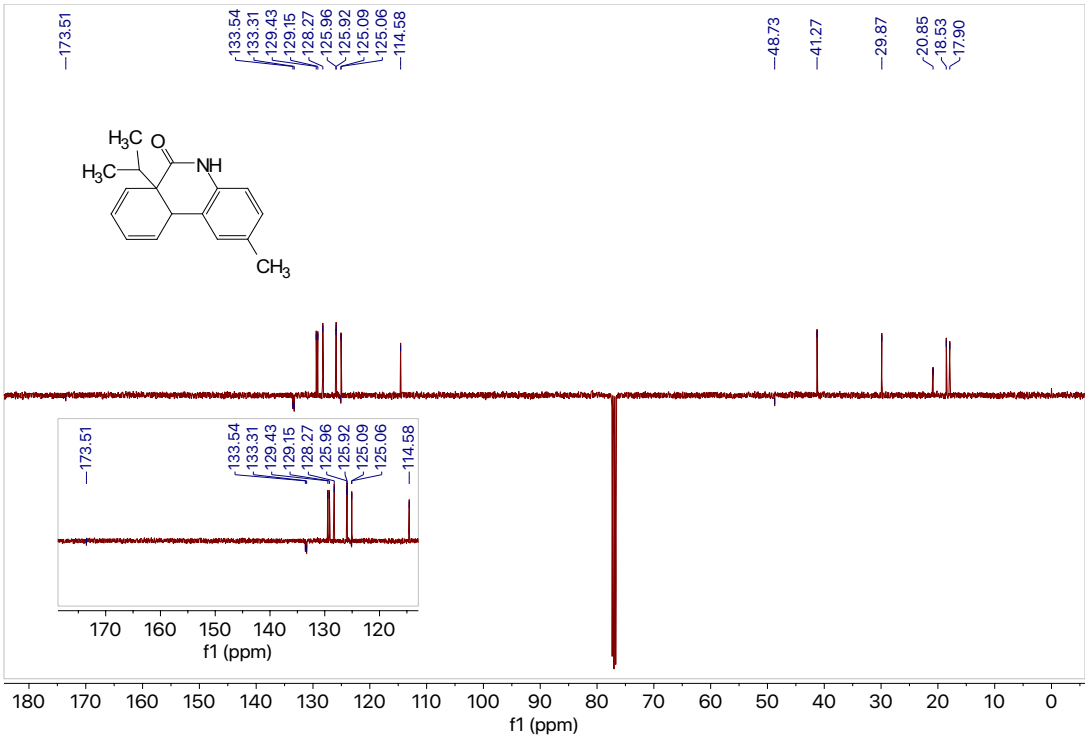

Figure 7.301 ^{13}C NMR (101 MHz, $CDCl_3$) of compound **10k**.

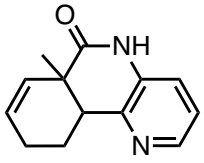

10m-2

6a-Methyl-6a,9,10,10a-tetrahydrobenzo[*c*][1,5]naphthyridin-6(5*H*)-one (10m-2). Using the general MOM-group deprotection procedure B with the MOM-protected Heck product **2m-2** (0.0323, 0.125 mmol, 1.0 equiv) in CH_3CN (4.3 mL, 0.03 M) afforded the crude deprotected product which was purified by column chromatography (silica, 3:2 hexanes: EtOAc) to obtain pure **10m-2** (0.0169 g, 0.0789 mmol) in 63% yield as a yellow solid, m.p.= 134.9 – 137.4°C.

^{1}H NMR (400 MHz, $CDCl_3$) δ 8.83 (s, 1H), 8.27 (dd, J = 3.8, 2.5 Hz, 1H), 7.15 – 7.12 (m, 2H), 5.95 – 5.85 (m, 2H), 2.92 (dd, J = 12.7, 3.1 Hz, 1H), 2.20 – 2.15 (m, 1H), 1.94 – 1.83 (m, 1H), 1.80 – 1.69 (m, 2H), 1.31 (s, 1H), 1.30 (s, 3H).

^{13}C NMR (101 MHz, $CDCl_3$) δ_u 144.3, 129.2, 128.3, 122.4, 121.9, 47.0, 42.3, 25.2; δ_d 175.6, 147.6, 131.5, 42.3, 25.7, 24.5.

GC (Method B) t_R = 2.294 min. EI-MS m/z (%): 214.0 (M^+,62), 199.0 (100), 185.0 (13), 171.0 (13), 161.0 (14), 156.0 (6), 131.0 (4), 91.0 (4), 77.0 (4).

HRMS (ESI) calculated for $C_{13}H_{15}ON_2$ $[M+H]^+$: 215.1184, found 215.1182.

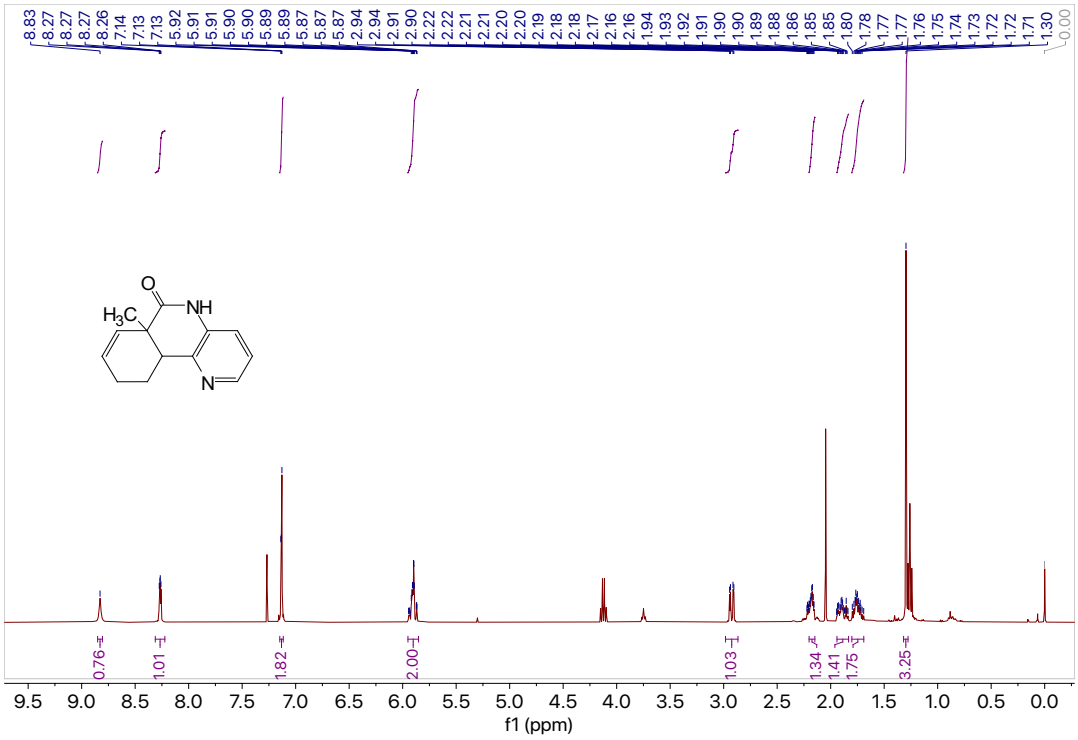

Figure 7.302 ^{1}H NMR (400 MHz, $CDCl_3$) of compound **10m-2**.

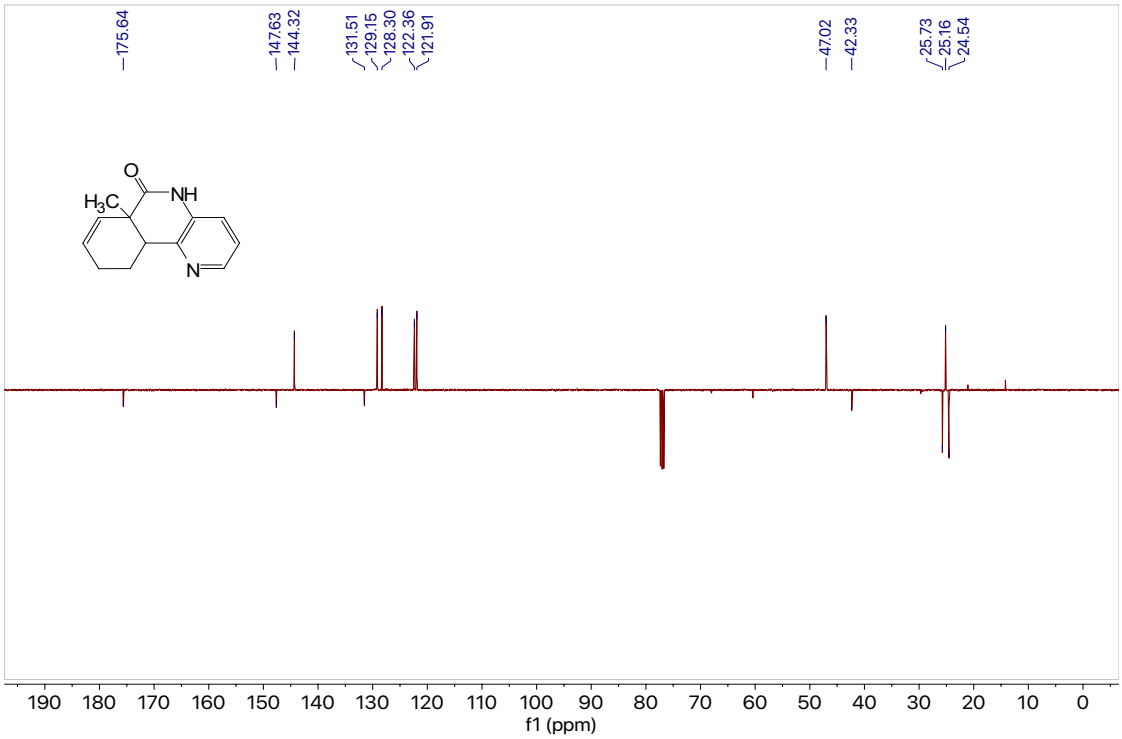

Figure 7.303 ^{13}C NMR (101 MHz, $CDCl_3$) of compound **10m-2**.

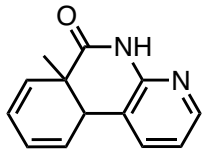

10n

6a-Methyl-6a,10a-dihydrobenzo[*c*][1,8]naphthyridin-6(5*H*)-one (10n): Using the general MOM-group deprotection procedure B with the MOM-protected Heck product **2n** (0.0301 g, 0.117 mmol, 1.0 equiv) in CH_3CN (3.9 mL, 0.03 M) afforded the crude deprotected product which was purified by column chromatography (silica, 3:2 hexanes: EtOAc) to obtain pure **10n** (0.0182 g, 0.0857 mmol) in 73% yield as a white solid, m.p.= 160.1 – 161.5°C.

^{1}H NMR (400 MHz, $CDCl_3$) δ 9.62 (s, 1H), 8.30 (dd, J = 5.0, 1.7 Hz, 1H), 7.61 – 7.56 (m, 1H), 7.02 – 6.99 (m, 1H), 6.14 – 6.04 (m, 2H), 5.87 – 5.82 (m, 1H), 5.68 – 5.61 (m, 1H), 3.58 – 3.52 (m, 1H), 1.36 (s, 3H).

^{13}C NMR (101 MHz, $CDCl_3$) δ_u 146.7, 136.8, 130.5, 126.9, 125.6, 124.6, 119.1, 42.7, 23.1; δ_d 174.8, 149.8, 120.2, 41.3.

GC (Method B) t_R = 1.999 min. EI-MS m/z (%): 211.0 (M-1$^+$,74), 197.0 (100), 183.0 (21), 168.0 (25), 160.0 (30), 154.0 (15), 140.0 (5), 131.0 (12), 115.0 (7), 91.0 (9), 84.0 (5), 77.0 (6), 63.0 (4), 51.0 (4).

HRMS (ESI) calculated for $C_{13}H_{13}ON_2$ $[M+H]^+$: 213.10279, found 213.10257.

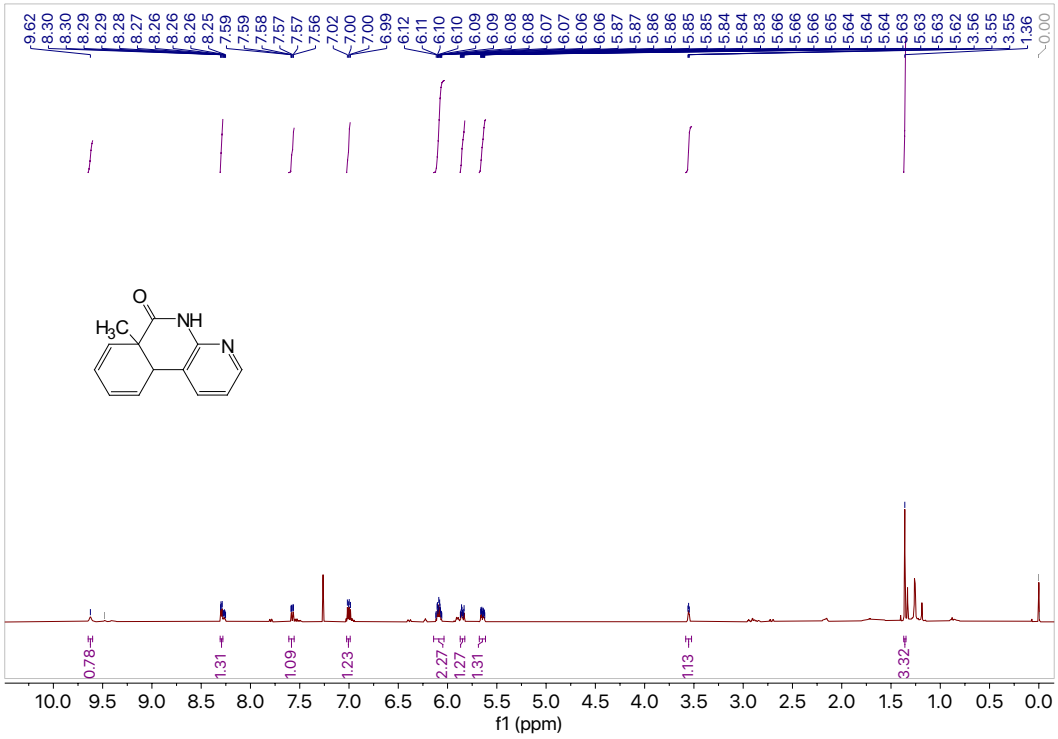

Figure 7.304 ^{1}H NMR (400 MHz, $CDCl_3$) of compound **10n**.

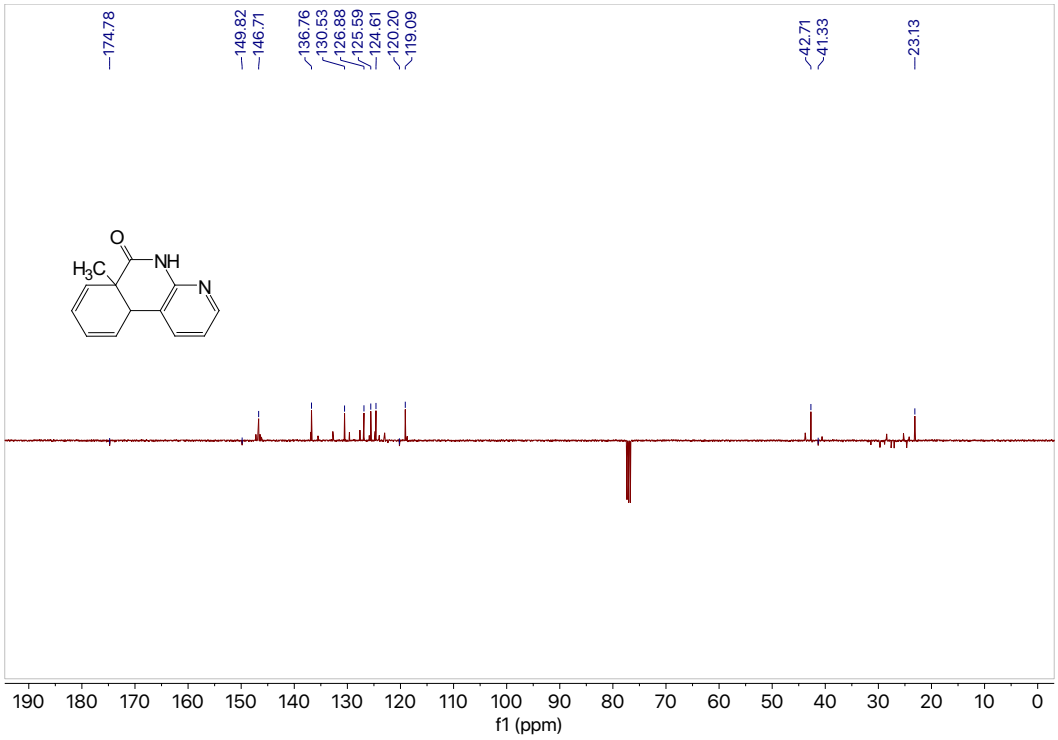

Figure 7.305 ^{13}C NMR (101 MHz, $CDCl_3$) of compound **10n**.

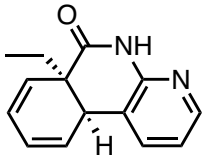

10o

(6aR,10aR)-6a-Ethyl-6a,10a-dihydrobenzo[c][1,8]naphthyridin-6(5H)-one (10o). Using the general MOM-group deprotection procedure B with the MOM-protected Heck product **2o** (0.0156, 0.0577 mmol, 1.0 equiv) in CH_3CN (1.9 mL, 0.03 M) afforded the crude deprotected product which was purified by column chromatography (silica, 3:2 hexanes: EtOAc) to obtain pure **10o** (0.0102 g, 0.0451 mmol) in 79% yield as a white solid, m.p.= 163.9 – 165.5°C.

^{1}H NMR (400 MHz, $CDCl_3$) δ 9.08 (s, 1H), 8.26 (dd, J = 5.0, 1.7 Hz, 1H), 7.60 – 7.54 (m, 1H), 7.00 (dd, J = 7.4, 5.0 Hz, 1H), 6.16 (m, 1H), 6.06 (m, 1H), 5.91 – 5.87 (m, 1H), 5.55 (m,1H), 3.77 – 3.71 (m, 1H), 1.70 – 1.61 (m, 2H), 0.95 (t, J = 7.5 Hz, 3H).

^{13}C NMR (101 MHz, $CDCl_3$) δ_u 146.8, 136.8, 128.9, 127.2, 125.6, 125.3, 119.2, 39.8, 9.2; δ_d 174.3, 149.7, 120.2, 45.6, 28.2.

GC (Method B) t_R = 2.237 min. EI-MS m/z (%): 225.0 ($M\text{-}1^+$, 20), 211.0 (4), 197.0 (100), 179.0 (6), 169.0 (11), 154.0 (15), 127.0 (8), 115.0 (4), 77.0 (4).

HRMS (ESI) calculated for $C_{13}H_{15}ON_2$ $[M+H]^+$: 227.1184, found 227.1183.

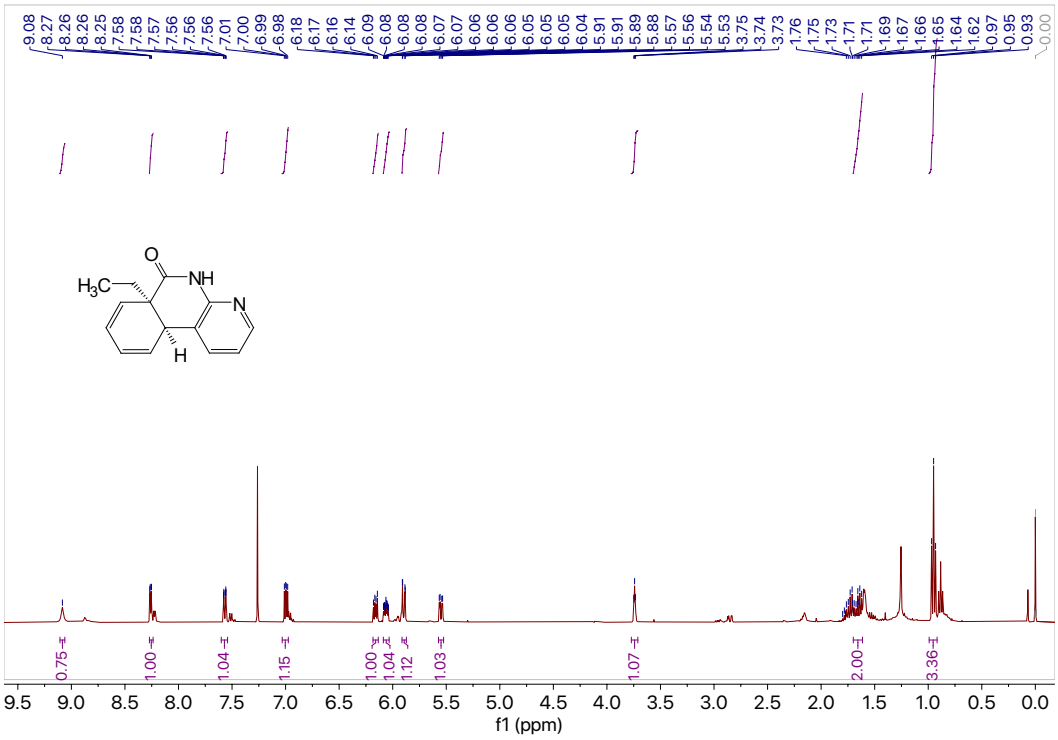

Figure 7.306 ^{1}H NMR (400 MHz, $CDCl_3$) of compound **10o**.

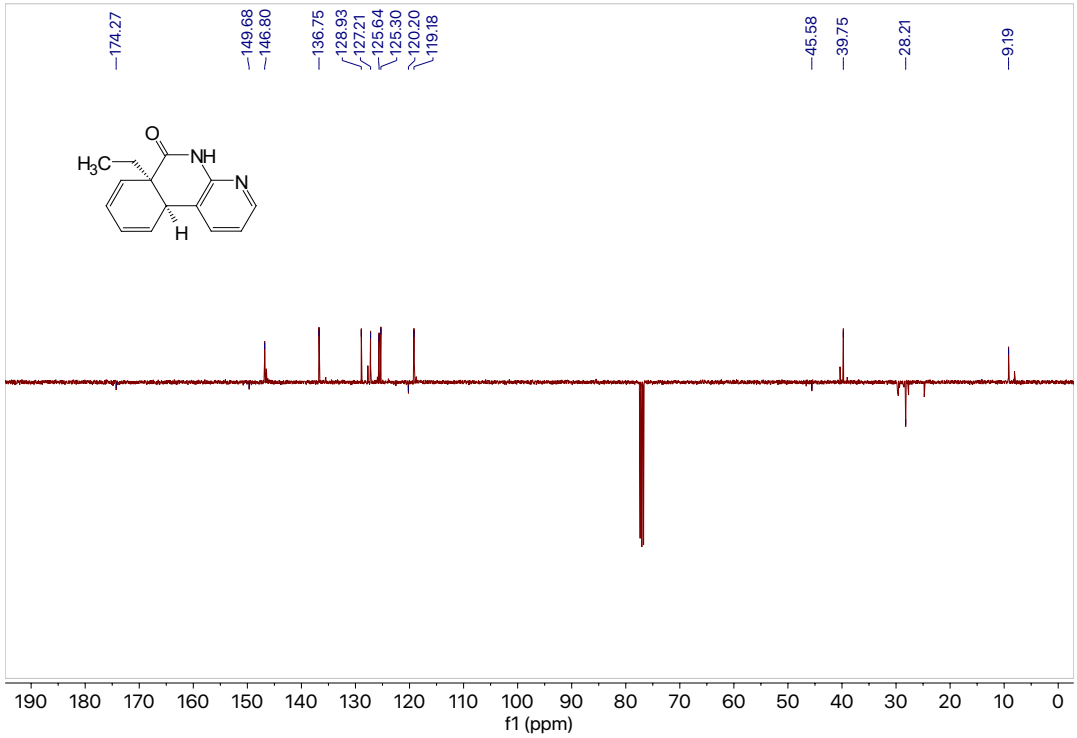

Figure 7.307 ^{13}C NMR (101 MHz, $CDCl_3$) of compound **10o**.

7.14 Alkene isomerization general procedures and data

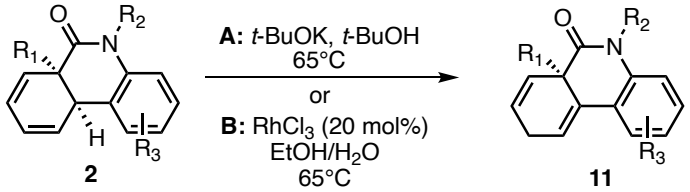

Scheme 7.22 Alkene isomerization general reaction.

General procedures and data

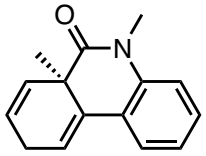

11a

(*R*)-5,6a-dimethyl-6a,9-dihydrophenanthridin-6(5*H*)-one (11a).

A: tBuOK/t-BuOH alkene isomerization

To a flame dried vial with a stir bar was added the Heck product **2a** (0.031 g, 0.14 mmol, 1.0 equiv) and *t*-BuOK (0.090 g, 0.80 mmol, 6.0 equiv), followed by *t*-BuOH (2.0 mL, 0.07 M). The vial was sealed with a pressure relief cap and stirred in a pre-heated (65°C) pie-block reactor overnight. Upon completion, the reaction mixture was cooled to room temperature, quenched with 10% HOAc (3.5 mL), stirred for 5-10 min and then transferred to a separatory funnel. The aqueous layer was extracted with diethyl ether. The combined organic layers were washed with a saturated $NaHCO_3$ solution and brine, dried over $MgSO_4$, and concentrated under reduced pressure. The crude product was purified by column chromatography (silica, 9:1 hexanes: EtOAc) to afford pure product **11a** (0.025 g, 0.11 mmol) as a yellow oil in 79% yield.

B: $RhCl_3 \bullet xH_2O$ catalyzed alkene isomerization

The Heck product **2a** (0.030 g, 0.13 mmol, 1.0 equiv) and $RhCl_3 \bullet xH_2O$ (0.006 g, 0.027, 0.2 equiv) were added to a vial with a stir bar and dissolved in 10:1 EtOH:H_2O (5.0 mL, 0.03 M). The vial was sealed with a pressure relief cap and stirred in a pre-heated (65°C) pie-block reactor overnight. Upon completion, the reaction mixture was cooled to room temperature, diluted in DCM, transferred to a round-bottom flask, and concentrated under reduced pressure. The crude product was purified by column chromatography (silica, 9:1 hexanes: EtOAc) to afford pure product **11a** (0.025 g, 0.11 mmol) as a yellow oil in 83% yield.

^{1}H NMR (400 MHz, $CDCl_3$) δ 7.55 (dd, J = 8.0, 1.0 Hz, 1H), 7.30 – 7.23 (m, 1H), 7.04 (t, J = 8.0 Hz, 1H), 6.98 (d, J = 8.0 Hz, 1H), 6.41 (d, J = 8.0 Hz, 1H), 6.07 – 6.01 (m, 2H), 5.89-5.83 (m, 1H), 3.37 (s, 3H), 2.7-2.71 (m, 2H), 1.26 (s, 3H).

^{13}C NMR (101 MHz, $CDCl_3$) δ_u 128.9, 125.5, 124.4, 123.5, 123.1, 117.9, 114.7, 39.9; δ_d 174.0, 138.2, 134.0, 122.4, 29.9, 22.4.

GC (method B) t_R = 2.33 min. EI-MS, m/z (%): 225.1 (M+, 10), 210.0 (100), 195.1 (39), 180.1 (11), 167.1 (14), 152.1 (13).
HRMS (ESI) calculated for $C_{15}H_{16}ON$ $[M+H]^+$: 226.1232, found 226.1228.

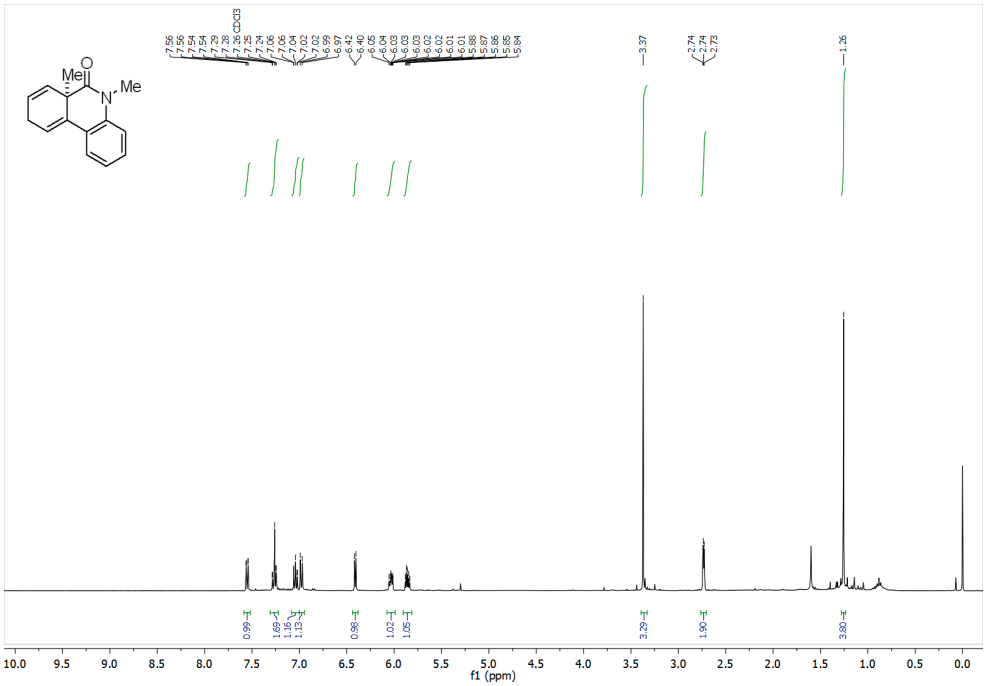

Figure 7.308 ^{1}**H** NMR (400 MHz, $CDCl_3$) of compound **11a**.

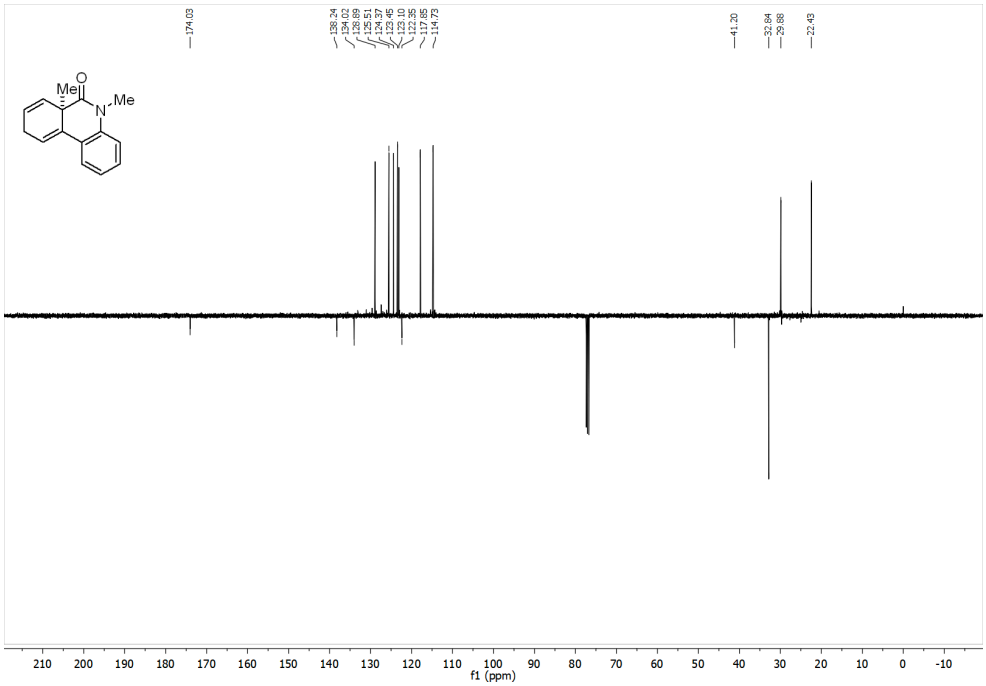

Figure 7.309 ^{13}C NMR (101 MHz, $CDCl_3$) of compound **11a**.

7.15 Synthesis of dienone and enone general procedures and data

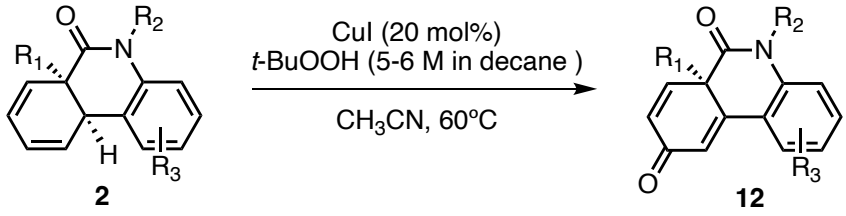

Scheme 7.23 Synthesis of dienone general reaction.

General procedure and data

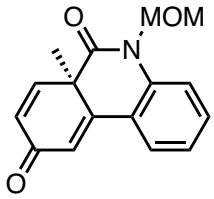

12b

(*R*)-5-(methoxymethyl)-6a-methylphenanthridine-6,9(5*H*,6a*H*)-dione (12b). To an argon-flushed flame dried vial with a stir bar, was added the Heck product **2b** (0.0300 g, 0.118 mmol, 1.0 equiv). The vial was imported in a glove box, where CuI (0.0045 g, 0.0236 mmol, 0.2 equiv) and CH_3CN (1.0 mL, 0.12 M) were added. The vial was sealed and exported outside the glovebox. The solution was stirred for a few minutes, then *t*BuOOH (0.24 mL, 11.8 mmol, 10 equiv) was added under argon. The reaction mixture was stirred in the pre-heated (60°C) pie-block reactor for 3 h or once determined to be complete by TLC and GC. Upon completion, the reaction mixture was cooled to room temperature, washed with 25 % ammonia and water, then extracted with diethyl ether, washed with brine, dried over $MgSO_4$, and concentrated under reduced pressure. The crude product was purified by column chromatography (silica, 4:1 hexanes: EtOAc) to afford pure product **12b** (0.0227 g, 0.084 mmol) as a yellow solid in 71% yield, m.p.=134.6-136.4°C.

^{1}H NMR (400 MHz, $CDCl_3$) δ 7.70 – 7.60 (m, 2H), 7.50 (ddd, J = 8.8, 7.3, 1.5 Hz, 1H), 7.41 (dd, J = 8.3, 1.2 Hz, 1H), 7.29 – 7.21 (m, 1H), 6.65 (d, J = 1.8 Hz, 1H), 6.44 (dd, J = 10.1, 1.8 Hz, 1H), 5.72 (d, J = 10.7 Hz, 1H), 5.02 (d, J = 10.8 Hz, 1H), 3.43 (s, 3H), 1.52 (s, 3H).

^{13}C NMR (101 MHz, $CDCl_3$) δ_u 148.4, 132.1, 128.5, 125.6, 124.6, 124.2, 116.3, 56.5, 28.6. δ_d 185.1, 169.6, 154.31, 137.4, 121.8, 74.6, 46.9.

GC (method B) t_R = 3.36 min. EI-MS, m/z (%): 269.1 (M^+, 100), 239.0 (56), 210.0 (39), 196.0 (11), 180.0 (18), 167.0 (22), 152.0 (13).

HRMS (ESI) calculated for C16H16O3N $[M+H]^+$: 270.1130, found 270.1126.

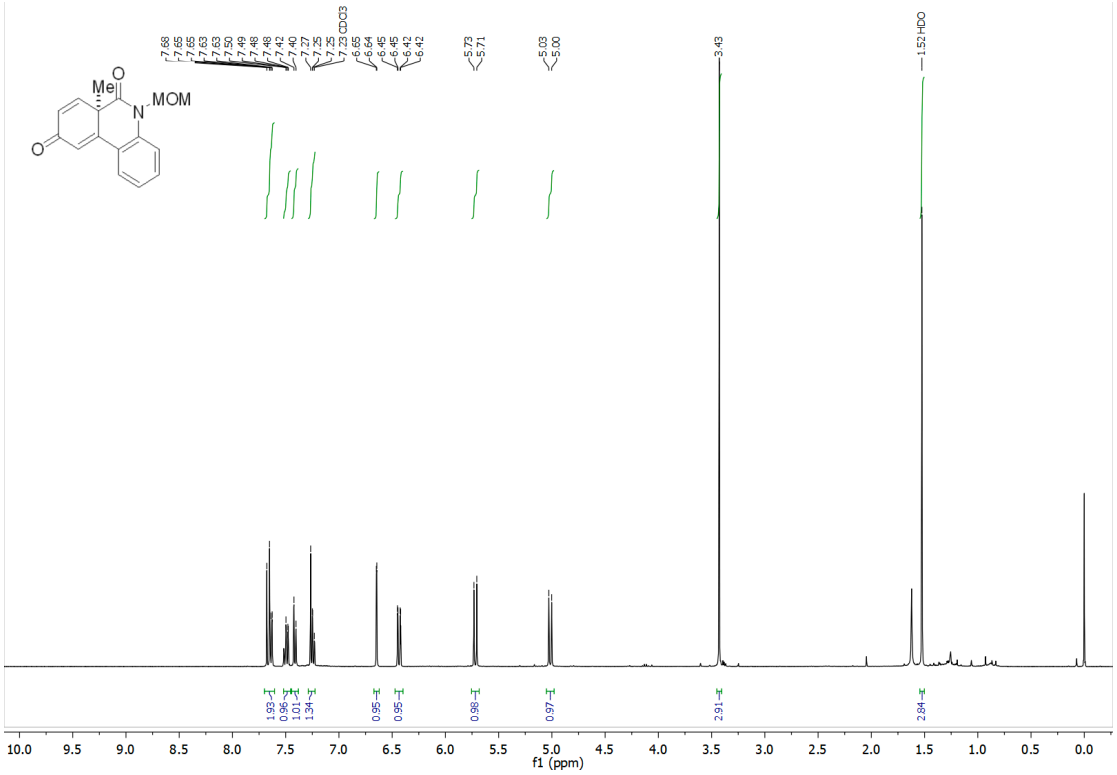

Figure 7.310 ^{1}H NMR (400 MHz, $CDCl_3$) of compound **12b**.

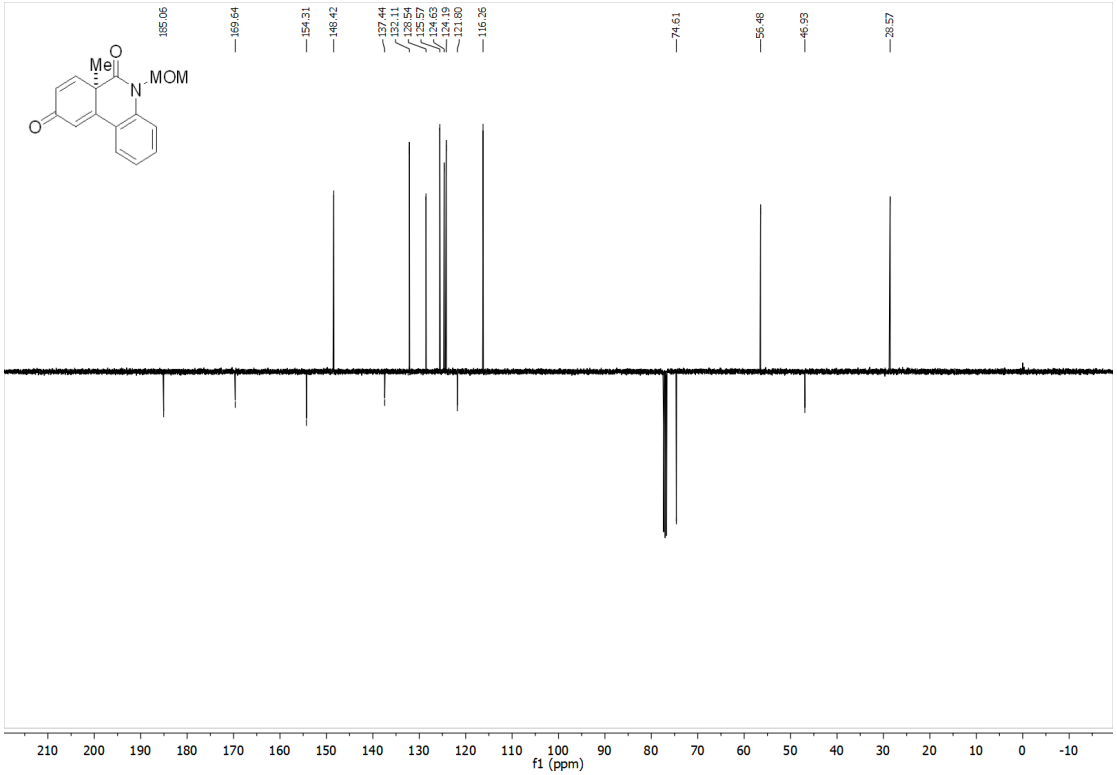

Figure 7.311 ^{13}C NMR (101 MHz, $CDCl_3$) of compound **12b**.

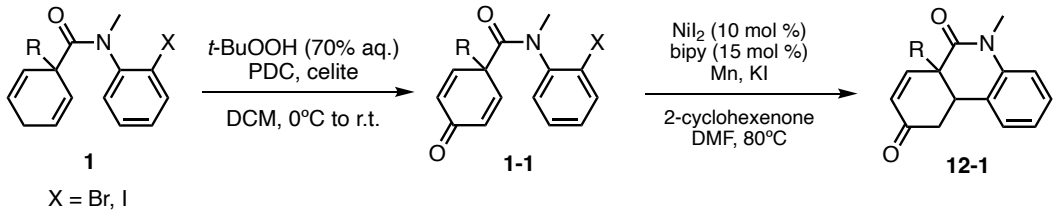

Scheme 7.24 Synthesis of enone general reaction sequence.

General procedures and data

PDC/*t*BuOOH oxidation

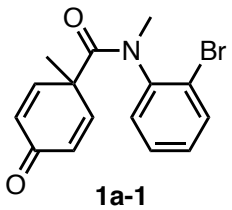

1a-1

***N*-(2-bromophenyl)-*N*,1-dimethyl-4-oxocyclohexa-2,5-diene-1-carboxamide (1a-1).** A round bottom flask with a stir bar, under argon, was charged with tertiary amide **1a** (0.102 g, 0.327 mmol, 1.0 equiv) in DCM (1 mL, 0.1 M). PDC (0.0127 g, 0.0327 mmol, 0.1 equiv) and celite (0.0127 g) were added and the solution was cooled to 0°C. *t*BuOOH (70% aq., 0.136 mL, 0.981 mmol, 3.0 equiv) was added dropwise and the solution was stirred at r.t. for 2 hrs. Upon completion, the reaction mixture was filtered using a pipet packed with celite, washed with excess DCM, and concentrated under reduced pressure. The crude product was purified by column chromatography (silica, 3:2 hexanes: EtOAc) to afford pure product **1a-1** (0.0705 g, 0.22 mmol) as a white solid in 67% yield.
^{1}H NMR (400 MHz, $CDCl_3$) δ 7.55 (dd, *J* = 8.1, 1.4 Hz, 1H), 7.25 – 7.17 (m, 1H), 7.14 – 7.02 (m, 2H), 6.94 (dd, *J* = 10.0, 3.0 Hz, 1H), 6.74 (dd, *J* = 10.1, 3.0 Hz, 1H), 6.08 (dd, *J* = 10.1, 1.9 Hz, 1H), 5.57 (dd, *J* = 10.1, 1.8 Hz, 1H), 3.20 (s, 3H), 1.52 (s, 3H).
^{13}C NMR (101 MHz, $CDCl_3$) δ_u 150.9, 149.2, 133.6, 131.2, 130.9, 128.6, 128.3, 126.1, 38.7, 26.5; δ_d 184.5, 169.5, 141.0, 124.2, 50.6.
GC (method B) t_R = 2.831 min. EI-MS, m/z (%): 319.1 (M^+, 1), 240.1 (13), 212.0 (100), 196.9 (9), 184.0 (21), 156.9 (5), 133.0 (10), 105.0 (13), 90.0 (4), 77.0 (15).

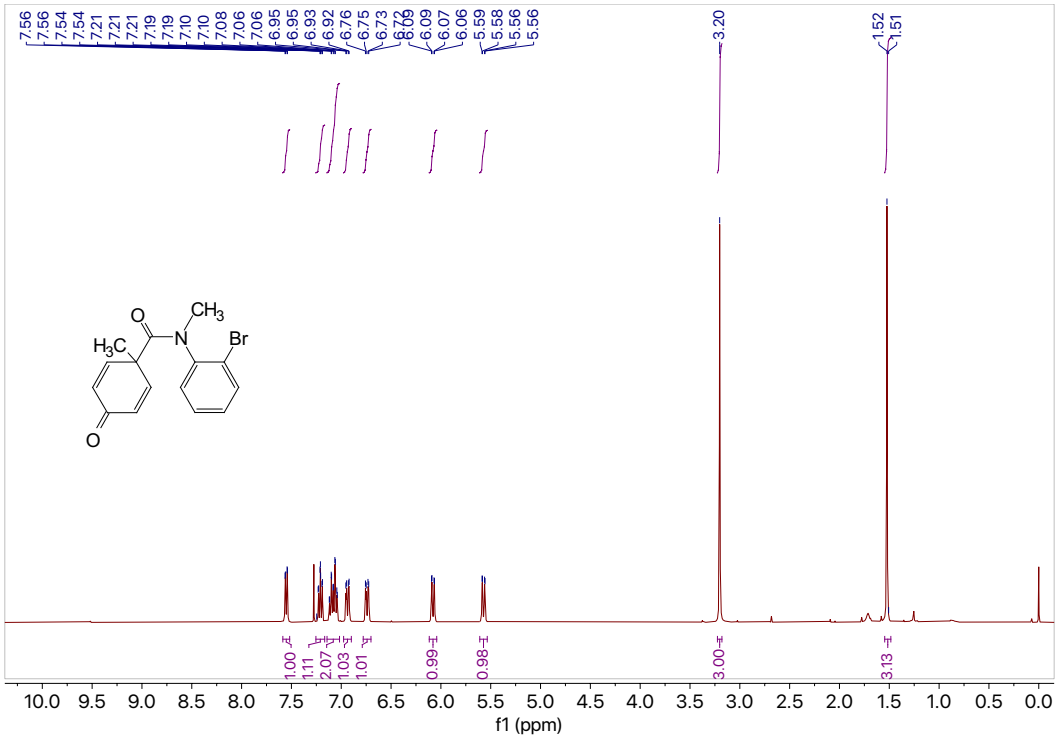

Figure 7.312 ^{1}H NMR (400 MHz, $CDCl_3$) of compound **1a-1**.

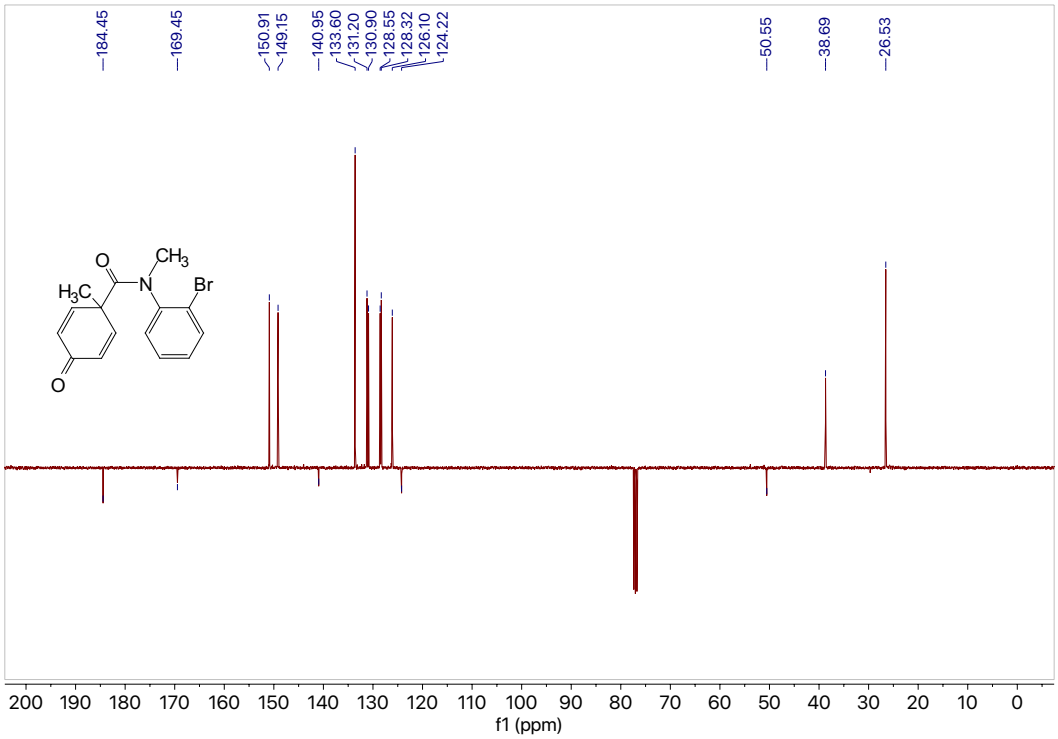

Figure 7.313 ^{13}C NMR (101 MHz, $CDCl_3$) of compound **1a-1**.

Ni-catalyzed Heck reaction

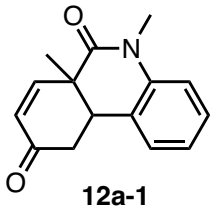

12a-1

(6a*R*)-5,6a-dimethyl-10,10a-dihydrophenanthridine-6,9(5*H*,6a*H*)-dione (1a-1). Using the general procedure for the Ni-catalyzed Heck reaction, aryl bromide dienone **1a-1** (0.065 g, 0.203 mmol, 1.0 equiv) in DMF (2.5 mL, 0.08 M) was subjected to the Heck reaction conditions with 10 mol% NiI_2/15 mol% 2,2'-bipyridine for h.The crude product was purified by column chromatography (silica, 4:1 hexanes: EtOAc) to afford **12a-1** (0.0387 g, 0.162 mmol) in 80% yield as a yellow oil. **^{1}H NMR** (400 MHz, $CDCl_3$) δ 7.34 (ddd, *J* = 8.2, 7.4, 1.7 Hz, 1H), 7.18 (dd, *J* = 7.5, 1.7 Hz, 1H), 7.13 – 7.08 (m, 2H), 7.04 (dd, *J* = 8.2, 1.0 Hz, 1H), 6.12 (dd, *J* = 10.1, 0.9 Hz, 1H), 3.41 (s, 3H), 3.19 (dd, *J* = 12.9, 5.2 Hz, 1H), 2.58 – 2.50 (m, 2H), 1.33 (s, 3H).**^{13}C NMR** (101 MHz, $CDCl_3$) δ_u 153.1, 128.6, 128.5, 128.3, 123.9, 115.0, 44.2, 29.8, 23.7; δ_d 197.0, 171.1, 138.3, 125.8, 41.7. **GC** (method B) t_R = 2.611 min. EI-MS, m/z (%): 241.1 (M^+, 100), 226.1 (10), 212.1 (12), 198.1 (26), 182.1 (14), 173.1 (12), 158.1 (7), 145.1 (14), 130.1 (10), 115.1 (8), 77.1 (7), 53.1 (5)

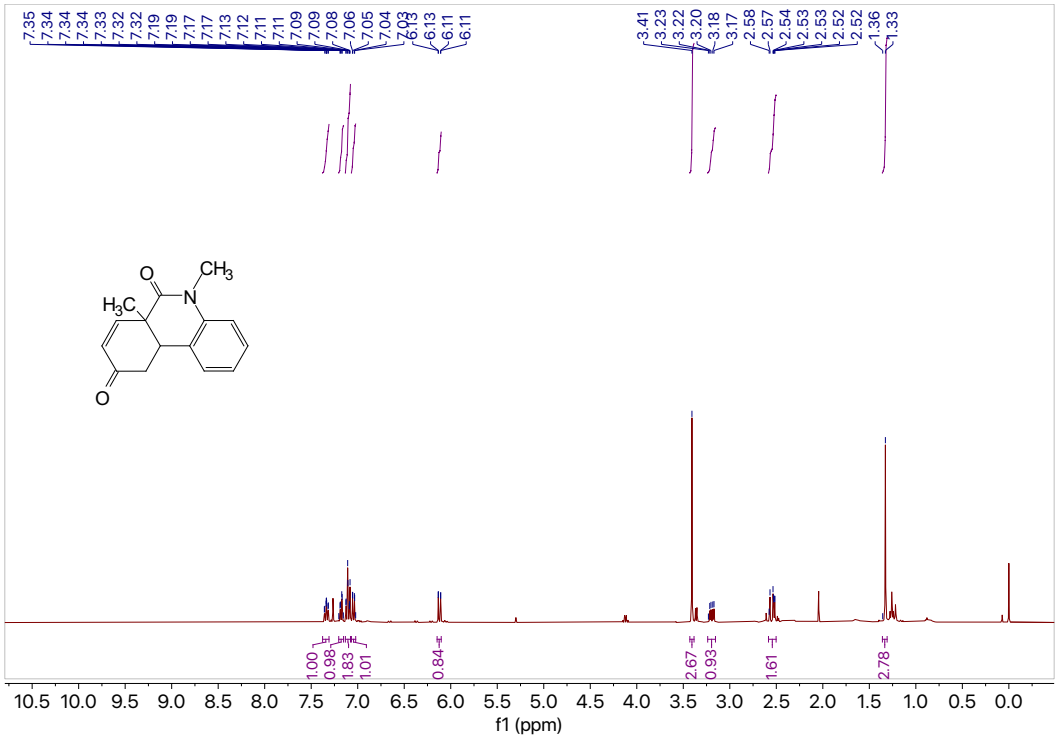

Figure 7.314 ^{1}H NMR (400 MHz, $CDCl_3$) of compound **12a-1**.

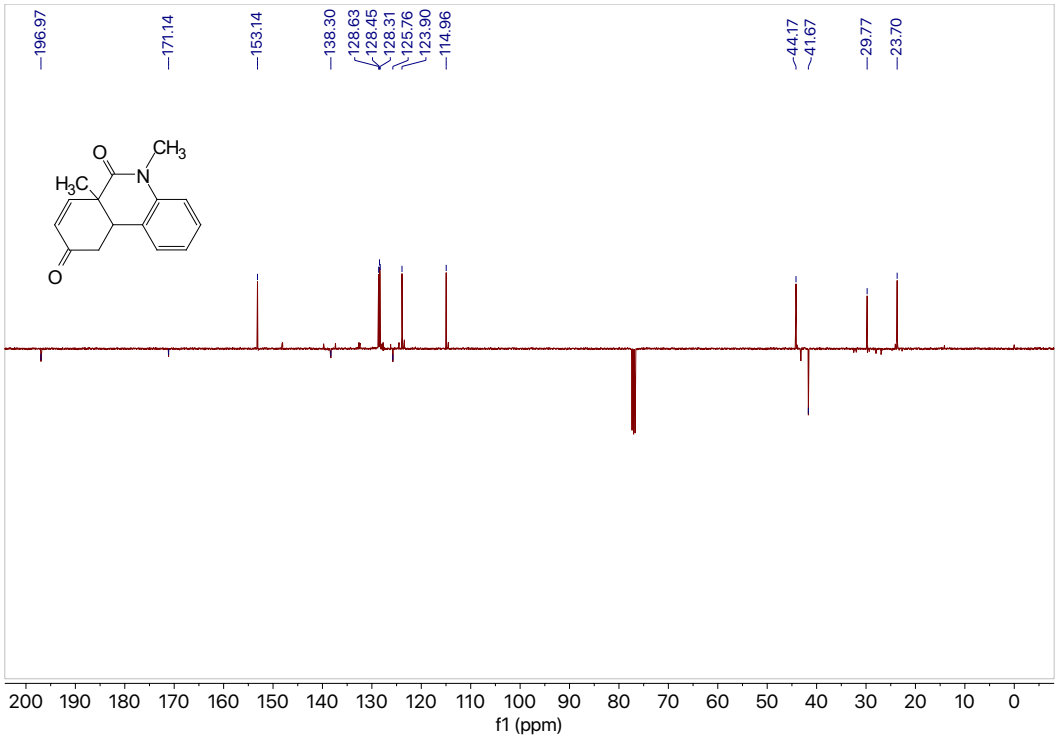

Figure 7.315 ^{13}C NMR (101 MHz, $CDCl_3$) of compound **12a-1**.

7.16 Cytotoxicity screening of phenanthridinone derivatives

34 phenanthridinone derivatives were evaluated for cytotoxicity by our biological collaborators at the Lankenau Institute of Medical Research (LIMR). Two human cell lines were employed: WI-38, a diploid human cell line composed of fibroblasts derived from lung tissue, which served as the normal cell line; and MCF-7, a breast cancer cell line. The compounds were screened using the Sulforhodamine B (SRB) assay.

Table 7.1 Cytotoxicity screening of phenanthridinone derivatives.

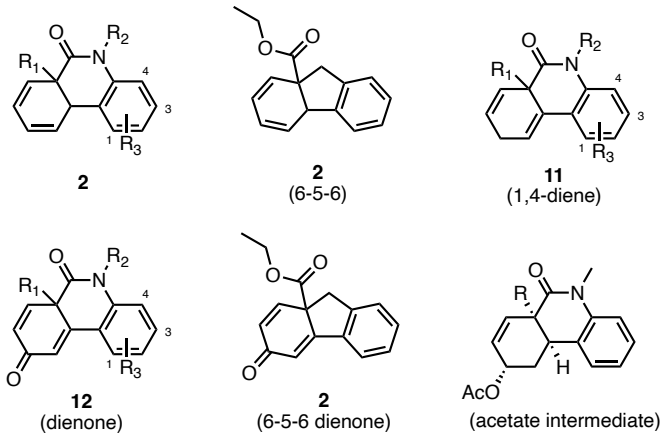

Compound	R_1	R_2	R_3
1	Me	Me	H
2	Me	MOM	H
3	Me	H	H
4	Me	MOM	3-F
5	Me	H	3-Me
6	Me	H	2-Cl
7	Et	H	H
8	Et	MOM	H
9	*i*-Pr	MOM	H
10	*i*-Pr	Me	H
11	*i*-Pr	MOM	3-F
12	*i*-Pr	MOM	3-Me
13	*i*-Pr	MOM	2-Cl
14	*i*-Pr	H	H
15	*i*-Pr	H	3-Me
16	*i*-Pr	H	3-F
17	*i*-Pr	H	2-Cl
18	Me	Bu	H
19	CH_2CO_2Et	Me	H
20	Me	MOM	2-Me
21	Me	MOM	2-Cl
22	Me	H	3-F
23	CO_2Et	6-5-6	H
24	Me (1,4-diene)	H	H
25	Me (1,4-diene)	Me	H
26	Me (1,4-diene)	H	3-F
27	Me (dienone)	Me	H
28	Me (dienone)	MOM	H
29	Et (dienone)	MOM	H
30	CH_2CO_2Et (dienone)	Me	H
31	Me (dienone)	MOM	3-F
32	Me (enone)	Me	H
33	CO_2Et (dienone)	6-5-6	H
34	Me (acetate interm.)	MOM	H

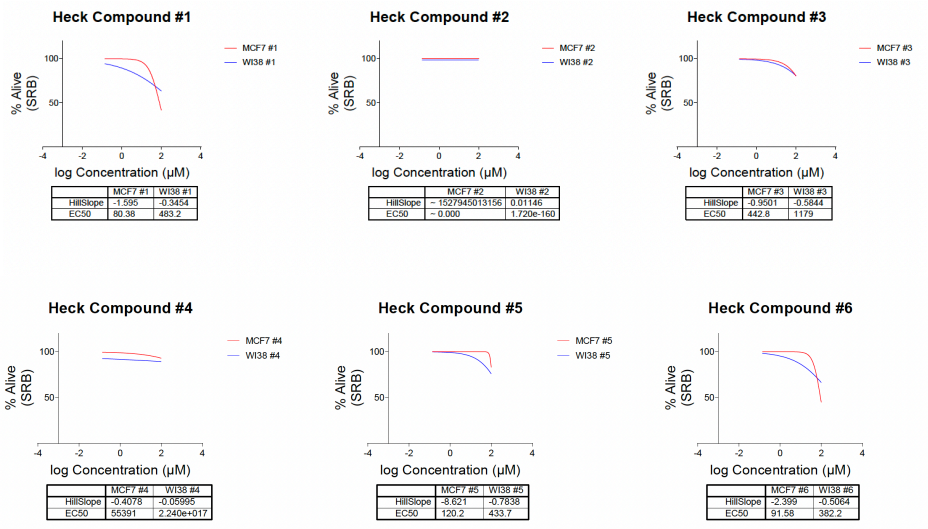

Heck Compound #7

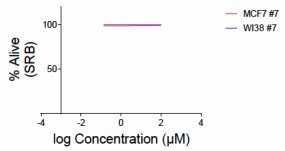

	MCF7 #7	WI38 #7
HillSlope	~ -489.6	0.03757
EC50	~	2.529e-050

Heck Compound #8

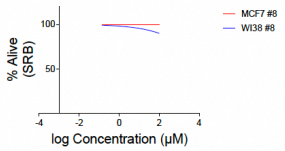

	MCF7 #8	WI38 #8
HillSlope	~ -1.199e+042	-0.3796
EC50	~	32622

Heck Compound #9

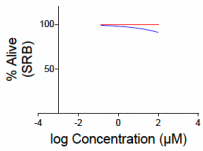

	MCF7 #9	WI38 #9
HillSlope	~ 56422	-0.3350
EC50	~ 0.000	102375

Heck Compound #10

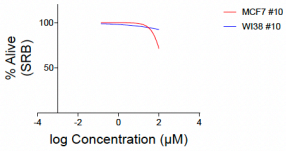

	MCF7 #10	WI38 #10
HillSlope	-1.629	-0.3040
EC50	175.1	374316

Heck Compound #11

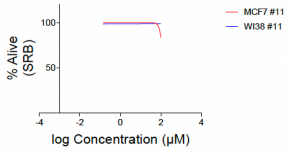

	MCF7 #11	WI38 #11
HillSlope	-5.596	0.04119
EC50	133.4	4.048e-047

Heck Compound #12

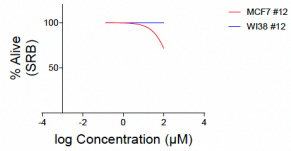

	MCF7 #12	WI38 #12
HillSlope	-1.054	~ 13.30
EC50	240.6	~ 3.175e-160

Heck Compound #13

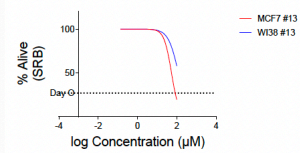

	MCF7 #13	WI38 #13
HillSlope	-2.299	-1.695
EC50	53.70	120.5

Heck Compound #14

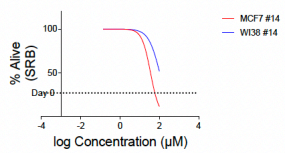

	MCF7 #14	WI38 #14
HillSlope	-1.980	-1.517
EC50	35.55	104.5

Heck Compound #15

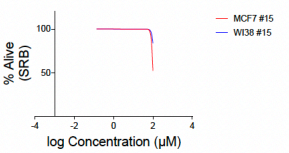

	MCF7 #15	WI38 #15
HillSlope	-9.530	~ -7.489
EC50	100.9	~ 124.4

Heck Compound #16

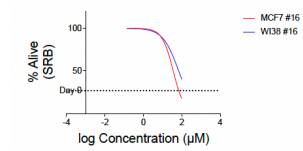

	MCF7 #16	WI38 #16
HillSlope	-1.502	-1.060
EC50	35.66	68.63

Heck Compound #17

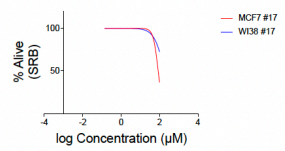

	MCF7 #17	WI38 #17
HillSlope	-3.396	-1.620
EC50	85.14	181.8

Heck Compound #18

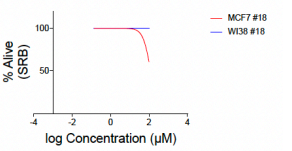

	MCF7 #18	WI38 #18
HillSlope	-2.211	~ 5.509
EC50	121.4	~ 1.918e-263

Heck Compound #19

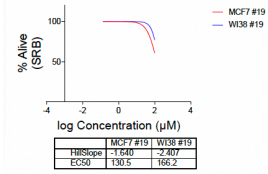

	MCF7 #19	WI38 #19
HillSlope	-1.640	-2.407
EC50	130.5	166.2

Heck Compound #20

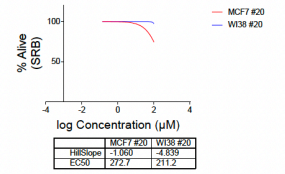

	MCF7 #20	WI38 #20
HillSlope	-1.060	-4.839
EC50	272.7	211.2

Heck Compound #21

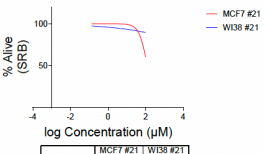

	MCF7 #21	WI38 #21
HillSlope	-1.977	-0.2216
EC50	124.0	1671647

Heck Compound #22

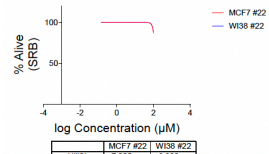

	MCF7 #22	WI38 #22
HillSlope	-7.205	-6.322
EC50	129.9	137.5

Heck Compound #23

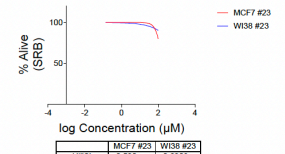

	MCF7 #23	WI38 #23
HillSlope	-2.580	-0.6903
EC50	171.1	2551

Heck Compound #24

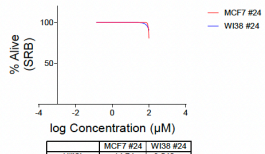

	MCF7 #24	WI38 #24
HillSlope	~ -14.74	-3.540
EC50	~ 110.2	190.1

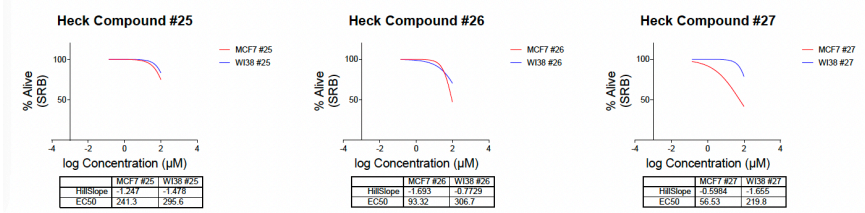
Heck Compound #25
MCF7 #25
WI38 #25
% Alive (SRB)
log Concentration (μM)
MCF7 #25 WI38 #25
HillSlope -1.247 -1.478
EC50 241.3 295.6
Heck Compound #26
MCF7 #26
WI38 #26
% Alive (SRB)
log Concentration (μM)
MCF7 #26 WI38 #26
HillSlope -1.693 -0.7729
EC50 93.32 306.7
Heck Compound #27
MCF7 #27
WI38 #27
% Alive (SRB)
log Concentration (μM)
MCF7 #27 WI38 #27
HillSlope -0.5984 -1.655
EC50 56.53 219.8

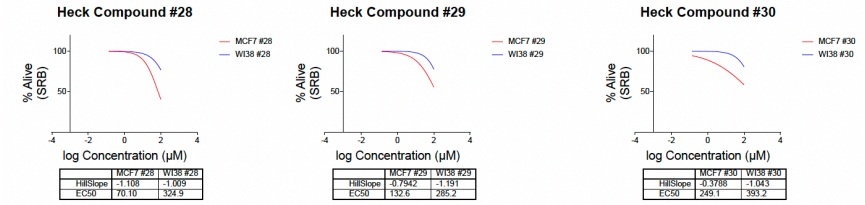
Heck Compound #28
MCF7 #28
WI38 #28
% Alive (SRB)
log Concentration (μM)
MCF7 #28 WI38 #28
HillSlope -1.108 -1.009
EC50 70.10 324.9
Heck Compound #29
MCF7 #29
WI38 #29
% Alive (SRB)
log Concentration (μM)
MCF7 #29 WI38 #29
HillSlope -0.7942 -1.191
EC50 132.6 285.2
Heck Compound #30
MCF7 #30
WI38 #30
% Alive (SRB)
log Concentration (μM)
MCF7 #30 WI38 #30
HillSlope -0.3788 -1.043
EC50 249.1 393.2

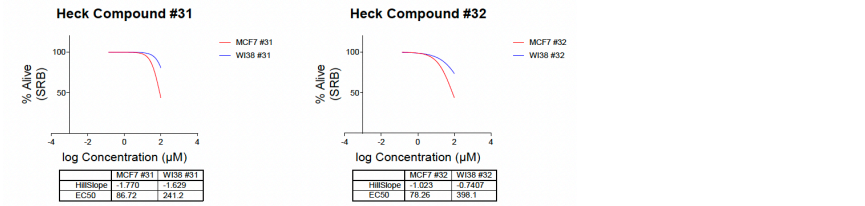
Heck Compound #31
MCF7 #31
WI38 #31
% Alive (SRB)
log Concentration (μM)
MCF7 #31 WI38 #31
HillSlope -1.770 -1.629
EC50 86.72 241.2
Heck Compound #32
MCF7 #32
WI38 #32
% Alive (SRB)
log Concentration (μM)
MCF7 #32 WI38 #32
HillSlope -1.023 -0.7407
EC50 78.26 398.1

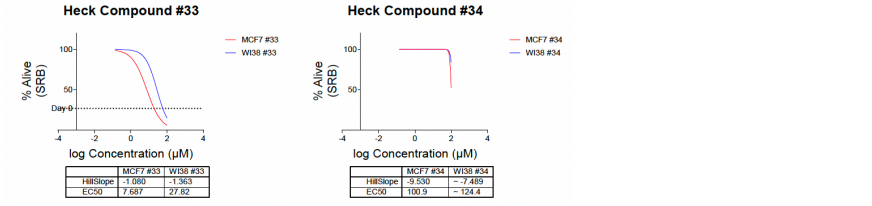
Heck Compound #33
MCF7 #33
WI38 #33
% Alive (SRB)
Day 0
log Concentration (μM)
MCF7 #33 WI38 #33
HillSlope -1.080 -1.363
EC50 7.687 27.82
Heck Compound #34
MCF7 #34
WI38 #34
% Alive (SRB)
log Concentration (μM)
MCF7 #34 WI38 #34
HillSlope -9.530 ~ -7.489
EC50 100.9 ~ 124.4

7.17 1,2-Dicarbofunctionalization of alkenes

7.17.1 Alkene arylalkylation general procedures and data

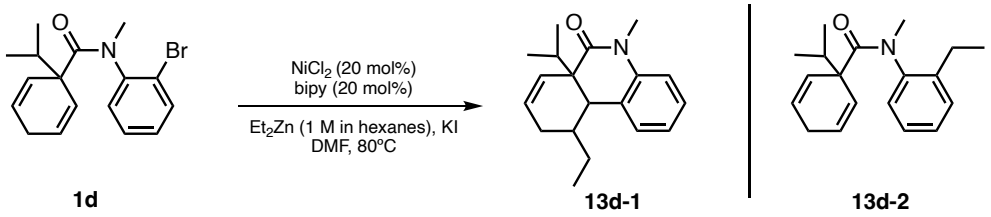

Scheme 7.25 Redox neutral alkene arylalkylation with Et_2Zn reaction.

General procedure and data

An oven-dried screw-cap vial, equipped with a magnetic stir bar, was charged with the aryl bromide diene **1d** (0.1 g, 0.299 mmol, 1.0 equiv) and then brought into a glovebox. An anhydrous $NiCl_2$ (0.0078 g, 0.0598 mmol, 20 mol %), bipy (0.0093 g, 0.0598 mmol, 25 mol %), KI (0.0496 g, 0.299 mmol, 1.0 equiv), Et_2Zn (1 M in hexanes, 1.8 mL, 1.794 mmol, 6.0 equiv), and DMF (3.7 mL, 0.08 M) were added, and the vial was sealed with a pressure relief cap and removed from the glovebox. The vial was stirred at 80˚C in a pie reactor for 3 h. Upon completion, the reaction mixture was filtered through an aluminum oxide plug and washed with EtOAc. The resulting organic solution was washed with 1 N HCl and brine, dried with $MgSO_4$, filtered, and concentrated in vacuo. The crude product was purified by column chromatography (silica, 4:1 hexanes: EtOAc) to afford **13d-2** as the major observed product (0.0686 g, 0.242 mmol) in 81% yield (95% purity by GCMS) as a yellow oil.

^{1}H NMR (400 MHz, $CDCl_3$) δ 7.26 – 7.20 (m, 2H), 7.04 – 7.01 (m, 2H), 5.46 (d, J = 10.4 Hz, 1H), 5.33 (dd, J = 15.5, 6.0 Hz, 1H), 5.18 (s, 2H), 3.15 (s, 3H), 2.56 (qd, J = 9.0, 4.0 Hz, 2H), 2.48 (q, J = 6.9 Hz, 1H), 2.29 (d, J = 23.0 Hz, 1H), 2.13 (d, J = 23.0 Hz, 1H), 1.23 (t, J = 7.6 Hz, 3H), 0.80 (d, J = 6.9 Hz, 3H), 0.71 (d, J = 6.9 Hz, 3H).
^{13}C NMR (101 MHz, $CDCl_3$) δ_u 129.0, 128.8, 128.2, 127.9, 126.2, 125.9, 124.4, 123.9, 40.0, 36.0, 17.7, 17.3, 13.8; δ_d 174.9, 143.1, 141.5, 53.9, 26.4, 23.2.
GC t_R = 2.397 min (Method B). EI-MS m/z (%): 283.1 (M^+, 5), 240.0 (25), 210.0 (5), 163.0 (100), 146.0 (70), 134.0 (34), 120.0 (20), 105.0 (56), 91.0 (8), 77.0 (35), 51(5).

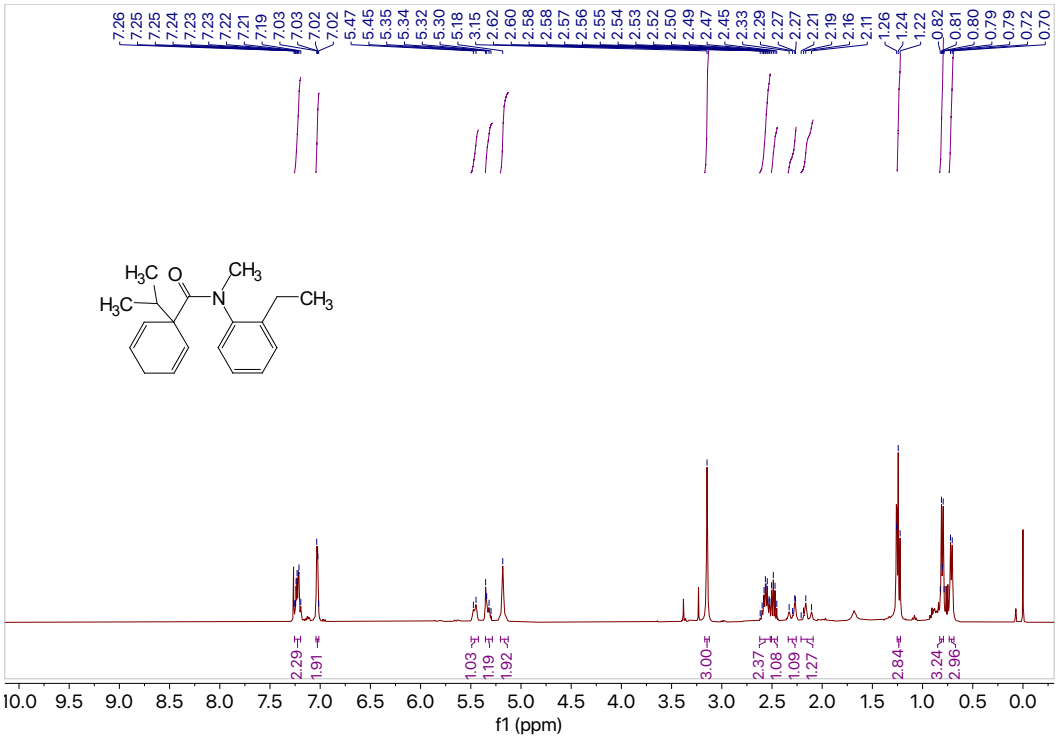

Figure 7.316 ^{1}H NMR (400 MHz, $CDCl_3$) of compound **13d-2**.

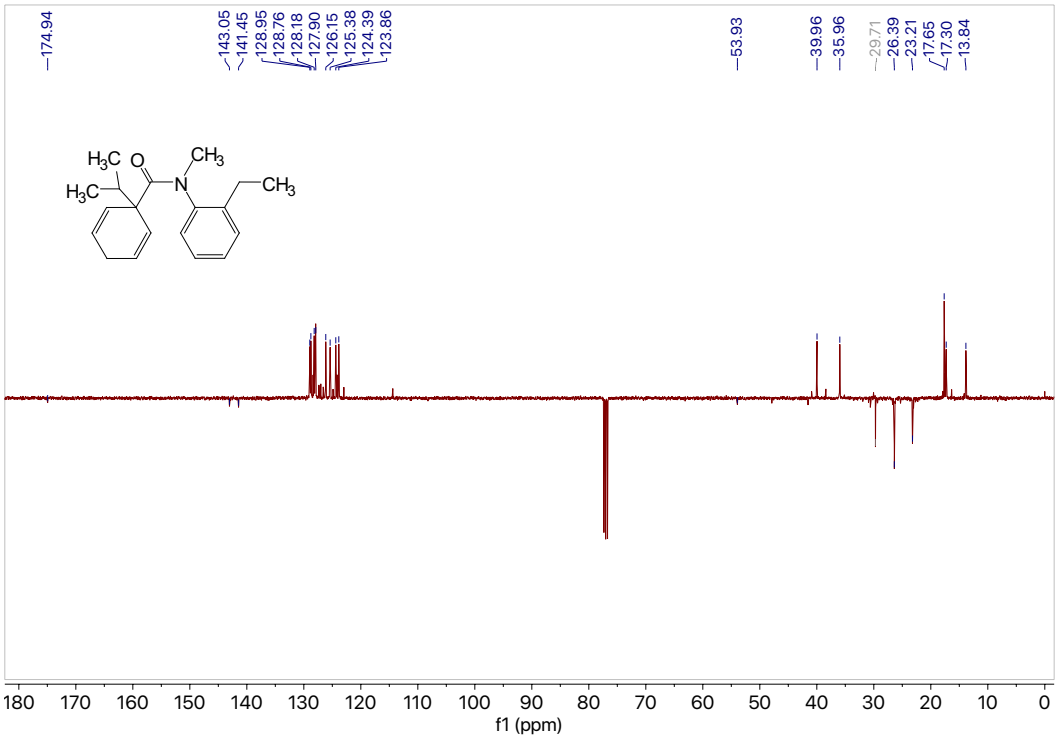

Figure 7.317 ^{13}C NMR (101 MHz, $CDCl_3$) of compound **13d-2**.

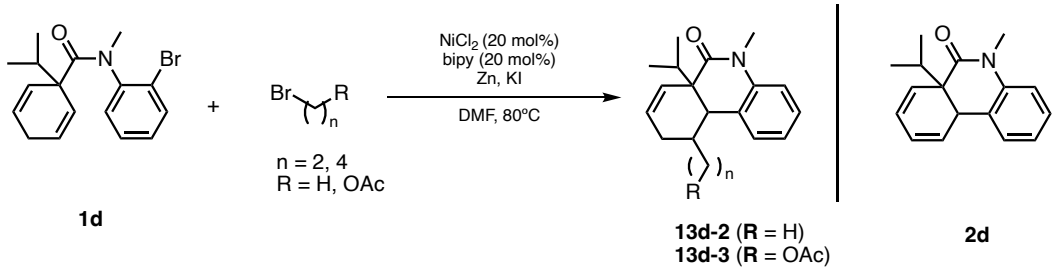

Scheme 7.26 Reductive alkene arylalkylation with bromobutane or 2-bromoethyl acetate.

General procedure and data[21]

An oven-dried screw-cap vial, equipped with a magnetic stir bar, was charged with the aryl bromide diene **1d** (0.020 g, 0.0598 mmol, 1.0 equiv) and then brought into a glovebox. An anhydrous $NiCl_2$ (0.0015 g, 0.0119 mmol, 20 mol %), bipy (0.0019 g, 0.01196 mmol, 20 mol %), Zn (0.0108 g, 0.179 mmol, 3.0 equiv), KI (0.0099 g, 0.0598 mmol, 1.0 equiv), bromobutane (13 µL, 0.0164 g, 0.119 mmol, 2.0 equiv) or 2-bromoethyl acetate (13 µL, 0.0199 g, 0.119 mmol, 2.0 equiv), and DMF (0.8 mL, 0.08 M) were added, and the vial was sealed with a pressure relief cap and removed from the glovebox. The vial was stirred at 80˚C in a pie reactor. After 3 hrs., the reaction mixture was filtered through an aluminum oxide plug, diluted with EtOAc, and analyzed by TLC/GCMS. The major observed species was the Heck diene product **2d** (68-70%)[GC]. **GC** (Method B) t_R = 2.294. EI-MS m/z (%): 253.1 (12, M^+).

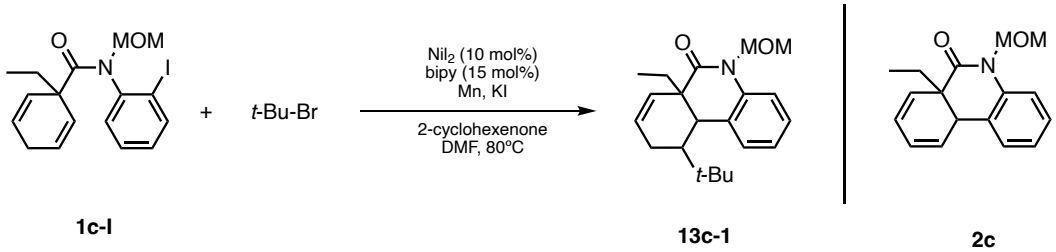

Scheme 7.27 Reductive alkene arylalkylation with tert-butyl bromide.

General procedure and data

An oven-dried screw-cap vial, equipped with a magnetic stir bar, was charged with the aryl iodide diene **1c-I** (0.0500 g, 0.126 mmol, 1.0 equiv) and then brought into a glovebox. An anhydrous NiI_2 (0.0039 g, 0.0126 mmol, 10 mol %), bipy (0.0029 g, 0.0189 mmol, 15 mol %), Mn (0.0210 g, 0.378 mmol, 3.0 equiv), KI (0.0209 g, 0.126 mmol, 1.0 equiv), tert-butyl bromide (43 µL, 0.052 g, 0.378 mmol, 3.0 equiv), 2-cyclohexenone (37 µL, 0.0363 g, 0.378 mmol, 3.0 equiv), and DMF (1.6 mL, 0.08 M) were added, and the vial was sealed with a pressure relief cap and removed from the glovebox. The vial was stirred at 80˚C in a pie reactor. After 2 hrs., the reaction mixture was filtered through an aluminum oxide plug, diluted with EtOAc, and analyzed by TLC/GCMS. The reaction mixture contained mostly the Heck diene product **2c** (95%)[GC]. **GC** (Method B) t_R = 2.380. EI-MS m/z (%): 269.1 (M^+, 36).

7.17.2 Alkene diarylation general procedures and data

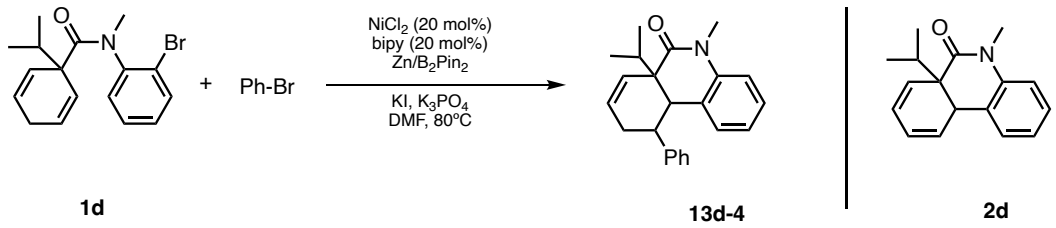

Scheme 7.28 Reductive alkene diarylation with bromobenzene.

General procedure and data[22]

An oven-dried screw-cap vial, equipped with a magnetic stir bar, was charged with the aryl bromide diene **1d** (0.0503 g, 0.1496 mmol, 1.0 equiv) and then brought into a glovebox. An anhydrous $NiCl_2$ (0.0039 g, 0.0299 mmol, 20 mol %), bipy (0.0047 g, 0.0299 mmol, 20 mol %), Zn (0.0196 g, 0.299 mmol, 2.0 equiv), B_2Pin_2 (0.0759 g, 0.299 mmol, 2.0 equiv), KI (0.0248 g, 0.1496 mmol, 1.0 equiv), K_3PO_4 (0.0630 g, 0.299 mmol, 2.0 equiv), bromobenzene (63 µL, 0.0934 g, 0.5984 mmol, 4.0 equiv) and DMF (2 mL, 0.08 M) were added, and the vial was sealed with a pressure relief cap and removed from the glovebox. The vial was stirred at 80˚C in a pie reactor. After 2 hrs., the reaction mixture was filtered through an aluminum oxide plug, diluted with EtOAc, and analyzed by TLC/GCMS. The major observed species was the Heck diene product **2d** (67%)[GC]. **GC** (Method B) t_R = 2.294. EI-MS m/z (%): 253.1 (M^+, 12).

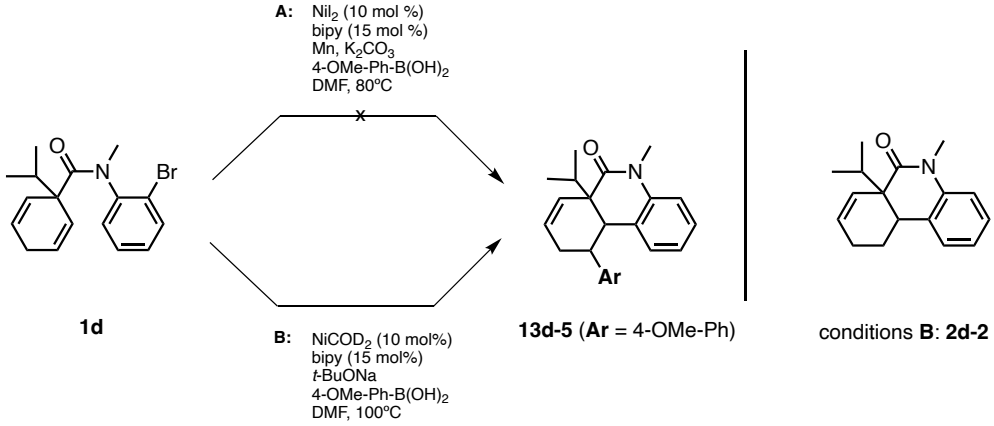

Scheme 7.29 Domino Heck cyclization/Suzuki coupling.

General procedure A and data[23]

An oven-dried screw-cap vial, equipped with a magnetic stir bar, was charged with the aryl bromide diene **1d** (0.0301 g, 0.0903 mmol, 1.0 equiv) and then brought into a glovebox. An anhydrous NiI_2 (0.0028 g, 0.009 mmol, 10 mol %), bipy (0.0021 g, 0.0135 mmol, 15 mol %), Mn (0.0149 g, 0.271 mmol, 3.0 equiv), K_2CO_3 (0.0249 g, 0.1806 mmol, 2.0 equiv), 4-OMe-Ph-$B(OH)_2$ (0.0274 g, 0.181 mmol, 2.0 equiv) and DMF (1.3 mL, 0.08 M) were added, and the vial was sealed with a pressure relief cap and removed

from the glovebox. The vial was stirred at 80˚C in a pie reactor. After 15 hrs., the reaction mixture was filtered through an aluminum oxide plug, diluted with EtOAc, and analyzed by TLC/GCMS. The reaction mixture contained only the starting material **1d** (>99%)^{GC}. **GC** (Method B) t_R = 2.692 min. EI-MS m/z (%): 333.1 (M-1$^+$, 2).

General procedure B and data[23]

An oven-dried screw-cap vial, equipped with a magnetic stir bar, was charged with the aryl bromide diene **1d** (0.0299 g, 0.0903 mmol, 1.0 equiv) and then brought into a glovebox. An anhydrous $NiCOD_2$ (0.0025 g, 0.009 mmol, 10 mol %), bipy (0.0021 g, 0.0135 mmol, 15 mol %), NaO*t*Bu (0.0217 g, 0.226 mmol, 2.5 equiv), 4-OMe-Ph-$B(OH)_2$ (0.0343 g, 0.226 mmol, 2.5 equiv) and DMF (1.3 mL, 0.08 M) were added, and the vial was sealed with a pressure relief cap and removed from the glovebox. The vial was stirred at 80˚C in a pie reactor. After 1 hr, the reaction mixture was filtered through an aluminum oxide plug, diluted with EtOAc, and analyzed by TLC/GCMS. The major observed species was the Heck alkene product **2d-2** (55%)^{GC}.
GC (Method B) t_R = 2.313 min. EI-MS m/z (%): 255.1 (M$^+$, 5).

7.17.3 Oxidative boron Heck reaction general procedures and data

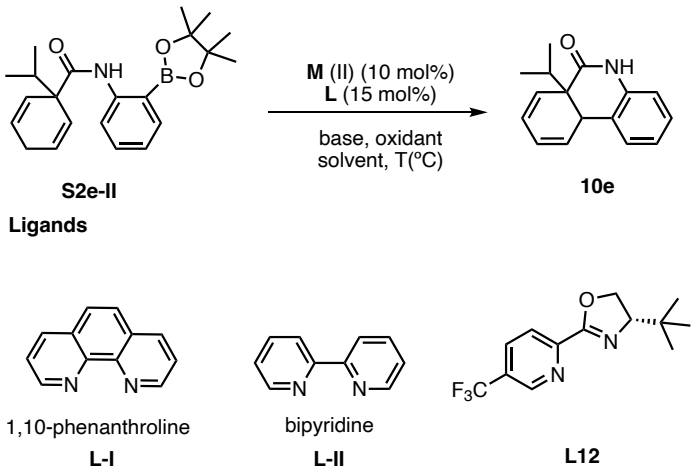

Scheme 7.30 Oxidative Boron Heck reactions.

General procedure A and data

An oven-dried screw-cap vial, equipped with a magnetic stir bar, was charged $Pd(OAc)_2$ (0.0031 g, 0.0136 mmol, 10 mol%) and 1,10-phenanthroline **L-I** (0.0037 g, 0.0204 mmol, 15 mol%) in DMF (1.7 mL, 0.08 M). The resulting mixture was stirred at r.t. for 30 minutes and then, aryl boronic ester **S2e-II** (0.0500 g, 0.136 mmol, 1.0 equiv) was added. The reaction mixture was stirred at 70˚C in a pie reactor with an O_2 balloon for 24 hrs., then filtered through a celite plug, diluted with EtOAc, and analyzed by TLC/GCMS. The reaction mixture contained only the starting material **S2e-II** (>99%)^{GC}.
GC (Method A) t_R = 18.38 min. EI-MS m/z (%): 367.3 (M$^+$, 6).

General procedure B[24] and data

An oven-dried screw-cap vial, equipped with a magnetic stir bar, was charged $Pd(TFA)_2$ (0.0045 g, 0.0136 mmol, 10 mol%) and **L12** (0.0055 g, 0.0201 mmol, 15 mol%) in DCE (2.7 mL, 0.05 M). The resulting mixture was stirred at r.t. for 30 minutes and then, aryl boronic ester **S2e-II** (0.0500 g, 0.136 mmol, 1.0 equiv) and Na_2CO_3 (0.0288, 0.272 mmol, 2.0 equiv) were added. The reaction mixture was stirred at 50˚C in a pie reactor with an O_2 balloon for 24 hrs., then filtered through a celite plug, diluted with EtOAc, and analyzed by TLC/GCMS. The reaction mixture contained mostly the starting material **S2e-II** (92%)^{GC}.

GC (Method A) t_R = 18.38 min. EI-MS m/z (%): 367.3 (M^+, 6).

General procedure C and data

An oven-dried screw-cap vial, equipped with a magnetic stir bar, was charged with aryl boronic ester **S2e-II** (0.0588 g, 0.160 mmol, 1.0 equiv) and then brought into a glovebox. An anhydrous NiI_2 (0.0051 g, 0.0016 mmol, 10 mol %), bipy **L-II** (0.0049 g, 0.032 mmol, 20 mol %), Cs_2CO_3 (0.0782 g, 0.24 mmol, 1.5 equiv), DDQ (0.0726 g, 0.32 mmol, 2.0 equiv), and DMF (0.8 mL, 0.2 M) were added. The vial was sealed with a pressure relief cap, removed from the glovebox, and stirred at 80˚C in a pie reactor for 24 hrs. The reaction mixture was filtered through a celite plug, diluted with EtOAc, and analyzed by TLC/GCMS. The reaction mixture contained mostly the starting material **S2e-II** (89%)^{GC}.

GC (Method A) t_R = 18.38 min. EI-MS m/z (%): 367.3 (M^+, 6).

7.18 Mechanistic studies general procedures and data

Control experiments of aryl halides with Mn and Zn

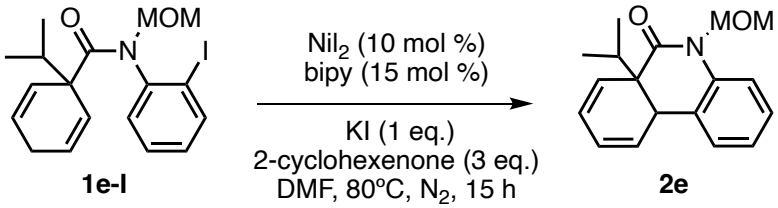

1e-I **2e**

Scheme 7.31 Control experiment in the absence of Mn.

An oven-dried screw-cap vial, equipped with a magnetic stir bar was charged with the aryl iodide diene **1e-I** (0.020 g, 0.049 mmol, 1.0 equiv) and then brought into a glovebox. An anhydrous NiI_2 (0.0015 g, 0.0049 mmol, 10 mol %), bipy (0.0011 g, 0.0074 mmol, 15 mol %), KI (0.0081 g, 0.049 mmol, 1.0 equiv), 2-cyclohexenone (14 µL, 0.0141 g, 0.147 mmol, 3.0 equiv), and DMF (0.6 mL, 0.08 M) were added, and the vial was sealed with a pressure relief cap and removed from the glovebox. The vial was stirred at 80˚C in a pie reactor for 15 h, then filtered through an aluminum oxide plug, diluted with EtOAc, and analyzed by TLC/GCMS. However, the formation of desired product **2e** was not observed and only the starting material **1e-I** (>99%)^{GC} was present in the reaction mixture.

GC (Method B) t_R = 3.438 min (**1e-I**). EI-MS m/z (%): 411.1 (M^+, 1), 379.1 (4), 292.0 (8), 260.1 (10), 252.1 (8), 230.9 (100), 202.9 (5), 164.0 (34), 121.1 (10), 105.0 (50), 90.0 (7), 79.0 (26), 51.0 (4).

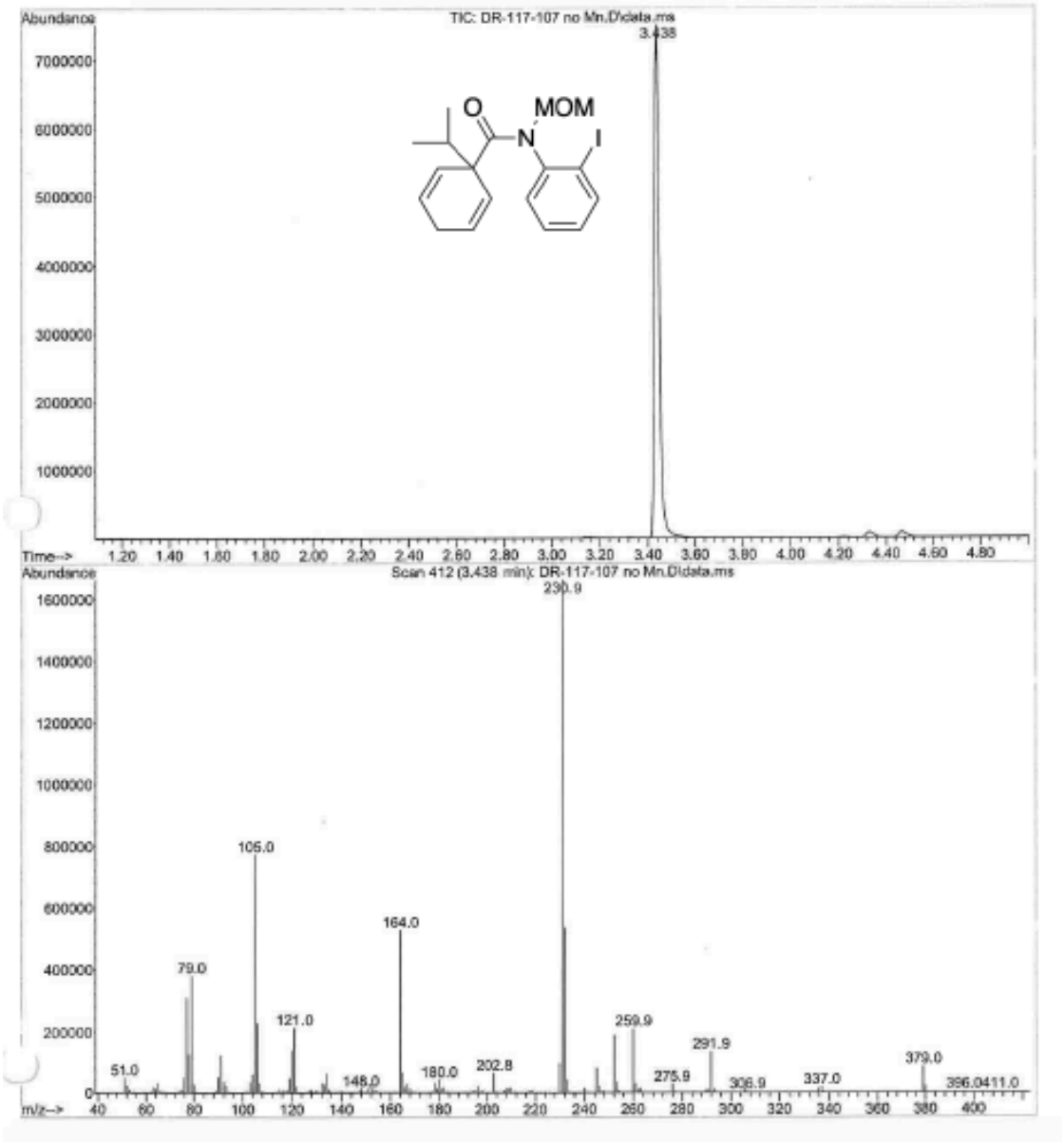

Figure 7.318 GCMS data for the control experiment in the absence of Mn.

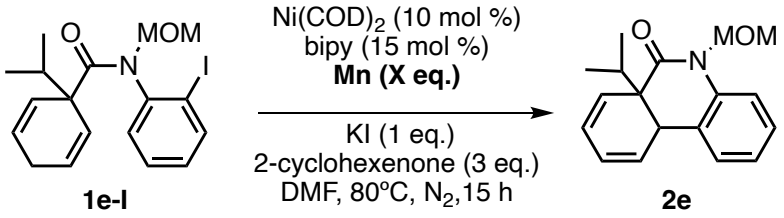

Scheme 7.32 Control experiments using $Ni(COD)_2$.

An oven-dried screw-cap vial, equipped with a magnetic stir bar was charged with the aryl iodide diene **1e-I** (0.020 g, 0.049 mmol, 1.0 equiv) and then brought into a glovebox. An anhydrous $Ni(COD)_2$ (0.0013 g, 0.0049 mmol, 10 mol %), bipy (0.0011 g, 0.0074 mmol, 15 mol %), **Mn** (reaction 1: **0 equiv**) or (reaction 2: 0.0080 g, 0.147 mmol, **3.0 equiv**), KI (0.0081 g, 0.049 mmol, 1.0 equiv), 2-cyclohexenone (14 µL, 0.0141 g, 0.147 mmol, 3.0 equiv), and DMF (0.6 mL, 0.08 M) were added, and the vial was sealed with a pressure relief cap and removed from the glovebox. The vial was stirred at 80˚C in a pie reactor for 15 h, then filtered through an aluminum oxide plug, diluted with EtOAc, and analyzed by TLC/GCMS.

Reaction 1 (no Mn): The reaction mixture contained the desired product **2e** (8%)^{GC} and the starting material **1e-I** (>90%)^{GC}.

GC (Method B) t_R = 2.546 min (**2e**). EI-MS m/z (%): 283.1 (M^+, 17), 251.0 (12), 240.0 (15), 224 (10), 208.0 (100), 196.0 (99), 178 (67), 167 (10), 152.0 (12), 139 (4), 115.0 (4), 105.0 (4), 77.0 (6).

GC (Method B) t_R = 3.439 min (**1e-I**). EI-MS m/z (%): 411.1 (M^+, 1), 379.1 (4), 292.0 (8), 260.1 (10), 252.1 (8), 230.9 (100), 202.9 (5), 164.0 (34), 121.1 (10), 105.0 (50), 90.0 (7), 79.0 (26), 51.0 (4).

Reaction 2 (with Mn): The reaction mixture contained the desired product **2e** (78%)^{GC}.

GC (Method B) t_R = 2.546 min (**2e**). EI-MS m/z (%): 283.1 (M^+, 17), 251.0 (12), 240.0 (15), 224 (10), 208.0 (100), 196.0 (99), 178 (67), 167 (10), 152.0 (12), 139 (4), 115.0 (4), 105.0 (4), 77.0 (6).

peak #	R.T. min	first scan	max scan	last scan	PK TY	peak height	corr. area	corr. % max.	% of total
1	2.546	251	256	271	rBV	648018	790696	9.02%	8.277%
2	3.439	406	412	443	rBV	6805478	8762312	100.00%	91.723%

Sum of corrected areas: 9553008

AK1.M Fri Mar 10 14:55:31 2023

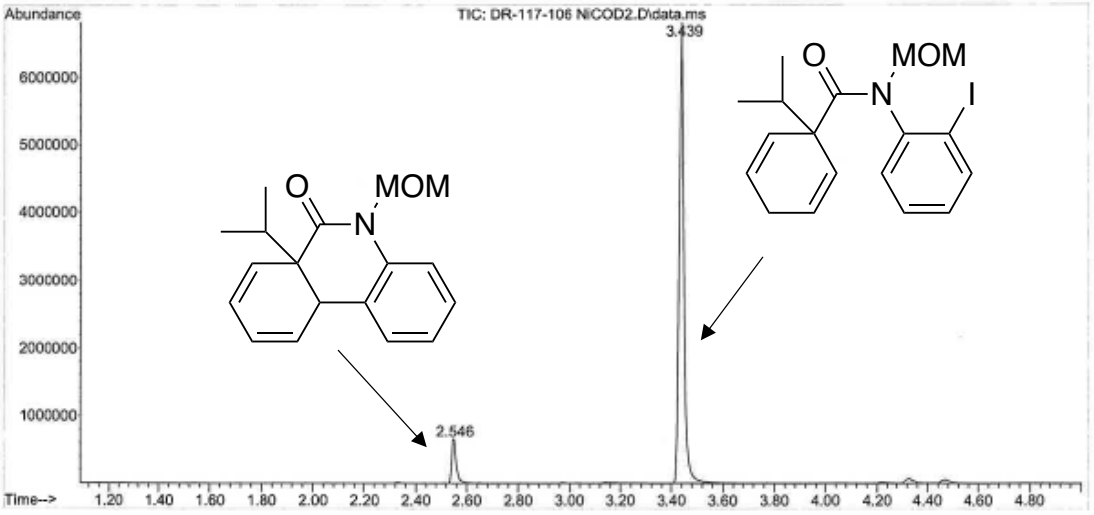

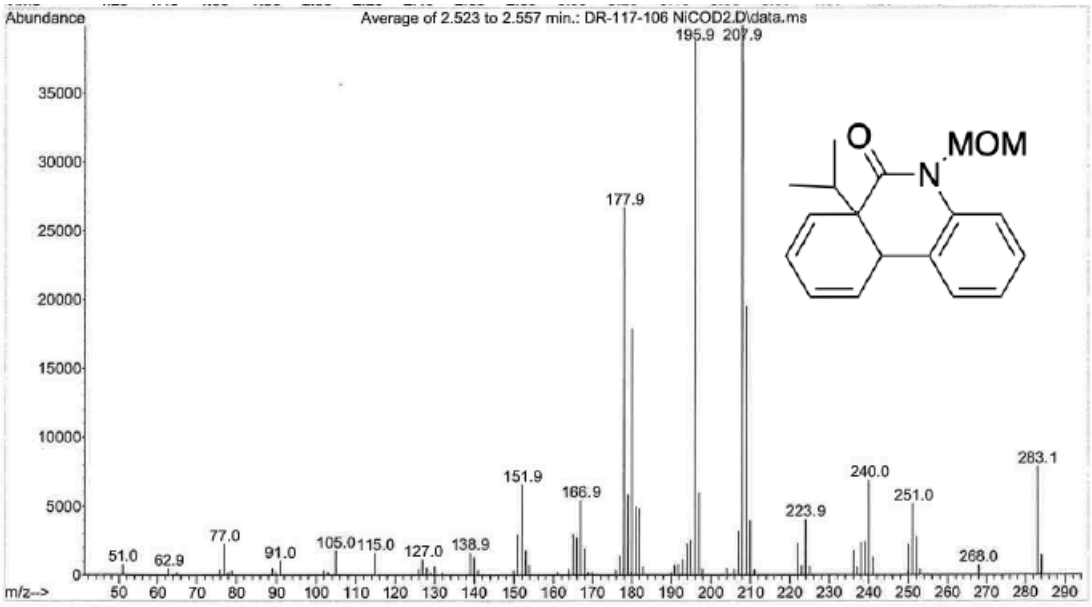

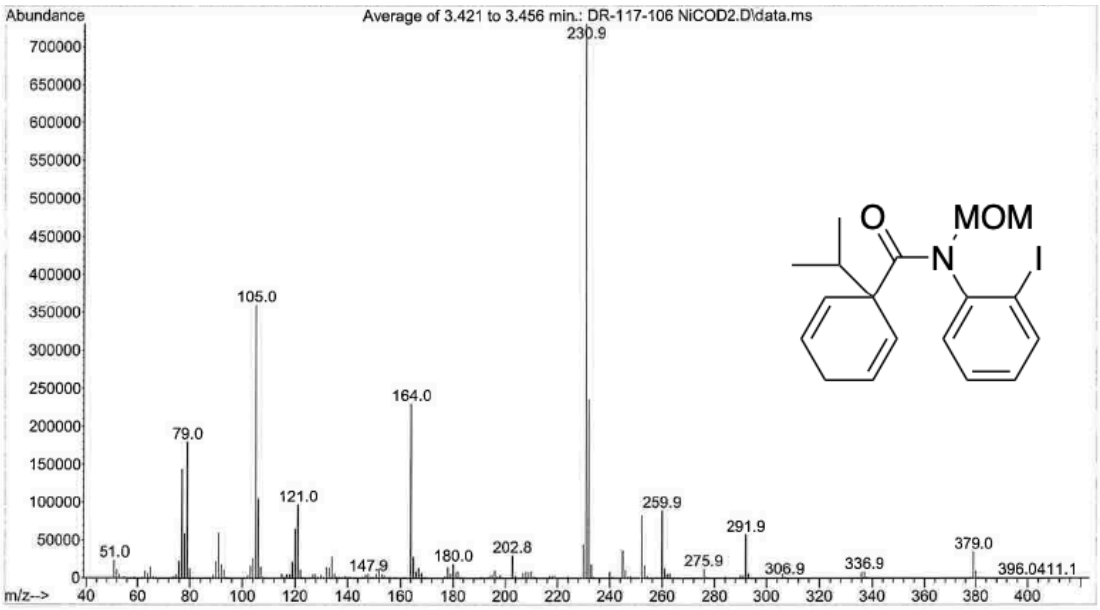

Figure 7.319 GCMS data for the control experiment using $Ni(COD)_2$ in the absence of Mn (reaction 1).

peak #	R.T. min	first scan	max scan	last scan	PK TY	peak height	corr. area	corr. % max.	% of total
1	1.653	97	100	114	rVB	286010	482657	7.87%	6.146%
2	1.825	127	130	158	rVB	664557	1235721	20.14%	15.735%
3	2.546	250	256	270	rBV	5636612	6135189	100.00%	78.120%

Sum of corrected areas: 7853567

AK1.M Fri Mar 10 14:57:49 2023

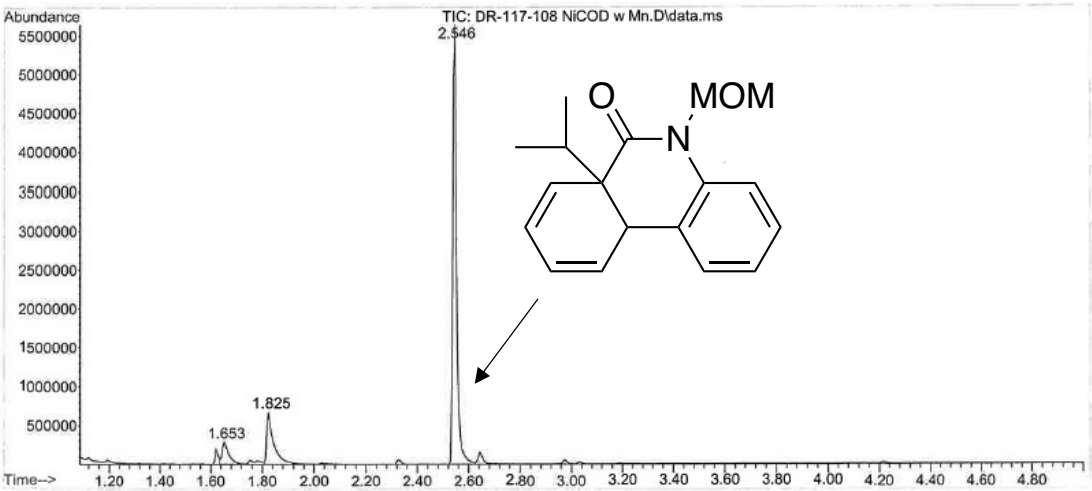

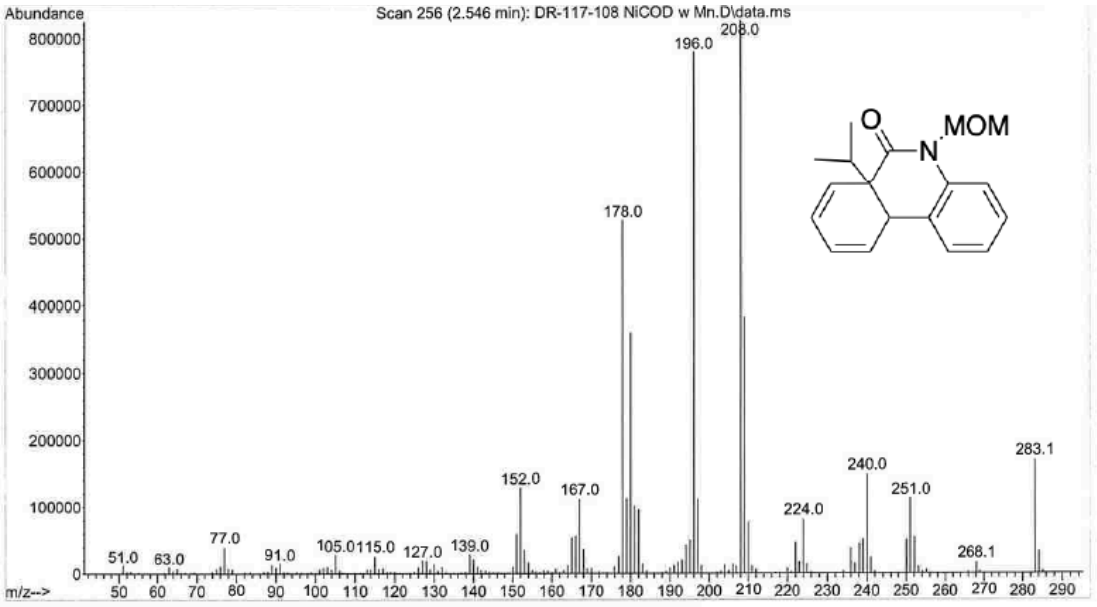

Figure 7.320 GCMS data for the control experiment using $Ni(COD)_2$ in the presence of Mn (reaction 2)

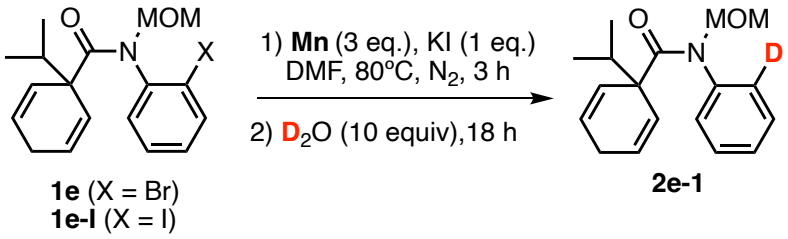

Scheme 7.33 Control experiments using D_2O and Mn.

Reaction 1: with aryl bromide **1e**

An oven-dried screw-cap vial, equipped with a magnetic stir bar was charged with the aryl bromide diene **1e** (0.020 g, 0.055 mmol, 1.0 equiv) and then brought into a glovebox. Mn (0.0091 g, 0.165 mmol, 3.0 equiv), KI (0.0091 g, 0.055 mmol, 1.0 equiv), and DMF (0.66 mL, 0.08 M) were added, and the vial was sealed with a pressure relief cap and removed from the glovebox. The vial was stirred at 80˚C. After 3 h, D_2O (0.01 mL, 0.55 mmol, 10.0 equiv) was added and the mixture was heated at 80˚C for additional 18 h. The reaction mixture was filtered through an aluminum oxide plug, diluted with EtOAc, and analyzed by TLC/GCMS. The reaction mixture contained only the starting material **1e** (>99%)^{GC}.

GC (Method B) t_R = 3.032 min (**1e**). EI-MS m/z (%): 363.1 ($M\text{-}1^+$, 1), 331.1 (7), 243.9 (10), 227.9 (4), 213.9 (15), 183.0 (68), 164.1 (64), 121.1 (21), 105.1 (100), 91.0 (12), 79.1 (47), 51.1 (5).

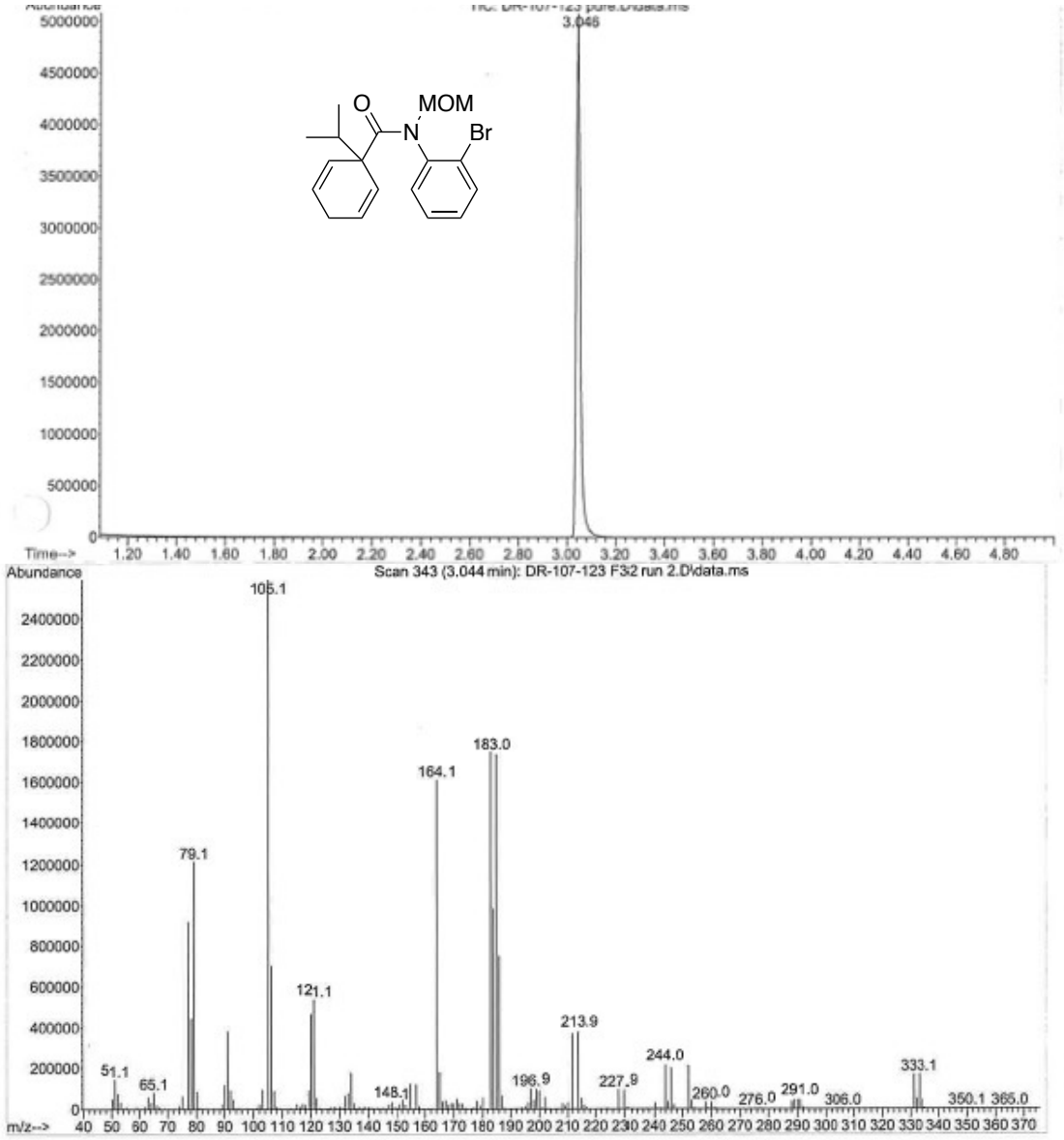

Figure 7.321 GCMS of the starting material **1e.**

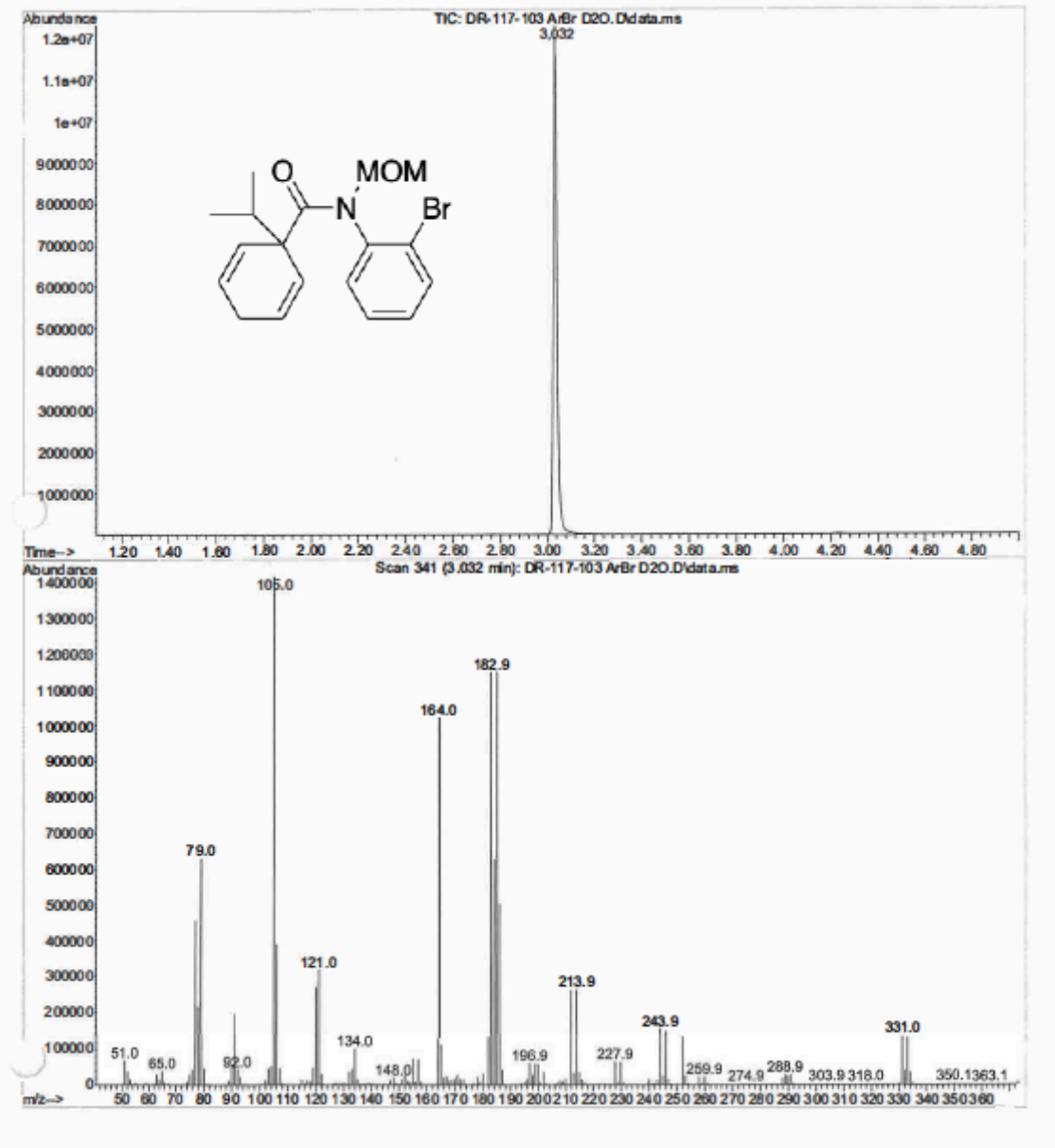

Figure 7.122 GCMS data of the control experiment with **1e** (reaction 1).

Reaction 2: with aryl iodide **1e-I**

An oven-dried screw-cap vial, equipped with a magnetic stir bar was charged with the aryl bromide diene **1e-I** (0.020 g, 0.049 mmol, 1.0 equiv) and then brought into a glovebox. Mn (0.0080 g, 0.147 mmol, 3.0 equiv), KI (0.0081 g, 0.049 mmol, 1.0 equiv), and DMF (0.6 mL, 0.08 M) were added, and the vial was sealed with a pressure relief cap and removed from the glovebox. The vial was stirred at 80˚C. After 3 h, D_2O (0.01 mL, 0.49 mmol, 10.0 equiv) was added and the mixture was heated at 80˚C for additional 18 h. The reaction mixture was filtered through an aluminum oxide plug, diluted with EtOAc, and analyzed by TLC/GCMS. The reaction mixture contained the deuterated dehalogenated side product-D_1 **2e-1** (13%)^{GC} and the starting material **1e-I** (87%)^{GC}.

GC (Method B) t_R = 2.323 min (**2e-1**). EI-MS m/z (%): 254.0 (M-32$^+$, 21), 211.0 (5), 166.0 (30), 150.9 (23), 135.0 (5), 121.0 (20), 106.0 (100), 91.0 (6), 79.0 (36). 51.0 (5).
GC (Method B) t_R = 3.439 min (**1e-I**). EI-MS m/z (%): 379.1 (M-32$^+$, 4), 291.9 (7), 259.9 (12) 252.1 (0), 244.8 (4), 230.9 (100), 202.9 (4), 164.0 (33), 121.1 (12), 105.0 (50), 79.0 (26), 51.0 (4).

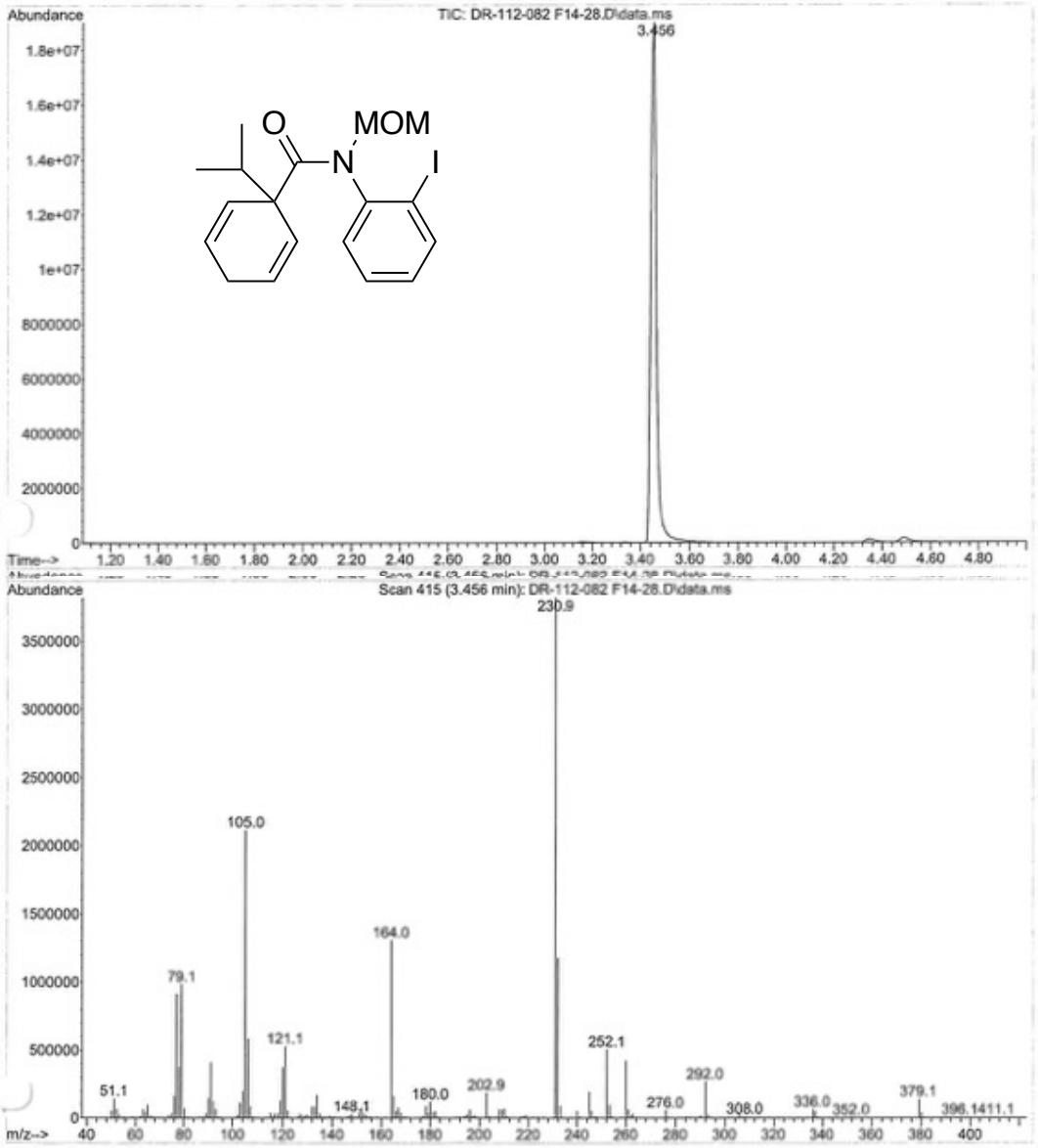

Figure 7.323 GCMS of the starting material **1e-I**.

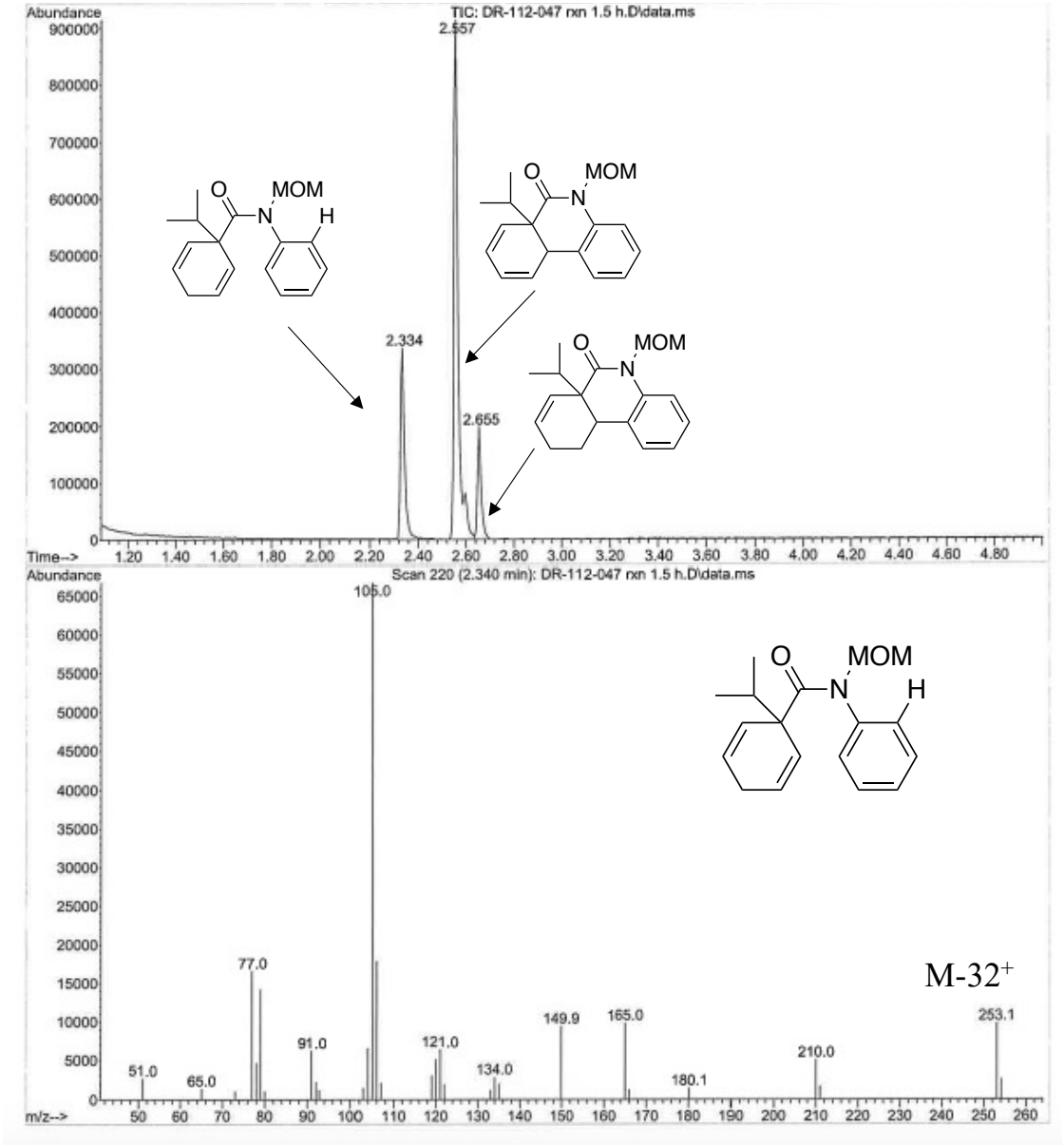

Figure 7.324 GCMS data for the crude Heck reaction with **1e-I** (non-deuterated reference).

peak #	R.T. min	first scan	max scan	last scan	PK TY	peak height	corr. area	corr. % max.	% of total
1	2.323	211	217	232	rBV	770405	891210	15.37%	13.322%
2	3.439	406	412	441	rBV	4039574	5798656	100.00%	86.678%

Sum of corrected areas: 6689866

AK1.M Fri Mar 10 15:05:49 2023

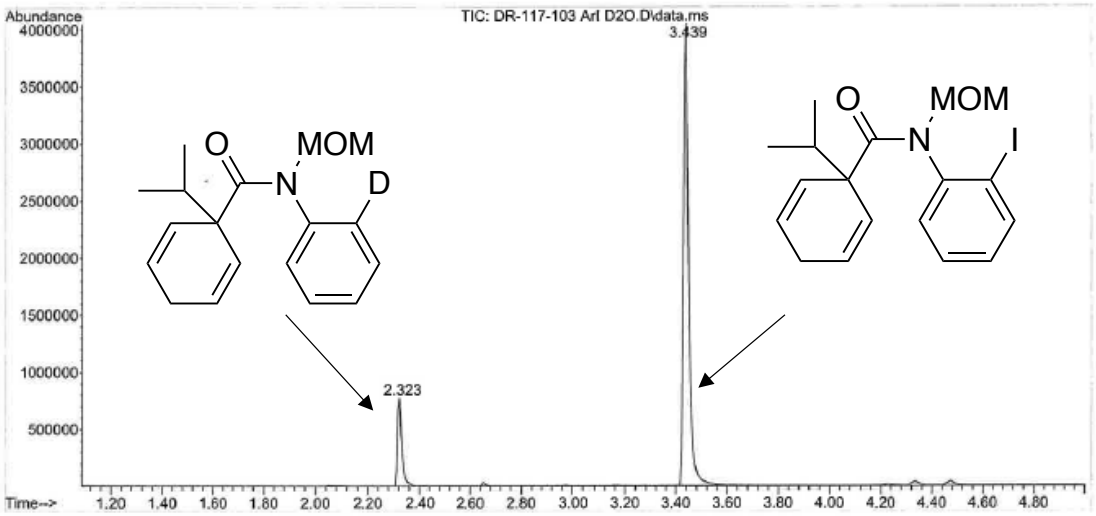

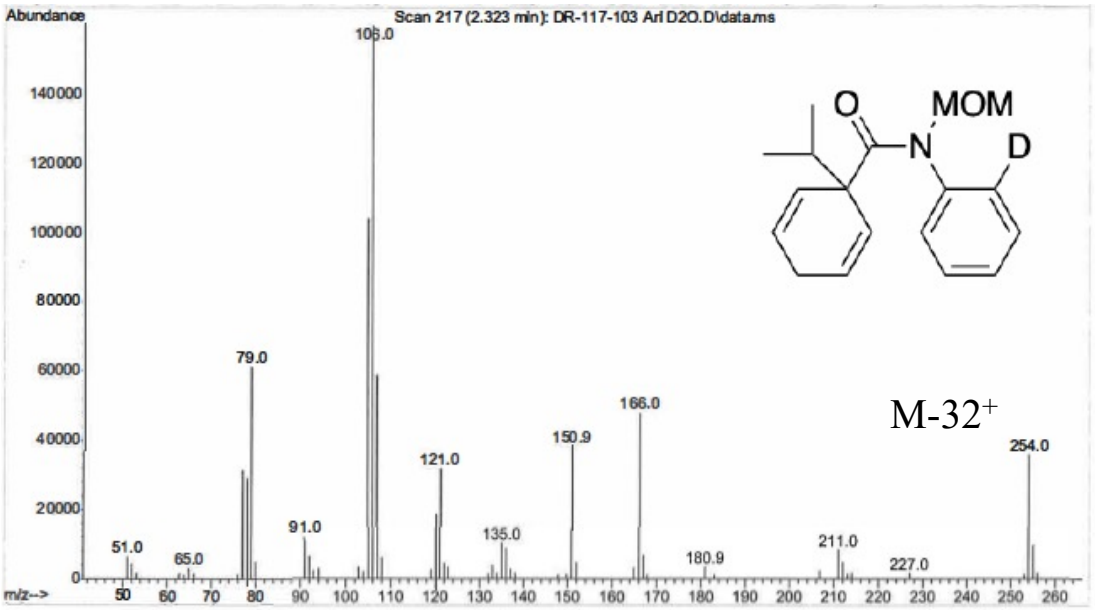

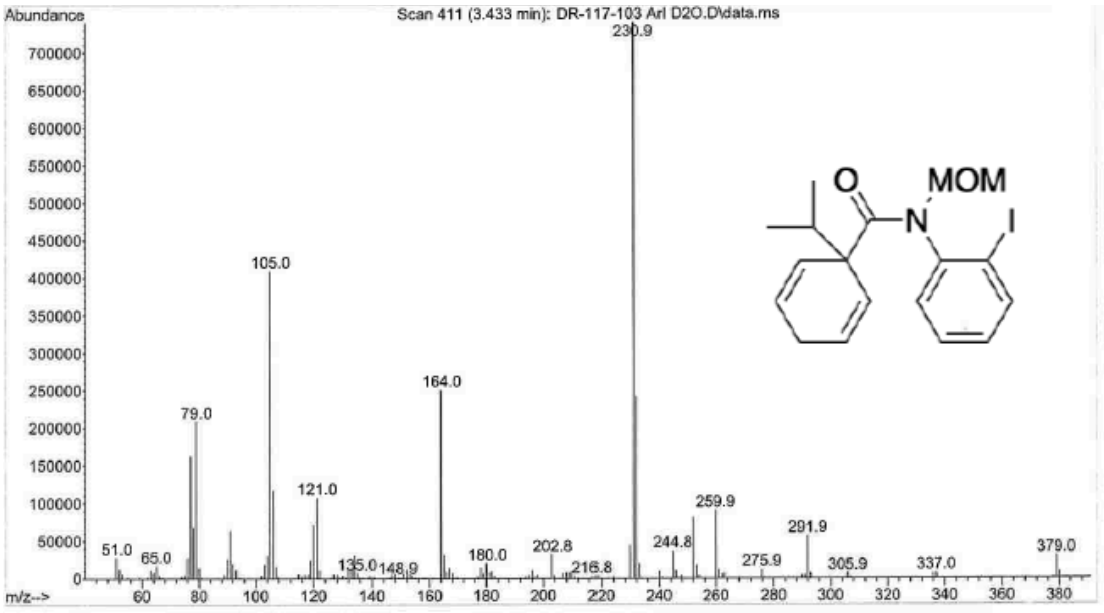

Figure 7.325 GCMS data of the control experiment with **1e-I** (reaction 2).

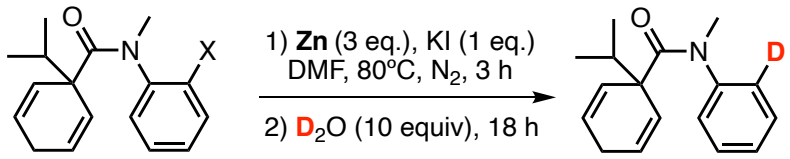

1d (X = Br)
1d-I (X = I)

2d-1

Scheme 7.34 Control experiments using D_2O and Zn

Reaction 1: with aryl bromide **1d**

An oven-dried screw-cap vial, equipped with a magnetic stir bar was charged with the aryl bromide diene **1d** (0.025 g, 0.075 mmol, 1.0 equiv) and then brought into a glovebox. Zn (0.0146 g, 0.224 mmol, 3.0 equiv), KI (0.0124 g, 0.075 mmol, 1.0 equiv), and DMF (0.9 mL, 0.08 M) were added, and the vial was sealed with a pressure relief cap and removed from the glovebox. The vial was stirred at 80˚C. After 3 h, D_2O (0.014 mL, 0.75 mmol, 10 equiv) was added and the mixture was heated at 80˚C for additional 18 h. The reaction mixture was filtered through an aluminum oxide plug, diluted with EtOAc, and analyzed by TLC/GCMS. The reaction mixture contained only the starting material **1d** (>99%)^{GC}.

GC (Method B) t_R = 2.677 min (**1d**). EI-MS m/z (%): 333.1 (M-1$^+$, 3), 290.0 (23), 214.0 (63), 197 (5), 185.0 (17), 134.0 (100), 121.1 (10), 105.0 (74), 91.0 (9), 77.1 (39), 51.0 (6).

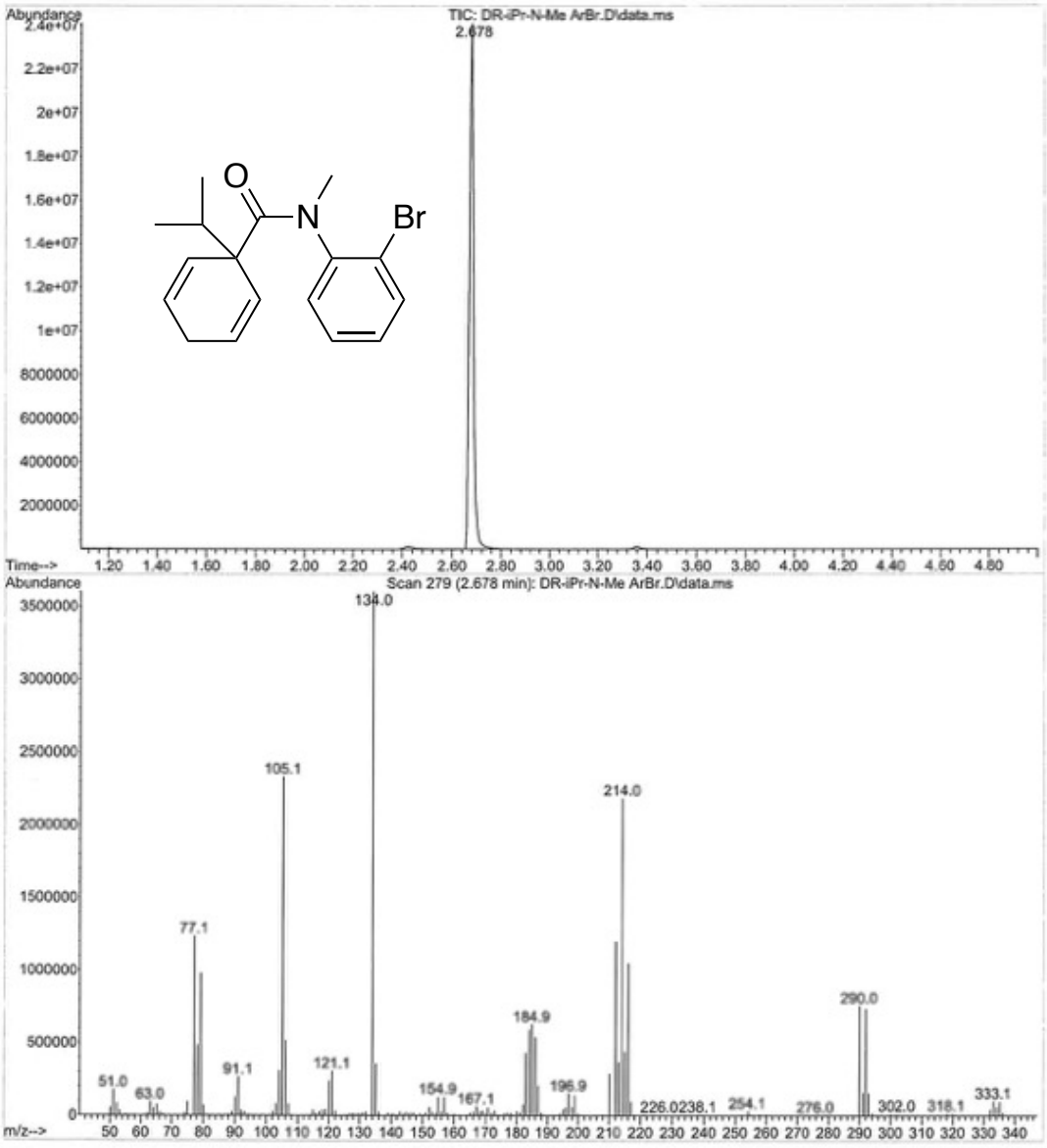

Figure 7.326 GCMS of the starting material **1d**.

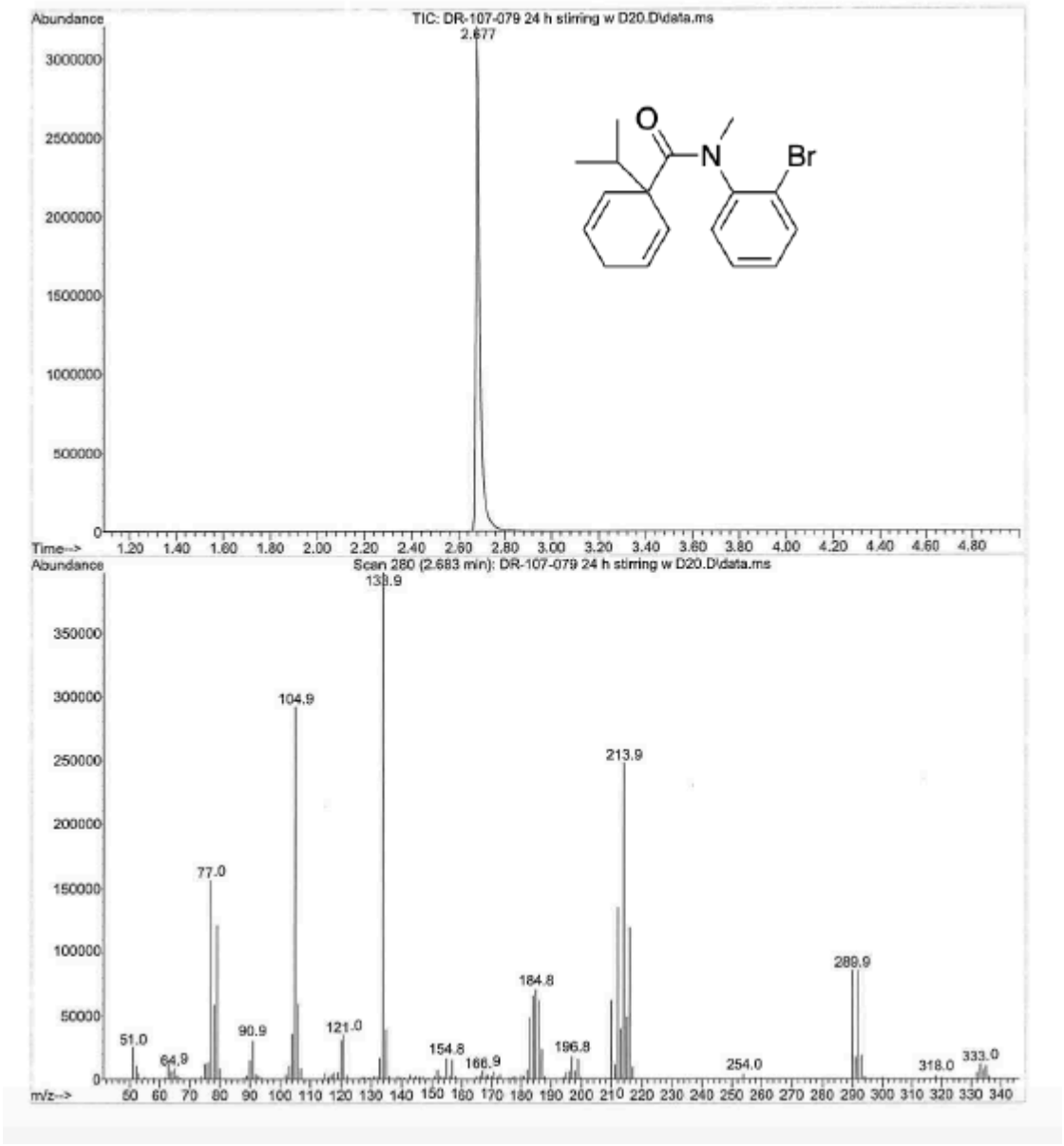

Figure 7.327 GCMS data of the control experiment with **1d** (reaction 1).

Reaction 2: with aryl iodide **1d-I**

An oven-dried screw-cap vial, equipped with a magnetic stir bar was charged with the aryl iodide diene **1d-I** (0.025 g, 0.066 mmol, 1.0 equiv) and then brought into a glovebox. Zn (0.0129 g, 0.197 mmol, 3.0 equiv), KI (0.0111 g, 0.066 mmol, 1.0 equiv), and DMF (0.8 mL, 0.08 M) were added, and the vial was sealed with a pressure relief cap and removed from the glovebox. The vial was stirred at 80˚C. After 3 h, D_2O (0.012 mL, 0.66 mmol, 10 equiv) was added and the mixture was heated at 80˚C for additional 18 h. The reaction mixture was filtered through an aluminum oxide plug, diluted with EtOAc, and analyzed by TLC/GCMS. The reaction mixture contained the deuterated dehalogenated side product-D_1 **2d-1** (82%)^{GC}. The organic layer was washed with 1 N HCl (twice) and

brine, dried with $MgSO_4$, and filtered and concentrated *in vacuo.* The crude residue was purified by column chromatography (silica, 4:1 hexanes: EtOAc) to afford **2d-1** in 65% yield (0.011 g, 0.043 mmol) as a yellow oil.
^{1}H NMR (400 MHz, $CDCl_3$) δ 7.28 – 7.20 (m, 3H), 7.15 – 7.09 (m, 1H), 5.35 (s, 4H), 3.23 (s, 3H), 2.49 (hept, J = 6.9 Hz, 1H), 2.37 – 2.07 (m, 2H), 0.76 (d, J = 6.9 Hz, 6H).
^{13}C NMR (101 MHz, $CDCl_3$) δ_u 128.8, 128.7, 128.4, 127.9, 127.0, 124.1, 40.9, 35.9, 17.5; δ_d 174.9, 145.0, 128.1, 53.9, 26.3.
GC (Method B) t_R = 1.951 min (**2d-1**). EI-MS m/z (%): 256.0 (M^+, 6), 213.0 (28), 136.0 (100), 121.0 (14), 105.0 (54), 95.0 (10), 79.0 (45), 51.0 (6).

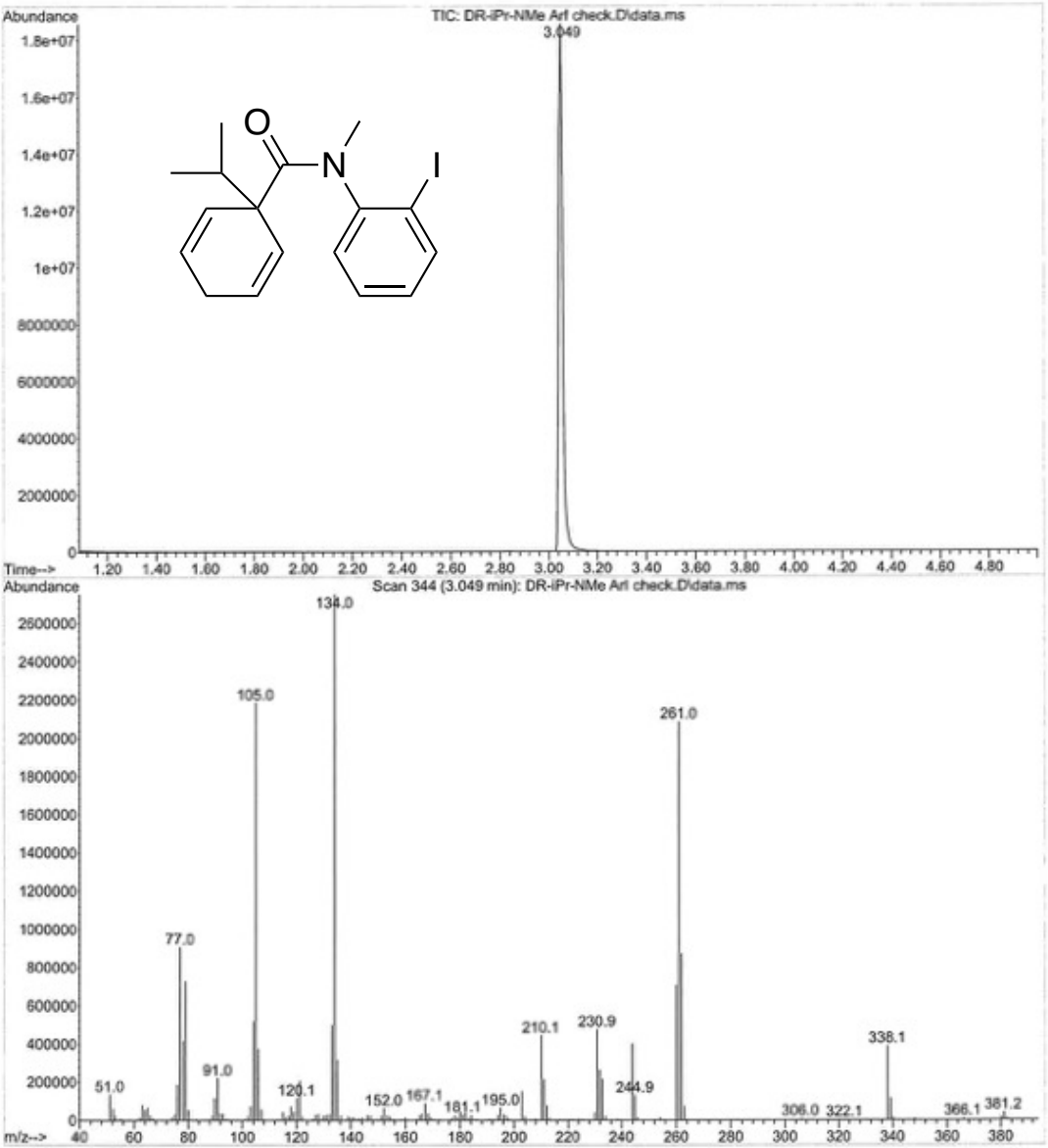

Figure 7.328 GCMS of the starting material **1d-I**.

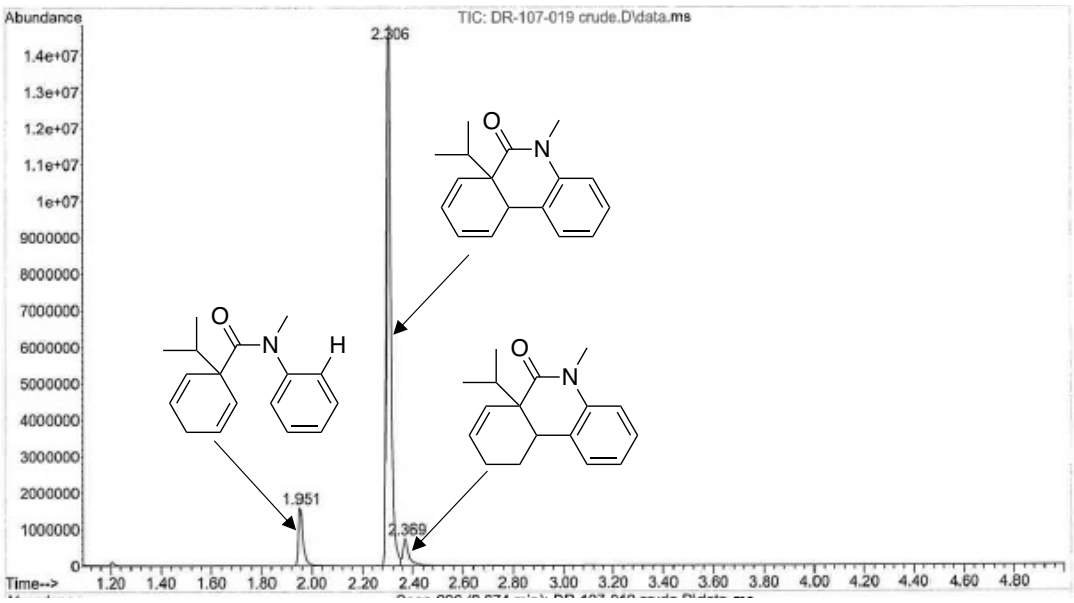
Abundance
TIC: DR-107-019 crude.D\data.ms
2.306
1.951
2.369
Time-->

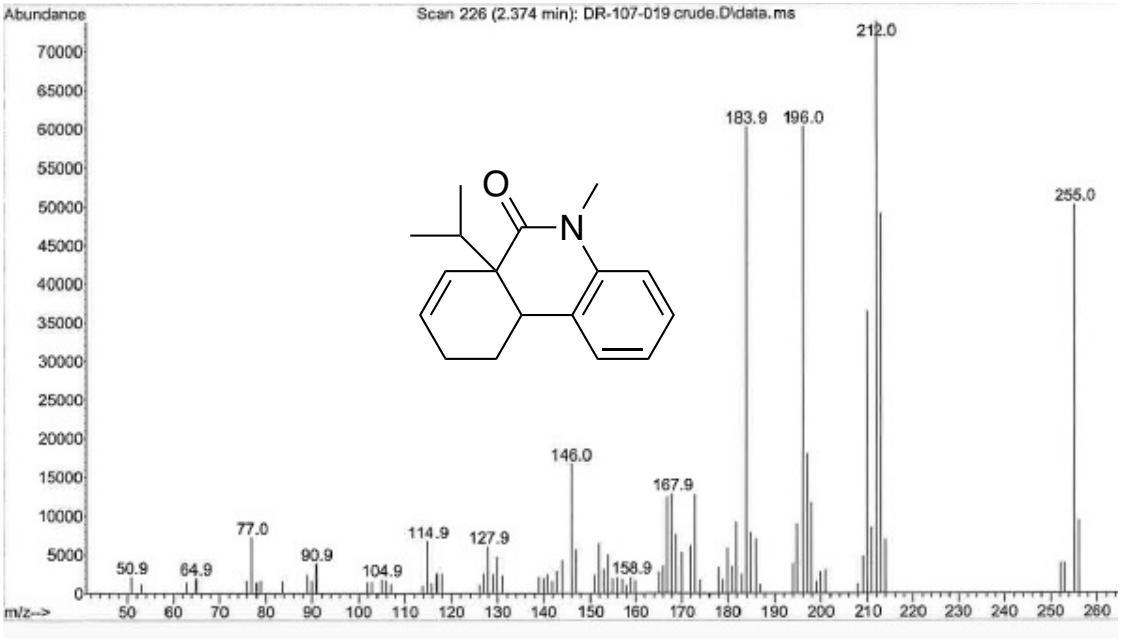
Abundance
Scan 226 (2.374 min): DR-107-019 crude.D\data.ms
212.0
183.9
196.0
255.0
146.0
167.9
77.0
114.9
127.9
90.9
50.9
64.9
104.9
158.9
m/z-->

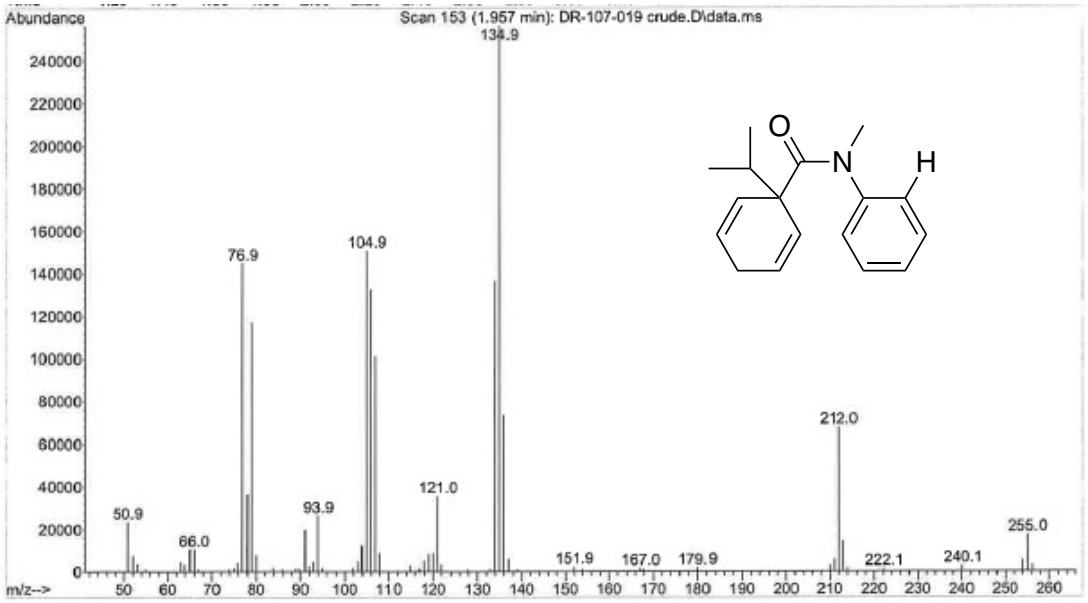

Figure 7.329 GCMS data of the crude Heck reaction with **1d-I** (non-deuterated reference).

peak #	R.T. min	first scan	max scan	last scan	PK TY	peak height	corr. area	corr. % max.	% of total
1	1.951	147	152	183	rBV	7055466	6868842	100.00%	81.943%
2	2.368	221	225	245	rBB	1454169	1513635	22.04%	18.057%

Sum of corrected areas: 8382477

AK1.M Wed Mar 15 10:01:10 2023

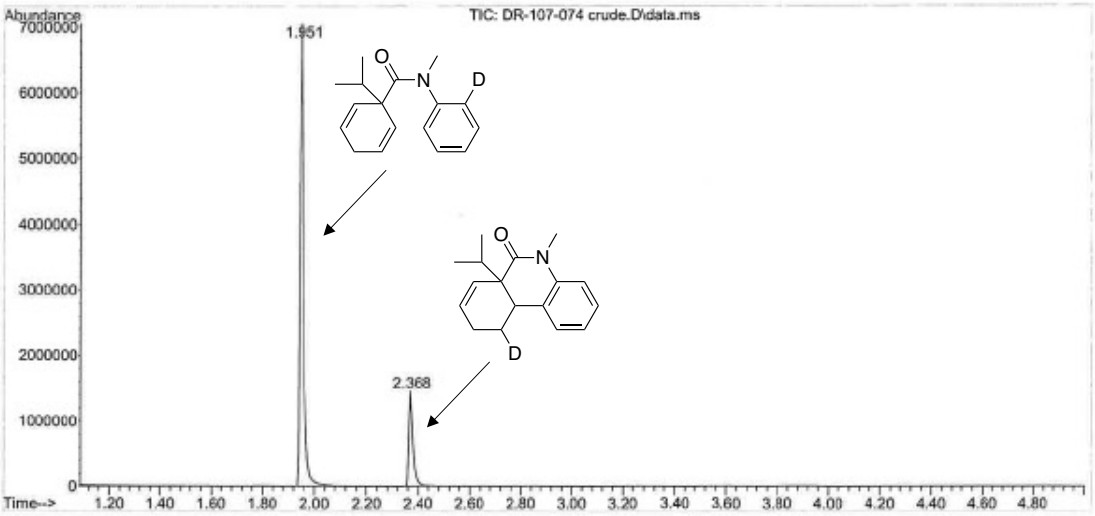

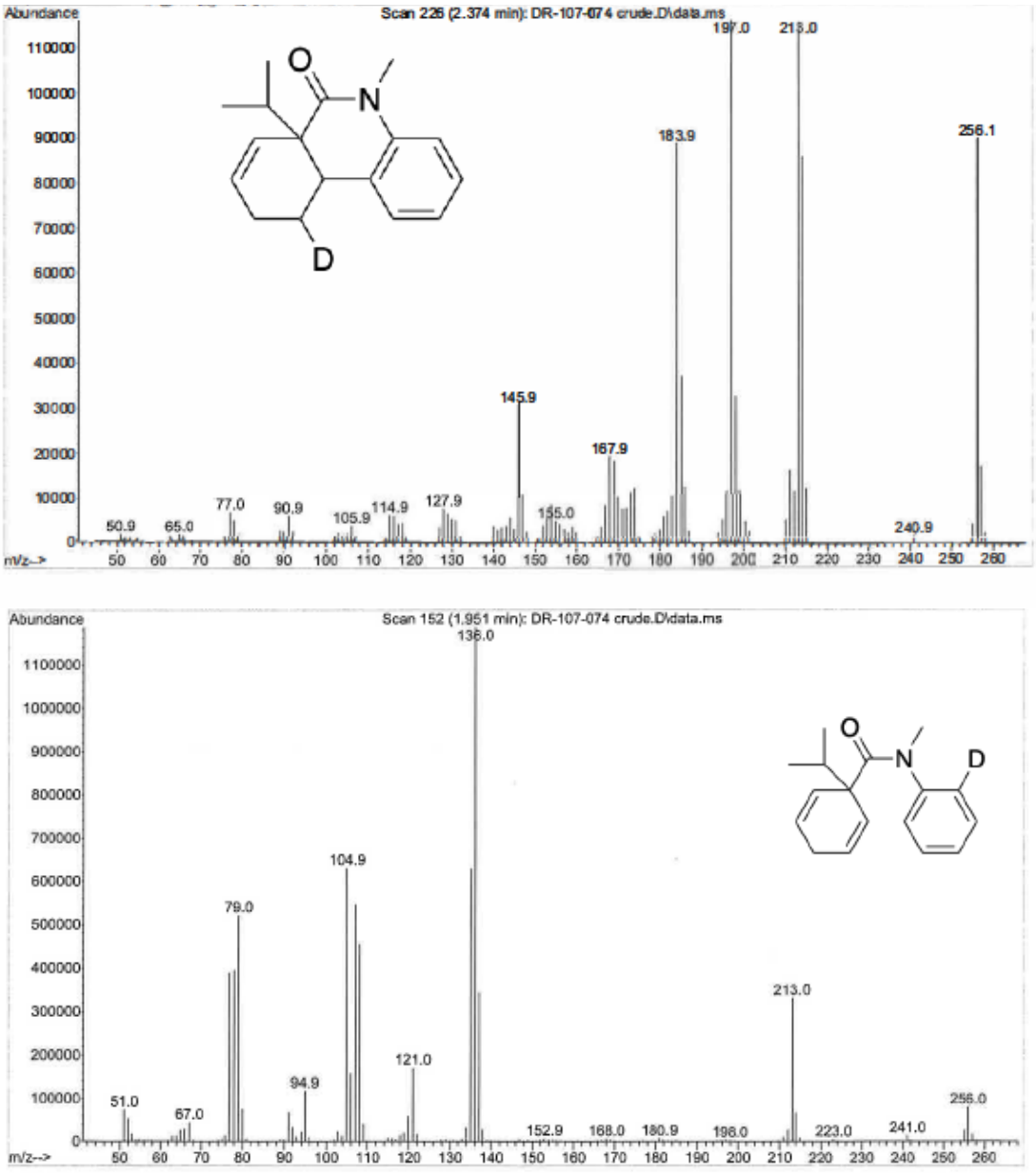

Figure 7.330 GCMS data of the control experiment with **1d-I** (reaction 2).

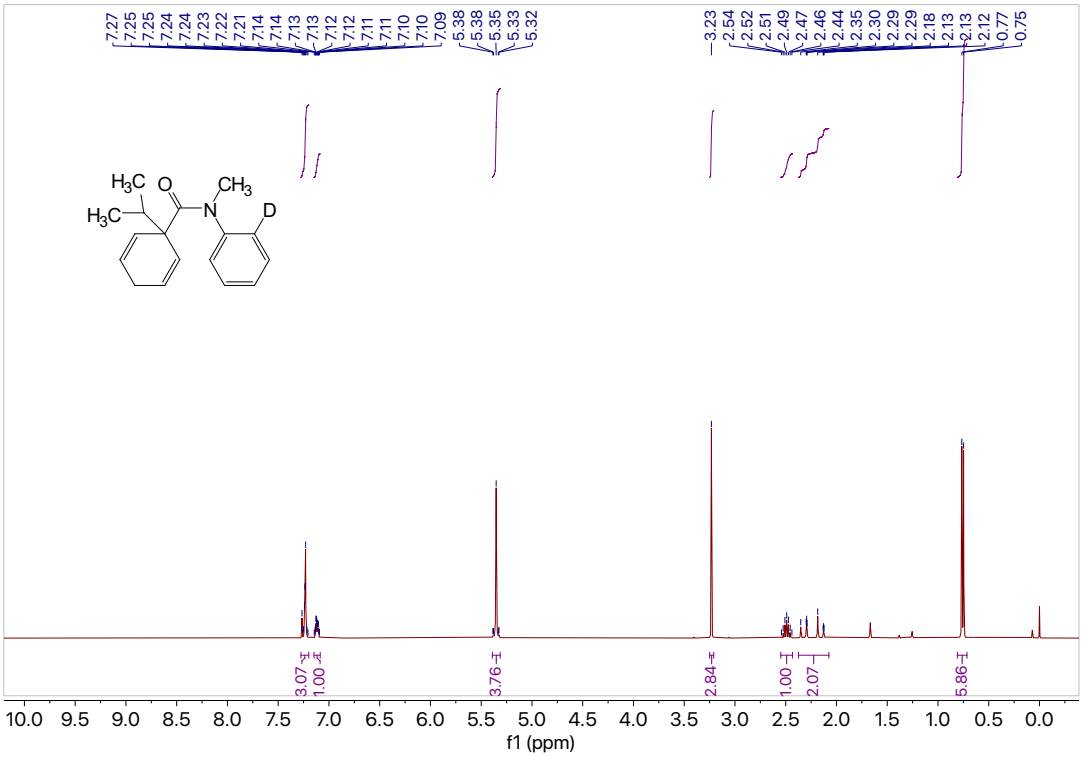

Figure 7.331 ^{1}H NMR (400 MHz, $CDCl_3$) of compound **2d-1**.

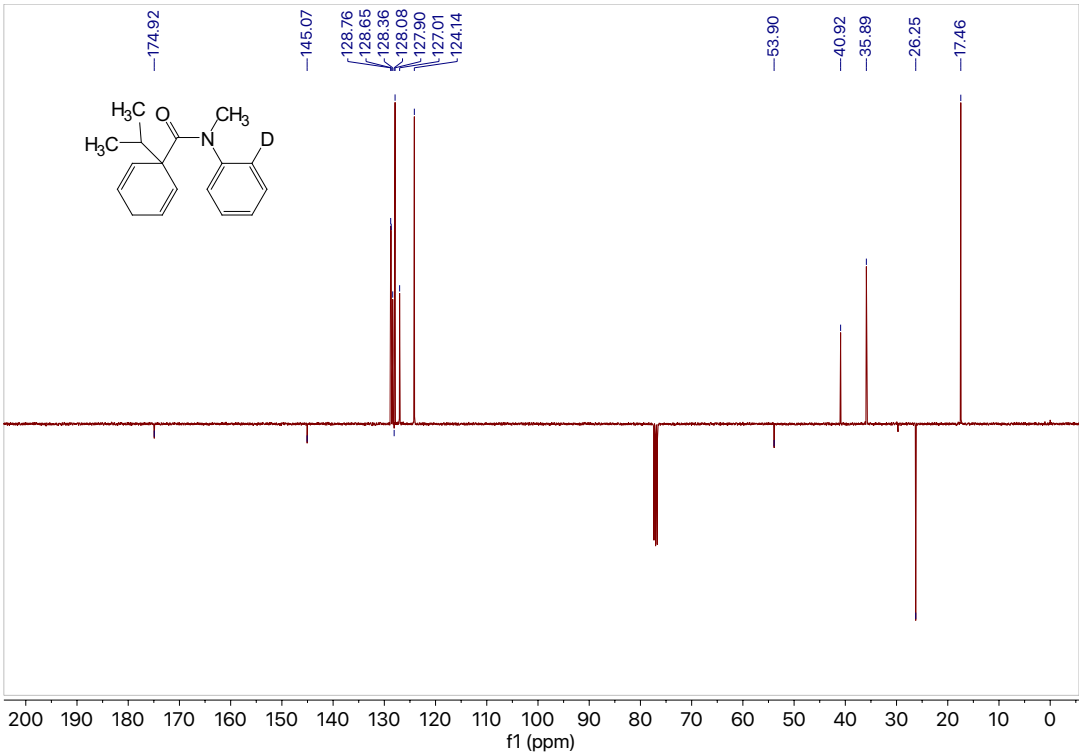

Figure 7.332 ^{13}C NMR (101 MHz, $CDCl_3$) of compound **2d-1**.

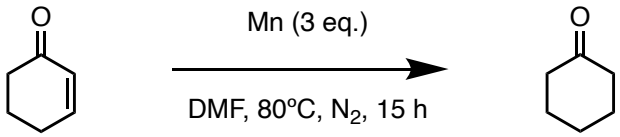

Scheme 7.35 Control experiment using 2-cyclohexenone and Mn.

An oven-dried screw-cap vial, equipped with a magnetic stir bar was charged with 2-cyclohexenone (50 µL, 0.05 g, 0.52 mmol, 1.0 equiv), Mn (0.057 g, 1.04 mmol, 2.0 equiv) and DMF (2 mL, 0.26 M) in a glovebox. The vial was sealed with a pressure relief cap, removed from the glovebox and stirred at 80˚C for 15 h. The reaction mixture was filtered through an aluminum oxide plug, diluted with EtOAc, and analyzed by TLC/GCMS. The reaction mixture contained only the starting material, **2-cyclohexenone** (>99%)[GC].

GC (Method B) t_R = 1.970 min (**2-cyclohexenone)**. EI-MS m/z (%): 96.0 (M^+, 41), 73.0 (4), 68.0 (100), 55.0 (5).

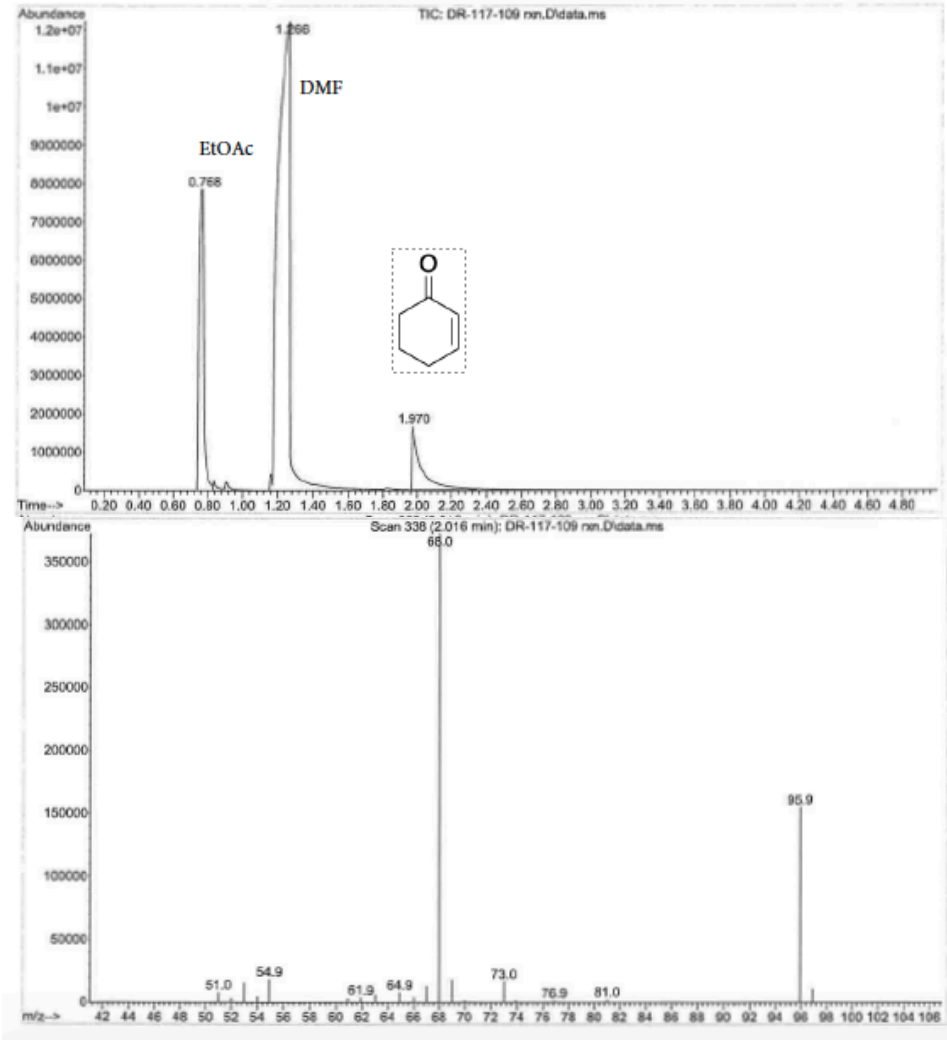

Sample Name: DR-2-cyclohexenone control
Misc Info :

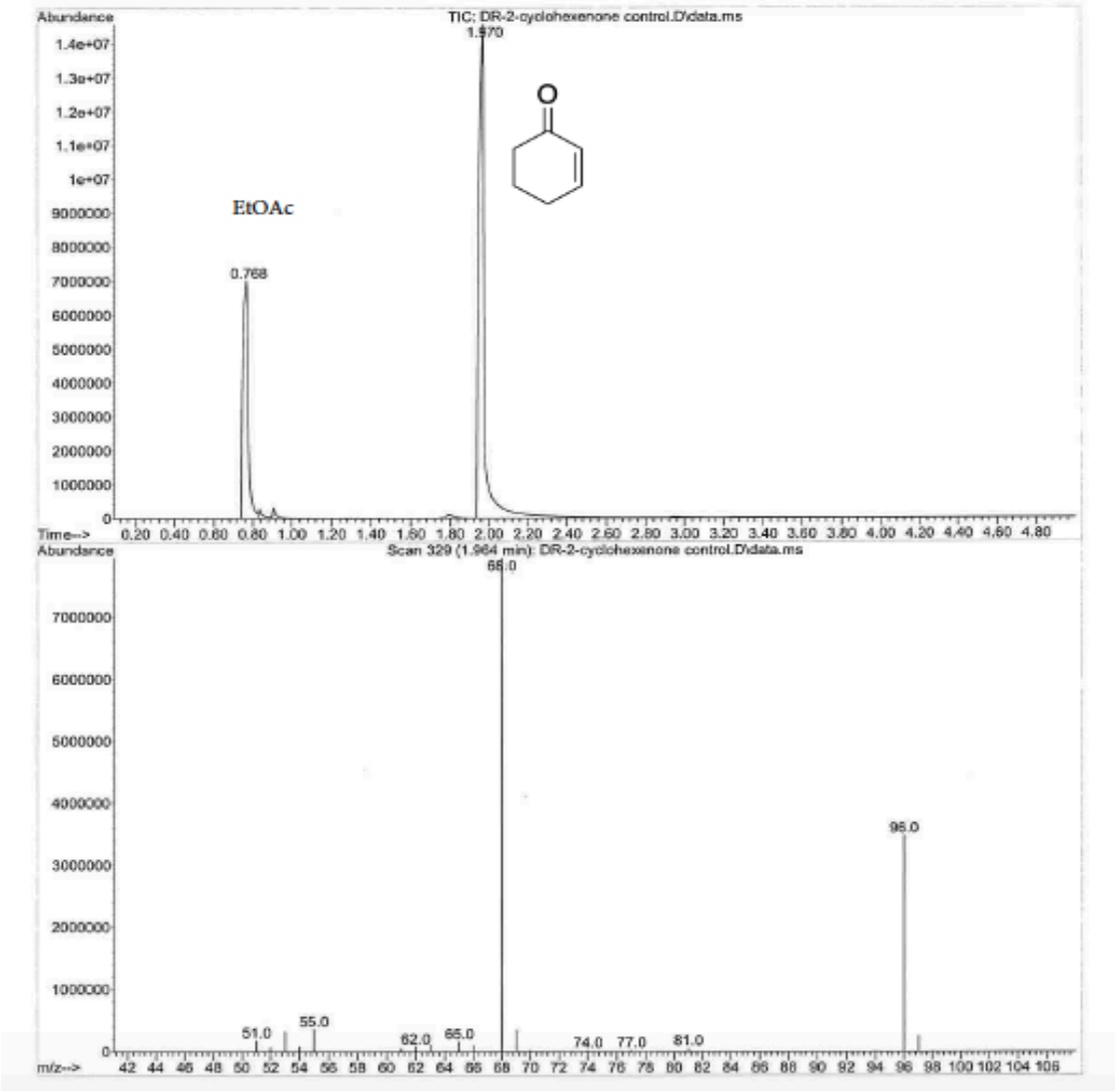

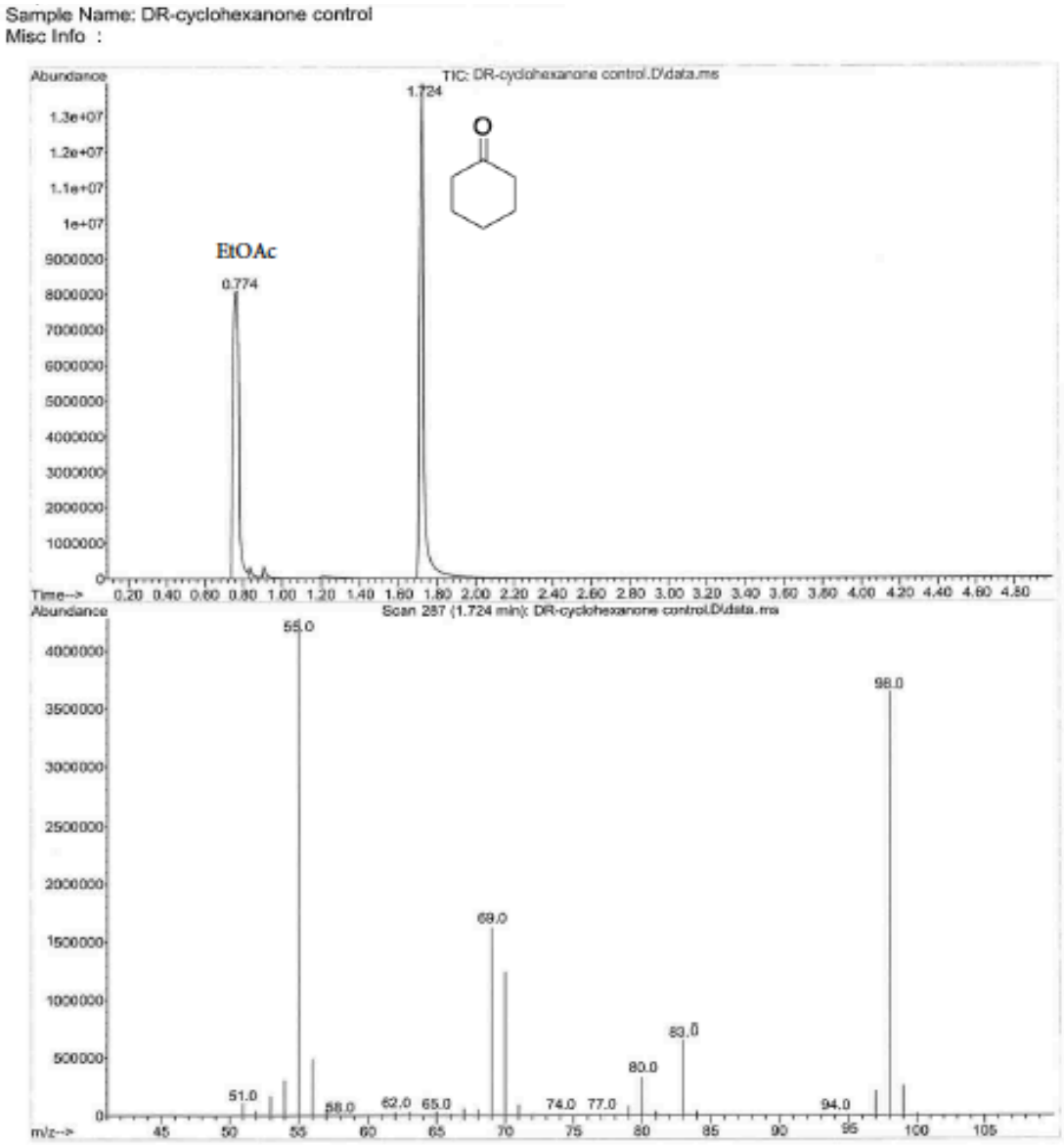

Figure 7.333 GCMS data for the control experiment using 2-cyclohexenone and Mn.

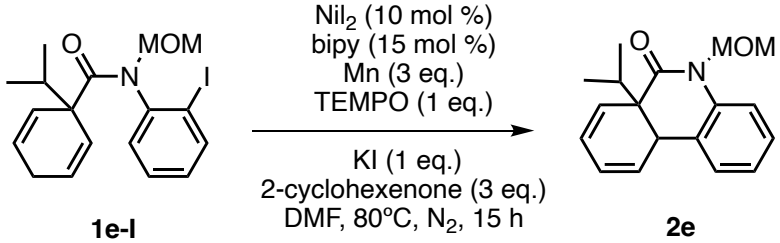

1e-I **2e**

Scheme 7.36 Control experiment using TEMPO.

An oven-dried screw-cap vial, equipped with a magnetic stir bar was charged with the aryl iodide diene **1e-I** (0.020 g, 0.049 mmol, 1.0 equiv) and then brought into a glovebox. An anhydrous NiI_2 (0.0015 g, 0.0049 mmol, 10 mol %), bipy (0.0011 g, 0.0074 mmol, 15 mol %), Mn (0.0080 g, 0.147 mmol, 3.0 equiv), KI (0.0081 g, 0.049 mmol, 1.0 equiv), 2-cyclohexenone (14 µL, 0.0141 g, 0.147 mmol, 3.0 equiv), TEMPO (0.0077 g, 0.049 mmol, 1.0 equiv), and DMF (0.6 mL, 0.08 M) were added. The vial was sealed with a pressure relief cap and removed from the glovebox. The vial was stirred at 80˚C in a pie reactor for 15 h. After completion, the reaction mixture was filtered through an aluminum oxide plug, diluted with EtOAc, and analyzed by TLC/GCMS. The reaction mixture contained the desired product **2e** (94%)[GC].

GC (Method B) t_R = 2.546 min (**2e**). EI-MS m/z (%): 283.1 (M^+, 17), 251.0 (12), 240.0 (15), 224 (10), 208.0 (100), 196.0 (99), 178 (67), 167 (10), 152.0 (12), 139 (4), 115.0 (4), 105.0 (4), 77.0 (6).

peak #	R.T. min	first scan	max scan	last scan	PK TY	peak height	corr. area	corr. % max.	% of total
1	2.020	159	164	182	rBV	149144	299156	6.93%	6.477%
2	2.546	250	256	271	rBV	3940128	4319310	100.00%	93.523%

Sum of corrected areas: 4618466

AK1.M Fri Mar 10 15:09:24 2023

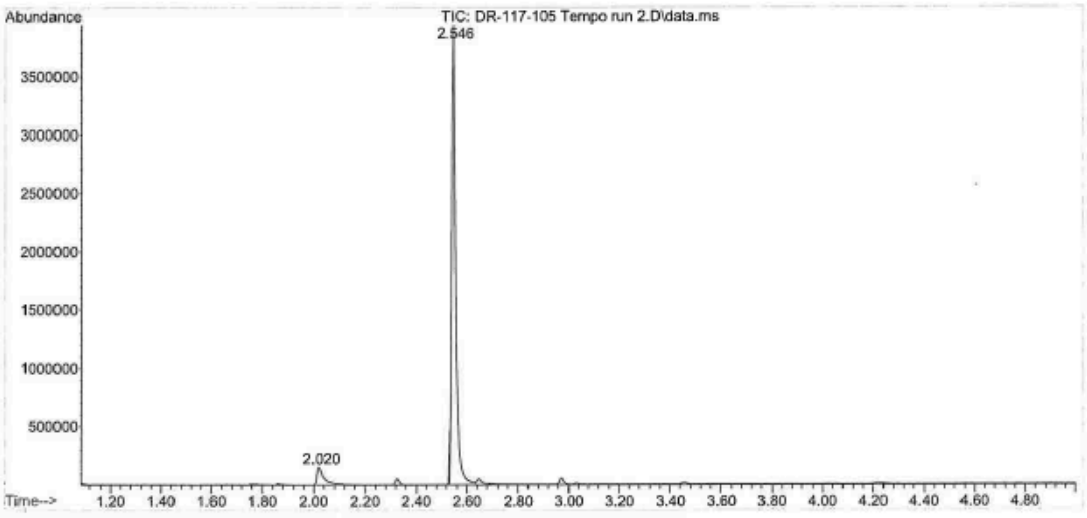

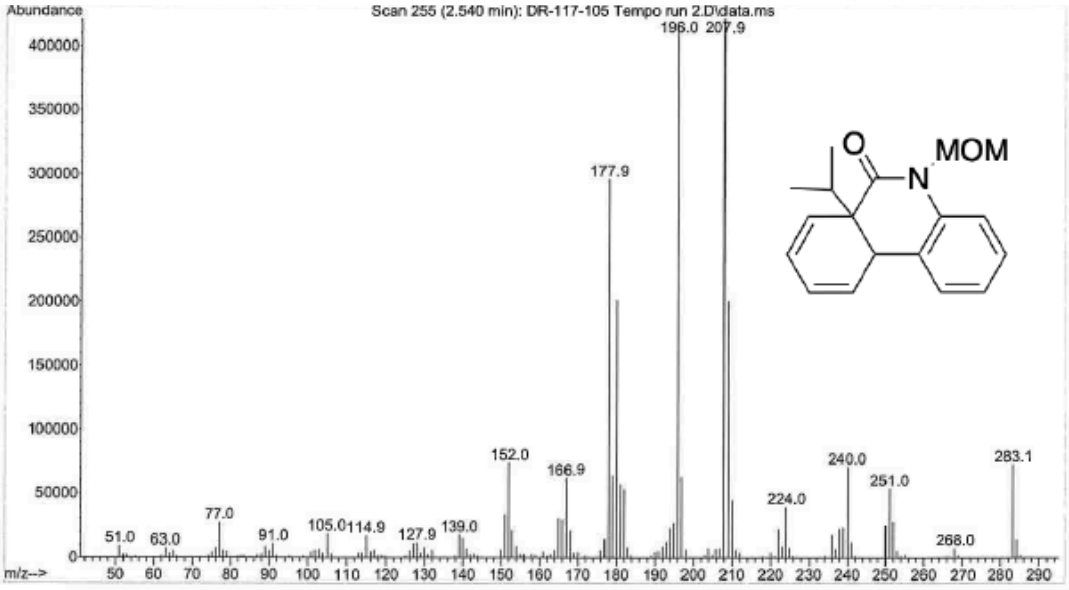

Figure 7.334 GCMS data for the control experiment using TEMPO.

7.19 Cost comparison of the Pd- vs Ni-catalyzed Heck reaction.

Pd-Catalyzed Heck Reaction

*(Cost of 1mmol scale)**

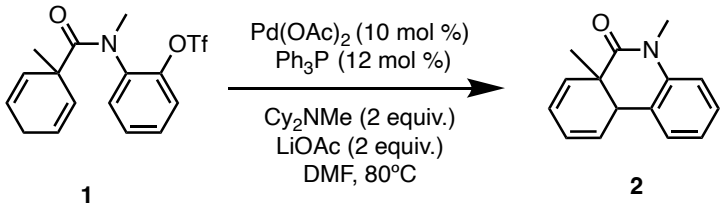

1 **2**

	1	**Pd(OAc)$_2$**	**Ph$_3$P**	**Cy$_2$NMe**	**LiOAc**	**Product**
MW(g/mol)	375.36	224.51	262.29	195.34	65.99	211.26
mmol	1.0	0.1	0.12	2.0	2.0	1.0
eq	1.0	0.1	0.12	2.0	2.0	1.0
g	0.375	0.0225	0.0315	0.391	0.132	0.211
mL	-	-	-	0.428	-	-
density (g/mL)	-	-	-	0.912	-	-
cost ($/mmol)	-	$17.03	$0.15	$0.08	$0.07	-
actual cost ($)	-	$1.70	$0.02	$0.15	$0.14	**$2.02**

*excluding the cost of aryl triflate **1** and DMF. All reagent costs are based on Sigma Aldrich Catalog.

Pd(OAc)$_2$ (205869-25G): $1890.00
Ph$_3$P (T84409-100G): $59.70
Cy$_2$NMe (294942-250G): $97.40
LiOAc (517992-100G): $106.00

Ni-Catalyzed Heck Reaction

*(Cost of 1mmol scale)**

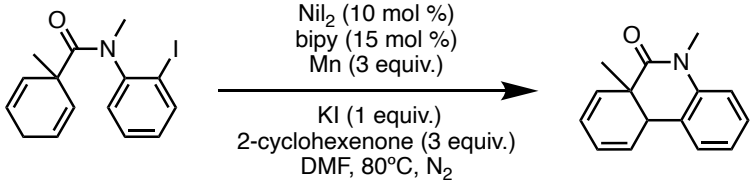

1 **2**

	1	**NiI$_2$**	**bipy**	**Mn**	**KI**	**cyclohexenone**	**Product**
MW(g/mol)	353.20	312.50	156.18	54.94	166.0	96.13	211.26
mmol	1.0	0.1	0.15	3.0	1.0	3.0	1.0
eq	1.0	0.1	0.15	3.0	1.0	3.0	1.0
g	0.353	0.0313	0.0234	0.165	0.166	0.288	0.211
mL	-	-	-	-	-	0.290	-
density (g/mL)	-	-	-	-	-	0.993	-
cost ($/mmol)	-	$1.89	$0.43	$0.01	$0.06	$0.13	-
actual cost ($)	-	$0.19	$0.06	$0.03	$0.06	$0.39	**$0.73**

*excluding the cost of aryl iodide **1** and DMF. All reagent costs are based on Sigma Aldrich Catalog.

NiI$_2$ (400777-25G): $151.00
Bipy (D216305-100G): $273.00
Mn (266132-250G): $67.60
KI (207969-500G): $182.00
2-cyclohexenone (C102814-100ML): $135.00

7.20 Computational data (by Prof. Paul Rablen)

Conformational Changes:
"**R**" = parent configuration
"**A**" = Ni complexed to other **a**lkene of cyclohexadiene (compared to parent)
"**F**" = tBu-(6)CH3iQuinox ligand **f**lipped ~180° (compared to parent)
"**T**" = amide **t**wisted other way (compared to parent)

Numbers in parentheses are the Gibbs free energies (in kcal/mol) of the transition structures relative to the global minimum for intermediate B.

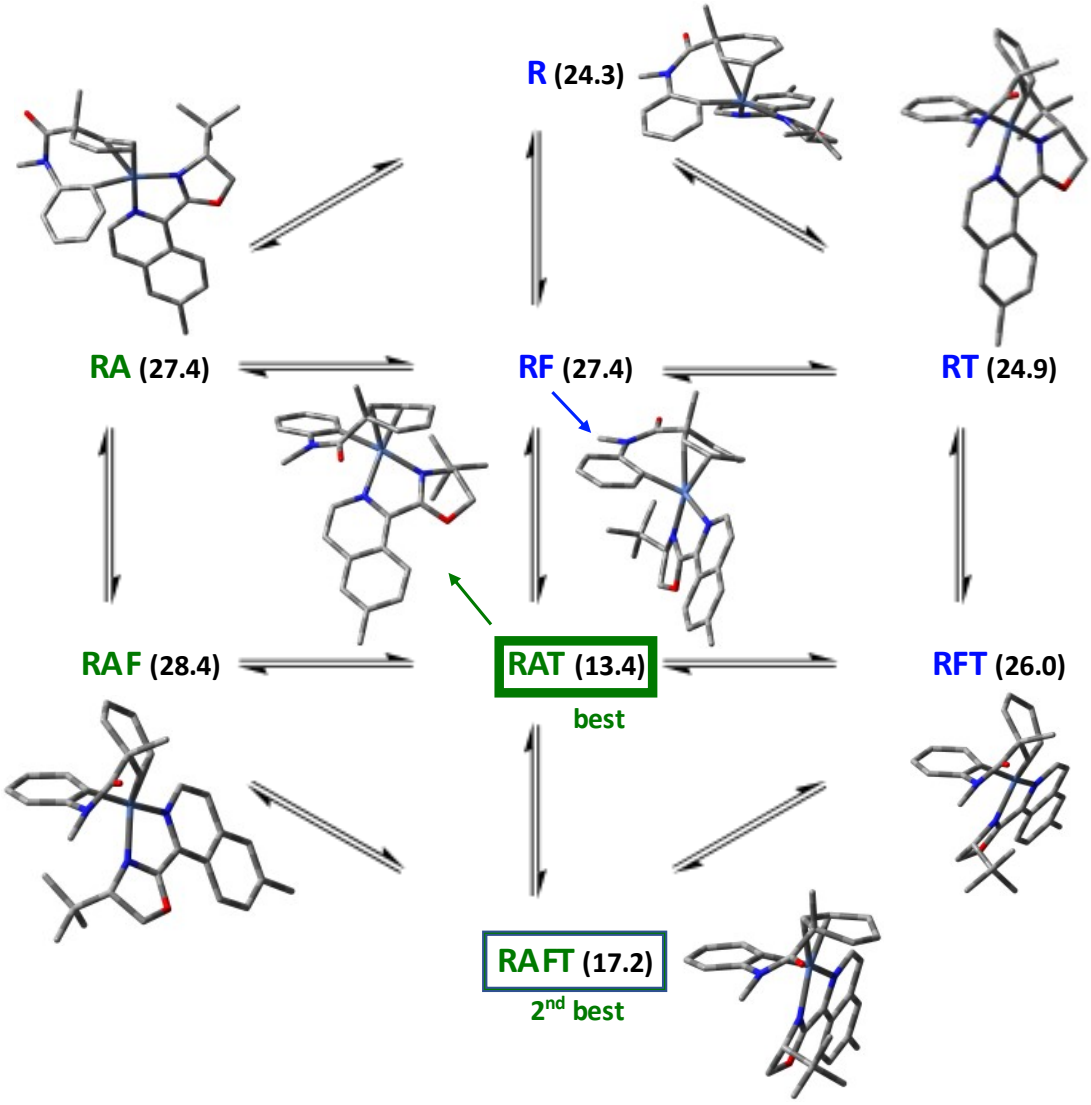

RA, RAF, RAT, and RAFT proceed to the observed **(S,S)** stereochemistry of product.

R, RF, RT, and RFT proceed to the unobserved **(R,R)** stereochemistry of product.

Figure 7.335 Conformation images and relative energy.

Table 7.2 Computational analysis – calculated results.

Mizoroki-Heck Cyclization																
Ni-Catalyzed																
B3LYP/Def2SVP EmpiricalDispersion=GD3BJ optimization								**B3LYP/Def2TZVPP EmpiricalDispersion=GD3BJ single-point**								Resulting stereochemistry in intC
								(thermodynamic corrections from the optimization at left)								1st = cabon bearing R1 (CH3 in this case) adjacent to C=O
R1=R2=CH3; R3=H																2nd = next carbon
L=bpy	**E (elec)**	**H**	**G**	**ΔE**	**ΔH**	**ΔG**		**E (elec)**	**H**	**G**	**ΔE**	**ΔH**	**ΔG**			
intB	-2713.85740	-2713.39213	-2713.47368	0.0	0.0	0.0		-2715.37357	-2714.90830	-2714.98985	0.0	0.0	0.0			
intB_to_intC_ts	-2713.85665	-2713.39236	-2713.47183	0.5	-0.1	1.2		-2715.37164	-2714.90734	-2714.98682	1.2	0.6	1.9			
intC	-2713.89035	-2713.42323	-2713.50331	-20.7	-19.5	-18.6		-2715.40473	-2714.93760	-2715.01768	-19.6	-18.4	-17.5			
L=tBu-(6)CH3iQuinox																
Nomenclature of stereoisomers:																
R configuration of cabon bearing tBu group.																
"R" = parent configuration																
"A" = Ni complexed to other alkene of cyclohexadiene (compared to parent)																
"F" = tBu-(6)CH3iQuinox ligand flipped ~180° (compared to parent)																
"T" = amide twisted other way (compared to parent)																
intB_tBuMeQ_R	-3062.84891	-3062.19526	-3062.29875	20.6	20.4	19.4		-3064.75092	-3064.09727	-3064.20077	20.7	20.5	19.5			
intB_to_intC_ts_tBuMeQ_R	-3062.84524	-3062.19198	-3062.29252	22.9	22.4	23.3		-3064.74585	-3064.09259	-3064.19313	23.9	23.4	24.3			
intC_tBuMeQ_R	-3062.92196	-3062.26600	-3062.36458	-25.2	-24.0	-21.9		-3064.81819	-3064.16223	-3064.26081	-21.5	-20.3	-18.2	R	R	
intB_tBuMeQ_RA	-3062.88010	-3062.22605	-3062.32799	1.0	1.0	1.0		-3064.78137	-3064.12732	-3064.22926	1.6	1.6	1.6			
intB_to_intC_ts_tBuMeQ_RA	-3062.83982	-3062.18731	-3062.28692	26.3	25.3	26.8		-3064.74103	-3064.08852	-3064.18813	26.9	25.9	27.4			
intC_tBuMeQ_RA	-3062.88813	-3062.23063	-3062.33071	-4.0	-1.8	-0.7		-3064.78922	-3064.13173	-3064.23181	-3.3	-1.2	0.0	S	S	
intB_tBuMeQ_RF	-3062.84325	-3062.18866	-3062.29050	24.1	24.5	24.5		-3064.74667	-3064.09208	-3064.19392	23.4	23.7	23.8			
intB_to_intC_ts_tBuMeQ_RF	-3062.84188	-3062.18835	-3062.28764	25.0	24.7	26.3		-3064.74229	-3064.08876	-3064.18805	26.1	25.8	27.4			
intC_tBuMeQ_RF	-3062.91393	-3062.25805	-3062.35794	-20.2	-19.0	-17.8		-3064.81135	-3064.15546	-3064.25535	-17.2	-16.1	-14.8	R	R	
intB_tBuMeQ_RT	-3062.88173	-3062.22770	-3062.32961	0.0	0.0	0.0		-3064.78390	-3064.12987	-3064.23178	0.0	0.0	0.0	Lowest energy intermediate B		
intB_to_intC_ts_tBuMeQ_RT	-3062.84354	-3062.19106	-3062.29098	24.0	23.0	24.2		-3064.74458	-3064.09211	-3064.19202	24.7	23.7	24.9			
intC_tBuMeQ_RT	-3062.88453	-3062.22918	-3062.33082	-1.8	-0.9	-0.8		-3064.78534	-3064.12999	-3064.23163	-0.9	-0.1	0.1	R	R	
intB_tBuMeQ_RAF	-3062.87955	-3062.22540	-3062.32672	1.4	1.4	1.8		-3064.78126	-3064.12710	-3064.22842	1.7	1.7	2.1			
intB_to_intC_ts_tBuMeQ_RAF	-3062.83851	-3062.18622	-3062.28597	27.1	26.0	27.4		-3064.73901	-3064.08673	-3064.18648	28.2	27.1	28.4			
intC_tBuMeQ_RAF	-3062.88548	-3062.22837	-3062.32992	-2.4	-0.4	-0.2		-3064.78644	-3064.12932	-3064.23087	-1.6	0.3	0.6	S	S	
intB_tBuMeQ_RAT	-3062.86461	-3062.21017	-3062.31281	10.7	11.0	10.5		-3064.76580	-3064.11136	-3064.21400	11.4	11.6	11.2			
intB_to_intC_ts_tBuMeQ_RAT	-3062.86328	-3062.20989	-3062.31047	11.6	11.2	12.0		-3064.76323	-3064.10984	-3064.21043	13.0	12.6	13.4	Lowest energy pathway		
intC_tBuMeQ_RAT	-3062.89586	-3062.24059	-3062.34182	-8.9	-8.1	-7.7		-3064.79386	-3064.13860	-3064.23983	-6.3	-5.5	-5.1	S	S	
intB_tBuMeQ_RFT	-3062.87927	-3062.22487	-3062.32524	1.5	1.8	2.7		-3064.78087	-3064.12647	-3064.22684	1.9	2.1	3.1			
intB_to_intC_ts_tBuMeQ_RFT	-3062.84275	-3062.19034	-3062.28995	24.5	23.4	24.9		-3064.74323	-3064.09082	-3064.19042	25.5	24.5	26.0			
intC_tBuMeQ_RFT	-3062.88913	-3062.23248	-3062.33310	-4.6	-3.0	-2.2		-3064.79050	-3064.13385	-3064.23447	-4.1	-2.5	-1.7	R	R	
intB_tBuMeQ_RAFT	-3062.86555	-3062.21078	-3062.31094	10.2	10.6	11.7		-3064.76850	-3064.11373	-3064.21390	9.7	10.1	11.2			
intB_to_intC_ts_tBuMeQ_RAFT	-3062.85700	-3062.20365	-3062.30321	15.5	15.1	16.6		-3064.75809	-3064.10474	-3064.20430	16.2	15.8	17.2	Second lowest energy pathway		
intC_tBuMeQ_RAFT	-3062.89821	-3062.24291	-3062.34230	-10.3	-9.5	-8.0		-3064.79610	-3064.14080	-3064.24019	-7.7	-6.9	-5.3	S	S	
Energy Conversion	627.51															

7.21 References

1. Frisch, M. J.; Trucks, G. W.; Schlegel, H. B.; Scuseria, G. E.; Robb, M. A.; Cheeseman, J. R.; Scalmani, G.; Barone, V.; Petersson, G. A.; Nakatsuji, H.; et al. *Gaussian 16*; Gaussian, Inc., **2016**.
2. Wu, X.; Turlik, A.; Luan, B.; He, F.; Qu, J.; Houk, K. N.; Chen, Y. Nickel-Catalyzed Enantioselective Reductive Alkyl-Carbamoylation of Internal Alkenes. *Angew.Chem.Int.* **2022**, *61*, e2022075.
3. Becke, A. D. Density-functional thermochemistry. III. The role of exact exchange. *J. Chem. Phys.* **1993**, *98*, 5648–5652.
4. Weigend, F. Accurate Coulomb-fitting basis sets for H to Rn . *Phys. Chem. Chem. Phys.* **2006**, *8* (9), 1057–1065.
5. Weigend, F.; Ahlrichs, R. Balanced basis sets of split valence, triple zeta valence and quadruple zeta valence quality for H to Rn: Design and assessment of accuracy . *Phys. Chem. Chem. Phys.* **2005**, *7* (18), 3297–3305.
6. Grimme, S.; Antony, J.; Ehrlich, S.; Krieg, H. A consistent and accurate ab initio parametrization of density functional dispersion correction (DFT-D) for the 94 elements H-Pu. *J. Chem. Phys.* **2010**, *132* (15), 154104.
7. Grimme, S.; Ehrlich, S.; Goerigk, L. Effect of the damping function in dispersion corrected density functional theory. *J. Comput. Chem.* **2011**, *32* (7), 1456 –1465.
8. Joo, W.; Wang, W.; Mesch, R.; Matsuzawa, K.; Liu, D.; Willson, C. G. Synthesis of Unzipping Polyester and a Study of its Photochemistry. *J. Am. Chem. Soc.* **2019**, *141* (37), 14736–14741. DOI: 10.1021/jacs.9b06285.
9. Jackson, L. V.; Walton, J. C. Homolytic dissociation of 1-substituted cyclohexa-2,5-diene-1-carboxylic acids: an EPR spectroscopic study of chain propagation. *J. Chem. Soc., Perkin Trans.* **2001** *2*(9), 1758-1764. DOI: 10.1039/b104859g.
10. Sexton, M.; Malachowski, W. P.; A., G. Y. P.; Rachii, D.; Feldman, G.; Krasley, A.; Chen, Z.; Tran, M.; Wiley, K.; Matei, A.; et al. Catalytic Enantioselective Birch−Heck Sequence for the Synthesis of Phenanthridinone Derivatives with an All-Carbon Quaternary Stereocenter. *J. Org. Chem.* **2022**, *87* (2), 1154–1172.
11. Krasley, A. T.; Malachowski, W. P.; Hannah, T. M.; Tran Tien, S. Catalytic Enantioselective Birch–Heck Sequence for the Synthesis of Tricyclic Structures with All-Carbon Quaternary Stereocenters. *Org. Lett.* **2018**, *20* (7), 1740–1743.
12. Krasley, A. T. Exploration of Synthetic Pathways to Quaternary Carbon Stereocenters and Fused Ring Systems via Birch Reductions. Bryn Mawr College, Scholarship, Research, and Creative Work at Bryn Mawr College, **2017**
13. Peng, Q.; Hu, J.; Yuan, H.; Xu, L.; Pan, X. Cp*Rh(iii) catalyzed *ortho*-halogenation of *N*-nitrosoanilines by solvent-controlled regioselective C–H functionalization. *Org. Biomol. Chem.* **2018**, *16* (24), 4471–4481. DOI: 10.1039/C8OB00601F.

14. Geerts, J. P.; Rasmussen, C. A. H.; van der Plas, H. C.; van Veldhuizen, A. PMR-studies on the formation of adducts between 4-substituted-5-bromopyrimidines and potassium amide in liquid ammonia. *Recl. Trav. Chim. Pays-Bas* **1974**, *98* (8), 231–233. .
15. White, W. L.; Filler, R. New reactions of polyfluoroaromatic compounds. Part II. Polyfluoroaralkyl amines. *J. Chem. Soc.* **1971**, 2062–2068.
16. Stoltz, B. M.; Holder, J. C.; Shockley, S. E.; Wiesenfeldt, M. P.; Shimizu, H. Preparation of (S)- t*ert* -ButylPyOx and Palladium-catalyzed Asymmetric Conjugate Addition of Arylboronic Acids. *Organic Synth.* **2016**, *92*, 1–16.
17. Hickey, D. P.; Rhodes, C. S. Z.; Gensch, T.; Fries, L.; Sigman, M. S.; Minteer, S. D. Investigating the Role of Ligand Electronics on Stabilizing Electrocatalytically Relevant Low-Valent Co(I) Intermediates. *J. Am. Chem. Soc.* **2019**, *141* (3), 1382–1392.
18. Sarmah, B. K.; Konwar, M.; Bhattacharyya, D.; Adhikari, P.; Das, A. Regioselective Cyanation of Six-Membered N -Heteroaromatic Compounds Under Metal-, Activator-, Base- and Solvent-Free Conditions. *Adv. Synth. Catal.* **2019**, *361*, 5616–5625.
19. Klapars, A.; Buchwald, S. L. Copper-Catalyzed Halogen Exchange in Aryl Halides: An Aromatic Finkelstein Reaction. *J. Am. Chem. Soc.* **2002**, *124* (50), 14844–14845.
20. Gonda, Z.; Kovács, S.; Wéber, C.; Gáti, T.; Mészáros, A.; Kotschy, A.; Novák, Z. Efficient Copper-Catalyzed Trifluoromethylation of Aromatic andHeteroaromatic Iodides: The Beneficial Anchoring Effect of Borates. *Org. Lett.* **2014**, *16* (16), 4268–4271.
21. Jin, Y.; Wang, C. Ni-catalysed reductive arylalkylation of unactivated alkenes. *Chem. Sci.* **2019**, *10*, 1780–1785
22. Wang, K.; Kong, W. Enantioselective Reductive Diarylation of Alkenes by Ni-Catalyzed Domino Heck Cyclization/Cross Coupling. *Synlett* **2019**, *30* (9), 1008–1014.
23. Li, Y.; Wang, K.; Ping, Y.; Wang, Y.; Kong, W. Nickel-Catalyzed Domino Heck Cyclization/Suzuki Coupling for the Synthesis of 3,3-Disubstituted Oxindoles . *Org. Lett.* **2018**, *20* (4), 921–924.
24. Chen, G.; Cao, J.; Wang, Q.; Zhu, J. Desymmetrization of Prochiral Cyclopentenes Enabled by Enantioselective Palladium-Catalyzed Oxidative Heck Reaction. *Org. Lett.* **2020**, *22* (1), 322–325.